frontiers | Research Topics

Environmental influences on the host-associated microbiomes

Edited by
Sandip Paul, Punyasloke Bhadury, Juan Sun and Yi Luo

Published in
Frontiers in Microbiology

ISSN 1664-8714
ISBN 978-2-8325-2710-8
DOI 10.3389/978-2-8325-2710-8

About Frontiers

Frontiers is more than just an open access publisher of scholarly articles: it is a pioneering approach to the world of academia, radically improving the way scholarly research is managed. The grand vision of Frontiers is a world where all people have an equal opportunity to seek, share and generate knowledge. Frontiers provides immediate and permanent online open access to all its publications, but this alone is not enough to realize our grand goals.

Frontiers journal series

The Frontiers journal series is a multi-tier and interdisciplinary set of open-access, online journals, promising a paradigm shift from the current review, selection and dissemination processes in academic publishing. All Frontiers journals are driven by researchers for researchers; therefore, they constitute a service to the scholarly community. At the same time, the *Frontiers journal series* operates on a revolutionary invention, the tiered publishing system, initially addressing specific communities of scholars, and gradually climbing up to broader public understanding, thus serving the interests of the lay society, too.

Dedication to quality

Each Frontiers article is a landmark of the highest quality, thanks to genuinely collaborative interactions between authors and review editors, who include some of the world's best academicians. Research must be certified by peers before entering a stream of knowledge that may eventually reach the public - and shape society; therefore, Frontiers only applies the most rigorous and unbiased reviews. Frontiers revolutionizes research publishing by freely delivering the most outstanding research, evaluated with no bias from both the academic and social point of view. By applying the most advanced information technologies, Frontiers is catapulting scholarly publishing into a new generation.

What are Frontiers Research Topics?

Frontiers Research Topics are very popular trademarks of the *Frontiers journals series*: they are collections of at least ten articles, all centered on a particular subject. With their unique mix of varied contributions from Original Research to Review Articles, Frontiers Research Topics unify the most influential researchers, the latest key findings and historical advances in a hot research area.

Find out more on how to host your own Frontiers Research Topic or contribute to one as an author by contacting the Frontiers editorial office: frontiersin.org/about/contact

Environmental influences on the host-associated microbiomes

Topic editors
Sandip Paul — JIS Institute of Advanced Studies and Research, India
Punyasloke Bhadury — Indian Institute of Science Education and Research Kolkata, India
Juan Sun — Qingdao Agricultural University, China
Yi Luo — Nankai University, China

Topic Coordinator
Paltu Kumar Dhal — Jadavpur University, India

Citation
Paul, S., Bhadury, P., Sun, J., Luo, Y., eds. (2023). *Environmental influences on the host-associated microbiomes*. Lausanne: Frontiers Media SA.
doi: 10.3389/978-2-8325-2710-8

Table of contents

frontiers | Frontiers in Microbiology

ORIGINAL RESEARCH
published: 12 July 2022
doi: 10.3389/fmicb.2022.934232

Contrasting Diversity and Composition of Human Colostrum Microbiota in a Maternal Cohort With Different Ethnic Origins but Shared Physical Geography (Island Scale)

Wanying Xie[1†], Huimin Zhang[2†], Yongqing Ni[2] and Yunhua Peng[1,3*]*

[1] Department of Obstetrics and Gynecology, Hainan Medical University, Haikou, China, [2] School of Food Science and Technology, Shihezi University, Xinjiang, China, [3] The First Affiliated Hospital of Hainan Medical University, Haikou, China

OPEN ACCESS

Edited by:
Yi Luo,
Nankai University, China

Reviewed by:
Fengwei Tian,
Jiangnan University, China
Lei Yan,
Heilongjiang Bayi Agricultural University, China

***Correspondence:**
Yongqing Ni
niyqlzu@sina.com
Yunhua Peng
2008pengyh@163.com

[†]These authors share first authorship

Specialty section:
This article was submitted to Microbial Symbioses, a section of the journal Frontiers in Microbiology

Received: *02 May 2022*
Accepted: *22 June 2022*
Published: *12 July 2022*

Citation:
Xie W, Zhang H, Ni Y and Peng Y (2022) Contrasting Diversity and Composition of Human Colostrum Microbiota in a Maternal Cohort With Different Ethnic Origins but Shared Physical Geography (Island Scale). Front. Microbiol. 13:934232. doi: 10.3389/fmicb.2022.934232

Colostrum represents an important source for the transfer of important commensal bacteria from mother to newborn and has a strong impact on the newborn's health after birth. However, the composition of the colostrum microbiome is highly heterogeneous due to geographic factors and ethnicity (maternal, cultural, and subsistence factors). By analyzing the colostrum 16S rRNA gene full-length sequencing dataset in 97 healthy mothers (60 from Han, 37 from Li) from the Hainan island of China, we showed that the ethnic differences of the colostrum microbiome in a maternal cohort with different ethnic origins shared physical geography. Results indicated that the richness of microbial community in colostrum of Han women was higher than that of Li women, but there was no significant difference in Shannon index and invsimpson index between the two groups. Visualization analysis based on the distance showed an obvious ethnicity-associated structural segregation of colostrum microbiota. The relative abundance of *Firmicutes* was higher in the microbiota of the Han group than in Li's, while *Proteobacteria* was on the contrary. At the genus level, the most dominant members of the Han and Li ethnic groups were *Acinetobacter* and *Cupriavidus*, two common environmental bacteria, respectively, although skin-derived *Staphylococcus* and *Streptococcus* were still subdominant taxa. *Cupriavidus lacunae* was the most dominant species in the Li group, accounting for 26.10% of the total bacterial community, but only 3.43% for the Han group with the most dominant *Staphylococcus petrasii* (25.54%), indicating that human colostrum microbiome was more susceptible to local living environmental factors. Hence, the ethnic origin of individuals may be an important factor to consider in human milk microbiome research and its potential clinical significance during the perinatal period in ethnic-diverse societies, even within a small geographic scale.

Keywords: 16S rRNA gene, ethnicity, colostrum microbiome, Island scale, diversity

INTRODUCTION

Colostrum is the first milk sucked by a baby after birth, and it is usually produced within 4–5 days after the mother has given birth (Fernández and Rodríguez, 2020; Stinson et al., 2021). Human milk (HM) contains the considerable beneficial nutrients and biologically active factors (Andreas et al., 2015; Williams et al., 2017), and it is universally considered the optimal source of nutrition for almost all healthy infants (Hunt et al., 2011; Lloyd-Price et al., 2016). In the meantime, increasing evidence shows that HM contains a diverse range of microbes (Oikonomou et al., 2020; Zimmermann and Curtis, 2020), which has important health implications for both mothers (mammary gland health) and infants (protection from diarrheal and respiratory diseases) (Lyons et al., 2020). Studies have shown that the relative abundance of potentially beneficial microbiota *Lactobacillus* and *Bifidobacterium* in exclusively breastfed infants is significantly higher than that in mixed-fed and formula-fed infants (Fehr et al., 2020; Lyons et al., 2020). Therefore, breastfeeding is one of the most optimum feeding regimes for newborn infants.

The maternal gut is thought to be the most important source of bacteria that are detectable in HM (*via* an entero-mammary pathway). However, it is incredible that more than 1,300 species and 3,500 operational taxonomic units of bacteria have been reported to be present in HM, even implying that the bacterial diversity in breast milk appears to be higher than in infant or maternal feces (Zimmermann and Curtis, 2020). Obviously, not all the bacteria detected in breast milk are considered inherent inhabitants of the mammary gland, and instead, a fairly large number of them come from environmental exposure (skin microbiota of the mother and the oral cavity of the infant), leading to significant differences between ethnic groups and/or even inter-individuals (Pannaraj et al., 2017). According to existing data, colostrum is characterized by higher diversity and more significant disparity in microbiome composition, compared with mature milk.

Depending on the source of bacteria, multiple factors could contribute to shaping the milk microbiota (Andreas et al., 2015; Zimmermann and Curtis, 2020). On the one hand, the microbial composition and diversity of breast milk may be influenced by maternal characteristics, including ethnicity (Deschasaux et al., 2018; Xu et al., 2020; Shafiee et al., 2022), pregnancy age, body mass index (BMI) (Cabrera-Rubio et al., 2012), mode of delivery (Cabrera-Rubio et al., 2012), parity, and intake of intrapartum antibiotics or probiotics (de Andrade et al., 2021). Meanwhile, several studies have reported differences in the microbiota composition of HM in different geographic locations, just as they do in the human skin metagenome (Gupta et al., 2017). Geography is an ensemble of multiple factors responsible for geography-based alterations in microbiota, including environmental (temperature, humidity, and altitude), population genetic, and cultural factors. In terms of microbiome studies, host surface-associated microbiomes could respond strongly to variations in environmental factors (Woodhams et al., 2020). Therefore, it is reasonable to speculate that bioclimatic factors would shape the composition of the human breast milk microbiome by exerting a force over skin microorganisms.

Modern molecular techniques, especially next-generation sequencing (NGS), are a more sensitive and less biased analytical method than the culture-based method and have been adopted for characterization of the composition and diversity of the human microbiome by using the 16S rRNA gene (Bardanzellu et al., 2017). To date, most of the studies utilized a shorter variation region of the 16S rRNA gene to profile human breast milk microbiota, such as the 16s rRNA gene V4 or V4-V5 region (Kumar et al., 2016; Ojo-Okunola et al., 2018) and the V1-V3 region (Williams et al., 2017). Due to the drawback of the short reading length, the composition of breast milk microbes cannot be exactly documented (Jost et al., 2012; Walker et al., 2015). By contrast, 16S rRNA gene full-length amplicon sequencing could achieve more accurate representation by providing species-level microbiome data (Lopez Leyva et al., 2021).

Human Milk presents an interplay between a mother and her infant from an evolutionary perspective. The various components of colostrum have a great impact on the newborn's health after birth. Among them, the human milk oligosaccharides (HMOs) are thought to play a role in preventing pathogenic bacterial adhesion and orchestrating the development of the microbiota (Cheema et al., 2022; Sprenger et al., 2022). Particularly, bacteria in colostrum can stimulate the anti-inflammatory response by stimulating the production of specific cytokines, gradually promoting the maturation of the newborn's immune system, although most of them might not be residents of infant gut microbiota. However, the high heterogeneity is characteristic of the composition of the colostrum microbiome depending on geographical and ethnic variations (maternal, cultural, and subsistence factors) (Gupta et al., 2017). So, parsing the appreciable disparity of colostrum microbiome between sub-populations in the same locality helps understand the clinical significance of breast milk microbiota in the perinatal period.

In the present study, we analyzed the NGS datasets of bacterial 16S rRNA full-length gene of colostrum samples in a maternal cohort containing two different ethnic groups, which included 97 healthy mothers (60 from Han and 37 from Li) from Hainan Island, the southernmost province in China. Historically, Li ethnic group is an indigenous people who live mostly in rural areas; Most of the Han Chinese are immigrants and live in cities or towns. We aimed to gain insight into the colostrum microbiome patterns of different sub-populations with shared physical climate in the narrow region (Island scale) and to assess how ethnicity (maternal, cultural factors, and subsistence) influences microbiota in the breast milk of healthy mothers.

MATERIALS AND METHODS

Sample Collection

In this study, a total of 97 mothers (18–41 years old, with an average age of 28 years) after childbirth were recruited. The above volunteers all lived in Hainan for a long time. Among them, 37 mothers are of Li nationality and 60 mothers of Han nationality. Demographic data about the volunteer mothers' BMI, delivery mode, and the use of antibiotics and probiotics during pregnancy were summarized in **Table 1**. When collecting samples, they have

informed and signed an informed consent form for themselves and their family members. In addition, this study has also been approved by the ethics committee of Shihezi University.

Colostrum samples were collected into sterile tubes by manual expression using sterile gloves after nipples and areolas were cleaned with a swab soaked in sterile water or saline (Rodriguez-Cruz et al., 2020); the first 1–2 mL of milk was discarded to avoid contamination from the environment as much as possible (Douglas et al., 2020). Then, 5–15 mL of milk was collected and was immediately frozen and stored at −80°C until DNA extraction.

DNA Extraction

FastPure Bacteria DNA Isolation Mini Kit (Vazyme, Nanjing, China) was used for the extraction of breast milk DNA with slight modification and combined with the glass bead beating method (Cheema et al., 2021; Lyons et al., 2021). About 1 mL of breast milk was centrifuged at 12,000 rpm (∼13,400 × *g*) for 10 min at 4°C, and the fat was removed with a sterile cotton swab and the supernatant was discarded (Ojo-Okunola et al., 2020). Add lysozyme (100 mg/mL) to the centrifuge tube and bath at 37°C for 30 min to achieve the purpose of enzymatic hydrolysis; then add 0.25 g zirconium beads (0.1 mm) and use a cell tissue disruptor to physically break the cell wall. After the fragmentation is completed, add 250 μL of Buffer GB, shake and mix, and incubate at 70°C for 10 min; add 4 μL RNase A to the digestion solution and heat at 65°C for 10 min to remove the RNA and obtain pure DNA as much as possible; add Proteinase K (20 mg/mL) to the sample and incubate at 58°C for 30 min to make it fully active (Hunt et al., 2011); then follow the steps in the instructions for column purification. Each DNA pellet was resuspended in 50–100 μL of Elution Buffer.

The DNA was quantified using a NanoDrop ND-2000 spectrophotometer (NanoDrop Technologies, Wilmington, DE, United States), and the remaining DNA was stored in a refrigerator at −20°C until the next step.

TABLE 1 | Demographic characteristics of the mothers in the study population.

Characteristics and demographic data	Values or (%)
Ethnicity	
Li	37 (38.1%)
Han	60 (61.9%)
Age	
18–25	21 (21.6%)
26–35	67 (69.1%)
36–45	9 (9.3%)
Maternal BMI condition	
Normal (18.0–23.9)	24 (24.7%)
Slightly fat (24.0–26.9)	28 (28.8%)
Obesity (27.0–29.9)	30 (30.9%)
Severe obesity (≥ 30.0)	16 (15.6%)
Lifestyle	
Farmer	51 (52.6%)
Urban	46 (47.4%)
Delivery mode	
Vaginal	70 (72.2%)
Cesarean	27 (27.8%)
Intrapartum antibiotics	
Received	18 (18.5%)
Not received	79 (81.5%)
Parity	
0	38 (39.2%)
1	46 (47.4%)
2–3	13 (13.4%)

The 16S rRNA Full-Length Amplicon Sequencing

The microbial library construction and sequencing of the total DNA of 97 colostrum samples were completed by Shanghai Personal Biotechnology Co., Ltd. (Shanghai, China). PCR amplification of full-length 16S rRNA gene was performed using a forward primer PB_16s_Bac-F (5′-AGAGTTTGATCMTGGCTCAG-3′) and a reverse primer PB_16s_Bac-R (5′-ACCTTGTTACGACTT-3′). To distinguish each sample, a unique barcode was added to each sample for specific amplification. The PCR amplification system was 25 μL, including 5 × reaction buffer 5 μL, 5 × GC buffer 5 μL, dNTP (2.5 mM) 2 μL, barcoded primers with forward primer (10 μM) 1 μL, reverse primer (10 μM) 1 μL, DNA template 2 μL, double distilled water (ddH_2O) 8.75 μL, and Q5 DNA Polymerase 0.25 μL. The PCR conditions were as follows: 98°C for 2 min, 30 cycles at 98°C for 15 s, 55°C for 30 s, and 72°C for 30 s, and final extension at 72°C for 5 min. Sequencing was performed with PacBio Sequel sequencer.

Raw Sequence Analysis

The original data files are converted into FASTQ format files and saved by using CCS v 4.0.0 [Generate Highly Accurate Single-Molecule Consensus Reads (HiFi Reads) software]. Use Perl[1] script to divide the barcode sequence at both ends of the sequence, remove the barcode, and then transpose the reverse complementary sequence to the forward direction according to the primer sequence. Raw sequences were processed by using a pipeline combining USEARCH 11.0 Linux 64-bit and QIIME2. High-quality reads, as selected using the default values in USEARCH, were binned into amplicon sequence variants (ASVs) according to the denoising (error-correcting) Illumina amplicon reads using Unoise3, through an open-reference strategy. Taxonomic identification of ASVs for the sequences was assigned using the Naive Bayes classifier of the Ribosomal Database Project (RDP) against the Greengenes database and generated the feature table for subsequent analysis.

Diversity Analysis and Significant Difference Analysis Between Ethnic Groups

Alpha diversity indices were calculated in QIIME2 from rarefied samples using the Chao1 and ACE indexes for richness, and the Shannon and invsimpson indexes for diversity, and

[1]https://github.com/torognes/vsearch/wiki/VSEARCH-pipeline

statistics and the difference check box plot were performed using the personalbio genescloud platform.[2] Beta diversity was calculated using Bray–Curtis distance, and principal coordinates analysis (PCoA) was performed. VENN analyses were also conducted using the R package Statistical analyses between different groups and were analyzed using ANOVA (Liu et al., 2021). Cytoscape_v3.8.2 was used to draw the network diagram. Mann–Whitney U-test was used for diversity and taxonomic comparisons between groups at different levels (phylum, genus, and species). Based on the standardized matrix and grouping information, STAMP 2.1.3 was used to analyze different genus and species. Linear discriminant analysis (LDA) effect size (LEfSe) analysis was performed at http://www.ehbio.com/Cloud_Platform/front (Liu et al., 2021). IBM SPSS statistical 26 was used to calculate the p-value. The $p < 0.05$ was considered statistically significant.

RESULTS

Description of the Study Population

The socio-demographic characteristics of Li ($n = 37$) and Han's mothers ($n = 60$) are summarized in **Table 1**. The mean maternal age in both groups was 28 years old. The average BMI was 27.1 and 25.5 for women in the Li and Han ethnic groups, respectively.

Table 2 showed the significant analysis results of the interaction between ethnic and other mother-related factors. BMI was significantly correlated with ethnic factors and the same as the mode of delivery ($p < 0.05$). There were extremely significant differences between the Li and Han groups in the mother's lifestyle and the use of intrapartum antibiotics (Chi-square, both $p = 0.001$). There were no significant differences in maternal age and parity between Li and Han ethnic groups (all $p > 0.05$).

At the same time, we conducted a multivariate analysis of variance. The results of the analysis are shown in **Supplementary Table 1**. We did not discuss the effects between the two groups in detail when considering the distribution of the sample and the effects of the statistical test.

[2]https://www.genescloud.cn/login

TABLE 2 | Socio-demographic characteristics of subjects.

Characteristics	Li ($n = 37$)	Han ($n = 60$)	p-value
Age (mean ± SD, range)[1]	27.9 ± 5.7 (18–41)	29.2 ± 4.1 (21–41)	0.267
18–25	11 (29.7%)	10 (16.7%)	
26–35	21 (56.8%)	46 (76.7%)	
36–45	5 (13.5%)	4 (6.7%)	
Maternal BMI condition (mean ± SD, range)[1]	25.5 ± 3.1 (19–31)	27.1 ± 3.4 (21.5–35)	0.023*
Normal weight (18.0–23.9)	11 (29.7%)	13 (21.7%)	
Slightly fat (24.0–26.9)	15 (40.5%)	16 (26.7%)	
Obesity (27.0–29.9)	7 (18.9%)	19 (31.7%)	
Severe obesity (≥ 30.0)	4 (10.8%)	12 (20.0%)	
Lifestyle[2]			0.001***
Farmer	37 (100%)	13 (21.7%)	
Urban	0 (0%)	47 (78.3%)	
Delivery mode[2]			0.009**
Vaginal delivery	32 (86.5%)	37 (61.7%)	
C-section	5 (13.5%)	23 (38.3%)	
Intrapartum antibiotics[2]			0.001***
Received	0 (0%)	18 (30.0%)	
Not received	37 (100%)	42 (70.0%)	
Parity[2]			0.065
0	10 (27.0%)	28 (46.7%)	
1	19 (51.4%)	27 (45.0%)	
2–3	8 (21.6%)	5 (8.3%)	

*[1]t-test; [2]Chi-square. *p < 0.05, **p < 0.01, ***p < 0.001.*

DNA Sequencing and Filtering

A total of 859,638 16S rRNA raw reads were generated from the 97 samples. After filtering low-quality sequences, 859,345 filtered sequences were retained with lengths measuring 1,200–1,500 bp. All 859,345 high-quality sequences were clustered into ASVs at 100% sequence similarity using Quantitative Insights Into Microbial Ecology (QIIME2) software. An average number of high-quality sequences in each sample reached 17,543 and a total of 789 ASVs were discovered in 97 samples.

Diversities of Bacterial Communities of Colostrum Across Two Ethnic Groups

According to the number of ASVs, the alpha diversity of microflora in colostrum was calculated under different maternal-related factor grouping (**Supplementary Table 2**). Results showed that ethnicity, age, and lifestyle had a significant effect on the microbial richness of colostrum, among which the ethnic factor had the most significant impact on the richness. Then, when we grouped by ethnicity, the chao1 of colostrum microbiome in Han's mothers (151.54 ± 60.86) was significantly ($p = 0.001$) higher than the index of colostrum in Li's mothers (106.75 ± 40.06) (**Figure 1A**), and the same trend was observed in the index of ace (Li 108.99 ± 39.46 vs. Han 152.65 ± 59.29) (**Figure 1B**). However, we did not find a significant difference in the Shannon and invsimpson index (**Figures 1C,D**). (Li 2.76 ± 0.69 vs. Han 2.82 ± 0.81) (Li 10.15 ± 4.97 vs. Han 11.15 ± 9.14). To investigate the taxonomic structural distinctiveness of colostrum microbial communities between Li and Han Ethnic Groups, beta-diversity analysis was conducted based on the Bray–Curtis distance (**Figure 1E**). There is an obvious structural separation between the two ethnic groups.

Impact of Ethnic and Delivery Mode on Microbial Diversity in Colostrum

When we grouped all the data by the mode of delivery (vaginal vs. cesarean), the diversity of the cesarean group was higher than that of the vaginal group (**Supplementary Table 2**). Based on the ethnicity (Han vs. Li) and the mode of delivery (vaginal vs. cesarean), 97 samples were divided into four groups (Han_vaginal and Han_cesarean and Li_vaginal and

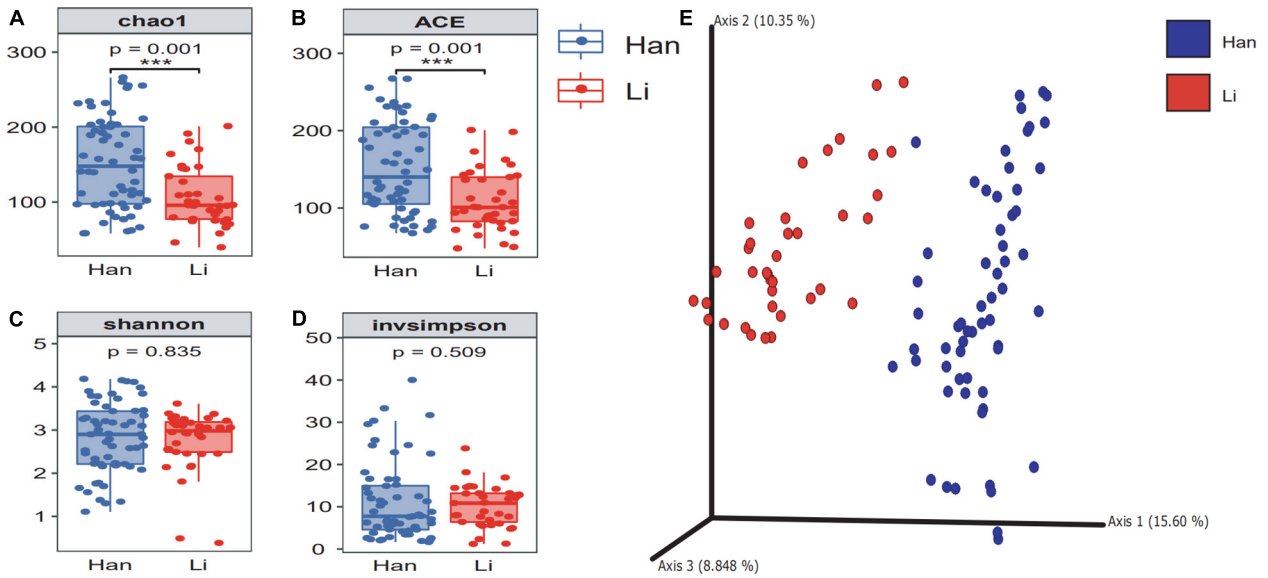

FIGURE 1 | The α diversity and β diversity of colostrum microbiota of two ethnic groups. The difference check box plot shows the alpha diversity between the Li and Han ethnic groups. chao1 **(A)** and ACE **(B)** can reflect the abundance, and Shannon **(C)** and invsimpson **(D)** can reflect the diversity between Li and Han's mothers analyzed by 16S rRNA gene sequencing. **(E)** Principal coordinate analysis plot of Bray–Curtis distance.

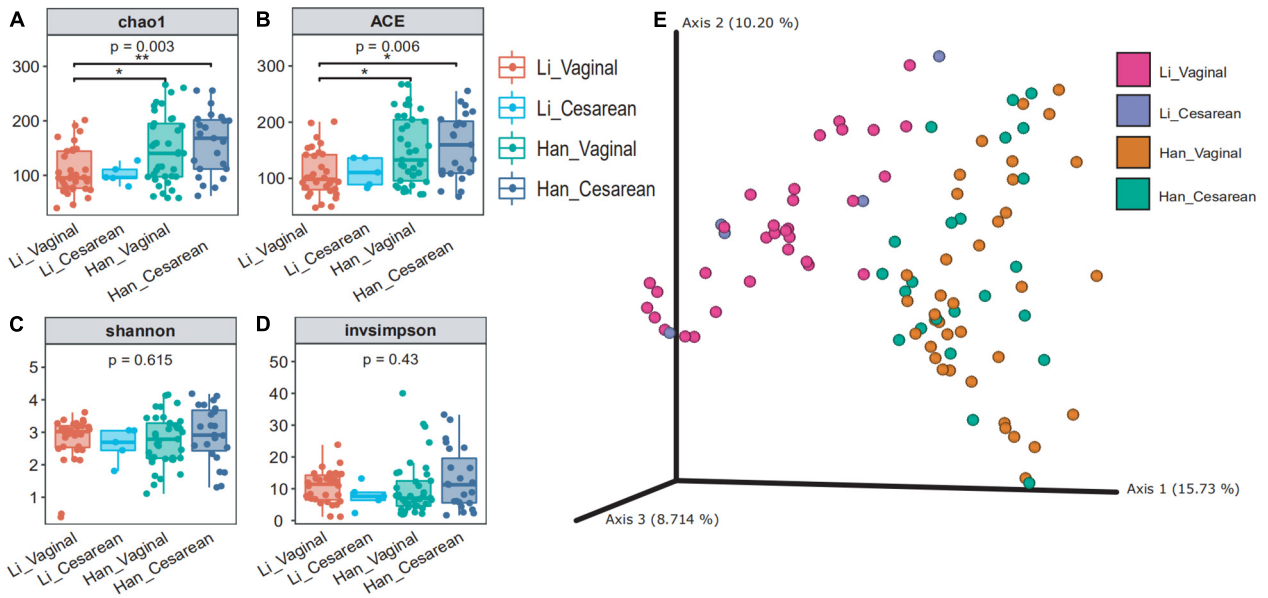

FIGURE 2 | Colostrum microbial diversity in China's Hainan cohort grouped by ethnicity (Han/Li) and mode of delivery (cesarean/vaginal). chao1 **(A)** and ACE **(B)** reflected the abundance of the four groups (Li_Vaginal and Li_Cesarean and Han_Vaginal and Han_Cesarean), and Shannon **(C)** and invsimpson **(D)** reflected the diversity. **(E)** Bray–Curtis distance of the 97 samples using the full set of ASVs. The percentage of the variation explained by the plotted principal coordinates (PCs) was shown in parentheses.

Li_cesarean). The chao1 and ace indexes showed that there were significant differences between the colostrum microbial α-diversity of the mothers of the Li_vaginal group and the Han_vaginal group (**Figures 2A,B**). When we consider the richness of microbiota, the results showed that the richness indexes (chao1 and ace) of the Han_cesarean group were the highest, followed by the Han_vaginal group. Different from the Han ethnic group, the diversity index of the Li_vaginal group was higher than that of the Li_cesarean group. The Shannon and invsimpson index showed that there was no significant difference among the four groups (**Figures 2C,D**). β-diversity analysis showed that the two groups of the same ethnic group among the

four groups were gathered, that is, the Han_vaginal group and the Han_cesarean group were clustered together and the Li_vaginal group and the Li-cesarean group were gathered (**Figure 2E**). In conclusion, PCA showed that there was an obvious division in the diversity of colostrum microbes between Li and Han ethnic groups regardless of the grouping of delivery modes.

Colostrum Microbiota Compositional Analysis

We profiled the bacterial composition of colostrum microbiota between different groups at the level of phylum, genus, and species. Bacterial taxa with a relative abundance of less than 1% in individual samples were categorized into the "others" group.

The results of the phylum level show that the most dominant phyla in Li colostrum is *Proteobacteria* (66.5%), followed by *Firmicutes* (29.5%). Interestingly, the results of the dominant phylum in the microbial composition of breast milk in the Han population are completely opposite; *Firmicutes* is the most dominant phylum with a relative abundance of 46.5% and *Proteobacteria* with a relative abundance of 43.7% (**Table 3** and **Supplementary Figure 1A**). When analyzing at the genus level, *Cupriavidus* (26.28%), *Staphylococcus* (17.36%), and *Streptococcus* (13.11%) were relatively abundance genera in the Li population cohort; while in Han colostrum, *Acinetobacter* (28.72%), *Staphylococcus* (28.38%), and *Streptococcus* (9.45%) were dominant genera. **Table 3** and **Supplementary Figure 1C** showed that the microbial components of colostrum between the two ethnic groups are more abundant and diverse at the species level. Among the Li population, species with a relative abundance above 1% were *Cupriavidus lacunae* (26.10%), *Staphylococcus petrasii* (16.60%), *Enterobacter hormaechei* (7.83%), *Streptococcus himalayensis* (5.50%), and *Streptococcus panodentis* (1.09%). In the Han group, there were eight species with an abundance of more than 1%, namely *Staphylococcus petrasii* (25.54%), *Streptococcus himalayensis* (4.37%), *Citroniella saccharovorans* (4.11%), *Cupriavidus lacunae* (3.43%), *Enterobacter hormaechei* (2.67%), *Staphylococcus pseudoxylosus* (1.96%), *Streptococcus panodentis* (1.93%), and *Klebsiella aerogenes* (1.01%).

Core Microbiota Analysis of Colostrum Based on Amplicon Sequence Variant Level

The core composition of colostrum bacteria and specific ASVs or species with a relative abundance of more than 0.1% were screened from 97 samples. The overlapping areas of the circles in the Venn diagram represent the core microbiome, which is generally defined as a shared group of microbiome members from similar habitats. As shown in the Venn diagram, a total of 32 ASVs were observed as common ASVs, 96 ASVs in the Han ethnic group, and 60 ASVs in the Li ethnic group (**Figure 3A**). The 32 ASVs assigned to the eight-core genera were *Staphylococcus*, *Acinetobacter*, *Streptococcus*, *Cutibacterium*, *Cupriavidus*, *Enterobacter*, *Rhodopseudomonas,* and *Paucibacter*. Among the 16 ASVs belonging to *Staphylococcus*, 14 ASVs can be classified to the *Staphylococcus* species level: *Staphylococcus pseudoxylosus* (ASV_59 and ASV_83) and *Staphylococcus petrasii* (ASV_3, ASV_4, ASV_18, ASV_34, ASV_62, ASV_65, ASV_66, ASV_74, ASV_75, ASV_82, ASV_124, and ASV_282). The four ASVs of Acinetobacter were divided into two species: *Acinetobacter courvalinii* (ASV_5 and ASV_10) and *Acinetobacter oleivorans* (ASV_21 and ASV_78). Among the 3 ASVs belonging to *Streptococcus*, ASV_29 and ASV_72 were classified as *Streptococcus himalayensis*, while ASV_9 could not be classified to the species level. ASV_47 and ASV_60 both belonged to *Cutibacterium acnes.* In addition, *Cutibacterium modestum* (ASV_26) could also be detected in our study. Other ASVs that can be identified include *Cupriavidus lacunae* (ASV_1), *Cupriavidus nantongensis* (ASV_80), *Enterobacter bugandensis* (ASV_15), *Rhodopseudomonas boonkerdii* (ASV_31), and *Paucibacter oligotrophus* (ASV_6).

When considering the mode of delivery and the ethnic factor, network analysis revealed the total number of ASVs among the four groups (Han_Cesarean, Han_Vaginal, Li_Cesarean, and Li_Vaginal). There were 42 ASVs in Han_Cesarean and Han_Vaginal groups, belonging to 11 genera: *Acinetobacter*, *Staphylococcus*, *Enterococcus*, *Streptococcus*, *Thermus*, *Meiothermus*, *Diaphorobacter*, *Cutibacterium*, *Brucella*, *Chryseobacterium,* and *Brachybacterium.* In the Li_Cesarean and Li_Vaginal groups, 10 ASVs were identified as *Acinetobacter*, *Enterococcus,* and *Streptococcus*, another 10 ASVs belong to *Novosphingobium*, *Ruegeria*, *Agrobacterium*, *Phytobacter*, *Delftia*, *Serratia,* and *Cupriavidus*. Only ASV_141 (*Corynebacterium*) belongs to the Cesarean group; while the vaginal group had four specific ASVs, including *Streptococcus himalayensis* (ASV_46 and ASV_72) and *Staphylococcus petrasii* (ASV_55), and ASV_124 could only be assigned into the *Staphylococcus* (**Figure 3B**).

Microbial Signatures in Different Ethnic Group Samples

Linear discriminant analysis effect size (LEfSe) analysis of ASVs, with an average relative abundance of$>$0.01%, was further conducted to detect microbial signatures in the colostrum of Han and Li ethnic groups. **Figure 4A** was a histogram of LDA value distribution, showing species with LDA Score greater than 3.0. The significant biomarkers in the entire Han and Li groups were mainly distributed in *Proteobacteria* and just several significant biomarkers were distributed in *Actinobacteria*, *Firmicutes,* and *Deinococcus_Thermus*. Analysis of the different species in Li people showed that they were all belonging to *Proteobacteria.* In the Li group, the LDA score was highest in *Burkholderiales*. The highest LDA score was found in the Acinetobacter of Han ethnicity. The LEfSe cladogram analysis revealed that 39 biomarkers of different classification levels were significantly different among the two groups (**Figure 4B**). Notably, we did not find any differences in biomarkers at the species level.

Using the stamp software and the Benjamin FDR method, the extend-bar plot showed the difference between the two groups. Overall, 17 distinct genera and 25 distinct species were identified. *Cupriavidus* and *Enterobacter* were the two most significant genera in the Li ethnic group. *Staphylococcus*

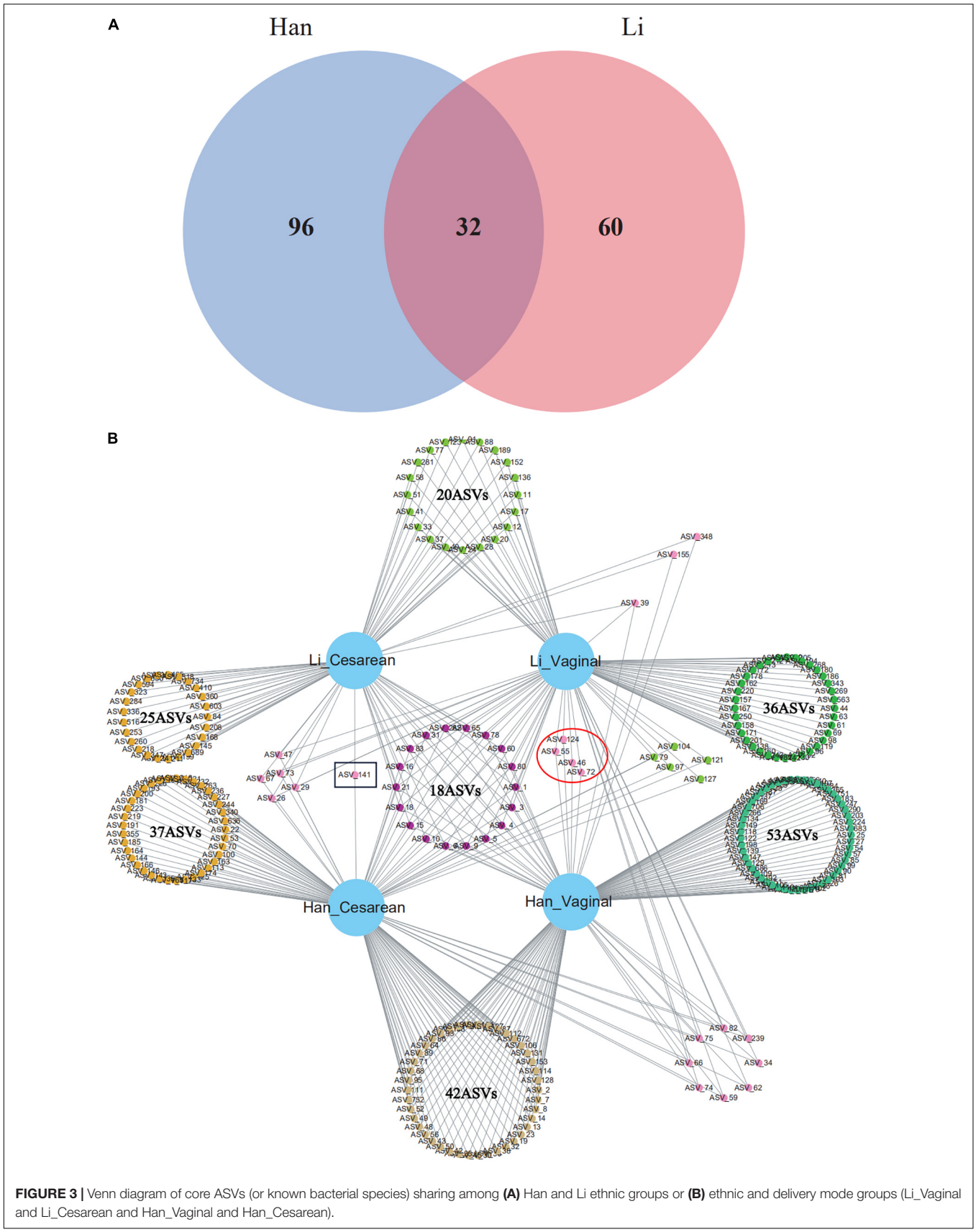

FIGURE 3 | Venn diagram of core ASVs (or known bacterial species) sharing among **(A)** Han and Li ethnic groups or **(B)** ethnic and delivery mode groups (Li_Vaginal and Li_Cesarean and Han_Vaginal and Han_Cesarean).

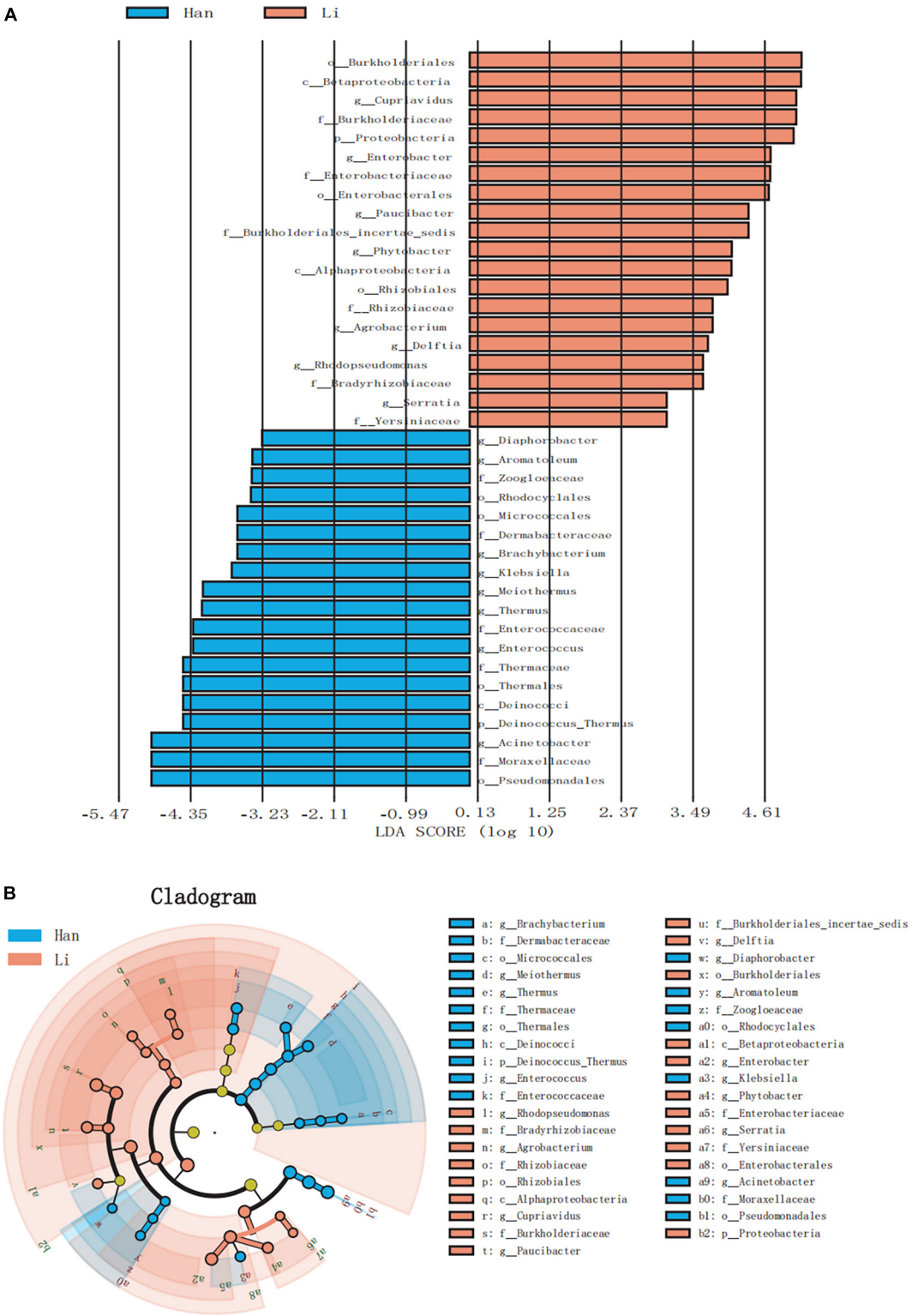

FIGURE 4 | LEfSe based on bacterial communities in colostrum samples from two different ethnic groups. **(A)** Histogram of LDA value distribution (LDA score > 3.0). **(B)** LEfSe analysis evolutionary branch diagram.

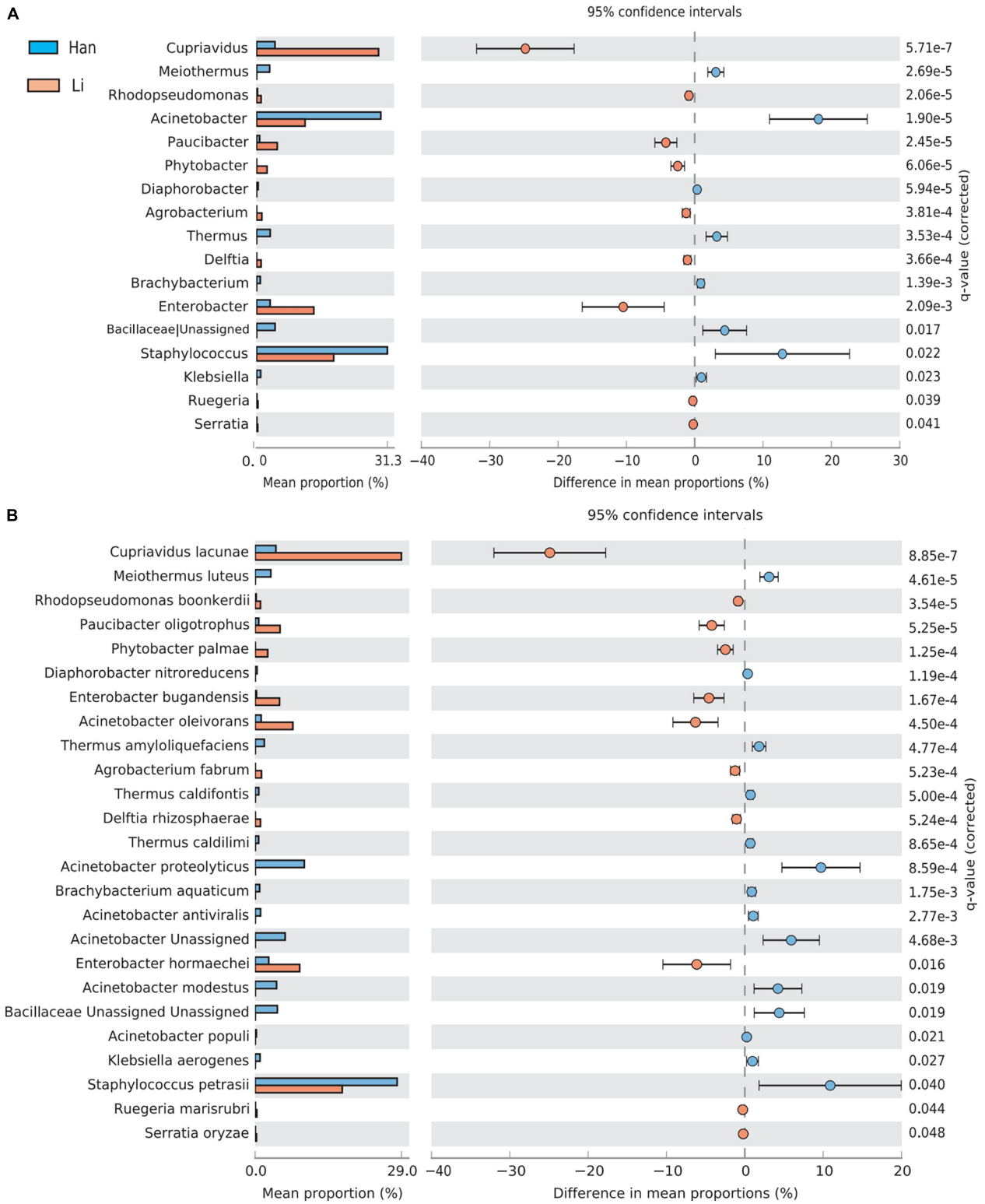

FIGURE 5 | Analysis of the difference of taxa between groups at the genus **(A)** and species level **(B)**. Different colors represent different groups. The left figure in the picture shows the abundance ratio of different taxa in the two groups of samples, the middle shows the difference ratio of functional abundance in the 95% confidence interval, and the right value is the *p*-value.

TABLE 3 | Associations between maternal characteristics and top 4 phyla, 11 genera, and 11 species.

	All	Han	Li	Han-vaginal	Han-cesarean	Li-vaginal	Li-cesarean
Phylum	%						
Firmicutes	45.90	47.10	34.43	45.54	49.62	34.54	33.76
Proteobacteria	36.50	43.02	61.54	46.12	38.03	61.28	63.18
Actinobacteria	9.90	3.46	2.61	2.70	4.67	2.69	2.11
Bacteroidetes	5.20	0.58	1.22	0.34	0.96	1.27	0.88
Genus							
Streptococcus	17.70	9.45	13.11	10.36	7.99	12.88	14.58
Acinetobacter	10.00	28.72	10.41	30.08	26.54	10.59	9.26
Staphylococcus	9.60	28.38	17.36	27.54	29.75	17.52	16.35
Pseudomonas	3.70	0.02	0.85	0.02	0.03	0.88	0.65
Corynebacterium	2.90	0.55	0.33	0.16	1.19	0.27	0.69
Enterobacter	2.40	3.25	12.13	4.69	0.92	12.07	12.51
Prevotella	2.30	0.04	0.97	0.05	0.03	0.99	0.80
Cutibacterium	1.10	1.42	1.82	1.08	1.97	1.99	1.22
Cupriavidus	0.90	3.74	26.28	2.57	5.61	25.74	29.72
Rhodopseudomonas	0.40	0.17	0.91	0.11	0.27	0.97	0.51
Paucibacter	0.30	0.64	4.17	0.38	1.67	4.16	4.24
Species							
Streptococcus himalayensis	9.90	4.37	5.50	3.62	5.56	5.78	3.69
Staphylococcus petrasii	7.00	25.54	16.06	24.97	26.45	16.15	15.49
Streptococcus panodentis	2.40	1.93	1.09	2.61	0.83	0.66	3.84
Enterobacter hormaechei	1.80	2.67	7.83	3.91	0.69	7.73	8.49
Citroniella saccharovorans	1.60	4.11	0.04	5.62	1.68	0.04	0.05
Klebsiella aerogenes	1.60	1.01	0.18	1.50	0.23	0.20	0.01
Staphylococcus pseudoxylosus	1.50	1.96	0.88	1.59	2.56	0.90	0.73
Escherichia/Shigella coli	1.50	0.80	0.07	1.16	0.21	0.08	0.07
Acinetobacter pseudolwoffii	1.10	0.19	0.02	0.18	0.20	0.02	0.05
Acinetobacter modestus	1.60	0.09	0.51	0.04	0.18	0.41	1.16
Cupriavidus lacunae	0.60	3.43	26.10	2.30	5.25	25.57	29.50
Unassigned	30.40	18.40	11.54	20.14	15.59	11.82	9.74

and *Actinobacteria* were the two most abundant genera in the Han ethnic group (**Figure 5A**). There were 11 species with higher abundance in the Li ethnic group and 14 species with higher abundance in the Han ethnic group (**Figure 5B**). *Cupriavidus lacunae* were the dominant species and the most distinct species in the Li ethnicity. In the meantime, *Enterobacter hormaechei* was rich in the Li group. The different species in the Han group were *Staphylococcus petrasii* and *Acinetobacter proteolyticus*.

Lactobacillaceae and *Bifidobacterium* Profiles Identified by 16S rRNA Gene Sequencing

A total of 17 ASVs were identified as members of the *Lactobacillaceae, including Limosilactobacillus*, *Lactobacillus*, *Lacticaseibacillus*, *Levilactobacillus*, *Lactiplantibacillus,* and *Leuconostoc.* Among them, 13 ASVs were classified into the species, including *Leuconostoc mesenteroides* (ASV_164 and ASV_251), *Limosilactobacillus reuteri* (ASV_303, ASV_529, ASV_541, and ASV_637), *Lacticaseibacillus rhamnosus* (ASV_575), *Limosilactobacillus caviae* (ASV_385 and ASV_754), *Lactobacillus colini* (ASV_452), *Levilactobacillus bambusae* (ASV_419), and *Lactobacillus acidophilus* (ASV_447 and ASV_464). Only three samples (HNa10, HNa17, and HNa31) and ten samples (16.67%) from the Li and Han ethnic groups contained *Lacticaseibacillus rhamnosus*, respectively. As for *Limosilactobacillus reuteri*, the detection rate in Han ethnic group was 11.67% and the relative abundance was 0.05–0.10%; while in the Li ethnic group, we did not detect it.

In the present study, to obtain more accurate taxonomic results at the species level, the representative sequences of all five ASVs were identified as members of the *Bifidobacterium* genus. Due to the resolving power of the 16S rRNA gene in the identification of different bacteria species, four out of five ASVs were assigned to the *Bifidobacterium* species level: *Bifidobacterium castoris* (ASV_225), *Bifidobacterium longum* (ASV_461), and *Bifidobacterium scaligerum* (ASV_307 and ASV_647), respectively. ASV_607 can be only classified into the *Bifidobacterium* genus. In the Li ethnic group, *Bifidobacterium* did not detect in the colostrum of the Li ethnic group. While in the Han ethnic group, *Bifidobacterium* was detected in 35 samples, and the detection rate of *Bifidobacterium* was 60%. Overall, five samples (HNb15, HNb21 HNb27, HNb30, and

HNb41) contained *B. castoris*, *B. longum*, and *B. scaligerum* with mean relative abundance ranging from 0.05 to 0.90%.

DISCUSSION

The breast milk microbiome can have a profound impact on human health by affecting the establishment of the neonatal intestinal flora and the development of the immune system (Fernández and Rodríguez, 2020; Yi and Kim, 2021). Some of the ethnic variations in microbiome structure have been attributed to differences in host genetics and innate/adaptive immunity, while in many other cases, maternal factors (age, BMI, mode of delivery, etc.), cultural features (diet, hygiene, environmental exposure, etc.), and subsistence factors overshadow genetics (Gupta et al., 2017). We focused on the ethnic group, which represents a highly diverse demographic character of the Chinese population (**Table 1**). A total of 97 Li and Han's mothers, who lived in Hainan of China for a long time, were selected to collect their milk within 2–5 days after delivery and were used to compare the composition and diversity of colostrum microbiota.

Maternal factors, including pre-gestational BMI, age or mode of delivery, and other related factors have been proposed to influence colostrum microbiota composition (Zimmermann and Curtis, 2020). Our results showed that BMI and parity had no significant effect on the alpha-diversity of the colostrum microbial community (**Supplementary Table 1**). In terms of the delivery mode, our results reported a higher alpha-diversity in the colostrum of women delivered cesarean, which was consistent with the result of the study on the diversity of breast milk microbes in Taiwan and Mainland China (Li et al., 2017). However, the other two studies (84 and 393 participants, respectively) did not confirm this (Kumar et al., 2016; Moossavi et al., 2019). Previous studies also reported higher alpha-diversity and richness in the HM microbiota of women receiving intrapartum antibiotics (Hermansson et al., 2019). Our results suggest that intrapartum antibiotics had no significant influence on the diversity of colostrum microbiota. This could be attributed to the fact that women who have c-sections have a high rate of taking antibiotics during the perinatal period. It is now generally believed that the establishment of the human gut microbiota was influenced by the host's genetics and diet and environmental exposure. The maternal gut is thought to be the most important source of bacteria in HM (*via* an entero-mammary pathway). So, the mother's diet might influence the HM microbiota diversity by modifying the composition of the maternal gut microbiota (Biagi et al., 2017; Padilha et al., 2019).

Most studies reported consistently *Firmicutes* and *Proteobacteria* to be the most predominant phyla in both mature milk and colostrum (Sakwinska et al., 2016; Biagi et al., 2017). However, at the genus and species levels, there are significant differences in the composition of breast milk microbiome reported, with many genera found in less than 10% of studies. In addition, to distinguish stable and permanent microbiome members from the highly complex colostrum microbiota, which includes thousands of different species, we aimed to use the concept of the core microbiome (Lemanceau et al., 2017; Toju et al., 2018). Due to the resolution limits of DNA-based analyses, core microbiota had been predominantly defined using genus-level discrimination of a population. Nevertheless, a core microbiota of seven to nine bacterial genera was often proposed based on sample abundance (intestinal microbes, environmental microbes, and other related fields). In our study, using the 16S rRNA full-length amplicon technique, *Staphylococcus*, *Acinetobacter*, *Streptococcus*, *Cutibacterium*, *Cupriavidus*, *Enterobacter*, *Rhodopseudomonas, and Paucibacter* (**Table 3**) were selected as the core microbiota in 97 maternal colostrums from Hainan province according to the relative abundance of microbiota. Among them, *Cupriavidus*, being the most abundant genera in the Li ethnic group, was often found in soil (Estrada-de Los Santos et al., 2014), with isolates of *Cupriavidus lacunae* recovered in pond-side soil (Feng et al., 2019). Similarly, *Paucibacter* was also an environmental bacteria found in aquatic sediment.

Environmental exposure during the perinatal period (skin microbiota of the mother and the oral cavity of the infant) may be the main reason for broad differences in breast milk microbiome. Based on published data, colostrum displayed higher diversity and more significant disparity in microbiome composition than mature milk across geographically different populations, characterized by a higher prevalence of environmental bacteria. Indeed, the oral and skin microbiome are the next most diverse. In the case of the skin microbiome, rural and urban Chinese populations show variation in the abundance of some taxa, such as *Trabulsiella* and *Propionibacterium* (Gupta et al., 2017). Generally, host surface-associated microbiomes, such as skin microbiome, might respond strongly to variations in bioclimatic factors, thereby they may shape the composition of the human breast milk microbiome (Woodhams et al., 2020). In our study, Hainan Island of China has a tropical monsoon climate, characterized by hot and humid year-round, abundant rainfall. Interestingly, some thermotolerant environmental bacteria taxa first isolated from a hot spring, such as *Thermus amyloliquefaciens*, *Thermus caldifontis,* and *Meiothermus luteus* (Yu et al., 2015; Habib et al., 2017; Khan et al., 2017), were found in the most of Hainan colostrum samples. Moreover, another peculiarity from our data was the prevalence of other soil environmental bacteria in colostrum samples of Li's mothers, such as the genus *Agrobacterium*. In fact, previous multiple studies showed that about half of dominant genera in colostrum belonged to environmental bacteria ubiquitous in soil and water, such as *Pseudomonas*, *Rhizobium*, *Acinetobacter, Alcaligenes,* and so on (Drago et al., 2017; Toscano et al., 2017). Consequently, some of the ethnic variations in the colostrum microbiome could be attributed to differences in cultural features/subsistence like diet, hygiene, and labor practice. This result is also consistent with the fact that most mothers the Li ethnic group recruited live mostly in rural areas and are engaged in farming. In other words, for most of the studies on breast milk microbiome, alcohol disinfection

is not effective in preventing the detection of skin-associated microorganisms probably derived from exposed environment (soil and vegetation).

Based on the excessive presence of exogenous bacteria in breast milk, the most prevalent genera in breast milk microbiota were generally distinct from the most prevalent genera of the infant gut (Pannaraj et al., 2017; Fehr et al., 2020). However, there is a consensus that the first beneficial bacteria that enters the infant's gut should be from the colostrum. Particularly, the commensal bacteria in colostrum could be selected to serve as seeds for newborns to initially establish a healthy gut microbiome. Several studies have shown that *Bifidobacterium* and *Lactobacillus* are highly present in the gut microbiota of infants and have been considered to be transmitted from mother to infants shortly after birth by breastfeeding, which can effectively avert irritable bowel syndrome and contribute to the development and balance of intestinal flora for infants (Yassour et al., 2018). Therefore, these potential probiotic commensal bacteria in colostrum are of particular concern, especially *Bifidobacterium, Lactobacillus,* and so on.

By reviewing the existing literature, the presence of *Bifidobacterium* and *Lactobacillus* was sporadically reported in a few colostrum samples or not at all (Gupta et al., 2017). In our study, about 48.5% of colostrum samples were retrieved using the 16S rRNA ASVs corresponding to family *Lactobacillaceae,* with about 0.28% mean relative abundance. According to NCBI BLAST homology search of 16S rRNA gene full-length sequencing, ASVs belonging to five new genera revised of the family *Lactobacillaceae* were retrieved, including *Limosilactobacillus*, *Lactobacillus*, *Lacticaseibacillus*, *Levilactobacillus*, *Lactiplantibacillus,* and *Leuconostoc* (Zheng et al., 2020). Taxa identified at the species level were *Limosilactobacillus reuteri*, *Limosilactobacillus caviae*, *Lactobacillus colini*, *Lactobacillus acidophilus*, *Lacticaseibacillus rhamnosus*, and *Levilactobacillus bambusae*. Surprisingly, *Bifidobacterium* did not detect in the colostrum of the Li ethnic group, but the detection rate was nearly 60% in the Han group, with mean relative abundance ranging from 0.05 to 0.9%. The *Bifidobacterium* species identified mainly included *B. longum*, *B. castoris, and B. scaligerum*. To date, most studies on breast milk using the NGS of different 16S variable gene regions reported their presence only at the taxonomic level of genus, with significantly different results. For example, in a study based on the V4 variable region of the 16S rRNA gene, the average relative abundances ranged from 0.1 to 1% for *Bifidobacterium* and from 0.1 to 0.3% for *Lactobacillus* (Padilha et al., 2019). In another study based on the V3-V4 region of the 16S rRNA gene, investigators reported around 2% average relative abundances of *Bifidobacterium* and *Lactobacillus* in the first weeks after delivery (Murphy et al., 2017). Intriguingly, an ASV affiliated with *Akkermansia* (as a kind of emerging candidate probiotics) was also detected in eight colostrum samples of the Han ethnic group (0.1%), belonging to *Akkermansia glycaniphila.* This was the first report that *Akkermansia* was detected in breast milk (Ouwerkerk et al., 2016).

To the best of our knowledge, this is the first study to reveal the composition and diversity of colostrum microbiome in different ethnic groups living in narrow geographical areas on an island scale. We tried to understand the influence of ethnicity on the colostrum microbiome in different sub-populations with shared physical geography by minimizing environmental factors. In fact, it is hard to tease out the relative contributions of geography and ethnicity to the breast milk microbiome, which are intertwined. Our study has limitation concerning the sample size and cohort populations. We will recruit multiple cohorts, including different cohorts of the same ethnic groups with different subsistence and living environments, and different ethnic groups sharing similar subsistence and living environments.

CONCLUSION

In the present study, by analyzing the colostrum 16S rRNA gene full-length sequencing dataset in 97 healthy mothers (60 from Han, 37 from Li) from the Hainan island of China, we show the ethnic differences of the colostrum microbiome in a maternal cohort with shared physical geography. The analysis based on the Bray–Curtis distance showed an obvious ethnicity-associated structural segregation of colostrum microbiota. The human colostrum microbiome is more susceptible to local living environmental factors, although skin-derived *Staphylococcus* and *Streptococcus* are still subdominant taxa. Probably, environmental exposure during the perinatal period may be the main reason for broad differences in the colostrum microbiome. Consequently, colostrum displayed higher diversity and more significant disparity in microbiome composition than mature milk, characterized by a higher prevalence of environmental bacteria. In addition, despite the low relative abundance and presence of inter-population differences, the potential probiotic bacteria do exist in colostrum, especially *Bifidobacterium* and *Lactobacillus*. Our results suggest that the ethnic origin of individuals may be an important factor to consider in HM microbiome research and its potential clinical significance during the perinatal period in ethnic-diverse societies, despite a small geographic scale. Finally, further research is needed to tease out the relative contributions of geography and ethnicity to the breast milk microbiome.

DATA AVAILABILITY STATEMENT

The datasets presented in this study can be found in online repositories. The names of the repository/repositories and accession number(s) can be found below: NCBI - PRJNA845888, SRR19548162 - SRR19548258.

ETHICS STATEMENT

The studies involving human participants were reviewed and approved by the Ethics Committee of the First Affiliated Hospital, Shihezi University School of Medicine (KJ2022-080-01). The patients/participants provided their written informed consent to participate in this study.

AUTHOR CONTRIBUTIONS

WX: resources, methodology, investigation, and writing. HZ: formal analysis, methodology, validation, and writing—original draft. YN: conceptualization and supervision. YP: conceptualization, project administration, and funding acquisition. All authors contributed to the article and approved the submitted version.

FUNDING

This work was supported by the High Level Talent Project of Hainan Natural Science Foundation (No. 821RC691), Hainan Province Key Research and Development Program (No. ZDYF2022SHFZ071), the Joint Key Funds of the National Natural Science Foundation of China, and the Autonomous Region Government of Xinjiang, China (No. U1903205).

ACKNOWLEDGMENTS

We would like to thank the mothers who participated in this study and also thank the Personalbio help with sequencing-related experiments.

SUPPLEMENTARY MATERIAL

The Supplementary Material for this article can be found online at: https://www.frontiersin.org/articles/10.3389/fmicb.2022.934232/full#supplementary-material

REFERENCES

Andreas, N. J., Kampmann, B., and Mehring Le-Doare, K. (2015). Human breast milk: a review on its composition and bioactivity. *Early Hum Dev.* 91, 629–635. doi: 10.1016/j.earlhumdev.2015.08.013

Bardanzellu, F., Fanos, V., and Reali, A. (2017). "Omics" in human colostrum and mature milk: looking to old data with new eyes. *Nutrients* 9:843. doi: 10.3390/nu9080843

Biagi, E., Quercia, S., Aceti, A., Beghetti, I., Rampelli, S., Turroni, S., et al. (2017). The bacterial ecosystem of mother's milk and infant's mouth and gut. *Front. Microbiol.* 8:1214. doi: 10.3389/fmicb.2017.01214

Cabrera-Rubio, R., Collado, M. C., Laitinen, K., Salminen, S., Isolauri, E., and Mira, A. (2012). The human milk microbiome changes over lactation and is shaped by maternal weight and mode of delivery. *Am. J. Clin. Nutr.* 96, 544–551. doi: 10.3945/ajcn.112.037382

Cheema, A. S., Stinson, L. F., Lai, C. T., Geddes, D. T., and Payne, M. S. (2021). DNA extraction method influences human milk bacterial profiles. *J. Appl. Microbiol.* 130, 142–156. doi: 10.1111/jam.14780

Cheema, A. S., Trevenen, M. L., Turlach, B. A., Furst, A. J., Roman, A. S., Bode, L., et al. (2022). Exclusively breastfed infant microbiota develops over time and is associated with human milk oligosaccharide intakes. *Int. J. Mol. Sci.* 23:2804. doi: 10.3390/ijms23052804

de Andrade, P., Maria, E. S. J., Carregaro, V., Sacramento, L. A., Roberti, L. R., Aragon, D. C., et al. (2021). Efficacy of probiotics in children and adolescents with atopic dermatitis: a randomized, double-blind, placebo-controlled study. *Front. Nutr.* 8:833666. doi: 10.3389/fnut.2021.833666

Deschasaux, M., Bouter, K. E., Prodan, A., Levin, E., Groen, A. K., Herrema, H., et al. (2018). Depicting the composition of gut microbiota in a population with varied ethnic origins but shared geography. *Nat. Med.* 24, 1526–1531. doi: 10.1038/s41591-018-0160-1

Douglas, C. A., Ivey, K. L., Papanicolas, L. E., Best, K. P., Muhlhausler, B. S., and Rogers, G. B. (2020). DNA extraction approaches substantially influence the assessment of the human breast milk microbiome. *Sci. Rep.* 10:123. doi: 10.1038/s41598-019-55568-y

Drago, L., Toscano, M., De Grandi, R., Grossi, E., Padovani, E. M., and Peroni, D. G. (2017). Microbiota network and mathematic microbe mutualism in colostrum and mature milk collected in two different geographic areas: Italy versus Burundi. *ISME J.* 11, 875–884. doi: 10.1038/ismej.2016.183

Estrada-de Los Santos, P., Solano-Rodriguez, R., Matsumura-Paz, L. T., Vasquez-Murrieta, M. S., and Martinez-Aguilar, L. (2014). *Cupriavidus plantarum* sp. nov., a plant-associated species. *Arch. Microbiol.* 196, 811–817. doi: 10.1007/s00203-014-1018-7

Fehr, K., Moossavi, S., Sbihi, H., Boutin, R. C. T., Bode, L., Robertson, B., et al. (2020). Breastmilk feeding practices are associated with the co-occurrence of bacteria in mothers' milk and the infant gut: the CHILD cohort study. *Cell Host Microbe* 28, 285.e284–297.e284. doi: 10.1016/j.chom.2020.06.009

Feng, T., Kim, K. H., Oh, J., and Jeon, C. O. (2019). *Cupriavidus lacunae* sp. nov., isolated from pond-side soil. *Antonie Van Leeuwenhoek* 112, 543–551. doi: 10.1007/s10482-018-1187-5

Fernández, L., and Rodríguez, J. M. (2020). Human milk microbiota: origin and potential uses. *Nestle Nutr. Inst. Workshop Ser.* 94, 75–85. doi: 10.1159/000505031

Gupta, V. K., Paul, S., and Dutta, C. (2017). Geography, ethnicity or subsistence-specific variations in human microbiome composition and diversity. *Front. Microbiol.* 8:1162. doi: 10.3389/fmicb.2017.01162

Habib, N., Khan, I. U., Hussain, F., Zhou, E. M., Xiao, M., Dong, L., et al. (2017). *Meiothermus luteus* sp. nov., a slightly thermophilic bacterium isolated from a hot spring. *Int. J. Syst. Evol. Microbiol.* 67, 2910–2914. doi: 10.1099/ijsem.0.002040

Hermansson, H., Kumar, H., Collado, M. C., Salminen, S., Isolauri, E., and Rautava, S. (2019). Breast milk microbiota is shaped by mode of delivery and intrapartum antibiotic exposure. *Front. Nutr.* 6:4. doi: 10.3389/fnut.2019.00004

Hunt, K. M., Foster, J. A., Forney, L. J., Schütte, U. M., Beck, D. L., Abdo, Z., et al. (2011). Characterization of the diversity and temporal stability of bacterial communities in human milk. *PLoS One* 6:e21313. doi: 10.1371/journal.pone.0021313

Jost, T., Lacroix, C., Braegger, C. P., and Chassard, C. (2012). New insights in gut microbiota establishment in healthy breast fed neonates. *PLoS One* 7:e44595. doi: 10.1371/journal.pone.0044595

Khan, I. U., Habib, N., Hussain, F., Xian, W. D., Amin, A., Zhou, E. M., et al. (2017). *Thermus caldifontis* sp. nov., a thermophilic bacterium isolated from a hot spring. *Int. J. Syst. Evol. Microbiol.* 67, 2868–2872. doi: 10.1099/ijsem.0.002037

Kumar, H., du Toit, E., Kulkarni, A., Aakko, J., Linderborg, K. M., Zhang, Y., et al. (2016). Distinct patterns in human milk microbiota and fatty acid profiles across specific geographic locations. *Front. Microbiol.* 7:1619. doi: 10.3389/fmicb.2016.01619

Lemanceau, P., Blouin, M., Muller, D., and Moënne-Loccoz, Y. (2017). Let the core microbiota be functional. *Trends Plant Sci.* 22, 583–595. doi: 10.1016/j.tplants.2017.04.008

Li, S. W., Watanabe, K., Hsu, C. C., Chao, S. H., Yang, Z. H., Lin, Y. J., et al. (2017). Bacterial composition and diversity in breast milk samples from mothers living in taiwan and mainland china. *Front. Microbiol.* 8:965. doi: 10.3389/fmicb.2017.00965

Liu, Y. X., Qin, Y., Chen, T., Lu, M., Qian, X., Guo, X., et al. (2021). A practical guide to amplicon and metagenomic analysis of microbiome data. *Protein Cell* 12, 315–330. doi: 10.1007/s13238-020-00724-8

Lloyd-Price, J., Abu-Ali, G., and Huttenhower, C. (2016). The healthy human microbiome. *Genome Med.* 8:51. doi: 10.1186/s13073-016-0307-y

Lopez Leyva, L., Brereton, N. J. B., and Koski, K. G. (2021). Emerging frontiers in human milk microbiome research and suggested primers for 16S rRNA gene analysis. *Comput. Struct. Biotechnol. J.* 19, 121–133. doi: 10.1016/j.csbj.2020.11.057

Lyons, K. E., Fouhy, F., Ca, O., Shea, C. A., Ryan, C. A., Dempsey, E. M., et al. (2021). Effect of storage, temperature, and extraction kit on the phylogenetic composition detected in the human milk microbiota. *Microbiologyopen* 10:e1127. doi: 10.1002/mbo3.1127

Lyons, K. E., Ryan, C. A., Dempsey, E. M., Ross, R. P., and Stanton, C. (2020). Breast milk, a source of beneficial microbes and associated benefits for infant health. *Nutrients* 12:1039. doi: 10.3390/nu12041039

Moossavi, S., Sepehri, S., Robertson, B., Bode, L., Goruk, S., Field, C. J., et al. (2019). Composition and variation of the human milk microbiota are influenced by maternal and early-life factors. *Cell Host Microbe* 25, 324.e324–335.e324. doi: 10.1016/j.chom.2019.01.011

Murphy, K., Curley, D., O'Callaghan, T. F., O'Shea, C. A., Dempsey, E. M., O'Toole, P. W., et al. (2017). The composition of human milk and infant faecal microbiota over the first three months of life: a pilot study. *Sci. Rep.* 7:40597. doi: 10.1038/srep40597

Oikonomou, G., Addis, M. F., Chassard, C., Nader-Macias, M. E. F., Grant, I., Delbès, C., et al. (2020). Milk microbiota: what are we exactly talking about? *Front. Microbiol.* 11:60. doi: 10.3389/fmicb.2020.00060

Ojo-Okunola, A., Claassen-Weitz, S., Mwaikono, K. S., Gardner-Lubbe, S., Zar, H. J., Nicol, M. P., et al. (2020). The influence of dna extraction and lipid removal on human milk bacterial profiles. *Methods Protoc.* 3:39. doi: 10.3390/mps3020039

Ojo-Okunola, A., Nicol, M., and du Toit, E. (2018). Human breast milk bacteriome in health and disease. *Nutrients* 10:1643. doi: 10.3390/nu10111643

Ouwerkerk, J. P., Aalvink, S., Belzer, C., and de Vos, W. M. (2016). *Akkermansia glycaniphila* sp. nov., an anaerobic mucin-degrading bacterium isolated from reticulated python faeces. *Int. J. Syst. Evol. Microbiol.* 66, 4614–4620. doi: 10.1099/ijsem.0.001399

Padilha, M., Danneskiold-Samsoe, N. B., Brejnrod, A., Hoffmann, C., Cabral, V. P., Iaucci, J. M., et al. (2019). The human milk microbiota is modulated by maternal diet. *Microorganisms* 7:502. doi: 10.3390/microorganisms7110502

Pannaraj, P. S., Li, F., Cerini, C., Bender, J. M., Yang, S., Rollie, A., et al. (2017). Association between breast milk bacterial communities and establishment and development of the infant gut microbiome. *JAMA Pediatr.* 171, 647–654. doi: 10.1001/jamapediatrics.2017.0378

Rodriguez-Cruz, M., Alba, C., Aparicio, M., Checa, M. A., Fernandez, L., and Rodriguez, J. M. (2020). Effect of sample collection (manual expression vs. pumping) and skimming on the microbial profile of human milk using culture techniques and metataxonomic analysis. *Microorganisms* 8:1278. doi: 10.3390/microorganisms8091278

Sakwinska, O., Moine, D., Delley, M., Combremont, S., Rezzonico, E., Descombes, P., et al. (2016). Microbiota in breast milk of chinese lactating mothers. *PLoS One* 11:e0160856. doi: 10.1371/journal.pone.0160856

Shafiee, N. H., Razalli, N. H., Muhammad Nawawi, K. N., Mohd Mokhtar, N., and Raja Ali, R. A. (2022). Implication of food insecurity on the gut microbiota and its potential relevance to a multi-ethnic population in Malaysia. *JGH Open* 6, 112–119. doi: 10.1002/jgh3.12709

Sprenger, N., Tytgat, H. L. P., Binia, A., Austin, S., and Singhal, A. (2022). Biology of human milk oligosaccharides: from basic science to clinical evidence. *J. Hum. Nutr. Diet.* 35, 280–299. doi: 10.1111/jhn.12990

Stinson, L. F., Sindi, A. S. M., Cheema, A. S., Lai, C. T., Mühlhäusler, B. S., Wlodek, M. E., et al. (2021). The human milk microbiome: who, what, when, where, why, and how? *Nutr. Rev.* 79, 529–543. doi: 10.1093/nutrit/nuaa029

Toju, H., Peay, K. G., Yamamichi, M., Narisawa, K., Hiruma, K., Naito, K., et al. (2018). Core microbiomes for sustainable agroecosystems. *Nat Plants* 4, 247–257. doi: 10.1038/s41477-018-0139-4

Toscano, M., De Grandi, R., Peroni, D. G., Grossi, E., Facchin, V., Comberiati, P., et al. (2017). Impact of delivery mode on the colostrum microbiota composition. *BMC Microbiol.* 17:205. doi: 10.1186/s12866-017-1109-0

Walker, A. W., Martin, J. C., Scott, P., Parkhill, J., Flint, H. J., and Scott, K. P. (2015). 16S rRNA gene-based profiling of the human infant gut microbiota is strongly influenced by sample processing and PCR primer choice. *Microbiome* 3:26. doi: 10.1186/s40168-015-0087-4

Williams, J. E., Carrothers, J. M., Lackey, K. A., Beatty, N. F., York, M. A., Brooker, S. L., et al. (2017). Human milk microbial community structure is relatively stable and related to variations in macronutrient and micronutrient intakes in healthy lactating women. *J. Nutr.* 147, 1739–1748. doi: 10.3945/jn.117.248864

Woodhams, D. C., Bletz, M. C., Becker, C. G., Bender, H. A., Buitrago-Rosas, D., Diebboll, H., et al. (2020). Host-associated microbiomes are predicted by immune system complexity and climate. *Genome Biol.* 21:23. doi: 10.1186/s13059-019-1908-8

Xu, J., Lawley, B., Wong, G., Otal, A., Chen, L., Ying, T. J., et al. (2020). Ethnic diversity in infant gut microbiota is apparent before the introduction of complementary diets. *Gut Microbes* 11, 1362–1373. doi: 10.1080/19490976.2020.1756150

Yassour, M., Jason, E., Hogstrom, L. J., Arthur, T. D., Tripathi, S., Siljander, H., et al. (2018). Strain-level analysis of mother-to-child bacterial transmission during the first few months of life. *Cell Host Microbe* 24, 146.e144–154.e144. doi: 10.1016/j.chom.2018.06.007

Yi, D. Y., and Kim, S. Y. (2021). Human breast milk composition and function in human health: from nutritional components to microbiome and MicroRNAs. *Nutrients* 13:3094. doi: 10.3390/nu13093094

Yu, T. T., Ming, H., Yao, J. C., Zhou, E. M., Park, D. J., Hozzein, W. N., et al. (2015). *Thermus amyloliquefaciens* sp. nov., isolated from a hot spring sediment sample. *Int. J. Syst. Evol. Microbiol.* 65, 2491–2495. doi: 10.1099/ijs.0.000289

Zheng, J., Wittouck, S., Salvetti, E., Franz, C. M. A. P., Harris, H. M. B., Mattarelli, P., et al. (2020). A taxonomic note on the genus *Lactobacillus*: description of 23 novel genera, emended description of the genus *Lactobacillus* Beijerinck 1901, and union of *Lactobacillaceae* and *Leuconostocaceae*. *Int. J. Syst. Evol. Microbiol.* 70, 2782–2858. doi: 10.1099/ijsem.0.004107

Zimmermann, P., and Curtis, N. (2020). Breast milk microbiota: a review of the factors that influence composition. *J. Infect.* 81, 17–47. doi: 10.1016/j.jinf.2020.01.023

Conflict of Interest: The authors declare that the research was conducted in the absence of any commercial or financial relationships that could be construed as a potential conflict of interest.

frontiers | Frontiers in Microbiology

REVIEW
published: 14 July 2022
doi: 10.3389/fmicb.2022.916488

Root Exudates: Mechanistic Insight of Plant Growth Promoting Rhizobacteria for Sustainable Crop Production

Sudhir K. Upadhyay[1]*, *Abhishek K. Srivastava*[2], *Vishnu D. Rajput*[3], *Prabhat K. Chauhan*[1], *Ali Asger Bhojiya*[4], *Devendra Jain*[5], *Gyaneshwer Chaubey*[6], *Padmanabh Dwivedi*[7]*, *Bechan Sharma*[8] *and Tatiana Minkina*[3]

[1] Department of Environmental Science, V.B.S. Purvanchal University, Jaunpur, India, [2] Department of Biotechnology, M.H.P.G. College, Jaunpur, India, [3] Academy of Biology and Biotechnology, Southern Federal University, Rostov-on-Don, Russia, [4] Department of Agriculture and Veterinary Sciences, Mewar University, Chittorgarh, India, [5] Department of Molecular Biology and Biotechnology, Maharana Pratap University of Agriculture and Technology, Udaipur, India, [6] Cytogenetics Laboratory, Department of Zoology, Banaras Hindu University, Varanasi, India, [7] Department of Plant Physiology, Institute of Agricultural Sciences, Banaras Hindu University, Varanasi, India, [8] Department of Biochemistry, Faculty of Science, University of Allahabad, Allahabad, India

OPEN ACCESS

Edited by:
Sandip Paul,
JIS Institute of Advanced Studies and Research, India

Reviewed by:
Divjot Kour,
Eternal University, India
José David Flores Félix,
Universidade da Beira Interior, Portugal

***Correspondence:**
Sudhir K. Upadhyay
sku.env.lko@gmail.com
orcid.org/0000-0002-2228-8063
Padmanabh Dwivedi
pdwivedi25@rediffmail.com

Specialty section:
This article was submitted to Microbial Symbioses, a section of the journal Frontiers in Microbiology

Received: 09 April 2022
Accepted: 09 June 2022
Published: 14 July 2022

Citation:
Upadhyay SK, Srivastava AK, Rajput VD, Chauhan PK, Bhojiya AA, Jain D, Chaubey G, Dwivedi P, Sharma B and Minkina T (2022) Root Exudates: Mechanistic Insight of Plant Growth Promoting Rhizobacteria for Sustainable Crop Production. Front. Microbiol. 13:916488. doi: 10.3389/fmicb.2022.916488

The breaking silence between the plant roots and microorganisms in the rhizosphere affects plant growth and physiology by impacting biochemical, molecular, nutritional, and edaphic factors. The components of the root exudates are associated with the microbial population, notably, plant growth-promoting rhizobacteria (PGPR). The information accessible to date demonstrates that PGPR is specific to the plant's roots. However, inadequate information is accessible for developing bio-inoculation/bio-fertilizers for the crop in concern, with satisfactory results at the field level. There is a need to explore the perfect candidate PGPR to meet the need for plant growth and yield. The functions of PGPR and their chemotaxis mobility toward the plant root are triggered by the cluster of genes induced by the components of root exudates. Some reports have indicated the benefit of root exudates in plant growth and productivity, yet a methodical examination of rhizosecretion and its consequences in phytoremediation have not been made. In the light of the afore-mentioned facts, in the present review, the mechanistic insight and recent updates on the specific PGPR recruitment to improve crop production at the field level are methodically addressed.

Keywords: chemoattractant, PGPR recruitment, plant-microbes interaction, root-exudate, rhizosphere

INTRODUCTION

According to the World Health Organization (WHO), the food shortage for sustaining the human population is on a steep upward trajectory, mainly owing to the quickly booming human population that is expected to cross the 10 billion mark by 2050 (DESA UN, 2015). Both WHO and the United Nations have proposed to intensify global food production by 50% in the near future. The agriculturally important microorganisms (AIMs) can play a pivotal role in realizing this colossal target considering the fact that fertile lands are sharply shrinking owing to urbanization and industrialization.

AIMs not only improve plant growth and yield but provide sustained protection against a variety of phytopathogens (Bhattacharyya and Jha, 2012; Glick, 2012; Compant et al., 2019). The beneficial microbes of the rhizosphere zone interact positively with mutually guided components of root exudates, i.e., rhizodeposits (Hassan et al., 2019). During the rhizodeposition process, the plant roots secrete carbohydrates, fatty acids, essential amino acids, organic acids, hydrolytic enzymes, growth-regulating hormones, vitamins, nucleotides, flavonoids, polyphenols, sterols, and volatile organic compounds (Hartmann et al., 2009; Hu et al., 2018; Ankati and Podile, 2019).

In the last century, the word "rhizosphere" was introduced as a microbial hot spot in the area of the rootsystem (Hartmann et al., 2008). The rhizospheric region, a specific zone around the root and harbors various kinds of microorganisms, primarily bacteria, fungi, nematodes, insect larvae, mites, amoebas, and protozoa (Bonkowski et al., 2009). The bacterial colonies residing in the rhizospheric zone are called rhizobacteria (Hartmann et al., 2009). The rhizospheric zone supports the plant root system (Ahemad and Kibret, 2014) and modulates the physico-chemical and biological properties of the soil (Ahemad and Kibret, 2014; Zhalnina et al., 2018).

The rhizosphere zone provides a shelter for the exchange of biochemical components that establish inter-species relationships between the roots and microorganisms (Gupta et al., 2020). Plant roots release various types of enzymes/compounds in the soil that mediate the interaction between microorganisms and plants (Ankati and Podile, 2019). Factors influencing soil microbial population include soil quality, soil moisture, soil pH, and rhizospheric secretion (Bagyalakshmi et al., 2012; Upadhyay and Singh, 2015; Hu et al., 2018). There are various physical and chemical parameters of the rhizospheres that impact the function of microorganisms, which ultimately affect several mechanisms, such as the respiratory process, the secretion of organic acids by the roots, the breakdown of soil organic matter, nutrient uptake, symbiotic nitrogen fixation, etc. (Reinhold-Hurek et al., 2015; Mahmud et al., 2021).

The rhizosphere plays an important role in root excretion, microbial activity, genetic exchange, improving nutrient use efficiency, and gradient diffusion, which are jointly referred to as the rhizosphere effect (Badri and Vivanco, 2009; Ladygina and Hedlund, 2010; Mendes et al., 2013). Rhizobacteria associated with the plant root are often referred to as plant growth-promoting rhizobacteria (PGPR). The functions of plant growth-promoting rhizobacteria, such as direct and indirect mechanism, metabolism, chemotaxis, secretion, antibiotic production, etc., are mediated by its gene cluster that triggers host–PGPR interactions (Mark et al., 2005; Matilla et al., 2007; Ramachandran et al., 2011; Zhang et al., 2015; Bashir et al., 2021; South et al., 2021). Ultrastructure of the root cell wall mediated PGPR interaction, which was induced by the gene expression of the plant. Ryu et al. (2003) demonstrated that out of 38 genes, 30 genes of *Bacillus subtilis*-GB03 were associated with a change in the *Arabidopsis* root-ultrastructure and promote plant growth. *Azospirillum irakense* vitalized polygalacturonase gene (PG genes) in the roots of rice plant (Sekar et al., 2000). Among PG genes, PbrPG6 is responsible for fruit-soothe (Zhang et al., 2019). The root exudation and root exudates are relevant for the survivability of plants against various environmental conditions. The root exudates aid in the selection of microbial populations around the rhizosphere (Mendes et al., 2013; Zhang et al., 2015). In the purview to tackle this aspect, the review discusses the mechanisms of root exudation, the current updates on the selective plant growth-promoting rhizobacteria aggregation and their role in plant–microbe interface, and most importantly, the future developments in plant–PGPR interactions for sustainable agriculture.

ROOT EXUDATES AND PLANT GROWTH-PROMOTING RHIZOBACTERIA

Plant root secretes 5–21% of photosynthetic matter such as carbohydrates, proteins, secondary metabolites, etc., into the rhizospheric soil environment, generally known as root exudates (Badri et al., 2013; **Figure 1**). The coping mechanism of plants under diverse environmental conditions mainly rests on the root acquisition of soil resources and their surroundings (Gupta et al., 2020). In the mid twentieth century, the world population increased quickly and posed various problems related to food, fiber, fuel, homeland, etc., which has consequences for hunger, poverty, water scarcity, and environmental degradation. The scarcity of food is a burgeoning challenge for humans that has been classified as goal number two of the Zero Hunger of the United Nations Sustainable Development Goals 2030.

Recently, the researchers have introduced an eco-friendly concept based on free-living bacteria called PGPR (plant-growth promoting rhizobacteria). The plant growth-promoting rhizobacteria are soil-borne or root-colonizing rhizobacteria (Upadhyay et al., 2009, 2012a,b; Singh et al., 2017; Numana et al., 2018; Upadhyay and Chauhan, 2022), which play a functional role in plant growth through several mechanisms in terrestrial ecosystems. Plant-growth promoting rhizobacteria significantly reduce the dependence on chemical fertilizers and pesticides (Liu et al., 2017). Plant growth-promoting rhizobacteria promote plant growth through root-hair proliferation, enhancing root hair branching; increase in seedling emergence; early nodulation; nodule functioning; enhanced leaf surface area; improvement in vigor and biomass; increased indigenous plant hormones levels; and most importantly, by improving nutrient use efficiency (Vocciante et al., 2022). The plant growth-promoting rhizobacteria induce the accumulation of carbohydrates in plants and consequently the yield of various plant species (Bhattacharyya and Jha, 2012; **Table 1**). The most dominant endophytic plant growth-promoting rhizobacteria phyla are Proteobacteria and Actinobacteria, followed by Bacteroidetes and Firmicutes (Ray et al., 2017). Endophytic bacteria enter the plant tissues by the lateral root cracks, wounds, lenticels, germinating radicles, and other parts of the plant body (Chaturvedi et al., 2016). Endophytic-rhizospheric bacteria are involved in several functions such as internal protection of the environment (Santos et al., 2018), metabolism of carbon compounds, nitrogen fixation by nitrogenase (Santoyo et al., 2016), and capability for germination of nodes (Yousaf et al., 2017).

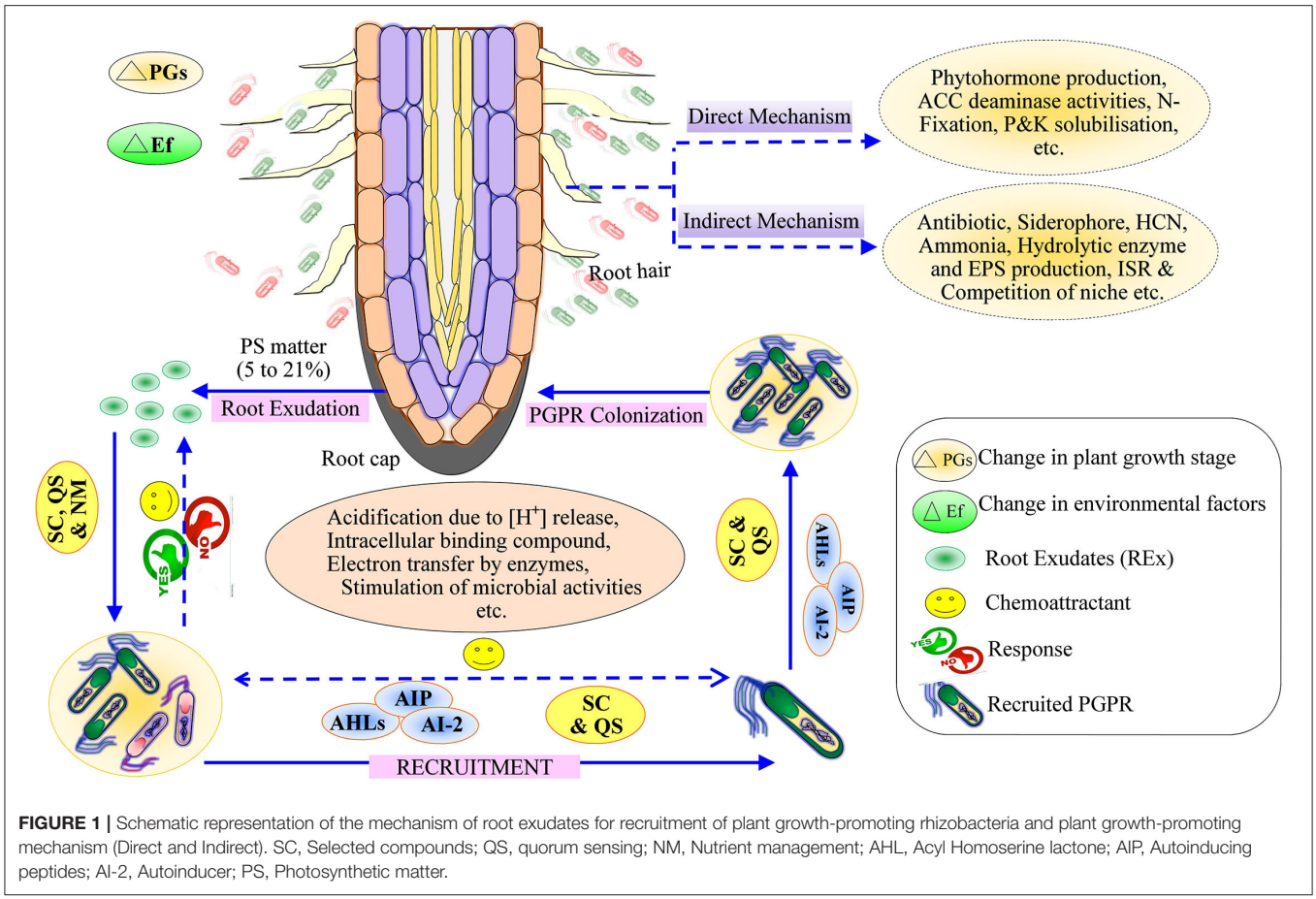

FIGURE 1 | Schematic representation of the mechanism of root exudates for recruitment of plant growth-promoting rhizobacteria and plant growth-promoting mechanism (Direct and Indirect). SC, Selected compounds; QS, quorum sensing; NM, Nutrient management; AHL, Acyl Homoserine lactone; AIP, Autoinducing peptides; AI-2, Autoinducer; PS, Photosynthetic matter.

The PGPR leads to increased soil fertility, plant growth promotion, and suppression of phytopathogens. These are involved in different functions of the soil ecosystem, nutrient availability, bioremediation of toxic heavy metals, degradation of pesticides, etc. (Chandler et al., 2008; Braud et al., 2009; Rajkumar et al., 2010; Paul et al., 2020; Bhojiya et al., 2021). The PGPR induces plant growth under varied environmental conditions, and the functional roles of bacteria vary with a specific plant (**Table 1**). The studies demonstrated that root exudates recruited microbial species that are more favorable for plant growth and productivity (Chowdhury et al., 2015; Zhang et al., 2015).

PLANT–MICROBE INTERACTIONS

Several researchers have reported that the population of microorganisms differs in the soil, for example, 12×10^8 bacteria/g dry soil, 12×10^5 fungi/g dry soil, 5×10^5 algae/g dry soil, and 46×10^6 actinomycetes/g dry soil; the bacterial population is highest followed by fungi, algae, and actinomycetes, as a general rule of the thumb (Yadav et al., 2015). Biotic interactions between the plants and microbes occur through communication that requires two essential conditions: one is the production of a specific signal, and another is the behavioral response generated from the signals (Keller and Surette, 2006). Plants communicate to rhizobacteria by secreting specific signaling molecules, viz. lectine enzymes, which are retraced by the bacterial species (Keller and Surette, 2006). *B. subtilis* detects only secondary metabolites as signals and produces a response against the secondary metabolites (Shank and Kolter, 2011; Singh et al., 2019). The behavior between the plants and the PGPR is mediated through root exudates, quorum sensing, cross-talk, electron-transfer mechanism, etc. (Tashiro et al., 2013; Singh et al., 2017; Keswani et al., 2020a). Positive plant–microbe interactions can be observed with PGPR, nitrogen-fixing bacteria, endo- and ecto-mycorrhizal fungi, whereas negative plant–microbe interactions are exhibited by pathogenic microbes (Haldar and Sengupta, 2015; Compant et al., 2019; Bashir et al., 2021; South et al., 2021). The legume rhizobia is an example of symbiotic interactions (Cai et al., 2009); the plant's secondary metabolite secretes flavonoids that activate a cascade of transcriptional events and mediates rhizobial nodulation signals commonly known as *Nod*-factors or lipo-chitooligosaccharides (Spaink, 2000). These factors trigger plant growth, leading to morphological changes in root hairs of legumes and the development of root nodules, while *Nod*-factors play a significant role in symbiotic nitrogen fixation (D'Haeze et al., 1998). The rhizospheric microbes act as biological control agents (BCA) that regulate plant pathogens. Thus, BCA

ultimately increases plant productivity through the production of antimicrobial secondary metabolites (Weller, 2007; Singh et al., 2019), production of hydrolytic enzymes (Adesina et al., 2007), effectors (Rezzonico et al., 2005), and hyperparasitism (Harman et al., 2004). Plant growth-promoting microorganisms (PGPM) affect plant growth directly or indirectly through biofertilizers (Mahmud et al., 2021) and/or phytostimulators (Spaepen et al., 2007), as well as biocontrol activity (**Figure 1**).

The functional genes of *B. amyloliquefaciens* strains CAUB946, YAUB9601-Y2, and FZB42 are involved in the synthesis of phytohormones, and other gene clusters are involved in disease control (Chen et al., 2007; Borriss, 2011; Blom et al., 2012; Hao et al., 2012). The selection of the perfect candidate PGPR can be a remarkable development for biofertilizer technology. Zhang et al. (2015) demonstrated that *B. amyloliquefaciens* (SQR9) is an ideal and more efficient PGPR than other strains of *Bacillus* strains (**Table 2**). Thirteen unique mobile genomic islands (GIs) were observed for the SQR9 strain. These GIs were found to be involved in the synthesis of many known and unidentified novel compounds. A recent report also demonstrated that maize root exudates regulate 98 genes in SQR9 for carbohydrate and amino acid metabolism. The set of the genome in SQR9 performed several functions like extracellular matrix production and regulated gene expression (**Table 2**), which revealed a high density (1.8×10^6 CFU g^{-1} root) of SQR9 in the maize rhizosphere, and triggers plant growth (Zhang et al., 2015).

MECHANISTIC INSIGHT OF PLANT GROWTH-PROMOTING RHIZOBACTERIA

Root Exudation

Narasimhan et al. (2003) reported two groups of root-exudates:(i) low molecular weight (LMW) such as sugars, amino acids, phenolics, secondary metabolites, and organic acids (citric, malic, oxalic, pyruvic, and succinic, etc.), and (ii) high molecular weight (HMW) that include proteins and complex carbohydrates. The nature and specificity of root exudates are dependent on the host species, plant developmental stages, physio-chemical nature of the soil, and surrounding microbial diversity (Hu et al., 2018; Singh et al., 2022). The maximum concentration of root exudates is found at the root tips and the lateral branching of the roots. Its amount also attenuates with increasing root surface (Compant et al., 2019), diffusion and degradation through sorption, deposition, or microbial consumption (Reinhold-Hurek et al., 2015). The microbial consumption contributes to the extravagance of root exudates owing to the valuable source of nutrition and energy for the rhizospheric microbes (Compant et al., 2019). The difference in the amount and nature of root exudates determines nutrient mobility, microbial population, and microbial diversity (Chamam et al., 2013; Bowya and Balachandar, 2020; Korenblum et al., 2020; Singh et al., 2022). Plant roots secrete root exudates in the rhizospheric region through passive (ion channels, vesicular transport, and diffusion) and active (secretion) mechanisms (Rohrbacher and St-Arnaud, 2016). LMW compounds are released through passive transport while HMW compounds through active transport mechanisms (Rohrbacher and St-Arnaud, 2016). The root exudates and solutes from cell membranes develop equilibrium between exterior and interior molecular transport (Weston et al., 2012; Cesari et al., 2019). In the passive mechanism, polar molecules and ions diffuse through the membrane using channels/permeases through a process called facilitated diffusion. These channels act as a passage for small ions like Na^+, K^+, Cl^-, etc., and water, which aid in maintaining intra-cellular pH, membrane potential, osmotic status, and stabilized volume of the cell (Lee et al., 2007). The small polar and uncharged molecules can transport through direct passive diffusion depending on membrane permeability (Weston et al., 2012; Rohrbacher and St-Arnaud, 2016). The non-polar molecules pass through without using channels or transfer proteins (Weston et al., 2012). The electrochemical gradient arises owing to charged molecules or ions like amino acids, sugars, carboxylates ions, etc. (Rohrbacher and St-Arnaud, 2016). Passive transport across the membrane through channels is driven by an electrochemical gradient (Rohrbacher and St-Arnaud, 2016). Without any expense of energy, the movement based on an electrochemical gradient is called passive transport. The transport that requires energy from ATP for several ions or molecules against the concentration gradient or electrochemical gradient is called active transport (Rohrbacher and St-Arnaud, 2016). Plants have different coping mechanisms against the environment and secrete a large number of compounds that may require many transporters (Weston et al., 2012; Rohrbacher and St-Arnaud, 2016; Korenblum et al., 2020), and these transporters are capable of root exudation of aggregates into the rhizo-microbiome.

Weston et al. (2012) reported that the root exudates from root cells are transported by membrane transport proteins (MTPs). The ATP-binding cassette transporter helps in the phytochemical secretion from roots. Besides, Badri et al. (2013) have also described that out of 129 genes, 25 are significant for root exudation in *Arabidopsis thaliana*. A single gene mutation may influence the interaction among the microbial group of soil in *A. thaliana* (Badri et al., 2013). The MTPs include ABC transporter, multidrug and toxic compound extrusion (MATEs), major facilitator superfamily (MFS), and aluminum-activated malate transporter (ALMT). MATE transporter in rice root promotes exudation of polyphenolic compounds (Baetz and Martinoia, 2014). Recently, Wanga et al. (2018) reported that the aluminum exclusion from the root is facilitated by ALMT and citrate exudation through the MATE citrate transporter.

The Action of Root Exudates

Root exudates can mediate neutral, useful, or harmful interections between plant microbes and inter-species of microorganisms (Mendes et al., 2013; Hu et al., 2018). The secretion of root exudates rests on plant needs, and the rate of exudation is modified to cope with different biotic and abiotic stresses (Badri and Vivanco, 2009; Vardharajula et al., 2011). The root-driven changes in the microbial community observed by Donn et al. (2015) in the wheat rhizosphere demonstrated ten times more bacterial abundance than the bulk soil. Specific microbes like *Burkholderiales*, *Sphingobacterium,*

TABLE 1 | Compounds from plant root exudates recruit perfect plant growth-promoting rhizobacteria (PGPR) improving plant growth performance.

Plant	Compounds from root exudates	Recruited PGPR	Plant growth performance	Condition	References
Groundnut (*Arachis hypogaea*)	Naringenin, oleic, citric, and lactic acid	*Bradyrhizobium-Azospirillum brasilense*	Enhance root exudation and PGPR interaction	Water deficit condition	Cesari et al., 2019
	Threonine and glycoxylicoxime acid	*Pseudomonas aeruginosa* (RP2)	Enhance growth and yields of groundnut	field study	Ankati and Podile, 2019
	Serine, pentanoic acid, glycopyranoside, tartaric acid, and 2-pyrrolidinone	*Bacillus sonorensis* (RS4) and *Pseudomonas aeruginosa* (RP2)			
	Polyphenol oxidase and phenylalanine	*Pseudomonas aeruginosa* (P4)	Significantly enhance seed germination, seedling, and shoot- root length and dry weight	*in vitro*	Gupta et al., 2020
	N-acylhomoserine lactones (AHLs)	*Bradyrhizobia*	Induces nitrogen fixation and PGPR colonization	*in vitro*	Nievas et al., 2012
Wheat (*Triticum* sp.)	2,4 diacetylphloroglucinol (DAPG)	*Pseudomanas* (F113) *and Azospirillum* sp.	Enhances phyto-stimulation effect by *Azospirillum* Sp245-Rif (Root-proficient, spontaneous rifampicin-resistant mutant of Sp245) gene, and PGPR colonization	*in vitro*	Combes-Meynet et al., 2011
	2,4-diacetylphloroglucinol (DAPG)	*Fluorescent Pseudomonas* sp	Act as a bio-control	*in vitro*	Bonsall et al., 1997
	Organic acids (acetic acid, oxalic acid, succinic acid, and tartaric acid)	*Arthrobacter*, *Bacillus* and *Devosia*	Enhance the Organic compounds concentration mediates root exudation and PGPR colonization	field study	Chen et al., 2019
Rice (*Oryza sativa*)	Carbohydrates, histidine, proline, valine, alanine, and glycine	*Azospirillum brasilense*	Rice exudates significantly induce attraction of the endophytic bacteria *Corynebacterium flovesence* and *Bacillus pumilus*. *Bacillus* sp. was less attracted than endophytes while the *Azospirillum brasilense* showed higher chemotactic response	Hydrponic condition	Bacilio-Jimenez et al., 2003
	Salicylic acid (SA)	*Pseudomonas chlororaphis* (ZSB15-M2)	Increases rhizospheric colonization on foliar spray of SA or *Corynebacterium glutamicum* cell extract (CGCE) Soil organic carbon, microbial biomass carbon, soil protein was increased with 21.86, 9.68, and 11.57%, respectively Available form of nitrogen, phosphorus, potassium, and zinc was increase with 21.83, 28.83, 23.95, and 61.94% over the control in the rhizosphere	field study	Bowya and Balachandar, 2020
	Flavonoids and hydroxycinnamic	*Azospirillum*	Enhance metabolites activities and plant growth	field study	Chamam et al., 2013
	N-acyl homoserinelactones (AHLs)	*Azospirillum lipoferum* (TVV3)	Ability to enhance chemotactic interaction	*in vitro*	Vial et al., 2006

(Continued)

TABLE 1 | Continued

Plant	Compounds from root exudates	Recruited PGPR	Plant growth performance	Condition	References
Tomato (*Solanum lycopersicum*)	Organic acids (Citric, succinic, and malic acids)	*Pseudomonas fluorescens* (WCS365)	Act as bio-control agent and increase the biomass	*In vivo*	Kamilova et al., 2006b
	Azelaic acid	*Bacillus* spp.	Acts as a bio-control through ISR and enhance plant growth performance	*in vitro*	Korenblum et al., 2020
Maize (Zea *mays*)	Humic acid	*Herbaspirillum seropedicae*	Enhances the production of border cells (involve at prime stage of plant soil ecosystem, including signaling and sense response) followed by root colonization of nitrogen fixer *Herbaspirillum seropedicae*	*in vitro*	Canellas and Olivares, 2017
	Amino acids, proline, total soluble sugar, and exopolysaccharides	*Bacillus* spp.	Enhance seedling and plant growth	Drought stress	Vardharajula et al., 2011
Pigeon pea (*Cajanus cajan*)	Tryptophan	*Rhizobium* spp.	IAA production that significantly enhance plant growth	*in vitro*	Ghosh et al., 2013
Banana (*Musa* sp.)	Oxalic, malic, furmaric, and several organic acids	*Bacillus amyloliquefaciens* (NJN-6)	Chemotactic response by malic acids and fumaric acids induced 20.7–27.3% biofilm formation	*in vitro*	Yuan et al., 2015
Common glasswort (*Salicornia europaea*)	*N*-acylhomoserine lactones (AHLs)	*Pseudomonas segetis* (P6)	Act as quorum quenching and bio-control agent. Increases height and weight of tomato plant	*In vivo*	Rodriguez et al., 2020
Alfalfa (*Medicago sativa* L.)	Flavonoids	*Rhizobium melilofi*	Chemoattractants and *nod* gene inducers for the symbiotic *Rhizobium*	Aeroponic system	Coronado et al., 1995
	7,4- Dihydroxyflavone and Naringeni	Acidobacteria	Induced colonization of PGPR with addition of enhancing *nod* gene expression	*in vitro*	Szoboszlay et al., 2016
	N-acyl homoserine lactones (AHLs)	*Sinorhizobium meliloti*	Induce nitrogen fixation and PGPR colonization	*in vitro*	Marketon et al., 2002
Soybean (*Glycine max*)	Isoflavonoid	Rhizobia	Helps in plant defense and also facilitate symbiotic interaction among soybean root and rhizobial communities	*in vitro*	White et al., 2017
Cucumber (*Cucumis sativus*)	Citric and fumaric acids	*Bacillus amyloliquefaciens* (SQR-9)	Induces colonization of *Bacillus amyloliquefaciens* SQR-9 and mitigate against pathogen *Fusarium oxysporum*	*in vitro*	Liu et al., 2014
Arabidopsis (*Arabidopsis thaliana*)	L-malic acid	*Bacillus subtilis* (FB17)	L-malic acid enhance boifilm formation chemotactically	*in vitro*	Rudrappa et al., 2008
Sugar beet (*Beta vulgaris*)	2,4-diacetylphloroglucinol (DAPG)	*Pseudomonas* spp. (F113)	Acts as a inhibitor of plant pathogens	*in vitro*	Shanahan et al., 1992

TABLE 2 | Root exudates of maize plant recruit *B. amyloliquefaciens* strain. The whole genome sequence of *B. amyloliquefaciens* revealed that the group of genes induced by root exudates and its functional gene triggers rhizoadaptation, phytostimulation, bioferlilizer, and biocontrol activity.

Gene	Functions
fZB42, ysnE, yhcX, and *dhaS*	Tryptophane dependent indol-3-acetic acid (IAA)
alsRSD operon	2, 3-butanediol biosynthesis
phy	Phosphate solubilization
gap and *fbaB*	Embden-Meyerhof-Parnas pathway
sucC	Tricarboxylic acid cycle
iol cluster	Inositol
mtlD	Mannitol
hxlA	Hexulose
dat, *alaT*	Alanine
gltD, *gltA*	Glutamate
kamA	Lysine
dapG	Aspartate
pTS	Phosphotransferase system or sugar transporter
citH	Citrate transporter
glnQHM, *yveA*, *appC*, etc	Amino acid/Peptide
yclN, *yclO*	Ferrichrome
sapB	Mg^{2+}
pst cluster	Phosphate
epsA-O	Exopolysaccharides synthesis
tapAsipW-tasA	Extracellular protein production
bslA	Self-assembling the bacterial hydrophobin that coats the biofilm
spo0A ∼ *p-AbrB/sinI-sinR*	Regulatory genes
degQ	Stimulates phosphotransfer from DegS ∼ P to DegU; enhanced the biofilm formation and root colonization of SQR9
bglC, *bglS*, *bglA*, *licH* etc	Cellulose degradation
xynA, *xynB*, *xylR* and *xylAB*	Xylan transport
bglS and *bglA*	Significantly induced by root
cheA, *cheB*, *cheW*, *mcpB*, and *mcpC*	Involve in chemotaxis
fliF-L, *flgD*, *flgG*, *flhA*, *flhF*	Flagella synthesis

(Source: Wang et al., 2009; Zhang et al., 2015; Wanga et al., 2018; Zhalnina et al., 2018).

and *Xanthomonadales* are dominant in the rhizospheres of *Brachypodium distachyon* in comparison to bulk soil (Kawasaki et al., 2016). Similar observations were recorded by Zhalnina et al. (2018) while studying the chemistry of root exudates of *Avenabarbata* where root-exudates were preferred as substrates for the specific bacterial community in the rhizospheres. The beneficial rhizobacterium *Pseudomonas putida* KT2440 is chemotactically attracted by 2-4-dihydroxy-7methoxy-1,4-benzoxazin-3-one from root exudates of *Zea mays* (Neal et al., 2012). The root exudate compounds like flavonoids act as signaling molecules, regulate *nod*-gene expression, activate *nod*-factors (lipochito-oligosaccharide), and trigger nodulation establishment in legumes (Abdel-Lateif et al., 2012; **Figure 2**). The flavonoids are released due to overcoming nitrogen deficiency in soil (Coronado et al., 1995). The flavonoid 7,4-dihydroxyflavone, from the root exudates of *Medicago sativa,* can mediate interaction with a diverse range of acid bacteria along with the induction of the *nod*-gene in the legumes (Szoboszlay et al., 2016). Strigolactone stimulates hyphal branching in mycorrhiza (Akiyama et al., 2005), and malic acid helps in the recruitment of plant growth-promoting rhizobacteria (Rudrappa et al., 2008). On the other hand, root-exudates have antimicrobial secondary metabolites such as benzoxazinoids (BXs), which can trim actinobacteria, proteobacteria, and pathogenic microbial populations in the maize rhizosphere (Hu et al., 2018). Root exudates influence the recruitment and make-up of microbiota in the plant rhizosphere (Hartmann et al., 2009; Ladyginaand Hedlund 2010; Reinhold-Hurek et al., 2015; **Table 1**). The ability of *A. brasilense* to modulate the plant root architecture was reported by Creus et al. (2005). Molina-Favero et al. (2008) observed that *A. brasilense* can synthesize nitric oxide (NO) aerobically, which mediates the IAA signaling pathway, leading to lateral and adventitious root formation in tomatoes. In *Arabidopsis,* under drought stress, root colonization of *P. chlororaphis* increases the expression of genes associated with ROS (reactive oxygen species) defense, auxin, jasmonic acid, and salicylic acid synthesis (Cho et al., 2013). *P. chlororaphis* also decreases the expression of ethylene and abscisic acid genes in *Arabidopsis* under drought stress (Cho et al., 2013; **Figure 2**). The roots of watermelon secrete more trans-chlorogenic acid and caffeic acid, followed by trans-cinnamic acid, which induced resistance against *Fusarium oxysporum* (Ling et al., 2013). Cai et al. (2009) reported that leguminous plant roots secrete canavanine, which recruits beneficial microorganisms. Canavanine favors the growth of selective rhizobia and also acts as an antimicrobial for pathogenic bacteria (Cai et al., 2009). Sugars and strigolactone, viz. 5-dexystrigal, components of non-legume root exudates mediate symbiotic association with mycorrhizal fungi (Fang and St Leger, 2010). Nguema-Ona et al., 2013 observed that AGPs (arabinogalactans protein) of root exudates also attract plant growth-promoting rhizobacteria through the chemo-attractant mechanism, and the maximum amount of AGPs was found at the root tip regions of the plants (Cannesan et al., 2012). AGPs induce a population of beneficial microbes in leguminous and non-leguminous plants (Xie et al., 2012; Vieira et al., 2020). The VOCs, *myc*-factors, *nod*-factors, exopolysaccharides, etc. are signaling components associated with rhizospheric microbes (Goh et al., 2013). VOCs (acetoin, 2-3-butanediol) mediate communication between plant microbes, induce ISR (induced systemic resistance) as bio-protestants (Ryu et al., 2004), and plant growth promotion. Ankati and Podile (2019) reported that threonine and glyoxylic oxime acid from root-exudates of groundnut influenced *Pseudomonas aeruginosa* (RP2), while serine, pentanoic acid, glucopyranoside, tartaric acid, and 2-pyrrolidinone influenced both *P. aeruginosa* (RP2) and *B. sonorensis* (RS4). These findings demonstrated that a specific component of root-exudates was responsible for selective PGPR interaction. Thus, the products of root exudates could be an effective agent for improving crop yield at the field level by enhancing PGPR colonization.

Quorum sensing (QS) helps in establishing root microbe assemblage in the rhizosphere. The root exudates mimic QS signals of bacteria to repress QS-regulated responses of

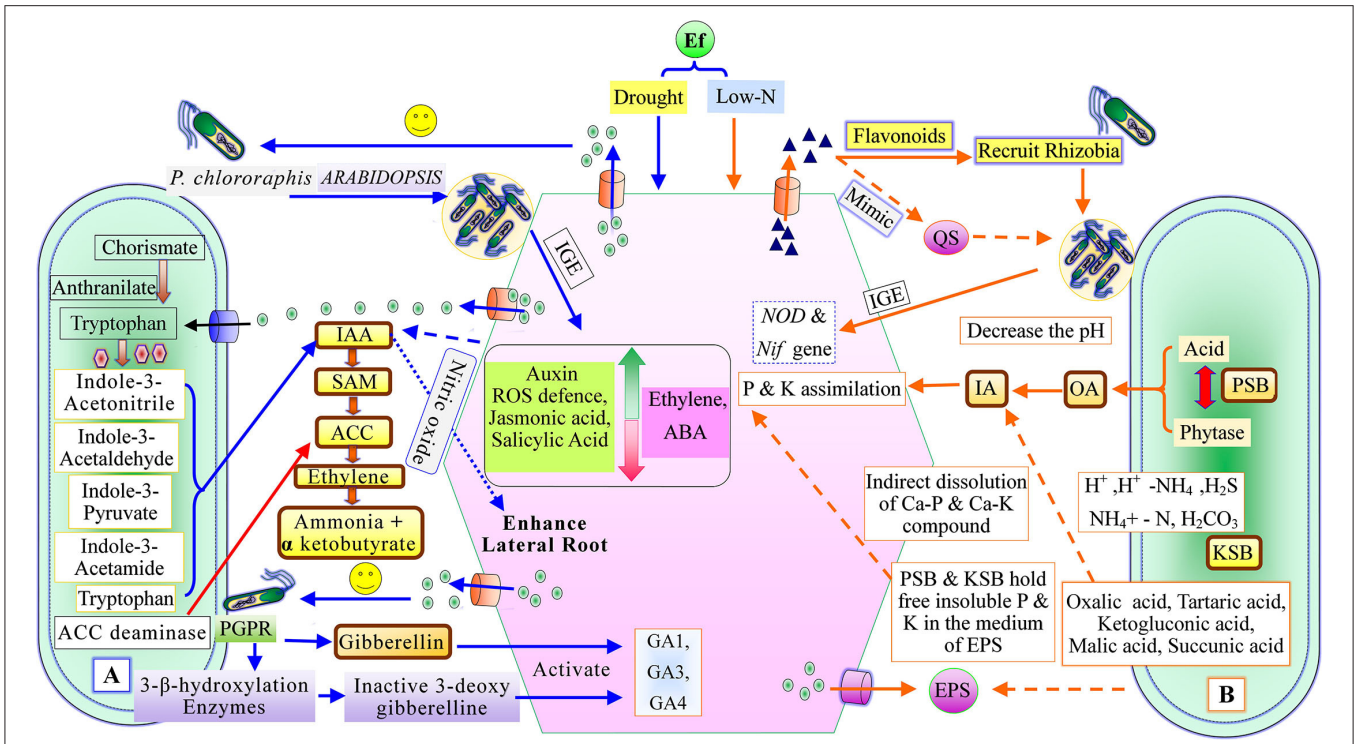

FIGURE 2 | Plant growth-promoting mechanism of recruited plant growth-promoting rhizobacteria, **(A)** Phytostimulation, and **(B)** Biofertilizer activity [QS, Quorum sensing; IAA, indole-3-acetic acid; SAM, S-adenosyl methionine; ACC, 1-aminocyclopropane-1-carboxylate; IGE, Induce gene expression; ABA, Abscisic acid; GA1, GA2, and GA4, (Types of gibberellin); PSB, Phosphate solubilizing bacteria; KSB, Potassium solubilizing bacteria; EPS, exo-polysaccharides; OA, Organic acid; and IA, Inorganic acid].

associated/adjacent bacteria. The root exudates have primary and secondary metabolites along with proteins (Korenblum et al., 2020). Some reports demonstrated that these proteins influenced the selective recruitment of useful bacteria (De-la-Pena et al., 2008). The QS compound in the root exudates of groundnut plants selects microbes and induces their population (Ankati and Podile, 2019). Bacteria communicate within the system through a density-dependent mechanism known as QS (Reinhold-Hurek et al., 2015). The QS regulates the metabolic as well as the behavioral activities of the bacterial community (Marketon et al., 2002; Nievas et al., 2012; Liu et al., 2014; Korenblum et al., 2020). This sort of interaction occurs through a dialect of chemical signals called autoinducers (AHLs: acyl homoserine lactones), autoinducing peptides (AIP), and autoinducer-2; furanone (AI-2), synthesized by bacteria (**Figure 1**). AHLs mediate signaling in gram-negative bacteria (Vial et al., 2006). AIP requires specialized membrane transport protein for signaling in the gram-positive bacteria, whereas AI-2 is required for both gram-positive and gram-negative bacteria (Abisado et al., 2018). Bacterial QS occurs through various complex pathways depending upon species diversity (Reinhold-Hurek et al., 2015). Therefore, the cognizance of the QS enables the regulation, thereby constraining bacterial communication (**Figure 1**). The inhibition strategies of QS are jointly called quorum-quenching, through which bacteria are ineffective in their interplay with each other. QS-mediates bacterial processes like growth, conjugation, bioluminescence, biofilm formation, siderophore production, and swarming (Barriuso et al., 2008). The threshold level of the initial plant growth-promoting rhizobacteria inoculum mediated by QS molecules strongly induces plant growth performance (Rodriguez et al., 2020). The plant rhizospheric region has a higher amount of AHL in comparison to the bulk soil, suggesting that these trigger bacterial colonization and establish a strong association between bacteria and plant roots (Vial et al., 2006).

Plant Growth-Promoting Rhizobacteria

Menendez and Garcia-Fraile (2017) classified plant growth-promoting rhizobacteria into extracellular plant growth-promoting rhizobacteria (e-PGPR) and intracellular plant growth-promoting rhizobacteria (i-PGPR). The plant growth-promoting rhizobacteria stimulate plant growth directly by the activity of phytostimulation and bio-fertilization, whereas indirectly through biopesticides or bio-control agents (Dwivedi and Dwivedi, 2002; Glick et al., 2007; Glick, 2012; Ngoma et al., 2012). The direct mechanism of plant growth-promoting rhizobacteria facilitates nutrient uptake or improvement in nutrient availability by nitrogen fixation (Cheng, 2008; Glick, 2012), solubilization of phosphorus and mineral nutrients, mineralizing organic compounds (Khan et al., 2010; Sharma et al., 2013), and phytohormones production including, IAA, ethylene, cytokinins, and gibberellins (Pliego et al., 2011; Upadhyay et al., 2016, 2019; South et al., 2021; **Figure 2**). On

the basis of PGPR function, siderophore production may be considered as both a direct and an indirect mechanism (Ahmed and Holmstrom, 2014). The indirect mechanisms include antibiotic production (Sindhu et al., 2009), hydrolytic enzyme production (Dubey et al., 2014), induced systemic resistance (ISR), and exo-polysaccharides (EPS) production (Upadhyay et al., 2011; **Figure 3**).

DIRECT MECHANISMS

IAA Production

IAA (indole-3-acetic acid), a product of the amino acid L-tryptophan (Yu et al., 2017), acts as a plant growth regulator. The IAA regulates the plant-growth through several cellular functions such as cell division, cell elongation and differentiation, increase in root length and root surface area, and the development of flowers (Gravel et al., 2007; Santner et al., 2009). About 80% of rhizobacteria produce auxins of microbial origin but with analogous functions, such as the auxins of plant origin (Patten and Glick, 1996; Ahemad and Kibret, 2014; Myresiotis et al., 2015; Keswani et al., 2020b. The IAA plays a crucial role in the interaction between plant and rhizobacteria and is synthesized by the associated plants and many microbes like plant growth-promoting rhizobacteria (Upadhyay et al., 2009). Several studies have demonstrated that the IAA production system was present in many bacterial species such as *Agrobacterium tumefaciens*, *Alcaligenes faecalis, Agrobacterium tumefaciens* (Costacurta and Vanderleyden, 1995), *Pseudomonas syringae* (Kosuge and Sanger, 1987), *Streptomyces* sp., *B. subtilis* spp. (Swain et al., 2007), *Pseudomonas fluorescens* (Oberhansli et al., 1991), and *B. megaterium* (Nghia et al., 2017).

Ethylene Production

Ethylene is a unique type of plant hormone secreted by plants and plant growth-promoting rhizobacteria (Babalola, 2010). Ethylene regulates plant physiological processes such as seed dormancy, enhances the formation of an adventitious root, leaf abscission, senescence of flower and leaf, and fruit ripening (Abeles et al., 1992). Different environmental conditions like salinity, drought, low temperature, pathogenic attack, and chemical exposure alter ethylene production and plant growth (Babalola, 2010). The optimum concentration of ethylene induces positive growth and development of plants (Saleem et al., 2007). Ethylene production directly depends on ACC production (Shaharoona et al., 2006).

Gibberellins and Cytokinin Production

Gibberellin (GA) is a tetracyclic di-terpenoid compound that acts as a plant hormone and is synthesized by many plant growth-promoting rhizobacteria. GA regulates many plant functions, such as fruit ripening, cell division, plant growth, etc. (Martinez et al., 2016; Plackett and Wilson, 2016). The endogenous GA concentration is raised by GA-producing plant growth-promoting rhizobacteria in the rhizospheric zone and it induces plant growth; for example, *Leifsonia soli*-SE134 and *Enterococcus faecium*-LKE12 in rice plant (Kang et al., 2014; Lee et al., 2015). Cytokinin is a plant hormone and is also synthesized by plant growth-promoting rhizobacteria. It is a member of adenine derivatives of the N-6 substituted group (Tsukanova et al., 2017), promotes cell cycle of the plant (Schaller et al., 2014), regulates plant growth and biosynthesis of chlorophyll (Cortleven and Schmülling, 2015). Plant growth-promoting rhizobacteria can produce Cytokinin and cause an increase in plant growth even under stressed conditions (O'Brien and Benkova, 2013). Tahir et al. (2017) demonstrated that *B. subtilis*-SYST2 induces the expression of cytokinin gene (*s1CKX1*) in tomato plants (Tahir et al., 2017). The plant growth-promoting rhizobacteria like *Rhizobium* sp., *Azotobacter* sp., *Pantoea agglomerans*, *Pseudomonas fluorescens*, *Rhodospirillum rubrum*, *B. subtilis,* and *Paenibacillus polymyxa* secrete cytokinins and/or gibberellins that promote plant growth (Kang et al., 2010).

Availability of Nutrients

The soil acts as a buzzword source of macro- and micro-nutrients for plant growth, while the compatible form of nutrients is a question of their availability to the plant. Most of the microorganisms can enhance the availability of nutrients in their compatible form to the plants (Upadhyay et al., 2019). Thus, soil fertility is one of the significant factors that governs diverse mechanisms of microorganisms. Nitrogen occurs in 78% of total atmospheric gases and cannot be utilized by higher plants directly. The nitrogen is utilized when it becomes fixed in the form of nitrogenous salt or ammonium ion. In nature, two kinds of N_2 fixation occurs i.e., biological and non-biological (Raza et al., 2021). The biological nitrogen fixation (BNF) is carried out with the aid of bacteria, fungi, and algae, etc., which makes the atmospheric nitrogen available in the form of nitrogenous salt through the action of several plant growth-promoting rhizobacteria and blue-green algae (Dwivedi and Dwivedi, 2004). The BNF is borne out by two kinds of microbes, e.g., symbiotic and non-symbiotic (Tang et al., 2020; Raza et al., 2021). Symbiotic-BNF, a mutualistic link between the microbe and the plant, occurs in leguminous plants such as pea, chickpea, etc. (Cheng, 2008). In symbiotic-BNF, microbes enter the root and induce nodule formation (Cheng, 2008; Singh et al., 2022). Free nitrogen peroxide is converted into ammonia by nitrogen-fixing microorganisms and makes it available to the host (Ahemad and Kibret, 2014). This process involves a complex enzyme system known as nitrogenase (Gaby and Buckley, 2012), and the *nif*-gene, found in symbiotic as well as free-living bacterial systems (Reed et al., 2011). Nitrogen-fixing plant growth-promoting rhizobacteria such as *Azospirillum* (Montanez et al., 2009), *Klebsiella* (Arruda et al., 2013), *Burkholderia* (Chelius and Triplett, 2001), *Bacillus* (Zakry et al., 2012), and *Pseudomonas* (Piromyou et al., 2011) can significantly enhance crop productivity. *Bacillus* is associated with N_2-fixing bacteria promoting plant growth and enhances the yield in non-leguminous cereals (Cakmakci et al., 2001; Ramirez and Mellado, 2005) such as maize (Pal, 1998), sugar beet, and barley (Sahin et al., 2004).

Mostly, phosphorus exists in the insoluble complex form like calcium phosphates in saline soil (Goldstein and Krishnaraj, 2007) and iron phosphates and aluminum phosphates in acidic soil (Mullen, 2005). Phosphorus is commonly present in soil

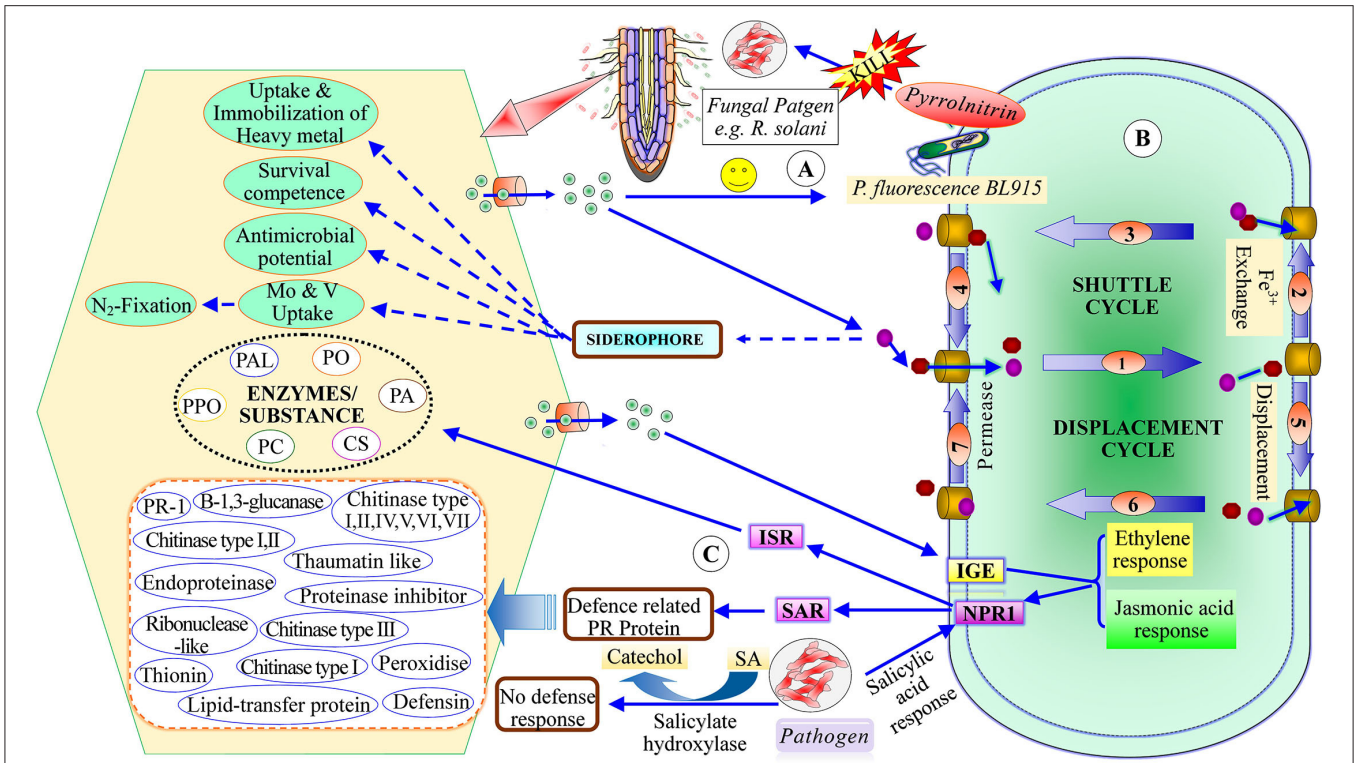

FIGURE 3 | Indirect mechanism of plant growth-promoting rhizobacteria **(A)** recruited PGPR to produce antibiotic **(B)** siderophore production and plant growth-promotion, **(C)** mechanism of induced systematic resistance [ISR, induced systemic resistance; SAR, Systematic acquired resistance; IGE, Induce gene expression; NPRI, Non-expresser pathogenesis-related gene; SA, salicylic acid; PAL, phenylalanine amonislyase; PO, peroxidase; PPO, polyphenol oxidase; PC, poly-phenolic compounds; CS, chalcone synthase; PA, phytoalaxine.

in the range of 400–1,200 mg kg^{-1} (Fernández et al., 1988). Earth rocks are rich sources of phosphorus, in the form of primary apatites, and other primary minerals that previously existed in the geological age (Fernández et al., 1988). Indian soils are commonly deficient in phosphorus (Johri et al., 2003), and there are about 40 million tons of phosphorus deposits in India (Roychoudhury and Kaushik, 1989). Phosphate solubilizing bacteria (PSB), actinomycetes, and phosphate solubilizing fungi (PSF) solubilize the complex form of phosphates in the soil (Khan et al., 2007). The plant growth-promoting rhizobacteria induce the availability of phosphorus through mineralization and solubilization of the compounds of rock phosphates (organic and inorganic phosphorus; Nahas, 1996; Hilda and Fraga, 2000; Khiari and Parent, 2005). Bacterial species are superior phosphorus solubilizers than fungal species (Alam et al., 2002); PSB involves about 1–50% phosphorus solubilization followed by PSF, i.e., about 0.1–0.5% (Chen et al., 2006). *Pseudomonas*, *Bacillus*, *Rhizobium,* and *Enterobacter,* and fungal genera such as *Penicillium* and *Aspergillus* are the most efficient phosphate solubilizers (Kucey et al., 1989; Rodriguez and Fragal, 1990).

About 90% of potassium (K) in the soil exists in its complex form and is not available to the plants (Yadegari and Mosadeghzad, 2012; Zhang et al., 2013). Therefore, the solubilization of potassium is essential for K uptake by plants. K enhances seed germination, plant growth productivity, seedling vigor, and plantbiomass (Awasthi et al., 2011; Lynn et al., 2013; Meena et al., 2014; Zhang and Kong, 2014). The plant growth-promoting rhizobacteria can solubilize potassium rock (e.g., biotite, feldspar, illite, muscovite, orthoclase, and mica) into an available form of potassium for the plant. Potassium solubilizing plant growth-promoting rhizobacteria releases organic acids (e.g., oxalic acid, tartaric acids, gluconic acid, 2-ketogluconic acid, citric acid, malic acid, succinic acid, lactic acid, propionic acid, glycolic acid, malonic acid, fumaric acid, etc.) and inorganic acids (Awasthi et al., 2011; Etesami et al., 2017), which play an effective role in releasing K from K-bearing minerals (Hu et al., 2006; Liu et al., 2012; Keshavarz et al., 2013; Saiyad et al., 2015).

Different types of organic acids are involved in potassium solubilization, but the most prominent acids are tartaric acid, citric acid, succinic acid, α-ketogluconic acid, and oxalic acid released by KSB (Meena et al., 2014). Both aerobic and anaerobic plant growth-promoting rhizobacteria act as KSB, but most frequently aerobic bacteria that act as potassium solubilizers are *Acidothiobacillus ferrooxidans*, *B. edaphicus*, *B. mucilaginosus*, *Burkholderia*, *Paenibacillus* sp., and *Pseudomonas* (Etesami et al., 2017). Saprophytic bacteria, fungal strains, and actinomycetes also participate in K solubilization in a wide range (Gundala et al., 2013; Meena et al., 2014; Bakhshandeh et al., 2017). Thus, KSB–PGPR acts as a biofertilizer that improves soil fertility and plant growth. KSB is commonly

found in different soil environments and can be isolated from rhizospheric and non-rhizospheric soil, including paddy soil (Bakhshandeh et al., 2017) and saline soil (Bhattacharya et al., 2016). KSB–PGPR is more effective for potassium solubilization (4.90 mg l^{-1}) at a specific pH range of 6.5–8.0 (Badr et al., 2006). Similarly, *Bacillus* sp., *Burkholderia* sp., and *Pseudomonas* sp. can solubilize potassium at different temperatures and carbon sources from tea (*Camellia sinensis;* Bagyalakshmi et al., 2012).

DIRECT/INDIRECT MECHANISM

Siderophore Production

Plant growth-promoting rhizobacteria secrete a low molecular weight (500–2,000 Da) iron-chelating compound called siderophore (Ahmed and Holmstrom, 2014). Siderophores are involved in the transportation and uptake of iron elements in the plant cells (Singh et al., 2022) and induce plant growth (Schwyn and Neilands, 1987; Hider and Kong, 2010; Ahmed and Holmstrom, 2014). *Pseudomonas* sp., *Enterobacter* genera, *Bacillus,* and *Rhodococcus* have a special capacity for binding iron through siderophores or siderochromes (Sah and Singh, 2015). Those microorganisms which cannot produce siderophores but use siderophores produced by other microorganisms are called xenosiderophores (Ahmed and Holmstrom, 2014). Production of siderophores occurs at specific conditions such as pH, temperature, and iron-concentration. The bacteria *P.chlororaphis* PCL1391 strain of rhizospheric roots of tomato plants can solubilize iron from the insoluble ferric oxides at neutral pH (Hernandez et al., 2004; Haas and Defago, 2005). Similarly, Sinha et al. (2018) reported that *Psychrobacter piscatorii* and *Enterococcus casseliflavus* from the Kerguelen Islands and *B. cereus, Pseudoalteromonas tetraodonis*, *Psychrobacter pocilloporae*, *Pseudomonas weihenstephanensis,* and *Micrococcus aloeverae* from the Prydz-Bay produced either hydroxamate-type siderophore or catecholate-type siderophores at 15–25°C with pH 8.5. Siderophores are produced by both aerobic and facultative anaerobic types of bacteria under the iron stress habitats (Neilands, 1995). Facultative aerobic bacterium such as *Pseudomonas stutzeri* CCUG 36651 produced siderophores under both aerobic and anaerobic conditions (Essen et al., 2007), *Pseudomonas stutzeri* CCUG 36651 produced four types of ferrioxamine siderophores under aerobic conditions but ferrioxamines siderophores under anaerobic conditions (Essen et al., 2007). Siderophore tightly binds with iron (Fe^{+3}), then Fe^{+3}-chelates move inside the cell through the cell membrane with the help of specific siderophore receptors (Haas and Defago, 2005). There are several types of siderophore binding proteins, such as permeases and ATPases involved in the transport of Fe^{+3} chelating compounds in the cell membrane, reported in gram-positive bacteria (Ahmed and Holmstrom, 2014). Gram-negative bacteria release many enzymes including periplasmic binding protein, outer membrane receptors, and cytoplasmic membrane protein, which help in the transport of iron-chelating compounds (Ahmed and Holmstrom, 2014).

Indirect Mechanisms of Plant Growth-Promoting Rhizobacteria

Indirect mechanisms involve antibiotics production, and hydrogen cyanide (HCN), ISR, and EPS production. The secretion of lytic enzymes of plant growth-promoting rhizobacteria induces plant growth (Maksimov et al., 2011; Upadhyay et al., 2016). The production of antibiotics is one of the most powerful bio-control tools for plant pathogens. Antibiotics are heterogeneous, low molecular weight, organic compounds secreted by microorganisms that help plant growth and metabolic activities (Duffy, 2003). The first antibiotic used as bio-control for plants was isolated from the bacterial species of fluorescent pseudomonads (Weller and Cook, 1983). Based on the mode of action, there are six classes of antibiotics, namely, phenazines, phloroglucinols, pyoluteorin, pyrrolnitrin, cyclic lipopeptides, and hydrogen cyanide (Haas and Defago, 2005). A large number of bacterial and fungal species secrete various types of antibiotics which induce plant growth by the suppression of phytopathogens (Maksimov et al., 2011). Pyrrolnitrin, an antibiotic isolated from *P. fluorescens* BL915 strain suppresses the growth of the fungal pathogen *Rhizoctonia solani* in cotton plants (Hill et al., 1994). Bacterial species of *Pseudomonas* secretes phenazine antibiotics that suppress various fungal pathogens including *F. oxysporum* and *Gaeumannomyces graminis* (Chin-A-Woeng et al., 2003). *Bacillus* sp. produces many types of antibiotics such as polymyxin, circulin, and colistin that suppress many plant diseases (Maksimov et al., 2011).

Hydrogen cyanide is a volatile secondary metabolite secreted by several gram-positive and gram-negative bacteria such as *P.fluorescens*, *P. aeruginosa, Chromobacteria violaceum,* etc. (Morrison and Askeland, 1983) that act as bio-control agents against soil-borne phytopathogens (Haas and Defago, 2005). HCN acts as a powerful inhibitor of various metallic enzymes including copper-bearing cytochrome C oxidase (Cho et al., 2013). HCN prevents many plant diseases like root-rot and black-rot diseases of tomato plants (Voisard et al., 1989) and also has nematicidal activities (Kang et al., 2010; Anderson and Kim, 2018). It is also very useful in agriculture and forestry due to the control of subterranean termites, *Odontotermes obesus* (Devi et al., 2007).

Induced systemic response (ISR) suppresses the disease of plants and animals that induces resistance against diseases (Van Loon et al., 1998). ISR induced by rhizobacteria shows resistance to several pathogens such as bacteria, fungi, and viruses (Korenblum et al., 2020). The plant growth-promoting rhizobacteria strain secretes salicylic acid that produces resistance to plant diseases, indicating that PGPR induces ISR (Krause et al., 2003; Idris et al., 2004). The treatment of tobacco plants with *Bacillus* rhizobacteria suppressed the impact of TMV (Tobacco Mosaic Virus) and also enhanced the height, weight, and yield of tobacco plants (Kloepper et al., 2004; Wang et al., 2009).

Exo-polysaccharides is a very active constituent of soil organic matter (Gouzou et al., 1993) produced by plant growth-promoting rhizobacteria under different soil environments like salinity (Upadhyay et al., 2011; Mohammed, 2018), drought, and normal conditions (Alami et al., 2000). EPS is the most important

component of the extracellular matrix that shows two characters, slimy EPS and capsular EPS. EPS plays a significant role in several functions like biofilm formation (Bhaskar and Bhosle, 2005), bacterial cell protection (Mohammed, 2018), pollutants degradation (Fusconi and Godinho, 2002), plasma substituting capacity and bioremediation (Mohammed, 2018), maintenance of primary function of the cell, and antibacterial activity (Alami et al., 2000; Mohammed, 2018). EPS-producing PGPR influences root-adhering soils and establishes a balance between plant roots and microbial populations (Alami et al., 2000; Upadhyay et al., 2011).

Hydrolytic enzymes (HEs), mainly chitinase, glucanase, protease, and cellulase can hydrolyze chemical bonds of a wide variety of polymeric compounds including chitin, proteins, cellulose, hemicelluloses, and phytopathogenic DNA (Jadhav and Sayyed, 2016). HEs are capable of controlling phytopathogens through the hydrolysis of the cell wall, proteins, and DNA of pathogens. Thus, HEs play a major role in bio-control (Prathap and Ranjitha, 2015; Jadhav and Sayyed, 2016). The plant growth-promoting rhizobacteria act as an effective BCA through the lysis of phytopathogenic DNA (Garbeva et al., 2004). Microbial strains such as *S. marcescens*, *B. cereus*, *B. subtilius,* and *B. thuringiensis* can produce HEs that can control several phytopathogens namely *R. solani*, *F. oxysporum*, *S. rolfsii*, *P. ultimum,* etc. through different mechanisms (Someya et al., 2000).

Selective Recruitment of Plant Growth-Promoting Rhizobacteria

It is appealing to discuss what triggers the recruitment of microbiome in the rhizosphere. Microbiome in the rhizosphere affects plant growth and yield of the crop. There are two possibilities: (i) plant root creates an environment in the rhizosphere and attracts the useful microorganism/bacteria in the rhizosphere, (ii) soil already has a specified microbial population that allows the growth of selective plants. Here, we will discuss the first possibility which is more relevant to the root exudates and relevant to the remit of this review. Several previous reports demonstrated that the composition of root exudates varies with plant species, soil type, pH, and developmental stage (Berg and Smalla, 2009). The specific components of plant exudates promote the recruitment of specific microbiome/PGPR (Kamilova et al., 2006a). It is well-recognized that the microbial community in the rhizosphere is highly distinguished in different plant species (Edwards et al., 2015), the reason being the availability of different genotypes of the host plant. Based on the knowledge till date, the repertoire of the microbial community (especially the PGPR) around the plant root can be managed. It has been stated that some workers induced the recruitment of plant growth-promoting rhizobacteria by mutating the ABC transporter gene in plants (Badri et al., 2009). These results suggest the growth of a disease-resistant plant by influencing the root exudate components for the recruitment of plant growth-promoting rhizobacteria (Wei and Jousset, 2017). Natural disease-suppressive soil (term defined by Baker and Cook, 1974) can be achieved by manipulating the plant exudate resulting in the recruitment of the required PGPR (Exposito et al., 2017). Thus, differential components in plant exudates recruit microbial communities with a certain degree of specificity.

FUTURE PERSPECTIVES

Many pieces of research demonstrated the diverse compounds of root exudates and their sensing toward beneficial microbes studied under confined and controlled laboratory conditions. Therefore, elucidation of the function of chemotaxis behavior of microbe-mediated compounds of root exudates is necessary for future research to make the success story at the field level. This will provide the structural foundation for a wide range of PGPR recognition by specific compounds (chemoattractants) of plant root exudates, respectively, and induce the growth of sustainable agriculture by chemotaxis to genetically modified plant growth-promoting rhizobacteria under degraded soil. Despite little knowledge of chemoattractant compounds of plant's root exudates, there are scopes for more researches for getting diverse advantages of root exudates through the application of emerging technology. Biotechnology is the utilization of biological resources for human welfare and industrial use. Plants have a well-developed system for the secretion of root exudates. Whether this secretion system can be utilized for biotechnological application is the central issue. Undoubtedly, there are several published reports, but the most fitting domains are (i) rhizosecretion and (ii) phytoremediation. Rhizosecretion is an alternative platform for manufacturing a large amount of pure target proteins (Drake et al., 2009). Borisjuk et al. (1999) demonstrated the production of recombinant proteins in plant root exudates. For this purpose, a genetically engineered plant with increased root mass can be used (Gaume et al., 2003). Rhizosecretion has been utilized for the production of antibodies. Madeira et al. (2016) have demonstrated that hyposecretion is an efficient and economical method for monoclonal antibody production. Catellani et al. (2020) recently evaluated the production of anti-fungal antibody scFvFc 2G8 using the root hair secretion system in *Nicotiana benthamiana* and *Solanum lycopersicum*. Another example of next-generation human therapeutic antibody production was demonstrated by Lonoce et al. (2016). They showed the production of tumor-targeting human-compatible monoclonalantibody H10 in hairy root plants (Lonoce et al., 2016).

Environmental pollution is the most devastating condition in the present ecological perspective. Phytoremediation is the process of removal of water and soil contaminants, especially by using the plant root system (Upadhyay and Edrisi, 2021). The role of root exudate in the removal of soil and water contaminants has been reported outstandingly (Gleba et al., 1999; Ma et al., 2016; Chen et al., 2020). Different components of root exudates play a specific role in the removal of certain contaminants from the soil and groundwater. Lu et al. (2017) reported that glucose present in plant exudates can remove the soil pyrene by promoting soil dehydrogenase activity. Palmitic acid present in plant exudates of tall fescue showed promising results in the removal of petroleum contaminants from the soil

(Liu et al., 2015). Similarly, by manipulating the components of root exudates, it can be used for the removal of targeted pollutants from the soil and ground water. There are two main types of phytoremediation processes exploiting the plant exudates (i) rhizosphere biodegradation (plant root exudate recruited microbe mediated degradation of pollutants) and (ii) phytostabilization (plant exudate components immobilize the pollutants).

CONCLUDING REMARKS

Since the 1980s, plant growth-promoting rhizobacterial inoculants have been developed, but few of them revealed irregular performance at the field level. Although several researchers have developed the consortia of plant growth-promoting rhizobacteria, but with more or less similar outcomes in the farmer's field, the solution to these problems is somehow hidden in the root exudates and root microenvironment. Thus, the present review has concentrated on the remarkable views for future research to manage the challenges at the field level with PGPR inoculants. Several components of root exudates have functional interplay with PGPR either directly or through their gene expression. The recruitment of plant growth-promoting rhizobacteria through root exudates can enhance plant growth-promoting rhizobacteria root colonization, specifically, and induce close sustainable relationships between them for a long time. The hypothesis of specific recruitment would address the key gap for warranting the perfect plant growth-promoting rhizobacteria candidate and opening a new horizon of research in biofertilizer technology. It would be a promising technique for reducing the asymmetrical performance of plant growth-promoting rhizobacteria in the farmer's field.

AUTHOR CONTRIBUTIONS

SU, AS, PC, PD, and AB contributed to conceptualization and visualization of the present review and writing the original draft. SU and AS designed the figures and tables. DJ, PD, and GC contributed to re-structuring the review. PD, BS, VDR, and TM contributed special remarks and edited the review for final submission. All authors contributed to the article and approved the submitted version.

ACKNOWLEDGMENTS

This review work was supported by the Department of Environmental Science, V.B.S. Purvanchal University, Jaunpur, India. VDR and TM would like to recognize the support from the Ministry of Science and Higher Education of the Russian Federation (no. 220-5234-7520), laboratory "Soil Health" Southern Federal University.

REFERENCES

Abdel-Lateif, K., Bogusz, D., and Hocher, V. (2012). The role of flavonoids in the establishment of plant roots endosymbioses with arbuscular mycorrhiza fungi, rhizobia and frankia bacteria. *Plant Signal Behav*. 7, 636–641. doi: 10.4161/psb.20039

Abeles, F. B., Morgan, P. W., and Saltveit, M. E. Jr. (1992). *Ethylene in Plant Biology, 2nd Edn*. San Diego, CA: Academic Press.

Abisado, R. G., Benomar, S., Klaus, J. R., Dandekar, A. A., and Chandler, J. R. (2018). Bacterial quorum sensing and microbioll community interactions. *mBio* 9, e01749–18. doi: 10.1128/mBio.01749-18

Adesina, M. F., Lembke, A., Costa, R., Speksnijder, A., and Smalla, K. (2007). Screening of bacterial isolates from various European soils for *in vitro* antagonistic activity towards *Rhizoctonia solani* and *Fusarium oxysporum*: site dependent composition and diversity revealed. *Soil Biol. Biochem*. 39, 2818–2828. doi: 10.1016/j.soilbio.2007.06.004

Ahemad, M., and Kibret, M. (2014). Mechanisms and applications of plant growth promoting rhizobacteria: current perspective. *J. King Saud Univer. Sci.* 26, 1–20. doi: 10.1016/j.jksus.2013.05.001

Ahmed, E., and Holmstrom, S. J. (2014). Siderophores in environmental research: roles and applications. *Microbiol. Biotechnol*. 7, 196–208. doi: 10.1111/1751-7915.12117

Akiyama, K., Matsuzaki, K., and Hayashi, H. (2005). Plant sesquiterpenes induce hyphal branching in arbuscular mycorrhizal fungi. *Nature* 435, 824–827. doi: 10.1038/nature03608

Alam, S., Khalil, S., Ayub, N., and Rashid, M. (2002). *in vitro* solubilization of inorganic phosphate by phosphate solubilizing microorganism (PSM) from maize rhizosphere. *Int. J. Agric. Biol*. 4, 454–458.

Alami, Y., Achouk, W., Marol, C., and Heulin, T. (2000). Rhizosphere soil aggregation and plant growth promotion of sunflowers by an exopolysaccharide-producing *Rhizobium* sp. strain isolated from sunflower roots. *Appl. Environ. Microbiol*. 66, 3393–3398. doi: 10.1128/AEM.66.8.3393-3398.2000

Anderson, A. J., and Kim, Y. C. (2018). Biopesticides produced by plant-probiotic *Pseudomonas chlororaphis*isolates. *Crop Prot*. 105, 62–69. doi: 10.1016/j.cropro.2017.11.009

Ankati, S., and Podile, A. R. (2019). Metabolites in the root exudates of groundnut changes during interection with plant growth promoting rhizobacteria in a strain-specific manner. *J. Plant Physiol*. 24, 153057. doi: 10.1016/j.jplph.2019.153057

Arruda, L., Beneduzi, A., Martins, A., Lisboa, B., Lopes, C., and Bertolo, F. (2013). Screening of rhizobacteria from maize (*Zea mays* L.) in Rio Grande do Sul State (South Brazil) and analysis of their potential to improve plant growth. *Appl. Soil Ecol*. 63, 15–22. doi: 10.1016/j.apsoil.2012.09.001

Awasthi, R., Tewari, R., and Nayyar, H. (2011). Synergy between plants and P-solubilizing microbes in soils: effects on growth and physiology of crops. *Int. Res. J. Microbiol*. 2, 484–503.

Babalola, O. O. (2010). Ethylene quantification in three rhizobacterial isolates from Striga hermonthica-infested maize and sorghum Egypt. *J. Biol*. 12, 1–5.

Bacilio-Jimenez, M., Aguilar-Flores, S., Ventura-Zapata, E., Perez-Campos, E., Bouquelet, S., and Zenteno, E. (2003). Chemical characterization of root exudates from rice (*Oryza sativa*) and their effects on the chemotactic response of endophytic bacteria. *Plant Soil* 249, 271–277. doi: 10.1023/A:1022888900465

Badr, M. A., Shafei, A. M., and Sharaf El-Deen, S. H. (2006). The dissolution of K and P-bearing minerals by silicate dissolving bacteria and their effect on sorghum growth. *Res. J. Agri. Biol. Sci*. 2, 5–11.

Badri, D. V., Chaparro, J. M., Zhang, R., Shen, Q., and Vivanco, J. M. (2013). Application of natural blends of phytochemicals derived from the root exudates of *Arabidopsis* to the soil reveal that phenolic-related compounds predominantly modulate the soil microbiome. *J. Biol. Chem*. 288, 4502–4512. doi: 10.1074/jbc.M112.433300

Badri, D. V., Quintana, N., El Kassis, E. G., Kim, H. K., Choi, Y. H., Sugiyama, A., et al. (2009). An ABC transporter mutation alters root exudation of

phytochemicals that provoke an overhaul of natural soil microbiota. *Plant Physiol*. 151, 2006–2017. doi: 10.1104/pp.109.147462

Badri, D. V., and Vivanco, J. M. (2009). Regulation and function of root exudates. *Plant Cell Environ*. 32, 666–681. doi: 10.1111/j.1365-3040.2009.01926.x

Baetz, U., and Martinoia, E. (2014). Root exudates: the hidden part of plant defense. *Trends Plant Sci*. 2, 90–98. doi: 10.1016/j.tplants.2013.11.006

Bagyalakshmi, B., Ponmurugan, P., and Balamurugan, A. (2012). Impact of different temperature, carbon and nitrogen sources on solubilization efficiency of native potassium solubilizing bacteria from tea (*Camellia sinensis*). *J. Biol. Res* 3, 36–42.

Baker, K. F., and Cook, R. J. (1974). *Biological Control of Plant Pathogens*. San Fransisco, CA: Freeman and Company.

Bakhshandeh, E., Pirdashti, H., and Lendeh, K. S. (2017). Phosphate and potassium-solubilizing bacteria effect on the growth of rice. *Ecol. Eng*. 103, 164–169. doi: 10.1016/j.ecoleng.2017.03.008

Barriuso, J., Solano, B. R., Fray, R. G., Camara, M., Hartmann, A., and Gutierrez, M. F. J. (2008). Transgenic tomato plants alter quorum sensing in plant growth-promoting rhizobacteria. *Plant Biotechnol*. 6, 442–452. doi: 10.1111/j.1467-7652.2008.00331.x

Bashir, S., Iqbal, A., Hasnain, S., and White, J. F. (2021). Screening of sunfower associated bacteria as biocontrol agents for plant growth promotion. *Arch. Microbiol*. 203, 4901–4912. doi: 10.1007/s00203-021-02463-8

Berg, G., and Smalla, K. (2009). Plant species and soil type cooperatively shape the structure and function of microbial communities in the rhizosphere. *FEMS Microbiol. Ecol*. 68, 1–13. doi: 10.1111/j.1574-6941.2009.00654.x

Bhaskar, P. V., and Bhosle, N. B. (2005). Microbial extracellular polymeric substances in marine biogeochemical processes. *Curr. Sci*. 88, 45–53.

Bhattacharya, S., Bachani, P., Jain, D., Patidar, S. K., and Mishra, S. (2016). Extraction of potassium from K-feldspar through potassium solubilization in the halophilic acinetobacter soli (MTCC 5918) isolated from the experimental salt farm. *Int. J. Min. Proc*. 152, 53–57. doi: 10.1016/j.minpro.2016.05.003

Bhattacharyya, P. N., and Jha, D. K. (2012). Plant growth-promoting rhizobacteria (PGPR): emergence in agriculture. *World J. Microbiol. Biotechnol*. 28, 1327–1350. doi: 10.1007/s11274-011-0979-9

Bhojiya, A. A., Joshi, H., Upadhyay, S. K., Srivastava, A. K., Pathak, V. V., Pandey, V. C., et al. (2021). Screening and optimization of zinc removal potential in *Pseudomonas aeruginosa*-HMR1 and its plant growth-promoting attributes. *Bull. Environ. Contam. Toxicol*. 108, 468–477. doi: 10.1007/s00128-021-03232-5

Blom, J., Rueckert, C., Niu, B., Wang, Q., and Borriss, R. (2012). The complete genome of *Bacillus amyloliquefaciens* sub sp. *plantarum* CAU B946 contains a gene cluster for non ribosomal synthesis of iturin A. *J. Bacteriol*. 194, 1845–1846. doi: 10.1128/JB.06762-11

Bonkowski, M., Villenave, C., and Griffiths, B. (2009). Rhizosphere fauna: the functional and structural diversity of intimate interactions of soil fauna with plant roots. *Plant Soil*. 321, 213–233. doi: 10.1007/s11104-009-0013-2

Bonsall, R. F., Weller, D. M., and Thomashow, L. S. (1997). Quantification of 2,4-diacetylphloroglucinol produced by fluorescent *Pseudomonas* spp. *in vitro* and in the rhizosphere of wheat. *Appl. Environ. Microbiol*. 63, 951–955. doi: 10.1128/aem.63.3.951-955.1997

Borisjuk, N. V., Borisjuk, L. G., Logendra, S., Petersen, F., Gleba, Y., and Raskin, I. (1999). Production of recombinant proteins in plant root exudates. *Nat. Biotechnol*. 17, 466–469. doi: 10.1038/8643

Borriss, R. (2011). "Use of plant-associated Bacillus strains as biofertilizers and biocontrol agents in agriculture," in *Bacteria in Agrobiology: Plant Growth Responces*, ed D. K. Maheshwari (Berlin: Springer), 41–76. doi: 10.1007/978-3-642-20332-9_3

Bowya, T., and Balachandar, D. (2020). Rhizosphere engineering through exogenous growth-regulating small molecules improves the colonizing efficiency of a plant growth-promoting rhizobacterium in rice. *3 Biotech* 10, 277. doi: 10.1007/s13205-020-02275-5

Braud, A., Jezequel, K., Bazot, S., and Lebeau, T. (2009). Enhanced phytoextraction of an agricultural Cr-, Hg- and Pb-contaminated soil by bio-augmentation with siderophore producing bacteria. *Chemosphere* 74, 280–286. doi: 10.1016/j.chemosphere.2008.09.013

Cai, T., Cai, W., Zhang, J., Zheng, H., Tsou, A. M., Xiao, L., et al. (2009). Host legume-exuded antimetabolites optimize the symbiotic rhizosphere. *Mol. Microbiol*. 73, 507–517. doi: 10.1111/j.1365-2958.2009.06790.x

Cakmakci, R., Kantar, F., and Sahin, F. (2001). Effect of N2-fixing bacterial inoculations on yield of sugar beet and barley. *J. Plant Nutr. Soil Sci*. 164, 527–531. doi: 10.1002/1522-2624(200110)164:5<527::AID-JPLN527>3.0.CO;2-1

Canellas, L. P., and Olivares, F. L. (2017). Production of border cells and colonization of maize root tips by *Herbaspirillumseropedicae* are modulated by humic acid. *Plant Soil*. 417, 403–413. doi: 10.1007/s11104-017-3267-0

Cannesan, M. A., Durand, C., Burel, C., Gangneux, C., Lerouge, P., Ishii, T., et al. (2012). Effect of arabinogalactan proteins from the root caps of pea and *Brassica napus* on *Aphanomyces euteiches* zoospore chemotaxis and germination. *Plant Physiol*. 159, 1658–1670. doi: 10.1104/pp.112.198507

Catellani, M., Lico, C., Cerasi, M., Massa, S., Bromuro, C., Torosantucci, A., et al. (2020). Optimised production of an anti-fungal antibody in Solanaceae hairy roots to develop new formulations against *Candida albicans*. *BMC Biotechnol*. 20, 15. doi: 10.1186/s12896-020-00607-0

Cesari, A., Paulucci, N., Lopez-Gomez, M., Hidalgo-Castellanos, J., Pla, C. L., and Dardanelli, M. S. (2019). Restrictive water condition modifies the root exudates composition during peanut-PGPR interaction and conditions early events, reversing the negative effects on plant growth Plant. *Physiol. Biochem*. 142, 519–527. doi: 10.1016/j.plaphy.2019.08.015

Chamam, A., Sanguin, H., Belllvert, F., Meiffren, G., Comte, G., Wisniewski-Dye, F., et al. (2013). Plant secondary metabolite profiling evidences strain-dependent effect in the *Azospirillum- Oryza sativa* association. *Phytochemistry* 87, 65–77. doi: 10.1016/j.phytochem.2012.11.009

Chandler, D., Davidson, G., Grant, W. P., Greaves, J., and Tatchell, G. M. (2008). Microbial biopesticides for integrated crop management: an assessment of environmental and regulatory sustainability. *Trends Food Sci. Tech*. 19, 275–283. doi: 10.1016/j.tifs.2007.12.009

Chaturvedi, H., Singh, V., and Gupta, G. (2016). Potential of bacterial endophytes as plant growth promoting factors. *J. Plant Pathol. Microbiol*. 7, 1–6. doi: 10.4172/2157-7471.1000376

Chelius, M. K., and Triplett, E. W. (2001). The diversity of archaea and bacteria in association with the roots of *Zea mays* L. *Microb. Ecol*. 3, 252–263. doi: 10.1007/s002480000087

Chen, C., Li, Z., Li, S., Deng, N., and Mei, P. (2020). Effects of root exudates on the activation and remediation of cadmium ion in contaminated soils. *Environ. Sci. Pollut. Res. Int*. 27, 2926–2934. doi: 10.1007/s11356-019-07263-8

Chen, S., Waghmode, T. R., Sun, R., Kuramae, E. E., Hu, C., and Liu, B. (2019). Root-associated microbiomes of wheat under the combined effect of plant development and nitrogen fertilization. *Microbiome* 7, 136. doi: 10.1186/s40168-019-0750-2

Chen, X. H., Koumoutsi, A., Scholz, R., Eisenreich, A., Schneider, K., Heinemeyer, I., et al. (2007). Comparative analysis of the complete genome sequence of the plant growth-promoting bacterium *Bacillus amyloliquefaciens* FZB42. *Nat. Biotechnol*. 25, 1007–1014. doi: 10.1038/nbt1325

Chen, Y. P., Rekha, P. D., Arunshen, A. B., Lai, W. A., and Young, C. C. (2006). Phosphate solubilizing bacteria from subtropical soil and their tricalcium phosphate solubilizing abilities. *Appl. Soil Ecol*. 34, 33–41. doi: 10.1016/j.apsoil.2005.12.002

Cheng, Q. (2008). Perspectives in biological nitrogen fixation research. *J. Integr. Plant Biol*. 50, 786–798. doi: 10.1111/j.1744-7909.2008.00700.x

Chin-A-Woeng, T. F., Bloemberg, G. V., and Lugtenberg, B. J. (2003). Phenazines and their role in biocontrol by *Pseudomonas* bacteria. *New Phytol*. 157, 503–523. doi: 10.1046/j.1469-8137.2003.00686.x

Cho, S. M., Kim, Y. H., Anderson, A. J., and Kim, Y. C. (2013). Nitric oxide and hydrogen peroxide production are involved in systemic drought tolerance induced by 2R, 3R-butanediol in *Arabidopsis thaliana*. *Plant Pathol*. 29, 427–434. doi: 10.5423/PPJ.OA.07.2013.0069

Chowdhury, S. P., Hartmann, A., Gao, X., and Borriss, R. (2015). Biocontrol mechanism by root-associated *Bacillus* amyloliquefaciens FZB42 – a review. *Front. Microbiol*. 6, 780. doi: 10.3389/fmicb.2015.00780

Combes-Meynet, E., Potheir, J., Moenne-Loccoz, Y., and Prigent-Combaret, C. (2011). The pseudomonas secondary metabolite 2, 4-diacetylphloroglucinol is a signal inducing rhizoplane expression of azospirillum genes involve in plant-growth promotion. *Mol. Plant Microbe Interact*. 24, 271–284. doi: 10.1094/MPMI-07-10-0148

Compant, S., Samad, A., Faist, H., and Sessitsch, A. (2019). A review on the plant microbiome: ecology, functions, and emerging trends in microbial application. *J. Adv. Res*. 19, 29–37. doi: 10.1016/j.jare.2019.03.004

Coronado, C., Zuanazzi, J. A. S., Sallaud, C., Quirion, J. C., Esnault, R., Husson, H. P., et al. (1995). Alfalfa root flavonoid production 1s nitrogen regulated. *Plant Physiol*. 108, 533–542. doi: 10.1104/pp.108.2.533

Cortleven, A., and Schmülling, T. (2015). Regulation of chloroplast development and function by cytokinin. *J. Exp. Bot*. 66, 4999–5013. doi: 10.1093/jxb/erv132

Costacurta, A., and Vanderleyden, J. (1995). Synthesis of phytohormones by plant associated bacteria. *Crit. Rev. Microbiol*. 2, 1–18. doi: 10.3109/10408419509113531

Creus, M. C., Graziano, M., Casanovas, E. M., Pereyra, M. A., Simontacchi, M., Puntarulo, S., et al. (2005). Nitric oxide is involved in the *Azospirillum brasilense*-induced lateral root formation in tomato. *Planta* 221, 297–303. doi: 10.1007/s00425-005-1523-7

De-la-Pena, C., Lei, Z., Watson, B. S., Sumner, L. W., and Vivanco, J. M. (2008). Root-microbe communication through protein secretion. *J. Biol. Chem*. 283, 25247–25255. doi: 10.1074/jbc.M.801967200

DESA UN (2015). *World Population Prospects: The 2015 Revision, Key Findings and Advance Tables. Working Paper No ESA/P/WP,* 241. New York, NY: United Nations, Department of Economic and Social Affairs, Population Division.

Devi, K. K., Seth, N., Kothamasi, S., and Kothamasi, D. (2007). Hydrogen cyanide producing rhizobacteria killsubterranean termite *Odontotermesobesus*(Rambur) by cyanide poisoning under in Vitroconditions. *Curr. Microbiol*. 54, 74–78. doi: 10.1007/s00284-006-0473-z

D'Haeze, W., Gao, M., De, R., Rycke, Van, M., Montagu, E. G., and Holsters, M. (1998). Roles for azorhizobial nod factors and surface polysaccharides in intercellular invasion and nodule penetration, respectively. *Mol. Plant Microbe Interact*. 11, 999–1008. doi: 10.1094/MPMI.1998.11.10.999

Donn, S., Kirkegaard, J. A., Perera, G., Richardson, A. E., and Watt, M. (2015). Evolution of bacterial communities in the wheat crop rhizosphere. *Environ. Microbiol*. 17, 610–621. doi: 10.1111/1462-2920.12452

Drake, P. M. W., Barbi, T., Sexton, A., McGowan, E., Stadlmann, J., Navarre, C., et al. (2009). Development of rhizo secretion as a production system for recombinant proteins from hydroponic cultivated tobacco. *FASEB J*. 23: 3581–3589. doi: 10.1096/fj.09-131771

Dubey, R. C., Khare, S., Kumar, P., and Maheshwari, D. K. (2014). Combined effect of chemical fertilisers and rhizosphere-competent *Bacillus subtilis* BSK17 on yield of *Cicer arietinum*. *Arch. Phytopathol. Plant Protect*. 47, 2305–2318. doi: 10.1080/03235408.2013.876744

Duffy, B. (2003). Pathogen self-defense: mechanisms to counteract microbial antagonism. *Annu. Rev. Phytopathol*. 41, 501–538. doi: 10.1146/annurev.phyto.41.052002.095606

Dwivedi, P., and Dwivedi, S. K. (2002). "Biopesticidal management of plant diseases," in *Microbial Diversity: Status and Potential*, eds S. C. Tiwari, and G. D. Sharma (Guwahati: Scientific Book Publishers), 220–235.

Dwivedi, P., and Dwivedi, S. K. (2004). "Nitrogen fixation and biofertilizers," in *Environmental Microbiology and Biotechnology*, eds D. P. Singh, and S. K. Dwivedi (New Delhi: New Age International Pvt Ltd), 126–148.

Edwards, J., Johnson, C., Santos-Medellin, C., Lurie, E., Podishetty, N. K., Bhatnagar, S., et al. (2015). Structure, variation, and assembly of the root-associated microbiomes of rice. *Proc. Natl. Acad. Sci. U.S.A*. 112, 911–920. doi: 10.1073/pnas.1414592112

Essen, S. A., Johnsson, A., Bylund, D., Pedersen, K., and Lundstrom, U. S. (2007). Siderophore production by *Pseudomonas stutzeri* under aerobic and anaerobic conditions. *Appl. Environ. Microbiol*. 73, 5857–5864. doi: 10.1128/AEM.00072-07

Etesami, H., Emami, S., and Alikhani, H. A. (2017). Potassium solubilizing bacteria (KSB): mechanisms, promotion of plant growth, and future prospects - a review. *J. Soil Sci. Plant Nutr*. 17, 897–911. doi: 10.4067/S0718-95162017000400005

Exposito, R. G., de Bruijn, I., Postma, J., and Raaijmakers, J. M. (2017). Current insight into the role of rhizospheric bacteria in disease suppressive soil. *Front. Microbiol*. 8, 2529. doi: 10.3389/fmicb.2017.02529

Fang, W., and St Leger, R. J. (2010). Mrt a gene unique to fungi, encodes an oligosaccharide transporter and facilitates rhizosphere competency in *Metarhiziumrobertsii*. *Plant Physiol*. 154,1549–1557. doi: 10.1104/pp.110.163014

Fernández, C., Novo, R., Microbiana, V., and Suelo, E. (1988). II. La habana: Editorial Puebloy Educación fibroblasts. *Life Sci*. 52, 1909–1915.

Fusconi, R., and Godinho, M. J. L. (2002). Screening for exopolysaccharide producing bacteria from sub- tropical polluted groundwater. *Braz. J. Biol*. 62, 363–369. doi: 10.1590/S1519-69842002000200020

Gaby, J. C., and Buckley, D. H. (2012). A comprehensive evaluation of PCR primers to amplify the *nif* H gene of nitrogenase. *PLoS ONE* 7, e42149. doi: 10.1371/journal.pone.0042149

Garbeva, P., van Veen, J. A., and Elas, J. D. (2004). Assessment of the diversity, and antagonism towards *Rhizoctonia solani* AG3, of *Pseudomonas* species in soil from different agricultural regimes. *FEMS Microbiol. Ecol*. 47, 51–64. doi: 10.1016/S0168-6496(03)00234-4

Gaume, A., Komarnytsky, S., Borisjuk, N., and Raskin, I. (2003). Rhizosecretion of recombinant proteins from plant hairy roots. *Plant Cell Rep*. 21,1188–1193. doi: 10.1007/s00299-003-0660-3

Ghosh, P. K., Saha, P., Mayilraj, S., and Maiti, T. K. (2013). Role of IAA metabolizing enzymes on production of IAA in root, nodule of *Cajanus cajan*and its PGP *Rhizobium* sp. *Biocatal. Agric. Biotechnol*. 2, 234–239. doi: 10.1016/j.bcab.2013.04.002

Gleba, D., Borisjuk, N. V., Borisjuk, L. G., Kneer, R., Poulev, A., Skarzhinskaya, M., et al. (1999). Use of plant roots for phytoremediation and molecular farming. *Proc. Natl. Acad. Sci. U.S.A*. 96, 5973–5977. doi: 10.1073/pnas.96.11.5973

Glick, B. R. (2012). Plant growth-promoting bacteria: mechanisms and applications. *Scientifica* 12, 1–15. doi: 10.6064/2012/963401

Glick, B. R., Todorovic, B., Czarny, J., Cheng, Z., and Duan, J. (2007). Promotion of plant growth by bacterial ACC deaminase. *Crit. Rev. Plant Sci*. 26, 227–242. doi: 10.1080/07352680701572966

Goh, C. H., Veliz, V. D. F., Nicotra, A. B., and Mathesius, U. (2013). The impact of beneficial plant-associated microbes on plant phenotypic plasticity. *J. Chem. Ecol*. 7, 826–839. doi: 10.1007/s10886-013-0326-8

Goldstein, A. H., and Krishnaraj, P. U. (2007). "Phosphate solubilizing microorganisms vs. phosphate mobilizing microorganisms: what separates a phenotype from a trait?" in *First International Meeting on Microbial Phosphate Solubilization*, eds E. Velazquez, and C. Rodriguez-Barrueco (Dordrecht: Springer), 203–213. doi: 10.1007/978-1-4020-5765-6_31

Gouzou, L., Burtin, R., Philippy, R., Bartoli, F., and Heulin, T. (1993). Effect of inoculation with bacillus polymyxa on soil aggregation in the wheat rhizosphere: preliminary examination. *Geoderma* 56, 479–491. doi: 10.1016/0016-7061(93)90128-8

Gravel, V., Antoun, H., and Tweddell, R. J. (2007). Growth stimulation and fruit yield improvement of greenhouse tomato plants by inoculation with *Pseudomonas putida* or *Trichoderma atroviride*: Possible role of indole acetic acid (IAA) soil. *Biol. Biochem*. 39, 1968–1977. doi: 10.1016/j.soilbio.2007.02.015

Gundala, P. B., Chinthala, P., and Sreenivasulu, B. (2013). A new facultative alkaliphilic, potassium solubilizing, *Bacillus* Sp. SVUNM9 isolated from mica cores of Nellore District, Andhra Pradesh, India. *Res. Rev. J. Microbiol. Biotechnol*. 2, 1–7.

Gupta, V., Kumar, G. N., and Buch, A. (2020). Colonization by multi-potential *Pseudomonas aeruginosa* P4 stimulates (*Arachis hypogaea* L.) growth, defence physiology and root system functioning to benefit the root-rhizobacterial interface. *J. Plant Physiol*. 248, 153144. doi: 10.1016/j.jplph.2020.153144

Haas, D., and Defago, G. (2005). Biological control of soil-borne pathogens by *fluorescent pseudomonads*. *Nat. Rev. Microbiol*. 3, 307–319. doi: 10.1038/nrmicro1129

Haldar, S., and Sengupta, S. (2015). Plant-microbe cross-talk in the rhizosphere: insight and biotechnological potential. *Open Microbiol. J*. 9, 1–7. doi: 10.2174/1874285801509010001

Hao, K., He, P., Blom, J., Rueckert, C., Mao, Z., Wu, Y., et al. (2012). The genome of plant growth-promoting *Bacillus amyloliquefaciens* sub sp. plantarum strain YAU B9601-Y2 contains a gene cluster for mersacidin synthesis. *J. Bacteriol*. 194, 3264–3265. doi: 10.1128/JB.00545-12

Harman, G. E., Howell, C. R., Viterbo, A., Chet, I., and Lorito, M. (2004). Trichoderma species-opportunistic, avirulent plant symbionts. *Nat. Rev. Microbiol*. 2, 43–56. doi: 10.1038/nrmicro797

Hartmann, A., Rothballer, M., Schmid, M., and Lorenz, H. (2008). A pioneer in rhizosphere microbial ecology and soil bacteriology research. *Plant Soil* 312, 7–14. doi: 10.1007/s11104-007-9514-z

Hartmann, A., Schmid, M., Tuinen, D., and Berg, G. (2009). Plant-driven selection of microbes. *Plant Soil* 321, 235–275. doi: 10.1007/s11104-008-9814-y

Hassan, M. K., McInroy, J. A., and Kloepper, J. W. (2019). The interactions of rhizodeposits with plant growth-promoting rhizobacteria in the rhizosphere: a review. *Agriculture* 9, 142. doi: 10.3390/agriculture9070142

Hernandez, M. E., Kappler, A., and Newman, D. K. (2004). Phenazines and other redox-active antibiotics promote microbial mineral reduction. *Appl. Environ. Microbiol*. 70, 921–928. doi: 10.1128/AEM.70.2.921-928.2004

Hider, R. C., and Kong, X. (2010). Chemistry and biology of siderophores. *Nat. Product Rep*. 27, 637–657. doi: 10.1039/b906679a

Hilda, R., and Fraga, R. (2000). Phosphate solubilizing bacteria and their role in plant growth promotion. *Biotech. Adv*. 17, 319–359.

Hill, D. S., Stein, J. I., Torkewitz, N. R., Morse, A. M., Howell, C. R., Pachlatko, J. P., et al. (1994). Cloning of genes involved in the synthesis of pyrrolnitrin from *Pseudomnas fluorescens* and role of pyrrolnitrin synthesis in biological control of plant disease. *Appl. Environ. Microbiol*. 60, 78–85. doi: 10.1128/aem.60.1.78-85.1994

Hu, L., Robert, C. A. M., Cadot, S., Zhang, X., M., Ye, Li, B., et al. (2018). Root exudate metabolites drive plant-soil feedbacks on growth and defense by shaping the rhizosphere microbiota. *Nat. Commun.* 9, 2738. doi: 10.1038/s41467-018-05122-7

Hu, X., Chen, J., and Guo, J. (2006). Two phosphate-and potassium-solubilizing bacteria isolated from Tianmu Mountain, Zhejiang, China. *World J. Microbiol. Biotechnol*. 22, 983–990. doi: 10.1007/s11274-006-9144-2

Idris, E. E. S., Bochow, H., Ross, H., and Borriss, R. (2004). Use of *Bacillus subtilis* as biocontrol agent. Phytohormone-like action of culture filtrates prepared from plant growth-promoting *Bacillus amyloliquefaciens* FZB24, FZB42, FZB45 and *Bacillus subtilis* FZB37. *J. Plant Dis. Prot*. 111, 583–597.

Jadhav, H. P., and Sayyed, R. Z. (2016). Hydrolytic enzymes of rhizospheric microbes in crop protection. *MOJ Cell Sci. Rep.* 3, 135–136. doi: 10.15406/mojcsr.2016.03.00070

Johri, B. N., Sharma, A., and Virdi, J. S. (2003). Rhizobacterial diversity in India and its in?uence on soil and plant health. *Adv. Biochem. Eng. Biotechnol*. 8, 49–89. doi: 10.1007/3-540-36488-9_2

Kamilova, F., Kravchenko, L. V., Shaposhnikov, A. I., Azarova, T., Makarova, N., and Lugtenberg, B. (2006b). Organic acids, sugars, and l-tryptophane in exudates of vegetables growing on stonewool and their effects on activities of rhizosphere. *Bacter. Mol. Plant Microbe Interact*. 19, 250–256. doi: 10.1094/MPMI-19-0250

Kamilova, F., Kravchenko, L. V., Shaposhnikov, A. I., Makarova, N., and Lugtenberg, B. (2006a). Effects of the tomato pathogen *Fusarium oxysporum* f. sp. *radicis-lycopersici* and of the biocontrol bacterium *Pseudomonas fluorescens* WCS365 on the composition of organic acids and sugars in tomato root exudates. *Mol. Plant Microbe Interact.* 19, 1121–1126. doi: 10.1094/MPMI-19-1121

Kang, B. G., Kim, W. T., Yun, H. S., and Chang, S. C. (2010). Use of plant growth-promoting rhizobacteria to control stress responses of plant roots. *Plant Biotechnol. Rep.* 4, 179–183. doi: 10.1007/s11816-010-0136-1

Kang, S. M., Khan, A. L., You, Y. H., Kim, J. G., Kamran, M., and Lee, I. J. (2014). Gibberellin production by newly isolated strain *Leifsonia soli* SE134 and its potential to promote plant growth. *J. Microbiol. Biotechnol*. 24,106–112. doi: 10.4014/jmb.1304.04015

Kawasaki, A., Donn, S., Ryan, P. R., Mathesius, U., Devilla, R., Jones, A., et al. (2016). Microbiome and exudates of the root and rhizosphere of *Brachypodiumdistachyon*, a model for wheat. *PLoS ONE* 11, e0164533. doi: 10.1371/journal.pone.0164533

Keller, L., and Surette, M. G. (2006). Communication in bacteria: an ecological and evolutionary perspective. *Nat. Rev. Microbiol*. 4, 249–258. doi: 10.1038/nrmicro1383

Keshavarz, Z. J., Aliasgharzad, N., Oustan, S., Emadi, M., and Ahmadi, A. (2013). Isolation and characterization of potassium solubilizing bacteria in some Iranian soils. *Arch. Agron. Soil Sci*. 59, 1713–1723. doi: 10.1080/03650340.2012.756977

Keswani, C., Singh, H. B., García-Estrada, C., Caradus, J., He, Y. W., Mezaache-Aichour, S., et al. (2020a). Antimicrobial secondary metabolites from agriculturally important bacteria as next-generation pesticides. *Appl. Microbiol. Biotechnol.* 104, 1013–1034. doi: 10.1007/s00253-019-10300-8

Keswani, C., Singh, S. P., Cueto, L., Garcia-Estrada, C., Mezaache-Aichour, S., Glare, T. R., et al. (2020b). Auxins of microbial origin and their use in agriculture. *Appl. Microbiol. Biotechnol.* 104, 8549–8565. doi: 10.1007/s00253-020-10890-8

Khan, M. S., Zaidi, A., Ahemad, M., Oves, M., and Wani, P. A. (2010). Plant growth promotion by phosphate solubilizing fungi-current perspective. *Arch. Agron. Soil Sci*. 56, 73–98. doi: 10.1080/03650340902806469

Khan, M. S., Zaidi, A., and Wani, P. A. (2007). Role of phosphate-solubilizing microorganisms in sustainable agriculture - a review. *Agron. Sustain. Dev*. 27, 29–43. doi: 10.1051/agro:2006011

Khiari, L., and Parent, L. E. (2005). Phosphorus transformations in acid light-textured soils treated with dry swine manure. *Can. J. Soil Sci*. 85, 75–87. doi: 10.4141/S03-049

Kloepper, J. W., Ryu, C. M., and Zhang, S. (2004). Induced systemic resistance and promotion of plant growth by *Bacillus* spp. *Phytopathology* 94, 1259–1266. doi: 10.1094/PHYTO.2004.94.11.1259

Korenblum, E., Donga, Y., Szymanski, J., Panda, S., Jozwiak, A., Massalha, H., et al. (2020). Rhizosphere microbiome mediates systemic root metabolite exudation by root-to-root signaling. *PNAS* 117, 3874–3883. doi: 10.1073/pnas.1912130117

Kosuge, T., and Sanger, M. (1987). Indole acetic acid, its synthesis and regulation: basis for tumorigen city in plant disease. *Recent. Adv. Phytochem*. 20, 147–161. doi: 10.1007/978-1-4684-8056-6_6

Krause, M. S., De Ceuster, T. J. J., Tiquia, S. M., Michel, J.r, F., C., Madden, L. V., et al. (2003). Isolation and characterization of rhizobacteria from composts that suppress the severity of bacterial leaf spot of radish. *Phytopathology* 93, 1292–1300. doi: 10.1094/PHYTO.2003.93.10.1292

Kucey, R. M. N., Janzen, H. H., and Legget, M. E. (1989). Microbial mediated increases in plant available phosphorus. *Adv. Agron*. 42, 199–228. doi: 10.1016/S0065-2113(08)60525-8

Ladygina, N., and Hedlund, K. (2010). Plant species influence microbial diversity and carbon allocation in the rhizosphere. *Soil Biol. Biochem*. 42, 162–168. doi: 10.1016/j.soilbio.2009.10.009

Lee, K. E., Radhakrishnan, R., Kang, S. M., You, Y. H., Joo, G. J., Lee, I. J., et al. (2015). *Enterococcus faecium* LKE12 cell-free extract accelerates host plant growth via gibberellin and indole-3-acetic acid secretion. *J. Microbiol. Biotechnol*. 25, 1467–1475. doi: 10.4014/jmb.1502.02011

Lee, Y. H., Foster, J., Chen, J., Voll, L. M., Weber, A. P. M., and Tegeder, M. (2007). App1 transports uncharged amino acids into roots of arabidopsis. *Plant J*. 50, 305–319. doi: 10.1111/j.1365-313X.2007.03045.x

Ling, N., Zhang, W., Wang, D., Mao, J., Huang, Q., Guo, S., et al. (2013). Root exudates from grafted-root watermelon showed a certain contribution in inhibiting *Fusarium oxysporum* f. sp. niveum. *PLoS ONE* 8, e63383. doi: 10.1371/journal.pone.0063383

Liu, D., Lian, B., and Dong, H. (2012). Isolation of *Paenibacillus* sp. and assessment of its potential for enhancing mineral weathering. *Geomicrobiol J*. 29, 413–421. doi: 10.1080/01490451.2011.576602

Liu, K., Newman, M., McInroy, J. A., Hu, C. H., and Kloepper, J. W. (2017). Selection and assessment of plant growth-promoting rhizobacteria (PGPR) for biological control of multiple plant diseases. *Phytopathology* 107, 928–936. doi: 10.1094/PHYTO-02-17-0051-R

Liu, W., Hou, J., Wang, Q., Yang, H., Luo, Y., and Christi, P. (2015). Collection and analysis of root exudates of *Festuca arundinacea* L. and their role in facilitating the phytoremediation of petroleum-contaminated soil. *Plant Soil*. 389, 109–119. doi: 10.1007/s11104-014-2345-9

Liu, Y., Zhang, N., Qiu, M., Feng, H., Vivanco, J. M., Shen, Q., et al. (2014). Enhanced rhizosphere colonization of beneficial *Bacillus amyloliquefaciens* SQR9 by pathogen infection. *FEMS Microbiol. Lett*. 353, 49–56. doi: 10.1111/1574-6968.12406

Lonoce, C., Salem, R., Marusic, C., Jutras, P. V., Scaloni, A., Salzano, A. M., et al. (2016). Production of a tumour-targeting antibody with a human-compatible glycosylation profile in *N. benthamiana* hairy root cultures. *Biotechnol. J.* 11, 1209–1220. doi: 10.1002/biot.201500628

Lu, H., Sun, J., and Zhu, L. (2017). The role of artificial root exudate components in facilitating the degradation of pyrene in soil. *Sci. Rep*. 7, 7130. doi: 10.1038/s41598-017-07413-3

Lynn, T. M., Win, H. S., Kyaw, E. P., Latt, Z. K., and Yu, S. S. (2013). Characterization of phosphate solubilizing and potassium decomposing strains and study on their effects on tomato cultivation. *Int. J. Innov. Appl. Stud.* 3, 959–966.

Ma, Y., Rajkumar, M., Zhang, C., and Freitas, H. (2016). Beneficial role of bacterial endophytes in heavy metal phytoremediation. *J. Environ. Manage.* 174, 14–25. doi: 10.1016/j.jenvman.2016.02.047

Madeira, L. M., Szeto, T. H., Henquet, M., Raven, N., Runions, J., Huddleston, J., et al. (2016). High-yield production of a human monoclonal IgG by rhizosecretion in hydroponic tobacco cultures. *Plant Biotechnol J.* 14, 615–624. doi: 10.1111/pbi.12407

Mahmud, A. A., Upadhyay, S. K., Srivastava, A. K., and Bhojiya, A. A. (2021). Biofertilizers: a nexus between soil fertility and crop productivity under abiotic stress. *Curr. Res. Environ. Sust.* 3, 100063. doi: 10.1016/j.crsust.2021.100063

Maksimov, I. V., Abizgildina, R. R., and Pusenkova, L. I. (2011). Plant growth promoting rhizobacteria as alternative to chemical crop protectors from pathogens (review). *Appl. Biochem. Microbiol.* 47, 333–345. doi: 10.1134/S0003683811040090

Mark, G. L., Dow, J. M., Kiely, P. D., Higgins, H., Haynes, J., Baysse, C., et al. (2005). Transcriptome profiling of bacterial responses to root exudates identifies genes involved in microbe-plant interactions. *Proc. Natl. Acad. Sci. U.S.A.* 102, 17454–17459. doi: 10.1073/pnas.0506407102

Marketon, M. M., Gronquist, M. R., Eberhard, A., and Gonzalez, J. E. (2002). Characterization of the *Sinorhizobiummelilotis*inR/sinI locus and the production of novel N-Acyl homoserine lactones. *J. Bacteriol.* 184, 5686–5695. doi: 10.1128/JB.184.20.5686-5695.2002

Martinez, C., Espinosa-Ruiz, A., and Prat, S. (2016). Gibberellins and plant vegetative growth. *Ann. Plant Rev.* 49, 285–322. doi: 10.1002/9781119210436.ch10

Matilla, M. A., Espinosa-Urgel, M., Rodriguez-Herva, J. J., Ramos, J. L., and Ramos-Gonzalez, M. L. (2007). Genomic analysis reveals the major driving forces of bacterial life in the rhizosphere. *Genome Biol.* 8, 179. doi: 10.1186/gb-2007-8-9-r179

Meena, V. S., Maurya, B. R., and Verma, J. P. (2014). Does a rhizospheric microorganism enhance K^+ availability in agricultural soils. *Microbiol. Res.* 169, 337–347. doi: 10.1016/j.micres.2013.09.003

Mendes, R., Garbeva, P., and Raaijmakers, J. M. (2013). The rhizosphere microbiome: significance of plant beneficial, plant pathogenic, and human pathogenic microorganisms. *FEMS Microbiol. Rev.* 37, 634–663. doi: 10.1111/1574-6976.12028

Menendez, E., and Garcia-Fraile, P. (2017). Plant probiotic bacteria: solutions to feed the world. *AIMS Microbiol.* 3, 502–524. doi: 10.3934/microbiol.2017.3.502

Mohammed, A. F. (2018). Effectiveness of exopolysaccharides and biofilm forming plant growth promoting rhizobacteria on salinity tolerance of faba bean (*Vicia faba* L.). *Afr. J. Microbiol. Res.* 12, 399–404. doi: 10.5897/AJMR2018.8822

Molina-Favero, C., Creus, C. M., Simontacchi, M., Puntarulo, S., and Lamattina, L. (2008). Aerobic nitric oxide production by *Azospirillumbrasilense* Sp245 and its influence on root architecture in tomato. *Mol. Plant Microbe Interact.* 21, 1001–1009. doi: 10.1094/MPMI-21-7-1001

Montanez, A., Abreu, C., Gill, P. R., Hardarson, G., and Sicardi, M. (2009). Biological nitrogen fixation in maize (*Zea mays* L.) by N-15 isotope-dilution and identification of associated culturable diazotrophs. *Biol. Fert. Soil* 45, 253–263. doi: 10.1007/s00374-008-0322-2

Morrison, S. M., and Askeland, R. A. (1983). Cyanide production by *Pseudomonas fluorescens* and *Pseudomonas aeruginosa*. *Appl. Environ. Microbiol.* 45, 1802–1807. doi: 10.1128/aem.45.6.1802-1807.1983

Mullen, M. D. (2005). "Phosphorus in soils: biological interactions," in *Encyclopedia of Soils in the Environment*, eds D. Hillel, C. Rosenzweig, D. Powlson, K. Scow, M. Singer, and D. Sparks (Oxford: Academic Press, Elsevier, Ltd), 210–215. doi: 10.1016/B0-12-348530-4/00161-2

Myresiotis, C. K., Vryzas, Z., and Papadopoulou-Mourkidou, E. (2015). Effect of specific plant-growth-promoting rhizobacteria (PGPR) on growth and uptake of neonicotinoid insecticide thiamethoxam in corn (*Zea mays* L.) seedlings. *Pest Manag. Sci.* 71, 1258–1266. doi: 10.1002/ps.3919

Nahas, E. (1996). Factors determining rock phosphate solubilization by microorganism isolated from soil. *World J. Microb. Biotechnol.* 12, 18–23. doi: 10.1007/BF00327716

Narasimhan, K., Basheer, C., Bajic, V. B., and Swarup, S. (2003). Enhancement of plant-microbe interactions using a rhizosphere metabolomics-driven approach and its application in the removal of polychlorinated biphenyls. *Plant Physiol.* 132, 146–153. doi: 10.1104/pp.102.016295

Neal, A. L., Ahmad, S., Gordon-Weeks, R., and Ton, J. (2012). Benzoxazinoids in root exudates of maize attract *Pseudomonas putida* to the rhizosphere. *PLoS ONE* 7, e35498. doi: 10.1371/journal.pone.0035498

Neilands, J. B. (1995). Siderophores: structure and function of microbial iron transport compounds. *J. Biol. Chem.* 270, 26723–26726. doi: 10.1074/jbc.270.45.26723

Nghia, N. K., Tien, T. T., Oanh, N. K., and Nuong, N. K. (2017). Isolation and characterization of indole acetic acid producing halophilic bacteria from salt affected soil of Rice-Shrimp farming system in the Mekong Delta, Vietnam. *Agric. For. Fish.* 6, 69–77. doi: 10.11648/j.aff.20170603.11

Ngoma, L., Babalola, O. O., and Ahmad, F. (2012). Ecophysiology of plant growth promoting bacteria. *Sci. Res. Essays* 7, 4003–4013. doi: 10.5897/SRE12.646

Nguema-Ona, E., Vicre-Gibouin, M., Cannesan, M. A., and Driouich, A. (2013). Arabinogalactan proteins in root-microbe interactions. *Trends Plant Sci.* 18, 440–449. doi: 10.1016/j.tplants.2013.03.006

Nievas, F., Bogino, P., Sorroche, F., and Giordano, W. (2012). Detection, characterization, and biological effect of quorum-sensing signaling molecules in peanut-nodulating bradyrhizobia. *Sensors* 12, 2851–2873. doi: 10.3390/s120302851

Numana, M., Bashir, S., Khan, Y., Mumtaz, R., Shinwari, Z. K., Khan, A. L., et al. (2018). Plant growth promoting bacteria as an alternative strategy for salt tolerance in plants: a review. *Microbiol. Res.* 209, 21–32. doi: 10.1016/j.micres.2018.02.003

Oberhansli, T., Defago, G., and Haas, D. (1991). Indole-3-acetic acid (IAA) synthesis in the biocontrol strain CHAO of *Pseudomonas fluorescens*: role of tryptophan side chain oxidase. *J. Gen. Microbiol.* 137, 2273–2279. doi: 10.1099/00221287-137-10-2273

O'Brien, J. A., and Benkova, E. (2013). Cytokinin cross-talking during biotic and abiotic stress responses. *Front. Plant Sci.* 4, 451. doi: 10.3389/fpls.2013.00451

Pal, S. S. (1998). Interaction of an acid tolerant strain of phosphate solubilizing bacteria with a few acid tolerant crops. *Plant Soil* 198, 169–177. doi: 10.1023/A:1004318814385

Patten, C. L., and Glick, B. R. (1996). Bacterial biosynthesis of indole-3-acetic acid. *Can. J. Microbiol.* 42, 207–220. doi: 10.1139/m96-032

Paul, S., Singh, V., Chauhan, P. K., Srivastava, A. K., and Upadhyay, S. K. (2020). Assessment of carrot growth performance with inoculation of AsT-PGPR under arsenic infested zone. *G J. Environ. Sci. Technol.* 7, 78–84.

Piromyou, P., Buranabanyat, B., Tantasawat, P., Tittabutr, P., Boonkerd, N., and Teaumroong, N. (2011). Effect of plant growth promoting rhizobacteria (PGPR) inoculation on microbial community structure in rhizosphere of forage corn cultivated in Thailand. *Eur. J. Soil Biol.* 47, 44–54. doi: 10.1016/j.ejsobi.2010.11.004

Plackett, A. R. G., and Wilson, Z. A. (2016). Gibberellins and plant reproduction. *Ann. Plant Rev.* 49, 323–358. doi: 10.1002/9781119210436.ch11

Pliego, C., Kamilova, F., and Lugtenberg, B. (2011). "Plant growth-promoting bacteria: fundamentals and exploitation," in *Bacteria in Agrobiology: Crop Ecosystems*, ed D. K. Maheshwari (Berlin: Springer-Verlag), 295–343. doi: 10.1007/978-3-642-18357-7_11

Prathap, M., and Ranjitha, K. B. D. (2015). A critical review on plant growth promoting rhizobacteria. *J. Plant Pathol. Microbiol.* 6, 1–4. doi: 10.4172/2157-7471.1000266

Rajkumar, M., Ae, N., Prasad, M. N. V., and Freitas,. H. (2010). Potential of siderophore-producing bacteria for improving heavy metal phytoextraction. *Trends Biotechnol.* 28, 142–149. doi: 10.1016/j.tibtech.2009.12.002

Ramachandran, V. K., East, A. K., Karunakaran, R., Downie, J. A., and Poole, P. S. (2011). Adaptation of *Rhizobium leguminosarum* to pea, alfalfa and sugar beet rhizospheres investigated by comparative transcriptomics. *Genome Biol.* 12, R106. doi: 10.1186/gb-2011-12-10-r106

Ramirez, L. E. F., and Mellado, J. C. (2005). "Bacterial biofertilizers," in *PGPR: Biocontrol and Biofertilization,* ed Siddiqui ZA (Dordrecht: Springer), 143–172.

Ray, S., Singh, V., Bisen, K., Keswani, C., Singh, S., Singh, H. B., et al. (2017). "Endophytomicrobiont: a multifaceted beneficial interaction," in H. B. Singh, B. K. Sarma, and C. Keswani. *Advances in PGPR Research* (Wallingford: CABI), 218–233. doi: 10.1079/9781786390325.0218

Raza, A., Ejaz, S., Saleem, M. S., Hejnak, V., Ahmad, F., Ahmed, M. A. A., et al. (2021). Plant growth promoting rhizobacteria improve growth and yield related attributes of chili under low nitrogen availability. *PLoS ONE* 16, e0261468. doi: 10.1371/journal.pone.0261468

Reed, S. C., Cleveland, C. C., and Townsend, A. R. (2011). Functional ecology of free-living nitrogen fixation: a contemporary perspective. *Annu. Rev. Ecol. Evol. Syst*. 42, 489–512. doi: 10.1146/annurev-ecolsys-102710-145034

Reinhold-Hurek, B., Bunger, W., Burbano, C. S., Sabale, M., and Hurek, T. (2015). Roots shaping their microbiome: global hotspots for microbial activity. *Annu. Rev. Phytopathol*. 53, 403–424. doi: 10.1146/annurev-phyto-082712-102342

Rezzonico, F., Binder, C., Defago, G., and Moenne-Loccoz, Y. (2005). The type III secretion system of biocontrol *Pseudomonas fluorescens* KD targets the phytopathogenic *ChromistaPythium*ultimum and promotes cucumber protection. *Mol. Plant Microbe Interact*. 18, 991–1001. doi: 10.1094/MPMI-18-0991

Rodriguez, H., and Fragal, R. (1990). Phosphate solubilizing bacteria and their role in plant growth promotion. *Biotechnol. Adv*. 17, 319–339. doi: 10.1016/S0734-9750(99)00014-2

Rodriguez, M., Torres, M., Blanco, L., Bejar, V., Sampedro, I., and Llamas, I. (2020). Plant growth-promoting activity and quorum quenching mediated biocontrol of bacterial phytopathogens by *Pseudomonas segetis* strain P6. *Sci. Rep*. 10, 4121. doi: 10.1038/s41598-020-61084-1

Rohrbacher, F., and St-Arnaud, M. (2016). Root exudation: the ecological driver of hydrocarbon rhizoremediation. *Agronomy* 6, 19. doi: 10.3390/agronomy6010019

Roychoudhury, P., and Kaushik, B. D. (1989). Solubilization of mussorie rock phosphate by cyanobacteria. *Curr. Sci*. 58, 569–570.

Rudrappa, T., Czymmek, K. J., Pare, P. W., and Bais, H. P. (2008). Root-secreted malic acid recruits beneficial soil bacteria. *Plant Physiol*. 3,1547–1556. doi: 10.1104/pp.108.127613

Ryu, C. M., Farag, M. A., Hu, C. H., Reddy, M. S., Kloepper, J. W., and Pare, P. W. (2004). Bacterial volatiles induce systemic resistance in *Arabidopsis*. *Plant Physiology*. 134, 1017–1026. doi: 10.1104/pp.103.026583

Ryu, C. M., Farag, M. A., Hu, C. H., Reddy, M. S., Wei, H. X., Pare, P. W., et al. (2003). Bacterial volatiles promote growth in *Arabidopsis*. *Proc. Natl. Acad. Sci. U.S.A*. 100, 4927–4932. doi: 10.1073/pnas.0730845100

Sah, S., and Singh, R. (2015). Siderophore: structural and functional characterization – a comprehensive review. *Agriculture* 6, 97–114. doi: 10.1515/agri-2015-0015

Sahin, F. C., Akmakc, I. R., and Kantar, F. (2004). Sugar beet and barley yields in relation to inoculation with N_2-fixing and phosphate solubilizing bacteria. *Plant Soil* 265, 123–129. doi: 10.1007/s11104-005-0334-8

Saiyad, S. A., Jhala, Y. K., and Vyas, R. V. (2015). Comparative efficiency of five potash and phosphate solubilizing bacteria and their key enzymes useful for enhancing and improvement of soil fertility. *Int. J. Sci. Res. Public*. 5, 1–6.

Saleem, M., Arshad, M., Hussain, S., and Bhatti, A. S. (2007). Perspective of plant growth promoting rhizobacteria (PGPR) containing ACC deaminase in stress agriculture. *J. Indust. Microbiol. Biotechnol*. 34, 635–648. doi: 10.1007/s10295-007-0240-6

Santner, A., Calderon-Villalobos, L. I. A., and Estelle, M. (2009). Plant hormones are versatile chemical regulators of plant growth. *Nat. Chem. Biol*. 5, 301–307. doi: 10.1038/nchembio.165

Santos, M. L. D., Berlitz, D. L., Wiest, S. L. F., Schunemann, R., Knaak, N., and Fiuza, L. M. (2018). Benefits associated with the interaction of endophytic bacteria and plants. *Braz. Arch. Biol. Technol*. 61, 1–11. doi: 10.1590/1678-4324-2018160431

Santoyo, G., Moreno-Hagelsieb, G., Orozco-Mosqueda, M. D. C., and Glick, B. R. (2016). Plant growth-promoting bacterial endophytes. *Microbiol. Res*. 183, 92–99. doi: 10.1016/j.micres.2015.11.008

Schaller, G. E., Street, I. H., and Kieber, J. J. (2014). Cytokinin and the cell cycle. *Curr. Opin. Plant. Biol*. 21, 7–15. doi: 10.1016/j.pbi.2014.05.015

Schwyn, B., and Neilands, J. B. (1987). Universal chemical assay for the detection and determination of siderophores. *Anal. Biochem*. 160, 47–56. doi: 10.1016/0003-2697(87)90612-9

Sekar, C., Prasad, N. N., and Sundaram, M. D. (2000). Enhancement of polygalacturonase activity during auxin induced para nodulation and endorhizosphere colonization of *Azospirillum* in rice roots. *Indian J. Exp. Biol*. 38, 80–83.

Shaharoona, B., Arshad, M., and Zahir, Z. A. (2006). Effect of plant growth promoting rhizobacteria containing ACC-deaminase on maize (*Zea mays* L.) growth under axenic conditions and on nodulation in mung bean. *Lett. Appl. Microbiol*. 42, 155–159. doi: 10.1111/j.1472-765X.2005.01827.x

Shanahan, P., Osullivan, D. J., Simpson, P., Glennon, J. D., and O' Gara, F. (1992). Isolation of 2, 4-diacetylphloroglucinol from a *Fluorescent Pseudomonad* and investigation of physiological parameters influencing its production. *Appl. Environ. Microbiol*. 58, 353–358. doi: 10.1128/aem.58.1.353-358.1992

Shank, E. A., and Kolter, R. (2011). Extracellular signaling and multicellularity in *Bacillus subtilis*. *Curr. Opin. Microbiol*. 14, 741–747. doi: 10.1016/j.mib.2011.09.016

Sharma, S. B., Sayyed, R. Z., Trivedi, M. H., and Gobi, T. A. (2013). Phosphate solubilizing microbes: sustainable approach for managing phosphorus deficiency in agricultural soils. *Springerplus* 2, 587. doi: 10.1186/2193-1801-2-587

Sindhu, S. S., Rakshiya, Y. S., and Sahu, G. (2009). Biological control of soilborne plant pathogens with rhizosphere. *Bacter. Pest Technol*. 3, 10–21.

Singh, H. B, Keswani, C., Reddy, M. S., Royano, E. S., and García-Estrada, C. (Eds.). (2019). *Secondary Metabolites of Plant Growth Promoting Rhizomicroorganisms: Discovery and Applications*. Singapore: Springer-Nature.

Singh, R., Singh, J., Deval, R., Upadhyay, S. K., and Kumar, D. (2017). The potentiality of selected strain of PGPR: azotobacter, for sustainable agriculture in India. *G J. Environ. Sci. Technol*. 4, 49–53.

Singh, R. K., Singh, P., Sharma, A., Guo, D.-J., Upadhyay, S. K., Song, Q.-Q., et al. (2022). Unraveling nitrogen fixing potential of endophytic diazotrophs of different saccharum species for sustainable sugarcane growth. *Int. J. Mol. Sci.* 23, 6242. doi: 10.3390/ijms23116242

Sinha, A. K., Venkateswaran, B. P., Tripathy, S. C., Sarkar, A., and Prabhakaran, S. (2018). Effects of growth conditions on siderophore producing bacteria and siderophore production from Indian ocean sector of Southern ocean. *J. Basic Microbiol*. 59, 412–424. doi: 10.1002/jobm.201800537

Someya, N., Kataoka, N., Komagata, T., Hirayae, K., Hibi, T., and Akutsu, K. (2000). Biological control of cyclamen soil borne diseases by *Serratia marcescens* strain B2. *Plant Dis*. 84, 334–340. doi: 10.1094/PDIS.2000.84.3.334

South, K. A., Nordstedt, N. P., and Jones, M. L. (2021). Identification of plant growth promoting rhizobacteria that improve the performance of greenhouse-grown petunias under low fertility conditions. *Plants* 10, 1410. doi: 10.3390/plants10071410

Spaepen, S., Vanderleyden, J., and Remans, R. (2007). Indole-3-acetic acid in microbial and microorganism-plant signaling. *FEMS Microbiol. Rev*. 31, 425–448. doi: 10.1111/j.1574-6976.2007.00072.x

Spaink, H. P. (2000). Root nodulation and infection factors produced by rhizobial bacteria. *Annu. Rev. Microbiol*. 54, 257–288. doi: 10.1146/annurev.micro.54.1.257

Swain, M. R., Naskar, S. K., and Ray, R. C. (2007). Indole 3-acetic acid production and effect on sprouting of yam (*Dioscorearotundata L.*) Minisetts by *Bacillus subtilis* isolated from culturable cowdung microflora. *Pol. J. Microbiol*. 56, 103–110.

Szoboszlay, M., White-Monsant, A., and Moe, L. A. (2016). The effect of root exudate 7,40- dihydroxyflavone and naringenin on soil bacterial community structure. *PLoS ONE* 11, e0146555. doi: 10.1371/journal.pone.0146555

Tahir, H. A. S., Gu, Q., Wu, H., Raza, W., Hanif, A., Wu, L., et al. (2017). Plant growth promotion by volatile organic compounds produced by *Bacillus subtilis* SYST2. *Front. Microbiol*. 8, 171. doi: 10.3389/fmicb.2017.00171

Tang, A., Haruna, A. O., Majid, N. M. A., and Jalloh, M. B. (2020). Potential PGPR properties of cellulolytic, nitrogen-fixing, phosphate-solubilizing bacteria in rehabilitated tropical forest soil. *Microorganisms* 8, 442. doi: 10.3390/microorganisms8030442

Tashiro, Y., Yawata, Y., Toyofuku, M., Uchiyama, H., and Nomura, N. (2013). Interspecies interaction between *Pseudomonas aeruginosa* and other microorganisms. *Microbes Environ*. 28, 13–24. doi: 10.1264/jsme2.ME12167

Tsukanova, K. A., Chebotar, V. K., Meyer, J. J. M., and Bibikova, T. N. (2017). Effect of plant growth-promoting rhizobacteria on plant hormone homeostasis. *South Afr. J. Bot*. 113, 91–102. doi: 10.1016/j.sajb.2017.07.007

Upadhyay, S. K., and Chauhan, P. K. (2022). Optimization of eco-friendly amendments as sustainable asset for salt-tolerant plant growth-promoting bacteria mediated maize (*Zea Mays* L.) plant growth, Na uptake reduction and saline soil restoration. *Environ. Res.* 211,113081. doi: 10.1016/j.envres.2022.113081

Upadhyay, S. K., and Edrisi, S. A. (2021). Developing sustainable measures to restore fly ash contaminated lands: current challenges and future prospects. *Land Degrad. Dev.* 32, 4817–4831. doi: 10.1002/ldr.4090

Upadhyay, S. K., Maurya, S. K., and Singh, D. P. (2012a). Salinity tolerance in free living plant growth promoting rhizobacteria. *Indian J. Sci. Res.* 3, 73–78.

Upadhyay, S. K., Saxena, A. K., Singh,. J. S., and Singh, D. P. (2019). Impact of native ST-PGPR (*Bacillus pumilus*; EU927414) on PGP traits, antioxidants activities, wheat plant growth and yield under salinity. *Clim. Change Environ. Sust.* 7, 157–168. doi: 10.5958/2320-642X.2019.00021.8

Upadhyay, S. K., and Singh, D. P. (2015). Effect of salt-tolerant plant growth-promoting rhizobacteria on wheat plants and soil health in a saline environment. *Plant Biol.* 17, 288–293. doi: 10.1111/plb.12173

Upadhyay, S. K., Singh, D. P., and Saikia, R. (2009). Genetic diversity of plant growth promoting rhizobacteria isolated from rhizospheric soil of wheat under saline condition. *Curr. Microbiol.* 59, 489–496. doi: 10.1007/s00284-009-9464-1

Upadhyay, S. K., Singh, G., and Singh, D. P. (2016). "Mechanism and understanding of PGPR: an approach for sustainable agriculture under a biotic stresses," in *Microbes and Environmental Management*, eds J. S. Singh, and D. P. Singh (Stadum: Studium Press Pvt. Ltd), 225–254.

Upadhyay, S. K., Singh, J. S., Saxena, A. K., and Singh, D. P. (2012b). Impact of PGPR inoculation on growth and antioxidant status of wheat under saline conditions. *Plant Biol.* 14, 605–611. doi: 10.1111/j.1438-8677.2011.00533.x

Upadhyay, S. K., Singh, J. S., and Singh, D. P. (2011). Exopolysaccharide-producing plant growth-promoting rhizobacteria under salinity condition. *Pedosphere* 21, 214–222. doi: 10.1016/S1002-0160(11)60120-3

Van Loon, L. C., Bakker, P. A., and Pieterse, M. J. (1998). Systemic induced resistance by rhizosphere bacteria. *Annu. Rev. Phytopathol.* 36, 453–483. doi: 10.1146/annurev.phyto.36.1.453

Vardharajula, S., Alia, S. Z., Grover, M., Reddy, G., and Bandi, V. (2011). Drought-tolerant plant growth promoting *Bacillus* spp. effect on growth, osmolytes and antioxidant status of maize under drought stress. *J. Plant Interact.* 6, 1–14. doi: 10.1080/17429145.2010.535178

Vial, L., Cuny, C., Gluchoff-Fiasson, K., Comte, G., Oger, P. M., Faure, D., et al. (2006). N-acyl-homoserine lactone-mediated quorum-sensing in *Azospirillum*: an exception rather than a rule. *FEMS Microbiol. Ecol.* 58, 155–168. doi: 10.1111/j.1574-6941.2006.00153.x

Vieira, S., Sikorski, J., Dietz, S., Herz, K., Schrumpf, M., Bruelheide, H., et al. (2020). Drivers of the composition of active rhizosphere bacterial communities in temperate grasslands. *ISME J.* 14, 463–475. doi: 10.1038/s41396-019-0543-4

Vocciante, M., Grifoni, M., Fusini, D., Petruzzelli, G., and Franchi, E. (2022). The role of plant growth-promoting rhizobacteria (PGPR) in mitigating plant's environmental stresses. *Appl. Sci.* 12, 1231. doi: 10.3390/app1203 1231

Voisard, C., Keel, C., Haas, D., and Defago, G. (1989). Cyanide production by *Pseudomonas fluorescens* suppress black root rot of tobacco under gnotobiotic conditions. *EMBO J.* 8, 351–358. doi: 10.1002/j.1460-2075.1989.tb0 3384.x

Wang, S., Huijun, W., Junqing, Q., Lingli, M., Jun, L., Yanfei, X., et al. (2009). Molecular mechanism of plant growth promotion and induced systemic resistance to tobacco mosaic virus by *Bacillus* spp. *J. Microbiol. Biotechnol.* 10, 1250–1258. doi: 10.4014/jmb.0901.008

Wanga, Y., Cai, Y., Cao, Y., Liu, Y., and Jiping, L. (2018). Aluminum-activated root malate and citrate exudation is independent of NIP1; 2-facilitated root-cell-wall aluminum removal in *Arabidopsis*. *Plant Signal. Behav.* 1, e1422469. doi: 10.1080/15592324.2017.1422469

Wei, Z., and Jousset, A. (2017). Plant breeding goes microbial. *Trends Plant Sci.* 22, 555–558. doi: 10.1016/j.tplants.2017.05.009

Weller, D. M. (2007). Pseudomonas biocontrol agents of soilborne pathogens: looking back over 30 years. *Phytopathology* 97, 250–256. doi: 10.1094/PHYTO-97-2-0250

Weller, D. M., and Cook, R. J. (1983). Suppression of take-all of wheat by seed-treatment with *Fluorescent pseudomonads*. *Phytopathology* 73, 463–469. doi: 10.1094/Phyto-73-463

Weston, L. A., Ryan, P. R., and Watt, M. (2012). Mechanisms for cellular transport and release of allelochemicals from plant roots into the rhizosphere. *J. Exp. Bot.* 63, 3445–3454. doi: 10.1093/jxb/ers054

White, L. J., Ge, X., Brozel, V. S., and Subramanian, S. (2017). Root isoflavonoids and hairy root transformation influence key bacterial taxa in the soybean rhizosphere. *Environ. Microbiol* 19, 1391–1406. doi: 10.1111/1462-2920.13602

Xie, F., Murray, J. D., Kim, J., Heckmann, A. B., Edwards, A., Oldroyd, G. E., et al. (2012). Legume pectate lyase required for root infection by rhizobia. *Proc. Natl. Acad. Sci. U.S.A.* 109, 633–638 doi: 10.1073/pnas.1113992109

Yadav, B. K., Akhtar, M. S., and Panwar, J. (2015). "Rhizospheric plant-microbe interactions: key factors to soil fertility and plant nutrition," in *Plant Microbes Symbiosis: Applied Facets*, ed N. K. Arora (New Delhi: Springer), 127–145. doi: 10.1007/978-81-322-2068-8_6

Yadegari, M., and Mosadeghzad, Z. (2012). Biofertilizers effects on quantitative and qualitative yield of Thyme (*Thymus vulgaris*). *Afr. J. Agri. Res.* 7, 4716–4723. doi: 10.5897/AJAR11.2347

Yousaf, M., Rehman, Y., and Hasnain, S. (2017). High-yielding wheat varieties harbour superior plant growth promoting-bacterial endophytes. *Appl. Food Biotech.* 4, 143–154. doi: 10.22037/afb.v4i3.15014

Yu, X., Li, Y., Cui, Y., Liu, R., Li, Y., Chen, Q., et al. (2017). An indoleacetic acid-producing *Ochrobactrum*sp. MGJ11 counteracts cadmium effect on soybean by promoting plant growth. *J. Appl Microbiol.* 122, 987–996. doi: 10.1111/jam.13379

Yuan, J., Zhang, N., Huang, Q., Raza, W., Li, R., Vivanco, J. M., et al. (2015). Organic acids from root exudates of banana help root colonization of PGPR strain *Bacillus amyloliquefaciens* NJN-6. *Sci. Rep.* 5, 13438. doi: 10.1038/srep13438

Zakry, F. A. A., Shamsuddin, Z. H., Rahim, K. A., Zakaria, Z. Z., and Rahim, A. A. (2012). Inoculation of *Bacillus sphaericus* UPMB-10 to young oil palm and measurement of its uptake of fixed nitrogen using the 15N isotope dilution technique. *Microbes Environ.* 27, 257–262, doi: 10.1264/jsme2.ME11309

Zhalnina, K., Louie, K. B., Hao, Z., Mansoori, N., Rocha, U. N. D., Dhi, S., et al. (2018). Dynamic root exudate chemistry and microbial substrate preferences drive patterns in rhizosphere microbial community assembly. *Nat. Microbiol.* 3, 470–480. doi: 10.1038/s41564-018-0129-3

Zhang, A., Zhao, G., Gao, T., Wang, W., Li, J., Zhang, S., et al. (2013). Solubilization of insoluble potassium and phosphate by *Paenibacilluskribensis* CX-7: a soil microorganism with biological control potential. *Afr. J. Microbiol. Res.* 7, 41–47. doi: 10.5897/AJMR12.1485

Zhang, C., and Kong, F. (2014). Isolation and identification of potassium-solubilizing bacteria from tobacco rhizospheric soil and their effect on tobacco plants. *Appl. Soil. Ecol.* 82, 18–25. doi: 10.1016/j.apsoil.2014.05.002

Zhang, N., Yang, D., Wang, D., Miao, Y., Shao, J., Zhou, X., et al. (2015). Whole transcriptomic analysis of the plant-beneficial rhizobacterium *Bacillus amyloliquefaciens* SQR9 during enhanced biofilm formation regulated by maize root exudates. *BMC Genomics* 16, 685. doi: 10.1186/s12864-015-1825-5

Zhang, S., Ma, M., Zhang, H., Zhang, S., Qian, M., Zhang, Z., et al. (2019). Genome-wide analysis of polygalacturonase gene family from pear genome and identification of the member involved in pear softening. *BMC Plant Biol.* 19, 587. doi: 10.1186/s12870-019-2168-1

Conflict of Interest: The authors declare that the research was conducted in the absence of any commercial or financial relationships that could be construed as a potential conflict of interest.

Publisher's Note: All claims expressed in this article are solely those of the authors and do not necessarily represent those of their affiliated organizations, or those of the publisher, the editors and the reviewers. Any product that may be evaluated in this article, or claim that may be made by its manufacturer, is not guaranteed or endorsed by the publisher.

frontiers | Frontiers in Microbiology

ORIGINAL RESEARCH
published: 14 July 2022
doi: 10.3389/fmicb.2022.903136

The Native Microbial Community of Gastropod-Associated *Phasmarhabditis* Species Across Central and Southern California

Jacob Schurkman[1†], Rui Liu[2†], Salma Alavi[2], Irma Tandingan De Ley[1], Ansel Hsiao[2] and Adler R. Dillman[1*]*

[1]Department of Nematology, University of California Riverside, Riverside, CA, United States, [2]Department of Microbiology and Plant Pathology, University of California Riverside, Riverside, CA, United States

OPEN ACCESS

Edited by:
Yi Luo,
Nankai University, China

Reviewed by:
Claudia S. L. Vicente,
University of Évora, Portugal
Ahmed Elhady,
Julius Kühn-Institute, Germany
Olivera Topalovic,
Aarhus University, Denmark
Robbie Rae,
Liverpool John Moores University, United Kingdom

***Correspondence:**
Adler R. Dillman
adlerd@ucr.edu
Ansel Hsiao
ansel.hsiao@ucr.edu

†These authors have contributed equally to this work

Specialty section:
This article was submitted to Microbial Symbioses, a section of the journal Frontiers in Microbiology

Received: *23 March 2022*
Accepted: *17 May 2022*
Published: *14 July 2022*

Citation:
Schurkman J, Liu R, Alavi S, Tandingan De Ley I, Hsiao A and Dillman AR (2022) The Native Microbial Community of Gastropod-Associated Phasmarhabditis Species Across Central and Southern California. Front. Microbiol. 13:903136. doi: 10.3389/fmicb.2022.903136

Nematodes in the genus *Phasmarhabditis* can infect and kill slugs and snails, which are important agricultural pests. This useful trait has been commercialized by the corporation BASF after they mass produced a product labeled Nemaslug®. The product contains *Phasmarhabditis hermaphrodita*, which has been cultured with *Moraxella osloensis*, a bacterial strain that was originally thought to be responsible for causing mortality in slugs and snails. The exact mechanism leading to death in a *Phasmarhabditis* infected host is unknown but may involve contributions from nematode-associated bacteria. The naturally occurring microbial community of *Phasmarhabditis* is unexplored; the previous *Phasmarhabditis* microbial community studies have focused on laboratory grown or commercially reared nematodes, and in order to obtain a deeper understanding of the parasite and its host interactions, it is crucial to characterize the natural microbial communities associated with this organism in the wild. We sampled *Phasmarhabditis californica*, *Phasmarhabditis hermaphrodita*, and *Phasmarhabditis papillosa* directly from their habitats in Central and Southern California nurseries and garden centers and identified their native microbial community *via* 16S amplicon sequencing. We found that the *Phasmarhabditis* microbial community was influenced by species, location, and possibly gastropod host from which the nematode was collected. The predominant bacteria of the *Phasmarhabditis* isolates collected included *Shewanella*, *Clostridium perfringens*, Aeromonadaceae, Pseudomonadaceae, and *Acinetobacter*. *Phasmarhabditis papillosa* isolates exhibited an enrichment with species belonging to Acinetobacter or Pseudomonadaceae. However, further research must be performed to determine if this is due to the location of isolate collection or a species specific microbial community pattern. More work on the natural microbial community of *Phasmarhabditis* is needed to determine the role of bacteria in nematode virulence.

Keywords: ***Phasmarhabditis californica*, *Phasmarhabditis hermaphrodita*, *Phasmarhabditis papillosa*, microbiome, gastropods**

INTRODUCTION

Nematodes are one of the most ecologically diverse groups of organisms on Earth. They exist on every continent, surviving in all climates where decomposition occurs (Ingham, 1994; Bongers and Bongers, 1998; De Ley, 2006; Schafer, 2016). Some exist as free-living organisms like *Caenorhabditis elegans*, and many have evolved to form a variety of parasitic relationships like *Ascaris lumbricoides*, or the entomopathogenic nematode (EPN) *Steinernema feltiae* that has been utilized for biological control against pestiferous insects (Kaya, 1993; Riddle et al., 1997; Marilyn, 2008). EPNs have evolved specific mutualistic relationships with bacterial species in their gut that helps to kill various insects (Grewal and Georgis, 1997). Recent metagenomic analyses have indicated that the commensal microbial community of EPNs, the gut microbial community, is more complex than originally thought, leading to the possibility of a native EPN pathobiome that assists with insect killing (Ogier et al., 2020).

One nematode that has been successfully used as a biological control agent is *Phasmarhabditis hermaphrodita* (Wilson et al., 1993b). All members of the genus are gastropod-specific facultative parasites. *Phasmarhabditis hermaphrodita* was discovered in Europe and has been commercialized for biological control in Europe under the name Nemaslug®. *Phasmarhabditis* nematodes are effective at killing pestiferous gastropods in laboratory and agricultural settings such as nurseries and a variety of crops (Wilson et al., 1994a,b; Rae et al., 2007b; McDonnell et al., 2020; Tandingan De Ley et al., 2020; Schurkman et al., 2022a) but are safe to tested non-gastropod organisms (Grewal and Grewal, 2003; Iglesias et al., 2003; Rae et al., 2007a; Nardo et al., 2010). However, due to the discovery of *Phasmarhabditis* in Europe, its use has not yet been permitted in the United States since invasive species are not permitted for biological control use in the country.

It was originally thought that *Phasmarhabditis* nematodes kill their hosts in a manner similar to EPNs, which employ mutualistic and pathogenic microbes to assist with insect killing (Wilson et al., 1993b; Tan and Grewal, 2001a). This hypothesis came about upon the discovery that *P. hermaphrodita* cultured with *Moraxella osloensis* was highly pathogenic to the grey field slug *Deroceras reticulatum*, more so than when it was cultured on other bacteria (Wilson et al., 1995a; Tan and Grewal, 2001b). The selection of bacteria to test came from isolates identified in *P. hermaphrodita* infective juveniles (IJs), dead *D. reticulatum*, and xenic foam chip cultures (Wilson et al., 1993a, 1995a). The species identified and tested included *Aeromonas hydrophila*, *Aeromonas* sp., *Flavobacterium breve*, *Flavobacterium odoratum*, *M. osloensis*, *Providencia rettgeri*, *Pseudomonas fluorescens* (isolate no. 140), *P. fluorescens* (isolate no. 141), and *Serratia proteamaculans*. When these bacteria were injected into *D. reticulatum*, *A. hydrophila*, and *P. fluorescens* (isolate no. 140) caused the most mortality. However, *P. fluorescens* (isolate no. 140) was able to facilitate better growth when culturing *P. hermaphrodita*, which may be indicative of this bacterial species serving as an optimum food source. However, nematodes which were grown on *M. osloensis* exhibited the highest pathogenicity while also allowing for good nematode growth. Another experiment showed that axenic *P. hermaphrodita* did not cause mortality in *D. reticulatum* while those reared on *M. osloensis* did (Tan and Grewal, 2001b). These experiments led to the assumption that *P. hermaphrodita* likely has a natural association with *M. osloensis*, similar to EPNs' association with pathogenic bacteria (An et al., 2008; Wilson and Rae, 2015). After these experiments, it was generally accepted among the *Phasmarhabditis* community that these nematodes caused death in their gastropod hosts strictly through the utilization of the apparent commonly associated bacteria *M. osloensis*. However, the natural association of other bacteria with *Phasmarhabditis* in the wild and how this association contributes to nematode host virulence remained largely unexplored.

In 2010, it was shown that *P. hermaphrodita* associates with many bacterial species that do not affect its virulence (Rae et al., 2010), in contrast to the existing understanding of *Phasmarhabditis* virulence (Wilson et al., 1995a). Rae et al. (2010) suggested that *P. hermaphrodita* does not associate with specific bacteria due to the observation of inconsistent and varied bacterial assemblages with the nematode (Rae et al., 2010). However, the study was unable to identify key microbial species that regularly occur within *Phasmarhabditis*. This is because a limitation to PCR-DGGE is that specific bacterial species cannot be identified. Therefore, no conclusions were made on the presence of *M. osloensis* since that was not the goal of the study. The study only aimed to show that *Phasmarhabditis* associated with multiple bacterial assemblages. In another study, bacteria were analyzed from laboratory grown *Phasmarhabditis*, by allowing nematodes to crawl on LB agar plates and identifying some of the bacterial colonies that subsequently arose (Howe et al., 2020). Eight genera of bacteria were identified that were hypothesized to have come from the laboratory grown *Phasmarhabditis*. *Pseudomonas* was the only genus found in this most recent study that was also found in 1995 (Wilson et al., 1995a; Howe et al., 2020). *Moraxella osloensis*, which was expected to be identified, was not found. These mirror findings related to the native and naturally occurring microbial community of the model organism *C. elegans* (Dirksen et al., 2016), though prolonged *in vitro* growth in the laboratory raises the possibility of association with microbes not commonly found with *Phasmarhabditis* in the wild.

Describing the natural and infected microbial community of the host could help to distinguish whether microbes present within *Phasmarhabditis* originated from the host or from another source. Very little microbial community research has been done on *D. reticulatum*, the slug often used in *Phasmarhabditis* studies (Walker et al., 1999). However, gut microbial community metagenomic analyses have been performed on other slug species like *Ambigolimax valentianus* which identified a core microbial community of *Citrobacter*, *Delftia*, *Erwinia*, *Arthrobacter*, *Stenotrophomonas*, *Pseudomonas*, *Rhodococcus*, and *Bacillus*. *Arion ater*'s microbial community was also found to be influenced by the substrate they were on, while the soil microbial community itself could also be influenced by the introduction of the slug (Jackson, 2020; Jackson et al., 2021). A gut metagenomic analyses of the slug *A. ater* has also been performed. The most abundant bacterial genera in the gut of

A. ater included *Enterobacter*, *Citrobacter*, *Pseudomonas*, and *Escherichia* (Joynson et al., 2017).

All microbial community studies that have taken place involving *Phasmarhabditis* have used laboratory cultured nematodes, and the microbial community changes upon introduction to a laboratory environment, especially when the nematodes are grown on monoxenic cultures (Dirksen et al., 2016). Recently, three species of *Phasmarhabditis* were discovered during gastropod surveys of California nurseries and garden centers (Tandingan De Ley et al., 2014, 2016). Between 2018 and 2021 additional surveys for *Phasmarhabditis* nematodes were performed to determine the distribution of these species (Schurkman et al., 2022b). Newly-isolated nematodes collected during these most recent surveys were used to identify the natural microbial communities of *Phasmarhabditis* isolates across the Central and Southern California regions. Similarities or differences between *Phasmarhabditis* isolates could help to further the understanding of the potential role that the microbial community plays between *Phasmarhabditis* nematodes and their hosts. In this study, we aimed to determine if the *Phasmarhabditis* microbial community is species specific, and if it is influenced by gastropod hosts, geographic locality, and collection methods.

MATERIALS AND METHODS

Phasmarhabditis Survey Collection

Fourteen plant nurseries from Central California and five nurseries from Southern California were surveyed for gastropods infected with *Phasmarhabditis* as described in Schurkman et al. (2022b). In short, 1 person hour was spent searching for gastropods. Then, gastropods were sorted into containers by species and taken back to the laboratory at UC Riverside in coolers. Gastropods were decapitated and placed on 1% plain agar to create seed cultures (1 L: 10 g agar, 900 ml H_2O) and their bodies were observed for the presence of nematodes under a dissecting microscope. Upon finding a nematode(s) which phenotypically resembled a member of the *Phasmarhabditis* genus (i.e., the significant presence of phasmids), up to five individuals were placed on Nematode Growth Medium [NGM; 1 L: 3 g NaCl, 20 g Agar, 2.5 g Peptone, 975 ml deionized H_2O, and 10 ml Uracil (2 g/L) were added to a liter of deionized water, autoclaved, and let cool, to which were added 25 ml filtered KPO_4, 1 ml filtered $MgSO_4$, 1 ml $CaCl_2$, and 1 ml Cholesterol (5 mg/ml)] to create axenic cultures. All nematodes on axenic culture plates were considered as identical species of the same strain with further verification after single nematode DNA sequencing. The axenic culture plates were stored at 17°C. Individual nematodes suspected to be *Phasmarhabditis* were picked from axenic culture plates and were prepared for PCR and DNA sequencing of the D2-D3 domains of the rDNA LSU, as described in Tandingan De Ley et al. (2014). Contigs were assembled and compared by BLAST with published sequences on Genbank using CodonCode Aligner (CodonCode Corp., 58 Beech Street, Dedham, MA, United States) to identify nematode species. A percent identity match near 99% was required in order to indicate a species identification using BLAST or CodonCode Aligner.

Phasmarhabditis Treatment and Storage

All nematodes suspected to be a member of the *Phasmarhabditis* genus *via* microscopy were prepared for microbial community analysis. This preparation was done for each nematode picked from gastropod cadavers and before axenic culture plates were created. To prepare, nematodes in seed cultures which phenotypically matched those that were used for axenic culture were subjected to a rinse. When possible, at least one nematode from each seed culture was washed in sterile M9 buffer (1 L: 3 g KH_2PO_4, 6 g Na_2HPO_4, 5 g NaCl, 1 ml 1 M $MgSO_4$, and H_2O to 1 L) thrice and then placed inside of 10 µl of sterile H_2O in a 200 µl PCR tube, which was stored at −20°C for future use. These nematodes were labeled as washed nematodes. The washes were performed to rinse excess material from the cuticle of the nematode. When possible, at least one nematode was also not subjected to any treatment at all, and the nematode was immediately picked and placed inside of a 200 µl sterile microtube with 10 µl of sterile H_2O and stored at −20°C. These nematodes were labeled as unwashed nematodes. Lastly, 10 µl of dead and partially decomposed gastropod tissue was pipetted into 10 µl of sterile H_2O in a 200 µl PCR and was stored at −20°C. Comparisons to unwashed nematodes and decomposed slug tissue were done to observe whether the washes significantly altered the microbial community of *Phasmarhabditis*. Upon finding a *Phasmarhabditis* nematode *via* 28S sequencing, we used the corresponding nematode(s) previously frozen at −20°C for microbial community analysis.

DNA Extraction

Genomic DNA was extracted from all washed and unwashed nematodes, as well as from the decomposed dead gastropod tissue. The DNA extraction protocol included thawing samples on ice and breaking the individual nematodes into pieces within their PCR tube using a sterile 10 µl pipette tip. After breaking the nematodes, the total volume of all samples was brought up to 100 µl with sterile PCR grade water. An equal volume of phenol chloroform was then added to each sample. The contents of the small PCR tubes were then transferred to a 1.25-ml Eppendorf tube and were mixed *via* pipettor. The tubes were shaken by hand for 30 s and were then centrifuged at 12,000 rpm for 10 min at 4°C. After centrifugation, the aqueous phase of the solutions was removed and placed in a new 1.25-ml Eppendorf tube. The wash with phenol chloroform was repeated once more, and then 400 µl of isopropanol stored at −20°C was added to the solution. A 1:10 ratio of 3 M sodium acetate was then added to the solution and was mixed *via* pipetting up and down. The tubes were then shaken by hand for 30 s and to each tube, 1 µl of glycogen stored at −20°C was added before storing at −20°C for 24 h. The samples were then centrifuged at 13,000 rpm for 30 min at 4°C to form a pellet. All liquid was then removed from the tubes with a pipettor, being careful not to disturb the pellet at the base of the tube. Using a pipette, the pellet was carefully washed with

500 µl of ethanol which was immediately drawn from each tube. The tubes were then stored at 37°C in an incubator until no visible liquid was present. The pellet was then resuspended in 50 µl of sterile PCR grade water and the DNA was quantified using a Qubit 3 Fluorometer (Invitrogen by Thermo Fisher Scientific and life technologies, Waltham, MA, United States).

16S rRNA Gene Library Preparation and Sequencing

The bacterial 16S rDNA V4 region 515F-806R was amplified according to the earth microbial community project, 16S Illumina protocol (Thompson et al., 2017). Based on the concentrations of each single nematode DNA sample, 1–8 µl of the extracted DNA template, 10 µl Platinum Hot Start PCR Master Mix (ThermoFisher), and 0.5 µl of forward and reverse primers (10 µM) were added into the 25 µl PCR reaction system, with the barcode in the reverse primer. Thermocycler conditions were 4°C for 3 min, followed by 30 cycles (94°C for 45 s, 50°C for 60 s, 72°C for 90 s), and 72°C for 10 min. PCR products were pooled together and submitted to an Illumina MiSeq platform with 2 × 150 bp read lengths.

Data Analysis

Raw reads were processed using the open-source software QIIME2 (Bolyen et al., 2019) version 2021.2. Samples that had >1,000 reads were retained and denoised using dada2 with default settings. Taxonomic classification was performed using classify-sklearn command against the Greengenes 13_8 99% OTUs from 515F/806R region of sequences (MD5: 9e82e8969303b3a86ac941ceafeeac86) set trimmed to 250 bp of the V4 hypervariable region (McDonald et al., 2012; Bokulich et al., 2018; Robeson et al., 2020). An amplicon sequence variant (ASV) was defined as a group of sequences with a similarity of 100%. Alpha and beta diversity analyses were calculated in QIIME2 with rarefied sample depth of 1,000, and results were plotted in GraphPad Prism 9. The heatmap was generated using pheatmap package in R program, samples and species clustered using hclust.

The statistical calculations used in QIIME2 were: Kruskal-Wallis test for alpha diversity comparisons, and permANOVA for beta diversity. Mann–Whitney U tests were performed in GraphPad Prism 9 for taxa comparisons.

RESULTS

DNA Amplification and Total Reads

Of the total 146 samples from three different nematode species from various gastropod hosts collected during surveys between 2019 and 2020, 26 were amplified and sequenced successfully (**Supplementary Table 1**). In total 475,226 raw reads were obtained from 26 samples. A total of 397,685 high-quality reads were clustered into 337 ASVs at 100% similarity level. Twenty-two samples with read depth > 1,000 remained for subsequent analyses (**Supplementary Table 1**).

Alpha Diversity Analyses

Alpha diversity analysis showed that nematode species may be an important factor associated with the diversity of nematode microbial community's. According to observed features, Shannon index, and Faith's phylogenetic diversity (Faith pd), *P. californica* microbial community's exhibited higher richness than those of *P. hermaphrodita* and *P. papillosa* (**Figure 1A**). Meanwhile, Central California samples had significantly higher observed features and Faith pd. index than Southern California. However, this may reflect the fact that all nematodes collected from Southern California were *P. papillosa*, which had the lowest diversity of observed features (**Figure 1**). The host of the nematode was not associated with differences in microbial richness or evenness (**Figure 2A**). No alpha diversity differences were noted across nematodes that were washed in M9 thrice, unwashed, or collected from decomposed gastropod tissue (**Figure 2B**).

Microbial Community Structure Comparisons

The difference of overall microbial community structure showed similar trends with alpha diversity analyses. The PCoA plots based on Bray–Curtis distance between sample microbial community's revealed a significant separation of bacterial composition depending on *Phasmarhabditis* species, especially between *P. californica* and *P. papillosa* (q value = 0.015), while the *P. hermaphrodita* microbial community overlapped with the other two species (**Figure 3A**), suggesting that *P. hermaphrodita*'s microbial community shared some of the same bacterial features with both *P. californica* and *P. papillosa*; these differences were statistically significant when tested using permANOVA (**Table 1**). Geographical location also contributed to differences in the nematode microbial community (**Figure 3B**), while treatment by washing with M9 did not (**Figure 4B**). The gastropod host also showed a slight overall association ($p = 0.017$) with the nematode microbial community (**Figure 4A**; **Table 1**), but no pairwise comparison of the hosts showed significantly separation. From these data, we conclude that nematode species and location may play an important role in shaping the native *Phasmarhabditis* microbial community and perhaps the gastropod microbial community.

Taxonomic Composition of the Nematode Microbial Community

The species-level bacterial community composition in the nematodes was analyzed using the unsupervised hierarchical cluster analysis. For this analysis, all the samples were divided into four groups (**Figure 5**). Cluster IV consisted of *P. papillosa* samples from Southern California and exhibited enrichment with species belonging to genus Acinetobacter or family Pseudomonadaceae. Cluster III consisted of *P. californica* from Central California. Cluster II consisted of a mixture of *P. papillosa* from Southern California and *P. hermaphrodita* from Central California, which were all collected from the same gastropod host, *D. reticulatum*; in these microbial communities, members of genus *Shewanella* and family Aeromonadaceae were the

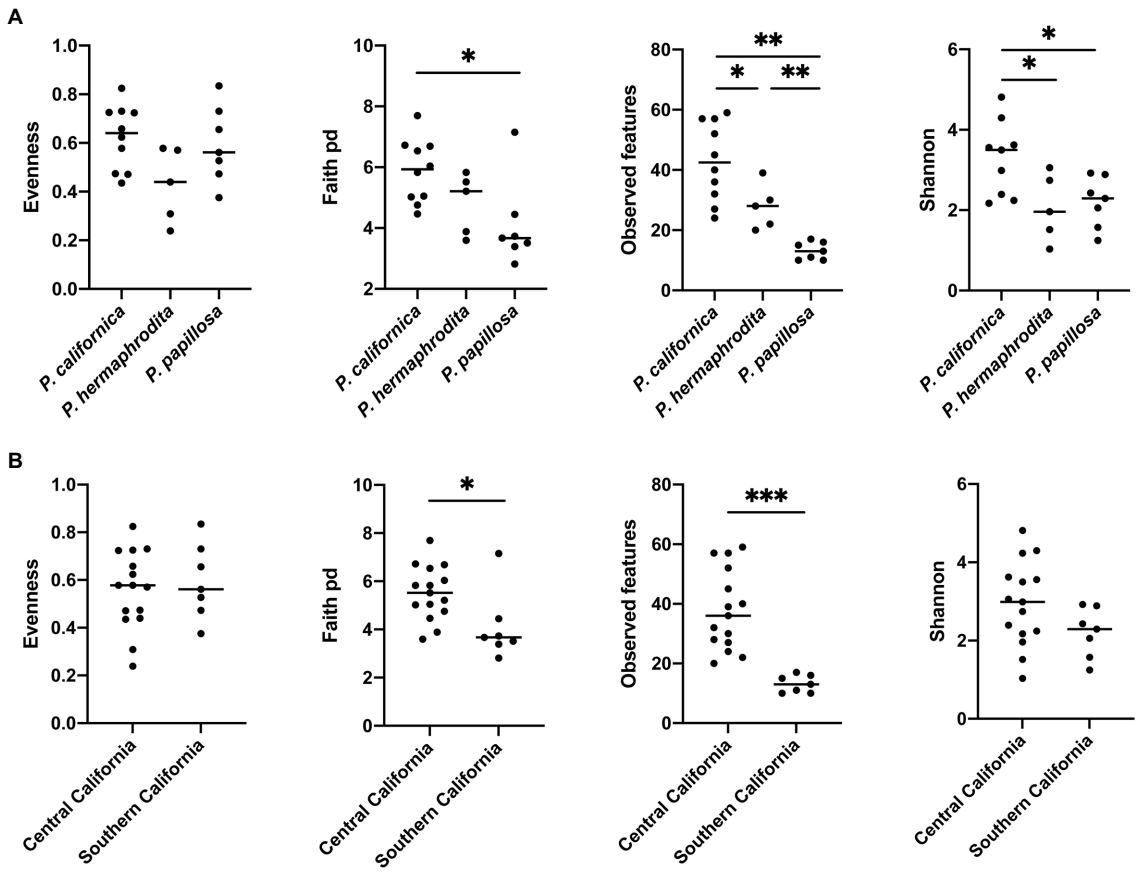

FIGURE 1 | The comparison of microbial community alpha diversity of nematode-associated microbial communities. **(A)** *Phasmarhabditis* species and **(B)** location affect the richness of the microbial composition in nematode. Kruskal-Wallis test, *$p < 0.05$; **$p < 0.01$; and ***$p < 0.001$.

dominant microbial members. No members of the genus *Moraxella* were identified. Cluster I microbial samples were dominated by a high proportion of *Clostridium perfringens*, though these samples were collected from multiple nematodes and gastropod hosts from Central California. Among the most abundant species, *Shewanella* sp. was significantly increased in cluster II compared to the other clusters; samples in cluster I had 48%–86% of *C. perfringens*, which was not shown in any other clusters; species from family Pseudomonadaceae and genus *Acinetobacter* were significantly enriched in cluster IV; while family Aeromonadaceae was evenly distributed in all clusters (**Figure 6**).

DISCUSSION

This study is the first analysis of the native microbial community of *Phasmarhabditis*. It assessed the microbial community of *Phasmarhabditis* in multiple nursery and garden center habitats and aimed to help identify core microbial communities of *Phasmarhabditis* utilizing 16S metabarcoding analysis. The previous *Phasmarhabditis* microbial community work had been done using nematodes which had been kept in culture, leaving the possibility of the nematode's microbial community being altered by laboratory conditions and frequent transfers (Wilson et al., 1993a, 1995b; Rae et al., 2010; Dirksen et al., 2016;Howe et al., 2020; Sheehy et al., 2022). Two other studies have used next generation sequencing techniques, however the studies did not use newly-recovered *Phasmarhabditis*, but instead utilized laboratory sub-cultured and maintained *Phasmarhabditis* (Howe et al., 2020; Sheehy et al., 2022). The most recent study by Sheehy et al. (2022) showed that *Phasmarhabditis* does not exclusively associate with a single bacterial species which it relies on for virulence. However, the study did not utilize native *Phasmarhabditis* and only utilized *Phasmarhabditis* nematodes which have been frequently cultured and transferred in laboratories (Sheehy et al., 2022). While some of the recent studies may suggest that *Phasmarhabditis* does not maintain a set core microbial community, understanding what microbes are naturally and commonly associated with *Phasmarhabditis* may help to solidify whether *Phasmarhabditis* utilizes any core microbial species which contributes to gastropod killing, similar to microbial contributors to EPN virulence. The findings may also reveal crucial bacterial species needed for *Phasmarhabditis* food consumption, survival, or host–parasite interactions. Our results suggest that the location, species, and possibly the gastropod host may affect the microbial diversity within the tested *Phasmarhabditis*.

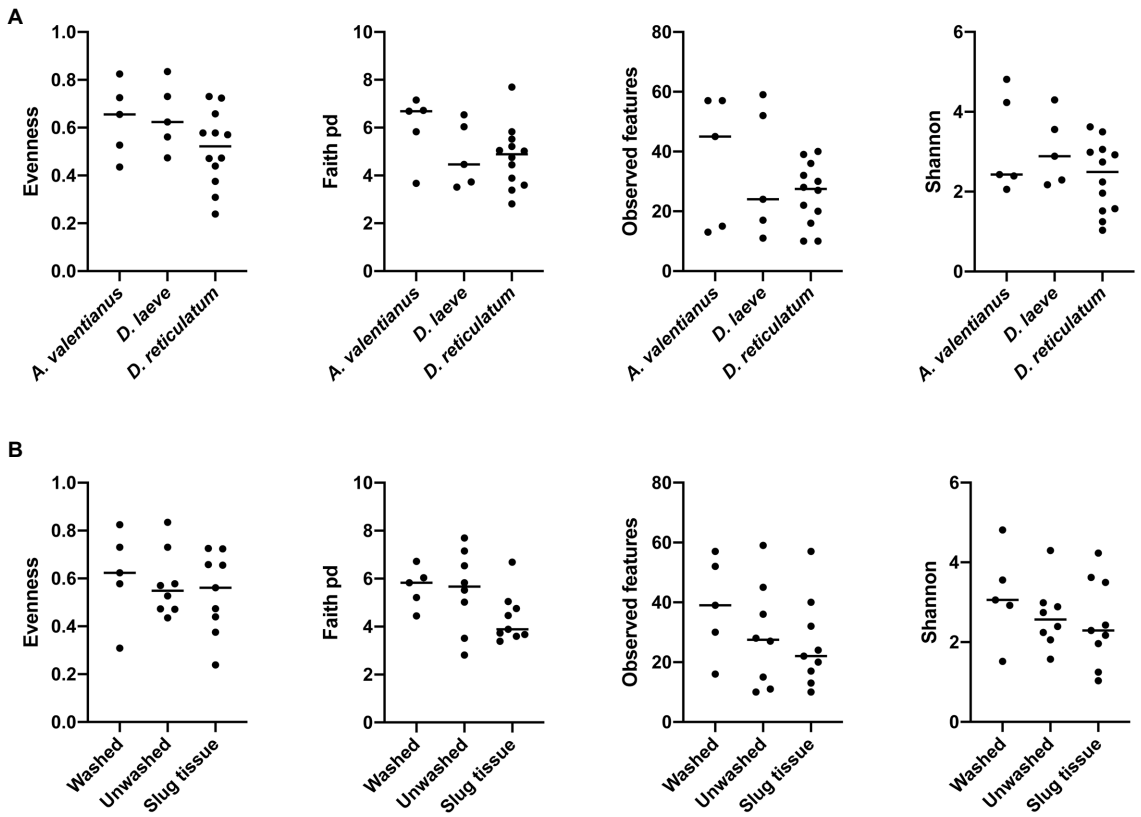

FIGURE 2 | Comparison of microbial community alpha diversity across different host species or sample collection strategy. **(A)** Gastropod host and **(B)** collection strategy are not associated with differences in the diversity of the *Phasmarhabditis* microbial community.

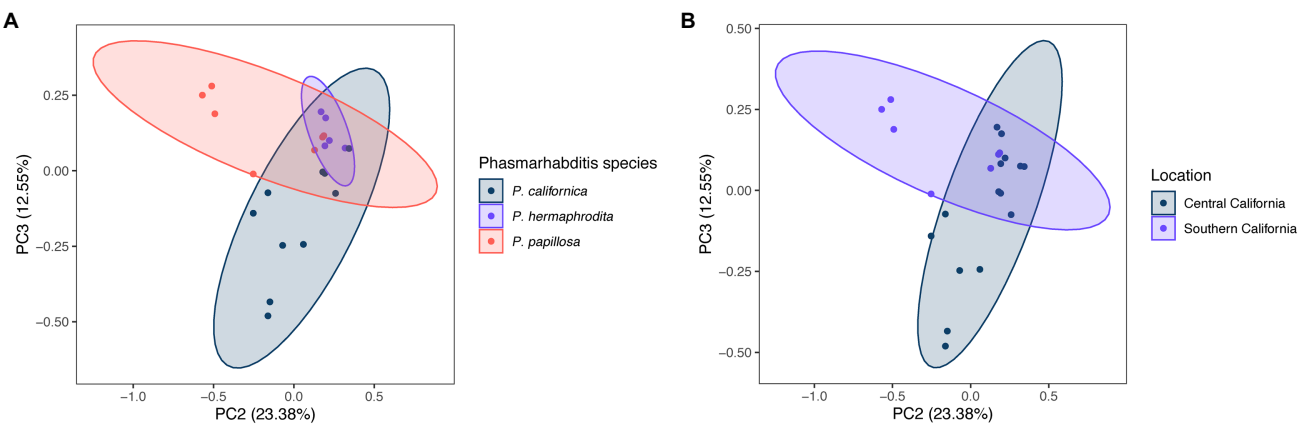

FIGURE 3 | Principal coordinate analysis (PCoA) plots of nematode microbial community's based on Bray Curtis distance. PCoA plots showing **(A)** *Phasmarhabditis* species and **(B)** location. Percent variance explained is shown in parentheses for each axis. Ellipses show 95% CI.

Our findings are not entirely congruent with the previous *Phasmarhabditis* microbial community work. Similar to previous studies, we identified *Acinetobacter* and *Pseudomonas* spp. occurring on *Phasmarhabditis*, however, no previous studies identified predominant bacteria like *Shewanella*, Aeromonadaceae, or *C. perfringens* which were identified in this study (Wilson et al., 1995a; Rae et al., 2010; Howe et al., 2020; Sheehy et al., 2022). Pseudomonaceae and *Acinetobacter* species were enriched in some clusters of *Phasmarhabditis* nematodes, specifically cluster IV which consisted of *P. papillosa* (**Figure 6**). *Acinetobacter* and Pseudomonaceae bacteria are commonly found in the soil and have been discovered in multiple gastropod species

TABLE 1 | permANOVA analysis reveals the microbial differences between gastropod hosts, locations, *Phasmarhabditis* species, or washed/unwashed/slug tissue.

	Overall value of *p*	Group 1	Group 2	Pseudo-F	*p*	*q*
Gastropod host	***p* = 0.017**	*Ambigolimax valentianus*	*Deroceras laeve*	0.834	0.578	0.578
		Ambigolimax valentianus	*Deroceras reticulatum*	2.569	**0.02**	0.06
		Deroceras laeve	*Deroceras reticulatum*	2.109	0.056	0.084
Location	***p* = 0.007**	Central California	Southern California	3.028	**0.007**	**0.007**
Phasmarhabditis species	***p* = 0.003**	*Phasmarhabditis californica*	*Phasmarhabditis hermaphrodita*	1.989	0.093	0.093
		Phasmarhabditis californica	*Phasmarhabditis papillosa*	3.148	**0.005**	**0.015**
		Phasmarhabditis hermaphrodita	*Phasmarhabditis papillosa*	2.303	0.056	0.084
Collection strategy	$p = 0.61$	Slug tissue	Unwashed	0.861	0.49	0.735
		Slug tissue	Washed	1.249	0.255	0.735
		Unwashed	Washed	0.473	0.877	0.877

Bolded values indicate statistical significance.

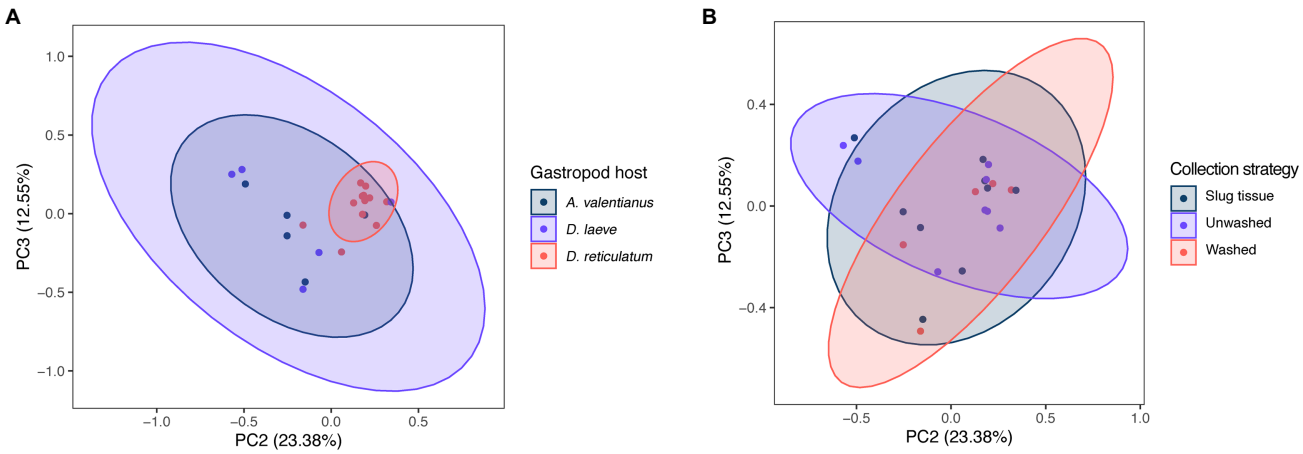

FIGURE 4 | PCoA plots of nematode microbial community of different gastropod hosts, based on Bray Curtis distance. PCoA plots with samples clustered by **(A)** gastropod host and **(B)** collection strategy; % variance explained shown in parentheses for each axis. Ellipses show 95% CI.

(Ducklow et al., 1981; Wilson et al., 1993a; Ekperigin, 2007; Villena et al., 2010; Joynson et al., 2017; Howe et al., 2020; Jackson, 2020). It was previously found that unhealthy *Biomphalaria glabrata* snails had a core microbial community predominantly made up of *Acinetobacter* and *Moraxella* spp.; however, healthy snails had a microbial community predominantly made up of *Pseudomonas* spp. (Ducklow et al., 1981). It is possible that *Phasmarhabditis* and gastropods thrive with *Pseudomonas* spp., and the presence of other species like *Acinetobacter* or *Moraxella* spp. (the bacterial species used to mass produce Nemaslug®) in *Phasmarhabditis* cause increased pathogenicity. However, this hypothesis is disputed from a finding that showed that rearing *Phasmarhabditis* on *Acinetobacter* had no effect on its virulence (Nermut et al., 2014). The interesting pattern in which only *P. papillosa* (discovered only in Southern California) have both increased Pseudomonaceae and *Acinetobacter* needs more study. This pattern may be due to the bacterial diversity and population and potential dominance at the collection site, or a species-specific relationship with *P. papillosa*. However, another possibility is that *Phasmarhabditis* uses some of the predominant bacterial species as a major food source, and others as contributors toward virulence, or perhaps some bacteria are used as both food and a driver for pathogenesis. Since *Acinetobacter* and Pseudomonaceae are frequently found in soils and are not commonly known as highly virulent bacteria, it is possible that these predominant bacteria are used as a food source rather than enhance or contribute to pathogenicity. This hypothesis is further supported by the observation that *Phasmarhabditis* grew exceptionally well on agar cultured with *P. fluorescens* (isolate 141) or *P. fluorescens* PSG strain compared to other bacterial species. The *Pseudomonas* bacteria was still not selected for use in the commercial production of Nemaslug® possibly because it was not associated with the highest mortality rates, suggesting its role as a food source for the nematodes rather than a source of virulence (Wilson et al., 1995a,b).

Shewanella has been discovered in multiple gastropod species where it causes increased pathogenicity, however all studies which identified this were performed in aquatic environments (Cai et al., 2006; Wang et al., 2008). The finding of an association of *Shewanella* with *Phasmarhabditis* has not previously been reported. The bacteria were not detected in any *P. californica* isolates (**Figure 5**). This may have been due to a limited sample size throughout the study, or due to a random association of bacteria with *Phasmarhabditis*, as hypothesized in 2010

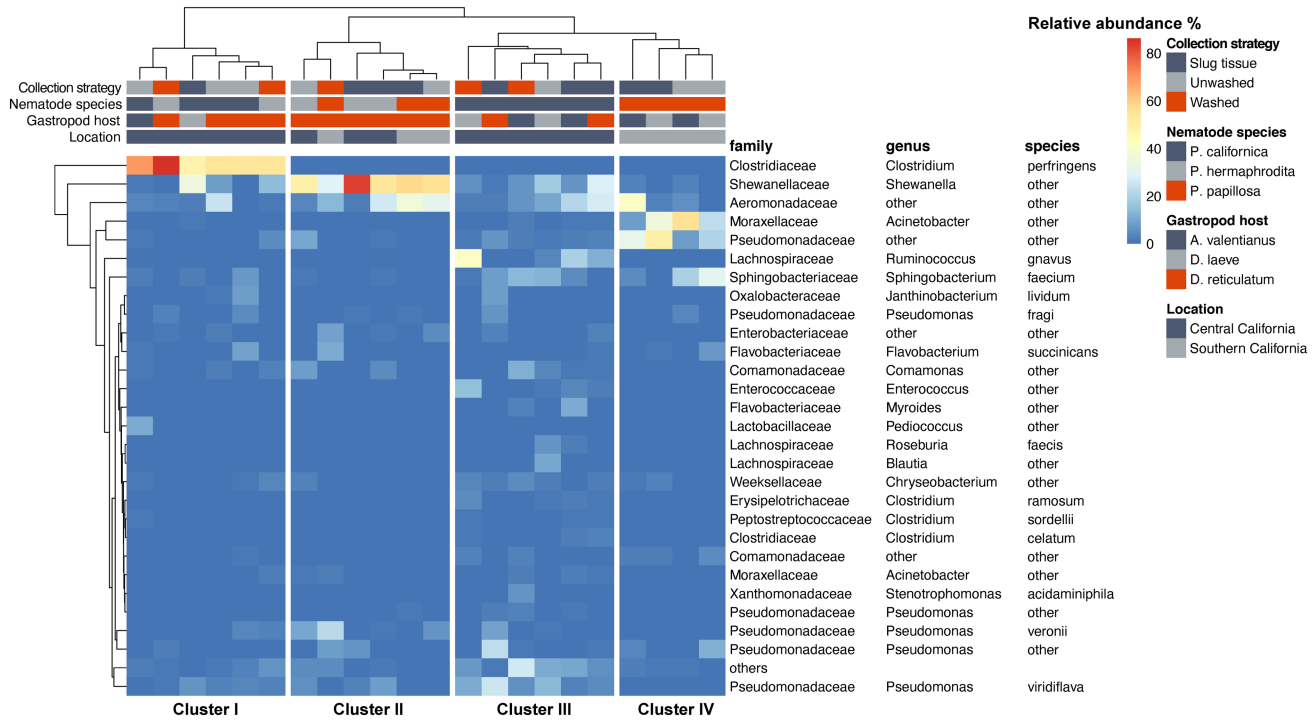

FIGURE 5 | Heatmap of the nematode microbial community at species level. Species with relative abundance >5% across all samples are displayed.

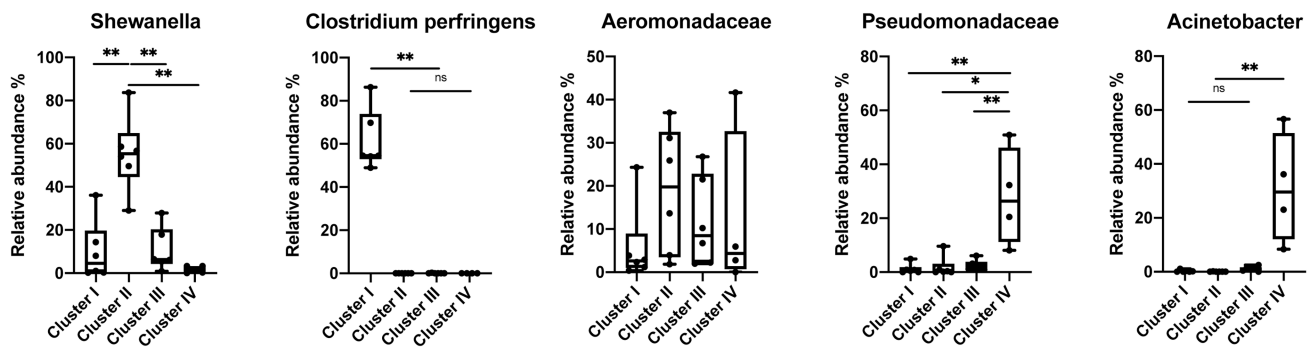

FIGURE 6 | Relative abundance of the most abundant species in the *Phasmarhabditis* species. Mann–Whitney U-test, $*p < 0.05$; $**p < 0.01$. Boxplots show inter-quartile range, whiskers minimum to maximum.

(Rae et al., 2010). However, *P. californica* had the largest representation throughout this study with a total of 10 utilized isolates (**Supplementary Table 1**). The occurrence of this predominant species may be indicative of it being used as a source of virulence toward the gastropod host; however further research is needed to assess this possibility.

Multiple gastropod species have been found associated with *Clostridium* bacteria (Charrier et al., 2006; Li, 2012). However, like *Shewanella*, the species *C. perfringens* had not previously been found in *Phasmarhabditis* or other nematodes. *C. perfringens* is most well known as a causative agent of food poisoning in mammals (Labbe, 1991). The species is frequently searched for and reported in foods for the sake of public health. There are over 1 million cases of poisoning from *C. perfringens* each year (Grass et al., 2013). A previous study demonstrated that *C. perfringens* enterotoxin could cause intestinal illness of mammals, and potentially fish and frogs (Robertson et al., 2010). However, it is not known how this bacterium affects gastropods and nematodes. *Phasmarhabditis* nematodes may serve as vectors for *C. perfringens*, using the bacteria as a weapon to kill their gastropod host. However, this seems less likely since it has been found that some gastropods can naturally harbor and vector the bacteria. It was previously thought that *C. perfringens* was only capable of reproducing in mammals and other endothermic organisms, and therefore only these organisms

could vector the pathogenic bacteria. More recently it was found that ectotherms such as gastropods, frogs, and fish can also vector the bacteria and therefore these organisms should be monitored as sources of contamination (Frick et al., 2018). Our finding of these bacteria furthers the claim that ectotherms, specifically gastropod-associated nematodes, can act as vectors. However, it was only discovered in cluster I which consisted of *P. californica* and *P. hermaphrodita*. It is possible that only *P. californica*, and *P. hermaphrodita* use *C. perfringens* as a source of virulence. However, further study is needed.

The most predominant bacterial family found throughout all *Phasmarhabditis* species was Aeromonadaceae. This family was found in similar abundance across all species and served as the only predominant commonality within the genus. The family has not previously been found within *Phasmarhabditis* and is not common in many nematodes, but it has been discovered within multiple gastropod species (Villena et al., 2010; Li et al., 2019). It is possible that *Phasmarhabditis* largely assumes the microbial diversity of its gastropod host. However, this hypothesis needs further experimentation. Since Aeromonadaceae is not commonly known to be highly pathogenic to a variety of organisms and it was the most predominant species across all *Phasmarhabditis* nematodes, it can be hypothesized that *Phasmarhabditis* species utilize the bacteria as a major food source rather than a source of virulence. *Phasmarhabditis hermaphrodita* and other members of the genus are known to be bacterivorous (Tan and Grewal, 2001b). However, their food preferences at collection sites are unknown. *Phasmarhabditis hermaphrodita* has been found to grow well when reared on monoxenic cultures of *P. fluorescens*, but this does not prove its preferred bacterial food source in a native setting (Wilson et al., 1995b). Further experimentation may draw out explanations for the clustering of Aeromonadaceae observed in clusters III and IV within *P. californica* and *P. papillosa* (**Figure 5**).

Future work to assess the microbial diversity of *Phasmarhabditis* needs to utilize next generation sequencing technology and nematodes which have not been maintained in culture for a long period of time. Further microbial community work with the species from this study (*P. californica*, *P. hermaphrodita*, and *P. papillosa*) should be done in order to obtain more isolates for statistical power in identifying the microbial community of the species. Further study would also lead to the possibility of work with less discrepancies in read counts as we observed. Study of other *Phasmarhabditis* species microbial community should also be assessed in order to determine other species-specific microbial patterns. It is likely that the maintenance of nematodes in culture on specific media can influence the microbiota (Dirksen et al., 2016). It was recently found that *C. elegans* native microbial community differs from the previously described microbial community, and its microbial community has some consistencies across time at the genus level but can be influenced by various substrates and present bacteria. Interestingly, one of the consistent genera in *C. elegans* is *Pseudomonas*, which was one of the predominant bacteria we identified which may serve as a major food source for *Phasmarhabditis* (Dirksen et al., 2016; Johnke et al., 2020). To understand the natural relationships and mechanisms between *Phasmarhabditis* and their hosts, native isolates must be utilized. Next generation sequencing technologies allow for rapid sequencing and identification of these isolates and their microbial communities upon collection, allowing for easy assessment of the native microbial flora and their potential interactions.

DATA AVAILABILITY STATEMENT

The datasets presented in this study can be found in online repositories. The names of the repository/repositories and accession number(s) can be found in the article/**Supplementary Material**. The 16S sequence data has been deposited in NCBI under BioProject PRJNA816167.

AUTHOR CONTRIBUTIONS

JS, IL, AH, and AD: conceptualization; JS, RL, SA, and AH: methodology and software; JS, RL, AH, and AD: validation and original draft preparation; JS, RL, and SA: formal analysis and investigation; IL, AH, and AD: resources and funding acquisition; JS, RL, and AH: data curation; JS, RL, SA, IL, AH, and AD: writing; JS, RL, IL, AH, and AD: writing—review and editing; JS and RL: visualization; and AH and AD: supervision and project administration. All authors have read and agreed to the published version of the manuscript.

FUNDING

The work was supported by the United States Department of Agriculture Specialty Crop Multi-State Program (USDA-SCMP) in partnership with CDFA (2018–2022 grant #12509488), a generous gift (2019–2022) from CANERS Foundation through the California Association of Nurseries and Garden Centers (CANGC), Plant California Alliance (PCA), and National Institutes of Health GM124724.

ACKNOWLEDGMENTS

We would like to acknowledge Rory McDonnell who has assisted in our project development as well as our identification of gastropods. We would also like to acknowledge Dee Denver for his assistance in project development, and Kyle Anesko for his assistance with gastropod maintenance.

SUPPLEMENTARY MATERIAL

The Supplementary Material for this article can be found online at: https://www.frontiersin.org/articles/10.3389/fmicb.2022.903136/full#supplementary-material

REFERENCES

An, R., Sreevatsan, S., and Grewal, P. S. (2008). *Moraxella osloensis* gene expression in the slug host *Deroceras reticulatum*. *BMC Microbiol.* 8:19. doi: 10.1186/1471-2180-8-19

Bokulich, N. A., Kaehler, B. D., Rideout, J. R., Dillon, M., Bolyen, E., Knight, R., et al. (2018). Optimizing taxonomic classification of marker gene amplicon sequences. *PeerJ* 6:p.e3208v2. doi: 10.1186/s40168-018-0470-z

Bolyen, E., Rideout, J. R., Dillon, M. R., Bokulich, N. A., Abnet, C. C., Al-Ghalith, G. A., et al. (2019). Reproducible, interactive, scalable and extensible microbiome data science using QIIME 2. *Nat. Biotechnol.* 37, 852–857. doi: 10.1038/s41587-019-0209-9

Bongers, T., and Bongers, M. (1998). Functional diversity of nematodes. *Appl. Soil Ecol.* 10, 239–251. doi: 10.1016/S0929-1393(98)00123-1

Cai, J., Chen, H., Thompson, K. D., and Li, C. (2006). Isolation and identification of *Shewanella* alga and its pathogenic effects on post-larvae of abalone *Haliotis diversicolor* supertexta. *J. Fish Dis.* 29, 505–508. doi: 10.1111/j.1365-2761.2006.00732.x

Charrier, M. Y., Fonty, G., Gaillard-Martinie, B., Ainouche, K., and Andant, G. (2006). Isolation and characterization of cultivable fermentative bacteria from the intestine of two edible snails, *Helixpomatia* and *Cornu aspersum* (Gastropoda: Pulmonata). *Biol. Res.* 39, 669–681. doi: 10.4067/S0716-97602006000500010

De Ley, P. (2006). "A quick tour of nematode diverity and the backbone of nematode phylogeny," in *Wormbook: The Online Review of C. elegans Biology* (Pasadena, CA: Wormbook), 2005–2018.

Dirksen, P., Marsh, S. A., Braker, I., Heitland, N., Wagner, S., Nakad, R., et al. (2016). The native microbiome of the nematode *Caenorhabditis elegans*: gateway to a new host-microbiome model. *BMC Biol.* 14, 1–16. doi: 10.1186/s12915-016-0258-1

Ducklow, H. W., Clausen, K., and Mitchell, R. (1981). Ecology of bacterial communities in the schistosomiasis vector snail *Biomphalaria glabrata*. *Microb. Ecol.* 7, 253–274. doi: 10.1007/BF02010308

Ekperigin, M. M. (2007). Preliminary studies of cellulase production by *Acinetobacter anitratus* and *Branhamella* sp. *Afr. J. Biotechnol.* 6, 634–649.

Frick, C., Vierhellig, J., Linke, R., Savio, D., Zornig, H., Antensteiner, R., et al. (2018). Poikilothermic animals as a previously unrecognized source of fecal indicator bacteria in a backwater ecosystem of a large river. *Appl. Environ. Microbiol.* 84, e00715–e00718. doi: 10.1128/AEM.00715-18

Grass, J. E., Gould, L. H., and Mahon, B. E. (2013). Epidemiology of foodborne disease outbreaks caused by *Clostridium perfringens*, United States, 1998-2010. *Foodborne Pathog. Dis.* 10, 131–136. doi: 10.1089/fpd.2012.1316

Grewal, P., and Georgis, R. (1997). "Entomopathogenic nematodes," in *Biopesticides: Use and Delivery*. *Vol. 5*. eds. F. R. Hall and J. J. Menn (Totowa, NJ: Humana Press), 271–299.

Grewal, S. K., and Grewal, P. S. (2003). Survival of earthworms exposed to the slug-parasitic nematode *Phasmarhabditis hermaphrodita*. *J. Invertebr. Pathol.* 82, 72–74. doi: 10.1016/S0022-2011(02)00200-8

Howe, D. K., Ha, A. D., Colton, A., Tandingan De Ley, I., Rae, R. G., Ross, J., et al. (2020). Phylogenetic evidence for the invasion of a commercialized European *Phasmarhabditis hermaphrodita* lineage into North America and New Zealand. *PLOS One* 15:e0237249. doi: 10.1371/journal.pone.0237249

Iglesias, J., Castillejo, J., and Castro, R. (2003). The effects of repeated applications of the molluscicide metaldehyde and the biocontrol nematode *Phasmarhabditis hermaphrodita* on molluscs, earthworms, nematodes, acarids and collembolans: a two year study in north-west Spain. *Pest Manag. Sci.* 59, 1217–1224. doi: 10.1002/ps.758

Ingham, R. E. (1994). "Nematodes," in *Methods of Soil Analysis, Part 2, Microbiological and Biochemical Properties*, eds. R. W. Weaver, J. S. Angle and P. S. Bottomley (Madison, WI: Soil Science Society of America), 459–490.

Jackson, D. (2020). *Elucidating the Influences of an Invasive Slug on Soil Bacterial Communities*. University of California, Riverside.

Jackson, D., Maltz, M. R., Freund, H. L., Borneman, J., and Aronson, E. (2021). Environment and diet influence the bacterial microbiome of *Ambigolimax valentianus*, and invasive slug in California. *Insects* 12:575. doi: 10.3390/insects12070575

Johnke, J., Dirksen, P., and Schulenburg, H. (2020). Community assembly of the native *C. elegans* microbiome is influenced by time, substrate, and individual bacterial taxa. *Environ. Microbiol.* 22, 1265–1279. doi: 10.1111/1462-2920.14932

Joynson, R., Pritchard, L., Osemwekha, E., and Ferry, N. (2017). Metagenomic analysis of the gut microbiome of the common black slug *Arion ater* in search of novel lignocellulose degrading enzymes. *Front. Microbiol.* 8:2181. doi: 10.3389/fmicb.2017.02181

Kaya, H. K. (1993). Entomopathogenic nematodes. *Annu. Rev. Entomol.* 38, 181–206. doi: 10.1146/annurev.en.38.010193.001145

Labbe, R. G. (1991). Clostridium perfringens. *J. Assoc. Off. Anal. Chem.* 74, 711–714. doi: 10.1093/jaoac/74.4.711

Li, K. (2012). Molecular analysis of intestinal bacterial communities in *Cipangopaludina chinensis* used in aquatic ecological restorations. *Ecol. Eng.* 39, 36–39. doi: 10.1016/j.ecoleng.2011.11.013

Li, L. H., Lv, S., Lu, Y., Bi, D. Q., Guo, Y. H., Wu, J. T., et al. (2019). Spatial structure of the microbiome in the gut of *Pomacea canaliculata*. *BMC Microbiol.* 19, 1–9. doi: 10.1186/s12866-019-1661-x

Marilyn, S. E. (2008). "*Ascaris lumbricoides*: a review of its epidemiology and relationship to other infections," in *Annales Nestle (English ed.)*, *Vol. 66*, 7–22. doi: 10.1159/000113305

McDonald, D., Price, M. N., Goodrich, J., Nawrocki, E. P., DeSantis, T. Z., Probst, A., et al. (2012). An improved greengenes taxonomy with explicit ranks for ecological and evolutionary analyses of bacteria and archaea. *ISME J.* 6, 610–618. doi: 10.1038/ismej.2011.139

McDonnell, R. J., Colton, A. J., Howe, D. K., and Denver, D. R. (2020). Lethality of four species of *Phasmarhabditis* (Nematoda: Rhabditidae) to the invasive slug, *Deroceras reticulatum* (Gastropoda: Agriolimacidae) in laboratory infectivity trials. *Biol. Control* 150:104349. doi: 10.1016/j.biocontrol.2020.104349

Nardo, E. A. B. d., Sindermann, A. B., Grewal, S. K., and Grewal, P. S. (2010). Non-susceptibility of earthworm *Eisenia fetida* to the Rhabditid nematode *Phasmarhabditis hermaphrodita*, a biocontrol agent of slugs. *Biocontrol Sci. Tech.* 14, 93–98. doi: 10.1080/09583150310001516 93

Nermut, J., Puza, V., and Mracek, Z. (2014). The effect of different growing substrates on the development and quality of *Phasmarhabditis hermaphrodita* (Nematoda: Rhabditidae). *Biocontrol Sci. Tech.* 24, 1026–1038. doi: 10.1080/09583157.2014.915926

Ogier, J. C., Pages, S., Frayssinet, M., and Gaudriault, S. (2020). Entomopathogenic nematode-associated microbiota: from monoxenic paradigm to pathobiome. *Microbiome* 8, 1–17. doi: 10.1186/s40168-020-00800-5

Rae, R. G., Robertson, J., and Wilson, M. J. (2007a). Susceptibility of indigenous UK earthworms and an invasive pest flatworm to the slug parasitic nematode *Phasmarhabditis hermaphrodita*. *Biocontrol Sci. Tech.* 15, 623–626. doi: 10.1080/09583150500086870

Rae, R. G., Tourna, M., and Wilson, M. J. (2010). The slug parasitic nematode *Phasmarhabditis hermaphrodita* associates with complex and variable bacterial assemblages that do not affect its virulence. *J. Invertebr. Pathol.* 104, 222–226. doi: 10.1016/j.jip.2010.04.008

Rae, R., Verdun, C., Grewal, P. S., Robertson, J. F., and Wilson, M. J. (2007b). Biological control of terrestrial molluscs using *Phasmarhabditis hermaphrodita* progress and prospects. *Pest Manag. Sci.* 63, 1153–1164. doi: 10.1002/ps.1424

Riddle, D., Blumenthal, T., Meyer, B. J., and James, R. (1997). *C. Elegans II. 2nd Edn*. Cold Spring Harbor, NY: Cold Spring Harbor Laboratory Press.

Robertson, S. L., Smedley, J. G. III, and McClane, B. A. (2010). Identification of a claudin-4 residue important for mediating the host cell binding action of *Clostridium perfringens* enterotoxin. *Infect. Immun.* 78, 505–517. doi: 10.1128/IAI.00778-09

Robeson, M. S., O'Rourke, D. R., Kaehler, B. D., Ziemski, M., Dillon, M. R., Foster, J. T., et al. (2020). RESCRIPt: reproducible sequence taxonomy reference database management for the masses. bioRxiv [Preprint]. doi: 10.1101/2020.10.05.326504

Schafer, W. (2016). Nematode nervous systems. *Curr. Biol.* 26, R955–R959. doi: 10.1016/j.cub.2016.07.044

Schurkman, J., Dodge, C., McDonnell, R., de Ley, I. T., and Dillman, A. R. (2022a). Lethality of *Phasmarhabditis* spp. (*P. hermaphrodita, P. californica, and P. papillosa*) nematodes to the grey field slug *Deroceras reticulatum* on canna lilies in a lath house. *Agronomy* 12:20. doi: 10.3390/agronomy12010020

Schurkman, J., Tandingan De Ley, I., Anesko, K., Paine, T., McDonnell, R., and Dillman, A. R. (2022b). Distribution of *Phasmarhabditis* (Nematoda:

Rhabditidae) and their gastropod hosts in California plant nurseries and garden centers. *Review* 13. doi: 10.3389/fpls.2022.856863

Sheehy, L., Cutler, J., Weedall, G. D., and Rae, R. (2022). Microbiome analysis of malacopathogenic nematodes suggests no evidence of a single bacterial symbiont responsible for gastropod mortality. *Front. Immunol.* 13:878783. doi: 10.3389/fimmu.2022.878783

Tan, L., and Grewal, P. S. (2001a). Infection behavior of the rhabditid nematode *Phasmarhabditis hermaphrodita* to the grey garden slug *Deroceras reticulatum*. *J. Parasitol.* 87, 1349–1354. doi: 10.1645/0022-3395(2001)087[1349:IBOTRN]2.0.CO;2

Tan, L., and Grewal, P. S. (2001b). Pathogenicity of *Moraxella osloensis*, a bacterium associated with the nematode *Phasmarhabditis hermaphrodita*, to the slug *Deroceras reticulatum*. *Appl. Environ. Microbiol.* 67, 5010–5016. doi: 10.1128/AEM.67.11.5010-5016.2001

Tandingan De Ley, I., Holovachov, O., McDonnell, R. J., Bert, W., Paine, T. D., and De Ley, P. (2016). Description of *Phasmarhabditis californica* n. sp. and first report of *P. papillosa* (Nematoda: Rhabditidae) from invasive slugs in the USA. *Nematology* 18, 175–193. doi: 10.1163/15685411-00002952

Tandingan De Ley, I., McDonnell, R., Lopez, S., Paine, T. D., and De Ley, P. (2014). *Phasmarhabditis hermaphrodita* (Nematoda: Rhabditidae), a potential biocontrol agent isolated for the first time from invasive slugs from North America. *Nematology* 16, 1129–1138. doi: 10.1163/15685411-00002838

Tandingan De Ley, I., Schurkman, J., Wilen, C., and Dillman, A. R. (2020). Mortality of the invasive white garden snail *Theba pisana* exposed to three US isolates of *Phasmarhabditis* spp (*P. hermaphrodita, P. californica, and P. papillosa*). *PLOS One* 15:e0228244. doi: 10.1371/journal.pone.0228244

Thompson, L. R., Sanders, J. G., McDonald, D., Amir, A., Ladau, J., Locey, K. J., et al. (2017). A communal catalogue reveals Earth's multiscale microbial diversity. *Nature* 551, 457–463. doi: 10.1038/nature24621

Villena, A. M., Morales, C. S., Soto, P. J., and Enciso, H. M. (2010). Bacterial flora in the digestive tract of *Helix aspersa* muller snails under two breeding systems. *Rev. de Investig. Vet. del Peru.* 21, 100–105.

Walker, A. J., Glen, D. M., and Shewry, P. R. (1999). Bacteria associated with the digestive system of the slug *Deroceras reticulatum* are not required for protein digestion. *Soil Biol. Biochem.* 31, 1387–1394. doi: 10.1016/S0038-0717(99)00054-1

Wang, X. J., Yu, R. C., Luo, X., Zhou, M. J., and Lin, X. T. (2008). Toxin-screening and identification of bacteria isolated from highly toxic marine gastropod *Nassarius semiplicatus*. *Toxicon* 52, 55–61. doi: 10.1016/j.toxicon.2008.04.170

Wilson, M. J., Glen, D. M., George, S. K., and Butler, R. C. (1993a). Mass cultivation and storage of the rhabditid nematode *Phasmarhabditis hermaphrodita*, a biocontrol agent for slugs. *Biocontrol Sci. Tech.* 3, 513–521. doi: 10.1080/09583159309355307

Wilson, M. J., Glen, D. M., George, S. K., Glen, D. M., and The, S. K. G. (1993b). The rhabditid nematode *Phasmarhabditis hermaphrodita* as a potential biological control agent for slugs. *Biocontrol Sci. Tech.* 3, 503–511. doi: 10.1080/09583159309355306

Wilson, M. J., Glen, D. M., George, S. K., and Pearce, J. D. (1995a). Selection of a bacterium for the mass production of *Phasmarhabditis hermaphrodita* (Nematoda: Rhabditidae) as a biocontrol agent for slugs. *Fundam. Appl. Nematol.* 18, 419–425.

Wilson, M. J., Glen, S. K., George, S. K., Pearce, J. D., and Wiltshire, C. W. (1994a). Biological control of slugs in winter wheat using the rhabditid nematode *Phasmarhabditis hermaphrodita*. *Ann. Appl. Biol.* 125, 377–390. doi: 10.1111/j.1744-7348.1994.tb04978.x

Wilson, M. J., Glen, D. M., Hughes, L. A., Pearce, J. D., and Rodgers, P. B. (1994b). Laboratory tests of the potential of entomopathogenic nematodes for the control of field slugs (*Deroceras reticulatum*). *J. Invertebr. Pathol.* 64, 182–187. doi: 10.1016/S0022-2011(94)90100-7

Wilson, M. J., Glen, D. M., Pearce, J. D., and Rodgers, P. B. (1995b). Monoxenic culture of the slug parasite *Phasmarhabditis hermaphrodita* (Nematoda: Rhabditidae) with different bacteria in liquid and solid phase. *Fundam. Appl. Nematol.* 18, 159–166.

Wilson, M. J., and Rae, R. (2015). "*Phasmarhabditis hermaphrodita* as a control agent for slugs," in *Nematode Pathogenesis of Insects and Other Pests. Sustainability in Plant and Crop Protection*. ed. R. Campos-Herrera (Cham: Springer).

Conflict of Interest: IL is a co-inventor on a patent entitled Mollusk-killing Biopesticide (WO2017059342A1).

The remaining authors declare that the research was conducted in the absence of any commercial or financial relationships that could be construed as a potential conflict of interest.

Publisher's Note: All claims expressed in this article are solely those of the authors and do not necessarily represent those of their affiliated organizations, or those of the publisher, the editors and the reviewers. Any product that may be evaluated in this article, or claim that may be made by its manufacturer, is not guaranteed or endorsed by the publisher.

frontiers | Frontiers in Microbiology

ORIGINAL RESEARCH
published: 18 July 2022
doi: 10.3389/fmicb.2022.914124

Insights of Host Physiological Parameters and Gut Microbiome of Indian Type 2 Diabetic Patients Visualized *via* Metagenomics and Machine Learning Approaches

Debjit De[1], *Tilak Nayak*[1], *Subhankar Chowdhury*[2] *and Paltu Kumar Dhal*[1]*

[1] *Department of Life Science and Biotechnology, Jadavpur University, Kolkata, India,* [2] *Department of Endocrinology, Institute of Post Graduate Medical Education and Research (IPGMER) and SSKM Hospital, Kolkata, India*

OPEN ACCESS

Edited by:
Punyasloke Bhadury, Indian Institute of Science Education and Research Kolkata, India

Reviewed by:
Sundus Javed, COMSATS University, Pakistan
Rebiya Nuli, Xinjiang Medical University, China

***Correspondence:**
Paltu Kumar Dhal
paltuk.dhal@jadavpuruniversity.in

Specialty section:
This article was submitted to Microbial Symbioses, a section of the journal Frontiers in Microbiology

Received: *06 April 2022*
Accepted: *13 June 2022*
Published: *18 July 2022*

Citation:
De D, Nayak T, Chowdhury S and Dhal PK (2022) Insights of Host Physiological Parameters and Gut Microbiome of Indian Type 2 Diabetic Patients Visualized via Metagenomics and Machine Learning Approaches. Front. Microbiol. 13:914124. doi: 10.3389/fmicb.2022.914124

Type 2 diabetes (T2D) is a serious public health issue and may also contribute to modification in the structure of the intestinal microbiota, implying a link between T2D and microbial inhabitants in the digestive tract. This work aimed to develop efficient models for identifying essential physiological markers for improved T2D classification using machine learning algorithms. Using amplicon metagenomic approaches, an effort has also been made to understand the alterations in core gut microbial members in Indian T2D patients with respect to their control normal glucose tolerance (NGT). Our data indicate the level of fasting blood glucose (FBG) and glycated hemoglobin (HbA1c) were the most useful physiological indicators while random forest and support vector machine with RBF Kernel were effective predictions models for identifications of T2D. The dominating gut microbial members *Allopreotella*, *Rikenellaceae RC9 gut group*, *Haemophilus*, *Ruminococcus torques group*, etc. in Indian T2D patients showed a strong association with both FBG and HbA1c. These members have been reported to have a crucial role in gut barrier breakdown, blood glucose, and lipopolysaccharide level escalation, or as biomarkers. While the dominant NGT microbiota (*Akkermansia*, *Ligilactobacillus*, *Enterobacter*, etc.) in the colon has been shown to influence inflammatory immune responses by acting as an anti-inflammatory agent and maintaining the gut barrier. The topology study of co-occurrence network analysis indicates that changes in network complexity in T2D lead to variations in the different gut microbial members compared to NGT. These studies provide a better understanding of the gut microbial diversity in Indian T2D patients and show the way for the development of valuable diagnostics strategies to improve the prediction and modulation of the T2D along with already established methods.

Keywords: type 2 diabetes, gut microbiota, machine learning, feature selection, microbial communities

INTRODUCTION

Type 2 diabetes (T2D) is a metabolic disorder that affects people all over the world and is caused by both inherited and environmental factors, such as physical inactivity, sedentary lifestyles, cigarette smoking, and excessive alcohol use because these factors create stress on a pancreatic β-cells resulting in decreased insulin sensitivity and production. Due to the β-cell dysfunction, both normal blood glucose level and insulin sensitivity are gradually hampered, resulting in pathophysiological changes and the development of several complications in patients (McIntyre et al., 2019). According to International Diabetes Federation (IDF) report, a total of 415 million people have diabetes globally (as of 2015) and this may increase to 642 million by 2040 because of T2D (Zhang et al., 2013, 2021a; Cho et al., 2018). Several mathematical and statistical models were established using human physiological parameters to predict the disease and/or risk of the disease, machine learning (ML) is one of them. Machine learning is a useful statistical method to analyze high-dimensional and multimodal biomedical data and disease diagnostics (Yu et al., 2020). Several studies endorsed the discrimination between T2D and normal person normal glucose tolerance (NGT) using different ML models based on patients' physiological conditions (Zhang et al., 2021b). However, most of those studied models made their observations based on the limited number of samples from a single geographical location. Additionally, none of them attempted to identify important physiological parameters out of their prediction model that significantly differentiates T2D disease from NGT. While best prediction model with high accuracy essentially needed a large sample size with variant coverage (Wei et al., 2013; Arbabshirani et al., 2017).

The recent developments have indicated that along with the host's genetics, gut microbiota plays a very important role in the establishment of obesity and T2D (Karlsson et al., 2013; Bhute et al., 2017; Sroka-Oleksiak et al., 2020). Over the past decade around the world, significant efforts have been given by various groups to define the structural and functional attributes of gut microbiota in T2D subjects to NGT to understand the disease progression (Bhute et al., 2017; Gaike et al., 2020). Most of these studies attempted to evaluate the differences in gut microbial members either between T2D and pre-T2D with NGT or between gut microbiome after the treatment of the disease. However, the deep study on predicting the most important influencing physiological factors and their association with gut microbes in disease states is incompletely explained while none from India have been reported. Nevertheless, this investigation attempted to make the following contributions:

1) Introduce the most effective machine learning (ML) methods for better T2D and NGT predictions, as well as the most critical physiological parameters for detecting the disease regardless of its geographical location.
2) Analyze the variations in core gut microbial members between Indian T2D and NGT, and discover the differentially abundant core gut microbial genera, as well as their relationship to key physiological parameters.
3) Identify the specific microbial genera for each group (T2D and NGT) as crucial indicators for disease prediction and diagnosis using established physiological measures.

MATERIALS AND METHODS

Feature Selection Approached Based on Machine Learning Techniques (MLT) and Evaluates the Prediction Model

Data Collection

For this study, the relevant physiological records of a total of 441 patient samples (T2D: 224 and NGT: 217) were considered. Among them, 345 data were obtained from Chinese cohorts (Qin et al., 2012) and 96 data from European cohorts (Karlsson et al., 2013). The physiological parameters included in our study were age, gender, body mass index (BMI), fasting blood glucose (FBG), fasting insulin (FI), hemoglobin A1c (HbA1c), cholesterol (CHL), high-density lipoproteins (HDL), low-density lipoproteins (LDL), triglycerides (TG), and C-peptide (CP).

Preparation of Training, Testing, and Blind/Identification Dataset

From 441 patients' physiological parameters data, we randomly generated a training dataset (with 150 samples) to train a prediction model and a testing dataset (with 150 samples) to assess the performance and ability to discriminate between two different classes (T2D and NGT) (Barman et al., 2014). A known blind/identification dataset was produced from the remaining 141 samples, but they were treated as an unknown dataset to evaluate the effectiveness of our predictive model. Finally, we applied this forecasting model to data obtained in Kolkata, West Bengal, and the surrounding areas (see sample collection section) to evaluate its performance on real-world unknown datasets.

Feature Selection and MLT

Feature selection improves the discrimination ability of the prediction model to relieve the over-fitting problem and help to better understand the data by examining the importance of the features (Saeys et al., 2007). Here, we used the recursive feature elimination (RFE) algorithm (Chen and Jeong, 2007) as a feature selection method to find out what was the best physiological parameters that showed higher discrimination ability between two classes using the "caret" R package (Kuhn, 2008). Random forest (RF) (Svetnik et al., 2003) and support vector machine (SVM) (Statnikov et al., 2013) were used for the prediction of T2D and NGT based on the physiological data. The prediction models were built up using 10-fold cross-validation methods.

Performance Checking of the Prediction Model

The performance of the prediction model was evaluated using the testing and blind datasets. To evaluate the performance of the prediction, they were assessed *via* sensitivity (SEN), specificity (SPF), accuracy (ACC), precision (PRC), and F1-score values. All these statistical analyses were performed in R (R, version 3.6.3) with the packages "randomForest" (Liaw and Wiener, 2002), "rfUtilities" (Evans and Murphy, 2019), "caret" (Kuhn, 2008),

"caTools" (Tuszynski and Tuszynski, 2007), "e1071" (Meyer et al., 2012), "verification" (Gilleland, 2015) and "pROC" (Robin et al., 2011).

Amplicon-Based Metagenomic Analysis of T2D and NGT Samples From West Bengal

Sample Selection and Collection

The samples were selected as per suggestion from the doctors of the endocrine department of IPGMER and SSKM Hospital, Kolkata, India based on World Health Organization (WHO) criteria, and anthropometric measurements were done from 34 samples (17 NGT and 17 T2D) from West Bengal at IPGMER and SSKM Hospital. Only newly diagnosed cases of T2D in males of age group above 25 years and up to 55 years, willing to take participation, were included in our study. The patients, in the age group below 25 years and above 55 years, already diagnosed or treated with insulin, were excluded from this study. The physiological parameters of all these samples were measured in the Endocrinology Lab of IPGMER and SSKM Hospital. The FI and CP were measured using Siemens Immulite Insulin and C-Peptide Kit and other remaining physiological data such as BMI, FBG, CHL, HDL, LDL, and TGL were measured by normal testing procedure (Zhang et al., 2013). The protocol and the project were approved by the ethics committee at SSKM Hospital.

The DNA Extraction and Amplicon Metagenomic Sequencing

The metagenomic DNA was extracted from the patients' fecal samples by using PowerFecal DNA Isolation Kit (Mo Bio, Catalog No. 12830-50) following the manufacturer's instructions. The extracted metagenomic DNA was pooled for the amplification of hypervariable V3–V4 regions of the bacterial 16S rRNA gene and sequenced them using the Illumina MiSeq platform (2×300 bp paired-end). The raw paired-end primer trimmed sequences were provided by Eurofins, India. All raw metagenomic DNA sequences were submitted to SRA–NCBI database (Accession No. PRJNA486712).

Sequence Processing and Taxonomy Classification

All the raw fastq datasets were processed by the following sequence processing protocol (Dhal et al., 2020; Nayak et al., 2021). For all 16S rRNA amplicon gene sequences from each sample, the quality screening was done by using Trimmomatic, version 0.33 (parameters: SLIDINGWINDOW: 4:15) (Bolger et al., 2014). High-quality sequence reads were then merged with PEAR, version 0.9.5 (Zhang et al., 2014), using default parameters. For operational taxonomy unit (OTU) clustering, SWARM, version 2.0, was used with default parameters (Mahé et al., 2014). Moreover, SINA tool was used for alignment and taxonomic classification using the SILVA ribosomal RNA gene database, version 138, as a reference sequence using the representative sequence per OTU (Pruesse et al., 2012). Absolute singletons OTUs, as well as unclassified sequences on phylum level, were removed from our dataset using our standardized R script.

Statistical Analysis

Principal component analysis (PCA) was done to understand the pattern among the two groups (T2D and NGT) of samples by utilizing their respective physiological data. To compare the physiological data of T2D and NGT groups, we used the Kruskal–Wallis rank–sum test.

Alpha (α) diversity analysis was done based on the rarefied data (minimum number of sequences among the samples) by sub-sampling the dataset. To assess the microbial communities' richness and evenness, OTU number (nOTU), inverse Simpson (invS), and Shannon diversity (shannon) were measured. The differences in α diversity between T2D and NGT were assessed by Wilcoxon rank–sum test. The unique and core bacterial members among the two groups (T2D and NGT) were identified by using Venny, version 2.1 (Oliveros, 2007), with genera that had >0.5% abundance. Spearman rank correlation was calculated to assess if there were any relationship between alpha-diversity and the physiological parameters and to identify the association between the physiological parameters and microbial genera.

For beta (β) diversity, OTUs data were pruned to exclude the rare biosphere by retaining OTUs that were present in one or more than one sequence in three or more than three samples. This reduction of the datasets did not change β diversity patterns (Mantel test; $r > 0.9$, $p = 0.001$). To test the differences in community-level (β diversity) among T2D and NGT groups permutational multivariate analysis of variance (PERMANOVA) was calculated. The contribution of physiological parameters for explaining the variation in community structure redundancy analysis (RDA) was calculated based on their centered log-transformed of pruned data using aldex.clr function with a median of 128 Monte Carlo Dirichlet of ALDEx2 R package. Forward model selection was carried out to assess which are the best physiological parameters to explain this variation in the community based on maximum adjusted R2 and minimum Akaike Information Criterion (AIC). The differentially abundant OTUs among the T2D and NGT groups were identified by using Dotplot. All statistical analyses, as well as figure visualizations, were performed in R, version 3.6.3, with the packages "vegan" (Oksanen et al., 2013) and "ALDEx2" (Fernandes et al., 2014), and the PCA plot was made using OriginPro 2021 software, version 9.8.0.200.

Co-Occurrence Network Analysis

The co-occurrence network analysis was performed to assess the complexity of the microbiome and identify potential keystone taxa for each group. The co-occurrence network was constructed with the OTUs that were present in 10% of samples and had more than 10 sequences for each group. We used Spearman's rank correlation to assess the association among microbial OTUs from each group. Moreover, $p = \leq 0.05$ and a Spearman's rank correlation coefficient, $\rho = \geq 0.6$ were selected as the thresholds between two OTUs (Jiao et al., 2016; Li et al., 2021). Two co-occurrence networks were built, the T2D co-occurrence network (TCN), and NGT co-occurrence network (NCN). The network's topology was measured by calculating the nodes, edges, average weighted degree, network diameter, graph density, modularity, average clustering coefficient, and average

TABLE 1 | Differences in physiological parameters between diabetes subjects and controls assess by Kruskal–Wallis rank–sum test.

Parameters	χ^2	DF	*p*
Body Mass Index (BMI)	0.001	1	0.9725
Fasting Blood Glucose (FBG)	11.640	1	0.0006*
Fasting Insulin (FI)	0.050	1	0.8228
Glycated hemoglobin (HbA1c)	13.233	1	0.0003*
C – Peptide (CP)	0.015	1	0.9040
Cholesterol (CHL)	0.323	1	0.5698
High Density Lipoprotein (HDL)	1.909	1	0.1671
Low Density Lipoprotein (LDL)	0.001	1	0.9725
Triglycerides (TGL)	0.058	1	0.8094

**Indicates highly significant.*

path length for each network. The network visualization and topology analysis were performed in the Gephi 0.9.2 (https://gephi.org/) visualization tool (Bastian et al., 2009). The role of nodes in individual co-occurrence network topology was determined by evaluating the within-module connectivity (Zi) and among-module connectivity (Pi) using a web-based tool, molecular ecological network analysis pipeline (MENAP) (http://ieg4.rccc.ou.edu/mena) (Deng et al., 2012; Qiu et al., 2022). Based on this analysis, the nodes are classified into the following four groups: (a) Peripheral nodes ($Zi < 2.5$, $Pi < 0.62$), (b) connectors ($Zi < 2.5$, $Pi > 0.62$), (c) module hubs ($Zi > 2.5$, $Pi < 0.62$), and (d) network hubs ($Zi > 2.5$, $Pi > 0.62$) (Qiu et al., 2022). The module hubs are densely connected to many nodes within *r* own modules, whereas the network hubs serve as both connectors and module hubs. Together with network hubs, module hubs, and connectors were termed an keystone nodes/taxa (Olesen et al., 2007; Zhou et al., 2010; Deng et al., 2012; Qiu et al., 2022).

RESULTS

Physiological Parameters of Indian T2D and NGT Samples

The pathophysiological conditions of diabetes patients were assessed *via* nine different parameters (BMI, FBG, FI, HbA1c, CP, CHL, HDL, LDL, and TGL) of T2D with respect to NGT (**Supplementary Table S1**). Among them, the average level of FBG and HbA1c in the T2D group (168 mg/dl and 8.1% respectively) were found significantly higher ($p \leq 0.05$) than NGT (**Table 1**). The PCA analysis indicates first three principal components accounted for 72.8% variation among the two groups of samples based on their measured physiological parameters (**Figure 1**). The PC1 alone explained 33.1% variation, majorly contributed by BMI, CP, CHL, and LDL; PC2 explained 23.7% of the total variation that was mainly driven by FBG, HbA1c, and TGL; and PC3 was responsible for the remaining 16% variation explained by FI and HDL. It was also evident that the T2D group was separated as a single cluster from the NGT group along the FBG and HbA1c parameters.

Selection of Optimal Features, Construction, and Performance Evaluation of MLT Models to Classify Between T2D and NGT

Feature selection (FS) is a pattern recognition application to remove the irrelevant or noise from the original features data. The RFE FS is a multivariate approach that incorporates all variables in the algorithm and gradually excludes those variables which are not able to discriminate between the different classes. In this study, nine physiological parameters (BMI, FBG, HbA1c, FI, CP, CHL, HDL, LDL, and TGL) of a total of 441 samples were considered to identify the best physiological parameters having the discriminatory ability between T2D and NGT and we have found five best physiological parameters (through RFE FS) that includes FBG, HbA1c, CP, FI, and CHL with high accuracy (ACC = 95%).

For this investigation, those five important physiological parameters were further used to build as well as to evaluate the performance of the prediction models using three different MLT methods, i.e., RF, SVM–L, and SVM–R. The prediction models were built with 150 training datasets (75 T2D and 75 NGT) and performance of these prediction models were tested using the same number of the testing datasets (75 T2D and 75 NGT) by measuring their SEN, SPF, ACC, and PRC with 10-fold cross-validation. However, the best prediction models were measured by their performance checking of precision (PRC) and recall (also known as SEN) since they were directly proportional to the true positive (Barman et al., 2014). All the prediction models worked very well and the values of SEN, SPF, and ACC of the three prediction models were nearly the same. However, the PRC score in SVM–L (100%) was higher than RF (94%) and SVM–R (94%), while the recall score of RF (100%) was higher than the SVM–L and SVM–R (**Table 2**). However, they were further evaluated to confirm their discriminatory abilities between T2D and NGT using a blind dataset.

Evaluation of Prediction Methods With Blind Dataset and Classification of Unknown Samples

We used the same approach to avoid any bias in the performance of our proposed models and observed how well they could distinguish between the two classes. Our analysis reported that all three prediction models worked very well to classify the T2D and NGT blind. Both RF and SVM–R models were able to identify the total 74 T2D samples correctly, (100% SEN values) while SVM–L showed the best prediction efficiency (97% SPF value) compared to the other two (**Table 2**). Overall, this investigation reported that the best two effective prediction models are random forest (RF) and SVM–R (SVM with RBF Kernel) as indicated on precision (PRC) and recall (SEN) values.

The collected physiological parameters of 34 samples (17 T2D and 17 NGT), as unknown datasets, were used to further evaluate the efficiency of RF and SVM–R prediction models using the top-five physiological data that were identified in RFE–FS. Both prediction models were successful in classifying all T2D samples as a true positive with 100% SEN or

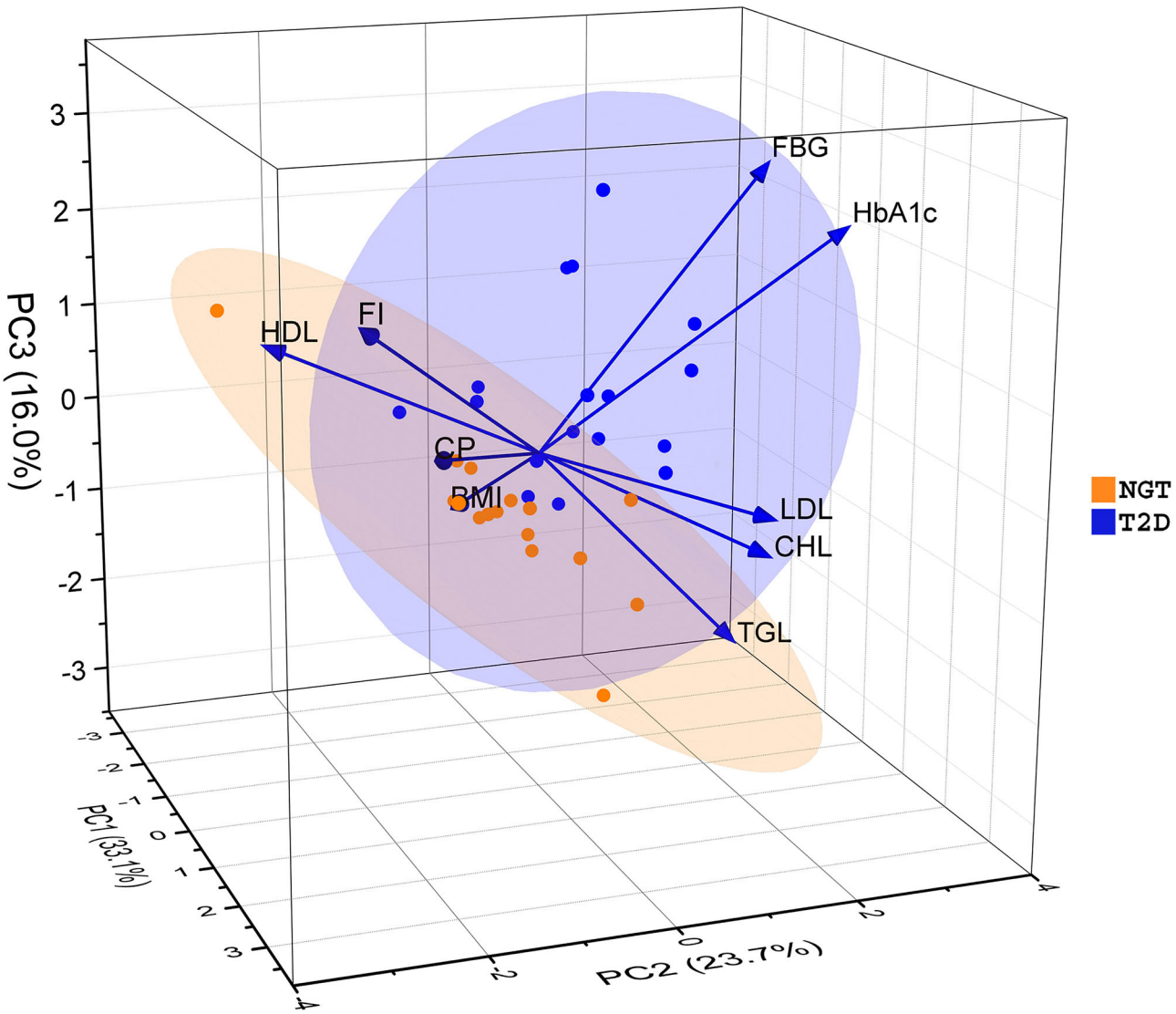

FIGURE 1 | Principal Component Analysis (PCA) based on physiological parameters of the Indian diabetes subjects and controls. The samples were divided into two groups along with three principal components (PCs). PC1, PC2, and PC3 explained 33.1, 23.7, and 16 percent of the total variation respectively. Here BMI, Body Mass Index; FBG, Fasting Blood Glucose; FI, Fasting Insulin; HbA1c, Glycated Hemoglobin; CP, C – Peptide; CHL, Cholesterol; HDL, High-Density Lipoprotein; LDL, Low-Density Lipoprotein; TGL, Triglyceride.

TABLE 2 | Comparative performance measurement among three different MLT methods using three different datasets with 10-fold cross-validation.

Datasets	MLT	Sensitivity	Specificity	Accuracy	Precision
Test dataset	RF	1.00	0.98	0.97	0.94
	SVM–L	0.97	1.00	0.98	1.00
	SVM–R	0.98	0.94	0.96	0.94
Blind dataset	RF	1.00	0.88	0.94	0.90
	SVM–L	0.81	0.97	0.88	0.96
	SVM–R	1.00	0.88	0.94	0.90
Unknown dataset	RF	1.00	0.52	0.76	0.68
	SVM–R	1.00	0.35	0.67	0.60

RF, Random forest; SVM–L, Support vector machine with linear Kernel; SVM–R, Support vector machine with RBF Kernel.

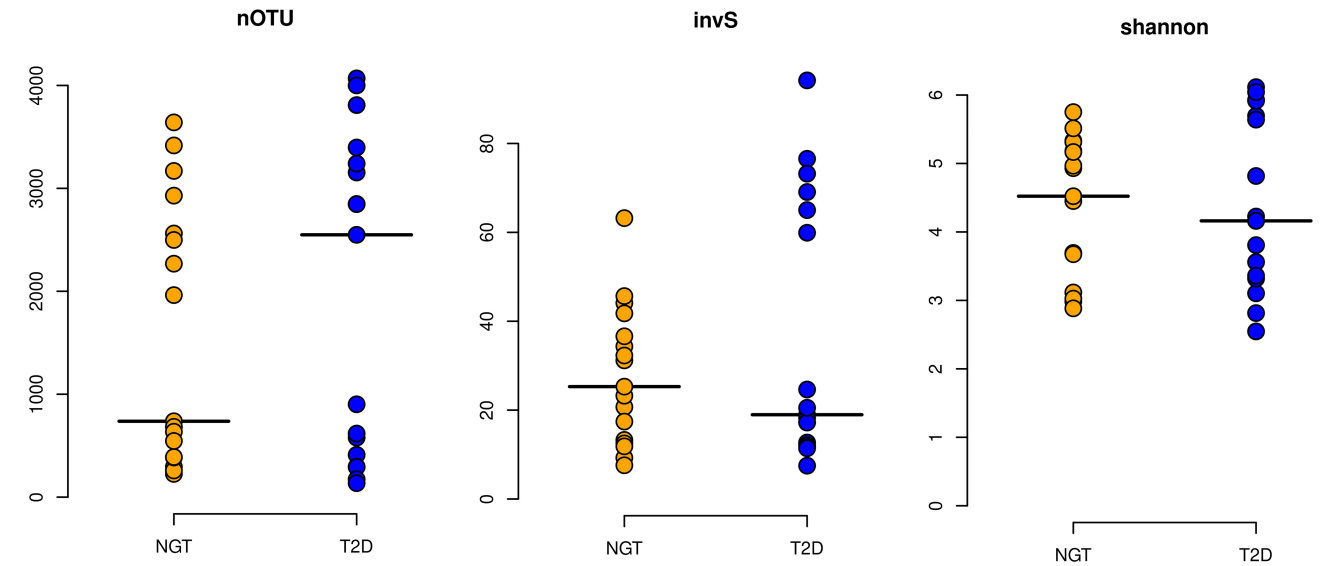

FIGURE 2 | Alpha diversity Indices. The alpha diversity of the studied groups was measured based on their richness [nOTU and inverse Simpson index (invS)] and evenness [Shannon Index (shannon)]. Here horizontal lines in the plot represent their respective mean value.

recall (**Table 2**). Interestingly, from the above study, it is observed that FBG and HbA1c were demonstrated as the most important discriminative parameters with the highest mean decrease scores (95.2 and 75.2%, respectively) among the two study groups.

Diversity Analysis and Taxonomy Composition of the Indian T2D and NGT

By removing primer sequences of microbial hypervariable V3–V4 region of 16S rRNA gene amplicon sequences, a total of 71,30,226 clipped pair-end reads were generated. After trimming and merging the paired-end reads, a total of 44,00,731 merged sequences were obtained (**Supplementary Table S2**). The high-quality reads were then clustered using > 97% sequence identity which generated 7,71,043 OTUs. A total of 43,467 swarm OTUs was obtained by removing the absolute singletons and unclassified sequence at the phylum level to avoid the rare biosphere, potential chimera effects, and PCR artifact (Dhal et al., 2020; Nayak et al., 2021).

α diversity i.e., diversity within the sample, was measured through nOTUs, Shannon diversity index as well as inverse Simpson index. It was observed that the average nOTU was higher in the T2D group (1960) than in the NGT (1565). Similar results were observed for Species richness and evenness in T2D and NGT groups as indicated by the Shannon diversity and inverse Simpson index (**Figure 2**). Spearman rank correlations test indicated a strong association of FBG with alpha diversity of the T2D group ($\rho = 0.54$, p-value ≤ 0.05) but none in NGT.

The bacterial communities of gut microbiota were dominated by the members of *Bacteroidota*, *Firmicutes*, *Proteobacteria,* and *Actinobacteria* which represented almost 97% of sequences (**Figure 3A**). In this study, we also observed 27 bacterial genera representing the core gut microbiome in the studied samples while each of 7 bacterial genera was found as unique for the T2D and NGT microbiome (**Figure 3B**). The core microbiome was mainly dominated by *Prevotella_9*, *Prevotella*, *Prevotellaceae Incertae Sedis*, *Bacteroides,* and *Alloprevotella* of *Bacteroidia*; *Lachnospiraceae Incertae Sedis*, *Roseburia,* and *Faecalibacterium* of *Clostridia*; *Megasphaera* of *Negativicutes* and *Succinivibrio* of *Gammaproteobacteria* (**Supplementary Figure S1**, **Supplementary Table S3**). The unique bacterial member for the T2D microbiome was composed of *Eubacterium eligens group*, *Lachnoclostridium*, *Ruminococcus torques group*, and *Clostridia vadinBB60 group Incertae Sedis,* and *Lachnospira* under the class *Clostridia*; *Haemophilus* of *Gammaproteobacteria* and *Catenibacterium* of *Bacilli* (**Supplementary Table S5**). While *Alistipes* and *Muribaculaceae Incertae Sedis* under the class *Bacteroidia*; *Ligilactobacillus* and *Holdemanella* of *Bacilli*; *Enterobacter* of *Gammaproteobacteria*; *Blautia* and *Coprococcus* of *Clostridia* were observed only in the NGT group (**Supplementary Table S4**).

Also, β diversity was a measure to determine the intra-sample variation of the gut microbial community using the pruned 6903 OTU datasets. The differential OTUs using the ALDEx2 test reported a total of 61 OTUs representing 68.1% of total communities for T2D and NGT gut microbiome that include classes *Bacteroidia* (34 OTUs), *Clostridia* (13 OTUs), *Gammaproteobacteria* (5 OTUs), *Negativicutes* (4 OTUs), *Spirochaetia* (2 OTUs), *Bacilli* (2 OTUs), and *Verrucomicrobiae* (1 OTU), which were deferred as differential abundant between T2D and NGT (**Supplementary Figure S2**).

Within *Bacteroidia*, OTU affiliated with genus *Prevotella_9* (15 OTUs), *Alloprevotella* (otu18 and otu36), *Bacteroides* (otu28), *Prevotella Incertae Sedis* (otu48), and *Rikenellaceae RC-9 gut group* (otu82) significantly enriched in the T2D microbiome whereas *Prevotella* (otu22, otu24, and otu116) significant

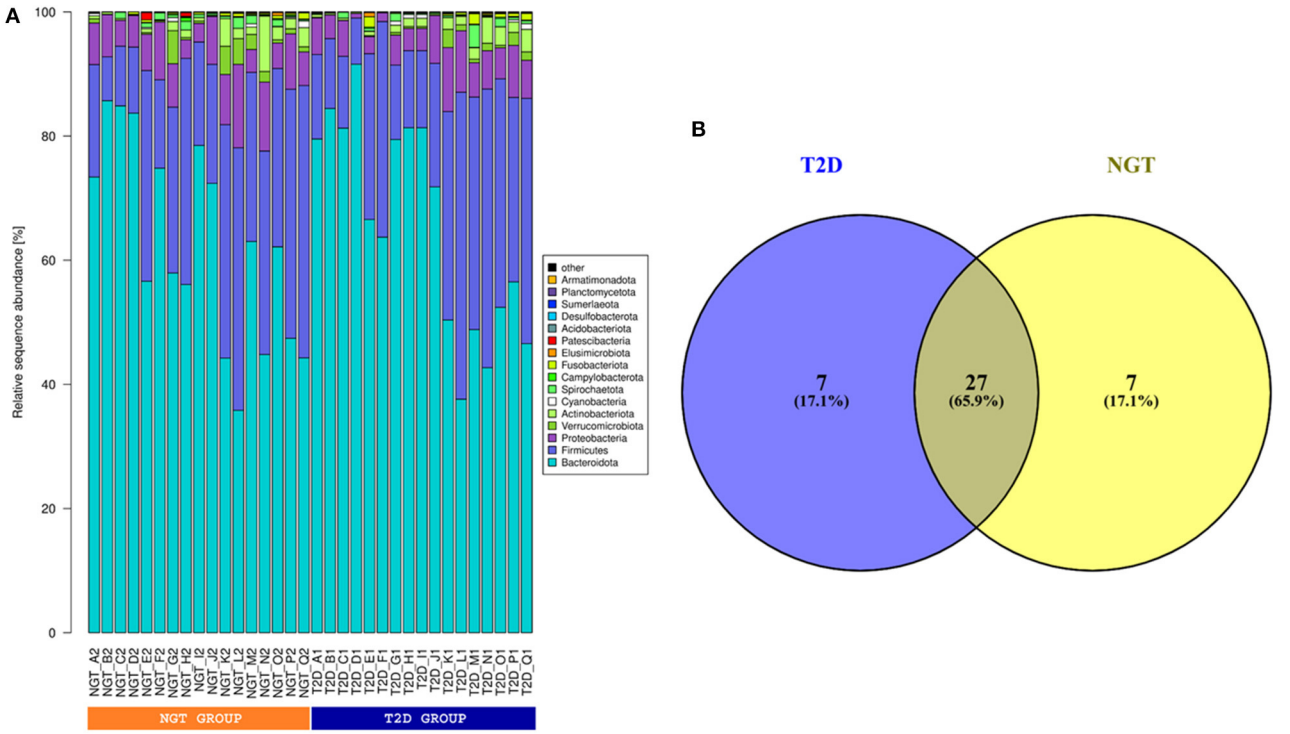

FIGURE 3 | (A) Phylum level taxonomic composition. Relative sequence abundance of most (top 10 based) dominant gut microbes in phylum level of studied samples. **(B)** Venn diagram for unique and common gut microbes. According to the Venn diagram, 27 gut microbes were common for both T2D and NGT groups, and 7 and 7 gut microbes were unique for T2D and NGT groups respectively.

enriched in NGT microbiome. Within the Clostridia class, *Eubacterium* (otu49 and otu59) and *UCG-002* (otu46) genera were found dominant in the T2D microbiome, whereas *Roseburia* (otu38 and otu51), *Lachnospiraceae Incertae Sedis* (otu43 and otu112), *Butyrivibrio* (otu55), and *Faecalibacterium* (otu42) genera were found significantly enriched in NGT microbiome. Similarly, *Gammaproteobacteria*, *Haemophilus* (otu237) showed dominance in the T2D microbiome whereas *Klebsiella* (otu83) and *Succinivibrio* (otu17) genera were found highly enriched in NGT. It was also observed that within *Negativicutes* genera, *Phascolarctobacterium* (otu33) was significantly dominant in the T2D microbiome, but in the same class, *Megasphaera* (otu25) and *Selenomonadaceae Incertae Sedis* (otu150) genera were significantly dominant in the NGT microbiome. Within *Bacilli*, the genus *Asteroleplasma* (otu64) significantly enriched in the T2D group whereas under the class *Spirochaetia* and *Verrucomicrobiae*, *Treponema* (otu81 and otu104), and *Akkermansia* (otu100) genera showed most dominance in the NGT group, respectively.

Similarities or dissimilarities between two groups were projected in an ordination space as well as their associated physiological parameters on the NMDS plot (**Figure 4**). Moreover, *Envfit* result showed that FBG ($R^2 = 0.2022$, $p = 0.025$) and HbA1c ($R^2 = 0.1480$, $p = 0.086$) coincided with microbial community composition, but the association seems to be weak. Redundancy analysis which was performed to assess the significant contribution of the tested parameters in describing the variation in microbial communities revealed that only HbA1c had the explanatory power for bacterial communities of T2D microbiota with 2.1% (Adj. $R^2 = 0.021$, $F = 1.34$, $AIC = 168.51$, $p = 0.05$). Together NMDS and RDA supported each other's results and suggested that HbA1c, as well as FBG, were the responsible variable among the parameters for variation in the microbial composition in the T2D group.

The significant correlation between the significant differentially abundant OTUs with the most important physiological parameters (FBG and HbA1c, as they were found as the most significant influence in our statistical analysis) was measured by calculating the Spearman correlation coefficient (SCC). As indicated in **Figure 5**, otu10, otu27, and otu231 represent *Prevotella_9*, otu28 represent the *Bacteroidandes*, otu48 represent the *Prevotella Incertae Sedis* showed a significantly positive correlation with FBG ($p \leq 0.05$) while out53, otu122, and otu231 representing *Prevotella_9*, otu64 representing *Asteroleplasma* and otu28 representing *Bacteroides* were highly positively correlated with the HbA1c ($p \leq 0.05$).

Co-Occurrence Network Analysis and Keystone Taxa of the Indian T2D and NGT

To understand the potential interactions among gut microbial community members for each group, we constructed co-occurrence networks based on OTU to OTU correlations.

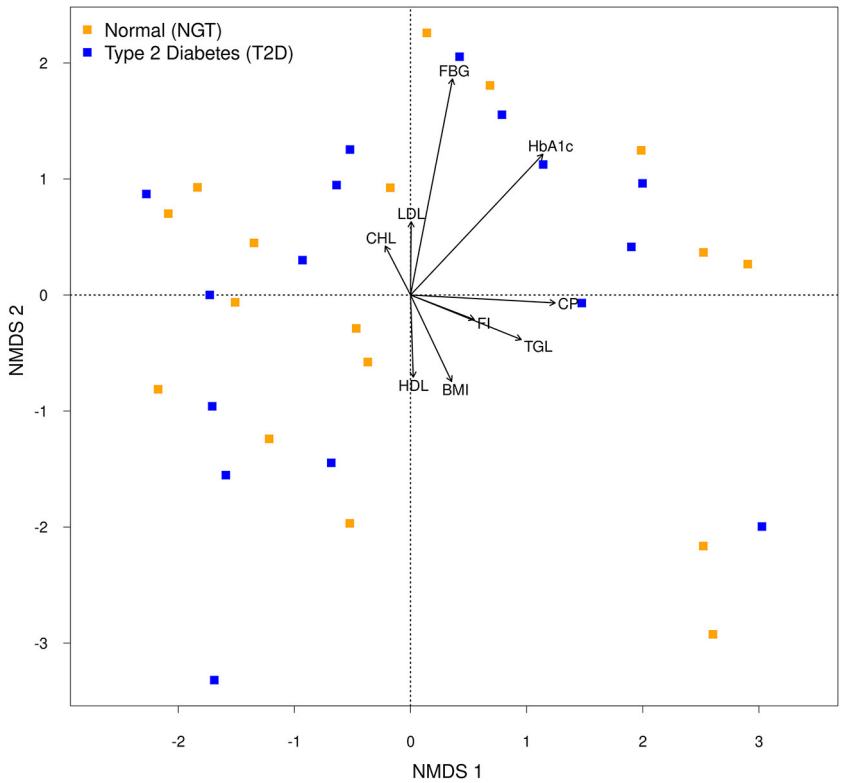

FIGURE 4 | Non-metric multidimensional scaling (NMDS) plot of the bacterial communities of each group. Arrows of the NMDS plot indicate *envfit* correlations of bacterial community composition with physiological parameters.

The T2D co-occurrence network (TCN) consisted of 168 nodes and 213 edges, while the NGT co-occurrence network (NCN) consisted of 217 nodes and 233 edges (**Table 3**). The modularity of TCN is 0.93 decreased from NCN modularity (0.96), accompanying the increase of average weighted degree in TCN (1.268) compared to NCN (1.074). The nodes present in both TCN and NCN networks were mostly dominated by phyla *Firmicutes*, *Bacteroidota*, *Proteobacteriota*, *Verrucomicrobiota*, *Spirochaetota*, *Fusobacteriota*, and *Desulfobacterota* (**Figures 6**, **7**). However, their percentage in each network was different, such as the *Firmicutes* present in TCN and NCN is 57.14 and 48.39%, respectively; the same trend was also observed in *Bacteroidota* (TCN *vs.* NCN: 28.57 *vs.* 36.87%), *Proteobacteria* (TCN *vs.* NCN: 8.33% *vs.* 7), *Actinobacteria* (TCN *vs.* NCN: 2.98 *vs.* 2.3%), *Verrucomicrobiota* (TCN *vs.* NCN: 1.19 *vs.* 0.46%), *Spirochaetota* (TCN *vs.* NCN: 0.6 *vs.* 0.46%), *Fusobacteriota* (TCN *vs.* NCN: 0.6 *vs.* 0.46%), and *Desulfobacterota* (TCN *vs.* NCN: 0.6 *vs.* 0.92%). *Cyanobacteria* (0.92%), *Campylobacterota* (0.46%), *Patescibacteria* (0.46%), and *Elusimicrobiota* (0.46%) gut microbial phyla were found only in the NCN, while none from TCN. We also identified 14 and 8 OTUs as keystone nodes from TCN and NCN networks, respectively, based on within-module connectivity (Zi) and among-module connectivity (Pi) values. Among them, six OTUs as module hubs and eight OTUs as connector nodes were identified in the TCN network, whereas in the NCN network, seven OTUs as module hubs and one OTU as connector node were identified. The identified keystone taxa, five OTUs were found under the phylum *Firmicutes*, four for *Bacteroidota*, three for *Proteobacteria*, one for *Actinobacteriota*, and one for *Spirochaetota* gut microbial phyla in TCN network. In contrast, two OTUs were found under the phylum *Bacteroidota*, three for *Firmicutes*, one for *Proteobacteria*, one for *Patescibacteria* and one for *Desulfobacterota* as keystone microbial phyla for NCN. Due to the decrease in network topology and different gut microbial compositions, the network stability also decreases in TCN compared to NCN.

DISCUSSION

Many reports endorsed the usefulness of different machine learning techniques to discriminate between T2D and NGT using a patient's physiological conditions, but none has attempted to identify the important parameters that can alone predict and diagnose the T2D (Choi et al., 2019; Tigga and Garg, 2020). In this study, we are the first to attempt to develop an MLT-based prediction model using the conventional classification algorithms as well as identification of the most important physiological

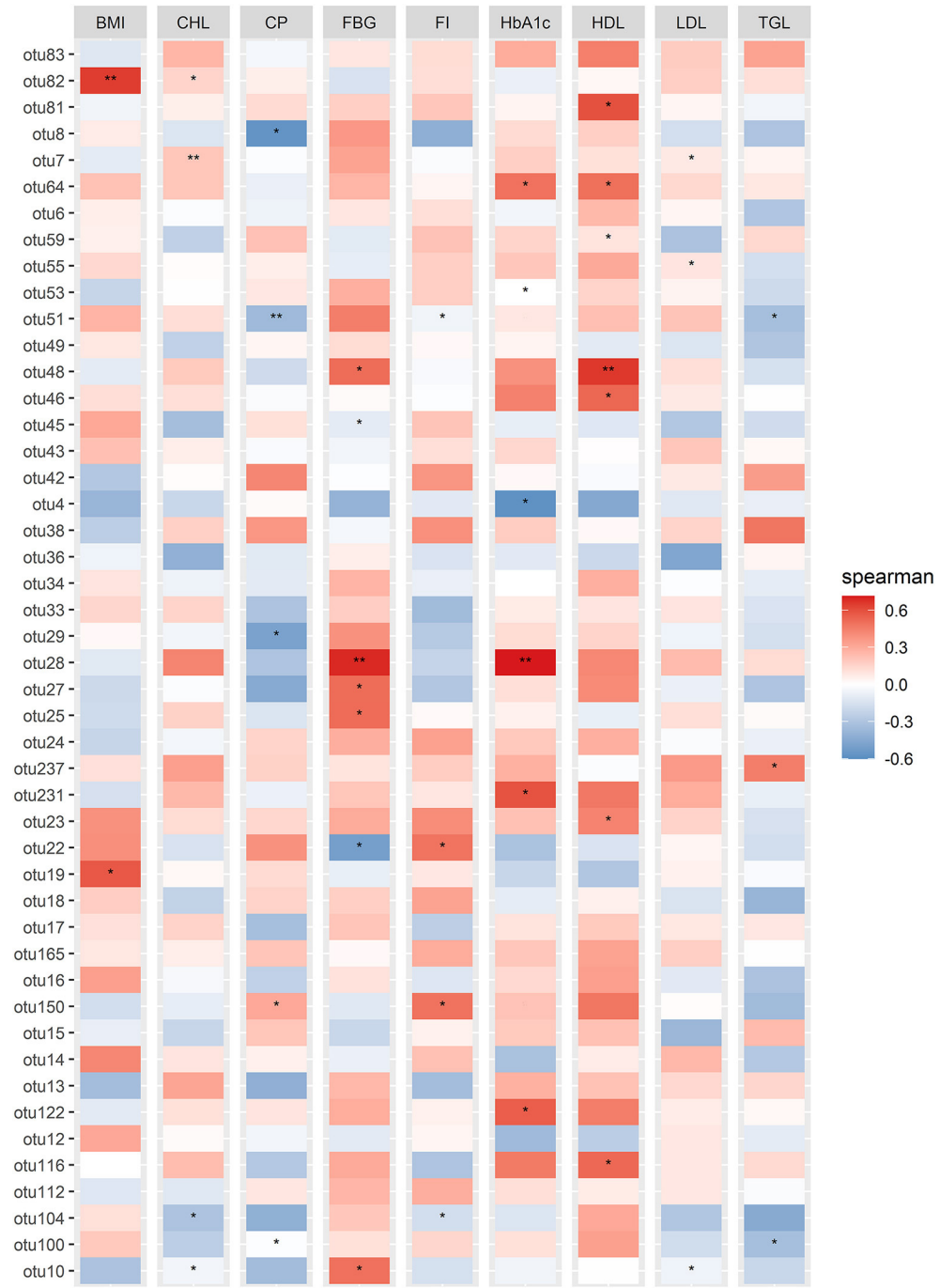

FIGURE 5 | Correlation Heatmap of physiological parameters with the significant differential abundant OTUs identified in DotPlot analysis. Spearman correlation analysis based on differentially abundant significant OTUs and the measured physiological parameters. Spearman correlation values were shown in the vertical heatmap panel to the right. $P \leq 0.05$ were indicated by the "*" symbols.

parameters (using the feature selection method, RFE) to classify diabetes status. Our prediction models are developed and verified using two different regions of datasets (Chinese and European) and applied these models to the studied Indian samples, to avoid any geographic biases. Our proposed prediction models, RF and SVM with RBF Kernel (SVM–R) have outperformed other already established models with high accuracy (94%) (Choi et al., 2019). Those models also identify the two most important physiological parameters, FBG and HbA1c, which have a greater role in the classification of T2D and diagnosis

of the disease which is in line with the American Diabetes Association (ADA) and the World Health Organization (WHO) recommendations as well as previous investigations, stating that both FBG and glycated hemoglobin (HbA1c) are critical to classify the T2D patients (Chaudhury et al., 2017; Deberneh and Kim, 2021).

Our statistical analysis also supports the result of MLT analysis by showing significant differences among FBG and HbA1c levels of the studied Indian T2D when compared to NGT, which have also separately ordinate from each other along with those parameters in the PCA plot. So, the significant changes in the level of both FBG and HbA1c can be used as critical physiological measurements to identify the T2D patients or risk of disease in impaired states of patients around the world.

TABLE 3 | Characteristics information of two gut microbial co-occurrence network; TCN–T2D co-occurrence network, NCN–NGT co-occurrence network.

Network Topology Parameters	NCN	TCN
Number of nodes	217	168
Number of edges	233	213
Average weighted degree	1.074	1.268
Network diameter	3	2
Graph density	0.005	0.008
Modularity	0.96	0.93
Average clustering co-efficient	0.226	0.208
Average path length	1.084	1.082

Alterations of gut microbiota and their association with T2D are well-established around the world (Karlsson et al., 2013; Bhute et al., 2017; Gaike et al., 2020; Sroka-Oleksiak et al., 2020). However, the microbial dynamism of T2D patients from normal as well as their correlation with the important physiological parameters (FBG and HbA1c) is not reported, which is another novelty of our investigation. In this study, we were the first to provide the preliminary information on the gut microbiome of T2D patients from the eastern region of the Indian Subcontinent, especially in and around Kolkata, West Bengal. The T2D patients from this region have unique dietary status compared to other regions and this seems to restrict us from collecting the samples from different regions which is also reflected in our sample size. The microbial community of the studied samples was dominated by the members of the bacterial groups under phylum *Bacteroidota*, *Firmicutes*, *Proteobacteria*, and *Actinobacteria*. *Bacteroidota* and *Firmicutes* are the well-known dominant bacteria phylum found in obesity, diabetes, and also in normal gut microbiome around the world (Gaike et al., 2020; Sroka-Oleksiak et al., 2020). Although there are reports on the differences in abundance among *Bacteroidota* and *Firmicutes* in T2D patients to NGT (Zhang et al., 2013; Ahmad et al., 2019). However, some other reports stated that such differences are not significant in T2D from NGT, which is in line with our results, as this investigation mostly focused on T2D irrespective of their obesity status (Turnbaugh et al., 2006; Ley et al., 2008; Zhang et al., 2013). The members of phyla *Firmicutes* play an important key role in fat digestion and their higher abundance is directly associated with obesity whereas *Bacteroidota* is associated with the production of short-chain fatty acids (SCFAs) (Ahmad et al., 2019).

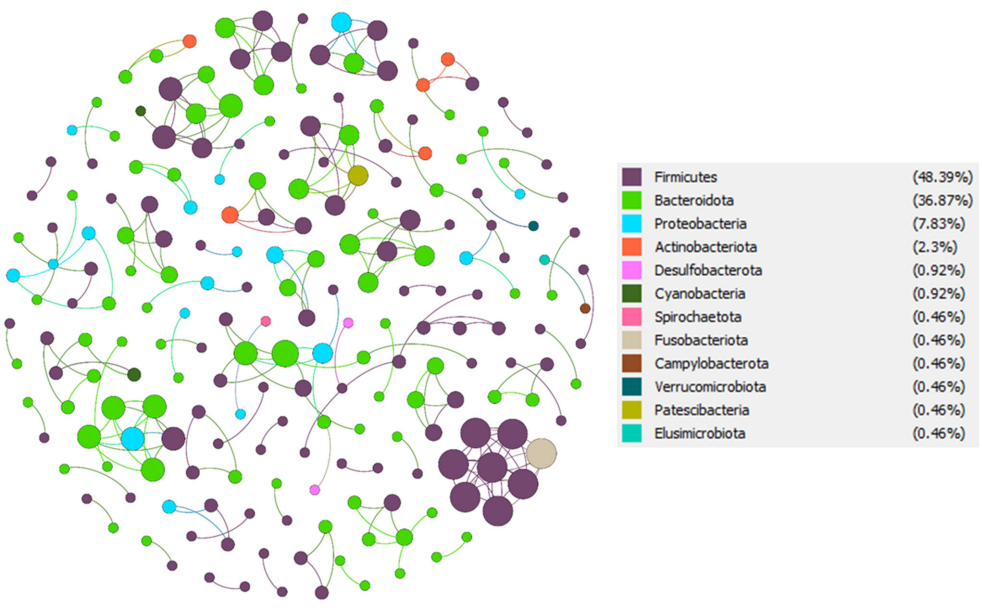

FIGURE 6 | NGT co-occurrence network (NCN). From total OTU abundance data, we select the NGT specific OTUs using the specified criteria, and a co-occurrence microbial network was constructed in Gephi.

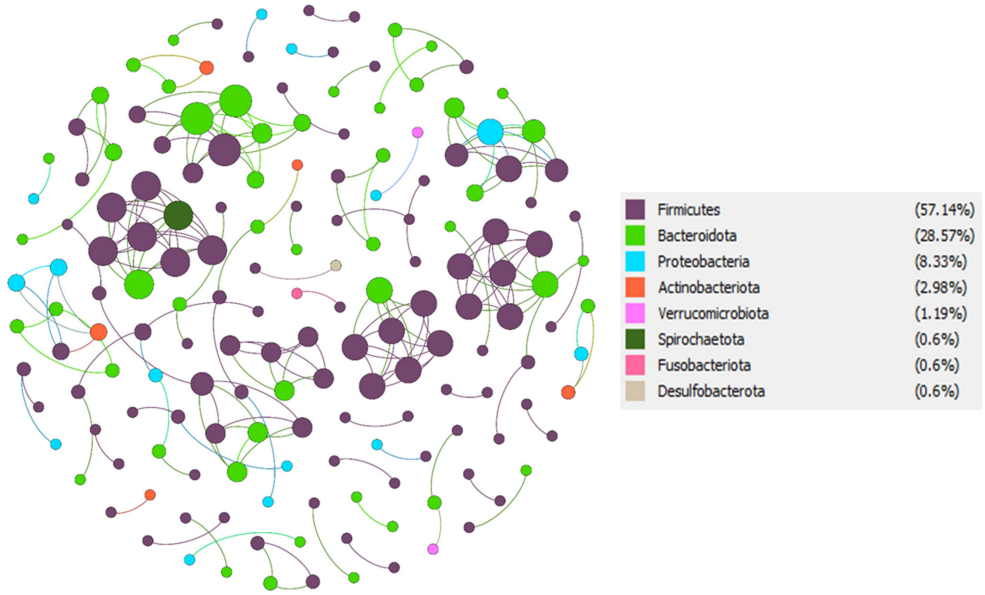

FIGURE 7 | T2D co-occurrence network (TCN). From total OTU abundance data, we select the T2D specific OTUs using the specified criteria, and a co-occurrence microbial network was constructed in Gephi.

Among the 27 core bacterial genera, the taxonomy of the associated genera with significantly dominated OTUs in studied T2D samples is *Prevotella_9*, *Alloprevotella*, *Bacteroides*, *Prevotella Incertae Sedis*, *Rikenellaceae RC-9 gut group*, *Eubacterium*, *UCG-002*, *Phascolarctobacterium*, and *Asteroleplasma*. They are also reported to be well-associated with T2D; for example, *Allopreotella* and *Bacteroides* are reported as risk factors for diabetes as these are reported to increase the level of lipopolysaccharides (LPS) and insulin resistance, which are detrimental to human health (Cheng et al., 2017; Wang et al., 2020). The *Prevotella_9* is reported to be associated with a plant-based low-fat diet and represents key bacterial members during human gut microbiota maturation in infants to young adults (Qian et al., 2018; Li et al., 2020b). However, the biological significance in the human gut enterocyte of both *Prevotella_9* and *Asteroleplasma* has not been well elucidated. While *Rikenellaceae RC9 gut group* bacterial genera showed an association with a high-fat diet and play an important role in lipid metabolism (Zhao et al., 2018). The genus *Phascolarctobacterium* is reported as an enriched bacterial genus in the T2D mice model and negatively correlated with fasting insulin (Naderpoor et al., 2019; Song et al., 2020). We found OTUs representing *Prevotella_9*, *Bacteroides*, *Prevotella Incertae Sedis* and *Asteroleplasma* bacterial genera have a significantly positive correlation with important established physiological parameters FBG and HbA1c. Interestingly, this observation supported the correlation analysis of alpha-diversity (richness and evenness) of the gut microbial community of studied T2D patients with FBG. Also, the results of NMDS *envfit* and RDA reflect that FBG and HbA1c both coincided most strongly with the microbial community composition of the T2D microbiome. On the other hand, *Prevotella*, *Roseburia*, *Lachnospiraceae Incertae Sedis*, *Butyrivibrio*, *Faecalibacterium*, *Klebsiella*, *Succinivibrio*, *Megasphaera*, *Selenomonadaceae Incertae Sedis*, *Treponema*, and *Akkermansia* genera are found as dominant bacterial genera in the NGT microbiome. A similar result was observed in the study by Almugadam et al. (2020) where they reported that short-chain fatty acid (SCFA) and butyrate producers such as *Faecalibacterium*, *Roseburia*, *Selenomonadaceae Incertae Sedis*, *Succinivibrio*, and *Megasphaera* genera were abundant in the healthy gut microbiome (Almugadam et al., 2020). *Prevotella*, *Succinivibrio*, *Treponema*, and *Lachnospiraceae* Incertae Sedis major contributes to inter-individual variation in gut microflora and are associated with better digestion of plant-derived complex carbohydrates and fibers diet for glucose homeostasis along with the production of butyric acid in the human colon for intestinal barrier protection (Arumugam et al., 2011; Schnorr et al., 2014; De Filippo et al., 2017; Zhao et al., 2020). Several investigators report the enrichment of butyrate-producing bacterial genera such as *Roseburia*, *Butyrivibrio*, *Faecalibacterium*, *Lachnospiraceae Incertae Sedis*, and *Megasphaera* are responsible for the reduction of inflammatory symptoms as well as insulin resistance. These bacterial genera play an important key role in intestinal health maintenance, immune defense, regulation of the dynamic balance of T-cells, and promote Treg cell differentiation by butyrate production (Canani et al., 2011; Karlsson et al., 2013). *Klebsiella* bacteria are also found in the healthy human intestines and are not reported to be pathogenic as long the person is sick because of pneumonia, bloodstream infections, wound, or surgical site infections, etc. (Canani et al., 2011). A high abundance of mucin degrading *Akkermansia* bacterial genus in

healthy human guts is well documented as they play a vital role in insulin resistance as well as intestinal barrier and LPS leakage reduction (Tanca et al., 2017; Gurung et al., 2020). Although some recent reports indicate that a decrease in this genus in diabetes is associated with inflammation and metabolic disorders in the mice model, it can be used as a biomarker for impaired glucose tolerance (Sonnenburg and Bäckhed, 2016; Plovier et al., 2017).

Several unique bacterial genera are identified in T2D compared to the NGT microbiome and probably play some roles in the structural and functional attributes of the gut microbes in the human intestine for the development of disease. The unique genera for the T2D microbiome are *Catenibacterium*, *Eubacterium eligens group*, *Lachnoclostridium*, *Ruminococcus torques group*, *Clostridia vadinBB60 group Incertae Sedis*, *Lachnospira*, and *Haemophilus*. Several investigators reported that a few of these bacterial genera such as *Ruminococcus torques group*, *Lachnospira*, and *Haemophilus* act in mucus degradation by decreasing the gut barrier integrity, and they can be used as bacterial biomarkers to study their involvement in the human gut or their uses as diagnostic tools should be encouraged (Chen et al., 2020; Vacca et al., 2020). *Haemophilus* bacterial genus reported highly abundant in the Chinese T2D cohort is a particular biomarker for them (Chen et al., 2020). While for NGT, the unique bacterial genera are *Enterobacter*, *Ligilactobacillus*, *Alistipes*, *Muribaculaceae Incertae Sedis*, *Blautia*, *Holdemanella*, and *Coprococcus* identified in this investigation. Few of those genera including, *Alistipes*, *Blautia*, and *Holdemanella* are observed in the normal human gastrointestinal tract and they have an important key role in protection from many diseases such as liver and cardiovascular fibrotic disorders and also from various pathogens (Arumugam et al., 2011; Parker et al., 2020). *Coprococcus*, *Muribaculaceae Incertae Sedis*, and *Enterobacter* bacterial genera are having the ability for metabolic improvements and consorted with a higher quality of life indicators supported by previous reports (Valles-Colomer et al., 2019; Wang et al., 2020).

Our co-occurrence network analysis showed that in T2D disease condition, significant changes in microbial network topological properties leads to a decrease in network stability and alteration in the microbial community in the human gastrointestinal tract, which is also in line with previous studies where they were reported, network complexity of the gut microbial community association was decreased in T2D (Li et al., 2020a). Interestingly co-occurrence network analysis also revealed that there are significant differences present in the proportion of taxonomic abundance of *Firmicutes* and *Bacteroidota* phylum in T2D compared to the NGT group which is also in line with the previously reported data (Turnbaugh et al., 2006; Ley et al., 2008; Zhang et al., 2013; Ahmad et al., 2019). The same trend was also observed in identified keystone taxa from the two co-occurrence networks and they might play an essential role in maintaining the microbial structure links, information transmission, and ecological function of the entire ecological communities in the gastrointestinal tract (Li et al., 2020a,b, 2021).

This investigation gives a well-resolved picture of the bacterial diversity and their correlation with important physiological parameters that influence the decrease of SCFA and butyrate-producing core bacteria which are beneficial for the human gut in T2D patients, in West Bengal, India. Also, we suggest that along with the well-established physiological parameters, the unique gut microbes can be used as a key biomarker to improve the disease diagnosis.

The Indian population size is large and has diverse dietary compositions or food habits with large metabolic differences. Recently, one report on the gut microbiota of T2D from the western part of India (Maharashtra, especially, in and around the city, Pune); however, none are from other regions/parts of this country (Gaike et al., 2020). In this study, we were the first to provide the preliminary information on the gut microbiome of Indian T2D patients from the eastern region of the Indian Subcontinent, especially, in and around the Kolkata, West Bengal, with almost similar dietary status and this seems to restrict us from increasing the sample size. This is a preliminary dataset that will help us formulate strategies to collect more samples from a diverse population for a deep understanding of the gut microbiome in Indian T2D patients. With the increase in the sample size, we will be able to perform more in-depth microbial diversity analysis and learn more about what governs the distribution of gut microbial taxa and how these distributions, as well as their ecosystem contributions in Indian T2D patients, will help to improve more accurate diagnosis of T2D disease in the future.

CONCLUSION

From the investigation in this study, following conclusions can be drawn:

1) Random forest (RF) and support vector machine with RBF Kernel (SVM–R) are the best prediction models to predict the T2D and normal state based on a patient's physiological condition.
2) Fasting blood glucose and HbA1c individually or together can be used for the T2D diagnosis as well as defining the disease in an impaired state. Also, both of these physiological parameters coincided with the microbial community composition of the T2D microbiome by decreasing the beneficiary core gut microbial members.
3) *Catenibacterium*, *Eubacterium eligens group*, *Lachnoclostridium*, *Ruminococcus torques group*, *Clostridia vadinBB60 group Incertae Sedis*, *Lachnospira*, and *Haemophilus* can be used as important biomarkers for Indian T2D patients.

DATA AVAILABILITY STATEMENT

The datasets presented in this study can be found in online repositories. The names of the repository/repositories and accession number(s) can be found below: https://www.ncbi.nlm.nih.gov/, PRJNA486712.

ETHICS STATEMENT

The studies involving human participants were reviewed and approved by Ethical Committee at SSKM Hospital. The patients/participants provided their written informed consent to participate in this study.

AUTHOR CONTRIBUTIONS

Conceptualization and supervision: PD. Data-curation: DD and PD. Formal analysis and writing the original draft: DD, TN, and PD. Methodology: PD, DD, and SC. Writing-review and editing: PD, DD, TN, and SC. All authors contributed to the article and approved the submitted version.

FUNDING

This work was supported by the UGC–BSR Start-up-grant and JU–RUSA 2.0, DST (Grant No.: R-11/446/19).

ACKNOWLEDGMENTS

The authors acknowledge the Science and Engineering Research Board (SERB), Ministry of Science and Technology (Grant No. EEQ/2018/000006) for the high-performance computing workstation facility. The authors are also thankful to JU-RUSA 2.0 for student fellowship (Grant No. R-11/183/19). We are grateful to Jadavpur University, Department of Life Sciences and Biotechnology, for providing lab space to carry out the work. We are also thankful to the doctors of IPGMER and SSKM Hospital, Department of Endocrine, for helping in interaction with patients and their family members and providing lab for testing the physiological parameters.

SUPPLEMENTARY MATERIAL

The Supplementary Material for this article can be found online at: https://www.frontiersin.org/articles/10.3389/fmicb.2022.914124/full#supplementary-material

Supplementary Table S1 | Physiological characteristics of type 2 diabetes and control used in this study: Age, Body Mass Index (BMI), Fasting Blood Glucose (FBG), Fasting Insulin (FI), HbA1c, C – Peptide (CP), Cholesterol (CHL), High Density Lipoprotein (HDL), Low Density Lipoprotein (LDL), Triglycerides (TGL).

Supplementary Table S2 | Step by step sequence processing information.

Supplementary Table S3 | Core taxonomic composition of most dominant gut microbes at genus level with their respective relative sequence abundance.

Supplementary Table S4 | Unique taxonomic composition of most dominant gut microbes at genus level with their respective relative sequence abundance for the NGT group.

Supplementary Table S5 | Unique taxonomic composition of most dominant gut microbes at genus level with their respective relative sequence abundance for the T2D group.

Supplementary Figure S1 | Taxonomic composition at the genus level. Relative sequence abundance of most (top 10 based) dominant gut microbes in genus level of studied samples.

Supplementary Figure S2 | Dominant bacterial community between two groups (T2D and NGT). Differentially abundant OTUs within two groups are represented in Dotplot using ALDEx2. Dotplot represents class level taxonomy on the left side and genus level on the right side. The size of each dot (0, 5, 10, 15) represents centered log-ratio (clr) – transformed sequence counts.

REFERENCES

Ahmad, A., Yang, W., Chen, G., Shafiq, M., Javed, S., Zaidi, S. S. A., et al. (2019). Analysis of gut microbiota of obese individuals with type 2 diabetes and healthy individuals. *PLoS ONE.* 14. doi: 10.1371/journal.pone.0226372

Almugadam, B. S., Liu, Y., Chen, S. M., Wang, C. H., Shao, C. Y., Ren, B. W., et al. (2020). Alterations of gut microbiota in type 2 diabetes individuals and the confounding effect of antidiabetic agents. *J. Diabetes Res.* 2020. doi: 10.1155/2020/7253978

Arbabshirani, M. R., Plis, S., Sui, J., and Calhoun, V. D. (2017). Single subject prediction of brain disorders in neuroimaging: promises and pitfalls. *Neuroimage.* 145, 137–165. doi: 10.1016/j.neuroimage.2016.02.079

Arumugam, M., Raes, J., Pelletier, E., Paslier, D., Le, Y. T., Mende, D. R., et al. (2011). Enterotypes of the human gut microbiome. *Nature.* 473, 174–180. doi: 10.1038/nature09944

Barman, R. K., Saha, S., and Das, S. (2014). Prediction of interactions between viral and host proteins using supervised machine learning methods. *PLoS ONE.* 9, e112034. doi: 10.1371/journal.pone.0112034

Bastian, M., Heymann, S., and Jacomy, M. (2009). Gephi : an open source software for exploring and manipulating networks visualization and exploration of large graphs. Available online at: www.aaai.org (accessed March 30, 2022).

Bhute, S. S., Suryavanshi, M. V., Joshi, S. M., Yajnik, C. S., Shouche, Y. S., and Ghaskadbi, S. S. (2017). Gut microbial diversity assessment of Indian type-2-diabetics reveals alterations in eubacteria, archaea, and eukaryotes. *Front. Microbiol.* 8, 1–15. doi: 10.3389/fmicb.2017.00214

Bolger, A. M., Lohse, M., and Usadel, B. (2014). Trimmomatic: a flexible trimmer for Illumina sequence data. *Bioinformatics* 30, 2114–2120. doi: 10.1093/bioinformatics/btu170

Canani, R. B., Di Costanzo, M., Leone, L., Pedata, M., Meli, R., and Calignano, A. (2011). Potential beneficial effects of butyrate in intestinal and extraintestinal diseases. *World J. Gastroenterol.* 17, 1519. doi: 10.3748/wjg.v17.i12.1519

Chaudhury, A., Duvoor, C., Reddy Dendi, V. S., Kraleti, S., Chada, A., Ravilla, R., et al. (2017). Clinical review of antidiabetic drugs: implications for type 2 diabetes mellitus management. *Front. Endocrinol. (Lausanne).* 8, 6. doi: 10.3389/fendo.2017.00006

Chen, B., Wang, Z., Wang, J., Su, X., Yang, J., Zhang, Q., et al. (2020). The oral microbiome profile and biomarker in Chinese type 2 diabetes mellitus patients. *Endocrine.* 68, 564–572. doi: 10.1007/s12020-020-02269-6

Chen, X., and Jeong, J. C. (2007). "Enhanced recursive feature elimination", in *Sixth International Conference on Machine Learning and Applications (ICMLA 2007).* p. 429–435. doi: 10.1109/ICMLA.2007.35

Cheng, W., Lu, J., Li, B., Lin, W., Zhang, Z., Wei, X., et al. (2017). Effect of functional oligosaccharides and ordinary dietary fiber on intestinal microbiota diversity. *Front. Microbiol.* 8, 1750. doi: 10.3389/fmicb.2017.01750

Cho, N. H., Shaw, J. E., Karuranga, S., Huang, Y., da Rocha Fernandes, J. D., Ohlrogge, A. W., et al. (2018). IDF Diabetes Atlas: Global estimates of diabetes prevalence for 2017 and projections for 2045. *Diabetes Res. Clin. Pract.* 138, 271–281. doi: 10.1016/j.diabres.2018.02.023

Choi, B. G., Rha, S.-W., Kim, S. W., Kang, J. H., Park, J. Y., and Noh, Y.-K. (2019). Machine learning for the prediction of new-onset diabetes mellitus during 5-year follow-up in non-diabetic patients with cardiovascular risks. *Yonsei Med. J.* 60, 191. doi: 10.3349/ymj.2019.60.2.191

De Filippo, C., Di Paola, M., Ramazzotti, M., Albanese, D., Pieraccini, G., Banci, E., et al. (2017). Diet, environments, and gut microbiota. A preliminary investigation in children living in rural and Urban Burkina Faso and Italy. *Front. Microbiol.* 8, 1979. doi: 10.3389/fmicb.2017.01979

Deberneh, H. M., and Kim, I. (2021). Prediction of type 2 diabetes based on machine learning algorithm. *Int. J. Environ. Res. Public Health* 18, 3317. doi: 10.3390/ijerph18063317

Deng, Y., Jiang, Y. H., Yang, Y., He, Z., Luo, F., and Zhou, J. (2012). Molecular ecological network analyses. *BMC Bioinformatics.* 13, 1–20. doi: 10.1186/1471-2105-13-113

Dhal, P. K., Kopprio, G. A., and Gärdes, A. (2020). Insights on aquatic microbiome of the Indian Sundarbans mangrove areas. *PLoS ONE.* 15, e0221543. doi: 10.1371/journal.pone.0221543

Evans, J. S., and Murphy, M. A. (2019). Package 'rfUtilities.'

Fernandes, A. D., Reid, J. N. S., Macklaim, J. M., McMurrough, T. A., Edgell, D. R., and Gloor, G. B. (2014). Unifying the analysis of high-throughput sequencing datasets: Characterizing RNA-seq, 16S rRNA gene sequencing and selective growth experiments by compositional data analysis. *Microbiome.* 2, 1–13. doi: 10.1186/2049-2618-2-15

Gaike, A. H., Paul, D., Bhute, S., Dhotre, D. P., Pande, P., Upadhyaya, S., et al. (2020). The gut microbial diversity of newly diagnosed diabetics but not of prediabetics is significantly different from that of healthy nondiabetics. *mSystems.* 5, 1–17. doi: 10.1128/mSystems.00578-19

Gilleland, E. (2015). *Verification: Weather forecast verification utilities (v1. 42)*. Available online at: https//cran.r-project.org/package=Verif.5

Gurung, M., Li, Z., You, H., Rodrigues, R., Jump, D. B., Morgun, A., et al. (2020). Role of gut microbiota in type 2 diabetes pathophysiology. *EBioMedicine.* 51, 102590. doi: 10.1016/j.ebiom.2019.11.051

Jiao, S., Liu, Z., Lin, Y., Yang, J., Chen, W., and Wei, G. (2016). Bacterial communities in oil contaminated soils: biogeography and co-occurrence patterns. *Soil Biol. Biochem.* 98, 64–73. doi: 10.1016/j.soilbio.2016.04.005

Karlsson, F. H., Tremaroli, V., Nookaew, I., Bergström, G., Behre, C. J., Fagerberg, B., et al. (2013). Gut metagenome in European women with normal, impaired and diabetic glucose *control*. doi: 10.1038/nature12198

Kuhn, M. (2008). Building predictive models in R using the caret package. *J. Stat. Softw.* 28, 1–26. doi: 10.18637/jss.v028.i05

Ley, R. E., Hamady, M., Lozupone, C., Turnbaugh, P. J., Ramey, R. R., Bircher, J. S., et al. (2008). Evolution of mammals and their gut microbes. *Science (80-.).* 320, 1647–1651. doi: 10.1126/science.1155725

Li, J., Lu, H., Wu, H., Huang, S., Chen, L., Gui, Q., et al. (2020a). Periodontitis in elderly patients with type 2 diabetes mellitus: impact on gut microbiota and systemic inflammation. *Aging (Albany. NY).* 12, 25959–25980. doi: 10.18632/aging.202174

Li, W.-Z., Stirling, K., Yang, J.-J., and Zhang, L. (2020b). Gut microbiota and diabetes: from correlation to causality and mechanism. *World J. Diabetes.* 11, 293–308. doi: 10.4239/wjd.v11.i7.293

Li, X., Wang, A., Wan, W., Luo, X., Zheng, L., He, G., et al. (2021). High salinity inhibits soil bacterial community mediating nitrogen cycling. *Appl. Environ. Microbiol.* 87, e0136621. doi: 10.1128/AEM.01366-21

Liaw, A., and Wiener, M. (2002). Classification and regression by randomForest. *R News.* 2, 18–22.

Mahé, F., Rognes, T., Quince, C., de Vargas, C., and Dunthorn, M. (2014). Swarm: Robust and fast clustering method for amplicon-based studies. *PeerJ.* 2014, e593. doi: 10.7717/peerj.593

McIntyre, H. D., Catalano, P., Zhang, C., Desoye, G., Mathiesen, E. R., and Damm, P. (2019). Gestational diabetes mellitus. *Nat. Rev. Dis. Prim.* 5, 1–19. doi: 10.1038/s41572-019-0098-8

Meyer, D., Dimitriadou, E., Hornik, K., Weingessel, A., Leisch, F., Chang, C. C., et al. (2012). *Functions for Latent Class Analysis, Short Time Fourier Transform, Fuzzy Clustering, Support Vector Machines, Shortest Path Computation, Bagged Clustering, Naive Bayes Classifier*.

Naderpoor, N., Mousa, A., Gomez-Arango, L. F., Barrett, H. L., Dekker Nitert, M., and de Courten, B. (2019). Faecal microbiota are related to insulin sensitivity and secretion in overweight or obese adults. *J. Clin. Med.* 8, 452. doi: 10.3390/jcm8040452

Nayak, T., De, D., Karmakar, P., Deb, A., and Dhal, P. K. (2021). Microbial communities of the drinking water with gradient radon concentration are primarily contributed by radon and heavy metal content. *Front. Environ. Sci.* 9, 1. doi: 10.3389/fenvs.2021.576400

Oksanen, J., Blanchet, F. G., Kindt, R., Legendre, P., Minchin, P. R., O'hara, R. B., et al. (2013). Community ecology package. *R Pack. Vers.* 2, 321–326.

Olesen, J. M., Bascompte, J., Dupont, Y. L., and Jordano, P. (2007). The modularity of pollination networks. *Proc. Natl. Acad. Sci. U. S. A.* 104, 19891–19896. doi: 10.1073/pnas.0706375104

Oliveros, J. C., and Venny, C. (2007). *An Interactive Tool for Comparing Lists with Venn's Diagrams*. BioinfoGP, CNB-CSIC.

Parker, B. J., Wearsch, P. A., Veloo, A. C. M., and Rodriguez-Palacios, A. (2020). The genus Alistipes: gut bacteria with emerging implications to inflammation, cancer, and mental health. *Front. Immunol.* 11. doi: 10.3389/fimmu.2020.00906

Plovier, H., Everard, A., Druart, C., Depommier, C., Van Hul, M., Geurts, L., et al. (2017). A purified membrane protein from Akkermansia muciniphila or the pasteurized bacterium improves metabolism in obese and diabetic mice. *Nat. Med.* 23, 107–113. doi: 10.1038/nm.4236

Pruesse, E., Peplies, J., and Glöckner, F. O. (2012). SINA: Accurate high-throughput multiple sequence alignment of ribosomal RNA genes. *Bioinformatics* 28, 1823–1829. doi: 10.1093/bioinformatics/bts252

Qian, L., Gao, R., Hong, L., Pan, C., Li, H., Huang, J., et al. (2018). Association analysis of dietary habits with gut microbiota of a native Chinese community. *Exp. Ther. Med.* 16, 856–866. doi: 10.3892/etm.2018.6249

Qin, J., Li, Y., Cai, Z., Li, S., Zhu, J., Zhang, F., et al. (2012). A metagenome-wide association study of gut microbiota in type 2 diabetes. *Nature.* 490, 55–60. doi: 10.1038/nature11450

Qiu, L., Kong, W., Zhu, H., Zhang, Q., Banerjee, S., Ishii, S., et al. (2022). Halophytes increase rhizosphere microbial diversity, network complexity and function in inland saline ecosystem. *Sci. Total Environ.*, 154944. doi: 10.1016/j.scitotenv.2022.154944

Robin, X., Turck, N., Hainard, A., Tiberti, N., Lisacek, F., Sanchez, J.-C., et al. (2011). pROC: an open-source package for R and S+ to analyze and compare ROC curves. *BMC Bioinformatics.* 12, 1–8. doi: 10.1186/1471-2105-12-77

Saeys, Y., Inza, I., and Larranaga, P. (2007). A review of feature selection techniques in bioinformatics. *Bioinformatics.* 23, 2507–2517. doi: 10.1093/bioinformatics/btm344

Schnorr, S. L., Candela, M., Rampelli, S., Centanni, M., Consolandi, C., Basaglia, G., et al. (2014). Gut microbiome of the Hadza hunter-gatherers. *Nat. Commun.* 5, 1–12. doi: 10.1038/ncomms4654

Song, Y., Wu, M., Tao, G., Lu, M., Lin, J., and Huang, J. (2020). Feruloylated oligosaccharides and ferulic acid alter gut microbiome to alleviate diabetic syndrome. *Food Res. Int.* 137, 109410. doi: 10.1016/j.foodres.2020.109410

Sonnenburg, J. L., and Bäckhed, F. (2016). Diet–microbiota interactions as moderators of human metabolism. *Nature.* 535, 56–64. doi: 10.1038/nature18846

Sroka-Oleksiak, A., Młodzińska, A., Bulanda, M., Salamon, D., Major, P., Stanek, M., et al. (2020). Metagenomic analysis of duodenal microbiota reveals a potential biomarker of dysbiosis in the course of obesity and type 2 diabetes: a pilot study. *J. Clin. Med.* 9, 369. doi: 10.3390/jcm9020369

Statnikov, A., Henaff, M., Narendra, V., Konganti, K., Li, Z., Yang, L., et al. (2013). A comprehensive evaluation of multicategory classification methods for microbiomic data. *Microbiome.* 1, 1–12. doi: 10.1186/2049-2618-1-11

Svetnik, V., Liaw, A., Tong, C., Christopher Culberson, J., Sheridan, R. P., and Feuston, B. P. (2003). Random forest: a classification and regression tool for compound classification and QSAR modeling. *J. Chem. Inf. Comput. Sci.* 43, 1947–1958. doi: 10.1021/ci034160g

Tanca, A., Abbondio, M., Palomba, A., Fraumene, C., Manghina, V., Cucca, F., et al. (2017). Potential and active functions in the gut microbiota of a healthy human cohort. *Microbiome* 5, 1–15. doi: 10.1186/s40168-017-0293-3

Tigga, N. P., and Garg, S. (2020). Prediction of type 2 diabetes using machine learning classification methods. *in* Procedia Computer Science (Elsevier B.V.). p. 706–716. doi: 10.1016/j.procs.2020.03.336

Turnbaugh, P. J., Ley, R. E., Mahowald, M. A., Magrini, V., Mardis, E. R., and Gordon, J. I. (2006). An obesity-associated gut microbiome with increased capacity for energy harvest. *Nature* 444, 1027–1031. doi: 10.1038/nature05414

Tuszynski, J., and Tuszynski, M. J. (2007). The caTools package. R Packag. version 1–8.

Vacca, M., Celano, G., Calabrese, F. M., Portincasa, P., Gobbetti, M., and De Angelis, M. (2020). The controversial role of human gut lachnospiraceae. *Microorganisms.* 8, 573. doi: 10.3390/microorganisms8040573

Valles-Colomer, M., Falony, G., Darzi, Y., Tigchelaar, E. F., Wang, J., Tito, R. Y., et al. (2019). The neuroactive potential of the human gut

microbiota in quality of life and depression. *Nat. Microbiol.* 4, 623–632. doi: 10.1038/s41564-018-0337-x

Wang, T. Y., Zhang, X. Q., Chen, A. L., Zhang, J., Lv, B. H., Ma, M. H., et al. (2020). A comparative study of microbial community and functions of type 2 diabetes mellitus patients with obesity and healthy people. *Appl. Microbiol. Biotechnol.* 104, 7143–7153. doi: 10.1007/s00253-020-10689-7

Wei, Z., Wang, W., Bradfield, J., Li, J., Cardinale, C., Frackelton, E., et al. (2013). Large sample size, wide variant spectrum, and advanced machine-learning technique boost risk prediction for inflammatory bowel disease. *Am. J. Hum. Genet.* 92, 1008–1012. doi: 10.1016/j.ajhg.2013.05.002

Yu, C. S., Lin, Y. J., Lin, C. H., Lin, S. Y., Wu, J. L., and Chang, S. S. (2020). Development of an online health care assessment for preventive medicine: a machine learning approach. *J. Med. Internet Res.* 22, e18585. doi: 10.2196/18585

Zhang, J., Kobert, K., Flouri, T., and Stamatakis, A. (2014). PEAR: a fast and accurate Illumina Paired-End reAd mergeR. *Bioinformatics* 30, 614–620. doi: 10.1093/bioinformatics/btt593

Zhang, J., Ni, Y., Qian, L., Fang, Q., Zheng, T., Zhang, M., et al. (2021a). Decreased Abundance of Akkermansia muciniphila Leads to the Impairment of Insulin Secretion and Glucose Homeostasis in Lean Type 2 *Diabetes*. doi: 10.1002/advs.202100536

Zhang, X., Shen, D., Fang, Z., Jie, Z., Qiu, X., Zhang, C., et al. (2013). Human Gut Microbiota Changes Reveal the Progression of Glucose Intolerance. *PLoS ONE.* 8, e71108. doi: 10.1371/journal.pone.0071108

Zhang, Z., Tian, T., Chen, Z., Liu, L., Luo, T., and Dai, J. (2021b). Characteristics of the gut microbiome in patients with prediabetes and type 2 diabetes. *PeerJ.* 9, e10952. doi: 10.7717/peerj.10952

Zhao, L., Zhang, F., Ding, X., Wu, G., Lam, Y. Y., Wang, X., et al. (2018). Gut bacteria selectively promoted by dietary fibers alleviate type 2 diabetes. *Science* 359, 1151–1156. doi: 10.1126/science.aao5774

Zhao, X., Zhang, Y., Guo, R., Yu, W., Zhang, F., Wu, F., et al. (2020). The alteration in composition and function of gut microbiome in patients with Type 2 diabetes. *J. Diabetes Res.* 2020. doi: 10.1155/2020/8842651

Zhou, J., Deng, Y., Luo, F., He, Z., Tu, Q., and Zhi, X. (2010). Functional molecular ecological networks. *MBio.* 1. doi: 10.1128/mBio.00169-10

Conflict of Interest: The authors declare that the research was conducted in the absence of any commercial or financial relationships that could be construed as a potential conflict of interest.

Publisher's Note: All claims expressed in this article are solely those of the authors and do not necessarily represent those of their affiliated organizations, or those of the publisher, the editors and the reviewers. Any product that may be evaluated in this article, or claim that may be made by its manufacturer, is not guaranteed or endorsed by the publisher.

frontiers | Frontiers in Microbiology

TYPE Original Research
PUBLISHED 19 July 2022
DOI 10.3389/fmicb.2022.923162

OPEN ACCESS

EDITED BY
Sandip Paul,
JIS Institute of Advanced Studies and Research, India

REVIEWED BY
Narendrakumar M. Chaudhari,
Friedrich Schiller University Jena, Germany
Zaki Saati Santamaría,
University of Salamanca,
Spain

*CORRESPONDENCE
Yin-yu Gu
guyy70@163.com

SPECIALTY SECTION
This article was submitted to Microbial Symbioses, a section of the journal Frontiers in Microbiology

RECEIVED 19 April 2022
ACCEPTED 01 July 2022
PUBLISHED 19 July 2022

CITATION
Chen C-j, Guo G, Li M, Liang X-y and Gu Y-y (2022) Diversity of endophytic bacteria of mulberry (*Morus* L.) under cold conditions.
Front. Microbiol. 13:923162.
doi: 10.3389/fmicb.2022.923162

Diversity of endophytic bacteria of mulberry (*Morus* L.) under cold conditions

Chuan-jie Chen, Guang Guo, Meng Li, Xiao-yan Liang and Yin-yu Gu*

Shandong Institute of Sericulture, Shandong Academy of Agricultural Sciences, Yantai, China

Endophytic bacteria are known to impact the growth and fitness of agriculturally relevant plants. However, there are limited reports describing endophytic bacteria related to mulberry (*Morus* L.). The present study used Illumina-based 16S rRNA gene sequencing to investigate the endophytic bacterial communities of two mulberry cultivars with differing resistance to low temperature, under cold conditions. In most cases, the bacterial communities of endophytes in the root exhibited higher richness compared with those in the stem, and the communities in resistant cultivar X792 exhibited higher richness compared with those of the sensitive cultivar "Da Shi" (DS). The difference in the proportion of unique operational taxonomic units showed the same trend. The number of genera with significant differences in abundance was greater between organs than between months, and greater between months than between cultivars. Microbial diversity analysis showed that Proteobacteria and Actinobacteria were the dominant phyla in all samples, while *Pseudomonas*, *Steroidobacter*, and *Rhodococcus* were the dominant genera in different samples. There were significant differences between cultivars DS and X792 in the relative abundance of *Pseudomonas*, *Acidibacter*, *Frigoribacterium*, *Gaiella*, and *Pseudokineococcus*. PICRUSt predictions indicated that the relative abundances of endophytic bacteria in membrane transport and signal transduction were significantly higher in the stem of resistant cultivar X792 in January compared with that of sensitive cultivar DS. Analysis of β-Diversity also revealed distinct differences in endophytic bacterial communities of stem and root, and communities of the stem in January and February. The complex correlation of the endophytic communities was higher in sensitive mulberry cultivar DS compared with resistant cultivar X792, in the stem compared with the root, and in January compared with February. Overall, findings from this study suggested that the diversity and community structure of endophytic bacteria in mulberry were significantly influenced by organs and months, followed by the host cultivar. The study provides insight into the complex microbial diversity of mulberry under cold conditions.

KEYWORDS

mulberry, endophytic, bacteria, diversity, cold condition

Introduction

Low-temperature stress leads to a series of molecular, biochemical, physiological, and morphological changes that adversely affect plant growth and productivity, and it is a major factor limiting the productivity of agricultural crops. Cold-resistant microorganisms play an important role in agricultural production by promoting nitrogen fixation, nutrient accumulation, and growth, and inhibiting harmful pathogens and insects (Barka et al., 2006). Many cold-tolerant, potential plant-growth-promoting bacteria (PGPB) including *Arthrobacter*, *Bacillus*, *Exiguobacterium*, *Pseudomonas*, and *Providencia* etc. have been reported from low-temperature environments (Mishra et al., 2011; Selvakumar et al., 2011; Bisht et al., 2013; Yadav et al., 2014, 2015, 2016).

Endophytes are a class of microorganisms that live in various groups of healthy plants and have a harmonious relationship with the host plant in the intercellular spaces or cells of the organs (Xie and Xia, 2008). Although De Bary (1866) put forward the concept of endophytes as early as 160 years ago, research on endophytes has only attracted attention for recent decades. Studies demonstrated that plant endophytes can promote plant growth and development (Hallmann et al., 1997), and enhance host resistance to biotic and abiotic stress (whether drought, salt, or cold/thermal stress; Bacon et al., 2015). When plants are in contact with a microbe, regardless of fungi or bacteria, either a pathogen or a mutualist, is in part correlated with an increase in antioxidant or osmolyte concentrations and/or in the activities of antioxidant enzymes (Singh et al., 2011; Chen et al., 2014; Harman et al., 2021; Zhou et al., 2021). Furthermore, some endophytic bacteria were shown to be involved in tolerance to low-temperature stress (Barka et al., 2006; Fernandez et al., 2012; Theocharis et al., 2012), such as *Burkholderia phytofirmans PsJN* (Barka et al., 2006) and *Clavibacter* sp. strain Enf12 (Ding et al., 2011), which can promote the growth, stimulate physiological activity and improve plant tolerance to chilling stress through enhancing the antioxidant defense system. 16S rRNA functional prediction demonstrated that hosts that adapted to lower temperatures recruited endophytic communities with a higher abundance of genes related to cold resistance (Wei et al., 2021).

Mulberry, belonging to the genus *Morus* of the family Moraceae, is a species native to China and has been widely cultivated in many regions including Asia, Africa, America, and Europe (Khan et al., 2013). Mulberry is one of the major commercialized, perennially grown tree plants and is cultivated worldwide mainly for its foliage, which is the food of the silkworm (*Bombyx mori* L.) that produces the cocoon for silk (Shukla et al., 2016). In many mulberry-growing countries, particularly India and China, mulberry is used to feed the silkworm, but in most European countries, including Turkey and Greece, mulberries are grown for fruit production rather than foliage (Ercisli and Orhan, 2007). Freezing or extremely low temperatures are key factors influencing plant growth, development, and productivity in temperate regions. Frost and low temperature adversely affect mulberry leaf production, which ultimately affects silkworm rearing. Some research revealed a correlation between mulberry cold resistance and genes (Ukaji et al., 2004; Checker et al., 2011; Saeed et al., 2016). However, there is currently limited information available regarding the endophytic bacterial community of the mulberry under cold conditions. Thus, this study aimed to explore the relationship between microorganisms and low-temperature resistance by examining the endophytic microbial diversity of mulberry trees under cold conditions. Two mulberry cultivars with different resistance to low temperature were selected according to the frozen shoot rate (Frozen withered shoot length/Total shoot length; Pan and Zhang, 2006), and the endophytic bacteria of the stem and root of resistant cultivar X792 and sensitive cultivar DS in January and February were analyzed. To the best of our knowledge, this is the first study to characterize endophytes related to the mulberry under cold conditions, and findings from the study provide new insights into this bacterial community and lay a foundation for future studies.

Materials and methods

Sample collection and surface sterilization

Two mulberry cultivars, "Da Shi" (DS) and "Xuan792" (X792), were used in the study. X792 is resistant to low temperature (frozen shoot rate 5.06%), while DS is sensitive to low temperature (frozen shoot rate 30.43%). Both varieties were sampled at the experimental farm of Shandong Sericulture Research Institute (37°08′25.44′N, 121°08′33.98′E) in Yantai, Shandong Province, China, and shared the same climatic conditions. The local area has a temperate maritime climate, possessing a mean air temperature of 14°C and average annual rainfall of approximately 700 mm, with a frost-free period of more than 210 days, and an annual sunshine duration of more than 2,100 h. The maximum and the minimum temperatures in January were 5.55 and −1.97°C, respectively, and in February were 6.97 and −0.10°C, respectively. The temperature of the sampling day in January was −4~3°C, and in February was 3~9°C.

Three replicates for each sample (2 cultivars × 2 months× 2 organs) were performed in the study. The samples were collected from 10-year-old trees of mulberry cultivars, with three healthy-looking, medium-growth plants randomly selected from each site in January and February of 2019. Plants were at least 2 m apart within an area of 100 m^2. Healthy branches approximately 180.0 cm in length and 1.5–1.8 cm in diameter, and roots approximately 30.0 cm in length and 0.3–0.8 cm in diameter, were collected from the three individual plants of each cultivar. Whole branches and roots were placed in Ziploc bags and stored at 4°C during transportation to the laboratory, then were processed within 24 h of collection. Branches and roots were washed in running tap water to remove surface debris and then the middle 60 cm of the branches were cut into several 5.0-cm segments,

while the middle 18 cm of the roots were cut into several 2.0-cm segments (15–20 cm depth). Six surface-sterilized segments of each cultivar were randomly selected, pooled, and served as one replicate for further endophyte enrichment (Nxumalo et al., 2020).

Plant materials were surface sterilized using the procedure of Du et al. (2020). Briefly, the stem and root were washed thoroughly with sterile water, then immersed in 70% ethanol for 3 min, washed with fresh sodium hypochlorite solution (2.5% available Cl^-) for 5 min with agitation, rinsed three times with 70% ethanol for 30 s, and finally washed five times with sterile distilled water. The sterile distilled water used in the final wash was cultivated to determine the success of the surface disinfection. Briefly, 100 µl of the final rinse water was plated on an LB medium and examined for bacterial growth after incubation at 30°C for 72 h. If there was no bacterial growth, the surface-sterilization procedure was confirmed to be effective and the samples were used for further analysis.

DNA extraction and PCR amplification

Genomic DNA of the microbial community of the mulberry plants was extracted from stems and roots using the E.Z.N.A.® soil DNA Kit (Omega Bio-tek, Norcross, GA, United States) according to the manufacturer's instructions. The quality of the extracted DNA was checked on a 1% agarose gel, and DNA concentration and purity were determined with a NanoDrop 2000 UV–vis spectrophotometer (Thermo Scientific, Wilmington, DE, United States). The hypervariable region V5–V7 of bacterial 16S rRNA genes was amplified by PCR using primer pairs 799F (5′-AACMGGATTAGATACCCKG-3′) and 1193R (5′-ACGTCATCCCCACCTTCC-3′; Beckers et al., 2017). The PCR mixtures contained 4 µl 5× *TransStart*FastPfu buffer, 2 µl of 2.5 mM dNTPs, 0.8 µl each primer (5 µM each), 0.4 µl *TransStart*FastPfu DNA Polymerase, 10 ng template DNA, and ddH_2O to 20 µl, and reactions were performed in triplicate. PCR cycling conditions comprised an initial denaturation at 95°C for 3 min, 27 cycles of denaturing at 95°C for 30 s, annealing at 55°C for 30 s, and extension at 72°C for 45 s, followed by a single extension at 72°C for 10 min and a continued hold at 4°C. The complete sequences generated in this study are available in the NCBI SRA database under accession number SRR18790631–SRR18790654.

Illumina MiSeq sequencing and processing of sequencing data

The resulting PCR products were extracted from 2% agarose gels, purified using the AxyPrep DNA Gel Extraction Kit (Axygen Biosciences, Union City, CA, United States) according to the manufacturer's instructions, and quantified using a Quantus™ Fluorometer (Promega, United States). Purified amplicons were pooled in equimolar ratios and paired-end sequenced by Majorbio Bio-Pharm Technology Co. Ltd. (Shanghai, China) using an Illumina MiSeq PE300 platform (Illumina, San Diego, CA, United States) according to standard protocols.

Raw 16S rRNA gene sequencing reads were demultiplexed, quality-filtered by fastq version 0.20.0 (Chen et al., 2018), and merged by FLASH version 1.2.7 (Magoč and Salzberg, 2011). Operational taxonomic units (OTUs) with a 97% similarity cut-off (Stackebrandt and Goebel, 1994; Edgar, 2013) were clustered using UPARSE version 7.1 (Edgar, 2013), and chimeric sequences were identified and removed. The taxonomy of each OTU representative sequence was analyzed by RDP Classifier version 2.2 (Wang et al., 2007) against the 16S rRNA database using a confidence threshold of 0.7 (Beckers et al., 2016).

Data analysis

Bacterial relative abundance, α-diversity, community composition, β-diversity, network structure, and functional analysis were performed using the free online Majorbio Cloud Platform.[1] Alpha diversity was calculated including Chao, ACE, Shannon, and Simpson indices using Mothur software (versionv.1.30.2). Rarefaction curves were also generated using Mothur at a 97% identity level. The Venn, Bar, and Heatmap diagram was generated using R script (version 3.3.1), and Silva (Release138; http://www.arb-silva.de) was used for taxonomic classification. β-diversity was visualized using principal coordinates analysis (PCoA) and non-metric multidimensional scaling (NMDS) based on the distance matrix, with the calculation of the Euclidean and Bray-Curtis algorithm, respectively. The potential function of bacterial communities was predicted using PICRUSt2 (Douglas et al., 2020; Phylogenetic Investigation of Communities by Reconstruction of Unobserved States), and the histogram was created using Graphypad Prism 9.3.1. The OTU abundance table was first normalised by PICRUSt2 (the PICRUSt process stores the COG information and KO information corresponding to the OTU), i.e., the influence of the number of copies of the 16S marker gene in the species genome was removed; then obtain the COG family information and KEGG Ortholog (KO) information corresponding to the OTU, and the abundance of each COG and the KO abundance were calculated; According to the information in the COG database, the description information of each COG and its function information can be parsed from the eggNOG database, so as to obtain the functional abundance spectrum; based on the information in the KEGG database, the KO, Pathway, and EC information can be obtained, and the abundance of each functional class can be calculated based on the OTU abundance. In addition, for Pathway, three levels of metabolic pathway information can be obtained by using PICRUSt2, and the abundance table of each level can be obtained respectively, significant differences were analyzed by TTEST in excel. The community differences for the 10 most abundant bacterial genera distributions were evaluated using the Student's *T* and one-way

1 www.majorbio.com

ANOVA, with values of $p < 0.05$ considered statistically significant. Finally, a network analysis was performed by spearman using Network × software to explore the complexity of the interactions among the microbial taxa, the absolute value of the correlation coefficient ≥0.7, $p < 0.05$, and the diagram was drawn by Cytoscape 3.5.1. All experiments were conducted in triplicate. Data are presented as means with SDs. Statistical analyses were performed using DPS Statistics 18.10 software.[2] Differences between the means of different treatments were determined using the Duncan test at $p < 0.05$. The OTU table with taxonomic annotations was provided as Supplementary Table S1.

Results

Sequence data and α-diversity index analysis

After read-quality filtering, a total of 1,059,743 high-quality sequences remained and were queried. The total number of bases was 399,174,839, and the average read length was 376.63 bp, (Supplementary Table S2). Rarefaction curves (Supplementary Figure S1), combined with the estimated coverage values (Table 1), suggested that the data were sufficiently large to capture most of the bacterial diversity in the samples. The number of OTUs obtained was highest in the stem of X792 in February, followed by that in the root of X792 in January, while the lowest number of OTUs was present in the stem of X792 in January.

The number of common and unique bacterial OTUs in the different samples was presented in Venn diagrams (Figure 1). The numbers of shared OTUs between January and February samples (983, Figure 1A) and between DS and X792 samples (932, Figure 1B) were both higher than the number of shared OTUs between stem and root samples (801, Figure 1C). For unique OTUs, the number obtained in January (332) was lower than the number obtained in February (667; Figure 1A); the number in the sensitive mulberry cultivar DS (302) was lower than the number in the resistant mulberry cultivar X792 (748; Figure 1B); and the number obtained from the stems (821) was higher than the number obtained from the roots (360; Figure 1C).

In addition, the number of OTUs shared between different organs and months for the DS cultivar (103; Figure 1D) was lower than that of the X792 cultivar (176; Figure 1E); the number shared between different organs and cultivars in January (97; Figure 1F) was lower compared with that in February (163; Figure 1G); and the number of OTUs shared between different months and cultivars for the stem samples (172; Figure 1H) was lower than that obtained for the root samples (260; Figure 1I). The number of unique OTUs in the roots of the DS cultivar in February (FRDS, 88) was lower than those of the other samples of the DS cultivar (JSDS, 178; JRDS, 145; and FSDS,174; Figure 1D); but when compared within stems (Figure 1H), or within February (Figure 1G), or within X792 (Figure 1E), the number of unique OTUs in the stems of X792 in February was the highest (516 in Figure 1E; 548 in Figure 1G; 636 in Figure 1H); and when compared within roots (Figure 1I), or within January (Figure 1F), the number of unique OTUs in the roots of X792 in January was the highest (219 in Figure 1F; 189 in Figure 1I).

These data suggest that month, mulberry cultivar., and organ all contributed to the observed variation in the composition of the mulberry endophytic bacterial OTUs.

Microbial taxonomic analysis at the phylum level

The obtained sequences were classified into 25 phyla, 56 classes, 169 orders, 325 families, and 647 genera. The bacterial composition and relative abundances varied across different samples. Figure 2 showed the diversity of bacterial communities in different samples at the phylum level. The dominant bacterial phyla were Proteobacteria and Actinobacteria across all samples; Actinobacteria was the predominant phylum in JSDS (45.88%), while Proteobacteria (47.65–88.44%) was the

2 www.dpsw.cn

TABLE 1 Operational taxonomic unit (OTU; 97% similarity cut-off) richness and diversity indices of different samples associated with mulberry.

Sample	OTUs observed	Shannon	Simpson	ACE	Chao	Coverage (%)
JSDS	285 ± 11 cd	3.13 ± 0.32 a	0.14 ± 0.08 b	308 ± 30 cd	336 ± 52 e	99.82
JS792	250 ± 28 d	2.70 ± 0.59 ab	0.20 ± 0.11 b	270 ± 50 d	290 ± 80 e	99.85
JRDS	353 ± 78 c	2.83 ± 0.47 ab	0.16 ± 0.08 b	645 ± 382 b	562 ± 110 bc	99.38
JR792	451 ± 98 b	3.16 ± 0.40 a	0.12 ± 0.03 b	687 ± 198 b	662 ± 205 b	99.26
FSDS	286 ± 70 cd	1.38 ± 0.77 c	0.55 ± 0.24 a	345 ± 67 cd	346 ± 63 de	99.64
FS792	682 ± 148 a	1.75 ± 0.40 c	0.50 ± 0.09 a	1,309 ± 672 a	1,076 ± 277 a	98.56
FRDS	323 ± 101 cd	2.57 ± 0.70 b	0.21 ± 0.17 b	621 ± 324 b	501 ± 219 cd	99.42
FR792	350 ± 160 c	3.14 ± 0.76 a	0.11 ± 0.1 b	564 ± 139 bc	494 ± 216 cd	99.42

Data are means ± SD of three replicates. Values within a column followed by different lowercase letters are significantly different ($p < 0.05$). JSDS, stem of DS in January; JS792, stem of X792 in January; JRDS, root of DS in January; JR792, root of X792 in January; FSDS stem of DS in February; FS792, stem of X792 in February; FRDS, root of DS in February; and FR792, root of X792 in February.

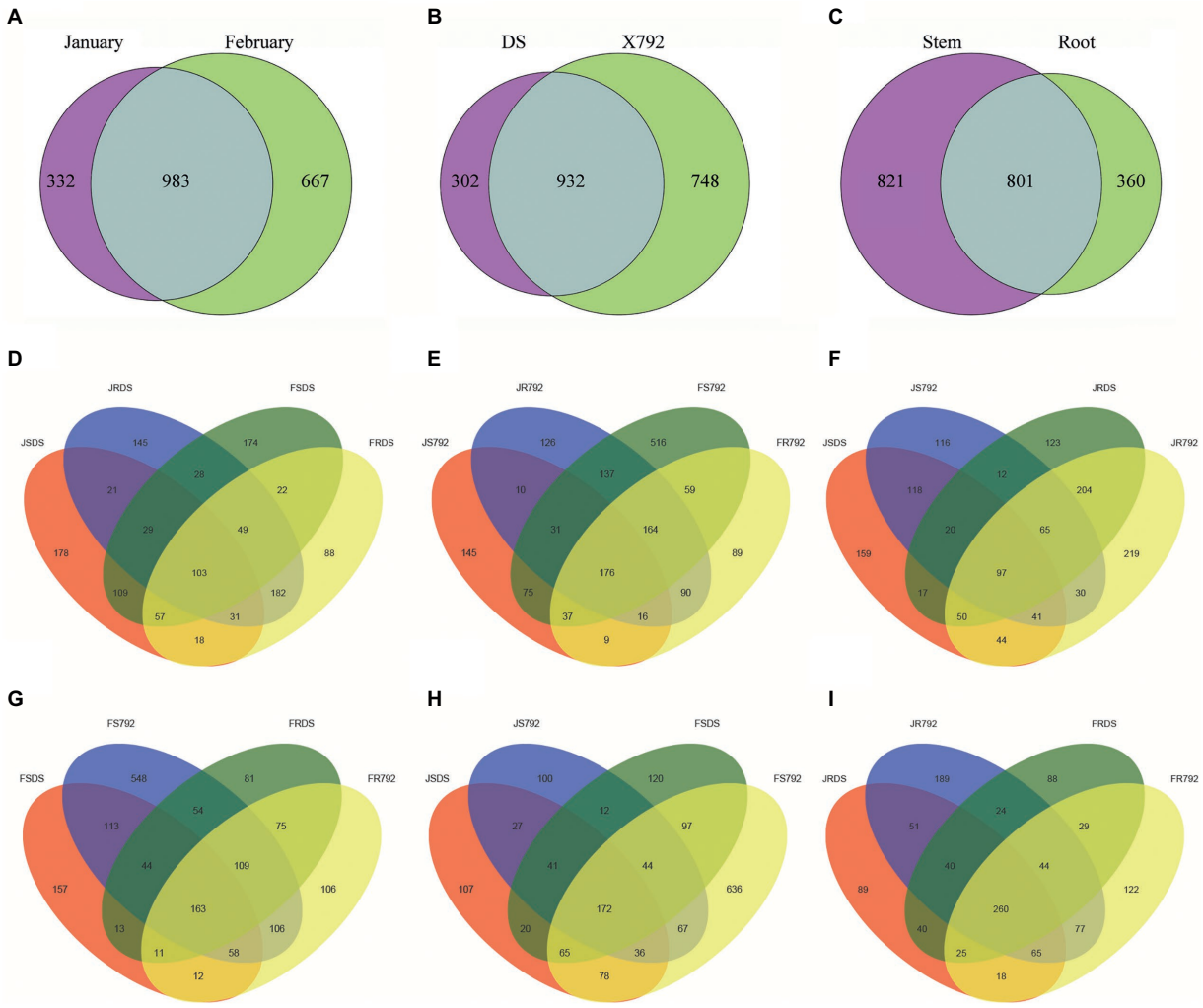

FIGURE 1
Venn diagrams of the number of operational taxonomic units (OTUs) obtained in different organs of different cultivars of mulberry in different months (January and Fabruary). Values represent the number of OTUs. **(A)** Grouping by month. January and February represent January bacterial communities and February bacterial communities of the two cultivars, respectively. **(B)** Grouping by cultivar. DS and X792 represent bacterial communities of cultivars "DS" and "X792" in 2months, respectively. **(C)** Grouping by organ. Stem and root represent bacterial communities from stem and root of two cultivars in 2months, respectively. **(D,E)** Grouping by different organs of DS **(D)** and X792 **(E)** in different months. **(F,G)** Grouping by different organs of different cultivars in January **(F)** and February **(G)**. **(H,I)** Grouping by stem **(H)** and root **(I)** of different cultivars in different months.

predominant phylum across all other samples. The relative abundance of Proteobacteria was higher in all cultivar X792 samples compared with the DS samples, except for the stem in February, while Actinobacteria showed the opposite trend. For Proteobacteria, Actinobacteria, and Firmicutes, there was no significant difference in relative abundance between mulberry cultivars; while there was a significant increase over relative abundance of Actinobacteria and Firmicutes in the stem of January compared with February ($p < 0.01$), and Proteobacteria showed the opposite trend, but not in root samples. Proteobacteria showed a significant increase in stems compared with roots in February ($p < 0.01$), and Actinobacteria showed the opposite trend, and Firmicutes showed significant increase in stems compared with roots in January ($p < 0.01$; Supplementary Table S3). These analyses indicated that the temperature had a greater influence on the endophytic bacterial content of the stem compared with that of the root.

Microbial taxonomic analysis at the genus level and core genus distribution

Clustering of the top 30 genera was shown in Figure 3 (with additional supporting data present in Supplementary Table S4). These 30 bacterial genera belonged to five phyla including Proteobacteria (15 genera), Actinobacteria (12), Firmicutes (1), Bacteroidetes (1), and unclassified_k_norank_d_Bacteria (1). *Pseudomonas*, *Steroidobacter*, *Rhodococcus*, *Ralstonia*, *Mycobacterium*, and *Cryptosporangium* were the most abundant (>0.1%) genera across all samples, but the genera distributions

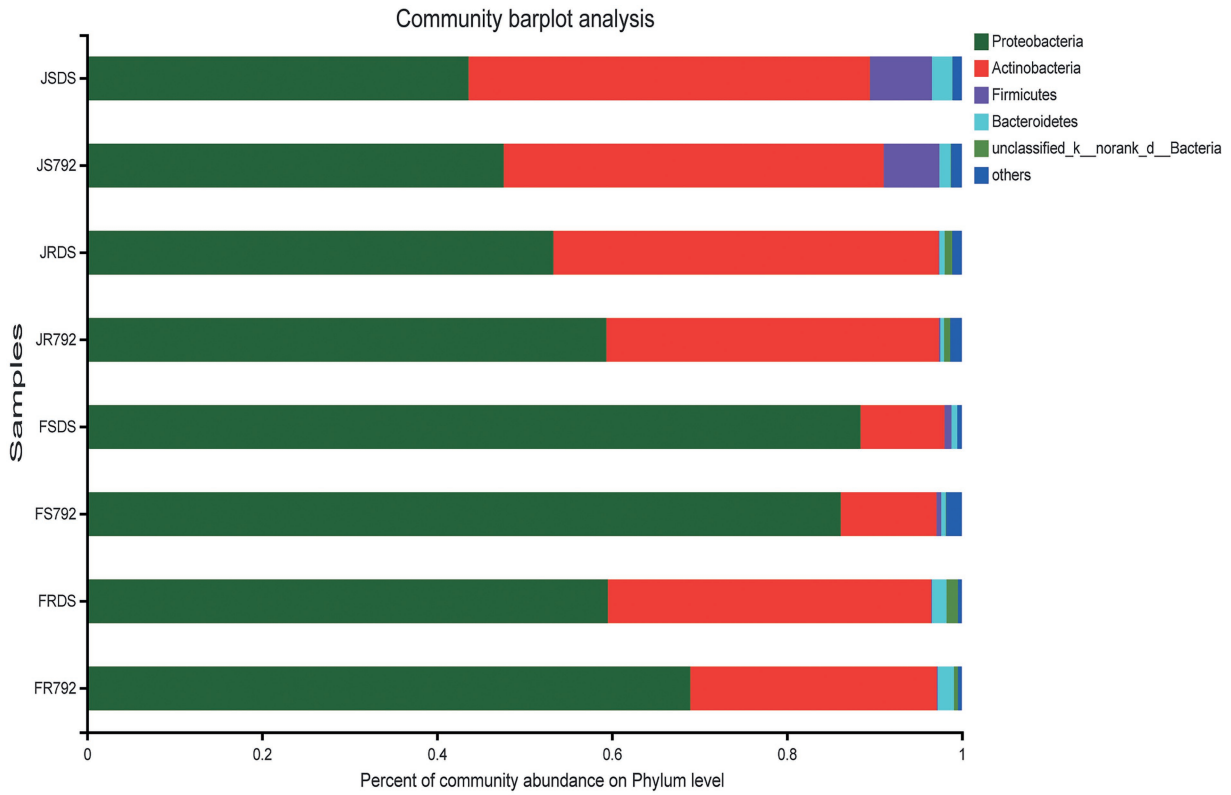

FIGURE 2
Relative abundance of endophytic bacteria from different communities at the phylum level. Taxa with an abundance <0.01 are included in "others." The *x*-axis represents different communities (month×organ×cultivar), and the *y*-axis represents the relative abundance of all communities.

differed greatly across different samples. *Pseudomonas* was the predominant genus in FSDS and FS792, while *Steroidobacter* was the most abundant genus in JRDS, JR792, FRDS, and FR792, and *Rhodococcus* was the predominant genus in JSDS and JS792. These results showed that the most predominant genus of the stem in January was *Rhodococcus*, and in February was *Pseudomonas*, while *Steroidobacter* was the predominant genus in the root, and there was no significant difference in the relative abundance of genus between mulberry cultivars. The clustering analysis showed a clear similarity among samples from each tissue (roots are similar and shoots are similar). For roots, two cultivars were gathered separately, and for stems, there were more similarities in January, and the same rule occurred in February.

The relative abundance of the top 15 core genera was also compared, and some differences were observed (Figure 4). The relative frequencies of *Frigoribacterium* ($p = 0.04$) and *Pseudokineococcus* ($p = 0.04$) were higher in JSDS compared with those in JS792 (Figure 4A), but there was no significant difference between JRDS and JR792 (Figure 4B), while that of the genus *Gaiella* ($p = 0.013$) was significantly lower in FSDS compared with that in FS792 (Figure 4C). The relative abundances of *Pseudomonas* ($p = 0.004$) and *Acidibacter* ($p = 0.012$) were significantly lower and significantly lower, respectively, in FRDS compared with those in FR792 (Figure 4D).

The relative abundance of *Pseudomonas* was also significantly lower in JSDS compared with that in FSDS ($p = 0.0002$), while that of *Ralstonia* was significantly higher in JSDS compared with that in FSDS ($p = 0.005$; Figure 4E). Moreover, the relative abundances of *Pseudomonas* ($p = 0.000009$) and *Rhodococcus* ($p = 0.0007$) were significantly lower and significantly higher, respectively, in JS792 compared with those in FS792, and that of *Ralstonia* was also significantly higher in JS792 compared with that in FS792 ($p = 0.004$; Figure 4F). *Pseudomonas* had a significantly lower abundance in JRDS compared with that in FRDS ($p = 0.012$; Figure 4G), and had a significantly lower relative abundance in JR792 compared with that in FR792 ($p = 0.002$; Figure 4H). The relative abundances of *Rhodococcus* ($p = 0.003$) and *Ralstonia* ($p = 0.001$) were significantly higher, and that of *Steroidobacter* was significantly lower, in JSDS compared with JRDS ($p = 0.01$; Figure 4I). In addition, the relative abundance of *Rhodococcus* was significantly higher in JS792 compared with that in JR792 ($p = 0.0003$), while that of *Steroidobacter* was significantly lower ($p = 0.003$), and those of *Ralstonia* ($p = 0.002$) and *Pseudomonas* ($p = 0.008$) were significantly higher, in JS792 compared with JR792 (Figure 4J). Furthermore, the genus *Pseudomonas* had a significantly higher relative abundance in FSDS compared with that in FRDS ($p = 0.0002$), while relative abundances of *Steroidobacter* ($p = 0.006$) and *Virgisporangium* were significantly

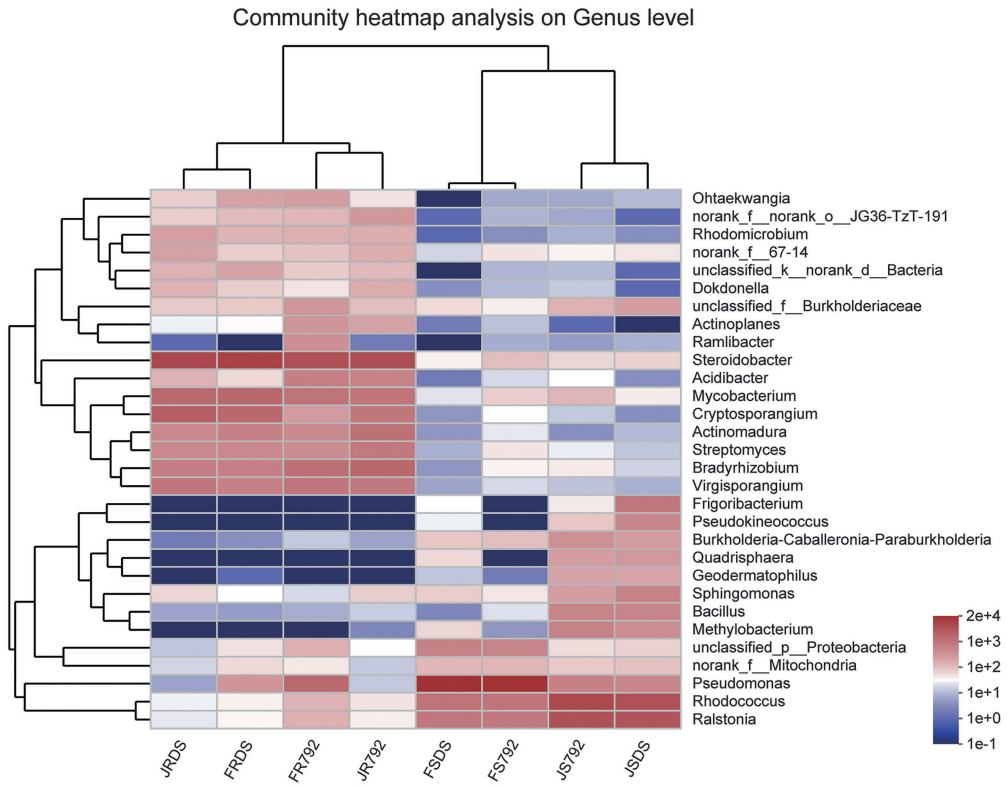

FIGURE 3
Heatmap displaying the relative abundances of the predominant genera (top 30) in each sample. The dendrogram represents complete-linkage agglomerative clustering, based on Euclidean dissimilarities.

lower in FSDS compared with those in FRDS ($p = 0.006$; Figure 4K). Finally, the relative abundances of *Pseudomonas* ($p = 0.00002$), *Rhodococcus* ($p = 0.0005$), and *Ralstonia* ($p = 0.00005$) were significantly higher, and that of *Bradyrhizobium* ($p = 0.0009$) was significantly lower, in FS792 compared with FR792, and that of *Steroidobacter* ($p = 0.007$) was significantly lower in FS792 compared with that in FR792 (Figure 4L). Overall, there were more significant differences in the relative abundances of the top 15 core genera between stem and root, especially in February, followed by the stem in January and February, while there were fewer significant differences between cultivars.

β-Diversity analysis

To further compare the relationship of endophytic bacteria populations among the stem and root of two mulberry cultivars in January and February, principal coordinates analysis (PCoA) based on Euclidean distances with arithmetic mean clustering was conducted using the genera. This analysis revealed the main variations in bacterial community composition and abundance among the samples. The PCoA results graphically demonstrated that organs or months were strong factors in accounting for the observed variations in the composition of the endophytic bacterial community, in which samples of the stem in January were placed at a higher PC 1 value (63.49%), while samples of the stem in February appeared a higher PC 2 value (27.54%), and root samples showed higher values of both PC 1 and PC 2 (Figure 5), and $p = 0.001$. Samples of the roots of different cultivars in different months clustered together, but the stems showed some separation, with samples of the stems in January and February clustering together, respectively. The PCoA results were supported by non-metric multidimensional scaling (NMDS) plots ($p = 0.001$; Supplementary Figure S2). In summary, these analyses revealed distinct differences in endophytic bacterial communities of stem and root, and stem of January and February, while no clustering was evident due to cultivars or root of January and February. This finding confirmed the results for the differential analysis of genera.

Network structure

To explore the complexity of the interactions within the endophytic communities among the different samples, a correlation network analysis was conducted, and its topological properties were calculated. The correlation network analysis revealed that there was a difference between January and February. The complexity and modular structure were higher in January (Figure 6A) compared with that in February (Figure 6B), specifically, the average number of connections per node was

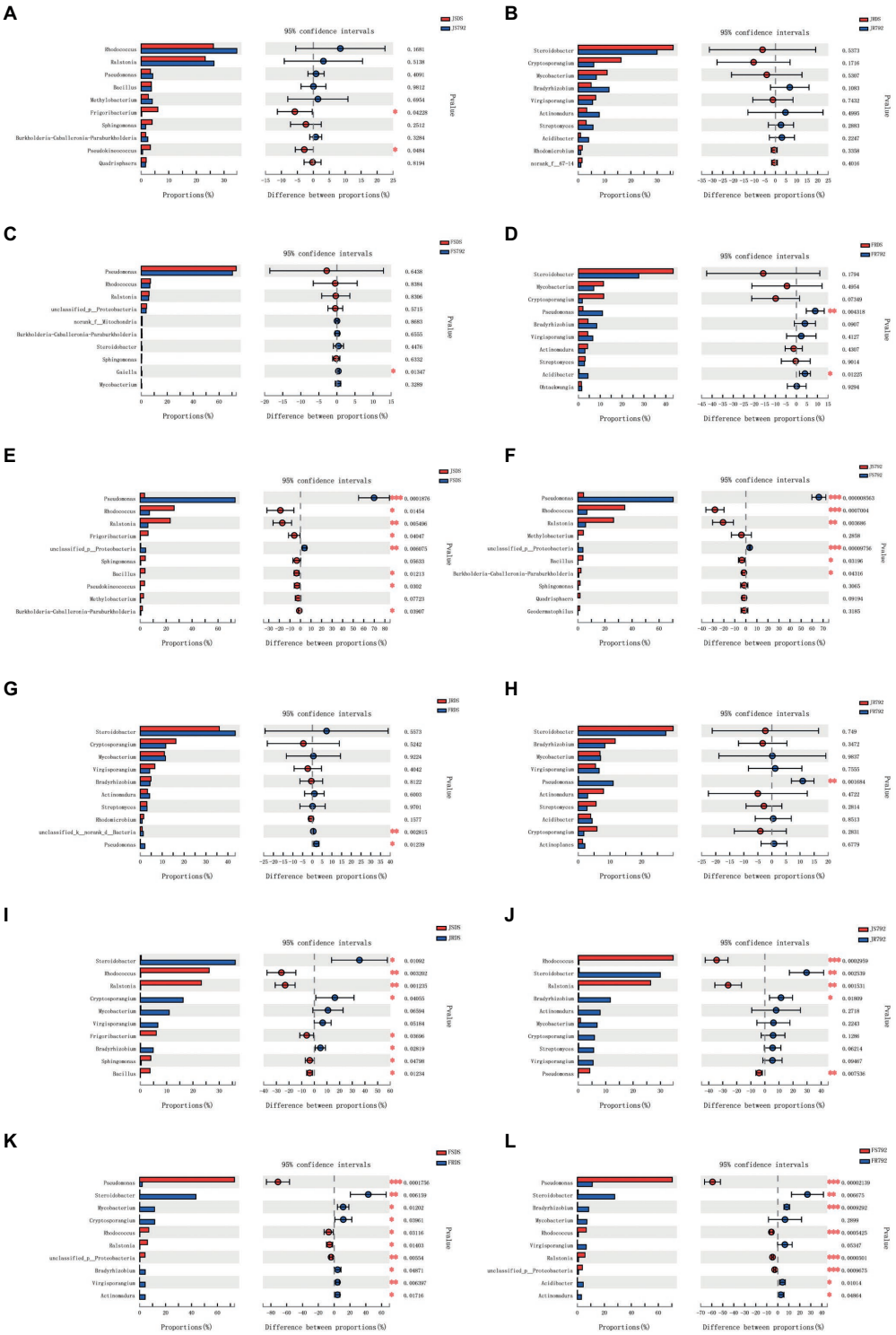

FIGURE 4
Comparison of the abundance of the top 10 dominant bacterial genera in different samples. *** indicates a significant difference at $p<0.001$, ** $p<0.01$, and * $p<0.05$. The x-axis represents the mean proportion of the genus and the y-axis shows the top 10 dominant bacterial genera. **(A)** Compared between different cultivars of stem in January. **(B)** Compared between different cultivars of root in January. **(C)** Compared between different cultivars of stem in February. **(D)** Compared between different cultivars of root in February. **(E)** Compared between different months of DS stem. **(F)** Compared between different months of X792 stem. **(G)** Compared between different months of DS root. **(H)** Compared between different months of X792 root. **(I)** Compared between different organs of DS in January. **(J)** Compared between different organs of X792 in January. **(K)** Compared between different organs of DS in February. **(L)** Compared between different organs of X792 in February.

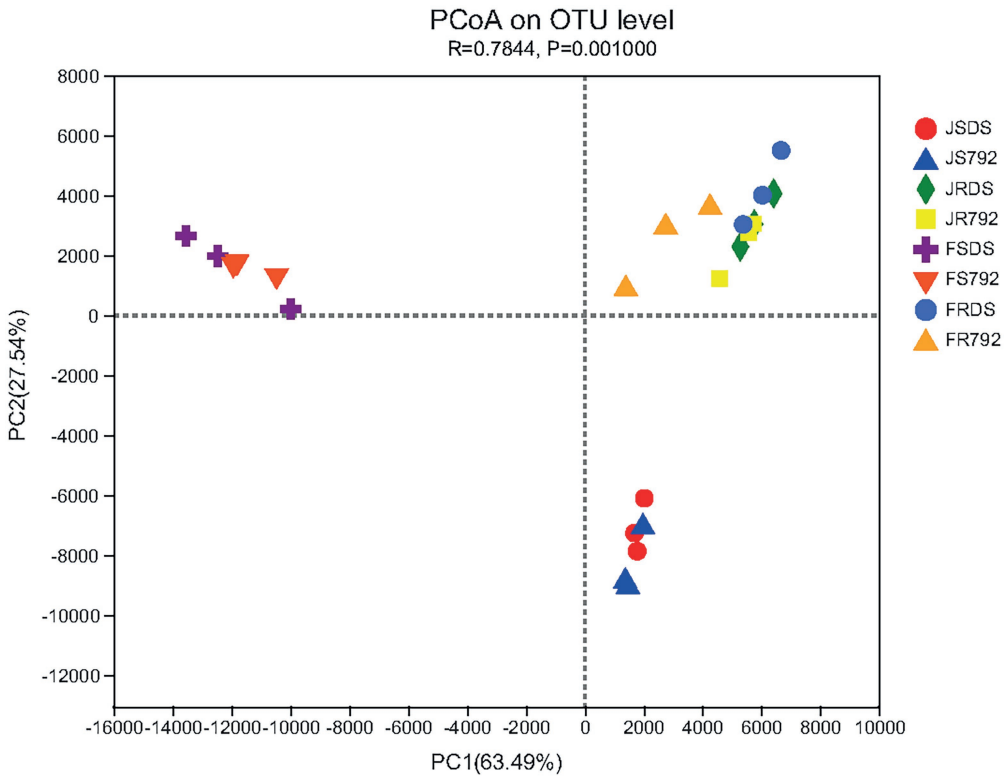

FIGURE 5
Principal coordinates analysis (PCoA) plot of the relationship between samples based on similarity in the community composition of bacterial OTUs. Two first components (PC1 and PC2) were plotted and represent 91.03% of the variation.

higher in January (node average degree = 26.60) relative to the February samples (node average degree = 21.57; Table 2). Furthermore, January also presented a higher number of negative correlations (negative edges = 210) compared with February (negative edges = 113) on the basis of the same number of positive correlations. Additionally, the correlation network analysis of microbial communities for the sensitive or resistant cultivar also revealed differences. The sensitive mulberry cultivar DS (Figure 6C) appeared to have a more complex correlation compared with the resistant mulberry cultivar X792 (Figure 6D). The node average degree, positive edges, and negative edges in DS (node average degree = 22.07, positive edges = 163, and negative edges = 168) were all higher than those in X792 (node average degree = 15, positive edges = 120, and negative edges = 90).

The correlation network analysis was performed to assess the complexity of the interactions among the microbial taxa, the results also revealed a strong difference between the communities based on organs, such as stem (Figure 6E) and root (Figure 6F). The edge number for stem (edge = 218) was much higher compared with that of root (edge = 28), with 130 positive edges (positive edges of stem = 160, positive edges of root = 30) and 26 negative edges (negative edges of stem = 58, negative edges of root = 32). Simultaneously, the average number of connections per node was also much higher in the stem (node average degree = 15.03) compared with that in the root (node average degree = 4.43). In summary, the correlation network indicated that the interaction degree of the microbial community of mulberry was strongly influenced by the month, cultivar resistance, and organs. January, sensitive mulberry cultivar., and stem possessed a greater microbial complexity and abundance compared with February, the resistant mulberry cultivar., and root. The nodes with the highest connections in January were *Quadrisphaera*, *Steroidobacter*, *Pseudokineococcus*, *Dokdonella*, *Streptomyces*, *Rhodomicrobium*, *Methylobacterium*, *Virgisporangium*, *Frigoribacterium*, and *unclassified_k__norank_d__Bacteria* with a degree of 29, and in February was *unclassified_p__Proteobacteria, unclassified_k__norank_d__Bacteria*, and *Pseudomonas* with the degree of 26. *Burkholderia-Caballeronia-Paraburkholderia, and unclassified_k__norank_d__Bacteria* were the genera with the highest degree of 23 in cultivar X792, and *Methylobacterium* was the genus with the highest degree of 23 in cultivar DS. *Ralstonia* (degree = 10) and *Pseudomonas* (degree = 24) were the genera with the highest connections in root and stem, respectively.

Potential functional consequences

Functions of microbial communities from all samples were predicted using PICRUSt2 on level 1 and level 2 (Figure 7; Supplementary Tables S10, S11). Genes associated with

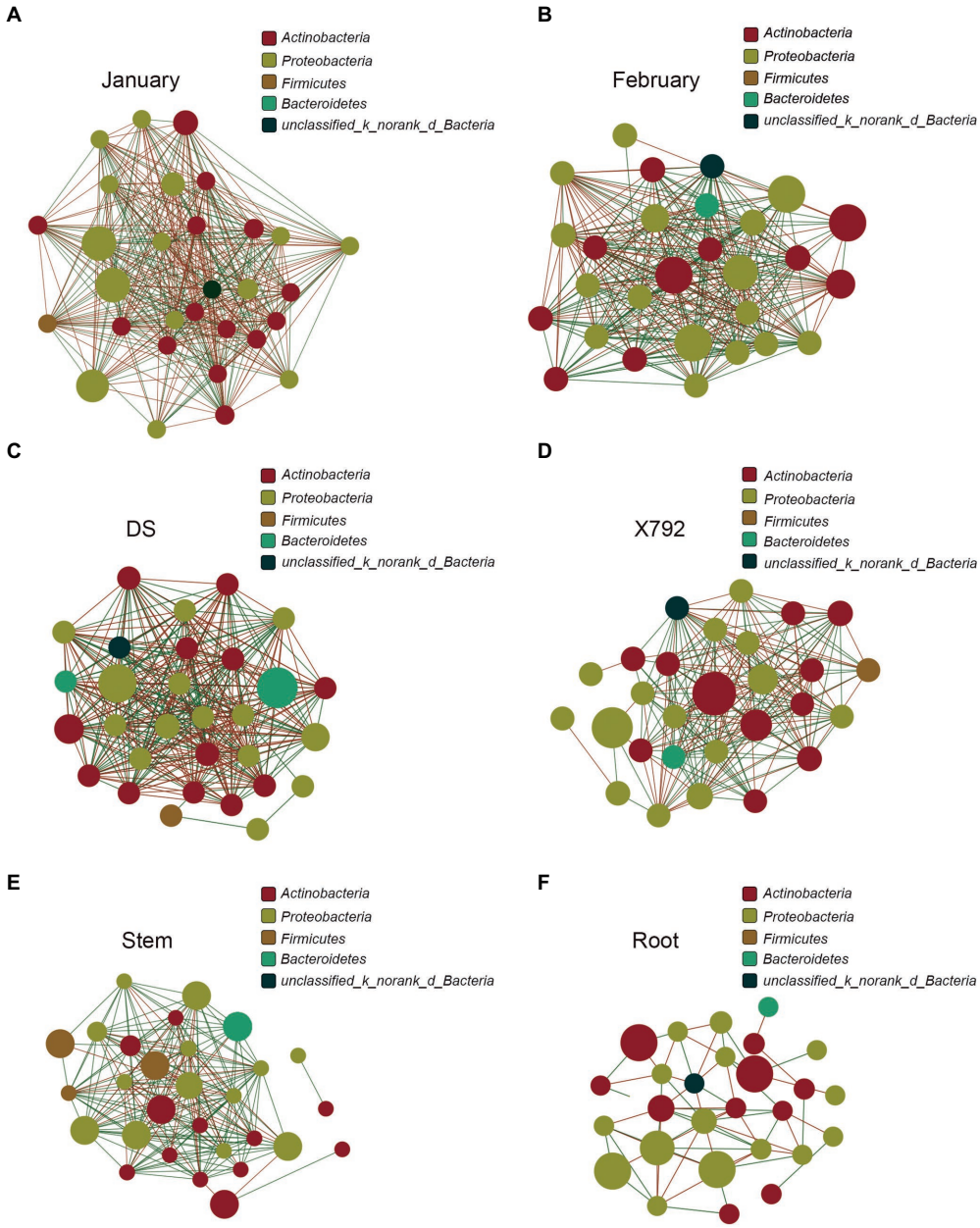

FIGURE 6
Correlation network analysis of microbial communities in January **(A)**, February **(B)**, DS **(C)**, X792 **(D)**, stem **(E)**, and root **(F)**. Node color represents phylum classification. The size of the node is proportional to the richness of bacteria. Edge color corresponds to positive (red) and negative (green) correlations, and the edge thickness is equivalent to the correlation values.

environmental information processing (level 1), membrane transport, and signal transduction (level 2) were significantly (95% CIs, $p < 0.05$) more abundant in the stem of resistant cultivar X792 compared with the sensitive cultivar DS in January, which may be related to low-temperature resistance, and warrants further research. Furthermore, Welch's *t*-test results (Supplementary Table S6) indicated that, except for the environmental information processing of stems in January, there were no significant differences in several predicted pathways (e.g., metabolism, environmental information processing, cellular processes, genetic information processing, human diseases, and organismal systems) among the other samples based on cultivars. In addition, there were no significant differences between the root of X792 in January and February for the five pathways on level 1, as well as the JRDS and FRDS for genetic information processing and organismal systems pathways, but there were significant or significant differences in the other samples based on months. Except for the genetic information processing pathway of the JS792 and JR792 samples, there were no significant differences among the

TABLE 2 Correlation network analysis of microbial communities.

	January	February	DS	X792	Stem	Root
Node numbers	30	28	30	28	29	28
Edge numbers	399	302	331	210	218	62
Node average degree	26.6	21.57	22.07	15	15.03	4.43
Positive edges	189	189	163	120	160	30
Negative edges	210	113	168	90	58	32

The correlation network indices were calculated based on the top 30 genera. The average number of connections per node in the network, that is, the node connectivity.

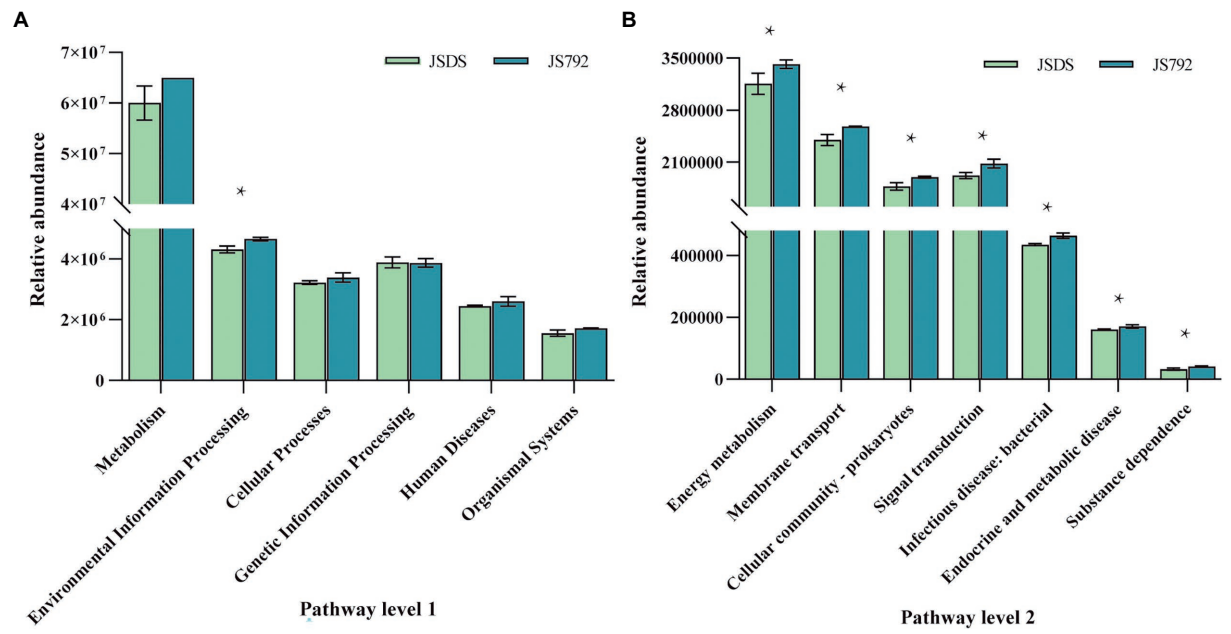

FIGURE 7
Functional analysis of microbial communities between mulberry cultivars. **(A)** Pathway level 1. **(B)** Pathway level 2. * indicates a significant difference at $p<0.05$.

other samples in January based on organs, but there were significant or significant differences throughout the five pathways in all samples in February. The stems of January and February had different degrees of significant differences in the five pathways, as did the stem and root of February. Overall, Environmental information processing was the pathway exhibiting the most differences, followed by the cellular process.

Discussion

Microbial endophytes play an important role in the ecology, health, and growth promotion of plants (Lodewyckx et al., 2002; Mahajan and Tuteja, 2005; Hardoim et al., 2015; Vandenkoornhuyse et al., 2015; Hassani et al., 2018). However, despite the importance of endophytes, there are limited reports concerning endophytic microbial populations in mulberry. Therefore, the diversity of endophytic bacteria of mulberry under cold conditions was investigated in the present study using Illumina Miseq sequencing of the V5–V7 variable region of the bacterial 16S rRNA gene.

Except for the stem of resistant mulberry cultivar X792 in February, all of the bacterial richness in the stem of the other samples was lower compared with that in the root, but cultivar DS did not reach a significant level. This was not entirely consistent with previous findings that bacterial communities of endophytes in the root exhibit higher richness than those in the stem (Ma et al., 2013; Beckers et al., 2017; Tian and Zhang, 2017; Table 1). The difference of X792 in February may be caused by the cultivar and environmental variability; the temperature rose in February and approached the critical point of germination, which resulted in a substantial increase in microbial richness. For cultivars, X792 samples had greater bacterial richness compared with DS samples of root in January and stem in February. This suggests that the richness in the resistant mulberry cultivar was higher than that in the sensitive cultivar in most cases. Richness in the stem of X792 in February was

much higher than that in January, while there was no significant change in richness in the stem of DS, which suggested that X792 reacted faster to high temperatures. Bacterial richness in the root of both cultivars in January was higher compared with that in February, albeit in different proportions, and this may be also caused by the temperature.

Previous studies showed that although most endophytic bacteria colonizing the host plant originate from the rhizosphere soil (Compant et al., 2010; Yang et al., 2017), some may originate elsewhere such as through colonization of the phyllosphere *via* aerosols (Fahlgren et al., 2010). It is hypothesized that endophytic bacteria colonize plants primarily through the root network *via* natural and artificial wound sites, root hairs, and epidermal junctions (Shi et al., 2014). In the current study, the root and stem shared about one-fifth to one-third of the OTUs, which may be migrating from root to stem (Supplementary Tables S7–S9). In January, the proportion of unique OTUs in the root of both cultivars was greater than that in the stem, while the opposite trend was observed in February. This may be due to the increased activity of microorganisms in the atmospheres as the temperature increases. In addition, the difference in the proportion of unique OTUs was much greater in resistant cultivar X792 compared with that in sensitive cultivar DS, and further research is required to determine whether this might be related to low-temperature resistance.

Proteobacteria have previously been reported as the predominant phylum of endophytic bacteria followed by Actinobacteria, and the richness of Proteobacteria in roots is higher than that in stems (Akinsanya et al., 2015; Tian and Zhang, 2017; Ou et al., 2019). Similar results were found in most samples of the current study, except in one January sample which the dominant bacterial phylum in the stem of sensitive cultivar DS was Actinobacteria, followed by Proteobacteria (Figure 2). This may be an individual case. The relative abundance of Proteobacteria was markedly higher than that of Actinobacteria in the stem of both cultivars in February, while there were no big differences among other samples; this difference might be caused by environmental variability.

The species composition of microbial communities can be affected by many factors. Hardoim et al. (2011) reinforced the importance of understanding the genetic and (bio)chemical mechanisms involved in the interplay between soil type, plant genotype, rhizosphere microbiome, plant growth, and plant health. The current study revealed that for the top 15 core genera, there were only five genera that had significant differences between the two mulberry cultivars. These genera were *Frigoribacterium* and *Pseudokineococcus*, which had significantly greater relative frequencies in the stem of sensitive cultivar DS compared with that in resistant cultivar X792, and *Gaiella*, which showed the opposite trend in the stem, *Pseudomonas* and *Acidibacter*, which also showed the opposite trend in the root (Figure 4). Egamberdieva (2009) revealed that *Pseudomonas* provided important benefits to plants by synthesizing phytohormones and improving host stress tolerance. *Pseudomonas* is a recognized psychrophile (Moyer and Morita, 2001), and well-characterized and reported from low-temperature environments (Yadav et al., 2016). *Frigoribacterium* also was one of the bacteria isolated from cold environments on Earth, such as permafrost, cold soils and deserts, glaciers, lakes, sea ice in the Arctic, Antarctic, and high mountains, as well as the deep sea, ice caves, and the atmospheric stratosphere etc. (Xin et al., 2013). *Acidibacter* was first isolated and identified by Falagán and Johnson (2014), from a pit lake in an abandoned metal mine in southwestern Spain. However, little has been reported on the function of *Pseudokineococc* and *Gaiella*. Additional work is required to elucidate whether the presence of the above five genera contributes to the low-temperature resistance. Ou et al. (2019) revealed that *Pantoea*, *Methylobacterium*, and *Pseudomonas* were the predominant genera in mulberry endophytic communities. *Pantoea* and *Methylobacterium* were not detected in the present study, and this may be caused by the sampling area and season. The number of genera with significant differences in abundance was greater between organs than between months, and greater between months than between cultivars. Among these genera, *Steroidobacter*, one of the dominant genera in the root (Tian and Zhang, 2017), and *Bradyrhizobium*, a nitrogen-fixing bacteria that has attracted a lot of attention (Saranraj et al., 2021), were more abundant in root than in stem, while *Rhodococcus* and *Ralstonia* were more abundant in stem compared with root. *Steroidobacter* also was the predominant genus in root both in January and February, but for the stem, *Rhodococcus* was the predominant genus in January and *Pseudomonas* was the predominant genus in February (Supplementary Tables S4, S5). Since abundant *Pseudomonas* and *Sphingomonas* were found to be harbored by aerosol (Fahlgren et al., 2010), enrichment of *Pseudomonas* in the stem endosphere may occur *via* dual origins, colonization of the rhizosphere, and/or stem stomatal colonization. *Rhodococcus* are gram-positive bacteria isolated from a variety of environments, such as soil and deep sea, and have a wide variety of species. *Rhodococcus* species are frequently studied because they possess multiple functions, and are meaningful for their environmental and industrial biotechnology applications (Abdelmohsen et al., 2010, 2014; Graça et al., 2015; Elsayed et al., 2017; Krivoruchko et al., 2019).

Correlation network analysis demonstrated that there was lower complexity in the network of the resistant cultivar X792 compared with sensitive cultivar DS, which was similar to the findings of Ou et al. (2019) but contrary to the observation of Mendes et al. (2018). Furthermore, the complexity in the network of the root was lower compared with stem, and lower in February compared with January.

Low temperature is a major environmental factor that limits plant growth, productivity, and distribution. To ensure optimal growth and survival, plants must respond and adapt to low-temperature stress using a variety of biochemical and physiological processes. The major detrimental effect of freezing is that it induces severe membrane damage, and this damage is largely due to the acute dehydration associated with freezing

(Steponkus, 1984; Steponkus et al., 1993). Furthermore, manipulation of signal transduction was shown to be an important way to make plants survive at low temperatures (Kim et al., 2003; Solanke and Sharma, 2008). Congruent with these observations, the function predictions obtained with PICRUSt in the current study indicated that the relative abundance of membrane transport and signal transduction (level 2), which belong to environmental information processing (level 1), was significantly higher in the stem of resistant cultivar X792 in January compared with that of sensitive cultivar DS. Since PICRUSt predictions are based on the use of a limited database to search for functions, these predictions can be biased and further study is required to reach more accurate conclusions.

Conclusion

This study is the first to elucidate the bacterial diversity and composition of mulberry under cold conditions using high-throughput sequencing methods. The endophytic bacterial community of the stem and root of two mulberry cultivars with differing resistance to low temperature was explored under cold conditions (January and February). Organ and month were found to play keys role in determining the diversity and community composition of endophytic bacteria in mulberry, followed by the host cultivar. *Pseudomonas*, *Steroidobacter*, and *Rhodococcus* were the predominant genera among the different samples, *Pseudomonas*, *Acidibacter*, *Frigoribacterium*, *Gaiella*, and *Pseudokineococcus* were genera that had significant differences in the relative abundance between cultivars DS and X792. There were different degrees of significant differences in five functional pathways between the stems of January and February, and between the stem and root of February samples. The relative abundance of endophytic bacteria that function as membrane transport and signal transduction was significantly higher in the stem of resistant cultivar X792 in January compared with that of sensitive cultivar DS. The present study significantly enhances understanding of the factors influencing the community structures of endophytic bacteria and lays the foundation for conducting research on the resistance of mulberry endophytes to low temperatures. Further studies are necessary to elucidate the low-temperature resistance properties or functional traits of mulberry endophytes and the functional roles of bacterial species in plant–microbe interactions in mulberry.

Data availability statement

The datasets presented in this study can be found in online repositories. The names of the repository/repositories and accession number(s) can be found in the article/**Supplementary Material**.

Author contributions

Y-yG contributed to the conception of the study and wrote the manuscript. C-jC, GG, ML, and X-yL performed the experiments and data analyses. All authors contributed to the article and approved the submitted version.

Funding

This work was supported by the Sericultural Industry Technical System of Shandong Province (Grant no. SDAIT-18-09).

Conflict of interest

The authors declare that the research was conducted in the absence of any commercial or financial relationships that could be construed as a potential conflict of interest.

Publisher's note

All claims expressed in this article are solely those of the authors and do not necessarily represent those of their affiliated organizations, or those of the publisher, the editors and the reviewers. Any product that may be evaluated in this article, or claim that may be made by its manufacturer, is not guaranteed or endorsed by the publisher.

Supplementary material

The Supplementary Material for this article can be found online at: https://www.frontiersin.org/articles/10.3389/fmicb.2022.923162/full#supplementary-material

References

Abdelmohsen, U. R., Pimentel-Elardo, S. M., Hanora, A., Radwan, M., Abou-El-Ela, S. H., Ahmed, S., et al. (2010). Isolation, phylogenetic analysis and anti-infective activity screening of marine sponge-associated Actinomycetes. *Mar. Drugs* 8, 399–412. doi: 10.3390/md8030399

Abdelmohsen, U. R., Yang, C., Horn, H., Hajjar, D., Ravasi, T., and Hentschel, U. (2014). Actinomycetes from red sea sponges: sources for chemical and phylogenetic diversity. *Mar. Drugs* 12, 2771–2789. doi: 10.3390/md12052771

Akinsanya, M. A., Goh, J. K., Lim, S. P., and Ting, A. S. Y. (2015). Metagenomics study of endophytic bacteria in *Aloe vera* using next-generation technology. *Genom. Data* 6, 159–163. doi: 10.1016/j.gdata.2015.09.004

Bacon, C. W., Palencia, E. R., and Hinton, D. M. (2015). "Abiotic and biotic plant stress-tolerant and beneficial secondary metabolites produced by endophytic *Bacillus* species," in *Plant Microbes Symbiosis: Applied Facets (Chapter 8)*. (New Delhi: Springer), 163–177.

Barka, E. A., Nowak, J., and Clement, C. (2006). Enhancement of chilling resistance of inoculated grapevine plantlets with a plant growth-promoting rhizobacterium, *Burkholderia phytofirmans* strain PsJN. *Appl. Environ. Microbiol.* 72, 7246–7252. doi: 10.1128/AEM.01047-06

Beckers, B., Beeck, M. O. D., Thijs, S., Truyens, S., Weyens, N., Boerjan, W., et al. (2016). Performance of 16s rDNA primer pairs in the study of rhizophere and endosphere bacterial microbiomes in metabarcoding studies. *Front. Microbiol.* 7:650. doi: 10.3389/fmicb.2016.00650

Beckers, B., Beeck, M. O. D., Weyens, N., Boerjan, W. V., and Angronsveld, J. (2017). Structural variability and niche differentiation in the rhizosphere and endosphere bacterial microbiome of field-grown poplar trees. *Microbiome* 5, 25. doi: 10.1186/s40168-017-0241-2

Bisht, S. C., Mishra, P. K., and Joshi, G. K. (2013). Genetic and functional diversity among root-associated psychrotrophic Pseudomonad's isolated from the Himalayan plants. *Arch. Microbiol.* 195, 605–615. doi: 10.1007/s00203-013-0908-4

Checker, V. G., Chhibbar, A. K., and Khurana, P. (2011). Stress-inducible expression of barley Hva1 gene in transgenic mulberry displays enhanced tolerance against drought, salinity and low temperature stress. *Transgenic Res.* 21, 939–957. doi: 10.1007/s11248-011-9577-8

Chen, X., Song, F., Liu, F., Tian, C., Liu, S., and Xu, H. (2014). Effect of different arbuscular mycorrhizal fungi on growth and physiology of maize at ambient and low temperature regimes. *Sci. World J.* 2014:956141. doi: 10.1155/2014/956141

Chen, S. F., Zhou, Y. Q., Chen, Y. R., and Gu, J. (2018). Fastp: an ultra-fast all-in-one FASTQ preprocessor. *Bioinformatics* 34, i884–i890. doi: 10.1093/bioinformatics/bty560

Compant, S., Clément, C., and Sessitsch, A. (2010). Plant growth-promoting bacteria in the rhizo-and endosphere of plants: their role, colonization, mechanisms involved and prospects for utilization. *Soil Biol. Biochem.* 42, 669–678. doi: 10.1016/j.soilbio.2009.11.024

De Bary, A. (1866). *Morphologie und Physiologie der Pilze, Flechten und Myxomyceten*. Leipzig: W. Engelmann, 1–360

Ding, S., Huang, C. L., Sheng, H. M., Song, C. L., Li, Y. B., and An, L. Z. (2011). Effect of inoculation with the endophyte *Clavibacter* sp. strain Enf12 on chilling tolerance in *Chorispora bungeana*. *Physiol. Plant.* 141, 141–151. doi: 10.1111/j.1399-3054.2010.01428.x

Douglas, G. M., Maffei, V. J., Zaneveld, J. R., Yurgel, S. N., Brown, J. R., Taylor, C. M., et al. (2020). PICRUSt2 for prediction of metagenome functions. *Nat. Biotechnol.* 38, 685–688. doi: 10.1038/s41587-020-0548-6

Du, J. J., Wang, T., Zhou, Q. X., Hu, X. G., Wu, J. H., Li, G. F., et al. (2020). Graphene oxide enters the rice roots and disturbs the endophytic bacterial communities. *Ecotoxicol. Environ. Saf.* 192:110304. doi: 10.1016/j.ecoenv.2020.110304

Edgar, R. C. (2013). UPARSE: highly accurate OTU sequences from microbial amplicon reads. *Nat. Methods* 10, 996–998. doi: 10.1038/nmeth.2604

Egamberdieva, D. (2009). Alleviation of salt stress by plant growth regulators and IAA producing bacteria in wheat. *Acta Physiol. Plant.* 31, 861–864. doi: 10.1007/s11738-009-0297-0

Elsayed, Y., Refaat, J., Abdelmohsen, U. R., and Fouad, M. A. (2017). The genus *Rhodococcus* as a source of novel bioactive substances: a review. *J. Pharm. Phytochem.* 6, 83–92.

Ercisli, S., and Orhan, E. (2007). Chemical composition of white (*Morus alba*), red (*Morus rubra*) and black (*Morus nigra*) mulberry fruits. *Food Chem.* 103, 1380–1384. doi: 10.1016/j.foodchem.2006.10.054

Fahlgren, C., Hagström, A., Nilsson, D., and Zweifel, U. L. (2010). Annual variations in the diversity, viability, and origin of airborne bacteria. *Appl. Environ. Microbiol.* 76, 3015–3025. doi: 10.1128/AEM.02092-09

Falagán, C., and Johnson, D. B. (2014). *Acidibacter ferrireducens* gen. nov., sp. nov.: an acidophilic ferric iron-reducing gammaproteobacterium. *Extremophiles* 18, 1067–1073. doi: 10.1007/s00792-014-0684-3

Fernandez, O., Theocharis, A., Bordiec, S., Feil, R., Jacquens, L., Clement, C., et al. (2012). *Burkholderiaphytofirmans* PsJN acclimates grapevine to low temperature by modulating carbohydrate metabolism. *Mol. Plant Microbe Interact. J.* 25, 496–504. doi: 10.1094/MPMI-09-11-0245

Graça, A. P., Viana, F., Bondoso, J., Correia, M. I., Gomes, L., Humanes, M., et al. (2015). The antimicrobial activity of heterotrophic bacteria isolated from the marine sponge *Erylus deficiens* (Astrophorida, Geodiidae). *Front. Microbiol.* 6:389. doi: 10.3389/fmicb.2015.00389

Hallmann, J., Quadt-Hallmann, A., Mahaffee, W. F., and Kloepper, J. W. (1997). Bacterial endophytes in agricultural crops can. *J. Microbiol.* 37, 361–370. doi: 10.1177/0095244305054674

Hardoim, P. R., Andreote, F. D., Reinhold-Hurek, B., Sessitsch, A., Overbeek, L. S., and Elsas, J. D. (2011). Rice root-associated bacteria: insights into community structures across 10 cultivars. *FEMS Microbiol. Ecol.* 77, 154–164. doi: 10.1111/j.1574-6941.2011.01092.x

Hardoim, P. R., Overbeek, L. S., Berg, G., Pirttil, A. M., Compant, S., Campisano, A., et al. (2015). The hidden world within plants: ecological and evolutionary considerations for defining functioning of microbial endophytes. *Microbiol. Mol. Biol. Rev.* 79, 293–320. doi: 10.1128/MMBR.00050-14

Harman, G., Khadka, R., Doni, F., and Uphoff, N. (2021). Benefits to plant health and productivity from enhancing plant microbial Symbionts. *Front. Plant Sci.* 11:610065. doi: 10.3389/fpls.2020.610065

Hassani, M. A., Durán, P., and Hacquard, S. (2018). Microbial interactions within the plant holobiont. *Microbiome* 6, 58. doi: 10.1186/s40168-018-0445-0

Khan, M. A., Rahman, A. A., Islam, S., Khandokhar, P., Parvin, S., Islam, M. B., et al. (2013). A comparative study on the antioxidant activity of methanolic extracts from different parts of *Morus alba* L. (moraceae). *BMC Res. Notes* 6, 24. doi: 10.1186/1756-0500-6-24

Kim, K. N., Cheong, Y. H., Grant, J. J., Pandey, G. K., and Luan, S. (2003). *CIPK3*, a calcium sensor-associated protein kinase that regulates abscisic acid and cold signal transduction in Arabidopsis. *Plant Cell* 15, 411–423. doi: 10.2307/3871874

Krivoruchko, A., Kuyukina, M., and Ivshina, I. (2019). Advanced *Rhodococcus* biocatalysts for environmental biotechnologies. *Catalysts* 9, 236. doi: 10.3390/catal9030236

Lodewyckx, C., Vangronsveld, J., Porteous, F., Moorea, E. R. B., Taghavi, S., Mezgeay, M., et al. (2002). Endophytic bacteria and their potential applications. *Crit. Rev. Plant Sci.* 21, 583–606. doi: 10.1080/0735-260291044377

Ma, B., Lv, X. F., Warren, A., and Gong, J. (2013). Shifts in diversity and community structure of endophytic bacteria and archaea across root, stem and leaf tissues in the common reed, *Phragmites australis*, along a salinity gradient in a marine tidal wetland of northern China. *Antonie Van Leeuwenhoek* 104, 759–768. doi: 10.1007/s10482-013-9984-3

Magoč, T., and Salzberg, S. L. (2011). FLASH: fast length adjustment of short reads to improve genome assemblies. *Bioinformatics* 27, 2957–2963. doi: 10.1093/bioinformatics/btr507

Mahajan, S., and Tuteja, N. (2005). Cold, salinity and drought stresses: an overview. *Arch. Biochem. Biophys.* 444, 139–158. doi: 10.1016/j.abb.2005.10.018

Mendes, L. W., Raaijmakers, M. R., Hollander, M., Mendes, R., and Tsai, S. M. (2018). Influence of resistance breeding in common bean on rhizosphere microbiome composition and function. *ISME J.* 12, 212–224. doi: 10.1038/ismej.2017.158

Mishra, P. K., Bisht, S. C., Ruwari, P., Selvakumar, G., Joshi, G. K., Bisht, J. K., et al. (2011). Alleviation of cold stress in inoculated wheat (*Triticum aestivum L.*) seedlings with psychrotolerant *Pseudomonads* from NW Himalayas. *Arch. Microbiol.* 193, 497–513. doi: 10.1007/s00203-011-0693-x

Moyer, C. L., and Morita, R. Y. (2001). *Psychrophiles and Psychrotrophs. Encyclopedia of Life Sciences* John Wiley & Sons, Ltd.

Nxumalo, C. I., Ngidi, L. S., Shandu, J. S. E., and Maliehe, T. S. (2020). Isolation of endophytic bacteria from the leaves of *Anredera cordifolia* CIX1 for metabolites and their biological activities. *BMC Complement. Med. Therap.* 20, 300. doi: 10.1186/s12906-020-03095-z

Ou, T., Xu, W. F., Wang, F., Strobel, G., Zhou, Z. Y., Xiang, Z. H., et al. (2019). A microbiome study reveals seasonal variation in endophytic bacteria among different mulberry cultivars. *Comput. Struct. Biotechnol. J.* 17, 1091–1100. doi: 10.1016/j.csbj.2019.07.018

Pan, Y. L., and Zhang, L. (2006). *Description Specifications and Data Standards of Mulberry Germplasm.* (Beijing: China agriculture press), 62–63.

Saeed, B., Baranwal, V. K., and Khurana, P. (2016). Comparative transcript omics and comprehensive marker resource development in mulberry. *BMC Genomics* 17, 16–24. doi: 10.1186/s12864-016-2417-8

Saranraj, P., Sivasakthivelan, P., Al-Tawaha, A. R. M., Sudha, A., Al-Tawaha, A. R., Sirajuddin, S. N., et al. (2021). Diversity and evolution of Bradyrhizobium communities relating to soybean cultivation: a review. *IOP Conf. Ser. Earth Environ. Sci.* 788:012208. doi: 10.1088/1755-1315/788/1/012208

Selvakumar, G., Joshi, P., Suyal, P., Mishra, P. K., Joshi, G. K., Bisht, J. K., et al. (2011). *Pseudomonas lurida* M2RH3 (MTCC 9245), a psychrotolerant bacterium from the Uttarakhand Himalayas, solubilizes phosphate and promotes wheat seedling growth. *World J. Microbiol. Biotechnol.* 27, 1129–1135. doi: 10.1007/s11274-010-0559-4

Shi, Y. W., Yang, H. M., Zhang, T., Sun, J., and Lou, K. (2014). Illumina-based analysis of endophytic bacterial diversity and space-time dynamics in sugar beet on the north slope of Tianshan mountain. *Appl. Microbiol. Biotechnol.* 98, 6375–6385. doi: 10.1007/s00253-014-5720-9

Shukla, P., Rohela, G. K., Shabnam, A. A., and Sharma, S. P. (2016). Prospect of cold tolerant genes and its utilization in mulberry improvement. *Indian Hortic. J.* 6, 127–129.

Singh, L. P., Gill, S. S., and Tuteja, N. (2011). Unraveling the role of fungal symbionts in plant abiotic stress tolerance. *Plant Signal. Behav.* 6, 175–191. doi: 10.4161/psb.6.2.14146

Solanke, A. U., and Sharma, A. K. (2008). Signal transduction during cold stress in plants. *Physiol. Mol. Biol. Plants* 14, 69–79. doi: 10.1007/s12298-008-0006-2

Stackebrandt, E., and Goebel, B. M. (1994). Taxonomic note: a place for DNA-DNA reassociation and 16S rRNA sequence analysis in the present species definition in bacteriology. *Int. J. Syst. Bacteriol.* 44, 846–849. doi: 10.1099/00207713-44-4-846

Steponkus, P. L. (1984). Role of the plasma membrane in freezing injury and low temperature acclimation. *Annu. Rev. Plant Physiol.* 35, 543–584. doi: 10.1146/annurev.pp.35.060184.002551

Steponkus, P. L., Uemura, M., and Webb, M. S. (1993). "A contrast of the cryostability of the plasma membrane of winter rye and spring oat-two species that widely differ in their freezing tolerance and plasma membrane lipid composition," in *Advances in Low-Temperature Biology. Vol. 2.* ed. P. L. Steponkus (London: JAI Press), 211–312.

Theocharis, A., Bordiec, S., Fernandez, O., Paquis, S., Dhondt-Cordelier, S., Baillieul, F., et al. (2012). *Burkholderia phytofirmans* PsJN primes *Vitis vinifera*L. and confers a better tolerance to low nonfreezing temperatures. *Mol. Plant Microbe Interact. J.* 25, 241–249. doi: 10.1094/MPMI-05-11-0124

Tian, X. Y., and Zhang, C. S. (2017). Illumina-based analysis of endophytic and rhizosphere bacterial diversity of the coastal halophyte *Messerschmidia sibirica*. *Front. Microbiol.* 8:2288. doi: 10.3389/fmicb.2017.02288

Ukaji, N., Kuwabara, C., Takezawa, D., Arakawa, K., and Fujikawa, S. (2004). Accumulation of pathogenesis-related (PR) 10/bet v 1 protein homologues in mulberry (*Morus* bombycis Koidz.) tree during winter. *Plant Cell Environ.* 27, 1112–1121. doi: 10.1111/j.1365-3040.2004.01216.x

Vandenkoornhuyse, P., Quaiser, A., Duhamel, M., Le Van, A., and Dufresne, A. (2015). The importance of the microbiome of the plant holobiont. *New Phytol.* 206, 1196–1206. doi: 10.1111/nph.13312

Wang, Q., Garrity, G. M., Tiedje, J. M., and Cole, J. R. (2007). Naive Bayesian classifier for rapid assignment of rRNA sequences into the new bacterial taxonomy. *Appl. Environ. Microbiol.* 73, 5261–5267. doi: 10.1128/AEM.00062-07

Wei, X. T., Jiang, F. G., Han, B., Zhang, H., Huang, D., Shao, X. Q., et al. (2021). New insight into the divergent responses of plants to warming in the context of root endophytic bacterial and fungal communities. *Peer J.* 9:e11340. doi: 10.7717/peerj.11340

Xie, J., and Xia, T. (2008). Research of mulberry endophytes and the prospect of their application. *Newslett. Sericult. Sci.* 28, 44–47.

Xin, Y. H., Zhou, Y. G., and Dong, X. Z. (2013). Biodiversity and cold adaptive mechanisms of psychrophiles. *Biodivers. Sci.* 21, 468–480. doi: 10.3724/SP.J.1003.2013.13040

Yadav, A. N., Sachan, S. G., Verma, P., and Saxena, A. K. (2014). Prospecting cold deserts of North-Western Himalayas for microbial diversity and plant growth promoting attributes. *J. Biosci. Bioeng.* 119, 683–693. doi: 10.1016/j.jbiosc.2014.11.006

Yadav, A. N., Sachan, S. G., Verma, P., and Saxena, A. K. (2016). Bioprospecting of plant growth promoting psychrotrophic Bacilli from the cold desert of north-western Indian Himalayas. *Indian J. Exp. Biol.* 54, 142–150. PMID: 26934782

Yadav, A. N., Sachan, S. G., Verma, P., Tyagi, S. P., Kaushik, R., and Saxena, A. K. (2015). Culturable diversity and functional annotation of psychrotrophic bacteria from cold desert of Leh Ladakh (India). *World J. Microbiol. Biotechnol.* 31, 95–108. doi: 10.1007/s11274-014-1768-z

Yang, R. X., Liu, P., and Ye, W. Y. (2017). Illumina-based analysis of endophytic bacterial diversity of tree peony (Paeonia sect. Moutan) roots and leaves. *Braz. J. Microbiol.* 48, 695–705. doi: 10.1016/j.bjm.2017.02.009

Zhou, L., Li, C., White, J. F., and Johnson, R. D. (2021). Synergism between calcium nitrate applications and fungal endophytes to increase sugar concentration in *Festuca sinensis* under cold stress. *Peer J.* 9:e10568. doi: 10.7717/peerj.10568

frontiers | Frontiers in Microbiology

TYPE Original Research
PUBLISHED 03 August 2022
DOI 10.3389/fmicb.2022.956489

OPEN ACCESS

EDITED BY
Juan Sun,
Qingdao Agricultural University, China

REVIEWED BY
Chao Yang,
Qingdao Agricultural University, China
Wu Zhang,
Lingnan Normal University, China

*CORRESPONDENCE
Pei Tian
tianp@lzu.edu.cn

SPECIALTY SECTION
This article was submitted to Microbial Symbioses, a section of the journal Frontiers in Microbiology

RECEIVED 30 May 2022
ACCEPTED 01 July 2022
PUBLISHED 03 August 2022

CITATION
Gao Y, Chen Y, Luo Y, Liu J, Tian P, Nan Z and Zhou Q (2022) The microbiota diversity of *Festuca sinensis* seeds in Qinghai-Tibet Plateau and their relationship with environments. *Front. Microbiol.* 13:956489. doi: 10.3389/fmicb.2022.956489

The microbiota diversity of *Festuca sinensis* seeds in Qinghai-Tibet Plateau and their relationship with environments

Yue Gao[1,2,3], Youjun Chen[4], Yang Luo[1,2,3], Junying Liu[1,2,3], Pei Tian[1,2,3]*, Zhibiao Nan[1,2,3] and Qingping Zhou[4]

[1]State Key Laboratory of Grassland Agro-Ecosystems, Lanzhou University, Lanzhou, China, [2]Key Laboratory of Grassland Livestock Industry Innovation, Ministry of Agriculture and Rural Affairs, Lanzhou University, Lanzhou, China, [3]College of Pastoral Agriculture Science and Technology, Lanzhou University, Lanzhou, China, [4]Institute of Qinghai-Tibetan Plateau, Southwest Minzu University, Chengdu, China

A total of 14 *Festuca sinensis* seed lots were collected from different geographical locations on the Qinghai-Tibet Plateau to study the seed microbiota and determine the abiotic (temperature, precipitation, and elevation) and biotic (*Epichloë sinensis* infection rate) factors likely to shape the seed microbiome. The 14 seed lots had different bacterial and fungal structures and significantly different diversities ($p < 0.05$). The α-diversity indices of the bacteria were significantly correlated with precipitation ($p < 0.05$), whereas those of the fungi were significantly correlated with temperature ($p < 0.05$). Microbiota analysis showed that Proteobacteria, Cyanobacteria, and Bacteroidetes were the most abundant bacteria at the phylum level in the seeds, and Ascomycota and Basidiomycota were the most abundant fungi. β-diversity analysis suggested large differences in the microbial communities of each sample. Redundancy analysis showed that temperature and precipitation were the main environmental factors that drive variations in the microbial community, at the medium-high elevation (3,000–4,500 m), the impact of temperature and precipitation on microbial community is different, and the other elevations that effect on microbial community were basically identical. Spearman's correlation analysis showed that the relative abundances of the most abundant bacterial phyla were significantly correlated with temperature ($p < 0.05$), whereas those of the most abundant fungal phyla were significantly correlated with precipitation ($p < 0.05$). *E. sinensis* infection rates were significantly correlated with elevation and temperature ($p < 0.05$). These results suggest that temperature and precipitation are the key factors driving the microbial community, that temperature and elevation also had a great influence on the *E. sinensis* infection rate, and that environmental factors (temperature and elevation) may further affect the microbial community by regulating the *E. sinensis* infection rate.

KEYWORDS

***Festuca sinensis*, seed microbiota, environmental factors, temperature, precipitation, *Epichloë sinensis* infection rate**

Introduction

Festuca sinensis, a native cool-season perennial grass species, is distributed across cold and semi-arid regions of China. It is important for grassland production and establishment, restoration of degraded grasslands, and ecological management of the Qinghai-Tibet Plateau of China (Lin et al., 2018). Seeds represent one of the most crucial stages in a plant's life history (Finch-Savage and Bassel, 2015). Microorganisms inside and on the surface of seeds play the important roles in the germination and development of seedlings (Nelson, 2018). During seed germination, a new compartment of microbiome is created. Recent omics-based analyses have shown that plant seeds contain beneficial plant-genotype-specific microbes, which can be vertically transmitted from one plant generation to the next (Johnston-Monje et al., 2016; Adam et al., 2018). Therefore, seed microbes play the important roles in the seed itself and in plant growth (Hashsham et al., 2000). Although studies have reported the importance of seed microbiota, there are no reports on the microbiota of *F. sinensis* seed. Therefore, research on *F. sinensis* seeds and their microbiota is of great significance for the production and applications of *F. sinensis*.

Some studies have shown that microbial communities are significantly affected by plant species, the host environment, host genotype, host age, and many other factors (Tannenbaum et al., 2020). Environmental factors, such as temperature, precipitation, and elevation, could be the main factors that affect microbial diversity (Jiang et al., 2016). However, most reports have only focused on the relationships between environmental factors and the soil microbial community. Some studies have found that the soil microbial community may be affected by total carbon (C) and total nitrogen (N) in the soil (Schimel et al., 2007). Some studies have shown that different tillage practices for wheat (*Triticum aestivum*) can change the microbial diversity in the soil (Lupwayi et al., 1998). However, few studies have highlighted the effects of environmental factors on the microbial diversity of seeds. Klaedtke et al. (2016) found that environmental factors had an important influence on the structure of seed microbiota. However, the relationships between environmental factors (such as temperature, precipitation, and elevation) and microbial diversity of *F. sinensis* seeds have not been reported.

F. sinensis is frequently infected by an asexual, symptomless *Epichloë* species that has been identified as *Epichloë sinensis* (Song et al., 2015; Tian et al., 2020). The recent studies have produced conflicting results regarding *Epichloë* endophytes in pasture microbiomes. For example, Nissinen et al. (2019) demonstrated that resident *E. coenophiala*, as a keystone species, had divergent effects on bacterial and fungal communities in the leaf endosphere of *F. arundinacea* and shaped fungal but not bacterial communities. However, Tannenbaum et al. identified the effects of *E. festucae* var. *lolii* on bacterial microbiomes of pooled young perennial ryegrass seedlings (Tannenbaum et al., 2020). These conflicting results suggest that more research on the influence of *Epichloë* endophytes on microbial communities is needed to understand their mechanisms. Therefore, it is of substantial importance to study the microbiota diversity of different *F. sinensis* seeds and their relationships with *E. sinensis* infection rates to clarify the effects of *Epichloë* endophyte infection on the host seed microbiota.

As environmental factors are very important for the formation of seed microbiota, we wanted to clarify the effects of varied environmental conditions on *F. sinensis* seed microbiota, using seeds collected from different locations in the Qinghai-Tibet Plateau. Therefore, the aims of this study were to 1) identify the seed microbiome diversity of *F. sinensis* seeds, 2) identify the abiotic and biotic factors that are likely involved in shaping the microbiome of *F. sinensis* seeds, and 3) reveal the relationships among *E. sinensis* infection rate, the microbiota, and environmental factors.

Materials and methods

Seed materials

A total of 14 seed lots of *F. sinensis* were collected from different locations on the Qinghai-Tibet Plateau, as shown in Table 1 and Supplementary Figure S1. The *E. sinensis* infection rate in these seed lots was detected by the aniline blue staining method (Nan, 1996). A total of 100 seeds per seed lot were tested, and the *E. sinensis* infection rate was calculated (Christensen et al., 2008).

DNA extraction

Each seed lot had three replicates, with 50 mg of seeds per replication. The total genomic DNA of each replication was extracted using the CTAB/SDS method after homogenization using a pestle and mortar (Ren et al., 2006). Seed powder (50 mg) was placed in a 2-ml microcentrifuge tube containing 1,000 μl of CTAB buffer and 20 μl of lysozyme. After the sample incubated at 65°C for 2–3 h with occasional mixing, the sample was vortexed briefly and then centrifuged for 10 min at 12,000 rpm. Then, 950 μl of the supernatant was mixed with 950 μl chloroform/isoamyl alcohol (24:25 v/v). Again, after totally mixing by vortexing, the sample was centrifuged for 10 min at 12,000 rpm. After repeating this step, the supernatant was mixed with ice-cold isopropanol (the volume of ice-cold isopropanol is three-quarters of the volume of the supernatant), and the tube was inverted five times to precipitate nucleic acids. The sample was centrifuged at 12,000 rpm for 10 min, and the precipitate was washed two times with 1 ml of 75% ethanol. The remaining

TABLE 1 Festuca sinensis seeds collected from different locations in Qinghai-Tibet Plateau.

Ecotypes	Elevation/m	*Epichloë sinensis* infection (%)	Longitude (E)	Latitude (N)	Location
S1	2,589	64	101°57′234″	36° 21′641″	Sanhe Town, Ping'an Country Qinghai
S2	2,741	80	101° 57′437″	36° 20′'047″	Sanhe Town, Ping'an Country Qinghai
S3	2,912	72	97° 99′044″	37° 17′138″	Keyukezhen Town, Delingha City Qinghai
S4	2,912	48	97° 99′044″	37° 17′138″	Keyukezhen Town, Delingha City Qinghai
S5	2,994	80	102°06′348″	36° 20′508″	Bazanggou Township, Ping'an Country Qinghai
S6	3,060	56	101° 58′846″	36° 17′059″	Gucheng Township, Ping'an Country Qinghai
S7	3,129	73	102° 06′214″	36° 20′021″	Bazanggou Township, Ping'an Country Qinghai
S8	3,534	74	93° 07′325″	29° 58′065″	Gubo'gyamda Country, Nyingchi City,Tibet
S9	4,003	32	91° 54′782″	29° 44′692″	Zhaxigang, Maizhokunggar County, Tibet
S10	4,542	0	91° 53′580″	31° 20′039″	Luoma Town, Naqu City, Tibet
S11	4,617	52	93° 57′485″	35° 32′876″	Qumahe Township, Qumaleb country Qinghai
S12	4,617	20	93° 57′485″	35° 32′876″	Qumahe Township, Qumaleb country Qinghai
S13	4,897	54	91° 50′961″	29° 46′564″	Zaxigang, Maizhokunggar County, Tibet
S14	5,197	0	91° 55′336″	32° 54′246″	Tanggula Mountains, Golmud City, Qinghai

small amount of liquid was collected by further centrifugation and then sucked out with a pipette tip. The pellets were air-dried for 2 h. Then, 50 μl ddH_2O was added to dissolve DNA samples. Then, 1 μl RNase A was added to digest RNA, and the mixture was incubated at 37°C for 15 min. DNA was diluted to 1 μg/L with sterile water after its purity was quantified using a NanoDrop 2000 spectrophotometer (Thermo Fisher Scientific, Waltham, MA, USA) (Zheng et al., 2018).

Polymerase chain reaction amplification and high-throughput sequencing

Specific primers with barcodes were synthesized to amplify the bacterial 16s rRNA V4–V5 region (515F:5'-ACTCCTACGGGAGCAGCA-3'; 806R:5'-GGACTACHVGGGTWTCTAAT-3') and the fungal ITS1 or ITS2 region (ITS5-1737F: 5'-CTTGGTCATTTAGAGGAAGTAA-3'; ITS2-2043R: 5'-GCTGCGTTCTTCATCGATGC-3') to assess the composition of both bacterial and fungal communities (Klindworth et al., 2013). Phusion® Hi-Fi PCR Master Mix (New England Biolabs, Ipswich, MA, USA) was used for all PCR. Each PCR mixture contained 5 μl genomic DNA (40–60 ng), 1.5 μl forward primer (10 μm), 1.5 μl reverse primer (10 μM), 1 μl Toyobo, 1 μl KOD FX Neo Buffer (2X), 10 μl dNTP (2 mM), and ddH_2O was added for a total volume of 50 μl. PCR was performed under the following conditions: one cycle at 95°C for 10 min, 15 cycles at 95°C for 1 min, 50°C for 1 min, 72°C for 1 min, and finally 72°C for 7 min. PCR products were subjected to 2% agarose gel electrophoresis for purification and magnetic beads were purified using a TruSeq® DNA PCR-Free Sample Preparation Kit (Illumina, San Diego, CA, USA). A DNA library was constructed after homogenization and quantified using Qubit and q-PCR (AB 9902). After the library was qualified, NovaSeq6000 was used for sequencing at Genepioneer Biotechnologies (Nanjing, China) with separate runs for the 16S rRNA and ITS amplicon pools (Reuter et al., 2015). All quality sequence files supporting the findings of this study are available in the NCBI Sequence Read Archive (SRA) under BioProject ID PRJNA844205.

Microbial diversity analysis

To maximize the quantity and quality of reliable sequences, the following protocols were performed. TrimGalore (version 0.4.2) software filtered out bases with a terminal mass of less than 20, which might comprise adapter and short sequences less than 100 bp in length. After merging *via* FLASH2 (V1.2.7) software and removing low-quality sequences, the primer sequences were trimmed using Mothur (version 1.41.1) (Schloss et al., 2009). Sequences less than 100 bp in length or with an error rate of more than two were discarded by USEARCH (version 10.0). High-quantity and high-reliability sequences were clustered into operational taxonomic units (OTUs) with 97% similarity using the UPARSE algorithm and singleton OTUs (with only one read) were removed.

Bacterial and fungal OTU representative sequences were classified taxonomically through BLAST alignment against the SSUrRNA database of SILVA138 (http://www.arb-silva.de/) and the Unit (v8.2) fungal ITS database (http://unite.ut.ee/), respectively (Bryant and Frigaard, 2006; Liu et al., 2012). The OTU tables were rarefied to the sample containing the lowest number of sequences, with a threshold of >10,000 sequences (all samples with < 10,000 sequences were removed from analyses

prior to the rarefaction step). A subsequent analysis of diversity was performed based on the output-normalized data. QIIME software (version 1.9.1) was used to compute the diversity indices of Chao1, Simpson, Shannon, and the abundance-based coverage estimator (ACE) based on OTU numbers to study the diversity and structure of the microbial community of *F. sinensis* seeds (Shade et al., 2017).

Unweighted pair-group method with arithmetic means (UPGMA) cluster analysis was performed to interpret the distance matrix using average linkage which conducted using the QIIME software (version 1.9.1). Principal component analysis (PCA) based on the unweighted UniFrac distances (Bray–Curtis) (QIIME software, version 1.9.1) was used to examine the differences in microbial community structures among 14 seed lot samples based on the relative abundances of OTUs. PCA was performed using the Ade4 package and ggplot2 package of R software (Version 2.15.3).

Statistical analysis

Meteorological data were obtained from the China Meteorological Center (http://data.cma.cn). Based on the longitude, latitude, and elevation of each sampling point, the thin plate smoothing spline algorithm in package Anusplin 4.4 (Version 4.4, Canberra, Australia http://fennerschool.anu.edu.au/files/anusplin44.pdf) was used to calculate the kriging difference to obtain the monthly mean temperature (MMT) and monthly mean precipitation (MMP) at each sampling point from 2006 to 2015. The growing season of *F. sinensis* is from April to August, and the average temperature and precipitation from April to August were calculated as the mean temperature and precipitation during the growing season. Microsoft Excel 2020 was used to calculate the MMT, MMP, growing monthly mean temperature (GMMT), and growing monthly mean precipitation (GMMP). Spearman's correlation analysis in SPSS 23.0 (version 23.0; SPSS Inc, Chicago, IL, USA) was used to analyze the relationship among environmental factors, *E. sinensis* infection rate, and microbial diversity, and statistical significance was set at $p < 0.05$.

One-way analysis of variance (ANOVA) was used to determine statistically significant differences in microbial community diversity among the 14 groups using SPSS 23.0 (version 23.0; SPSS Inc, Chicago, IL, USA). When ANOVA indicated a significant difference, Fisher's least significant difference (LSD) test was applied to conduct multiple pairwise comparisons, and statistical significance was set at $p < 0.05$.

Redundancy analysis (RDA) was performed using Canoco 5 software (Microcomputer Power, Ithaca, New York, USA), as discussed by Braak (1994). In RDA, microbial parameters were used as "species," and the ordination axes were constrained to be linear combinations of the environmental factors (i.e., MMT, MMP, GMMT, and GMMP). Thus, this analysis allowed the relationships between environmental factors and microbial parameters to be directly compared. Using the Monte Carlo permutation test (number of permutations), the significance of the environmental factors in accounting for the observed variance in the microbial parameters can be assessed with *p*-values. In the RDA diagram, positively correlated variables are indicated by arrows pointing in the same direction, negatively correlated variables point in opposite directions, and perpendicular variables are uncorrelated. In addition, the arrow length is a measure of the relative importance of environmental factors in explaining the variances of the microbial parameters. To more clearly understand the impacts of elevation, the samples were divided into 3 groups, including high elevation (2,500–3,000 m), medium-high elevation (3,000–4,500 m), and extremely high elevation (4,500–5,500 m). Additionally, a total of 14 samples were also analyzed together and compared.

Results

Sequencing annotation

After 16S rRNA sequencing, an average of 104,769 tags was detected for each sample, and 65,201 tags were obtained on average for each sample after quality control, with the efficiency of quality control reaching 62.28%. Sequences were clustered into OTUs with 97% identity, and a total of 3,003 OTUs were obtained. Taxonomic annotations of these OTUs were conducted using the SILVA138 database. There were 2,862 (95.30%) OTUs that could be annotated in the database.

After ITS sequencing, an average of 103,696 tags was detected for each sample. The quantity of effective data under quality control reached 65,156 for each sample, and the quality control efficiency reached 62.88%. The OTUs were clustered with 97% identity and 636 OTUs were identified. Taxonomic annotation was performed using the OTUs sequence and the UNITE databases, and 592 (93.08%) OTUs were annotated.

Microbiota diversity in seeds

OTUs level

Both the rarefaction of the sequencing depth (Supplementary Figure S2) and coverage estimators (Supplementary Table S2) indicated that the sequencing depth was sufficient to represent the microbial composition of the samples and to reveal the microbial community structure.

A total of 2,862 bacterial OTUs were obtained by clustering, whereas a total of 1,062 bacterial OTUs were obtained by clustering in the Venn petals (Figure 1A). In addition, 117 OTUs

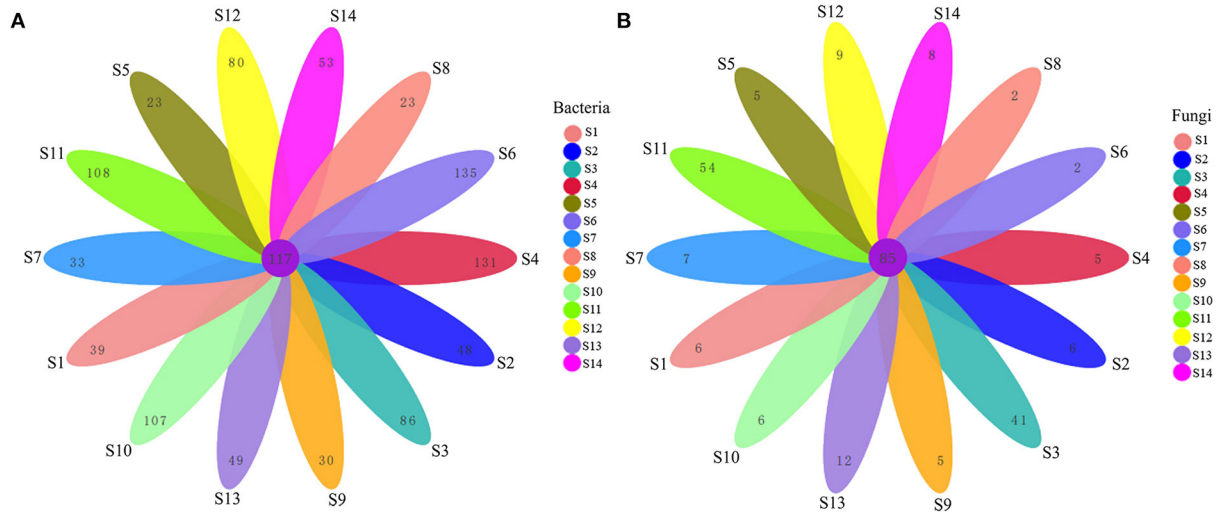

FIGURE 1
Venn petals of bacteria **(A)** and fungi **(B)** at the OTUS level showing the number of commonly and uniquely expressed genes collected the *Festuca sinensis* seeds from different geographical locations.

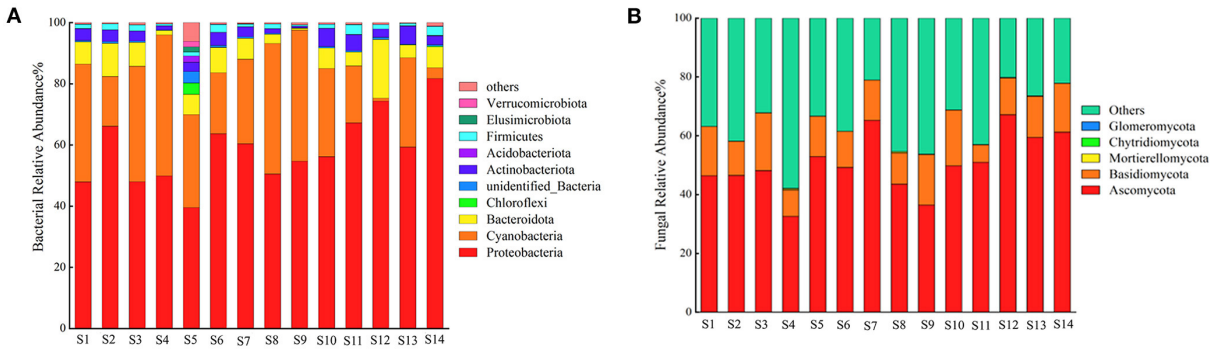

FIGURE 2
The relative abundance of the top 10 phyla of bacteria in seed lot from 14 ecotypes 16s ribosomal RNA sequencing **(A)** and fungi in seed lot from 14 ecotypes ITS sequencing **(B)**.

were shared by bacterial communities of these 14 seed lots, accounting for 11.02% of the total number of OTUs. Ecotype S6 had the largest number of unique OTUs (252), followed by ecotypes S4 (248), and S11 (225). Ecotypes S5 and S8 had the lowest numbers of unique OTUs (170), followed by ecotype S7 (180). A total of 592 fungal OTUs were obtained by clustering, whereas a total of 253 fungal OTUs were obtained by clustering in the Venn petals (Figure 1B), and 85 OTUs were shared by fungal communities of these 14 seed lots, accounting for 33.60% of the total number of OTUs. Ecotype S11 had the highest number of unique OTUs (139), followed by ecotype S3 (126). Ecotypes S6 (87), S8 (87), S9 (90), and S4 (90) had the lowest numbers of OTUs.

Relative abundance of the bacterial and fungal phyla

The relative abundances of the bacterial phyla are shown in Figure 2A. These phyla included Proteobacteria, Cyanobacteria, Bacteroidetes, Chloroflexi, Actinobacteria, Acidobacteria, Firmicutes, Elusimicrobiota, and Verrucomicrobiota. Proteobacteria, Cyanobacteria, and Bacteroidetes were the most abundant phyla. The microbiomes of each seed lot were different. The relative abundances of Proteobacteria in seeds of ecotypes S2, S6, S7, S11, S12, S14, S8, S9, S10, and S13 were over 50%, and Proteobacteria was the most abundant bacterial phylum in the seeds. The relative abundances of the three most abundant phyla in each seed lot are shown

in Supplementary Table S2. The relative abundances of Proteobacteria in the seeds of ecotype S13 were significantly higher than those in the seeds of ecotypes S1, S4, S3, S5, S7, S11, S12, S14, and S10 ($p < 0.05$). The relative abundance of Cyanobacteria in the seeds of ecotype S3 was significantly higher than those in the seeds of ecotypes S2, S9, and S13 ($p < 0.05$). The relative abundance of Bacteroidota in seeds of ecotype S9 was highest and was significantly higher than those in seeds of the other ecotypes ($p < 0.05$). The relative abundance of Chloroflexi in the seeds of ecotype S5 was significantly higher than those in the seeds of the other ecotypes ($p < 0.05$).

The relative abundances of the fungal phyla are shown in Figure 2B. These phyla include Ascomycota, Basidiomycota, Mortierellomycota, Chytridiomycota, and Glomeromycota. Ascomycota and Basidiomycota were the most abundant fungi, with relative abundances of > 50%. Ecotype S9 had the highest relative abundance of Ascomycota (Supplementary Table S2), which was significantly higher than those in seeds of ecotypes S3 and S12 ($p < 0.05$). The relative abundance of Ascomycota in seeds of ecotype S3 was significantly lower than those in seeds of ecotypes S7 and S9 ($p < 0.05$). The relative abundances of Basidiomycota in seeds of ecotypes S4 and S14 were significantly higher than those in seeds of ecotypes S3 and S8 ($p < 0.05$), and the relative abundance of Basidiomycota in seeds of ecotype S8 was significantly lower than that in seeds of ecotypes S1, S4, S12, and S14 ($p < 0.05$).

α-diversity of bacterial and fungal communities in seeds

There were significant differences among α-diversity indices of the bacteria of different ecotypes (Table 2). The Chao richness index of ecotype S116 was significantly higher than those of ecotypes S2, S12, S8, S9, and S13 ($p < 0.05$). The Shannon index of ecotype S9 was significantly higher than that of ecotype S14 ($p < 0.05$). The Simpson indices of ecotypes S2, S5, S6, S14, S8, and S9 were significantly higher than those of ecotypes S3 and S12 ($p < 0.05$). The ACE indices of ecotypes S4, S3, and S11 were significantly higher than those of ecotypes S2, S5, S12, S8, S9, S10, and S13 ($p < 0.05$).

The Chao richness index of fungi in ecotype S11 was significantly higher than that in ecotype S8 ($p < 0.05$; Table 2) and was not significantly different from that of other ecotypes. The Shannon indices of ecotypes S5 and S14 were significantly higher than those of ecotypes S8 and S13 ($p < 0.05$) and were not significantly different from those of the other ecotypes. Simpson indices of ecotypes S1, S2, S5, and S14 were significantly higher than those of ecotype S13 ($p < 0.05$) and were not significantly different from those of the other ecotypes. The ACE index of ecotype S11 was significantly higher than that of ecotype S8 ($p < 0.05$) and was not significantly different from those of the other ecotypes.

β-diversity of bacterial and fungal communities in seeds

A heat map of the beta diversity measurements is shown in Figure 3. For the bacterial community (Figure 3A), the distances of the samples based on weighted UniFrac were between 0.068 and 0.693, and the distances of the samples based on unweighted UniFrac were between 0.544 and 0.847. For the fungal community (Figure 3B), the distances of the samples based on weighted UniFrac were between 0.104 and 0.790, and the distances of the samples based on unweighted UniFrac were between 0.309 and 0.730. Overall, the UniFrac distances were relatively large.

UPGMA cluster and PCA

This study used both UPGMA cluster tree and PCA to cluster the *F. sinensis* seeds based on unweighted UniFrac (Figure 4). The UPGMA cluster analysis was performed using the unweighted UniFrac distance matrix, and the clustering results were integrated with the relative abundance column chart at the phylum taxon level for each sample. The phylogenetic tree showed that the bacterial communities were divided into four three groups (Figure 4A), and the fungal communities were divided into two major groups (Figure 4B), with each group containing samples from different areas of the Qinghai-Tibet Plateau. The KMO values for PCA of the bacteria (0.847, Supplementary Table S3) and fungi (0.938, Supplementary Table S3) are big enough to run multivariate analysis. For bacterial communities (Figure 4C), the first and second components explained 10.83 and 8.47% of the variances, respectively. For fungal communities (Figure 4D), the first and second components explained 9.66 and 7.4% of the variances, respectively. The results showed that the bacterial communities clustered more distinctively than the fungal communities. The bacterial communities of seed ecotypes S5, S1, S14, and S7 were less similar to those in seed ecotypes S8, S9, S2, S13, and S4, S11, S3, and S12, respectively. The fungal communities of seed ecotypes S11, S13, S12, and S3 were clustered together; however, they were less similar to those in seed ecotypes S10, S8, S6, S14, S9, S7, S1, S2, S4, and S5.

Correlation analysis

Correlation analysis between α-diversity and environmental factors

Analysis of correlations among α-diversity and environmental factors (Table 3) showed that the Chao richness index and ACE index of bacteria were significantly negatively correlated with MMP and GMMP ($p < 0.05$). However, the Simpson index of bacteria was significantly positively correlated with MMP and GMMP ($p < 0.05$).

TABLE 2 α-diversity of bacterial and fungal communities in seeds.

Ecotypes	Bacteria				Fungi			
	Chao1	Shannon	Simpson	ACE	Chao1	Shannon	Simpson	ACE
S1	505.6 ± 23.1 abcd	3.9 ± 0.8ab	0.8 ± 0.1abcd	513.6 ± 22.7abc	158.0 ± 3.9ab	3.7 ± 0.1ab	0.9 ± 0.0a	160.1 ± 4.1ab
S2	454.2 ± 31.0bcd	4.4 ± 0.6ab	0.8 ± 0.1ab	459.1 ± 31.7bc	161.0 ± 3.9ab	3.6 ± 0.1ab	0.9 ± 0.0a	163.3 ± 3.4ab
S3	571.9 ± 70.0abcd	2.8 ± 0.1ab	0.7 ± 0.0cd	589.3 ± 72.8ab	181.2 ± 18.9ab	3.3 ± 0.0abc	0.8 ± 0.0ab	179.6 ± 16.8ab
S4	680.8 ± 96.1a	4.1 ± 0.2ab	0.8 ± 0.0abc	692.5 ± 96.1a	159.0 ± 7.5ab	3.4 ± 0.1abc	0.8 ± 0.0ab	164.0 ± 8.1ab
S5	489.3 ± 21.3abcd	4.6 ± 1.1ab	0.8 ± 0.1ab	499.3 ± 19.4bc	172.3 ± 10.0ab	3.8 ± 0.1a	0.9 ± 0.0a	171.3 ± 8.7ab
S6	655.1 ± 112.6ab	4.3 ± 0.6ab	0.8 ± 0.1ab	581.8 ± 53.8abc	156.0 ± 9.6ab	3.5 ± 0.2abc	0.9 ± 0.0ab	158.9 ± 9.8ab
S7	529.8 ± 20.8abcd	4.0 ± 0.2ab	0.8 ± 0.0abc	542.5 ± 21.0abc	154.0 ± 10.4ab	3.4 ± 0.2abc	0.8 ± 0.0ab	157.0 ± 11.2ab
S8	389.6 ± 61.2d	4.0 ± 0.2ab	0.8 ± 0.0ab	392.5 ± 64.8c	129.7 ± 7.1b	3.1 ± 0.08bc	0.8 ± 0.01ab	126.3 ± 5.0b
S9	416.5 ± 49.5cd	5.1 ± 0.5a	0.9 ± 0.0a	422.7 ± 48.2bc	156.9 ± 5.4ab	3.5 ± 0.21abc	0.8 ± 0.03ab	160.5 ± 5.5ab
S10	471.8 ± 105.4abcd	3.6 ± 0.2ab	0.8 ± 0.0abcd	478.9 ± 109.1bc	176.5 ± 10.9ab	3.6 ± 0.20abc	0.8 ± 0.03ab	179.8 ± 10.6ab
S11	604.2 ± 55.5abc	3.3 ± 0.1ab	0.7 ± 0.01bcd	614.8 ± 56.9ab	205.7 ± 7.2a	3.4 ± 0.11abc	0.8 ± 0.02ab	210.7 ± 7.9a
S12	421.2 ± 41.2cd	2.5 ± 0.1ab	0.7 ± 0.0d	431.1 ± 38.9bc	178.5 ± 22.6ab	3.4 ± 0.20abc	0.8 ± 0.02ab	181.7 ± 23.1ab
S13	430.7 ± 55.1cd	4.2 ± 0.4ab	0.8 ± 0.0abc	435.5 ± 53.7bc	158.8 ± 28.2ab	2.9 ± 0.42c	0.7 ± 0.11b	161.1 ± 29.7ab
S14	551.2 ± 10.1abcd	4.1 ± 0.2b	0.8 ± 0.0ab	563.4 ± 9.3abc	185.7 ± 8.3ab	3.8 ± 0.06a	0.9 ± 0.01a	185.4 ± 5.5ab

The different lowercase letters in a column represent significant differences among treatments one-way ANOVA ($p < 0.05$).

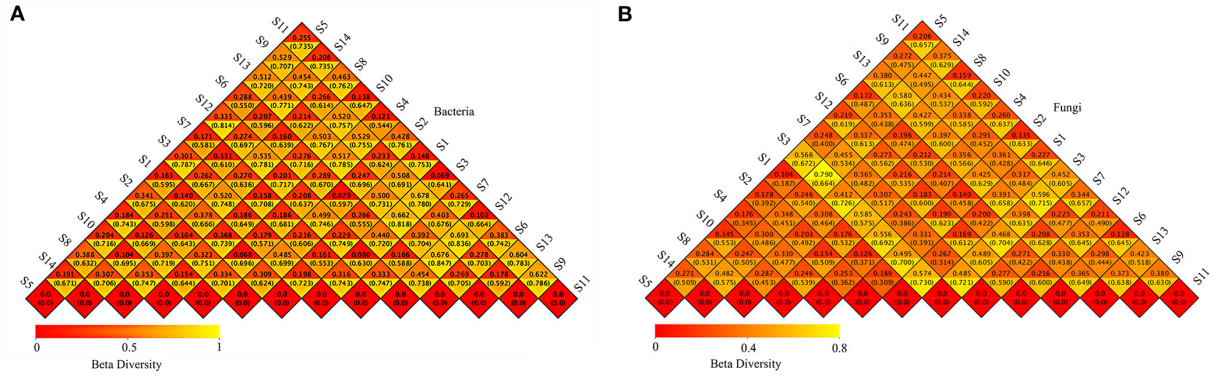

FIGURE 3
Beta diversity of bacterial **(A)** and fungal **(B)** heat map based on the UniFrac distance. The upper triangle is the weighted distance. The distance from the lower triangles is the unweighted distance.

The Chao richness index and the ACE index of fungi were significantly negatively correlated with MMT and GMMT ($p < 0.05$). The *E. sinensis* infection rate was significantly positively correlated with MMT and GMMT ($p < 0.05$) and significantly negatively correlated with elevation ($p < 0.05$).

Correlation analysis of the relative abundances of the most abundant bacteria and fungi with environmental factors

The correlation of the relative abundances of the three most abundant bacterial phyla (Proteobacteria, Cyanobacteria, and Bacteroidetes) with environmental factors was analyzed (Table 4). The relative abundance of Proteobacteria was significantly positively correlated with MMP and GMMP ($p < 0.05$). The relative abundance of Cyanobacteria was very significantly negatively correlated with MMP and GMMP ($p < 0.01$). The relative abundance of Bacteroidetes was significantly positively correlated with MMT and GMMT ($p < 0.05$). The correlation of relative abundances of the two most abundant fungal phyla (Ascomycota and Basidiomycota) with environmental factors was also analyzed (Table 4). The relative abundance of Ascomycota was significantly positively correlated with MMP and GMMP ($p < 0.05$).

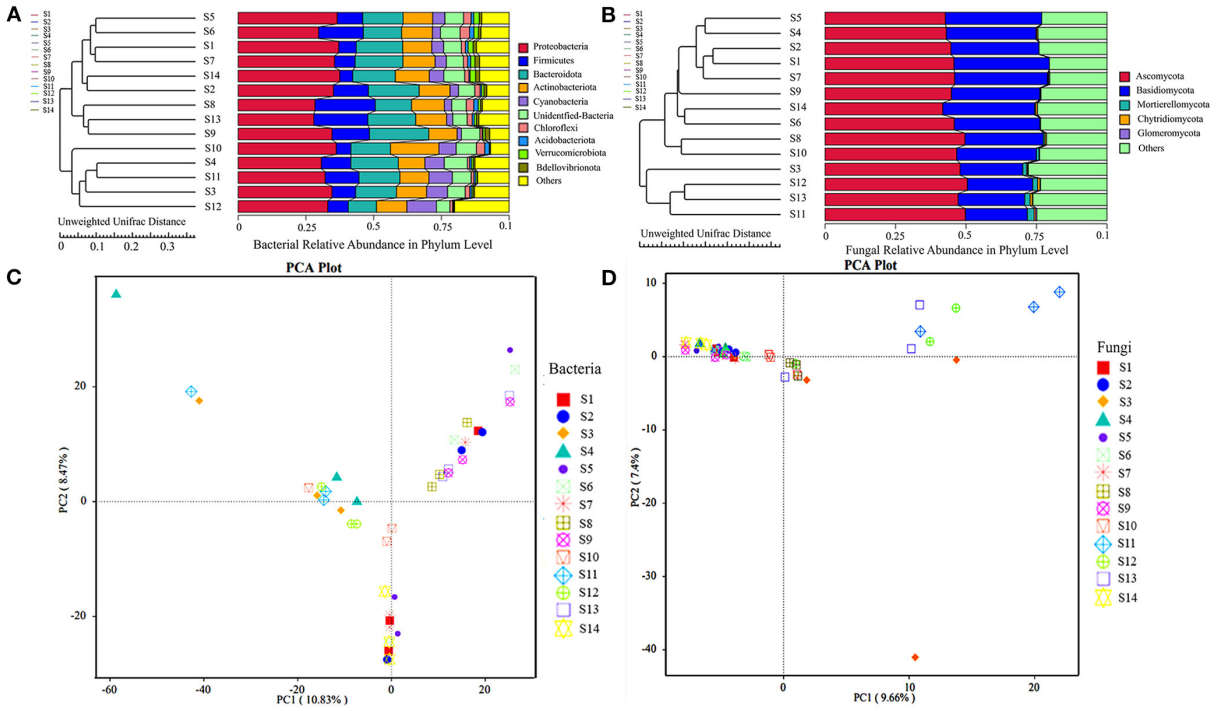

FIGURE 4
Analysis of *F. sinensis* seeds microbial communities with unweighted UniFrac. Principal component analysis (PCA) of bacterial **(A)** and fungal community **(B)** with unweighted UniFrac. Symbols represent different *F. sinensis* seeds. UPGMA tree based on unweighted UniFrac distance at the phylum level. Explanation: On the left is the UPGMA cluster tree structure, and on the right is the species relative abundance distribution at the phylum level for each sample. The phylogenetic relationship of the bacteria and fungi was determined by PCR sequencing portions of the 16S rRNA gene **(C)** and ITS gene **(D)**.

TABLE 3 Correlation coefficient between seed microbial α-diversity and environmental factors.

Environmental factors	Bacteria				Fungi				*Epichloë sinensis* infection rate
	Chao1	shannon	simpson	ACE	Chao1	shannon	simpson	ACE	
MMT	−0.254	0.479	0.216	−0.293	**−0.624***	0.251	0.280	**−0.675****	**0.652***
MMP	**−0.620***	0.483	**0.565***	**−0.642***	−0.461	0.128	0.108	−0.437	0.022
GMMT	−0.165	0.470	0.212	−0.223	**−0.642***	0.278	0.324	**−0.697****	**0.674****
GMMP	**−0.620***	0.483	**0.565***	**−0.642***	−0.461	0.128	0.108	−0.437	0.022
Elevation	−0.244	−0.117	−0.004	−0.231	0.302	−0.238	−0.280	0.407	**−0.636***
Epichloë sinensis infection rate	−0.077	0.262	0.131	−0.077	−0.399	−0.081	0.042	−0.526	x

"*" indicates a significant correlation at $p < 0.05$; "**" indicates a very significant correlation at $p < 0.01$.

The relationship between the composition of microbial communities and environmental factors

Through Monte Carlo permutation, the ranking results of the four axes could better reflect the relationship between environmental factors and microbial communities (Supplementary Tables S4–S7). The relationships between environmental factors and abundances of bacterial and fungal at the phylum and genus levels were analyzed on the overall elevation, high elevation, medium-high elevation, and extremely high elevation (Supplementary Table S8). On the overall elevation, MMP and GMMT had significant effects on the variation in the bacterial phyla and genera ($p < 0.05$), with explained degrees of variation being 42.4, 21.0, 48.4, and 17.9%, respectively (Supplementary Table S8). MMP and MMT had a significant influence on the variation in the fungal phyla ($p < 0.05$, Supplementary Table S8), and their explained

TABLE 4 Correlation coefficient between the relative abundance of the most abundance bacteria and fungi and environmental factors.

Environmental factors	Bacterial abundance			Fungal abundance	
	Proteobacteria	Cyanobacteria	Bacteroidota	Ascomyota	Basidiomycota
MMT	0.075	−0.395	**0.534***	0.324	−0.018
MMP	**0.547***	**−0.712****	0.291	**0.650***	0.088
GMMT	0.044	−0.364	**0.542***	0.271	−0.049
GMMP	**0.547***	**−0.712****	0.291	**0.650***	0.088
Epichloë sinensis infection rate	−0.040	−0.137	0.170	−0.128	−0.520
Elevation	0.390	−0.163	−0.383	0.385	0.143

Within a confidence interval of p = 0.05, "*" indicates a significant correlation, and "**" indicates a very significant correlation.

degrees of variation were 29.3 and 23.2%, respectively. MMP and GMMP had significant effects on the variation in the fungal genera, with explained degrees of variation of 21.7 and 17.8%, respectively (Supplementary Table S8). These results indicated that temperature and precipitation were the main environmental factors that affected the spatial differentiation of microbial communities. *E. sinensis* infection rates had a certain effect on the relative abundance of the phyla and genera of fungi (the explained degrees of variation were 7.4 and 9.2%, respectively). Elevation had the smallest effect on the phyla and genera of bacteria, with explained degrees of variation of only 1.0 and 0.4%, respectively. GMMT had the smallest effect on the phyla and genera of fungi, with explained degrees of variation of only 2.5 and 2.1%, respectively. On the high elevation, medium-high elevation and extremely high elevation the result of all axes were $F < 0.1$, $p = 1$ (Supplementary Table S8).

Redundancy analysis, as tested by Monte Carlo permutation on the bacterial phyla (Figure 5), fungal phyla (Figure 6), bacterial genera (Figure 7), and fungal genera (Figure 8) of samples at the overall elevation (2,589–5,197 m), high elevation (2,589–3,000 m), medium-high elevation (3,000–4,500 m), and extremely high elevation (4,500–5,197 m), identified the environmental factors (MMT, GMMT, MMP, and GMMP) that were significantly correlated with the microbial community. Environmental factors (GMMP, MMP, GMMT, and MMT) were positively correlated with the abundances of Chloroflexi, Elusimicrobiota, Acidobacteriota, Verrucomicrobiota, and Bateroidota at overall elevation (Figure 5A), high elevation (Figure 5B), and extremely high elevation (Figure 5D), however, negatively correlated with the abundance of Cyanobacteria at overall elevation, high elevation, and extremely high elevation (Figures 5A,B,D). The elevation was positively correlated with the abundances of Cyanobacteria at overall elevation and medium-high elevation (Figures 5A,C), whereas negatively correlated with the abundances of Cyanobacteria at high elevation and extremely high elevation (Figures 5B,D). At medium-high elevation group, GMMT and MMT were positively correlated with the abundance of Elusimicrobiota, Acidobacteriota, Chloroflexi, and Actinobacteriota; however, GMMP and MMP were negatively correlated with them (Figure 5C).

Environmental factors (MMT, GMMT, MMP, and GMMP) were significantly correlated with the fungal community at the phyla levels (Figure 6). Environmental factors (GMMP, MMP, GMMT, and MMT) were positively correlated with the abundances of Ascomycota (Figures 6A,B,D). The elevation was positively correlated with the abundance of Ascomycota, Basidiomycota, whereas *E. sinensis* infection rate was negatively correlated with the abundance of Ascomycota and Basidiomycota (Figures 6A,D). At the medium-high elevation, the GMMP and MMP were positively correlated with the abundance of Ascomycota, Chytridiomycota, and Mortierellomycota, whereas negatively correlated with the abundances of Basidiomycota and Glomeromycota (Figure 6C), GMMT and MMT were positively correlated with the abundances of Basidiomycota and Glomeromycota, whereas negatively correlated with the abundances of Ascomycota, Chytridiomycota, and Mortierellomycota (Figure 6C).

As shown in Figure 7, environmental factors (GMMP, MMP, GMMT, and MMT) were positively correlated with the abundances of *Amaricoccus, Sphingomonas, Pseudomonas, Paracoccus, Pedobacter, Massilia, Duganella, and Hymenobacter*, whereas negatively correlated with the abundances of *unidentified_Chloroplast* and *unidentified_Mitochondria* at overall elevation, high elevation, and extremely high elevation (Figures 7A,B,D). For all four groups, the elevation was positively correlated with the abundances of *Pseudomonas* and *Duganella*; however, *E. sinensis* infection rate was negatively correlated with them (Figure 7). At medium-high elevation group, GMMT and MMT were positively correlated with the abundance of *Pedobacter, Massilia, Amaricoccus, and Paracoccus,* whereas GMMP and MMP were negatively correlated with them (Figure 7C). The GMMP and MMP were positively correlated with the abundance of *Duganella, Pseudomonas,* and *Sphingomonas*; however, GMMP and MMP were negatively correlated with them (Figure 7C).

As shown in Figure 8, environmental factors (GMMP, MMP, GMMT, and MMT) were positively correlated with

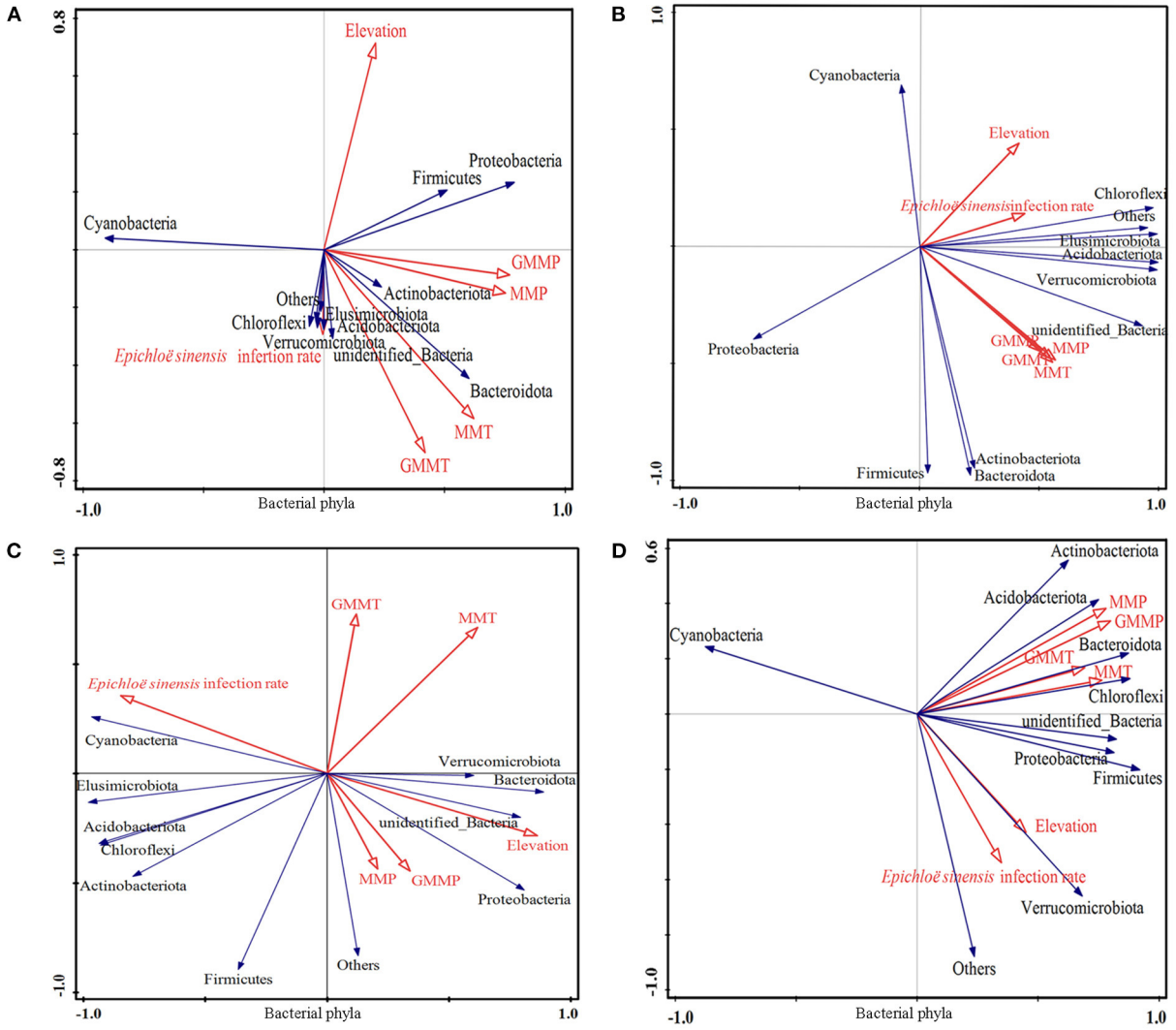

FIGURE 5
Effect of environmental factors on bacterial phyla. **(A)** on overall elevation (2,589–5,197 m). **(B)** on high elevation (2,589–3,000 m); **(C)** on medium-high elevation (3,000–4,500 m); **(D)** and on extremely high elevation (4,500–5,197 m). The microbial parameters (expressed as response variables in the RDA) were presented as black line vectors, and the environmental factors (explanatory variables) were presented as red line vectors. MMT, monthly mean temperature; MMP, monthly mean precipitation; GMMT, growing monthly mean temperature; GMMP, growing monthly mean precipitation.

the abundances of *Juncaceicola, Filobasidium, Microdochium, Fusarium,* and *Udeniomyces* at overall elevations, high elevations, and extremely high elevation (Figures 8A,B,D). For all four groups, elevation was positively correlated with the abundances of *Fusarium* and *Udeniomyces*, and *E. sinensis* infection rate was negatively correlated with the abundances of *Fusarium, Udeniomyces* (Figure 8). At the medium-high elevation, GMMP and MMP were positively correlated with the abundance of *Leptosphaerulina, Alternaria, Epicoccum,* and *Leptosphaeria,* whereas negatively correlated with the abundances of *Juncaceicola, Filobasidium, Microdochium*, and *Udeniomyces.* GMMP and MMP were positively correlated with the abundance of *Juncaceicola, Filobasidium, Microdochium*, and *Udeniomyces,* whereas negatively correlated with the abundances of *Leptosphaerulina, Alternaria, Epicoccum,* and *Leptosphaeria* (Figure 8C).

Discussion

There is a rich microbial community comprising a diverse range of bacteria (Truyens et al., 2015) and fungi (Shearin et al., 2018) on the surfaces and interiors of plant seeds. In this study, we characterized the seed microbiota from 14 different locations

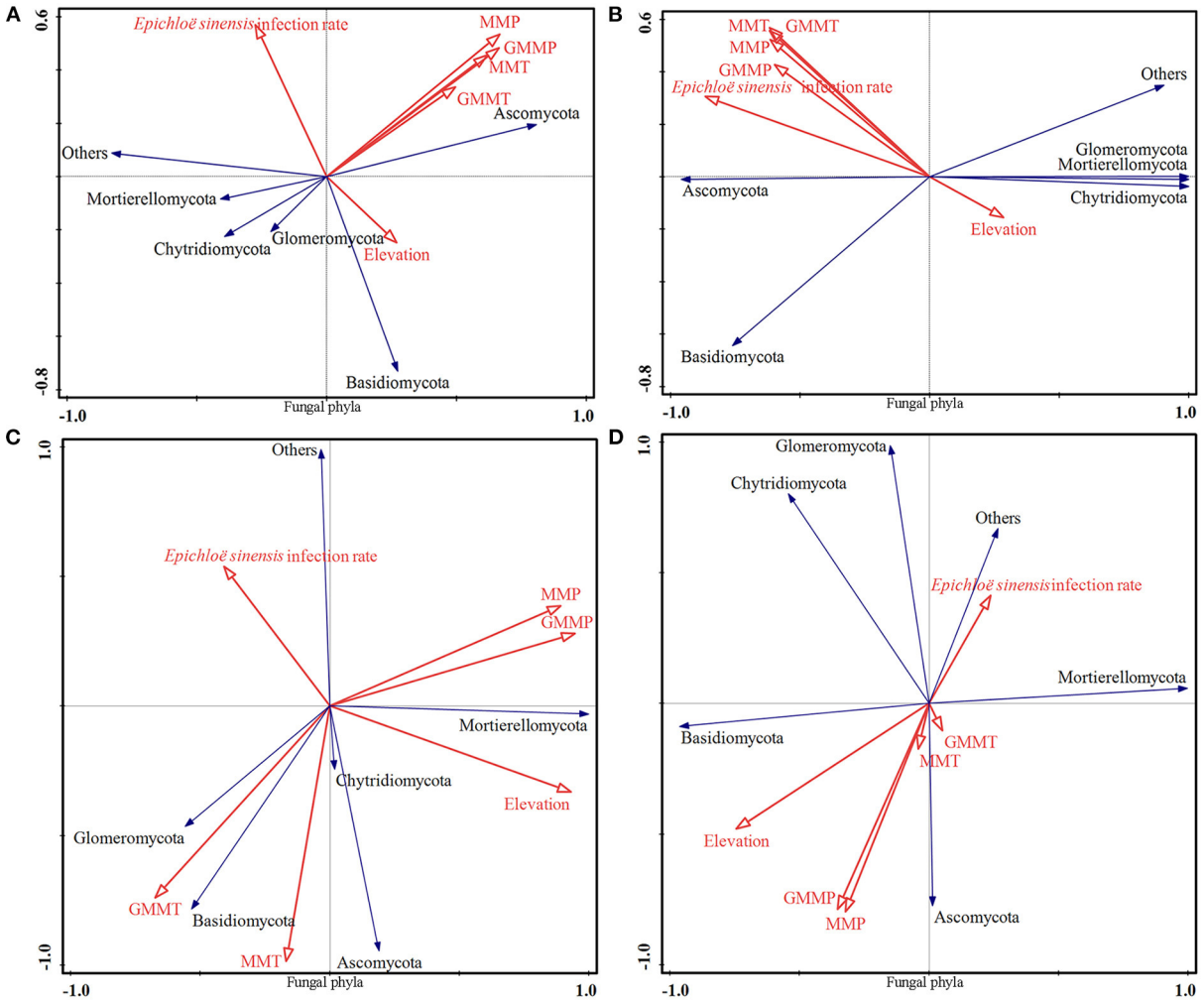

FIGURE 6
Effect of environmental factors on fungal phyla. **(A)** on overall elevation (2,589–5,197 m). **(B)** on high elevation (2,589–3,000 m); **(C)** on medium-high elevation (3,000–4,500 m); **(D)** and on extremely high elevation (4,500–5,197 m). The microbial parameters (expressed as response variables in the RDA) were presented as black line vectors, and the environmental factors (explanatory variables) were presented as red line vectors. MMT, monthly mean temperature; MMP, monthly mean precipitation; GMMT, growing monthly mean temperature; GMMP, growing monthly mean precipitation.

on the Qinghai-Tibet Plateau. A total of 64 bacterial phyla and six fungal phyla were found in the *F. sinensis* seeds by high-throughput sequencing. Moreover, α-diversity identified the important environment factors (temperature and precipitation) and β-diversity further showed that the microbial community structure varied greatly among different collection sites of the Qinghai-Tibet Plateau, which demonstrated that the microbiota diversity of *F. sinensis* seeds had a strong relationship with the geographical distribution. In general, the results suggested that the microbiome in different *F. sinensis* seed lots had different components. Previous research found a total of 54 genera and 129 species of bacteria were isolated from the surface and interior of more than 30 types of crop seeds. Among these bacteria, Proteobacteria was the main phylum, and Firmicutes, Actinobacteria, and Bacteroidetes were the second most common (Liu et al., 2012). Our study was consistent with the results of previous studies. Proteobacteria play a key role in phylogenetic, ecological, and pathogenic processes and participate in energy metabolism, including oxidation and photosynthesis of organic and inorganic compounds (Zhang et al., 2018). Cyanobacteria produce phycoerythrin and phycocyanin, two photosynthetic pigments characteristic of Rhodophyta or red algae, and one or two other smaller groups (Edelman et al., 1967). Cyanobacteria are also well recognized as producers of a wide array of bioactive metabolites including toxins and potential drug candidates (Walton and Berry, 2016). Thus, Cyanobacteria may improve plant growth and seed germination (Chua et al., 2019). Bacteroidetes are

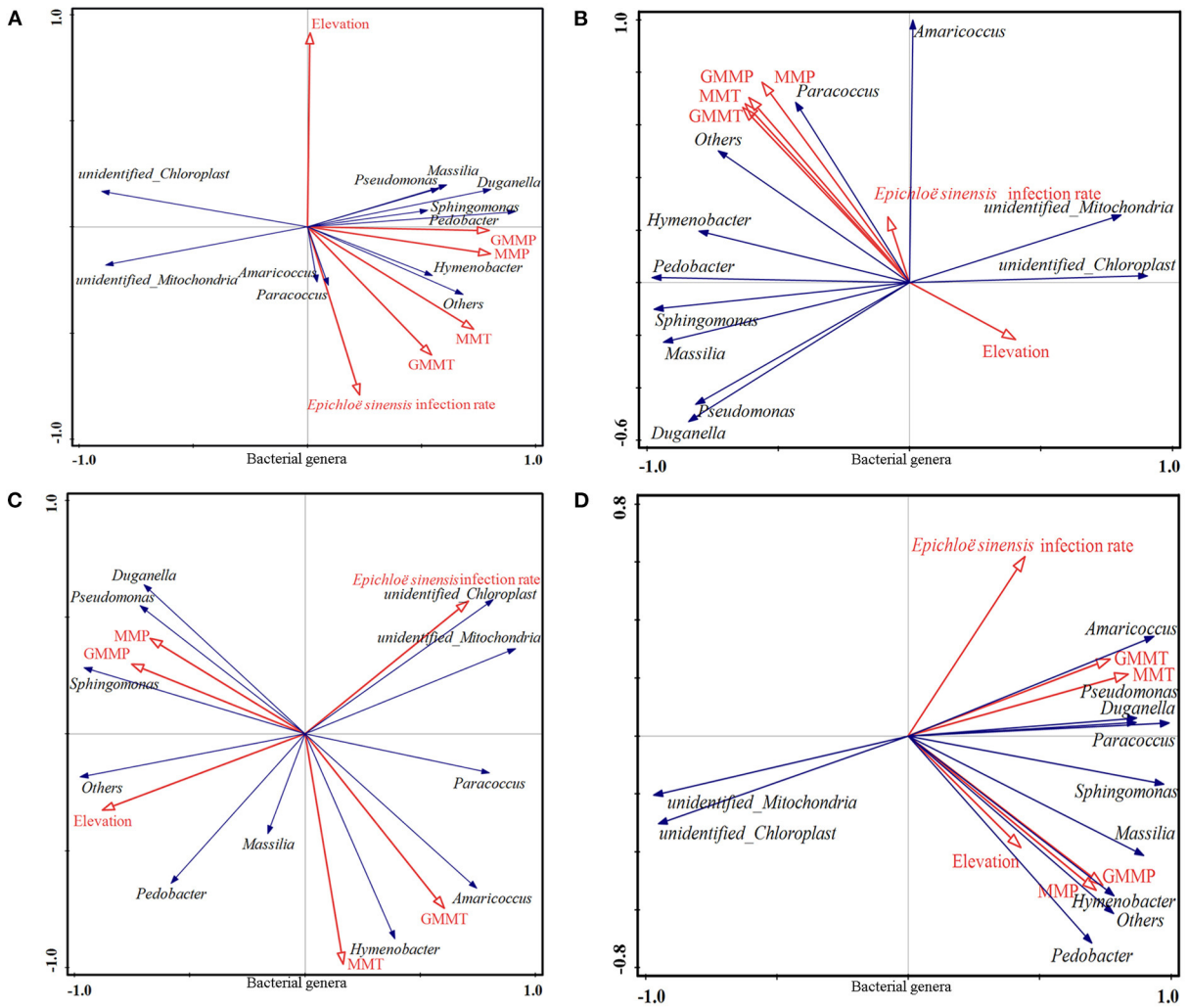

FIGURE 7
Effect of environmental factors on bacterial genera. **(A)** on overall elevation (2,589–5,197 m). **(B)** on high elevation (2,589–3,000 m); **(C)** on medium-high elevation (3,000–4,500 m); **(D)** and on extremely high elevation (4,500–5,197 m). The microbial parameters (expressed as response variables in the RDA) were presented as black line vectors, and the environmental factors (explanatory variables) were presented as red line vectors. MMT, monthly mean temperature; MMP, monthly mean precipitation; GMMT, growing monthly mean temperature; GMMP, growing monthly mean precipitation.

increasingly regarded as specialists in the degradation of high molecular weight organic matter, namely, proteins and carbohydrates (Thomas et al., 2011). A possible explanation for our findings is that the climate of the Qinghai-Tibet Plateau leads to more Cyanobacteria in the *F. sinensis* seeds. The higher amount of Cyanobacteria is more conducive to photosynthesis in *F. sinensis*, which makes it better adapted for growth in the Qinghai-Tibet Plateau. Ascomycota and Basidiomycota were the most abundant fungi, consistent with the previous studies conducted on alpine meadows in the Yushu Tibetan Autonomous Prefecture, which showed that most fungi belonged to Ascomycota (Chen et al., 2017), Ascomycota mainly decompose cellulose and lignin, and its growth may depend on more readily available energy sources, such as soluble carbohydrates (Osono and Takeda, 2002). Basidiomycota mainly produce lignin-modifying enzymes that degrade lignin (Osono et al., 2003). Ascomycota and Basidiomycota are widely distributed in plants, aquatic ecosystems, and soil, in different proportions (Vandenkoornhuyse et al., 2002). These microorganisms play the important roles in seed health and production.

The coexistence of microbial symbionts and hosts contributes to host adaptation to the natural environment. In turn, the composition of the plant microbial community responds to the environment and the host, making it possible for the plant to benefit. Seeds are involved in the transmission of microorganisms from one plant generation to another and consequently may act as the initial inoculum source for the plant

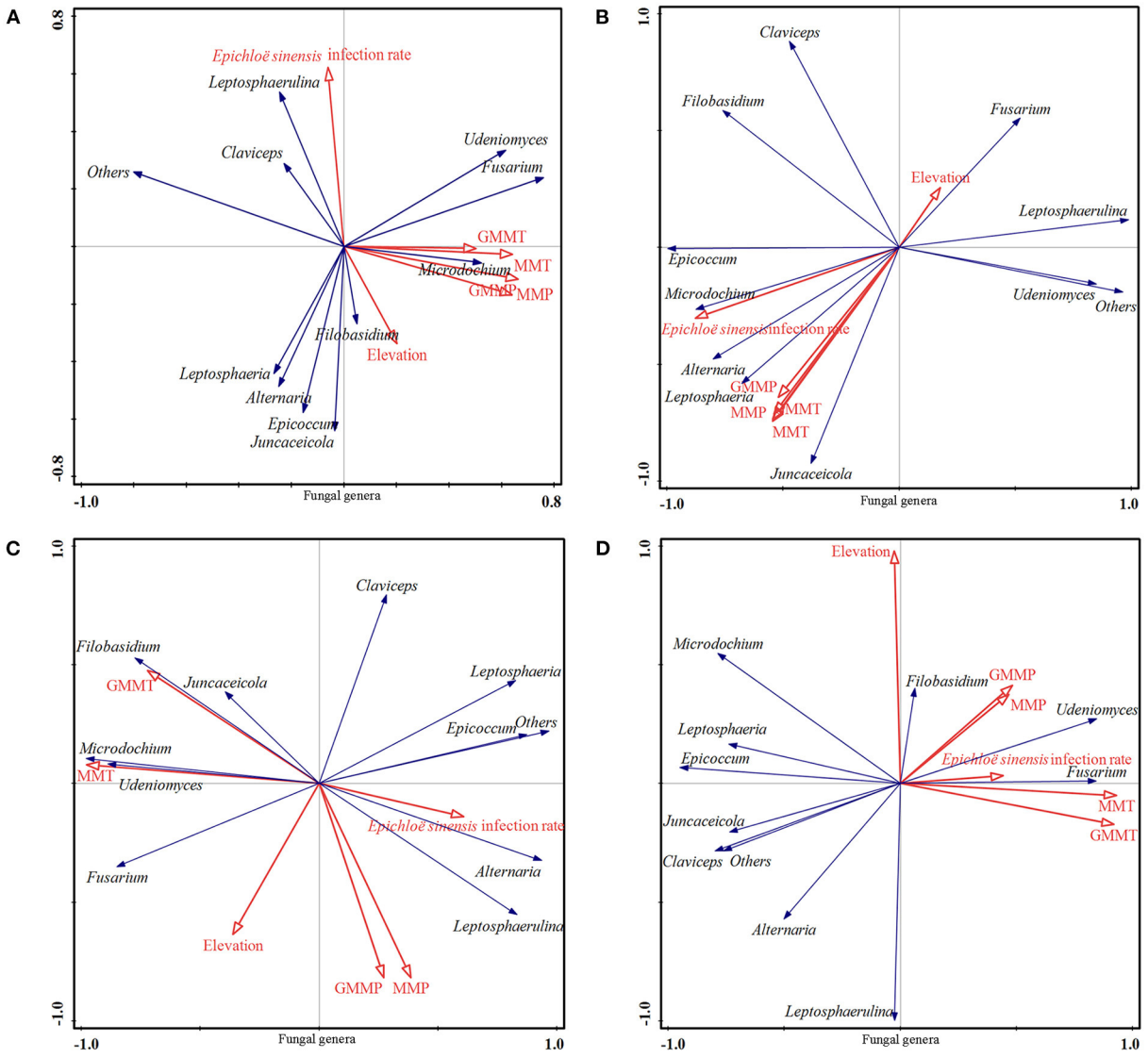

FIGURE 8
Effect of environmental factors on fungal genera. **(A)** on overall elevation (2,589–5,197 m). **(B)** on high elevation (2,589–3,000 m); **(C)** on medium-high elevation (3,000–4,500 m); **(D)** and on extremely high elevation (4,500–5,197 m). The microbial parameters (expressed as response variables in the RDA) were presented as black line vectors, and the environmental factors (explanatory variables) were presented as red line vectors. MMT, monthly mean temperature; MMP, monthly mean precipitation; GMMT, growing monthly mean temperature; GMMP, growing monthly mean precipitation.

microbiota (Rezki et al., 2018). Seeds have evolved in association with diverse microbial assemblages that may influence plant growth and health (Gibbons et al., 2013). Microbial communities and structures vary and can be influenced by many factors. Previous studies have found that both seed and soil types affect microbial communities (Buyer et al., 1999). Different environmental conditions affect the propagation, infection, and transmission of various microbes, and different species carry different types and numbers of microbes. The same seed can carry different fungi under different growth conditions (Thomas et al., 2016). Environmental factors have different effects on the abundance and diversity of seed microorganisms.

High-altitude ecosystems are generally characterized by low temperatures, variable precipitation, decreased atmospheric pressure, and soil nutrient stress, which have major impacts on biodiversity (Moran-Tejeda et al., 2013). We found that precipitation and temperature were the dominant drivers of the bacterial and fungal diversity gradients (Nottingham et al., 2018; Shen et al., 2020). Seeds of different ecotypes carried abundant amounts of different microorganisms that adapt to different environments, including elevation, temperature, and humidity. Some studies found that microbial species richness and diversity were closely correlated with temperature and that microbial diversity decreased under extreme and polar temperatures

(Sharp et al., 2014). In our study, temperature and precipitation were the main environmental factors that drive variations in the microbial community. Further correlation analysis showed that the most abundant bacterial phyla were significantly correlated with temperature and the most abundant fungal phyla were significantly correlated with precipitation.

A possible explanation is that temperature and precipitation became the dominant environmental factors that affect bacterial and fungal community diversity in the Qinghai-Tibet Plateau, which is characterized by low temperature and low precipitation due to high elevation. Precipitation has a strong impact on humidity, temperature, and other conditions in the air, which influence the growth of microorganisms. Some studies have shown that certain bacterial populations respond immediately to an increase in soil moisture once the monsoon rains arrive, although the relative abundances of most bacterial phyla showed less variation during the course of the study (McHugh et al., 2014). In this study, it is possible that precipitation affected local atmospheric conditions such as temperature and humidity, which further affected the abundance and diversity of the microbial communities. The *E. sinensis* infection rate in *F. sinensis* seeds on the Qinghai-Tibet Plateau was systematically investigated. The asexual *Epichloë* is extant in the embryos of seeds and is transmitted through the seeds (Wang et al., 2018). There have been extensive studies and reports on the influence of *Epichloë* endophytes on host performance, including disease and insect resistance, and cold and drought tolerance (Chen et al., 2016; Xia et al., 2018; Bu et al., 2019). However, there are relatively few reports on the effects of *Epichloë* endophytes on microbial communities, and research results are inconsistent. One study suggested that *Epichloë* endophytes can affect the microbial diversity in the roots and rhizosphere (Liu et al., 2021). Another study has reported that *E. festucae* var. *lolii* strains AR1 and AR37 significantly changed the rhizosphere bacterial community composition of the host perennial ryegrass but had no significant effect on the Pseudomonas community (Li et al., 2017). These studies have shown that *Epichloë* endophytes had different effects on different microbial communities. However, in this study, *E. sinensis* infection rate did not affect the relative abundance of the most abundant microbiota. In this study, *F. sinensis* seeds were obtained from a high-altitude areas of the Qinghai-Tibet Plateau, where the temperature and precipitation differ from those of the plain area. Correlation analysis showed that the *Epichloë sinensis* infection rate was significantly correlated with temperature and elevation, which further confirmed our hypothesis. Thus, this study provides some clues for studying the effects of *Epichloë* endophytes on seed microbiota.

The *E. sinensis* infection rate was also affected by environmental factors, which were significantly negatively correlated with elevation and positively correlated with temperature. Bacon and Siegel (1988) noted a decrease in the seed endophyte infection rate and vegetative tissue of tall fescue after the plants had experienced hot and dry summers and cold winters. Ju et al. found through growth chamber experiments that temperature appears to be a major variable that affects the fluctuation of endophyte frequency in plant tissues (Ju et al., 2006). Previous studies found that high concentrations of carbon dioxide significantly affect the infection frequency of endophytic fungi in tall fescue, and precipitation may promote this grass–fungal symbiosis, leading to higher endophyte infection frequency (Brosi et al., 2011). These studies indicate that endophytic fungi are susceptible to various environmental factors. In this study, *F. sinensis* seed lots were obtained from different sites on the Qinghai-Tibet Plateau; possibly, the combination of both host genotype and environment interactions led to the variations among the microbiomes of these 14 seed lots. The relationship between endophyte infection rate and host growth environment has not been confirmed as the research has been limited. Some reports have shown that endophyte infection rates of *Elymus tangutorum*, *Lolium rigidum,* and *F. rubra* decreased with increasing elevation (Bazely et al., 2007; Kirkby et al., 2011; Shi et al., 2020). However, other studies on *F. ovina*, *F. eskia*, *Deschampsia flexuosa,* and *Poa trivialis* did not find a relationship between endophyte infection rate and elevation (Bazely et al., 2007; Granath et al., 2007; Gonzalo-Turpin et al., 2010). Some studies have shown that the frequency of *E. alsodes* in *Poa alsodes* was positively correlated with July maximum temperatures, July precipitation, and soil nitrogen and phosphorous (Shymanovich and Faeth, 2019).

Conclusion

The microbiota of *F. sinensis* seeds of 14 different ecotypes collected from the Qinghai-Tibet Plateau were rich in diversity and were significantly affected by two environmental factors: temperature and precipitation; however, at the medium-high elevation (3,000–4,500 m), the impact of temperature and precipitation on microbial community is different. *E. sinensis* infection rates in the host *F. sinensis* seeds varied among different geographic locations, which varied in environmental factors affecting host growth, including elevation and temperature. However, the specific mechanisms of the variations require further investigation.

Data availability statement

The data presented in the study are deposited in the NCBI Sequence Read Archive (SRA) repository, accession number BioProject ID PRJNA844205.

Author contributions

PT designed the experiment, revised, and polished the manuscript and provide guidance for data analysis. YG

conducted data analysis and draft the manuscript. YC and QZ provided the experimental materials. ZN provided guidance for samples collection and experimental design. YL and JL helped in data analysis. All authors contributed to the article and approved the submitted version.

Funding

This study was supported by the National Nature Science Foundation of China (31971768), Gansu transportation department science and technology project 2021-07 and Gansu transportation department science and technology project 2021-28.

Conflict of interest

The authors declare that the research was conducted in the absence of any commercial or financial relationships that could be construed as a potential conflict of interest.

Publisher's note

All claims expressed in this article are solely those of the authors and do not necessarily represent those of their affiliated organizations, or those of the publisher, the editors and the reviewers. Any product that may be evaluated in this article, or claim that may be made by its manufacturer, is not guaranteed or endorsed by the publisher.

Supplementary material

The Supplementary Material for this article can be found online at: https://www.frontiersin.org/articles/10.3389/fmicb.2022.956489/full#supplementary-material

References

Adam, E., Bernhart, M., Müller, H., Winkler, J., and Berg, G. (2018). The *Cucurbita pepo* seed microbiome: genotype-specific composition and implications for breeding. *Plant Soil* 422, 35–49. doi: 10.1007/s11104-016-3113-9

Bacon, C. W., and Siegel, M. R. (1988). Endophyte parasitism of tall fescue. *J. Product. Agric.* 1, 45–55. doi: 10.2134/jpa1988.0045

Bazely, D. R., Ball, J. P., Vicari, M., Tanentzap, A. J., Bérenger, M., Rakocevic, T., et al. (2007). Broad-scale geographic patterns in the distribution of vertically-transmitted, asexual endophytes in four naturally-occurring grasses in Sweden. *Ecography* 30, 367–374. doi: 10.1111/j.0906-7590.2007.04985.x

Braak, C. J. F. (1994). Canonical community ordination. Part I: Basic theory and linear methods. *Ecoscience* 1, 127–140. doi: 10.1080/11956860.1994.11682237

Brosi, G. B., Mcculley, R. L., Bush, L. P., Nelson, J. A., Classen, A. T., and Norby, R. J. (2011). Effects of multiple climate change factors on the tall fescue–fungal endophyte symbiosis: infection frequency and tissue chemistry. *New Phytol.* 189, 797–805. doi: 10.1111/j.1469-8137.2010.03532.x

Bryant, D. A., and Frigaard, N. U. (2006). Prokaryotic photosynthesis and phototrophy illuminated. *Trends Microbiol.* 14, 488–496. doi: 10.1016/j.tim.2006.09.001

Bu, Y. Y., Guo, P., Ji, Y. L., Zhang, S. T., Yu, H. S., and Wang, Z. W. (2019). Effects of *Epichloë sinica* on *Roegneria kamoji* seedling physiology under PEG-6000 simulated drought stress. *Symbiosis* 77, 123–132. doi: 10.1007/s13199-018-0570-3

Buyer, J. S., Roberts, D. P., and Russek-Cohen, E. (1999). Microbial community structure and function in the spermosphere as affected by soil and seed type. *Can. J. Microbiol.* 45, 138–144. doi: 10.1139/w98-227

Chen, N., He, R. L., Chai, Q., Li, C. J., and Nan, Z. B. (2016). Transcriptomic analyses giving insights into molecular regulation mechanisms involved in cold tolerance by *Epichloë* endophyte in seed germination of *Achnatherum inebrians*. *Plant Growth Regul.* 80, 367–375. doi: 10.1007/s10725-016-0177-8

Chen, Y. L., Deng, Y., Ding, J. Z., Hu, H. W., Xu, T. L., Li, F., et al. (2017). Distinct microbial communities in the active and permafrost layers on the Tibetan Plateau. *Mol. Ecol.* 26, 6608–6620. doi: 10.1111/mec.14396

Christensen, M. J., Bennett, R. J., Ansari, H. A., Koga, H., Johnson, R. D., Bryan, G. T., et al. (2008). *Epichloë* endophytes grow by intercalary hyphal extension in elongating grass leaves. *Fungal Genet. Biol.* 45, 84–93. doi: 10.1016/j.fgb.2007.07.013

Chua, M., Erickson, T. E., Merritt, D. J., Chilton, A. M., Ooi M. K. J., and Muñoz-Rojas, M. (2019). Bio-priming seeds with cyanobacteria: effects on native plant growth and soil properties. *Restor. Ecol.* 28, S168–S176. doi: 10.1111/rec.13040

Edelman, M., Swinton, D., Schiff, J. A., Epstein, H., and Zeldin, B. (1967). Deoxyribonucleic acid of the blue-green algae (Cyanophyta). *Bacteriol. Rev.* 31, 315–331. doi: 10.1128/br.31.4.315-331.1967

Finch-Savage, W. E., and Bassel, G. W. (2015). Seed vigour and crop establishment: extending performance beyond adaptation. *J. Exp. Bot.* 67, 567–591. doi: 10.1093/jxb/erv490

Gibbons, S. M., Caporaso, J. G., Pirrung, M., Field, D., Knight, R., and Gilbert, J. A. (2013). Evidence for a persistent microbial seed bank throughout the global ocean. *Proc. Natl. Acad. Sci. U.S.A.* 110, 4651–4655. doi: 10.1073/pnas.1217767110

Gonzalo-Turpin, H., Barre, P., Gibert, A., Grisard, A., West, C. C., and Hazard, L. (2010). Co-occurring patterns of endophyte infection and genetic structure in the alpine grass, *Festuca eskia*: implications for seed sourcing in ecological restoration. *Conserv. Genet.* 11, 877–887. doi: 10.1007/s10592-009-9927-8

Granath, G., Vicari, M., Bazely, D. R., Ball, J. P., Puentes, A., and Rakocevic, T. (2007). Variation in the abundance of fungal endophytes in fescue grasses along altitudinal and grazing gradients. *Ecography* 30, 422–430. doi: 10.1111/j.0906-7590.2007.05027.x

Hashsham, S. A., Fernandez, A. S., Dollhopf, S. L., Dazzo, F. B., Hickey, R. F., Tiedje, J. M., et al. (2000). Parallel processing of substrate correlates with greater functional stability in methanogenic bioreactor communities perturbed by glucose. *Appl. Environ. Microbiol.* 66, 4050–4057. doi: 10.1128/AEM.66.9.4050-4057.2000

Jiang, L. F., Song, M. K., Yang, L., Zhang, D. Y., Sun, Y. T., Shen, Z. G., et al. (2016). Exploring the influence of environmental factors on bacterial communities within the rhizosphere of the cu-tolerant plant, *Elsholtzia splendens*. *Sci. Rep.* 6, 36302. doi: 10.1038/srep36302

Johnston-Monje, D., Lundberg, D. S., Lazarovits, G., Reis, V. M., and Raizada, M. N. (2016). Bacterial populations in juvenile maize rhizospheres originate from both seed and soil. *Plant Soil* 405, 337–355. doi: 10.1007/s11104-016-2826-0

Ju, H. J., Hill, N. S., Abbott, I., and Ingram, K. T. (2006). Temperature influences on endophyte growth in tall fescue. *Crop Sci.* 46, 404–412. doi: 10.2135/cropsci2005.0282

Kirkby, K. A., Pratley, J. E., Hume, D. E., Faville, M. J., An, M., and Wu, H. (2011). Incidence of endophyte neotyphodium occultans in *Lolium rigidum* from Australia. *Weed Res.* 51, 261–272. doi: 10.1111/j.1365-3180.2011.00846.x

Klaedtke, S., Jacques, M. A., Raggi, L., Préveaux, A., Bonneau, S., Negri, V., et al. (2016). Terroir is a key driver of seed-associated microbial assemblages. *Environ. Microbiol.* 18, 1792–1804. doi: 10.1111/1462-2920.12977

Klindworth, A., Pruesse, E., Schweer, T., Peplies, J., Quast, C., Horn, M., et al. (2013). Evaluation of general 16S ribosomal RNA gene PCR primers for classical and next-generation sequencing-based diversity studies. *Nucleic Acids Res.* 41, e1–e1. doi: 10.1093/nar/gks808

Li, F., Guo, Y. E., Christensen, M. J., Gao, P., Li, Y. Z., and Duan, T. Y. (2017). An arbuscular mycorrhizal fungus and *Epichloë festucae var.* lolii reduce *Bipolaris sorokiniana* disease incidence and improve perennial ryegrass growth. *Mycorrhiza* 28, 159–169. doi: 10.1007/s00572-017-0813-9

Lin, W. H., Wang, X. X., Wang, J. J., Nzabanita, C., Xu, W. B., Yang, L., et al. (2018). Intra- and interspecific competition of *Elymus Nutans griseb* and *Festuca Sinensis keng.* EX EB alexeev infected by *Epichloë* endophyte. *Bangladesh J. Bot.* 47, 699–709.

Liu, H., Wu, M., Liu, J. M., Gao, Y. B., and Ren, A. Z. (2021). Endophyte infection influences arbuscular mycorrhizal fungi communities in rhizosphere soils of host as opposed to non-host grass. *Eur. J. Soil Sci.* 72, 995–1009. doi: 10.1111/ejss.12996

Liu, Y., Zuo, S., Xu, L. W., Zou, Y. Y., and Song, W. (2012). Study on diversity of endophytic bacterial communities in seeds of hybrid maize and their parental lines. *Arch. Microbiol.* 194, 1001–1012. doi: 10.1007/s00203-012-0836-8

Lupwayi, N. Z., Rice, W. A., and Clayton, G. W. (1998). Soil microbial diversity and community structure under wheat as influenced by tillage and crop rotation. *Soil Biol. Biochem.* 30, 1733–1741. doi: 10.1016/S0038-0717(98)00025-X

McHugh, T. A., Koch, G. W., and Schwartz, E. (2014). Minor changes in soil bacterial and fungal community composition occur in response to monsoon precipitation in a semiarid grassland. *Microb. Ecol.* 68, 370–378. doi: 10.1007/s00248-014-0416-3

Moran-Tejeda, E., Ignacio Lopez-Moreno, J. I., and Beniston, M. (2013). The changing roles of temperature and precipitation on snowpack variability in Switzerland as a function of altitude. *Geophys. Res. Lett.* 40, 2131–2136. doi: 10.1002/grl.50463

Nan, Z. B. (1996). Incidence and distribution of endophytic fungi in seeds of some native and introduced grasses in China. *Acta Pratacult Sin.* 5, 13–17.

Nelson, E. B. (2018). The seed microbiome: Origins, interactions, and impacts. *Plant Soil* 422, 7–34. doi: 10.1007/s11104-017-3289-7

Nissinen, R., Helander, M., Kumar, M., and Saikkonen, K. (2019). Heritable *Epichloë* symbiosis shapes fungal but not bacterial communities of plant leaves. *Sci. Rep.* 9, 5253. doi: 10.1038/s41598-019-41603-5

Nottingham, A. T., Fierer, N., Turner, B. L., Whitaker, J., Ostle, N. J., McNamara, N. P., et al. (2018). Microbes follow Humboldt: temperature drives plant and soil microbial diversity patterns from the Amazon to the Andes. *Ecology* 99, 2455–2466. doi: 10.1002/ecy.2482

Osono, T., Fukasawa, Y., and Takeda, H. (2003). Roles of diverse fungi in larch needle-litter decomposition. *Mycologia* 95, 820–826. doi: 10.1080/15572536.2004.11833041

Osono, T., and Takeda, H. (2002). Comparison of litter decomposing ability among diverse fungi in a cool temperate deciduous forest in Japan. *Mycologia* 94, 421–427. doi: 10.1080/15572536.2003.11833207

Ren, X. L., Zhu, X. Y., Warndorff, M., Bucheli, P., and Shu, Q. Y. (2006). DNA extraction and fingerprinting of commercial rice cereal products. *Food Res. Int.* 39, 433–439. doi: 10.1016/j.foodres.2005.09.006

Reuter, J. A., Spacek, D. V., and Snyder, M. P. (2015). High-throughput sequencing technologies. *Mol. Cell* 58, 586–597. doi: 10.1016/j.molcel.2015.05.004

Rezki, S., Campion,. C., Simoneau,. P., Jacques, M. A., Shade, A., and Barret, M. (2018). Assembly of seed-associated microbial communities within and across successive plant generations. *Plant Soil* 422, 67–79. doi: 10.1007/s11104-017-3451-2

Schimel, J., Balser, T. C., and Wallenstein, M. (2007). Microbial stress-response physiology and its implications for ecosystem function. *Ecology* 88, 1386–1394. doi: 10.1890/06-0219

Schloss, P. D., Westcott, S. L., Ryabin, T., Hall, J. R., Hartmann, M., Hollister, E. B., et al. (2009). Introducing mothur: open-source, platform-independent, community-supported software for describing and comparing microbial communities. *Appl. Environ. Microbiol.* 75, 7537–7541. doi: 10.1128/AEM.01541-09

Shade, A., Jacques, M. A., and Barrett, M. (2017). Ecological patterns of seed microbiome diversity, transmission, and assembly. *Curr. Opin. Microbiol.* 37, 15–22. doi: 10.1016/j.mib.2017.03.010

Sharp, C. E., Brady, A. L., Sharp, G. H., Grasby, S. E., Stott, M. B., and Dunfield, P. F. (2014). Humboldt's spa: microbial diversity is controlled by temperature in geothermal environments. *ISME J.* 8, 1166–1174. doi: 10.1038/ismej.2013.237

Shearin, Z. R. C., Filipek, M., Desai, R., Bickford, W. A., Kowalski, K. P., and Clay, K. (2018). Fungal endophytes from seeds of invasive, non-native *Phragmites australis* and their potential role in germination and seedling growth. *Plant Soil* 422, 183–194. doi: 10.1007/s11104-017-3241-x

Shen, C. C., Gunina, A., Luo, Y., Wang, J. J., He, J. Z., Kuzyakov, Y., et al. (2020). Contrasting patterns and drivers of soil bacterial and fungal diversity across a mountain gradient. *Environ. Microbiol.* 22, 3287–3301. doi: 10.1111/1462-2920.15090

Shi, Q., Matthew, C., Liu, W. H., and Nan, Z. B. (2020). Alkaloid contents in *Epichloë* endophyte-infected *Elymus tangutorum* sampled along an elevation gradient on the Qinghai-Tibetan Plateau. *Agronomy-Basel* 10, 1812. doi: 10.3390/agronomy10111812

Shymanovich, T., and Faeth, S. H. (2019). Environmental factors affect the distribution of two *Epichloë* fungal endophyte species inhabiting a common host grove bluegrass (*Poa alsodes*). *Ecol. Evol.* 9, 6624–6642. doi: 10.1002/ece3.5241

Song, M. L., Chai, Q., Li, X. Z., Yao, X., Li, C. J., Christensen, M. J., et al. (2015). An asexual *Epichloë* endophyte modifies the nutrient stoichiometry of wild barley (*Hordeum brevisubulatum*) under salt stress. *Plant Soil* 387, 153–165. doi: 10.1007/s11104-014-2289-0

Tannenbaum, I., Kaur, J., Mann, R., Sawbridge, T., and Spangenberg, G. (2020). Profiling the *Lolium perenne* microbiome: from seed to seed. *Phytobiomes J.* 4, 281–289. doi: 10.1094/PBIOMES-03-20-0026-R

Thomas, D. C., Vandegrift, R., Ludden, A., Carroll, G. C., and Roy, B. A. (2016). Spatial ecology of the fungal genus xylaria in a tropical cloud forest. *Biotropica* 48, 381–393. doi: 10.1111/btp.12273

Thomas, F., Hehemann, J. H., Rebuffet, E., Czjzek, M., and Michel, G. (2011). Environmental and gut bacteroidetes: the food connection. *Front. Microbiol.* 2, 93. doi: 10.3389/fmicb.2011.00093

Tian, P., Xu, W. B., Li, C. J., Song, H., Wang, M. N., Schardl, C. L., et al. (2020). Phylogenetic relationship and taxonomy of a hybrid *Epichloë* species symbiotic with *Festuca sinensis*. *Mycol. Prog.* 19, 1069–1081. doi: 10.1007/s11557-020-01618-z

Truyens, S., Weyens, N., Cuypers, A., and Vangronsveld, J. (2015). Bacterial seed endophytes: genera, vertical transmission and interaction with plants. *Environ. Microbiol. Rep.* 7, 40–50. doi: 10.1111/1758-2229.12181

Vandenkoornhuyse, P., Baldauf, S. L., Leyval, C., Straczek, J., and Young, J. P. W. (2002). Extensive fungal diversity in plant roots. *Science* 295, 2051–2052. doi: 10.1126/science.295.5562.2051

Walton, K., and Berry, J. P. (2016). Indole alkaloids of the Stigonematales (Cyanophyta): chemical diversity, biosynthesis and biological activity. *Mar. Drugs* 14, 73. doi: 10.3390/md14040073

Wang, M. Y., McGill, C. R., Southward, R. C., He, X. Z., Card, S. D., and Rolston, M. P. (2018). *Epichloë* fungal endophyte colonisation and seed quality in developing grass florets-effect of different fertiliser applications. *N. Z. J. Agric. Res.* 61, 27–41. doi: 10.1080/00288233.2017.1383275

Xia, C., Li, N. N., Zhang, Y. W., Li, C. J., Zhang, X. X., and Nan, Z. B. (2018). Role of *Epichloë* endophytes in defense responses of cool-season grasses to pathogens: a review. *Plant Dis.* 102, 2061–2073. doi: 10.1094/PDIS-05-18-0762-FE

Zhang, B. G., Zhang, J., Liu, Y., Guo, Y. Q., Shi, P., and Wei, G. H. (2018). Biogeography and ecological processes affecting root-associated bacterial communities in soybean fields across China. *Sci. Total Environ.* 627, 20–27. doi: 10.1016/j.scitotenv.2018.01.230

Zheng, S., Shan, L. Y., Zhuang, Y. L., and Shang, Y. (2018). Identification of pyrg used as an endogenous reference gene in qualitative and real-time quantitative PCR detection of *Pleurotus ostreatus*. *J. Food Sci.* 83, 750–755. doi: 10.1111/1750-3841.14072

frontiers | Frontiers in Microbiology

TYPE Original Research
PUBLISHED 08 August 2022
DOI 10.3389/fmicb.2022.984757

OPEN ACCESS

EDITED BY
Punyasloke Bhadury,
Indian Institute of Science Education and Research Kolkata, India

REVIEWED BY
Junfeng Chen,
Qufu Normal University, China
Hailong Zhou,
Hainan University, China

*CORRESPONDENCE
Zhi-xun Xie
xiezhixun@126.com

†These authors have contributed equally to this work

SPECIALTY SECTION
This article was submitted to Microbial Symbioses, a section of the journal Frontiers in Microbiology

RECEIVED 02 July 2022
ACCEPTED 21 July 2022
PUBLISHED 08 August 2022

CITATION
Jiang J-y, Li W-h, Wu Y-y, Cheng C-x, Ye Q-q, Feng J-x and Xie Z-x (2022) Effects of cadmium exposure on intestinal microflora of *Cipangopaludina cathayensis*. *Front. Microbiol.* 13:984757. doi: 10.3389/fmicb.2022.984757

Effects of cadmium exposure on intestinal microflora of *Cipangopaludina cathayensis*

Jiao-yun Jiang[1,2,3†], Wen-hong Li[1,4†], Yang-yang Wu[3], Chun-xing Cheng[3], Quan-qing Ye[3], Jia-xun Feng[1] and Zhi-xun Xie[1,2*]

[1]College of Life Science and Technology, Guangxi University, Nanning, China, [2]Guangxi Key Laboratory of Veterinary Biotechnology, Guangxi Veterinary Research Institute, Nanning, China, [3]Key Laboratory of Ecology of Rare and Endangered Species and Environmental Protection, Ministry of Education, Guangxi Normal University, Guilin, China, [4]College of Animal Science and Technology, Guangxi University, Nanning, China

As one of the most environmentally toxic heavy metals, cadmium (Cd) has attracted the attention of researchers globally. In particular, Guangxi, a province in southwestern China, has been subjected to severe Cd pollution due to geogenic processes and anthropogenic activities. Cd can be accumulated in aquatic animals and transferred to the human body through the food chain, with potential health risks. The aim of the present study was to explore the effects of waterborne Cd exposure (0.5 mg/L and 1.5 mg/L) on the intestinal microbiota of mudsnail, *Cipangopaludina cathayensis*, which is favored by farmers and consumers in Guangxi. Gut bacterial community composition was investigated using high-throughput sequencing of the V3–V4 segment of the bacterial 16S rRNA gene. Our results indicated that *C. cathayensis* could tolerate low Cd (0.5 mg/L) stress, while Cd exposure at high doses (1.5 mg/L) exerted considerable effects on microbiota composition. At the phylum level, Proteobacteria, Bacteroidetes, and Firmicutes were the dominant phyla in the mudsnail gut microbiota. The relative abundances of Bacteroidetes increased significantly under high Cd exposure (H14) ($p < 0.01$), with no significant change in the low Cd exposure (L14) treatment. The dominant genera with significant differences in relative abundance were *Pseudomonas*, *Cloacibacterium*, *Acinetobacter*, *Dechloromonas*, and *Rhodobacter*. In addition, Cd exposure could significantly alter the pathways associated with metabolism, cellular processes, environmental information processing, genetic information processing, human diseases, and organismal systems. Notably, compared to the L14 treatment, some disease-related pathways were enriched, while some

xenobiotic and organic compound biodegradation and metabolism pathways were significantly inhibited in the H14 group. Overall, Cd exposure profoundly influenced community structure and function of gut microbiota, which may in turn influence *C. cathayensis* gut homeostasis and health.

KEYWORDS

cadmium, *Cipangopaludina cathayensis*, intestinal microbiota, high-throughput sequencing, microbial diversity

Introduction

In the wake of rapid industrialization, aquatic ecosystem pollution is becoming severe (Ali et al., 2022). As ubiquitous hazardous pollutants, heavy metals have attracted the attention or researchers globally due to their environmental toxicity. Cadmium (Cd), a non-essential element, usually exists as Cd (II). As one of the most toxic heavy metals, Cd is released into the environment mainly through anthropogenic activities, including electroplating, battery manufacturing, soldering, mining, and agriculture (Burger, 2008). Cd has numerous negative impacts on aquatic animals, including triggering histopathological changes, inducing oxidative stress, causing metabolic disorders, and altering gut microbial community structure (Chang et al., 2019; Liu et al., 2019; Cheaib et al., 2020; Wang et al., 2020a,b). Moreover, Cd is not easily degradable, and can be accumulated in aquatic animals followed by in the human body through the food chain, with potential human health risks (Wang et al., 2022).

Heavy metal pollution is a major environmental issue in China, and heavy metal pollution in aquatic environment is increasing in severity (Chen et al., 2022; Wang et al., 2022). Cd has been identified as one of the major soil contaminants in China (Ministry of Ecology and Environment of the People's Republic of China, 2014). In particular, Cd contamination in Guangxi province is significantly higher than in other regions in China due to high background geochemical concentrations in the region (Zhao et al., 2015; Wen et al., 2020). In addition, Guangxi province is a key non-ferrous metal production area in China, so that Cd pollution is a major challenge in the province. In early January 2012, the Longjiang River of Guangxi was exposed to serious Cd contamination following an accident, with long-term impacts on the regional aquatic ecosystems (Zhao et al., 2018; Cui et al., 2022). Cd is also the primary heavy metal pollutant in Chinese agricultural land, including paddy soils (Song et al., 2019; Yang et al., 2021). Indeed, people inhabiting such areas with high levels of Cd pollution may be exposed to Cd toxicity, with potential threats to human health (Xu et al., 2018).

The mudsnail, *Cipangopaludina cathayensis* (phylum Mollusca, Gastropoda, Prosobranchia, Mesogastropoda, Viviparidae, and *Cipangopaludina*), is a widely distributed species that can be found in Chinese rivers, lakes, ponds, and other water bodies (Lu et al., 2014). *C. cathayensis* has high protein and low fat content, is rich in umami amino acid, and has high nutritional value, so that it is highly favored among consumers and farmers in China (Luo et al., 2021). Moreover, *C. cathayensis* flesh has been reported to have diverse biological and physiological properties that are beneficial in human disease prevention and treatment (Wang et al., 2016; Zhao et al., 2021).

Indeed, *C. cathayensis* is one of the most popular aquatic animals in China. Particularly in Guangxi province, the snail family Viviparidae is a source of key components of a famous snack, "snail rice noodle," which represents one of the intangible cultural heritages in China (Luo et al., 2021). In recent years, with the continued increase in "snail rice noodle" consumption, demand for mudsnail and its production has been increasing. Paddy field culture is one of the major ways of mudsnail production in Guangxi. However, Cd pollution has been identified as a serious problem in Guangxi paddy soils and aquatic environments (Zhao et al., 2018; Song et al., 2019; Yang et al., 2021). In addition, considering mudsnail is a benthic organism that is closely associated with paddy soil, it could be exposed to high Cd concentrations, with major threats to food safety (Wang P. et al., 2019). At present, only a few studies had explored the adverse impacts of Cd exposure on the snail family Viviparidae. In addition, current studies have largely focused on the oxidative stress caused by Cd exposure (Hu and Tang, 2012; Zhou and Luo, 2018), so that further investigations on other adverse effects on snails need to be carried out.

The microbiomes associated with aquatic animals, particularly their gut systems, not only participate in digestion but also influence nutrition, growth, reproduction, the immune system, and host vulnerability to disease (Talwar et al., 2018; Chang et al., 2019; Paul and Small, 2019; Duan et al., 2020; Wang et al., 2020a; Diwan et al., 2021). Cd exposure has been reported to significantly affect the gut microbiota of numerous aquatic organisms (Chang et al., 2019; Wang et al., 2020b; Zhang Y. et al., 2020). However, the effects of Cd exposure on the intestinal microbiota of *C. cathayensis* remain unclear. To address the knowledge gap, in the present study, *C. cathayensis* individuals were exposed

to two doses (0.5 mg/L and 1.5 mg/L) of cadmium chloride ($CdCl_2 \cdot 2.5H_2O$) for > 14 days. The aim of the present study was to investigate the effect of Cd on *C. cathayensis* gut microbiota composition and diversity.

Materials and methods

Ethics statement

The experimental protocol for snail acclimation and experimentation was approved by the Animal Ethics committee of Guangxi Normal University, Guilin, Guangxi, China (No. 202207-02).

Experimental snail and treatment

Adult snails (*C. cathayensis*) were obtained from Juhe Agricultural Development Cooperatives (25.75° N, 109.38° E), Sanjiang District, Liuzhou City, Guangxi, China. They were then transferred to the laboratory, and acclimated to the experimental conditions at a temperature 24.0 ± 1.0°C, under a 12-h/12-h light/dark cycle in a 50-L (65 × 41 × 20 cm) plastic tank for 2 weeks. During the acclimation period, specimens were fed with commercial ground fish food (Tongwei, Chengdu, Sichuan, China) once a day at 0.5% of their body weight. The tank water was changed partially (30%) every day.

After a 2-week acclimation period, 225 snails were divided randomly into three groups and placed in plastic tanks, with three replicates (25 snails per tank) in each treatment. $CdCl_2 \cdot 2.5H_2O$ (Silong, Shantou, Guangdong, China) was dissolved in deionized water to prepare stock solution with a final concentration of 900 mg/L. The 0.5 mg/L and 1.5 mg/L Cd doses were selected according to previous studies (Hu and Tang, 2012). The three treatments in the present study included the control treatment (**CK14**: with no Cd supplementation), low Cd concentration exposure treatment (**L14**: 0.5 mg/L), and high Cd concentration exposure treatment (**H14**: 1.5 mg/L). Other experimental conditions were consistent with those in the acclimation phase. During the experimental period, one-third of the water in the tank was replaced every day by adding fresh water or water with a similar concentration. The experiment lasted 2 weeks, as severe mortality occurred at 14 -day in the H14 treatment (**Supplementary Table S1**).

Sample collection

Snail intestine samples were collected on day 14 and used to determine gut microbiota composition and diversity. The guts of three snails were pooled as a single sample, to ensure sample adequacy, with three biological replicates in each treatment. Briefly, the samples were wiped with 75% ethanol before the snails were removed from the shell. Subsequently, the snails were dissected and the guts extracted and rinsed with sterile water three times. The gut samples were flash frozen using liquid nitrogen and stored at −80°C for subsequent analyses.

DNA extraction, bacterial 16S rRNA amplification, and sequencing

Total genomic DNA (gDNA) of the gut microbiota were extracted using a Fast DNA SPIN Extraction Kit (MP Biomedicals, United States) according to the manufacturer's protocol. The V3–V4 regions of the bacterial 16S rRNA genes were amplified by PCR using universal bacterial primers (338F: 50-ACTCCTACGGGAGGGAGCA-30, 806R: 50-GGACTACHVGGGTWTCTAAT-30). The PCR cycle conditions for each sample were as follows: an initial denaturation at 95°C for 5 min; 25 cycles of denaturation at 95°C for 30 s, annealing at 55°C for 30 s, and extension at 72°C for 30 s, with a final extension at 72°C for 5 min. PCR products were purified and quantified using an AxyPrep DNA Gel Extraction Kit (Axygen, Union City, NJ, United States) and a Quant-iT PicoGreen dsDNA Assay Kit (Invitrogen, Waltham, MA, United States), respectively. A TruSeq Nano DNA LT Library Prep Kit (Illumina, United States) was used to establish the DNA library. The library was sequenced using a MiSeq Reagent Kit v3 (6,000-cycles-PE) (Illumina, United States) on a MiSeq platform by Personal Biotechnology Co., Ltd. (Shanghai, China). The raw reads were deposited into the NCBI Sequence Read Archive database (PRJNA837347).

Sequence processing

The sequencing data were processed using Quantitative Insights Into Microbial Ecology 2 (QIIME2 v2019.4[1]). Briefly, Cutadapt (version 3.7) was used to filter and trim PCR primers from the raw reeds. DADA2 was used for quality control (Callahan et al., 2016), removing chimera sequences, and determining the sequence variants. Taxonomy was assigned using the DADA2 pipeline, which implements the Naive Bayesian Classifier using the DADA2 default parameters based on the Greengenes database (Release 13.8[2]). Subsequently, the sequences were rarefied using the feature-table rarefy command in QIIME2.

1 http://qiime.org

2 http://greengenes.secondgenome.com/

Data analysis

All sequence analysis steps were performed using QIIME2 and R v3.2.0 (R Foundation for Statistical Computing, Vienna, Austria). The rarefaction curve was generated based on Amplicon Sequence Variants (ASVs) at a 97% similarity cut-off level. For alpha diversity analyses, Chao 1, Observed_species, Shannon, and Simpson indices were calculated using QIIME2 (for calculation methods[3]). Significance between groups was tested using the Kruskal–Wallis *H* test and the Dunn test. Beta diversity was calculated using weighted Bray-Curtis distance matrix and visualized with Principal Coordinates Analysis (PCoA). Hierarchical clustering using Bray–Curtis distances based on the relative abundances of species was performed to cluster the dataset. A Venn diagram was drawn using the "VennDiagram" package in R v3.2.0 (R Statistical Foundation). The functional profiles of microbial communities were predicted using PICRUSt2 (Phylogenetic Investigation of Communities by Reconstruction of Unobserved States[4]). The predicted genes and their respective functions were annotated using the Kyoto Encyclopedia of Genes and Genomes (KEGG) database[5]. Differences between populations were analyzed using one-way Analysis of Variance. Results were considering statistically significant at $p < 0.05$. The values are expressed as mean ± SD (Standard deviation).

Results

Relative abundance

After normalization, there were 833,989 sequences across all snail gut contents sampled, with an average of 92,665 sequences per sample (minimum of 55,824 sequences per sample and maximum of 145,373 sequences per sample, see **Supplementary Table S2**). Rarefaction curves indicated that all samples reached the saturation phase (**Supplementary Figure S1**). There were 14,951 ASVs derived from all samples; the CK14, L14, and H14 treatments had 4,625, 5,121, and 5,205 ASVs per sample, respectively. Moreover, 859 ASVs were shared among the three treatments, while 2,010, 2,029, and 2,386 ASVs were unique to the CK14, L14, and H14 treatments, respectively (**Figure 1**).

Intestinal microflora diversity

To compare bacterial community diversity across different groups, alpha-diversity and beta-diversity were evaluated.

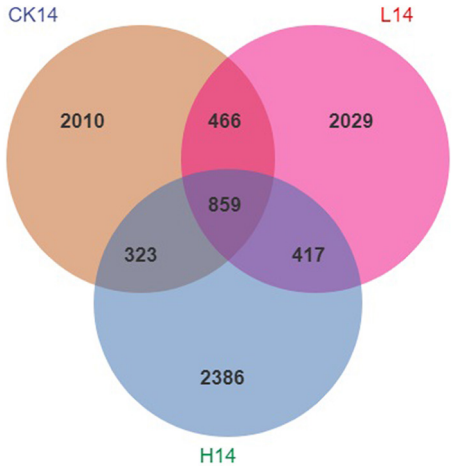

FIGURE 1
Venn diagram analysis depicting the numbers of shared and unique Amplicon Sequence Variants (ASVs) among the control (CK14), 0.5 mg/L (L14), and H14 (1.5 mg/L) treatments.

There were no significant differences in Chao 1 index, Observed_species index, Shannon index, and Simpson index among the three groups ($p > 0.05$) (**Figure 2A** and **Supplementary Table S3**). In a beta-diversity analysis (PCoA based on Bray–Curtis), the L14 and CK14 treatments were clustered together and could not be distinguished, whereas the H14 group was distinct from the L14 and CK14 groups, with the following main principal component (PC) scores: PC1 = 48.1%, PC2 = 25.7% (**Figure 2B**). In addition, according to the hierarchical clustering tree results, ASVs from *C. cathayensis* in the high Cd exposure group were clustered in one group based on similarity, while the control and low Cd exposure groups clustered into one independent group, excluding one control sample (**Figure 2C**). The results indicate that the high Cd exposure treatment had more severe effects on the diversity of the *C. cathayensis* microbiome than the low Cd exposure treatment.

Gut microbiota community structure

In total, 25 phyla, 50 classes, 115 orders, 185 families, 324 genera, and 90 species were identified. At the phylum level, Proteobacteria was the most abundant phylum across all three treatments (51.9% in CK14, 55.2% in L14, and 38.9% in H14), the other two prevalent phyla were Bacteroidetes and Firmicutes (**Figure 3A** and **Supplementary Table S4**). In addition, Bacteroidetes abundance in the H14 treatment was significantly higher than that in the C14 treatment ($p < 0.01$), although there was no significant difference between the L14 and control treatments (**Figure 3A** and **Supplementary Figure S2a**). At the genus level, *Pseudomonas, Cloacibacterium,*

3 http://scikit-bio.org/docs/latest/generated/skbio.diversity.alpha.html#module-skbio.diversity.alpha
4 https://github.com/picrust/picrust2
5 http://www.genome.jp/kegg/pathway.html

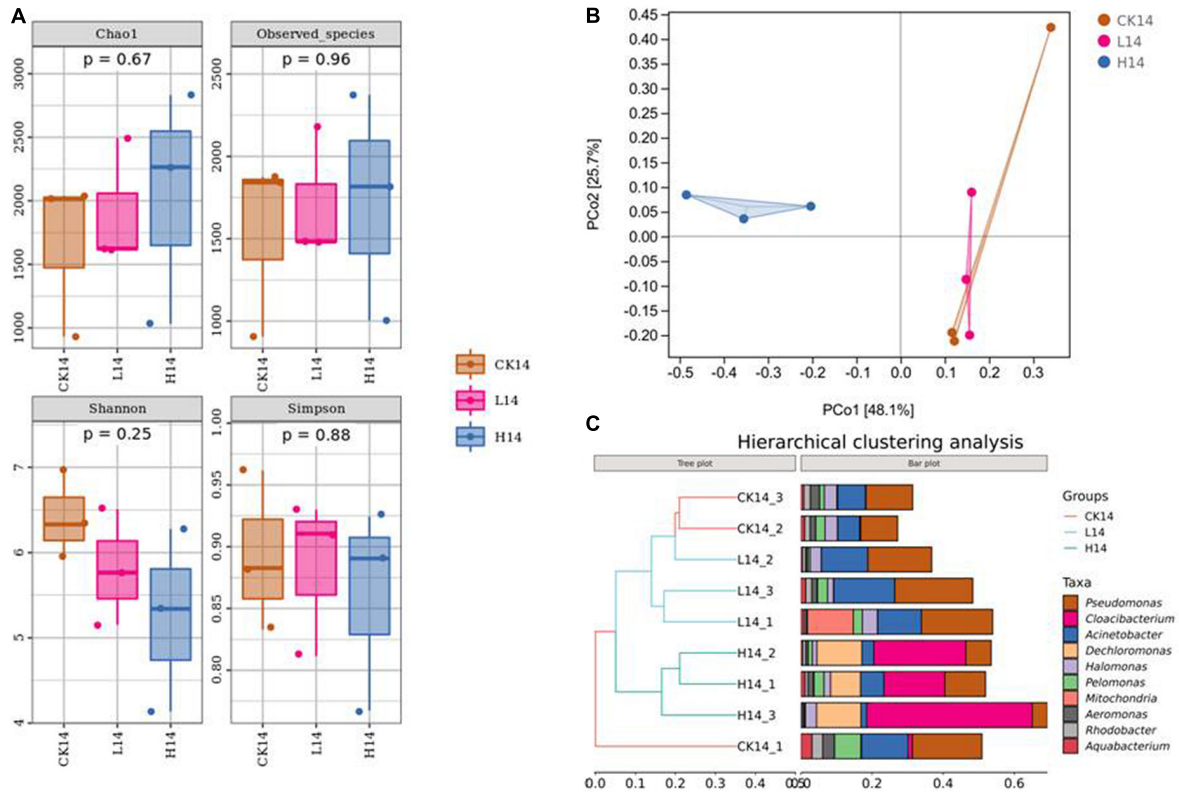

FIGURE 2
Intestinal microbiome diversity in the control (CK14), 0.5 mg/L (L14) and H14 (1.5 mg/L) groups. **(A)** α-diversity comparisons in the intestinal microflora among the CK14, L14, and H14 groups. **(B)** Bray–Curtis distances were calculated and visualized through Principal Coordinate Analysis (PCoA) (Ellipses were drawn with 95% confidence intervals). **(C)** Hierarchical cluster analysis of the Bray–Curtis distances generated from taxa tables showed Amplicon Sequence Variant (ASV) similarity across microbial communities among different groups.

Acinetobacter, Dechloromonas, Halomonas, Pelomonas, Mitochondria, Aeromonas, Rhodobacter, and *Aquabacterium* were the dominant (Figure 3B and Supplementary Table S5). *Pseudomonas* relative abundance was higher in the L14 treatment than in the C14 treatment, although the difference was not significant (Figure 3B and Supplementary Figure S2b). Conversely, *Pseudomonas* relative abundance was lower in the H14 treatment than in the C14 treatment, although the difference was not significant (Figure 3B and Supplementary Figure S2b). However, *Pseudomonas* relative abundance decreased with an increase in Cd concentration ($p < 0.01$) in the H14. *Acinetobacter* exhibited a similar trend (Figure 3B and Supplementary Figure S2c). In addition, *Rhodobacter* relative abundance was significantly lower in the H14 treatment than in the C14 treatment ($p < 0.05$). *Rhodobacter* relative abundance was also lower in the L14 treatment than in the C14 treatment, although the difference was not significant (Figure 3B and Supplementary Figure S2d). On the contrary, *Cloacibacterium* and *Dechloromonas* were significantly enriched in the H14 treatment ($p < 0.05$), although there was no significant indifference between the L14 treatment and the CK14 treatment (Figure 3B and Supplementary Figures S2e,f). The results were consistent with beta diversity analysis results (Figures 2B,C). Cd exposure at low doses had minimal effect on snail gut microbial diversity, whereas high Cd stress influenced snail gut microbial diversity considerably.

Prediction of microbial community function

PICRUSt functional prediction and KEGG pathway enrichment analysis results showed that the main functional categories included five cellular processes pathways, three environmental information processing pathways, four genetic information processing pathways, five human disease pathways, 11 metabolism pathways, and seven organismal system pathways (Figure 4). In the L14 treatment, the fluorobenzoate degradation pathway was enriched; on the contrary, carotenoid biosynthesis, steroid biosynthesis, and indole alkaloid biosynthesis pathways were significantly down-regulated in the L14 treatment compared with in the control treatment (Figures 5A,B). In the H14 treatment, five pathways (protein digestion and absorption, apoptosis, lysosome, other

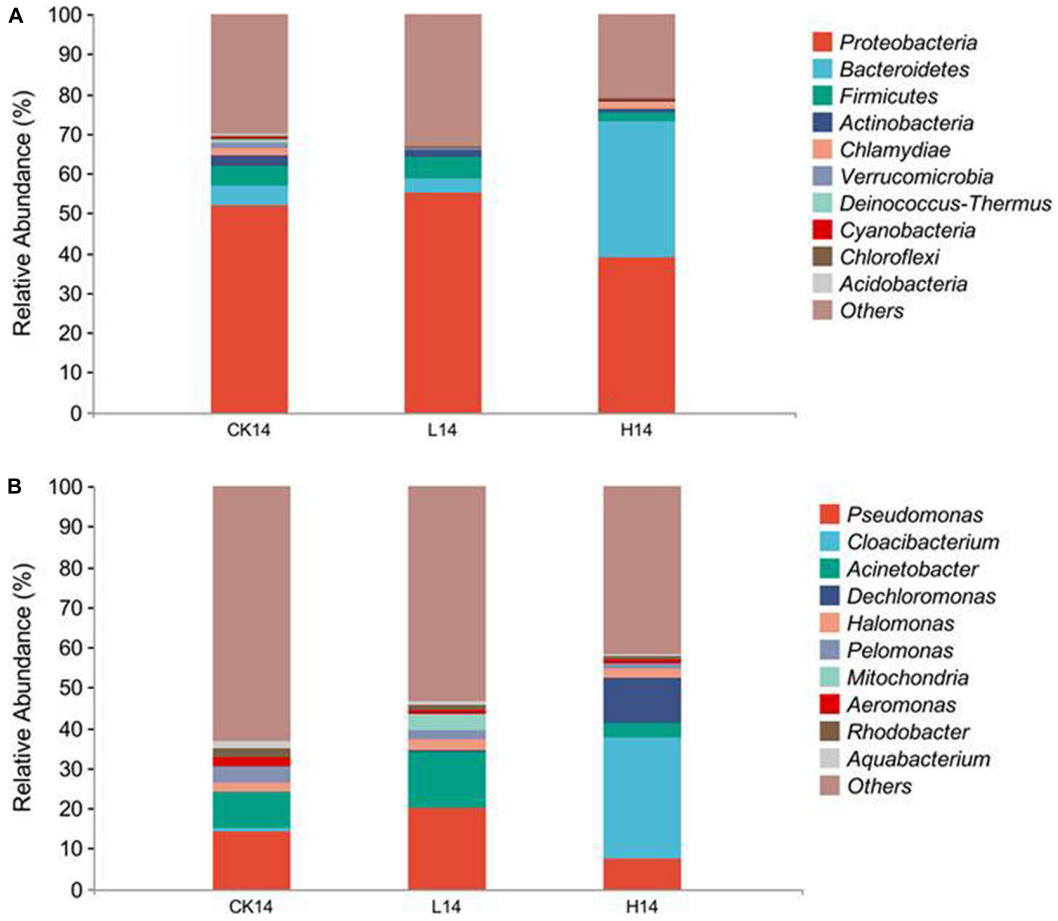

FIGURE 3
Compositions of the intestinal microflora among the control (CK14), 0.5 mg/L (L14), and H14 (1.5 mg/L) treatments. **(A)** Compositions of the intestinal microflora at the phylum level. **(B)** Compositions of the intestinal microflora at the genus level. The top ten abundant genera (higher than 1% in at least one sample) are shown in the figure and the rest are indicated as "Others."

glycan degradation, and pathways in cancer) were significantly up-regulated, whereas shigellosis and endocytosis pathways were decreased relative to the control group (**Figures 5A,C**). In addition, notably, compared with in the L14 treatment, some xenobiotic and organic compound biodegradation and metabolism pathways were significantly reduced in the H14 treatment (**Figures 5A,D**).

Discussion

Intestinal microbial diversity

Cadmium is undoubtedly an environmental contaminant. Previous studies have demonstrated that Cd exposure could alter intestinal flora composition in aquatic animals (Chang et al., 2019; Wang et al., 2020b; Zhang Y. et al., 2020). In the present study, intestinal microbiota in *C. cathayensis* was investigated using high-throughput 16S rRNA gene sequencing. Our results suggested no significant difference in alpha diversity among the three treatments (**Figure 2A**). The results are inconsistent with the findings of previous studies that have reported that Cd exposure altered the alpha diversity of gut microbiota (Ya et al., 2019; Zhang Y. et al., 2020), even under relatively low Cd concentration (Chang et al., 2019). Furthermore, the PCoA analysis results showed that gut microbial community structure in the high Cd exposure treatment was distinct from that in the low Cd exposure and control treatments, whereas the taxonomic groups in the latter two treatments were clustered together (**Figure 2B**). In addition, hierarchical clustering tree construction revealed that the intestinal samples of the three exposure treatments were clustered into two independent groups, excluding one control sample (**Figure 2C**), implying that Cd exposure at high dose (1.5 mg/L) exerted greater effects on the microbiota composition in *C. cathayensis*. The results indicate that *C. cathayensis* could potentially tolerate low Cd stress. Gut microbiome systems of aquatic animals participate in various processes, including

FIGURE 4
Functional annotations and abundance information about the intestinal microbiota at KEGG level 1 and level 2. The gene function is showed as color-bars (level 1). The detailed pathways are shown on the left side (level 2).

nutrition, growth, immunity, and disease resistance (Talwar et al., 2018; Chang et al., 2019; Paul and Small, 2019; Duan et al., 2020; Wang et al., 2020a; Diwan et al., 2021). In the present study, intestinal microbiota structure was altered in the *C. cathayensis* gut under high Cd exposure when compared with in the control treatment (**Figures 2B,C**). Consequently, alteration of intestinal microbial community structure following Cd exposure could induce adverse effects on *C. cathayensis* health.

Effects of Cd exposure on gut microbial community

In the present study, phylum Proteobacteria was the dominant phylum across all three groups. The results are consistent with the findings of recent studies in other *Cipangopaludina* species (Zhou K. Q. et al., 2022; Zhou Z. H. et al., 2022). The other two dominant phyla were Bacteroidetes

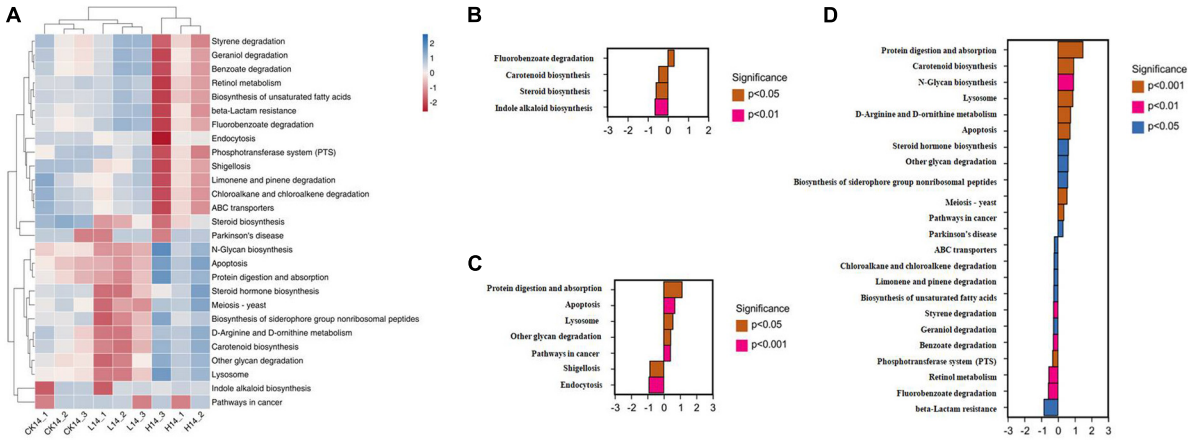

FIGURE 5
Intestinal microbiota predictive metabolic functions from the Kyoto Encyclopedia of Genes and Genomes (KEGG) database in all samples. **(A)** Heatmap of the significant differential pathways among the control (CK14), 0.5 mg/L (L14), and H14 (1.5 mg/L) treatments. **(B)** Significant different pathways between the control and L14 treatments. **(C)** Significantly different pathways between the control and H14 treatments. **(D)** Significantly different pathways between the L14 and H14 treatments.

and Firmicutes, which are consistent with the findings of previous studies that have reported that the major bacterial phyla in the gut of aquatic animals, including fish, crustaceans, and mollusks are Proteobacteria, Bacteroidetes, and Firmicutes (Chang et al., 2019; Liu et al., 2019; Wang et al., 2020b; Zhang Y. et al., 2020; Zhou Z. H. et al., 2022). However, the two phyla were not dominant in a closely related species, *Cipangopaludina chinensis* (Zhou K. Q. et al., 2022; Zhou Z. H. et al., 2022). The result implies that although the two species are closely related, they may have different strategies of responding to Cd stress. Nevertheless, further research is required to investigate the factors responsible for the difference between the two species. Compared to that in the control, the abundance of Bacteroidetes was significantly higher in the H14 treatment, although there was no significant difference between the L14 and control treatments. Bacteroidetes, the largest phylum of Gram-negative bacteria in the human gastrointestinal tract microbiome, has the potential to secrete surface lipopolysaccharides and toxic proteolytic peptides, which can cause inflammation in the gut (Lukiw, 2016). The elevated phylum Bacteroidetes abundance in H14 treatment indicated that high Cd exposure has potential adverse effects on *C. cathayensis* health.

Genus *Pseudomonas*, which has been identified as bacterial pathogen in teleosts, exists widely in aquatic environments and in the gut of aquatic animals (Llewellyn et al., 2014; Xu et al., 2015; Dehler et al., 2017; Diwan et al., 2021). *Pseudomonas* has also been observed to increase in the guts of different vertebrates, including fish and amphibians, following Cd exposure (Chang et al., 2019; Ya et al., 2019; Cheaib et al., 2020). Furthermore, *Pseudomonas* outbreaks have been reported in aquacultured animals (Llewellyn et al., 2014; Xu et al., 2015). However, *Pseudomonas* are also considered probiotics for application in aquaculture (Wang A. R. et al., 2019), that can chelate or oxidize heavy metals, thereby facilitating heavy metal excretion and minimizing the exposure of organisms to heavy metals (Duan et al., 2020; Arun et al., 2021). In the present study, *Pseudomonas* relative abundance in the L14 treatment was higher than that in the control treatment, although the difference was not significant. However, *Pseudomonas* relative abundance in the H14 treatment was lower than that in the control treatment, although not significant. Notably, *Pseudomonas* abundance decreased with an increase in Cd concentration, suggesting that *Pseudomonas* could play a role in Cd toxicity removal. However, probiotics contents decreased with an increase in Cd concentration, which could adversely affect Cd toxicity tolerance in mudsnail. Indeed, high snail mortality was observed in the H14 treatment but not in the L14 treatment. The results further confirm our postulation above that *C. cathayensis* could acclimate to low Cd concentration, potentially by accumulating *Pseudomonas*. *Acinetobacter* are putative pathogens. Their abundance increased significantly in the gut of Nile tilapia (Zhai et al., 2016) and common carp (Chang et al., 2019) following Cd exposure, and greatly increased in methyl-mercury (MeHg)-exposed fish (Bridges et al., 2018). Studies have shown that *Acinetobacter* may exert adverse effects on fish health (Wu et al., 2013; Wang et al., 2020c). Consistent with the previous findings, *Acinetobacter* increased in the L14 treatment, although not significantly. However, when Cd concentration reached 1.5 mg/L, *Acinetobacter* reduced considerably, which may be related to the extremely high Cd content (Wang et al., 2020c). Similarly, *Rhodobacter* significantly decreased in the H14 treatment. Decreased *Rhodobacter* abundance has been reported to reduce growth (Liu H. S. et al., 2021) and to have

adverse effects on fish innate immunity (Wang et al., 2020c), resulting in increased vulnerability to disease (She et al., 2017; Liu F. P. et al., 2021). Indeed, *Rhodobacter* is a candidate probiotic for fish (Ye et al., 2019). However, some studies have found that higher abundances of such bacteria could be associated with diseased intestines (Tran et al., 2018), and they could cause neurotoxicity in the hosts (Bridges et al., 2018; Arun et al., 2021). Such findings illustrate the importance of intestinal bacterial community homeostasis in hosts. Decreased *Rhodobacter* abundance in the present study suggest that intestinal function could have been impaired in *C. cathayensis* exposed to Cd, which could result in disease outbreaks under natural conditions (She et al., 2017; Liu F. P. et al., 2021).

In the present study, *Cloacibacterium*, a key genus in the phylum Bacteroidetes implicated in xenobiotic metabolism and metal removal (Nouha et al., 2016; Duan et al., 2020), increased significantly in the H14 treatment. *Cloacibacterium* has been used to detoxify MeHg in MeHg-exposed fish (Bridges et al., 2018). Enrichment of *Cloacibacterium* has been reported to be an important feature under MeHg-induced neurotoxicity (Bridges et al., 2018). In addition, in the present study, *Dechloromonas* abundance increased in the H14 treatment. *Dechloromonas*, which belongs to the phylum Proteobacteria and is considered a Cd-resistant microorganism (Zhang et al., 2019), could efficiently degrade polycyclic aromatic hydrocarbons during sludge composting (Lu et al., 2019; Che et al., 2021), and participate in organic matter degradation in aquaculture pond sediment (Zhang K. K. et al., 2020). *Cloacibacterium* and *Dechloromonas* enrichment in *C. cathayensis* gut in the present study highlight their potential roles in Cd detoxification, which merit further study.

Intestinal microbiome function

Our function prediction analysis of the gut microbiota showed that most of the genes encoded by the *C. cathayensis* gut microbiota were related to metabolism, followed by organismal systems, cellular processes pathways, human diseases pathways, genetic information processing pathways, and environmental information processing pathways (**Figure 4**). The intestines are essential organs involved in the metabolism of nutrients (Liu et al., 2022). The results suggest that Cd exposure may alter gut microbial function and host metabolism. In addition, function prediction results showed that, compared with the control treatment, only one pathway related to fluorobenzoate degradation was enriched in the L14 treatment, whereas more pathways were enriched in the H14 treatment (**Figure 5**), including protein digestion and absorption, apoptosis, lysosome, other glycan degradation, and pathways in cancer. Fluorobenzoate is the sole carbon and energy source for *Pseudomonas* (Kalpit et al., 1988). The fluorobenzoate degradation pathway was enriched in the L14 treatment, which is consistent with the increasing trends in *Pseudomonas* abundance observed in the treatment group. The cell apoptosis pathway is usually activated following disease infection (Qiu et al., 2020) or exposure to adverse environmental factors (Chen et al., 2021). Furthermore, lysosomes not only play a central role in cell decomposition but also participate in metabolism, membrane repair, and cell death (Serrano-Puebla and Boya, 2015), and lysosome metabolic pathways are closely related to cell apoptosis (Guo et al., 2017). In the present study, lysosome pathway and cell apoptosis pathway were both enriched in the H14 treatment, which suggests that high Cd exposure may exert more adverse effects on gut microbes of snails than low Cd exposure. Furthermore, pathways in cancer were also enriched in the H14 treatment. The results above partially explain our hypothesis above that *C. cathayensis* has a capacity to acclimate to low Cd stress.

It is also worth noting that pathways associated with xenobiotic and organic compound biodegradation and metabolism, including chloroalkane and chloroalkene degradation, benzoate degradation, fluorobenzoate degradation, styrene degradation, limonene and pinene degradation, geraniol degradation, were significantly inhibited in the H14 treatment in the present study, when compared to in the L14 treatment. Chloroalkane, chloroalkene, benzoate, fluorobenzoate and styrene are xenobiotics found in the environment (Vera et al., 2022). However, the pathways associated with the degradation of the xenobiotics were down-regulated in the H14 treatment, which suggested that the capacity of elimination of the compounds decreased following exposure to high Cd doses (Gu et al., 2017; Vera et al., 2022). Limonene and pinene are considered anti-inflammatory molecules; the down-regulation of the limonene and pinene degradation pathway in the H14 treatment could have increased the levels of limonene and pinene, which could have antagonized the inflammatory response caused by Cd stress (Han et al., 2021). Geraniol is another carbon and energy source for some *Pseudomonas* species (Vandenbergh and Wright, 1983; Zhu et al., 2020). The decline in the geraniol degradation pathway in the present study could be attributed to the decreased contents of the genus *Pseudomonas*. Overall, according to the results of the present study, Cd exposure disrupts gut microbial community structure and their potential functions, and could in turn, adversely influence *C. cathayensis* health.

Conclusion

Our results revealed that Cd exposure could significantly alter the structure and function of intestinal microbial communities, which may in turn influence *C. cathayensis* gut homeostasis and health. To the best of our knowledge, this is the first study to explore the effects of Cd exposure on the intestinal microbiota of *C. cathayensis*. The results obtained in

this study provide insights into the mechanisms associated with the response of the intestinal microbiota of *C. cathayensis* to Cd pollution. However, obtaining the 16S rRNA gene sequences through the Illumina HiSeq platform has limitations. In the present study, we did not isolate and identify the putatively pathogenic and putatively beneficial bacteria, which warrants further research.

Data availability statement

The datasets presented in this study can be found in online repositories. The names of the repository/repositories and accession number(s) can be found below: https://www.ncbi.nlm.nih.gov/, PRJNA837347.

Ethics statement

The animal study was reviewed and approved by Animal Ethics Committee of Guangxi Normal University.

Author contributions

Z-XX, J-XF, and J-YJ conceived and designed the study. Z-XX, J-YJ, and W-HL contributed reagents and materials. J-YJ and Y-YW analyzed the data. Y-YW and C-XC performed the gut extraction. Y-YW, C-XC, and Q-QY cultured the snails. J-YJ and W-HL wrote the manuscript. All authors read and approved the final manuscript.

Funding

This study was supported by the Guangxi BaGui Scholars Program Foundation (2019A50) and the National Key R&D Program of China (2021YFD1100106).

Acknowledgments

We thank all participants in this work, including staff at the Key Laboratory of Ecology of Rare and Endangered Species and Environmental Protection (Guangxi Normal University), Ministry of Education, and staff at Guangxi Key Laboratory of Veterinary Biotechnology, Guangxi Veterinary Research Institute.

Conflict of interest

The authors declare that the research was conducted in the absence of any commercial or financial relationships that could be construed as a potential conflict of interest.

Publisher's note

All claims expressed in this article are solely those of the authors and do not necessarily represent those of their affiliated organizations, or those of the publisher, the editors and the reviewers. Any product that may be evaluated in this article, or claim that may be made by its manufacturer, is not guaranteed or endorsed by the publisher.

Supplementary material

The Supplementary Material for this article can be found online at: https://www.frontiersin.org/articles/10.3389/fmicb.2022.984757/full#supplementary-material

SUPPLEMENTARY FIGURE S1
Rarefaction curves for all the analyzed samples. Different samples are represented by curves of different colors.

SUPPLEMENTARY FIGURE S2
Relative abundance of intestinal bacteria. **(a)** The relative abundance of phylum Bacteroidetes; **(b)** genus *Pseudomonas*; **(c)** genus *Acinetobacter*; **(d)** genus *Rhodobacter*; **(e)** genus *Cloacibacterium*; **(f)** and genus *Dechloromonas*. Asterisks (*) indicate p-values < 0.05.

References

Ali, M. M., Rahman, S., Islam, M. S., Rakib, M., Hossen, S., Rahman, M. Z., et al. (2022). Distribution of heavy metals in water and sediment of an urban river in a developing country: a probabilistic risk assessment. *Int. J. Sediment Res.* 37, 173–187.

Arun, K. B., Madhavan, A., Sindhu, R., Emmanual, S., Binod, P., Pugazhendhi, A., et al. (2021). Probiotics and gut microbiome-prospects and challenges in remediating heavy metal toxicity. *J. Hazard. Mater.* 420:126676. doi: 10.1016/j.jhazmat.2021.126676

Bridges, K. N., Zhang, Y., Curran, T. E., Magnuson, J. T., Venables, B. J., Durrer, K. E., et al. (2018). Alterations to the intestinal microbiome and metabolome of *pimephales promelas* and *mus musculus* following exposure to dietary methylmercury. *Environ. Sci. Technol.* 52, 8774–8784. doi: 10.1021/acs.est.8b01150

Burger, J. (2008). Assessment and management of risk to wildlife from cadmium. *Sci. Total Environ.* 389, 37–45.

Callahan, B. J., McMurdie, P. J., Rosen, M. J., Han, A. W., Johnson, A. J. A., and Holmes, S. P. (2016). DADA2: High-resolution sample inference from Illumina amplicon data. *Nat. Methods* 13, 581–583.

Chang, X. L., Li, H., Feng, J. C., Chen, Y. Y., Nie, G. X., and Zhang, J. X. (2019). Effects of cadmium exposure on the composition and diversity of the intestinal

microbial community of common carp (*cyprinus carpio* L.). *Ecotoxicol. Environ. Saf.* 171, 92–98. doi: 10.1016/j.ecoenv.2018.12.066

Che, J. G., Bai, Y. D., Li, X., Ye, J., Liao, H. P., Cui, P., et al. (2021). Linking microbial community structure with molecular composition of dissolved organic matter during an industrial-scale composting. *J. Hazard. Mater.* 405:124281. doi: 10.1016/j.jhazmat.2020.124281

Cheaib, B., Seghouani, H., Ijaz, U. Z., and Derome, N. (2020). Community recovery dynamics in yellow perch microbiome after gradual and constant metallic perturbations. *Microbiome* 8:14. doi: 10.1186/s40168-020-0789-0

Chen, G., Pang, M. X., Yu, X. M., Wang, J. R., and Tong, J. G. (2021). Transcriptome sequencing provides insights into the mechanism of hypoxia adaption in bighead carp (*Hypophthalmichthys nobilis*). *Comp. Biochem. Physiol. D Genom. Proteom.* 40:100891. doi: 10.1016/j.cbd.2021.100891

Chen, Y. F., Shi, Q. G., Qu, J. Y., He, M. X., and Liu, Q. (2022). A pollution risk assessment and source analysis of heavy metals in sediments: A case study of Lake Gehu, China. *Chin. J. Anal. Chem.* 50:100077.

Cui, Y. D., Wang, B. Q., Zhao, Y. J., Bond, N. R., and Wang, H. Z. (2022). Recovery time of macroinvertebrate community from Cd pollution in Longjiang River, Guangxi, China. *J. Oceanol. Limnol.* 40, 183–194.

Dehler, C. E., Secombes, C. J., and Martin, S. A. M. (2017). Environmental and physiological factors shape the gut microbiome of Atlantic salmon (*Salmo salar* L.). *Aquaculture* 467, 149–157.

Diwan, A. D., Harke, S. N., Gopalkrishna, and Panche, A. N. (2021). Aquaculture industry prospective from gut microbiome of fish and shellfish: An overview. *J. Anim. Physiol. Anim. Nutr.* 106, 441–469. doi: 10.1111/jpn.13619

Duan, H., Yu, L. L., Tian, F. W., Zhai, Q. X., Fan, L. P., and Chen, W. (2020). Gut microbiota: A target for heavy metal toxicity and a probiotic protective strategy. *Sci. Total Environ.* 742:140429. doi: 10.1016/j.scitotenv.2020.140429

Gu, X. Z., Fu, H. T., Sun, S. M., Qiao, H., Zhang, W. Y., Jiang, S. F., et al. (2017). Dietary cholesterol-induced transcriptome differences in the intestine, hepatopancreas, and muscle of Oriental River prawn *Macrobrachium nipponense*. *Comp. Biochem. Physiol. D Genom. Proteom.* 23, 39–48. doi: 10.1016/j.cbd.2017.06.001

Guo, Y. S., Ma, Y., Zhang, Y. W., Zhou, L., Huang, S. L., Wen, Y., et al. (2017). Autophagy-related gene microarray and bioinformatics analysis for ischemic stroke detection. *Biochem. Biophys. Res. Commun.* 489, 48–55. doi: 10.1016/j.bbrc.2017.05.099

Han, Y. J., Kang, L. L., Liu, X. H., Zhang, Y. H., Chen, X., and Li, X. Y. (2021). Establishment and validation of a logistic regression model for prediction of septic shock severity in children. *Hereditas* 158:45. doi: 10.1186/s41065-021-00206-9

Hu, R., and Tang, Z. Y. (2012). Effect of cadmium and mercury on superoxidedismutase activity of the mudsnail (*Cipangopaludina cahayensis*). *J. Sichuan Normal Univ.* 35, 690–693.

Kalpit, A. V., Singh, C., and Modi, V. V. (1988). Degradation of 2-fluorobenzoate by a pseudomonad. *Curr. Microbiol.* 17, 249–254.

Liu, H. S., Li, X., Lei, H. J., Li, D., Chen, H. X., Schlenk, D., et al. (2021). Dietary seleno-L-methionine alters the microbial communities and causes damage in the gastrointestinal tract of japanese medaka *Oryzias latipes*. *Environ. Sci. Technol.* 55, 16515–16525. doi: 10.1021/acs.est.1c04533

Liu, F. P., Xu, X. F., Chao, L., Chen, K., Shao, A., Sun, D. Q., et al. (2021). Alteration of the gut microbiome in chronic kidney disease patients and its association with serum free immunoglobulin light chains. *Front. Immunol.* 12:609700. doi: 10.3389/fimmu.2021.609700

Liu, J., Pang, J. J., Tu, Z. C., Wang, H., Sha, X. M., Shao, Y. H., et al. (2019). The accumulation, histopathology, and intestinal microorganism effects of waterborne cadmium on *carassius auratus gibelio*. *Fish Physiol. Biochem.* 45, 231–243. doi: 10.1007/s10695-018-0557-2

Liu, Y. Y., Cheng, J. X., Xia, Y. Q., Li, X. H., Liu, Y., and Liu, P. F. (2022). Response mechanism of gut microbiome and metabolism of European seabass (*Dicentrarchus labrax*) to temperature stress. *Sci. Total Environ.* 813:151786. doi: 10.1016/j.scitotenv.2021.151786

Llewellyn, M. S., Boutin, S., Hoseinifar, S. H., and Derome, N. (2014). Teleost microbiomes: The state of the art in their characterization, manipulation and importance in aquaculture and fisheries. *Front. Microbiol.* 5:207. doi: 10.3389/fmicb.2014.00207

Lu, H. F., Du, L. N., Li, Z. Q., Chen, X. Y., and Yang, J. X. (2014). Morphological analysis of the Chinese *Cipangopaludina* species (*Gastropoda*; *Caenogastropoda*: *Viviparidae*). *Zool. Res.* 35, 510–527.

Lu, Y., Zheng, G. Y., Zhou, W. B., Wang, J. J., and Zhou, L. X. (2019). Bioleaching conditioning increased the bioavailability of polycyclic aromatic hydrocarbons to promote their removal during co-composting of industrial and municipal sewage sludges. *Sci. Total Environ.* 665, 1073–1082. doi: 10.1016/j.scitotenv.2019.02.174

Lukiw, W. J. (2016). *Bacteroides* fragilis lipopolysaccharide and inflammatory signaling in alzheimer's disease. *Front. Microbiol.* 7:1544. 01544 doi: 10.3389/fmicb.2016

Luo, H., Chen, L. T., Jing, T. S., Sun, W. B., Li, Z., Zhou, M. R., et al. (2021). Muscle nutrition analysis of four snail species. *J. Fish. China 2021*. (in press). https://kns.cnki.net/kcms/ detail/31.1283.S.20211018.1713.002.html.

Ministry of Ecology and Environment of the People's Republic of China (2014). *National soil pollution survey communique*. Accessed online at: https://www.mee.gov.cn/gkml/sthjbgw/qt/201404/W020140417558995804588.pdf

Nouha, K., Kumar, R. S., and Tyagi, R. D. (2016). Heavy metals removal from wastewater using extracellular polymeric substances produced by cloacibacterium normanense in wastewater sludge supplemented with crude glycerol and study of extracellular polymeric substances extraction by different methods. *Bioresour. Technol.* 212, 120–129. doi: 10.1016/j.biortech.2016.04.021

Paul, J. S., and Small, B. C. (2019). Exposure to environmentally relevant cadmium concentrations negatively impacts early life stages of channel catfish (*Ictalurus punctatus*). *Comp. Biochem. Physiol. C Toxicol. Pharmacol.* 216, 43–51. doi: 10.1016/j.cbpc.2018.11.004

Qiu, Y., Yin, Y. H., Ruan, Z. Q., Gao, Y., Bian, C., Chen, J. M., et al. (2020). Comprehensive transcriptional changes in the liver of kanglang white minnow (*anabarilius grahami*) in response to the infection of parasite *ichthyophthirius multifiliis*. *Animals* 10:681. doi: 10.3390/ani10040681

Serrano-Puebla, A., and Boya, P. (2015). Lysosomal membrane permeabilization in cell death: New evidence and implications for health and disease. *Ann. N.Y.Acad. Sci.* 1371, 30–44. doi: 10.1111/nyas.12966

She, R., Li, T. T., Luo, D., Li, J. B., Yin, L. Y., Li, H., et al. (2017). Changes in the Intestinal Microbiota of Gibel Carp (*Carassius gibelio*) Associated with *Cyprinid herpesvirus* 2 (CyHV-2) Infection. *Curr. Microbiol.* 74, 1130–1136. doi: 10.1007/s00284-017-1294-y

Song, B., Wang, F. P., Zhou, L., Wu, Y., Pang, R., and Chen, T. B. (2019). Cd Content characteristics and ecological risk assessment of paddy soil in high cadmium anomaly area of Guangxi. *Environ. Sci.* 40, 2443–2452. doi: 10.13227/j.hjkx.201806202

Talwar, C., Nagar, S., Lal, R., and Negi, R. K. (2018). Fish gut microbiome: Current approaches and future perspectives. *Indian J. Microbiol.* 58, 397–414. doi: 10.1007/s12088-018-0760-y

Tran, N. T., Zhang, J., Xiong, F., Wang, G. T., Li, W. X., and Wu, X. G. (2018). Altered gut microbiota associated with intestinal disease in grass carp (*ctenopharyngodon idellus*). *World J. Microb. Biotechnol.* 34:71. doi: 10.1007/s11274-018-2447-2

Vandenbergh, P. A., and Wright, A. M. (1983). Plasmid involvement in acyclic isoprenoid metabolism by *Preudomonas putida*. *Appl. Environ. Microbiol.* 45, 1953–1955. doi: 10.1128/aem.45.6.1953-1955.1983

Vera, A., Wilson, F. P., and Cupples, A. M. (2022). Predicted functional genes for the biodegradation of xenobiotics in groundwater and sediment at two contaminated naval sites. *Appl. Microbiol. Biotechnol.* 106, 835–853. doi: 10.1007/s00253-021-11756-3

Wang, C., Liu, J., Huang, Y., and Zhang, X. (2016). In vitro polysaccharide extraction from *cipangopaludina cathayensis* and its pharmacological potential. *J. Environ. Biol.* 37, 1069–1072.

Wang, N., Jiang, M., Zhang, P. J., Shu, H., Li, Y. R., Guo, Z. Y., et al. (2020a). Amelioration of Cd-induced bioaccumulation, oxidative stress and intestinal microbiota by *bacillus cereus* in *carassius auratus gibelio*. *Chemosphere* 245:125613. doi: 10.1016/j.chemosphere.2019.125613

Wang, N., Guo, Z. Y., Zhang, Y. L., Zhang, P. J., Liu, J., Cheng, Y., et al. (2020b). Effect on intestinal microbiota, bioaccumulation, and oxidative stress of *carassius auratus gibelio* under waterborne cadmium exposure. *Fish Physiol. Biochem.* 46, 2299–2399. doi: 10.1007/s10695-020-00870-0

Wang, X. H., Hu, M. H., Gu, H. H., Zhang, L. B., Shang, Y. Y., Wang, T., et al. (2020c). Short-term exposure to norfloxacin induces oxidative stress, neurotoxicity and microbiota alteration in juvenile large yellow croaker *Pseudosciaena crocea*. *Environ. Pollut.* 267:115397. doi: 10.1016/j.envpol.2020.115397

Wang, P., Chen, H. P., Kopittke, P. M., and Zhao, F. J. (2019). Cadmium contamination in agricultural soils of China and the impact on food safety. *Environ. Pollut.* 249, 1038–1048.

Wang, A. R., Ran, C., Wang, Y. B., Zhang, Z., Ding, Q. W., Yang, Y. L., et al. (2019). Use of probiotics in aquaculture of china-a review of the past decade. *Fish Shellfish Immunol.* 86, 734–755. doi: 10.1016/j.fsi.2018.12.026

Wang, R., Xia, W., Eggleton, M. A., Qu, X., Liu, H., Xin, W., et al. (2022). Spatial and temporal patterns of heavy metals and potential human impacts in central yangtze lakes, China. *Sci. Total Environ.* 820:153368. doi: 10.1016/j.scitotenv.2022.153368

Wen, Y. B., Li, W., Yang, Z. F., Zhuo, X. X., Guan, D. X., Song, Y. X., et al. (2020). Evaluation of various approaches to predict cadmium bioavailability to rice grown in soils with high geochemical background in the karst region, Southwestern China. *Environ. Pollut.* 258:113645. doi: 10.1016/j.envpol.2019.113645

Wu, S. G., Tian, J. Y., Gatesoupe, F. J., Li, W. X., Zou, H., Yang, B. J., et al. (2013). Intestinal microbiota of gibel carp (*Carassius auratus gibelio*) and its origin as revealed by 454 pyrosequencing. *World J. Microbiol. Biotechnol.* 29, 1585–1595. doi: 10.1007/s11274-013-1322-4

Xu, J., Zeng, X. H., Jiang, N., Zhou, Y., and Zeng, L. B. (2015). Pseudomonas alcaligenes infection and mortality in cultured Chinese sturgeon, *Acipenser sinensis*. *Aquaculture* 446, 37–41.

Xu, X., Nie, S., Ding, H., and Hou, F. (2018). Environmental pollution and kidney diseases. *Nat. Rev. Nephrol.* 14, 313–324.

Ya, J., Ju, Z. Q., Wang, H. Y., and Zhao, H. F. (2019). Exposure to cadmium induced gut histopathological damages and microbiota alterations of Chinese toad (*Bufo gargarizans*) larvae. *Ecotox. Environ. Saf.* 180, 449–456. doi: 10.1016/j.ecoenv.2019.05.038

Yang, Q., Yang, Z. F., Zhang, Q., Liu, X., Zhuo, X. X., Wu, T. S., et al. (2021). Ecological risk assessment of Cd and other heavy metals in soil-rice system in the karst areas with high geochemical background of Guangxi. China. *Sci. China Earth Sci.* 64, 1126–1139.

Ye, Q., Feng, Y. Y., Wang, Z. L., Zhou, A. G., Xie, S. L., Fan, L. F., et al. (2019). Effects of dietary *gelsemium elegans* alkaloids on intestinal morphology, antioxidant status, immune responses and microbiota of *megalobrama amblycephala*. *Fish Shellfish Immunol.* 94, 464–478. doi: 10.1016/j.fsi.2019.09.048

Zhai, Q. X., Yu, L. L., Li, T. Q., Zhu, J. M., Zhang, C. C., Zhao, J. X., et al. (2016). Effect of dietary probiotic supplementation on intestinal microbiota and physiological conditions of Nile tilapia (‘) under waterborne cadmium exposure. *Antonie van Leeuwenhoek* 110, 501–513. doi: 10.1007/s10482-016-0819-x

Zhang, L. Q., Fan, J. J., Nguyen, H. N., Li, S. G., and Rodrigues, D. F. (2019). Effect of cadmium on the performance of partial nitrification using sequencing batch reactor. *Chemosphere* 222, 913–922.

Zhang, Y., Li, Z. Y., Kholodkevich, S., Sharov, A., Chen, C., Feng, Y. J., et al. (2020). Effects of cadmium on intestinal histology and microbiota in freshwater crayfish (*procambarus clarkii*). *Chemosphere* 242:125105. doi: 10.1016/j.chemosphere.2019.125105

Zhang, K. K., Zheng, X. F., He, Z. L., Yang, T., Shu, L. F., Xiao, F. S., et al. (2020). Fish growth enhances microbial sulfur cycling in aquaculture pond sediments. *Microb. Biotechnol.* 13, 1597–1610. doi: 10.1111/1751-7915.13622

Zhao, F. J., Ma, Y., Zhu, Y. G., Tang, Z., and McGrath, S. P. (2015). Soil contamination in China: Current status and mitigation strategies. *Environ. Sci. Technol.* 49, 750–759.

Zhao, T., Xiong, J. Q., Chen, W., Xu, A. H., Zhu, D., and Liu, J. T. (2021). Purification and characterization of a novel fibrinolytic enzyme from *cipangopaludina cahayensis*. *Iran. J. Biotechnol.* 19, 121–127. doi: 10.30498/IJB.2021.2805

Zhao, X., Yao, L. A., Ma, Q. L., Zhou, G., and Xu, Z. C. (2018). Distribution and ecological risk assessment of cadmium in water and sediment in Longjiang River, China: Implication on water quality management after pollution accident. *Chemosphere* 194:107. doi: 10.1016/j.chemosphere.2017.11.127

Zhou, K. Q., Qin, J. Q., Pang, H. F., Chen, Z., Huang, Y., Li, W. H., et al. (2022). Comparison of the composition and function of gut microbes between adult and juvenile *Cipangopaludina chinensis* in the rice snail system. *PeerJ* 10:e13042. doi: 10.7717/peerj.13042

Zhou, Z. H., Wu, H. W., Li, D. H., Zeng, W. L., Huang, J. L., and Wu, Z. J. (2022). Comparison of gut microbiome in the Chinese mudsnail (*Cipangopaludina chinensis*) and the invasive golden apple snail (*Pomacea canaliculata*). *PeerJ* 10:e13245. doi: 10.7717/peerj.13245

Zhou, Y. Y., and Luo, Z. M. (2018). Effects of cadmium on antioxidant enzymes activities and lipid peroxidation in mudsnail (*Cipangopaludina cathayensis*). *Sci. Technol. Food Ind.* 39, 43–47.

Zhu, C. S., Miller, M., Lusskin, N., Pinto, B. B., Maccario, L., Haggblom, M., et al. (2020). Snow microbiome functional analyses reveal novel aspects of microbial metabolism of complex organic compounds. *Microbiol. Open* 9:e1100. doi: 10.1002/mbo3.1100

frontiers | Frontiers in Microbiology

TYPE Original Research
PUBLISHED 22 August 2022
DOI 10.3389/fmicb.2022.895533

OPEN ACCESS

EDITED BY
Juan Sun,
Qingdao Agricultural University, China

REVIEWED BY
Chao Yang,
Qingdao Agricultural University, China
Liang Chen,
Institute of Microbiology (CAS), China

*CORRESPONDENCE
Qi Zhang
zhangqi@lzu.edu.cn
Huyuan Feng
fenghy@lzu.edu.cn

SPECIALTY SECTION
This article was submitted to Microbial Symbioses, a section of the journal Frontiers in Microbiology

RECEIVED 14 March 2022
ACCEPTED 29 July 2022
PUBLISHED 22 August 2022

CITATION
Meng Y, Zhang Q, Shi G, Liu Y, Du G and Feng H (2022) Can nitrogen supersede host identity in shaping the community composition of foliar endophytic fungi in an alpine meadow ecosystem?
Front. Microbiol. 13:895533.
doi: 10.3389/fmicb.2022.895533

Can nitrogen supersede host identity in shaping the community composition of foliar endophytic fungi in an alpine meadow ecosystem?

Yiming Meng[1], Qi Zhang[1]*, Guoxi Shi[2], Yongjun Liu[1,3,4], Guozhen Du[5,6] and Huyuan Feng[1,3]*

[1]Ministry of Education Key Laboratory of Cell Activities and Stress Adaptations, School of Life Sciences, Lanzhou University, Lanzhou, China, [2]College of Bioengineering and Biotechnology, Tianshui Normal University, Tianshui, China, [3]Center for Grassland Microbiome, Lanzhou University, Lanzhou, China, [4]State Key Laboratory of Grassland Agro-Ecosystems, Lanzhou University, Lanzhou, China, [5]School of Life Sciences, Lanzhou University, Lanzhou, China, [6]Key Laboratory of Arid and Grassland Ecology of Ministry of Education, School of Life Sciences, Lanzhou University, Lanzhou, China

The availability of limiting nutrients plays a crucial role in shaping communities of endophytes. Moreover, whether fungal endophytes are host-specific remains controversial. We hypothesized that in a harsh and nitrogen (N)-deficient area, diversity and community composition of foliar endophytic fungi (FEFs) varied substantially among plots with experimentally elevated levels of macronutrients, and thus, N availability, instead of host species identity, would have a greater influence in structuring fungal communities at different scales. We also expected an important subset of taxa shared among numerous host species and N gradients to form a community-wide core microbiome. We measured the leaf functional traits and community structures of FEFs of three commonly seen species in an alpine meadow nested with a long-term N fertilization experiment. We found that host plant identity was a powerful factor driving the endophytic fungal community in leaves, even in habitats where productivity was strongly limited by nitrogen ($p < 0.001$). We also found that within the same host, nitrogen was an important driving force for the composition of the endophytic fungi community ($p < 0.05$). In addition, the leaf carbon content was the most important functional trait that limited the diversity of endophytic fungi ($p < 0.001$). Finally, we documented a distinct core microbiome shared among our three focal species and N gradients.

KEYWORDS

foliar fungal endophytes, nitrogen deposition, Qinghai–Tibet Plateau, microbial community, host-specificity

Introduction

Ecosystems worldwide have been undergoing severe nitrogen (N) deposition over the last few decades (Cardinale et al., 2011; IPCC, 2014). In terrestrial ecosystems, N availability is supposed to be a primary limitation to plant growth (Vitousek and Howarth, 1991). Previous research has shown that N deposition, simulated by N fertilization experiments, increases plant growth and crop yields. However, N losses from industry and agriculture alter the plant community structure and reduce terrestrial biodiversity (Stevens et al., 2004; Bobbink et al., 2010). N deposition also results in an increase in air pollution (EPA, 2013) and soil acidification (Sullivan et al., 2013) and is hence considered a major threat to ecosystem functioning and services. While N deposition has declined in some parts of the world due to legislation, it is estimated that soil communities, ecosystem productivity, and nutrient cycling continue to be affected by historical soil nitrogen loads (Gilliam et al., 2019; Crawford et al., 2020).

Although the effect of atmospheric N deposition on plant ecology has been widely studied (Ellison and Gotelli, 2002; Scarpitta et al., 2017; Vallicrosa et al., 2022), our understanding of how N shapes the microbial community, particularly the fungal community, inside plants remains elusive. Plants do not exist as axenic organisms but are closely associated with large quantities of microorganisms. Leaves comprise one of the world's largest terrestrial habitats and provide a key location for interactions between plants and their associated microbiomes, yet we know relatively little about this association (Vacher et al., 2016). Foliar endophytic fungi (FEFs) spend all or part of their lifetime colonizing plant leaves and may increase, decrease, or show no apparent impact on host performance, as reviewed by Rodriguez et al. (2009) and Hardoim et al. (2015). Such mutualistic parasitic symbiosis depends on the host–endophyte genotype–genotype interaction, environmental conditions, and the state of the host's health (Stevens et al., 2004). However, the mechanism of this complex interactive network remains unclear. Moreover, although existing research indicates that FEFs mediate plant N uptake (Buckley et al., 2019; Christian et al., 2019), how N input affects the community structure of the FEF remains relatively unexplored. FEFs represent a ubiquitous and highly diversified fungal guild (Rodriguez et al., 2009) and a substantial and mostly under-explored microbiota critical for ecosystem functioning (Hardoim et al., 2015). Despite the ecological importance, the factors that shape FEF communities, either biotic or abiotic, are largely unknown.

Plant species shape biotic and abiotic environments in which the fungi live, and hence, different FEF species might be a function of host plant phylogeny (Apigo and Oono, 2018). However, the degree that FEFs are host-specific is controversial. Some endophytes were unique to divergent host clades in boreal and arctic sites (Higgins et al., 2007; Zhang and Yao, 2015), and they also showed a degree of host specificity in rainforest trees (Vincent et al., 2016), tropical trees (Arnold and Lutzoni, 2007), and grasses (Higgins et al., 2011, 2014). If high specificity is prevalent, this may have profound implications for plant–fungus coevolution, as plants can vary dramatically in susceptibility to their parasitic fungal companions, and plants prefer harboring mutualistic fungal companions (Clay and Schardl, 2002; Saikkonen et al., 2004; Chen et al., 2019; Razali et al., 2019). Conversely, it was also found that distantly related pine species hosted the same FEF species, indicating host species did not influence the microbial genetic structure (Oono et al., 2014). This might be explained by the fact that FEFs are often horizontally transmitted (Arnold et al., 2009; Rodriguez et al., 2009); thus, some populations may be panmictic, reflecting generalist associations with multiple host species (Dunham et al., 2013). Altogether, much evidence needs to be accumulated to understand the host specificity of FEF communities. Understanding the host specificity of FEFs will also provide critical insights into plant performance, competitive abilities among species, and the FEF dispersal strategy.

N input increases plant biomass and enhances plant growth. Changes in plant growth may further lead to variations in the plant-associated fungal community structure (Seghers et al., 2004; Larkin et al., 2012; Suryanarayanan and Shaanker, 2021). Furthermore, over different growth stages of the host plant, the plant endophytic fungal community is likely subject to dynamic changes over time (Singha et al., 2021; Sosso et al., 2021; Zheng et al., 2021). Several studies have provided some insights into how FEFs respond to high N supply. An inoculation experiment showed that endophyte (*Neotyphodium lolii*) concentration was reduced by 40% under high N supply in perennial ryegrass (*Lolium perenne*) cultivars (Rasmussen et al., 2007). Data from several sources also identified that FEFs enhanced plant N uptake and growth based on inoculation experiments (Newman et al., 2003; Knoth et al., 2013; Christian et al., 2019). However, all these conclusions were drawn based on greenhouse-based experiments with inoculation of specific species of endophytic fungi. How macronutrients, particularly N, regulate endophytic fungal communities in natural systems remains controversial. For example, Larkin et al. (2012) reported that nitrate in leaves was correlated with differences in the endophyte community, while in another study, Huang et al. (2016) found no correlation between foliar N and endophytic abundance or diversity in one host species, but a negative correlation with endophytic abundance in another species was found.

Independent of whether FEFs are highly host-specific, there still may be a subset of taxa that are shared among co-occurring host species. For example, Zhang and Yao (2015) found that 7.6% of total FEF operational taxonomic units (OTUs) were shared by all four plant species in the study of vascular plants in the high arctic zone. Thus, a very small group of fungi occurred repeatedly among plant species. Some subsets of fungi that comprise the shared OTUs (or, "core microbiome", see the explanation from Vandenkoornhuyse et al., 2015 and

Shade and Handelsman, 2012) may have traits that enhance their ability to colonize the interior of a phylogenetically diverse group of plant species, indicating their ecological competitiveness and importance. However, such investigations are very few, therefore, we cannot draw general conclusions on commonly shared FEF OTUs among plant species in different habitats.

The Qinghai–Tibet Plateau (QTP) is one of the hot spots for research, yet little is known about the endophytic fungal community and its response to global change in this region. Learning endophytic fungal host specificity and simulating the effects of N deposition on endophytic fungal communities will help us better identify the ecological and evolutionary constraints that limit symbiont distribution. To fill this knowledge gap, we established the following three hypotheses: (1) In alpine meadows on the QTP, FEFs vary substantially among different host plant species, (2) a subset of microbial taxa will be shared among all host plant species, and (3) FEF communities vary substantially among plots with experimentally elevated levels of N under N-deficient conditions, and nutrient availability would have a greater influence in structuring fungal communities than host identity. We assume that if phylogenetically conserved traits serve as biological filters for endophyte colonization and establishment, the endophytic fungal community may vary considerably in species with different morphology, structure, and tissue texture, as suggested by Zhang and Yao (2015). A study in southern Chile, on the other hand, found that the homogeneity of endophytic fungal communities might be due to the filtering effect of physical and chemical traits of leaves independent of the evolutionary history of the host (Gonzalez-Teuber et al., 2020). Therefore, we hypothesize that in alpine meadows on the QTP, where productivity is strongly limited by N availability (Xu et al., 2015), N will transcend host identity in shaping the community composition of FEFs. To address these hypotheses, we used high-throughput sequencing to characterize the FEF community composition of three grass species in 4-year N addition treatments in an alpine meadow ecosystem on the QTP. To our knowledge, this is the first study to explore the responses of FEF communities to N fertilization in an alpine meadow ecosystem. This research provides better understanding of the response of plant-associated fungi to changing global scenarios.

Materials and methods

Study site and sample collection

This study was conducted in 2014 at the Research Station of Alpine Meadow and Wetland Ecosystems of Lanzhou University, Maqu County, China. The study site is located in the eastern QTP (33°40′N, 101°51′E, altitude 3,500 m a.s.l, Supplementary Figure S1), with an average precipitation of 620 mm (mostly occurs in summer). The mean annual temperature is about 1.2°C (ranging from −10°C in winter to 11.7°C in summer), and the frost-free season lasts about 95 days (Wu et al., 2010). The mean aboveground primary productivity is 280–400 g m^{-2} (dry weight), and the species richness is, on average, 20–35 per 0.25 m^2 (Yang et al., 2011). The vegetation of the meadow is mainly dominated by *Kobresia capillifolia* (Cyperaceae), *Elymus nutans* Griseb (Poaceae), and *Anemone rivularis* Buch.-Ham. (Ranunculaceae). The soil type in the study area is Mattic Cryic Cambisols (Gong and Li, 2001). Total N deposition in this region is estimated to range from 14.26 to 18.65 kg ha^{-1} yr^{-1} (Lu and Tian, 2007).

The experimental site was used for grazing in the past and was fenced in 2011 to prevent grazing by large animals, such as yak and sheep. To understand how plants and related microorganisms respond to N addition in the field, NH_4NO_3 fertilizer was applied annually at the beginning of the growing season (usually in May) since then. The field experiment was a complete randomized block design, with 24 plots (20 × 10 m each, 1-m buffer strips) arranged in a regular 6 × 4 matrix. N gradients were generated with 0, 5, 10, and 15 g N (NH_4NO_3) m^{-2} yr^{-1} referring to N0 (control), N5, N10, and N15 treatments, and each treatment had six replicates (Supplementary Figure S1). After 4 years of N addition, available soil N concentration was increased significantly ($F = 11.1$, $p < 0.001$, Supplementary Table S1).

Samples were collected on 25 July 2014. We targeted three commonly observed plant species, namely, *A. rivularis*, *E. nutans*, and *Thermopsis lanceolata*. In each plot, six individuals of each species were randomly selected. For individuals of *A. rivularis* and *T. lanceolata*, five random mature leaves devoid of visible pathogen damage were collected from each individual. For individuals of *E. nutans*, the second leaf from the bottom of each individual was collected. The leaves collected from the same species in a plot were mixed as a sample. In total, we collected 71 samples (3 species × 24 plots, *T. lanceolata* was not found in one of the N15 plots). The samples were placed in zip-lock plastic bags and stored in coolers equipped with ice packs, transferred to the laboratory in 18 h, and stored at 4°C.

Sample preparation, DNA extraction, and Illumina sequencing

The leaves were thoroughly washed in tap water, patted dry, and divided into two subsamples: One subsample was sterilized for DNA extraction within 36 h of collection, and the other was stored at −20°C until the determination of the physical and chemical properties of the leaves. Before DNA extraction, the leaves were immersed in 75% ethanol for 1 min, in 1% sodium hypochlorite for 2 min, and in 75% ethanol for 30 s to eliminate microorganisms on leaf surfaces. The

surface-sterilized tissues were then rinsed with sterile water for 30 s three times and then patted dry with a sterile filter paper. Before sample grinding, ~1 ml of the final rinse water of each sample was plated on potato dextrose agar (PDA) and cultured in the dark to validate the effect of surface sterilization. The leaves were ground with liquid nitrogen using mortars and pestles in a sterile room. The mortars and pestles were sterilized before use and re-sterilized between samples to avoid cross-contamination.

Total genomic DNA was extracted using 100 mg leaf tissue powder from each sample using a Plant DNA Extraction Kit following the manufacturer's instructions (Tiangen Biotech, Beijing, China). The extracted DNA samples were frozen and shipped to Majorbio Bio-Pharm Technology Co., Ltd., Shanghai, China. Fungal diversity was determined by sequencing the internal transcribed spacer (ITS) region with primers ITS1F (CTTGGTCATTTAGAGGAAGTAA)/ITS2 (GCTGCGTTCTTCATCGATGC) (Gardes and Bruns, 1993) on an Illumina MiSeq platform (2 × 250 PE).

Sequence processing

Sequences were pre-processed using the Trimmomatic tool (v 0.36, Bolger et al., 2014). 3′ or 5′ ends with a Phred quality score lower than 20 were trimmed, and sequences of <200 bp in length and with an average quality score of <20 on a window of 50 bases were discarded. The remaining sequences were imported into QIIME2 version 2019.10 for bioinformatics analyses (Bolyen et al., 2019). The qiime2-dada2 plugin was used for denoising, dereplication, merging paired-end reads, and removing chimeras (Callahan et al., 2016). Molecular singletons were removed from the downstream analysis to minimize the possibility of sequencing artifacts (Unterseher et al., 2011). Taxonomic assignments were determined using the qiime2-feature-classifier (Bokulich et al., 2018) classify-sklearn against species hypotheses (SH) of UNITE's database version 8.2 (Koljalg et al., 2020). Click or tap here to enter text. Trained with the Naive Bayes classifier with a confidence threshold of 97%. All representative sequencing data were submitted to the National Center for Biotechnology Information (NCBI) under accession numbers OM744714-OM745695.

Leaf trait collection

The leaf traits were measured using the second subsample stored at −20°C. This work was completed within 10 days of sample collection. We focused on nitrogen and carbon fractions. Total leaf carbon and nitrogen per tree were determined using a C/N elemental analyzer, Vario MAXCN (Elementar, Hessia, Germany). Low-molecular weight (LMW) carbohydrates (mostly glucose, fructose, and sucrose) and high-molecular weight (HMW) carbohydrates (mainly fructans) were extracted and quantified from aboveground tissues, as previously described (Hunt et al., 2005; Rasmussen et al., 2007). Total free amino acids were analyzed from the ethanol fraction used for carbohydrate extraction and were determined colorimetrically with ninhydrin, as described previously (Yemm et al., 1955). Soluble proteins were extracted using 0.1% mercaptoethanol in 100 mM potassium phosphate buffer. Extracts were centrifuged, and the resulting supernatant was analyzed according to Bradford (1976) with absorbance measured at 595 nm using bovine serum albumin (BSA) as a standard.

Statistical analyses

The averages and standard deviations of the tree traits and leaf chemicals in each plot were calculated. Diversity assessment used Fisher's alpha (a richness index) and Shannon-index (considering both richness and abundance). Analyses were combined with ANOVA of the multivariate generalized linear models and randomized species accumulation curves. The abundance-based Bray–Curtis similarity coefficient was used to examine the dissimilarity of community composition and turnover. The distinctiveness of leaf endophytic fungi in different hosts and under different N conditions, and independence of the interactions of hosts and N were tested using a permutational multivariate analysis of variance (PERMANOVA) using the distance metrics mentioned earlier. The beta diversity of FEFs was analyzed using non-metric multidimensional scaling (NMDS) by R 4.1.1 statistical software (R Core Team, 2019). In addition, the environmental variables were screened using bioenv, mantel, and *vif.cca* functions, and the selected environmental variables were fitted onto the NMDS ordination plot using the *envfit* function in the vegan package v2.5 (Oksanen et al., 2019). A Mantel test was used in the vegan package to identify the plant traits that significantly correlated with the FEF community composition. Pearson's correlation analyses were used to identify the plant traits that significantly correlated with the FEF diversity indices in R. To reflect the OTU composition similarity among different samples or host identities, we performed network analysis. Sample-level OTUs by occurrence frequency were first filtered. A correlation between the two samples was considered statistically robust if Spearman's correlation coefficient (ρ) was >0.4 and the *P*-value was <0.05. All the robust correlations identified from pairwise comparison of OTU abundance form a correlation network, where each node represents one sample and each edge stands for a strong and significant correlation between nodes. Network analyses used the R packages vegan, igraph (Csardi and Nepusz, 2006), and Hmisc (Harrell and Dupont, 2018). Network visualization was then conducted using the interactive platform Gephi (Bastian et al., 2009).

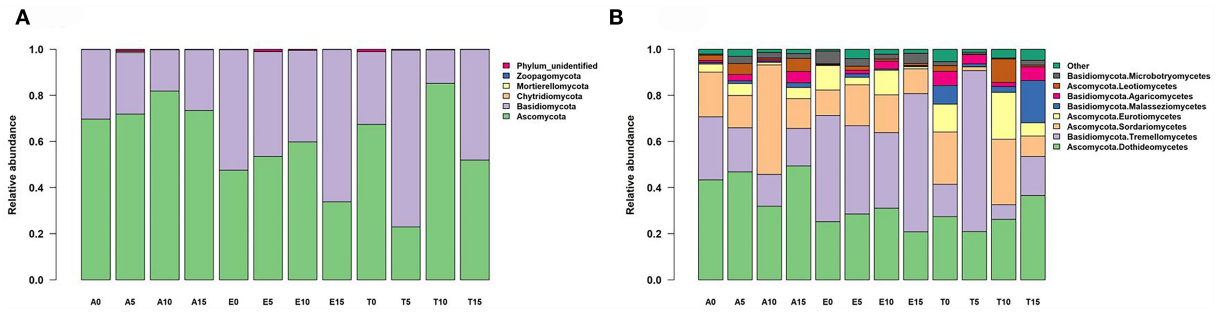

FIGURE 1
Taxonomic composition, **(A)** phylum level, and **(B)** class level of the fungal communities recovered from leaf interiors of three species along the nitrogen enrichment gradients in the study site. Bars show relative abundance of different taxonomic groups. The fungal endophyte classes with relative abundances of <0.1% were assigned to "Other". A, *Anemone rivularis*; E, *Elymus nutans*; T, *Thermopsis lanceolata*. 0 (control), 5, 10, and 15 referring to 0, 5, 10, and 15 g N (NH_4NO_3) m^{-2} yr^{-1} treatments, respectively.

All variables were transformed, where necessary. Prior to all analyses, data were rarefied to 1,944 sequence counts (minimum sequencing depth) using *rrarefy* function in the vegan package.

Results

Fungal OTU summary statistics

In total, 71 genomic DNA samples were sequenced, generating a total of 1,284,298 sequences after quality filtering. A total of 1,457 OTUs were clustered at the 97% sequence identity level. Of these, 475 (32.6%) OTUs were non-fungal taxa and were removed from the pool, the remaining 966,780 sequences; varied between 1,944 and 49,914 per sample; and clustered into 982 OTUs (Supplementary Figure S2a). Specifically, 337,614 sequences were observed in *A. rivularis*, 509,880 sequences were found in *E. nutans*, and 119,286 sequences were recovered in *T. lanceolata*, clustered into 505, 507, and 280 OTUs, respectively (Supplementary Table S2). The rarefaction curves of the observed OTU richness failed to approach the asymptote (Supplementary Figure S2b). This implies that a few rare fungal taxa were not observed, due to either insufficient sampling or sequencing depths. Nevertheless, valid comparisons can still be drawn at the species or at the plot level.

Endophytic fungal communities were strongly dominated by ascomycetes and basidiomycetes, together accounting for 99.4% of the sequences (Figure 1A; Supplementary Figure S3a; Supplementary Table S3). Members of those classified as "Basidiomycota" were present primarily in *E. nutans* and *T. lanceolata*, but ascomycetes are more prevalent in *A. rivularis* (Figure 1A). Early diverging lineages, including Chytridiomycota, Mortierellomycota, and Zoopagomycota (862 sequences, comprising 0.09% of the total sequences), were also observed (Supplementary Table S3). Unidentified OTUs (i.e., those classified as fungi but failed to be assigned to a phylum) comprised 0.51% of the total sequences (Supplementary Table S3). The most dominant class across our dataset, Dothideomycetes, comprised ∼35% of all assigned sequence reads, followed by Tremellomycetes (29.2%), Sordariomycetes (16.0%), and Eurotiomycetes [(6.1%), Figure 1B; Supplementary Figure S3b; Supplementary Table S4].

Fungal diversity patterns and community composition

Diversity measures displayed a significant difference among the three hosts. *A. rivularis* samples showed higher phylotype richness and Shannon diversity than *E. nutans* and *T. lanceolata* (Figure 2A). Statistical tests confirmed a significant effect of host types (GLM, $p < 0.01$, Table 1). N input showed a relatively weak effect on fungal diversity (Figure 2B; Table 1). However, at a smaller scale (i.e., within-host scale), N input decreased the fungal diversity of *A. rivularis* but increased that of *T. lanceolata* (Figure 3; Supplementary Table S5). Thus, fungal diversity can be maintained across the plot scale, except at the smaller, within-host scale under the background of N enrichment.

Composition of leaf mycobiome differed significantly among hosts (Figure 4A). However, the effects of fertilization led to overlapped fungal communities across the plot scale (Figure 4B). The dissimilarities of communities of FEFs among hosts, N gradients, and the interaction of the two factors were also confirmed by a multispecies generalized linear model calculation and a permutational multivariate analysis of variance (PERMANOVA) (Table 2). Community turnover in each host showed stronger clustering with N enrichment (Figure 4C; Supplementary Table S6).

10.3389/fmicb.2022.895533

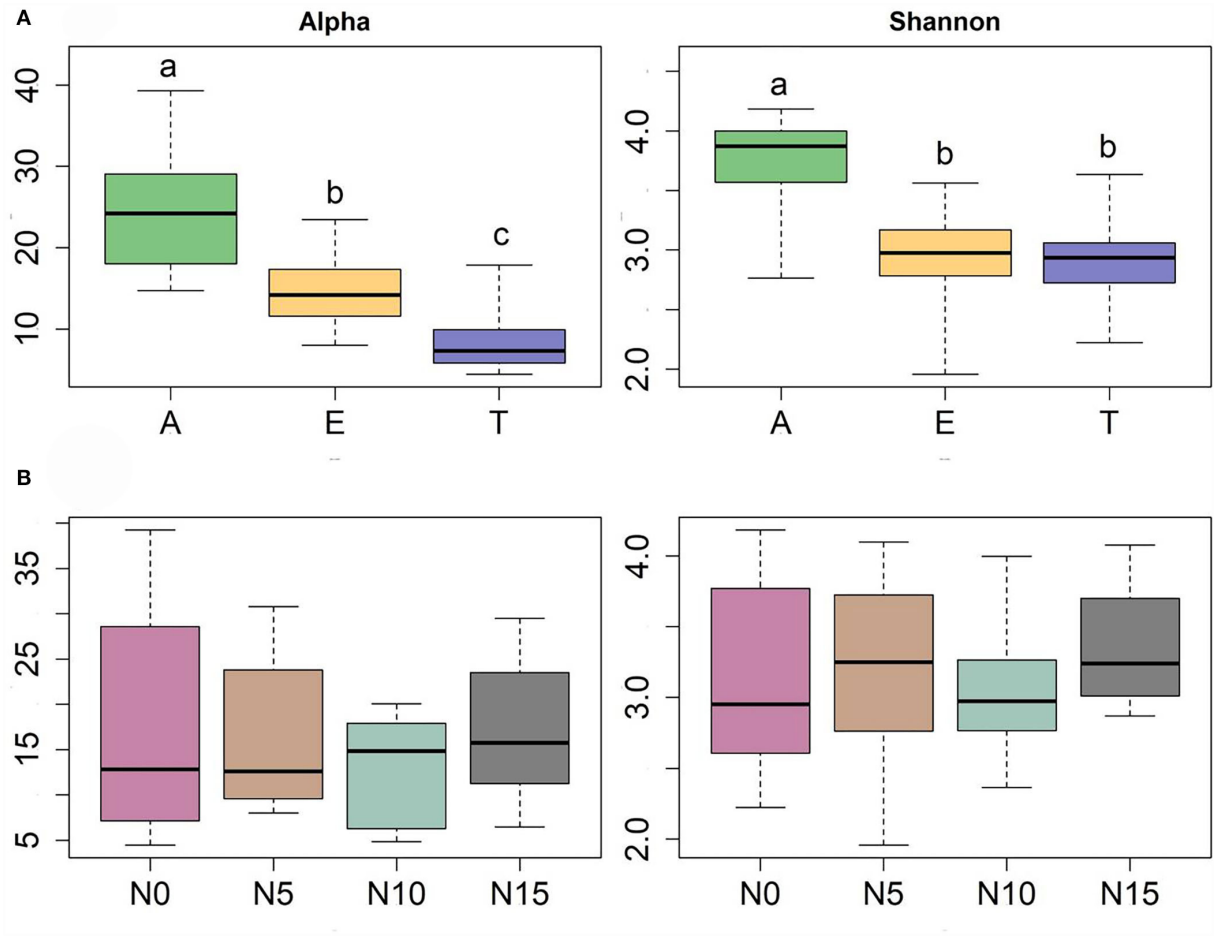

FIGURE 2
Diversity patterns of the entire fungal community of three species against host **(A)** and N gradients **(B)** based on linear models. Alpha is the number of observed species, and Shannon is the Shannon diversity index. The sequences were rarified to 1,944, $n = 71$. Significant differences of each variable are indicated by dissimilar letters above boxes. A, *Anemone rivularis*; E, *Elymus nutans*; T, *Thermopsis lanceolata*. N0, N5, N10, and N15 referring to 0, 5, 10, and 15 g N (NH_4NO_3) m^{-2} yr^{-1} treatments, respectively.

TABLE 1 Diversity statistics for the fungal endophytes in three hosts based on a multispecies generalized linear model.

	DF	Fisher's alpha			Shannon		
		Sum of squares	Dev	*p*	Sum of squares	Dev	*p*
Entire community							
Host	2	3,059.3	196.1	**0.001**	10.9	3.3	**0.001**
N input	3	190.4	12.7	**0.012**	1.2	0.4	0.399
Host × N input	6	562.7	30.9	**0.001**	1.2	0.4	0.864

Significance at 0.05 is highlighted in bold.

Plant functional trait variance along the N gradient

The effects of fertilization on plant measures varied among hosts. Only total free amino acids (Aa) and total soluble proteins (Pro) significantly changed in all three species with N fertilization (Supplementary Table S7). In *E. nutans*, both low-molecular weight (LMW) carbohydrates and high-molecular weight (HMW) carbohydrates decreased under high N treatment ($F = 3.783$, $p = 0.027$ and $F = 3.253$, $p = 0.043$, respectively). Although these water-soluble carbohydrates also decreased in *A. rivularis* and *T. lanceolata* under high

10.3389/fmicb.2022.895533

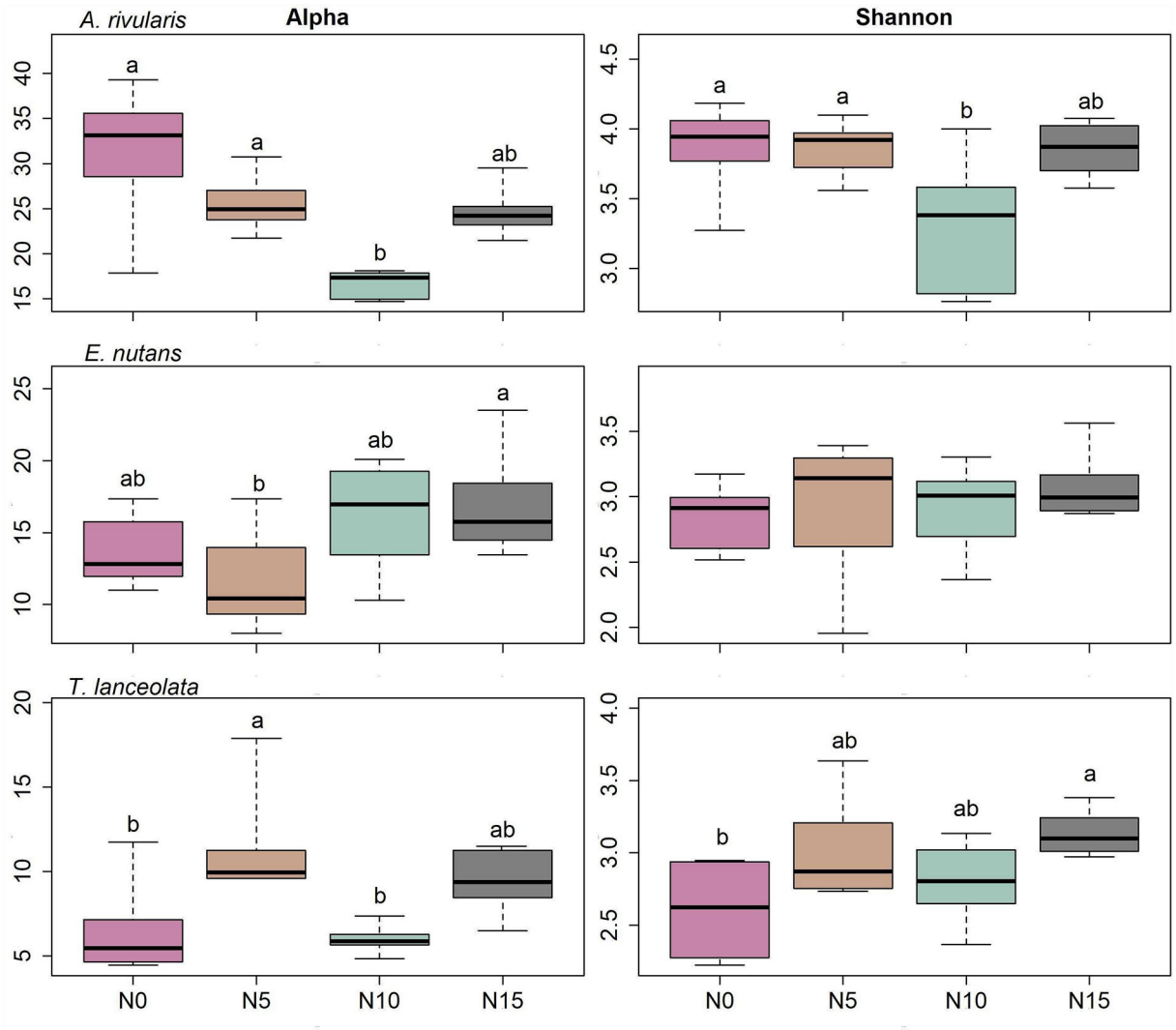

FIGURE 3
Diversity patterns of the fungal community within each host against N gradients. Alpha is the number of observed species, and Shannon is the Shannon diversity index. The sequences were rarified to 1,944, $n = 71$. Significant differences of each variable are indicated by dissimilar letters above boxes. N0, N5, N10, and N15 referring to 0, 5, 10, and 15 g N (NH_4NO_3) m^{-2} yr^{-1} treatments, respectively.

N conditions, only HMW sugars in *T. lanceolata* showed a significant response ($F = 7.547$, $p < 0.001$).

Unlike observations in soil (Supplementary Table S1), only tissue N in *E. nutans* was found increased under the high N condition ($F = 14.298$, $p < 0.001$), leading to a significant decrease in the tissue C/N ratio ($F = 18.287$, $p < 0.001$) and an increase in the tissue N/P ratio ($F = 4.129$, $p = 0.02$). An increased tissue N/P ratio was observed in *A. rivularis* ($F = 5.054$, $p = 0.009$) due to a decreased tissue P concentration ($F = 4.837$, $p = 0.011$). At the plot scale, elevated nutrient supply can cause a significant change in Pro ($F = 3.242$, $p = 0.04$), Aa ($F = 51.364$, $p < 0.001$), and tissue N/P ratio ($F = 5.854$, $p = 0.005$).

Effect of environmental variables on fungal diversity and community composition

Clearly, environmental variables were significantly correlated with both endophytic fungal diversity and community composition (Table 3). Pearson's correlation analyses showed that Pro, LMW sugars, tissue C, N, C/N ratio, and N/P ratio could be significantly related to the fungal alpha diversity indices to varying degrees (Table 3). There was a strong positive correlation between leaf carbon and endophytic fungal diversity indices, and LMW carbohydrates and Pro also showed a similar effect. Tissue N had a significant negative

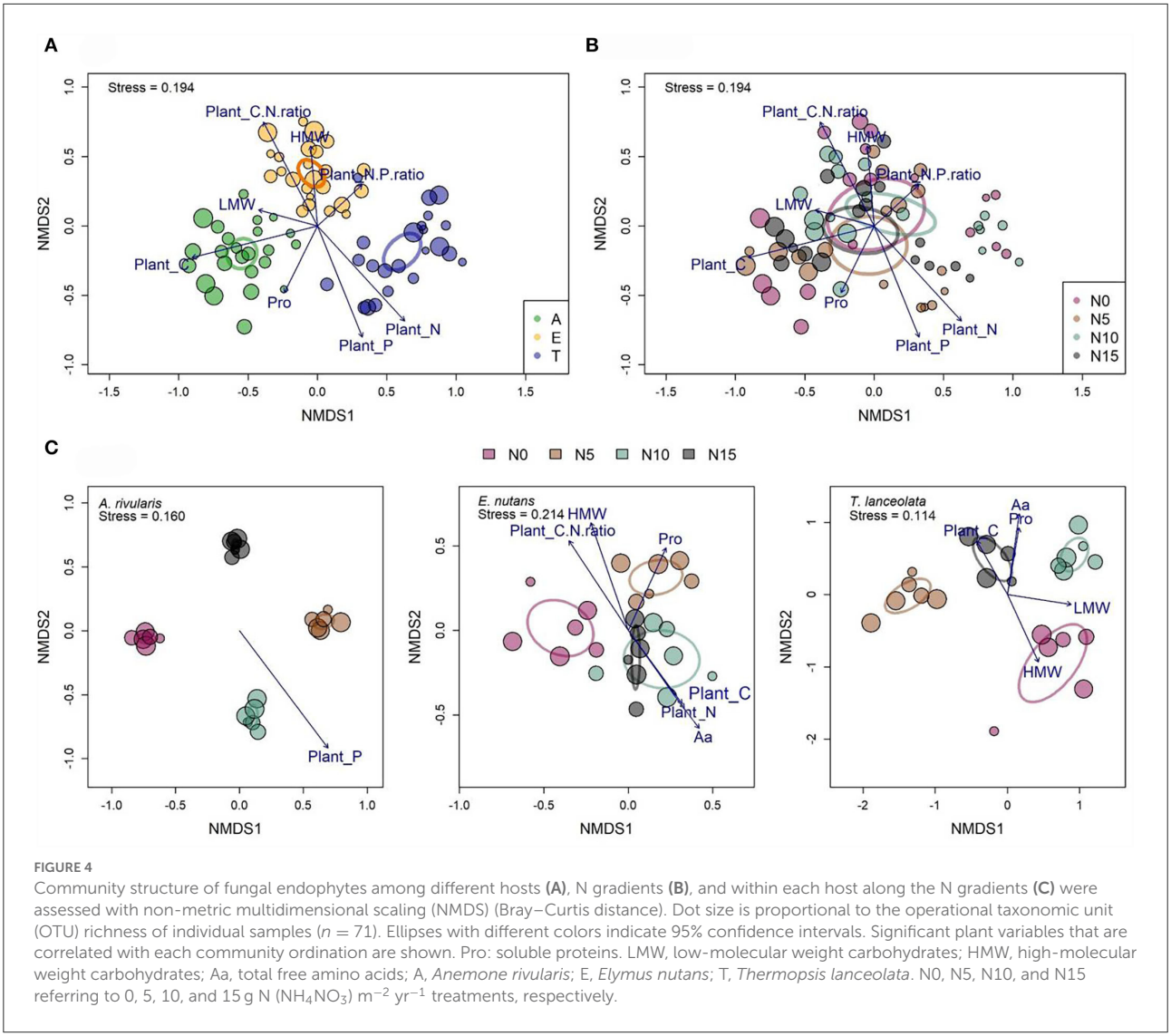

FIGURE 4
Community structure of fungal endophytes among different hosts **(A)**, N gradients **(B)**, and within each host along the N gradients **(C)** were assessed with non-metric multidimensional scaling (NMDS) (Bray–Curtis distance). Dot size is proportional to the operational taxonomic unit (OTU) richness of individual samples ($n = 71$). Ellipses with different colors indicate 95% confidence intervals. Significant plant variables that are correlated with each community ordination are shown. Pro: soluble proteins. LMW, low-molecular weight carbohydrates; HMW, high-molecular weight carbohydrates; Aa, total free amino acids; A, *Anemone rivularis*; E, *Elymus nutans*; T, *Thermopsis lanceolata*. N0, N5, N10, and N15 referring to 0, 5, 10, and 15 g N (NH_4NO_3) m^{-2} yr^{-1} treatments, respectively.

influence on endophytic fungal richness, but not on Shannon diversity. In addition, the leaf N/P ratio is negatively related to fungal diversity.

The Mantel test revealed a significant correlation between the fungal community composition and the following environmental variables (listed from highest to lowest Pearson's correlation coefficients): tissue C > N > P > C/N ratio (Table 3). With the *envfit* function in the vegan package (Oksanen et al., 2019) of R, Pro, LMW sugars, tissue C, N, P, C/N ratio, and N/P ratio were chosen to fit the NMDS plot (Figures 4A,B). When controlling for species, OTU assemblage was significantly correlated with tissue P in *A. rivularis*. Pro, Aa, HMW, tissue C, N, and C/N ratio were correlated with the fungal community in *E. nutans*, and ordination of *T. lanceolata* displayed the significance of five parameters, namely, Aa, Pro, LMW, and HMW sugars, and tissue C (Figure 4C). In summary, among all the measured indices, leaf carbon was considered the most significant factor constraining alpha and beta diversity.

Core microbiome and fungal co-occurrence network

Venn diagrams illustrated 927 OTUs (rarefied data) partitioning among the plant species and N gradients (Supplementary Figure S4). A total of 94 OTUs were shared among three species (10.14%, Supplementary Figure S4a), and 95 OTUs appeared in all treatment plots (10.25%, Supplementary Figure S4b). At the within-host scale, 47 (9.46%), 58 (11.79%), and 18 (6.43%) OTUs in *A. rivularis*, *E. nutans*, and *T. lanceolata* were shared among all N

TABLE 2 Statistical testing of fungal compositional dissimilarity based on a multispecies generalized linear model calculation (multispec.glm) and a permutational multivariate analysis of variance (PERMANOVA) using Bray–Curtis distance metrics.

	Multispec.glm		Permanova		
	Dev	*p*	*F*	R^2	*p*
Entire community					
Host	6,053	**0.003**	21.936	0.248	**0.001**
N input	5,036	**0.003**	7.959	0.136	**0.001**
Host × N input	3,259	**0.003**	8.353	0.283	**0.001**

Significance at 0.05 is highlighted in bold.

TABLE 3 Pearson's product–moment correlations between environmental variables and alpha (Fisher and Shannon indices) and beta diversity (Bray–Curtis distances) of fungal endophytes in three hosts.

Pearson *r*	Fisher's alpha	Shannon	Beta diversity
Pro	0.388**	0.471***	0.060
LMW	0.315**	0.285*	0.460
HMW	−0.112	−0.214	−0.010
Aa	−0.083	0.001	0.039
Plant_N	−0.466***	−0.188	0.373***
Plant_C	0.685***	0.570***	0.416***
Plant_P	−0.184	0.074	0.261***
Plant_C.N.ratio	0.251*	0.022	0.233***
Plant_N.P.ratio	−0.343**	−0.368**	0.006

The tested environmental variables included Soluble Pro, proteins; LMW, low-molecular weight carbohydrates; HMW, high-molecular weight carbohydrates; Aa, total free amino acids; plant total nitrogen; C, carbon; P, phosphorus; C/N ratio; and N/P ratio. Pearson's correlation coefficients (r) are shown.
*P < 0.05.
**P < 0.01.
***P < 0.001.

gradients, respectively (Supplementary Figure S5). We found evidence for a core microbiome, whereby nine OTUs were present among 90% or more of samples in the N0 (control) plot. These nine OTUs comprised ∼30% of the total reads (Supplementary Table S8), and taxonomic assignments were made using the National Center for Biotechnology Information (NCBI) nucleotide database. Most of the putative dominant fungi were previously found in close association with plants, which corroborated their potential symbiotic capability. In addition, among the 10 OTUs, seven were found among 90% or more of all individuals in all plots, indicating their prevalence in varied hosts along the environmental gradient.

For the network analysis of FEFs, 378 pairs of significant correlations were identified from 71 samples (Figure 5). Nodes of *A. rivularis* and *T. lanceolata* were highly interconnected (clustered) at each N level. Unique fungal taxon co-occurrence patterns were also found in *E. nutans* but were not affected by N input. Inter-host co-occurrence patterns were also observed; however, the correlations were relatively loose (18 edges), with Spearman's correlation coefficients ranging from 0.40 to 0.44. Overall, co-occurring FEFs tend to be tightly related to host identity, and the effect of N varied among species.

Discussion

Communities of FEFs in alpine meadows are highly diverse

E. nutans is dominant perennial grass in the QTP due to its high adaptability (Miao J. et al., 2011; Miao Q. et al., 2011), and *A. rivularis* and *T. lanceolata* are widespread forbs in this area. A recent survey on 596 publications on endophyte biodiversity revealed that forbs and graminoid-inhabiting fungal endophytes are largely understudied, especially in multiple hosts (Harrison and Griffin, 2020). In this study, diverse FEFs were found in three herbaceous hosts, suggesting a complex fungal network within QTP plant tissues, despite the geographic isolation and extreme environmental conditions. In a recent study, 210 endophytic fungal OTUs were identified in *E. nutans* collected from a nearby field site using similar study methods (Guo et al., 2021). Here, we identified 576 OTUs (492 OTUs after data rarefaction) in leaves of *E. nutans*, challenging the argument put forward by Harrison and Griffin (2020) that roots were the tissue that harbors the richest endophytes in graminoids. In terrestrial plants, environmental differences were proven to contribute to differences between organs in endophyte flora (Fisher et al., 1992). Higher fungal richness in leaves of *E. nutans* might be caused by the more dynamic aboveground environment, since environmental variability could promote diversity (Hutchinson, 1961; Chesson, 2000). During the short growing season in the QTP, leaves are more biochemically active than roots and may provide more available nutrients to attract microorganisms. Alternatively, low temperature can limit microbial activity, reducing the transmission of endophytes in QTP soil. Given the limited amount of published data on endophytes of alpine plants, it is difficult identify which patterns of distribution are normal.

To our knowledge, this is the first study to apply high-throughput sequencing to explore the endophyte communities in *A. rivularis* and *T. lanceolata*. Here, a taxonomically diverse assemblage of FEFs was recovered from *A. rivularis*, whereas by cultivation-dependent methods, only 23 fungal taxa were isolated from the leaves of Anemone tomentosa in a study in west China. We screened relatively less fungal taxa in *T. lanceolata* (280 OTUs), possibly due to the reduced abundance of *T. lanceolata* after N enrichment in the study site (Jiang et al., 2018). Abundant hosts have been proven to support a greater number and diversity of symbiotic fungi (Gilbert et al., 2007).

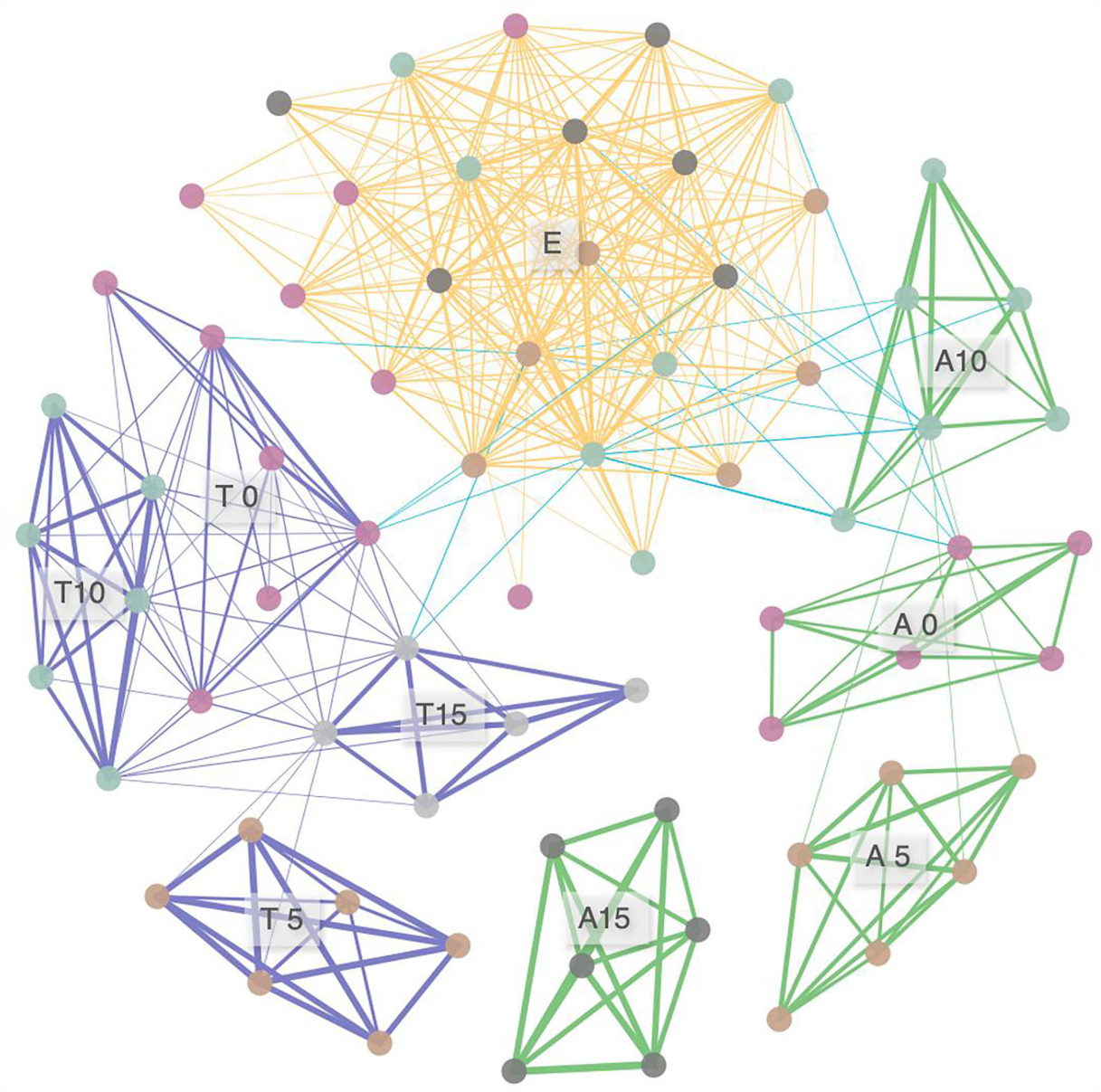

FIGURE 5
Networks of taxa similarity in three species along the nitrogen enrichment gradients, based on correlation analysis. A connection stands for a correlation with Spearman's $\rho > 0.4$ and $p < 0.05$. The thickness of each connection between two nodes (i.e., edge) is proportional to the value of Spearman's correlation coefficients ranging from 0.40 to 0.93. A, *Anemone rivularis*; E, *Elymus nutans*; T, *Thermopsis lanceolata*. 0 (control), 5, 10, and 15 referring to 0, 5, 10, and 15 g N (NH_4NO_3) m^{-2} yr^{-1} treatments, respectively.

Thus, we suggest that host abundance plays an important role in structuring endophytic microbiomes.

Ascomycota was described as the predominant endophytic fungal phyla in biomes ranging from tropical rainforests to harsh Antarctica in previous works (Arnold and Lutzoni, 2007; Zhang and Yao, 2015; Teasdale et al., 2018; Whitaker et al., 2020). Using 454 pyrosequencing, only 0.4% endophytic Basidiomycota was recovered from leaves of *Metrosideros polymorpha* in the tropics (Zimmerman and Vitousek, 2012). Conversely, 8.6% endophytic Basidiomycota was found in subalpine timberline ecotone (Yang et al., 2016), and 19.4% of FEFs in four species in a high arctic zone are basidiomycetous fungi (Zhang and Yao, 2015). Research on fungal endophytes has expanded dramatically in recent years, but the ecological roles of endophytic basidiomycetes are still unknown. Here, we found as high as 36.75% endophytic Basidiomycota, adding

evidence to the importance of Basidiomycota in high-altitude or high-latitude areas.

Effects of N modifications at plot and within-host scale

The impact of human development on endophyte biodiversity in wilderness areas remains understudied (Harrison and Griffin, 2020). We hypothesized that N could lead to significant community turnover at both plot and within-host scale. We found that fungal diversity for all samples (or all individuals) pooled was not dominantly shaped by N supply at the plot scale after 4 years of fertilization treatment (although some indices showed a significant effect of N, clearly lower deviances, F, and R^2 statistics were observed, cf. Tables 1, 2; Figures 2, 4). The findings agree with culture-based experimental evidence from Sweden recently (Witzell et al., 2022) that N input did not alter the total richness and Shannon diversity of FEFs in 12 aspen genotypes. We suggest that in the alpine meadow ecosystems, total fungal communities harbored in diverse groups of plants tend to persist under increasing N deposition. However, it is still not clear if plant microbiomes could be affected by anthropogenic environmental changes at larger spatial scales across the QTP landscapes. Further studies incorporating additional sites (or testing for spatial autocorrelation) are required in the QTP in order to make a strong inference or generalizations on these fungal communities.

In the present study, the effects of elevated N are more pronounced at the within-host scale (Supplementary Tables S5, S6; Figures 3–5). Fungal assemblages of *A. rivularis* exhibited decreased species diversity (Shannon diversity and richness) across the N enrichment gradients. However, an increased fungal diversity pattern was observed in *T. lanceolata* as compared to the control group. By contrast, FEF communities of *E. nutans* were not significantly affected by N. A study of root-associated arbuscular mycorrhizal (AM) fungi in *E. nutans* within the same experimental plots sampled at the same time found that N addition reduced AM fungal abundance (Jiang et al., 2018). These findings indicate that the effects of N input on plant microbiomes are multifarious and may depend upon host identity and tissue types. The multispecies generalized linear model, PERMANOVA model together with NMDS, and network analyses demonstrated that endophyte community composition varies significantly among host species, supporting findings of previous studies (e.g., Arnold and Lutzoni, 2007; Higgins et al., 2007; Dastogeer et al., 2018; Liu et al., 2019; Chen et al., 2020). Perennial hosts were suggested to cultivate and nurture their microbial surroundings (Baltrus, 2017). Thus, it was possible that in the stressful environment in the QTP, the fungal communities may have adapted to different types of leaves over evolutionary timescales. We reinforce the view that host plant identity is the significant driver of endophyte assemblage patterns, and we suggest host identity supersedes N supply in shaping the community composition of FEFs.

Host tissue C and related compounds significantly correlated with FEF diversity

Consistent with previous studies (Rasmussen et al., 2007; Ryan et al., 2014), leaf carbohydrates (LMW and HMW sugars) decreased with N input. Leaves provide shelter and nutrition for endophytes, and foliar carbon was known to correlate with plant function (Wright et al., 2004) and life history strategy (Wright et al., 2010), yet how leaf chemicals, especially leaf carbon, affect communities of fungal endophytes is not well studied. We found a strong relation between tissue carbon and communities of FEFs in the study site (Table 3). The NMDS plot with fitted environmental variables also showed that the carbon-associated factors, including tissue C, C/N ratio, and LMW and HMW sugar, significantly correlated with FEF community assemblages along the N gradient (Figures 4A,B). In addition, these carbon-associated factors correlated well with the dissimilarities among fungal assemblages in *E. nutans* and *T. lanceolata*. Similar trends were also found in the leaves of *Betula* (Yang et al., 2016) and *Ficus* (Liu et al., 2019), emphasizing the universal relationship between carbon source availability and this heterogeneous ecological guild in plants.

Core microbiomes exist among hosts and the N gradient

We demonstrated the existence of a fairly dominant core microbiome: three focal species shared one-third of all endophyte sequences, seven OTUs were prevalent in all sampled hosts along the N gradient, and two prevalent OTUs assigned to uncultured fungus in this study were also observed in the phyllosphere of trees in different ecosystems (Supplementary Table S8), indicating their potential wide niche range. Some subsets of fungi that comprise the core microbiome may have functional roles that enhance their ability to colonize the interior of a phylogenetically diverse group of plant species (Vandenkoornhuyse et al., 2015). These traits likely include high habitat adaptation (Pereira et al., 2019) and metabolite (enzymes or hormone) production that induces stomatal opening for fungi entry (Hardoim et al., 2015). The same microbial taxa may reach varied plant species in varied environmental conditions, and hence, searching for endophytes from the core microbiome of wild plants adapted to unhospitable habitats will provide solutions for the study of stress tolerance of plants.

Conclusion

This study provides insights into the changes in plant fungal microbiome in response to host identity and environmental conditions. We report two key findings: first, in the harsh habitat of the Qinghai–Tibetan Plateau, host identity, rather than N supply, is a stronger factor for driving communities of foliar fungal endophytes, even in an alpine meadow ecosystem where productivity is strongly limited by N availability; and second, N addition has varying effects on both α and β diversity of within-host scale fungal endophytes. We demonstrated leaf carbon and carbohydrates significantly affected fungal communities in host leaves, indicating FEFs may play a pivotal role in the carbon cycling of alpine meadow ecosystems. In addition, we found unequivocal evidence for a core microbiome present among 90% or more of all control samples, representing one-third of the total reads. The results suggest that even though soil resource availability often mediates plant performance, environmental modifications on fungal microbiomes likely depend on the host species. We suggest that future studies quantify the nutritional requirements of endophytes, at both small and large scales. The results implement theoretical frameworks of community ecology and gain new sights into the dynamics of endophyte communities in grasses and forbs driven by environment and host functional traits.

Data availability statement

The datasets presented in this study can be found in online repositories. The names of the repository/repositories and accession number(s) can be found below: https://www.ncbi.nlm.nih.gov/, OM744714:OM745695.

Author contributions

Conceptualization: HF, QZ, and YL. Methodology: GD, HF, and YL. Software, formal analysis, and visualization: YM. Investigation: GS, YL, QZ, and YM. Resources: GD. Data curation: QZ and YM. Original draft preparation: HF, QZ, and YM. Project administration: QZ and HF. All authors contributed to manuscript revision, read, and approved the submitted version.

Funding

This work was financially supported by the Second Tibetan Plateau Scientific Expedition and Research Program (2019QZKK0301) and the National Natural Science Foundation of China (31971445, 31870494, 31860146, 32171579, and U21A20186).

Acknowledgments

We thank the following members for assistance with fieldwork: Shengjing Jiang, Mingsen Qin, Yuxing Chai, and Jiajia Luo. YM is grateful to Sanni Färkkilä, Slendy Rodriguez, Iris Reinula, and Kai-Yun Li for their suggestions on writing this manuscript.

Conflict of interest

The authors declare that the research was conducted in the absence of any commercial or financial relationships that could be construed as a potential conflict of interest.

Publisher's note

All claims expressed in this article are solely those of the authors and do not necessarily represent those of their affiliated organizations, or those of the publisher, the editors and the reviewers. Any product that may be evaluated in this article, or claim that may be made by its manufacturer, is not guaranteed or endorsed by the publisher.

Supplementary material

The Supplementary Material for this article can be found online at: https://www.frontiersin.org/articles/10.3389/fmicb.2022.895533/full#supplementary-material

References

Apigo, A., and Oono, R. (2018). Dimensions of host specificity in foliar fungal endophytes. *Endop. Forest Trees Biol. Appl.* 86, 15–42. doi: 10.1007/978-3-319-89833-9_2

Arnold, A. E., and Lutzoni, F. (2007). Diversity and host range of foliar fungal endophytes: are tropical leaves biodiversity hotspots? *Ecology* 88, 541–549. doi: 10.1890/05-1459

Arnold, A. E., Miadlikowska, J., Higgins, K. L., Sarvate, S. D., Gugger, P., Way, A., et al. (2009). A phylogenetic estimation of trophic transition networks for ascomycetous fungi: are lichens cradles of symbiotrophic fungal diversification? *System. Biol.* 58, 283–297. doi: 10.1093/sysbio/syp001

Baltrus, D. A. (2017). Adaptation, specialization, and coevolution within phytobiomes. *Curr. Opin. Plant Biol.* 38, 109–116. doi: 10.1016/j.pbi.2017.04.023

Bastian, M., Heymann, S., and Jacomy, M. (2009). "Gephi: an open source software for exploring and manipulating networks," in *Proceedings of the International AAAI Conference on Web and Social Media, Vol. 3*, 361–362.

Bobbink, R., Hicks, K., Galloway, J., Spranger, T., Alkemade, R., Ashmore, M., et al. (2010). Global assessment of nitrogen deposition effects on terrestrial plant diversity: a synthesis. *Ecol. Appl.* 20, 30–59. doi: 10.1890/08-1140.1

Bokulich, N. A., Kaehler, B. D., Rideout, J. R., Dillon, M., Bolyen, E., Knight, R., et al. (2018). Optimizing taxonomic classification of marker-gene amplicon sequences with QIIME 2's q2-feature-classifier plugin. *Microbiome* 6, 90. doi: 10.1186/s40168-018-0470-z

Bolger, A. M., Lohse, M., and Usadel, B. (2014). Trimmomatic: a flexible trimmer for Illumina sequence data. *Bioinformatics* 30, 2114–2120. doi: 10.1093/bioinformatics/btu170

Bolyen, E., Rideout, J. R., Dillon, M. R., Bokulich, N. A., Abnet, C. C., Al-Ghalith, G. A., et al. (2019). Reproducible, interactive, scalable and extensible microbiome data science using QIIME 2 (vol 37, pg 852, 2019). *Nat. Biotechnol.* 37, 1091–1091. doi: 10.1038/s41587-019-0252-6

Bradford, M. M. (1976). A rapid and sensitive method for the quantitation of microgram quantities of protein utilizing the principle of protein-dye binding. *Anal. Biochem.* 72, 248–254. doi: 10.1016/0003-2697(76)90527-3

Buckley, H., Young, C. A., Charlton, N. D., Hendricks, W. Q., Haley, B., Nagabhyru, P., et al. (2019). Leaf endophytes mediate fertilizer effects on plant yield and traits in northern oat grass (*Trisetum spicatum*). *Plant Soil* 434, 425–440. doi: 10.1007/s11104-018-3848-6

Callahan, B. J., McMurdie, P. J., Rosen, M. J., Han, A. W., Johnson, A. J. A., and Holmes, S. P. (2016). DADA2: high-resolution sample inference from Illumina amplicon data. *Nat. Methods* 13, 581. doi: 10.1038/nmeth.3869

Cardinale, B. J., Matulich, K. L., Hooper, D. U., Byrnes, J. E., Duffy, E., Gamfeldt, L., et al. (2011). The functional role of producer diversity in ecosystems. *Am. J. Bot.* 98, 572–592. doi: 10.3732/ajb.1000364

Chen, J. H., Akutse, K. S., Saqib, H. S. A., Wu, X. L., Yang, F. Y., Xia, X. F., et al. (2020). Fungal endophyte communities of crucifer crops are seasonally dynamic and structured by plant identity, plant tissue and environmental factors. *Front. Microbiol.* 11, 01519. doi: 10.3389/fmicb.2020.01519

Chen, X. X., Luo, X. L., Fan, M. M., Zeng, W. L., Yang, C. R., Wu, J. R., et al. (2019). Endophytic fungi from the branches of *Camellia taliensis* (W. W. Smith) Melchior, a widely distributed wild tea plant. *World J. Microbiol. Biotechnol.* 35, 113. doi: 10.1007/s11274-019-2686-x

Chesson, P. (2000). Mechanisms of maintenance of species diversity. *Ann. Rev. Ecol. System.* 343–366. doi: 10.1146/annurev.ecolsys.31.1.343

Christian, N., Herre, E. A., and Clay, K. (2019). Foliar endophytic fungi alter patterns of nitrogen uptake and distribution in *Theobroma cacao*. *New Phytol.* 222, 1573–1583. doi: 10.1111/nph.15693

Clay, K., and Schardl, C. (2002). Evolutionary origins and ecological consequences of endophyte symbiosis with grasses. *Am. Natur.* 160, S99–S127. doi: 10.1086/342161

Crawford, J. T., Hinckley, E. L. S., and Neff, J. C. (2020). Long-term trends in acid precipitation and watershed elemental export from an alpine catchment of the colorado rocky mountains, USA. *J. Geophys. Res. Biogeosci.* 125, e2020JG005683. doi: 10.1029/2020JG005683

Csardi, G., and Nepusz, T. (2006). The igraph software package for complex network research. *Inter J. Complex Syst.* 1695, 1–9.

Dastogeer, K. M. G., Li, H., Sivasithamparam, K., Jones, M. G. K., and Wylie, S. J. (2018). Host specificity of endophytic mycobiota of wild nicotiana plants from arid regions of Northern Australia. *Microbial. Ecol.* 75, 74–87. doi: 10.1007/s00248-017-1020-0

Dunham, S. M., Mujic, A. B., Spatafora, J. W., and Kretzer, A. M. (2013). Within-population genetic structure differs between two sympatric sister-species of ectomycorrhizal fungi, *Rhizopogon vinicolor* and *R. vesiculosus*. *Mycologia* 105, 814–826. doi: 10.3852/12-265

Ellison, A. M., and Gotelli, N. J. (2002). Nitrogen availability alters the expression of carnivory in the northern pitcher plant, *Sarracenia purpurea*. *Proc. Natl. Acad. Sci. U. S. A.* 99, 4409–4412. doi: 10.1073/pnas.022057199

EPA (2013). *Reactive Nitrogen in the United States: An Analysis of Inputs, Flows, Consequences, and Management Options: A Report of the EPA Science Advisory Board*. Washington, DC: EPA.

Fisher, P. J., Petrini, O., and Scott, H. M. L. (1992). The distribution of some fungal and bacterial endophytes in maize (Zea-Mays L). *New Phytol.* 122, 299–305. doi: 10.1111/j.1469-8137.1992.tb04234.x

Gardes, M., and Bruns, T. D. (1993). Its primers with enhanced specificity for basidiomycetes - application to the identification of mycorrhizae and rusts. *Mol. Ecol.* 2, 113–118. doi: 10.1111/j.1365-294X.1993.tb00005.x

Gilbert, G. S., Reynolds, D. R., and Bethancourt, A. (2007). The patchiness of epifoliar fungi in tropical forests: host range, host abundance, and environment. *Ecology* 88, 575–581. doi: 10.1890/05-1170

Gilliam, F. S., Burns, D. A., Driscoll, C. T., Frey, S. D., Lovett, G. M., and Watmough, S. A. (2019). Decreased atmospheric nitrogen deposition in eastern North America: Predicted responses of forest ecosystems. *Environ. Pollut.* 244, 560–574. doi: 10.1016/j.envpol.2018.09.135

Gong, Z., and Li, F. (2001). *Chinese Soil Taxonomy*. Beijing: Science Press.

Gonzalez-Teuber, M., Vilo, C., Guevara-Araya, M. J., Salgado-Luarte, C., and Gianoli, E. (2020). Leaf resistance traits influence endophytic fungi colonization and community composition in a South American temperate rainforest. *J. Ecol.* 108, 1019–1029. doi: 10.1111/1365-2745.13314

Guo, J., Bowatte, S., and Hou, F. (2021). Diversity of endophytic bacteria and fungi in seeds of Elymus nutans growing in four locations of Qinghai Tibet Plateau, China. *Plant Soil* 459, 49–63. doi: 10.1007/s11104-020-04608-y

Hardoim, P. R., van Overbeek, L. S., Berg, G., Pirttila, A. M., Compant, S., Campisano, A., et al. (2015). The hidden world within plants: ecological and evolutionary considerations for defining functioning of microbial endophytes. *Microbiol. Mol. Biol. Rev.* 79, 293–320. doi: 10.1128/MMBR.00050-14

Harrell, F. E., and Dupont, C. (2018). *Hmisc: Harrell miscellaneous. R package version 4.1-1. R Found. Stat. Comput.* Avaible online at: https://CRAN.R-project.org/package=Hmisc (accessed February 16, 2018).

Harrison, J. G., and Griffin, E. A. (2020). The diversity and distribution of endophytes across biomes, plant phylogeny and host tissues: how far have we come and where do we go from here? *Environ. Microbiol.* 22, 2107–2123. doi: 10.1111/1462-2920.14968

Higgins, K. L., Arnold, A. E., Coley, P. D., and Kursar, T. A. (2014). Communities of fungal endophytes in tropical forest grasses: highly diverse host- and habitat generalists characterized by strong spatial structure. *Fungal Ecol.* 8, 1–11. doi: 10.1016/j.funeco.2013.12.005

Higgins, K. L., Arnold, A. E., Miadlikowska, J., Sarvate, S. D., and Lutzoni, F. (2007). Phylogenetic relationships, host affinity, and geographic structure of boreal and arctic endophytes from three major plant lineages. *Mol. Phylogen. Evol.* 42, 543–555. doi: 10.1016/j.ympev.2006.07.012

Higgins, K. L., Coley, P. D., Kursar, T. A., and Arnold, A. E. (2011). Culturing and direct PCR suggest prevalent host generalism among diverse fungal endophytes of tropical forest grasses. *Mycologia* 103, 247–260. doi: 10.3852/09-158

Huang, Y. L., Devan, M. M. N., U'Ren, J. M., Furr, S. H., and Arnold, A. E. (2016). Pervasive effects of wildfire on foliar endophyte communities in montane forest trees. *Microbial. Ecol.* 71, 452–468. doi: 10.1007/s00248-015-0664-x

Hunt, M. G., Rasmussen, S., Newton, P. C. D., Parsons, A. J., and Newman, J. A. (2005). Near-term impacts of elevated CO_2, nitrogen and fungal endophyte-infection on *Lolium perenne* L. growth, chemical composition and alkaloid production. *Plant Cell Environ.* 28, 1345–1354. doi: 10.1111/j.1365-3040.2005.01367.x

Hutchinson, G. E. (1961). The paradox of the plankton. *Am. Natur.* 95, 137–145. doi: 10.1086/282171

IPCC (2014). *Climate Change 2014 – Impacts, Adaptation and Vulnerability: Part A: Global and Sectoral Aspects: Working Group II Contribution to the IPCC Fifth Assessment Report: Volume 1: Global and Sectoral Aspects (Vol. 1)*. Cambridge; New York, NY: Cambridge University Press.

Jiang, S. J., Liu, Y. J., Luo, J. J., Qin, M. S., Johnson, N. C., Opik, M., et al. (2018). Dynamics of arbuscular mycorrhizal fungal community structure and functioning along a nitrogen enrichment gradient in an alpine meadow ecosystem. *New Phytol.* 220, 1222–1235. doi: 10.1111/nph.15112

Knoth, J. L., Kim, S. H., Ettl, G. J., and Doty, S. L. (2013). Effects of cross host species inoculation of nitrogen-fixing endophytes on growth and leaf physiology of maize. *Global Change Biol. Bioenergy* 5, 408–418. doi: 10.1111/gcbb.12006

Koljalg, U., Nilsson, H. R., Schigel, D., Tedersoo, L., Larsson, K. H., May, T. W., et al. (2020). The taxon hypothesis paradigm-on the unambiguous detection and communication of Taxa. *Microorganisms* 8, 910. doi: 10.3390/microorganisms8121910

Larkin, B. G., Hunt, L. S., and Ramsey, P. W. (2012). Foliar nutrients shape fungal endophyte communities in Western white pine (*Pinus monticola*) with implications for white-tailed deer herbivory. *Fungal Ecol.* 5, 252–260. doi: 10.1016/j.funeco.2011.11.002

Liu, J. W., Zhao, J., Wang, G., and Chen, J. (2019). Host identity and phylogeny shape the foliar endophytic fungal assemblages of Ficus. *Ecol. Evol.* 9, 10472–10482. doi: 10.1002/ece3.5568

Lu, C. Q., and Tian, H. Q. (2007). Spatial and temporal patterns of nitrogen deposition in China: Synthesis of observational data. *J. Geophys. Res. Atmosp.* 112, D22. doi: 10.1029/2006JD007990

Miao, J., Zhang, X., Chen, S., Ma, X., Chen, Z., Zhong, J., et al. (2011). Gliadin analysis of Elymus nutans Griseb. from the Qinghai–Tibetan Plateau and Xinjiang, China. *Grassland Sci.* 57, 127–134. doi: 10.1111/j.1744-697X.2011.00219.x

Miao, Q., Qin, S., Bian, G.-K., Yuan, B., Xing, K., Zhang, Y.-J., et al. (2011). Amycolatopsis endophytica sp. nov., a novel endophytic actinomycete isolated from oil-seed plant Jatropha curcas L. *Antonie van Leeuwenhoek* 100, 333–339. doi: 10.1007/s10482-011-9588-8

Newman, J. A., Abner, M. L., Dado, R. G., Gibson, D. J., Brookings, A., and Parsons, A. J. (2003). Effects of elevated CO_2, nitrogen and fungal endophyte-infection on tall fescue: growth, photosynthesis, chemical composition and digestibility. *Global Change Biol.* 9, 425–437. doi: 10.1046/j.1365-2486.2003.00601.x

Oksanen, J., Blanchet, F. G., Friendly, M., Kindt, R., Legendre, P., McGlinn, D., et al. (2019). *Vegan: Community Ecology Package (Version 2.5-6)*. The Comprehensive R Archive Network. Available online at: https://CRAN.R-project.org/package=vegan (accessed July 1, 2019).

Oono, R., Lutzoni, F., Arnold, A. E., Kaye, L., U'Ren, J. M., May, G., et al. (2014). Genetic variation in horizontally transmitted fungal endophytes of pine needles reveals population structure in cryptic species. *Am. J. Bot.* 101, 1362–1374. doi: 10.3732/ajb.1400141

Pereira, E., de Aldana, B. R. V., San Emeterio, L., and Zabalgogeazcoa, I. (2019). A survey of culturable fungal endophytes from festuca rubra subsp. pruinosa, a grass from marine cliffs, reveals a core microbiome. *Front. Microbiol.* 9, e03321. doi: 10.3389/fmicb,.2018.03321

R Core Team (2019). *R: A Language and Environment for Statistical Computing. In (Version 3.6.2) R Foundation for Statistical Computing*. Vienna: R Core Team.

Rasmussen, S., Parsons, A. J., Bassett, S., Christensen, M. J., Hume, D. E., Johnson, L. J., et al. (2007). High nitrogen supply and carbohydrate content reduce fungal endophyte and alkaloid concentration in Lolium perenne. *New Phytol.* 173, 787–797. doi: 10.1111/j.1469-8137.2006.01960.x

Razali, N. M., Cheah, B. H., and Nadarajah, K. (2019). Transposable elements adaptive role in genome plasticity, pathogenicity and evolution in fungal phytopathogens. *Int. J. Mol. Sci.* 20, 597. doi: 10.3390/ijms20143597

Rodriguez, R. J., White, J. F., Arnold, A. E., and Redman, R. S. (2009). Fungal endophytes: diversity and functional roles. *New Phytol.* 182, 314–330. doi: 10.1111/j.1469-8137.2009.02773.x

Ryan, G. D., Rasmussen, S., Xue, H., Parsons, A. J., and Newman, J. A. (2014). Metabolite analysis of the effects of elevated CO_2 and nitrogen fertilization on the association between tall fescue (*Schedonorus arundinaceus*) and its fungal symbiont Neotyphodium coenophialum. *Plant Cell Environ.* 37, 204–212. doi: 10.1111/pce.12146

Saikkonen, K., Wali, P., Helander, M., and Faeth, S. H. (2004). Evolution of endophyte-plant symbioses. *Trends Plant Sci.* 9, 275–280. doi: 10.1016/j.tplants.2004.04.005

Scarpitta, A. B., Bardat, J., Lalanne, A., and Vellend, M. (2017). Long-term community change: bryophytes are more responsive than vascular plants to nitrogen deposition and warming. *J. Veget. Sci.* 28, 1220–1229. doi: 10.1111/jvs.12579

Seghers, D., Wittebolle, L., Top, E. M., Verstraete, W., and Siciliano, S. D. (2004). Impact of agricultural practices on the Zea mays L. endophytic community. *Appl. Environ. Microbiol.* 70, 1475–1482. doi: 10.1128/AEM.70.3.1475-1482.2004

Shade, A., and Handelsman, J. (2012). Beyond the Venn diagram: the hunt for a core microbiome. *Environ. Microbiol.* 14, 4–12. doi: 10.1111/j.1462-2920.2011.02585.x

Singha, K. M., Singh, B., and Pandey, P. (2021). Host specific endophytic microbiome diversity and associated functions in three varieties of scented black rice are dependent on growth stage. *Sci. Rep.* 11, 12259. doi: 10.1038/s41598-021-91452-4

Sosso, J., Zakeel, M. C. M., and Akinsanmi, O. A. (2021). Culturable fungal endophytes in Australian macadamia nursery plants. *Austral. Plant Pathol.* 50, 739–746. doi: 10.1007/s13313-021-00824-x

Stevens, C. J., Dise, N. B., Mountford, J. O., and Gowing, D. J. (2004). Impact of nitrogen deposition on the species richness of grasslands. *Science* 303, 1876–1879. doi: 10.1126/science.1094678

Sullivan, T. J., Lawrence, G. B., Bailey, S. W., McDonnell, T. C., Beier, C. M., Weathers, K. C., et al. (2013). Effects of acidic deposition and soil acidification on sugar maple trees in the Adirondack Mountains, New York. *Environ. Sci. Technol.* 47, 12687–12694. doi: 10.1021/es401864w

Suryanarayanan, T. S., and Shaanker, R. U. (2021). Can fungal endophytes fast-track plant adaptations to climate change? *Fungal Ecol.* 50, 101039. doi: 10.1016/j.funeco.2021.101039

Teasdale, S. E., Caradus, J. R., and Johnson, L. J. (2018). Fungal endophyte diversity from tropical forage grass Brachiaria. *Plant Ecol. Diversity* 11, 611–624. doi: 10.1080/17550874.2019.1610913

Unterseher, M., Jumpponen, A., Opik, M., Tedersoo, L., Moora, M., Dormann, C. F., et al. (2011). Species abundance distributions and richness estimations in fungal metagenomics - lessons learned from community ecology. *Mol. Ecol.* 20, 275–285. doi: 10.1111/j.1365-294X.2010.04948.x

Vacher, C., Hampe, A., Porte, A. J., Sauer, U., Compant, S., and Morris, C. E. (2016). The phyllosphere: microbial jungle at the plant-climate interface. *Ann. Rev. Ecol. Evol. Syst.* 47, 1–24. doi: 10.1146/annurev-ecolsys-121415-032238

Vallicrosa, H., Sardans, J., Maspons, J., and Penuelas, J. (2022). Global distribution and drivers of forest biome foliar nitrogen to phosphorus ratios (N:P). *Global Ecol. Biogeogr.* 31, 861–871. doi: 10.1111/geb.13457

Vandenkoornhuyse, P., Quaiser, A., Duhamel, M., Le Van, A., and Dufresne, A. (2015). The importance of the microbiome of the plant holobiont. *New Phytol.* 206, 1196–1206. doi: 10.1111/nph.13312

Vincent, J. B., Weiblen, G. D., and May, G. (2016). Host associations and beta diversity of fungal endophyte communities in New Guinea rainforest trees. *Mol. Ecol.* 25, 825–841. doi: 10.1111/mec.13510

Vitousek, P. M., and Howarth, R. W. (1991). Nitrogen limitation on land and in the sea - how can it occur. *Biogeochemistry* 13, 87–115. doi: 10.1007/BF00002772

Whitaker, B. K., Christian, N., Chai, Q., and Clay, K. (2020). Foliar fungal endophyte community structure is independent of phylogenetic relatedness in an Asteraceae common garden. *Ecol. Evol.* 10, 13895–13912. doi: 10.1002/ece3.6983

Witzell, J., Decker, V. H. G., Agostinelli, M., Romeralo, C., Cleary, M., and Albrectsen, B. R. (2022). Aspen leaves as a "chemical landscape" for fungal endophyte diversity-effects of nitrogen addition. *Front. Microbiol.* 13, 846208. doi: 10.3389/fmicb.2022.846208

Wright, I. J., Reich, P. B., Westoby, M., Ackerly, D. D., Baruch, Z., Bongers, F., et al. (2004). The worldwide leaf economics spectrum. *Nature* 428, 821–827. doi: 10.1038/nature02403

Wright, S. J., Kitajima, K., Kraft, N. J. B., Reich, P. B., Wright, I. J., Bunker, D. E., et al. (2010). Functional traits and the growth-mortality trade-off in tropical trees. *Ecology* 91, 3664–3674. doi: 10.1890/09-2335.1

Wu, G. L., Liu, Z. H., Zhang, L., Chen, J. M., and Hu, T. M. (2010). Long-term fencing improved soil properties and soil organic carbon storage in an alpine swamp meadow of western China. *Plant Soil* 332, 331–337. doi: 10.1007/s11104-010-0299-0

Xu, D. H., Fang, X. W., Zhang, R. Y., Gao, T. P., Bu, H. Y., and Du, G. Z. (2015). Influences of nitrogen, phosphorus and silicon addition on plant productivity and species richness in an alpine meadow. *Aob Plants* 7, plv125. doi: 10.1093/aobpla/plv125

Yang, T., Weisenhorn, P., Gilbert, J. A., Ni, Y., Sun, R., Shi, Y., et al. (2016). Carbon constrains fungal endophyte assemblages along the timberline. *Environ. Microbiol.* 18, 2455–2469. doi: 10.1111/1462-2920.13153

Yang, Z., van Ruijven, J., and Du, G. (2011). The effects of long-term fertilization on the temporal stability of alpine meadow communities. *Plant Soil* 345, 315–324. doi: 10.1007/s11104-011-0784-0

Yemm, E. W., Cocking, E. C., and Ricketts, R. E. (1955). The determination of amino-acids with ninhydrin. *Analyst* 80, 209–214. doi: 10.1039/an9558000209

Zhang, T., and Yao, Y. F. (2015). Endophytic fungal communities associated with vascular plants in the high arctic zone are highly diverse and host-plant specific. *PLoS ONE* 10, e0130051. doi: 10.1371/journal.pone.0130051

Zheng, Y., Li, X., Cao, H., Lei, L., Zhang, X., Han, D., et al. (2021). The assembly of wheat-associated fungal community differs across growth stages. *Appl. Microbiol. Biotechnol.* 105, 7427–7438. doi: 10.1007/s00253-021-11550-1

Zimmerman, N. B., and Vitousek, P. M. (2012). Fungal endophyte communities reflect environmental structuring across a Hawaiian landscape. *Proc. Natl. Acad. Sci.* 109, 13022–13027. doi: 10.1073/pnas.1209872109

frontiers | Frontiers in Microbiology

TYPE Original Research
PUBLISHED 19 October 2022
DOI 10.3389/fmicb.2022.1013023

OPEN ACCESS

EDITED BY
Yi Luo,
Nankai University,
China

REVIEWED BY
Xingang Zhou,
Northeast Agricultural University,
China
Padmanabh Dwivedi,
Banaras Hindu University,
India

*CORRESPONDENCE
Yong Zhou
zhouyong275@sina.com

SPECIALTY SECTION
This article was submitted to Microbial Symbioses, a section of the journal Frontiers in Microbiology

RECEIVED 06 August 2022
ACCEPTED 04 October 2022
PUBLISHED 19 October 2022

CITATION
Xu L, Niu X, Li X, Zheng Y, Feng H, Fu Q and Zhou Y (2022) Effects of nitrogen addition and root fungal inoculation on the seedling growth and rhizosphere soil microbial community of *Pinus tabulaeformis*. *Front. Microbiol.* 13:1013023. doi: 10.3389/fmicb.2022.1013023

Effects of nitrogen addition and root fungal inoculation on the seedling growth and rhizosphere soil microbial community of *Pinus tabulaeformis*

Lingjie Xu[1], Xiaoyun Niu[1], Xia Li[2], Yanyan Zheng[1], Hualei Feng[1], Qiang Fu[1] and Yong Zhou[1]*

[1]Country College of Landscape Architecture and Tourism, Hebei Agricultural University, Baoding, China, [2]School of Life Sciences, Hebei University, Baoding, China

Nitrogen (N) availability is significant in different ecosystems, but the response of forest plant-microbial symbionts to global N deposition remains largely unexplored. In this study, the effects of different N concentration levels on four types of fungi, *Suillus granulatus* (Sg), *Pisolithus tinctorius* (Pt), *Pleotrichocladium opacum* (Po), and *Pseudopyrenochaeta* sp. (Ps), isolated from the roots of *Pinus tabulaeformis* were investigated *in vitro*. Then, the effects of the fungi on the growth performance, nutrient uptake, and rhizosphere soil microbial community structure of *P. tabulaeformis* under different N addition conditions (0, 40, and 80kg hm^{-2} $year^{-1}$) were examined. The biomass and phytohormone contents of the Sg, Pt and Po strains increased with increasing N concentration, while those of the Ps strain first increased and then decreased. All four fungal strains could effectively colonize the plant roots and form a strain-dependent symbiosis with *P. tabulaeformis*. Although the effects depended on the fungal species, the growth and root development of inoculated seedlings were higher than those of uninoculated seedlings under N deficiency and normal N supply conditions. However, these positive effects disappeared and even became negative under high N supply conditions. The inoculation of the four fungal strains also showed significant positive effects on the shoot and root nutrient contents of *P. tabulaeformis*. Fungal inoculation significantly increased different microbial groups and the total soil microorganisms but decreased the microbial diversity under N deficiency stress. In summary, exogenous symbiotic fungal inoculations could increase the growth performance of *P. tabulaeformis* under N deficiency and normal N supply conditions, but the effects were negative under excessive N addition.

KEYWORDS

dark septate endophytes, ectomycorrhizal fungi, growth characteristics, soil nutrients, soil microorganisms

Introduction

In recent years, atmospheric nitrogen (N) deposition has become one of the important phenomena of global climate change. Studies have shown that atmospheric N deposition has adverse effects on terrestrial ecosystems, and these effects are mainly related to soil N enrichment and increases in available N. In addition, N deposition can change the global carbon cycle and plant diversity, which will have a profound impact on the structure and function of terrestrial ecosystems (Schrijver et al., 2011; Phoenix et al., 2012; Liu et al., 2013). As an important part of terrestrial ecosystems, the soil microbial community plays an important role in the whole forest ecosystem. N deposition changes both the N pools and the carbon/nitrogen (C/N) ratio of the substrates where these microorganisms are found, resulting in corresponding changes in the structure and function of the soil microbial community (Compton et al., 2004; Zhou et al., 2020). The effects on specific microbial populations, such as ectomycorrhizal fungi and dark septate endophytes, will determine the forest plant community structure and key ecosystem processes, such as litter decomposition, N fixation and nitrification (Blaško et al., 2013). N utilization by symbiotic fungi of plant roots is an essential aspect of their ecosystem function, and it is important to understand how these changes affect the N forms used by fungi (Zhang et al., 2019). Therefore, it is extremely important to study the interaction between soil fungi and forest plants in response to the rapid increase in N deposition.

Previous studies showed that Pinaceae trees were obligate to ectomycorrhizal fungi, whereas recent research reported that dark septate endophytes were also the main root-associated fungi of pine (Deng et al., 2020; Gehring et al., 2020; Landolt et al., 2020; Chu et al., 2016, 2018, 2021). It is well known that ectomycorrhizal fungi have tremendous effects on plants, such as facilitating water and nutrient uptake in host plants, improving plant growth, aiding in the accumulation of metabolites, and conferring resistance to host plants against pathogens and other abiotic stresses (Smith and Read, 2008; van der Heijden et al., 2015; Sebastiana et al., 2019; Chu et al., 2021). Ectomycorrhizal fungi can not only affect the host plant but also change the soil microenvironment of the host (Talbot et al., 2008; Chu et al., 2021). Previous studies have found that mycorrhizal symbiosis is affected by N addition (Maaroufi, 2019). When the soil N content is limited or low, it can promote mycorrhizal growth (Nehls and Plassard, 2018). However, with the increase in N input, there were differences in the effects on mycorrhizal symbionts, and the degree of difference depended on the amount and time of N deposition in the ecosystem, initial soil N level, and vegetation type (Lilleskov et al., 2002; Maaroufi, 2019). Some studies have shown that the fruiting body yield and biomass of ectomycorrhizal fungi significantly decrease with the increase in N deposition and that long-term N excess can gradually reduce the species richness of ectomycorrhizal fungi, thus changing the community structure composition of ectomycorrhizal fungi (Lilleskov et al., 2002; Hasselquist and Högberg, 2014). At the same time, the soil microbial activity has a close relationship with the plants, soil pH and soil nutrient content, and thus, excessive N will not only directly affect the abundance, diversity and activities of soil microbes but may also indirectly affect plants or mycorrhizal symbionts by changing the mineral nutrient transformation and availability in soil (Leff et al., 2015; Chen et al., 2019). Therefore, we assume that ectomycorrhizal fungal inoculation under N deposition can not only affect the growth and physiological characteristics of host plants but also have an important impact on the soil microbial community in the forest ecosystem where the host is located.

Dark septate endophytes have a wide ecosystem distribution and variable effects on the growth of host plants (Ruotsalainen et al., 2021). Much research has indicated that dark septate endophytes have a similar function to mycorrhizal fungi (Jumpponen, 2011; Surono and Narisawa, 2017; Santos et al., 2021). Dark septate endophytes are a large group of endophytic fungi in plant roots. They mainly colonize the inside of root cells or their intercellular spaces and form dark septate mycelia and microsclerotia (Jumpponen et al., 1998; Mandyam and Jumpponen, 2005). Normally, dark septate endophytes are not limited to specific plant species, and can colonize plant roots in most taxonomic groups in all major biomes of the world, especially in heavy-metal-polluted, drought, alpine, polar and other adverse ecosystems (Barrow, 2003; Mandyam and Jumpponen, 2005; Knapp et al., 2012). The effects of dark septate endophytes on host plants are variable, depending on the combination of host symbiotic plants and fungal species (Newsham, 2011). Studies have shown that dark septate endophytes can significantly promote plant growth (Mayerhofer et al., 2013; Ban et al., 2017; Surono and Narisawa, 2017), nutrient absorption and the stress resistance of host plants (Mandyam et al., 2010; Vergara et al., 2017; Li et al., 2019). Previous studies on the effects of dark septate endophytic inoculation on host stress resistance mostly considered heavy metal pollution (Likar and Regvar, 2013; Berthelot et al., 2016), drought (Santos et al., 2017; Li et al., 2019; He et al., 2022) and pathogen stress (Khastini et al., 2012; Surono and Narisawa, 2018). For example, dark septate endophytes can be used as biocontrol agents for many pathogenic microorganisms and can reduce the adverse effects of plant diseases on plant growth (Terhonen et al., 2016; Surono and Narisawa, 2018). Additionally, dark septate endophytes can enhance photosynthesis, osmotic regulation, and the antioxidant capacity of host plants (Santos et al., 2017; Zhang Q. et al., 2017; Li et al., 2019) to improve the drought resistance of plants. However, the ecological roles of dark septate endophytes with regards to the soil N status are not well known.

Pinus tabulaeformis Carr., a coniferous evergreen tree of Pinaceae, is characterized by a well-developed root system, rapid growth, strong ecological adaptability and stress resistance and is a pioneer tree for vegetation restoration in a variety of stress environments (Liu et al., 2019; Zeng et al., 2020). Research has found that there are a variety of ectomycorrhizal fungi in the roots of *P. tabulaeformis* (Hibbett and Matheny, 2009; Wang and Guo, 2010). It has a strong dependence on ectomycorrhizal fungi to

absorb water and mineral nutrients through mycorrhizae and improve stress resistance (Huang et al., 2008; Zhang and Tang, 2012; Wen et al., 2017; Zhang H. et al., 2017). In addition to ectomycorrhizal fungi, dark septate endophytes also widely colonize the roots of *P. tabulaeformis*, but there are relatively few studies on the symbiotic relationship between dark septate endophytes and *P. tabulaeformis* at present (Gehring et al., 2020; Chu et al., 2021). The ecological function of dark septate endophytes and whether they affect the growth and stress resistance of mycorrhizal *P. tabulaeformis* require further research. Hence, in this study, we conducted two experiments using two ectomycorrhizal fungal strains and two dark septate endophyte strains isolated from *P. tabulaeformis* to test (1) the growth performance under different N addition levels in pure cultures and (2) the effects of inoculation with these fungi on the performance of *P. tabulaeformis* plants and the soil microbial community in an inoculation experiment under different N supply conditions. Improving the growth of *P. tabulaeformis* will also be a better use of plant root-associated fungal resources, providing a theoretical basis for maintaining the stability of forest ecosystems. We expect that our results will help determine which inoculated fungi could adapt to the change in the N environment and reveal whether they have the potential for improving the stress tolerance and symbiotic performance of plants under N content variation.

Materials and methods

Fungal isolates and plant materials

The four fungi applied in these experiments were isolated from the roots of *P. tabulaeformis* in the Wuling Mountain Nature Reserve, Hebei Province (117°17′–117°35′E, 40°29′–40°38′N) and were preserved in the Laboratory of Garden Plant Ecology, Hebei Agricultural University, China. These fungi were identified as two ectomycorrhizal fungi, *Suillus granulatus* (Sg) and *Pisolithus tinctorius* (Pt), and two dark septate endophytes, *Pleotrichocladium opacum* (Po) and *Pseudopyrenochaeta* sp. (Ps), by morphological characteristics and phylogenetic analyses of nuclear ribosomal DNA (nrDNA) internal transcribed spacer (ITS) sequences (Supplementary Figures S1,2). All strains were grown on potato dextrose agar (PDA) culture medium for 2 weeks at 27°C in the dark.

Mature seeds of *P. tabulaeformis* were also collected from natural populations in the Wuling Mountain Nature Reserve, China, and stored at 4°C. Before the experiment, the seeds were surface-sterilized for 1 h in 0.5% $KMnO_4$ solution and then washed 4 times with sterilized distilled water. After that, the seeds were immersed in 40°C sterilized distilled water for 24 h. The seeds were pregerminated on sterile gauze in Petri dishes (9 cm) at 25°C. During the incubation period, the seeds were rinsed with sterilized water twice a day. Seedlings with fully developed cotyledons were transferred to incubation plates containing autoclaved substrate and incubated in a greenhouse at room temperature. The seedlings were watered regularly to avoid water shortage.

Experiment 1

Effects of N addition on the fungi *in vitro*

The growth of the four isolates under different N addition conditions was tested in a preliminary experiment in liquid culture. The experiment was performed under sterile conditions, and the basal medium was a modification of modified Melin-Norkrans (MMN) medium (pH 5.5), in which NH_4NO_3 was the only N source. The different N concentrations tested were 0 (N free), 0.0053 (low N), 0.053 (medium N) and 0.530 (high N) $g l^{-1}$. Two disks of mycelium (5 mm) were cut from the edge of actively growing 21-day-old colonies of each isolate and inoculated into a 9-cm Petri dish containing 30 ml of MMN solid medium and into a 250-ml Erlenmeyer flask containing 100 ml of MMN liquid medium. Five replicates were performed per strain per N concentration. Then, the Petri dishes were placed in a thermostatic incubator and incubated on a shaker at 150 rpm at 27°C for 20 days in the dark. Upon harvest, the colony diameter on the solid medium was measured; the fungal mycelia in the liquid medium were filtered and washed with sterilized distilled water, and then the fungal mycelia were weighed after drying to a constant weight at 80°C to determine the biomass production. The filtrate was collected for the analysis of the hormone contents.

Determination of the hormone contents

The analysis of hormone contents (IAA and GA_3) was performed using high-performance liquid chromatography (HPLC). Briefly, after incubation for 20 days, 20 ml of filtrate of the liquid culture medium was collected and then purified and concentrated to 2.0 ml using a C18 solid-phase extraction column. HPLC was performed using a Thermo U3000 Syncronis C18 column (250 mm × 4.6 mm, particle size 5 μm) with deionized water and acetonitrile (volume ratio of 3:7) as the mobile phase. The flow rate, injection volume, detection wavelength, and column temperature were 1 ml min^{-1}, 20 μl, 210 nm and 30°C, respectively.

Experiment 2

Pot experiment of *Pinus tabulaeformis*

The pot experiment was performed in a greenhouse using a completely randomized design in a 5 × 3 factorial arrangement with fungal inoculation treatment (noninoculated control (CK), Sg, Pt, Po and Ps) and N addition treatment (N free; medium N;

high N) as the variables. Each treatment was replicated five times, totaling 75 experimental pots. Seedlings of *P. tabulaeformis* were cultured as previously described. Seedlings of uniform size were selected and transplanted into pots (15 cm in diameter and 18 cm in height, 3 seedlings per pot) containing 2 kg of autoclaved (90 min at 121°C) growth substrate, which consisted of a 1:1 (*v*/*v*) mixture of river sand and soil (< 2 mm). With respect to the fungal inoculation treatments, two 5-mm-diameter fungal mycelial discs cut from a 14-day-old PDA culture medium were inoculated within 1 cm of the roots of the *P. tabulaeformis* seedlings (Ban et al., 2017; Li et al., 2019). With respect to the noninoculated treatments, two 5-mm discs removed from PDA medium without any fungi were inoculated. All pots were placed in a greenhouse at a mean temperature of 27°C/22°C day/night, a 14 h/10 h photoperiod and 60% mean relative air humidity.

Thirty days after inoculation, the mycorrhizal infection rate was detected by microscopic examination and the staining methods of Phillips and Hayman (1970). After the formation of mycorrhizae was determined, the N addition treatments were conducted. The different N-level treatments were controlled by the addition of modified Hoagland nutrient solution, with NH_4NO_3 as the only N source. Three N concentrations (0 kg hm^{-2} $year^{-1}$, N free, 40 kg hm^{-2} $year^{-1}$, medium N; and 80 kg hm^{-2} $year^{-1}$, high N) were applied to the pots. During the experiment, 200 ml of nutrient solution was added once a week per pot. The positions of the pots were randomly rotated each week to minimize location effects. Finally, the plants were harvested after 6 months of treatment.

Plant biomass and root morphology traits

Prior to harvest, the plant height and ground diameter in each pot were recorded. Plant shoots and roots were subsequently harvested separately. The roots were washed carefully with deionized water and scanned with a desktop scanner (EPSON Perfection V800 Photo, Japan). Several morphological traits of roots (such as total root length, root surface area, root volume and average root diameter) were determined using the WinRHIZO image analysis system (Regent Instrument Inc., Quebec, Canada; Chen et al., 2012). The roots were collected after scanning, and a few root samples were randomly selected to analyze fungal colonization. The remaining roots and fresh shoots were dried at 80°C to constant weight for at least 48 h to calculate the dry weight and water content.

Fungal colonization rates

Ectomycorrhizal root colonization rates were estimated by microscopic examination of the root tips in six different root sections (3–4 cm) in each of the seedlings within each treatment. The percentage of root tips with distinct ectomycorrhizal structures was calculated by determining the number of mycorrhizal versus nonmycorrhizal root tips in each of the treatments (Brundrett et al., 1996). To evaluate whether the roots were colonized by dark septate endophytes, the fungal structures within the roots were stained with trypan blue (Phillips and Hayman, 1970) and observed under an optical microscope. For each treatment, approximately 30 1-cm segments of fine roots were randomly selected and placed on slides and then observed under a microscope.

Mycorrhizal growth response

The mycorrhizal growth response (MGR) of *P. tabulaeformis* was calculated according to the following equations based on van der Heijden (2002): if $M > NM_{mean}$, then $MGR\,(\%) = 100 \times (1 - NM_{mean}/M)$, but if $M < NM_{mean}$, then $MGR\,(\%) = 100 \times (-1 + M/NM_{mean})$, where M is the plant total dry weight in the given replicate of the fungal inoculation treatment and NM_{mean} is the mean total dry weight in the corresponding noninoculated treatment. Positive values for MGR indicated that plant growth was promoted by fungi, and negative values indicated that plant growth was suppressed by fungi.

Determination of plant nutrient contents

Dried powder samples (approximately 0.1 g) of shoots and roots were immersed in H_2SO_4 solution and heated for digestion until colorless and transparent. The cooled digestion solution was diluted to 100 ml by adding deionized water. The N concentrations of the plants were analyzed using the Kjeldahl method, the P concentrations were measured by the molybdenum-antimony colorimetric method, and the K concentrations were determined by atomic absorption spectrophotometry (Bao, 2000).

Soil microbial community composition

The composition of the rhizosphere soil microbial community was determined by phospholipid fatty acid (PLFA) analysis (Buyer and Sasser, 2012). PLFA analysis is widely used as a measurement of soil microbial biomass and community composition. The separation and identification of extracted fatty acids were performed on an Agilent 7,890 gas chromatograph and 5,975 mass spectrometer (Agilent Technologies, Wilmington, DE, United States) with 19-alkyl acid as the internal standard. The abundance of individual fatty acids was determined as the relative nmol per g of dry soil, and standard nomenclature was used. For the statistical analysis of the PLFA data, the concentrations of fatty acids were summed into different biomarker groups and used to estimate their respective biomasses. The gram-positive (G+) bacterial biomass was calculated as the sum of the PLFAs 14:1ω7c, iso14:0, anteiso14:0, iso15:1ω9c, and iso15:1ω6c. The gram-negative (G−) bacterial biomass was calculated as the sum of the PLFAs 14:1ω9c, 14:1ω8c, 14:1ω7c, 14:1ω5c, 15:1ω9c, 15:1ω8c,

TABLE 1 Analysis of variance (ANOVA) for the effects of fungal species (fungi) and nitrogen addition treatment (N) on the colony diameter, biomass and hormone contents (IAA and GA_3) of four fungi.

	Fungi		N		Fungi × N	
	F	*P*	*F*	*P*	*F*	*P*
Colony diameter	567.317	**<0.001**	136.240	**<0.001**	109.388	**<0.001**
Biomass	388.357	**<0.001**	211.756	**<0.001**	94.645	**<0.001**
IAA	0.962	0.422	14.638	**<0.001**	3.156	**0.008**
GA_3	2.997	**0.045**	251.392	**<0.001**	18.059	**<0.001**

Significant *p* values are in bold.

15:1ω7c, and 15:1ω6c. The actinomycete biomass was calculated as the sum of the PLFAs 16:0 10-methyl, 17:0 10-methyl, and 18:0 10-methyl. The fungal biomass was calculated as the sum of the PLFAs 18:1ω9c, 18:2ω6,9c, 18:3ω6,9,12c and 16:1ω5c (Rojas et al., 2016). The sum of the PLFA biomarkers detected in each sample was considered to represent the total biomass of the soil microbial community.

The soil microbial community diversity was calculated with the Shannon–Weaver diversity index (*H*) based on the PLFA profiles using the following formula: $H = -\Sigma P_i \ln P_i$, where P_i refers to the ratio of the concentration of each PLFA to the total PLFA concentration in one soil sample and *n* is the number of PLFAs detected in each soil sample. Each PLFA was considered to be representative of one species (Frostegård et al., 2010; Gui et al., 2017; Wang et al., 2019).

Statistical analyses

All analyses of variance (ANOVAs) were performed with SPSS software (Version 21.0, SPSS, Chicago, IL, United States). For the first experiment, two-way ANOVA was performed to analyze the effects of the fungal species (E) and N addition treatment (N) on the colony diameter, biomass and hormone content of the four fungi. For the second experiment, two-way ANOVA was performed to examine the effects of fungal inoculation (E), N addition treatment (N), and their interactions on the dry weight, root morphological traits, nutrient contents and soil microbial community structure. The effect of fungal inoculation on the soil microbial community composition consisting of all the PLFA markers was conducted by using principal coordinate analysis (PCoA) based on Bray–Curtis dissimilarity with R software (3.5.2; R Development Core Team 2015). Permutational multivariate analysis of variance (PERMANOVA) was used to test the effects of fungal inoculation and N addition treatment on community dissimilarity (Chen et al., 2019; Jin et al., 2022). All data in each experiment were tested for normality and homogeneity of variance before statistical analyses. The differences between the means among the different treatments were analyzed by Tukey's HSD *post hoc* tests. The criterion for statistical significance was $p < 0.05$.

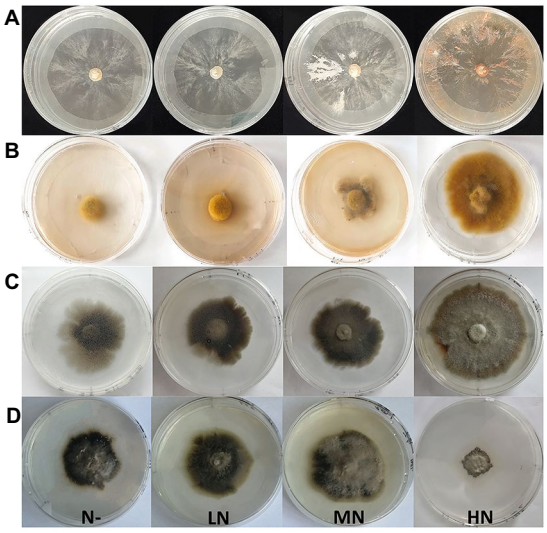

FIGURE 1
Colony morphology of four fungi under different nitrogen concentrations (N free, low N, medium N, high N). **(A-D)**, Colony morphology of Sg, Pt, Po and Ps under the nitrogen addition treatments. Sg, *Suillus granulatus*; Pt, *Pisolithus tinctorius*; Po, *Pleotrichocladium opacum*; Ps, *Pseudopyrenochaeta* sp.

Results

Experiment 1

Effects of N addition on the fungi *in vitro*

Different N concentrations had different effects on the colony diameters of the four fungi (Table 1; Figure 1). The colony diameters of the Sg, Pt and Po strains increased with increasing N concentration; in particular, the colony diameters of the three strains were significantly higher than those of the other treatments under the high N treatment (Figure 2A). The colony diameter of the Ps strain first increased and then decreased with increasing N concentration; the size was the largest under the medium N treatment and significantly smaller under the other N concentrations, particularly under the high N treatment (Figure 2A). The effect trend of the different N concentrations on the biomass of the four fungi was similar to that on the colony diameter. The biomass of the Sg, Pt and Po strains increased with increasing N concentration and was significantly higher under the high N treatment (Figure 2B). The biomass of the Ps strain first increased and then decreased with increasing N concentration, with the biomass of the Ps strain under the medium N treatment being significantly higher than that under the other treatments (Figure 2B). In general, the biomass accumulations of the two dark septate endophytes strains, Po and Ps, were better than those of the two ectomycorrhizal fungi strains, Sg and Pt, under all nitrogen concentrations.

The interaction between fungal species and nitrogen concentration significantly affected the contents of the two hormones (Table 1). The contents of IAA and GA_3 of the Sg, Pt

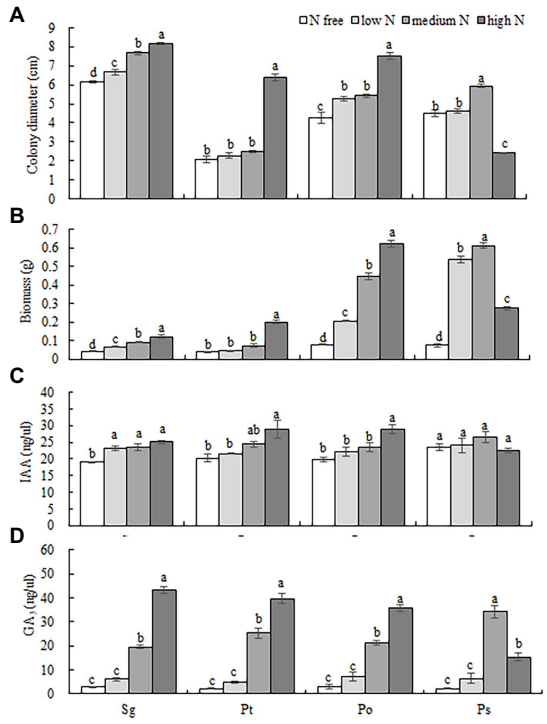

FIGURE 2
Effects of different nitrogen concentrations (N free, low N, medium N, high N) on the colony diameter **(A)**, biomass **(B)** and hormone contents (IAA and GA_3) **(C,D)** of four fungi. Different letters above the error bars indicate a significant difference at $p<0.05$. Sg, *Suillus granulatus*; Pt, *Pisolithus tinctorius*; Po, *Pleotrichocladium opacum*; Ps, *Pseudopyrenochaeta* sp.

and Po strains increased with increasing nitrogen concentration and reached their highest values under the high N treatment. However, the IAA content of the Ps strain showed no significant difference under different nitrogen concentrations, and the GA_3 content showed a trend of first increasing and then decreasing with increasing nitrogen concentration, with the GA_3 content under the medium N treatment being significantly higher than those under the other nitrogen levels (Figures 2C,D).

Experiment 2

Growth performance of *Pinus tabulaeformis*

Both Sg and Pt could form ectomycorrhizae with *P. tabulaeformis* seedlings (Supplementary Figures S3A–F). The front end of the root system of mycorrhizal seedlings was enlarged and thickened and round like a shield. The mycelia of the two dark septate endophytes invaded the cortical intercellular space of the seedling root, grew along the longitudinal axis and formed a loose network structure. Dark septate endophytes also invaded cells and formed a tightly packed cell cluster of enlarged, round, thickened cells inside cortical root cells, forming a microsclerotium structure (Supplementary Figures S3G,H). The noninoculated control did not form ectomycorrhizae or dark septate endophytes structures in the roots of *P. tabulaeformis* seedlings. Two-way ANOVA was conducted for each treatment of seedlings, and the results showed that the colonization rate of each treatment reached more than 60%. The seedling colonization rates of Sg, Pt and Po increased with increasing N concentration, while the seedling infection rates of Ps increased first and then decreased with increasing N concentration (Supplementary Figure S4).

The ground diameter of inoculated seedlings was significantly higher than that of noninoculated seedlings ($p < 0.05$; Table 2). The height, underground biomass and total biomass of seedlings were significantly affected by fungal inoculation, the N addition level and their interaction (Table 2). Under the N-free and medium N treatments, Sg and Pt inoculation significantly increased the plant height and underground and total biomass of *P. tabulaeformis* seedlings, while under the high N treatment, both Sg and Pt inoculation decreased the underground and total biomass of the seedlings. Under the N-free treatment, Po inoculation significantly increased the underground and total biomass of *P. tabulaeformis* seedlings, while Ps inoculation significantly increased the total biomass. Under the MH treatment, Po and Ps inoculation increased the plant height and underground and total biomass of the seedlings, but Po and Ps inoculation decreased the plant height and underground and total biomass under the high N treatment (Figures 3A–C).

There was a significant interaction between fungal inoculation and nitrogen addition treatment on the mycorrhizal growth response of seedlings (Table 2). With the increase in nitrogen concentration, the growth response of Sg seedlings first increased and then decreased, while the growth response of Pt, Po and Ps seedlings decreased (Figure 3D). Under the N-free and medium N treatments, the values of the mycorrhizal growth response were positive, indicating that inoculation had a positive effect on the growth of *P. tabulaeformis* seedlings, while the values of seedlings treated by all inoculations were negative under the high N treatment, indicating that inoculation had an inhibitory effect on the growth of seedlings when N was in excess. Under the N-free treatment, the mycorrhizal growth responses of Pt- and Po-inoculated seedlings were significantly higher than that of Sg-inoculated seedlings, while the growth response of Sg-inoculated seedlings was the highest and significantly higher than that of Po-inoculated seedlings under the medium N treatment, indicating that the Sg strain had a better growth effect under the medium N treatment. Under the high N treatment, the value of Pt inoculation was the highest and significantly higher than those of Po and Ps inoculation, while the mycorrhizal growth response of Ps inoculation was the lowest, indicating that Ps inoculation had the highest inhibitory effect on plants (Figure 3D).

TABLE 2 Analysis of variance (ANOVA) for the effects of fungal inoculation (Fungi) and nitrogen addition treatment (N) on growth and physiological parameters and microbial composition in the rhizosphere soil of *Pinus tabulaeformis*.

	Fungi		N		Fungi × N	
	F	*p*	*F*	*p*	*F*	*p*
Fungi colonization rate	45.881	**<0.001**	120.735	**<0.001**	79.895	**<0.001**
Plant height	19.885	**<0.001**	62.675	**<0.001**	6.060	**<0.001**
Ground diameter	8.220	**<0.001**	89.460	**<0.001**	1.975	0.084
Shoot dry weight	1.712	0.173	46.127	**<0.001**	2.140	0.063
Root dry weight	6.979	**<0.001**	115.226	**<0.001**	32.099	**<0.001**
Total dry weight	4.193	**<0.001**	96.866	**<0.001**	8.461	**<0.001**
Mycorrhizal growth response	5.561	**0.005**	179.965	**<0.001**	3.537	**0.012**
Total root length	21.519	**<0.001**	304.060	**<0.001**	4.048	**0.002**
Root surface area	41.821	**<0.001**	98.026	**<0.001**	17.421	**<0.001**
Root volume	27.442	**<0.001**	405.086	**<0.001**	45.573	**<0.001**
Average root diameter	12.492	**<0.001**	35.555	**<0.001**	28.349	**<0.001**
Shoot N concentration	3.311	**0.023**	170.377	**<0.001**	3.087	**0.012**
Shoot P concentration	20.156	**<0.001**	215.700	**<0.001**	3.746	**0.004**
Shoot K concentration	16.939	**<0.001**	251.842	**<0.001**	3.019	**0.013**
Root N concentration	20.005	**<0.001**	93.647	**<0.001**	2.359	**0.042**
Root P concentration	30.805	**<0.001**	210.569	**<0.001**	15.254	**<0.001**
Root K concentration	23.139	**<0.001**	463.239	**<0.001**	34.561	**<0.001**
Gram-positive bacteria	5.266	**0.002**	25.013	**<0.001**	1.919	0.094
Gram-negative bacteria	19.857	**<0.001**	45.345	**<0.001**	0.961	0.484
Fungi	3.807	**0.013**	21.142	**<0.001**	0.406	0.908
Actinomycetes	5.802	**0.001**	86.796	**<0.001**	3.114	**0.011**
Total PLFAs	29.905	**<0.001**	152.590	**<0.001**	2.528	**0.031**
Shannon–Weaver index	1.349	0.275	20.992	**<0.001**	3.203	**0.009**

Significant *p* values are in bold.

Root morphology and development of *Pinus tabulaeformis*

The total root length, root surface area, root volume and average root diameter of seedlings were significantly affected by fungal inoculation, nitrogen addition and their interaction (Table 2). The root indexes of inoculated seedlings first increased and then decreased with increasing nitrogen concentration (Figure 4). Under the N-free treatment, the root volume of Sg-inoculated seedlings was significantly higher than that under CK; the total root length, root surface area and root volume of Pt-inoculated seedlings were significantly higher than those under CK; the total root length and root volume of Po-inoculated seedlings were significantly higher than those under CK; and the root volume and average root diameter of P-inoculated seedlings were significantly higher than those under CK (Figure 4). Under the medium N treatment, the total root length, root surface area and root volume of Sg- and Pt-inoculated seedlings were significantly higher than those under CK, and the root surface area of plants inoculated with Pt was the largest; the total root length, root volume and average diameter of Po-inoculated seedlings were significantly higher than those under CK, and the total root length and average diameter were also significantly higher than those of the other inoculation treatments; and the total root length and root volume of Ps-inoculated seedlings were significantly higher than those under CK (Figure 4). Under the high N treatment, only the total root length of Po-inoculated seedlings was significantly higher than that under CK, while the root surface area, total volume and root diameter of the other fungus-inoculated seedlings were lower than those under CK (Figure 4).

Nutrient uptake of *Pinus tabulaeformis*

The effects of fungal inoculation, nitrogen addition treatment and their interaction on the nutrient concentrations in the shoots and roots of *P. tabulaeformis* seedlings were significant (Table 2). Under different nitrogen concentration conditions, the effects of inoculation on the nutrient concentrations of host plants were positive in most cases (Figure 5). Under the N-free treatment, the concentrations of N, P and K in Sg-, Pt- and Po-inoculated seedlings were higher than those under CK, and the concentrations of N and K in the shoots and roots of Ps-inoculated seedlings were significantly higher than those under CK (Figure 5). Under the medium N treatment, the N, P and K concentrations were higher than those under CK when the seedlings were inoculated with Sg

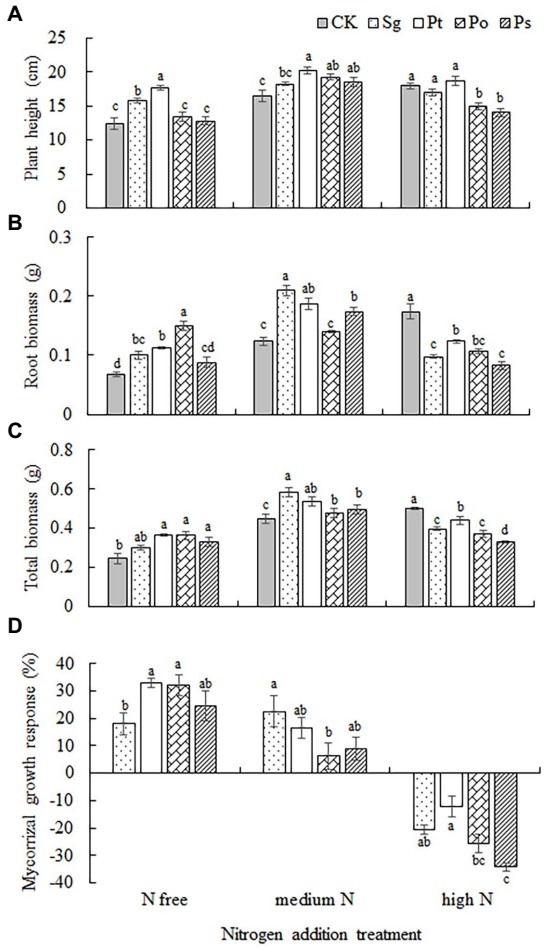

FIGURE 3
Growth performance of inoculated *Pinus tabulaeformis* under the nitrogen addition treatments (N free, medium N, high N). Different letters above the error bars indicate a significant difference at $p<0.05$. **(A)**, plant height; **(B),** root biomass; **(C)**, total biomass; and **(D)**, mycorrhizal growth response. Sg, *Suillus granulatus*; Pt, *Pisolithus tinctorius*; Po, *Pleotrichocladium opacum*; Ps, *Pseudopyrenochaeta* sp.

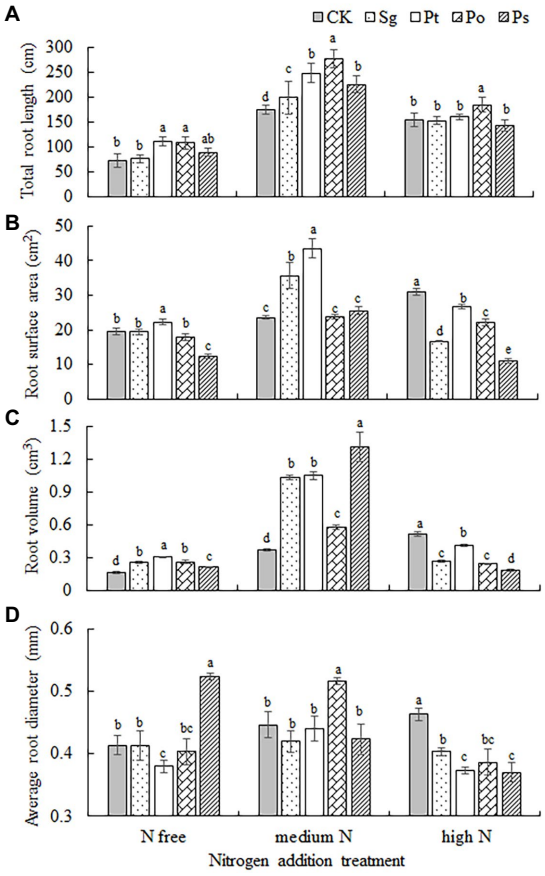

FIGURE 4
Root morphology of inoculated *Pinus tabulaeformis* under the nitrogen addition treatments (N free, medium N, high N). Different letters above the error bars indicate a significant difference at $p<0.05$. **(A)**, total root length; **(B)**, root surface area; **(C)**, root volume; and **(D)**, average root diameter. Sg, *Suillus granulatus*; Pt, *Pisolithus tinctorius*; Po, *Pleotrichocladium opacum*; Ps, *Pseudopyrenochaeta* sp.

and Po; the concentrations of N and shoot K in Pt-inoculated seedlings were significantly higher than those under CK, but the concentration of root K was significantly lower than that under CK; and the concentrations of root N, P and K in Ps-inoculated seedlings were significantly higher than those under CK (Figure 5). Under the high N treatment, the plant P and root N and K concentrations of Sg- and Po-inoculated seedlings were significantly higher than those under CK, and the root P and K concentrations of Pt- and Ps-inoculated seedlings were significantly higher than those under CK (Figure 5).

Soil microbial community composition

There were significant interaction effects between fungal inoculation and N addition treatment on the fatty acid contents of actinomycetes, total PLFAs and Shannon–Wiener index in rhizosphere soil of *P. tabulaeformis* seedlings (Table 2). Compared with CK, Pt and Po inoculation significantly increased the contents of G+ and G– bacterial fatty acids and fungal fatty acids in rhizosphere soil, and Ps inoculation significantly increased the content of G+ bacterial fatty acids regardless of N conditions (Figure 6A). Under the N-free treatment, fungal inoculation significantly increased the fatty acid contents of actinomycetes and total PLFAs compared with those under CK, especially when inoculated with Pt, while the Shannon–Wiener index of the soil microbial community was significantly lower than that under CK, indicating that fungal inoculation reduced the microbial diversity in the rhizosphere soil of seedlings (Figures 6B–D). Under the medium N treatment, the total PLFA contents in the rhizosphere soil of Sg-, Pt- and Po-inoculated seedlings were significantly higher than those of CK seedlings, and the same results were also found in the rhizosphere soil of Pt- and Po-inoculated seedlings under the high N treatment (Figure 6C). The results of the

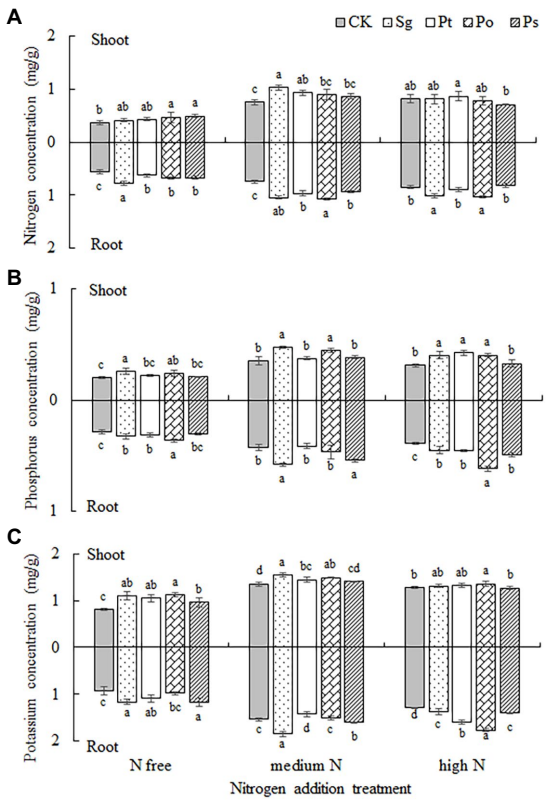

FIGURE 5
Plant **(A)** nitrogen, **(B)** phosphorus, and **(C)** potassium concentrations in the shoots and roots of inoculated *Pinus tabulaeformis* under the nitrogen addition treatments (N free, medium N, high N). Different letters above the error bars indicate a significant difference at $p<0.05$. Sg, *Suillus granulatus*; Pt, *Pisolithus tinctorius*; Po, *Pleotrichocladium opacum*; Ps, *Pseudopyrenochaeta* sp.

principal coordinate analysis (PCoA) showed that the soil microbial community composition of the CK treatment was clearly separated from those of the Pt and Po inoculation treatments (Figure 6E). PERMANOVA showed that fungal inoculation and N addition treatment significantly altered the soil microbial community β-diversity ($p<0.001$; Figure 6E).

Discussion

Under adverse conditions, mycelial biomass is one of the important indicators reflecting fungal resistance (Berthelot et al., 2019). Our results showed that the growth of fungi under different N concentrations was related to the fungal species, and the growth of the Sg, Pt and Po strains increased with increasing N concentration. Especially under the high N treatment, the colony diameter and biomass of the three strains were significantly higher than those of the other treatments. The biomass of the Ps strain first increased and then decreased with increasing N concentration. It has long been established that ectomycorrhizal fungi are of critical importance for improving the N nutrition of plants (Read and Perez-Moreno, 2003; Mikusinska et al., 2013). Ectomycorrhizal fungi increase the surface area for absorbing and can act as an extension of the root system (Wu, 2011; Laliberté, 2017), thus storing N nutrition in the mycelium. Dark septate endophytes can also contribute to the capacity of plants to tolerate abiotic stress (Santos et al., 2021). Dark septate endophytes have been isolated from plant roots in many different natural ecosystems, such as arid, temperate, arctic, tropical, boreal, and alpine ecosystems, which are often characterized by abiotic stress conditions (Jumpponen et al., 1998; Mandyam and Jumpponen, 2005; Rodriguez et al., 2009) and have also been found in anthropogenic ecosystems that lack abiotic stress (Andrade-Linares et al., 2011). Several dark septate endophytes were reported to display stress tolerance *in vitro* (Ban et al., 2012; Berthelot et al., 2016; Santos et al., 2017). Therefore, the complex ecological adaptations developed by dark septate endophytes over a long period of evolution contribute to their tolerance to low nutrient conditions. However, in high nitrogen environments, fungi may be limited by other factors, such as carbon (C; Alberton and Kuyper, 2009; Ekblad et al., 2016). The C to N ratio of the substrate has been hypothesized to affect N source absorption by fungi (Maaroufi, 2019). Therefore, in this study, the Ps strain may be limited by carbon in the substrate under the high N treatment, resulting in a decrease in biomass. Studies have found that some rhizosphere microorganisms can produce IAA, GA_3 and cytokinin substances, which can increase the surface area and number of roots to change the structure of the plant root system. These effects may improve the ability of plants to absorb nutrients from the soil, promote plant growth and development, and resist the negative impact of abiotic stress (Waqas et al., 2012; Priyadharsini and Muthukumar, 2017; Qiang et al., 2019). In this study, the IAA and GA_3 contents of the two ectomycorrhizal fungal strains (Sg and Pt) and two dark septate endophyte strains (Po and Ps) secreted different concentrations of IAA and GA_3 under different nitrogen concentrations, indicating that these fungi may have certain growth-promoting potential and produce plant hormones and then release them into the plant tissue.

Fungi can form complex symbiotic relationships with plants and are widely distributed in many ecosystems (Smith and Read, 2008). Studies have shown that a variety of fungi colonize the roots of *P. tabulaeformis* and improve the adaptability of host plants to different habitats through complex biological pathways (Huang et al., 2008; Wang and Guo, 2010; Zhang and Tang, 2012; Wen et al., 2017; Zhang H. et al., 2017). However, an understanding of the effects of both fungal colonization and N addition together is lacking. In this study, the four fungi successfully colonized the root tissues of *P. tabulaeformis* under all N treatments, and the colonization structures of ectomycorrhizal fungi and dark septate endophytes in the roots were observed, indicating that the changes in N conditions did not affect the effectiveness of colonization of the four fungi. Some previous studies have shown that the mycorrhizal infection rate decreases with increasing soil nitrogen availability (Nilsson et al.,

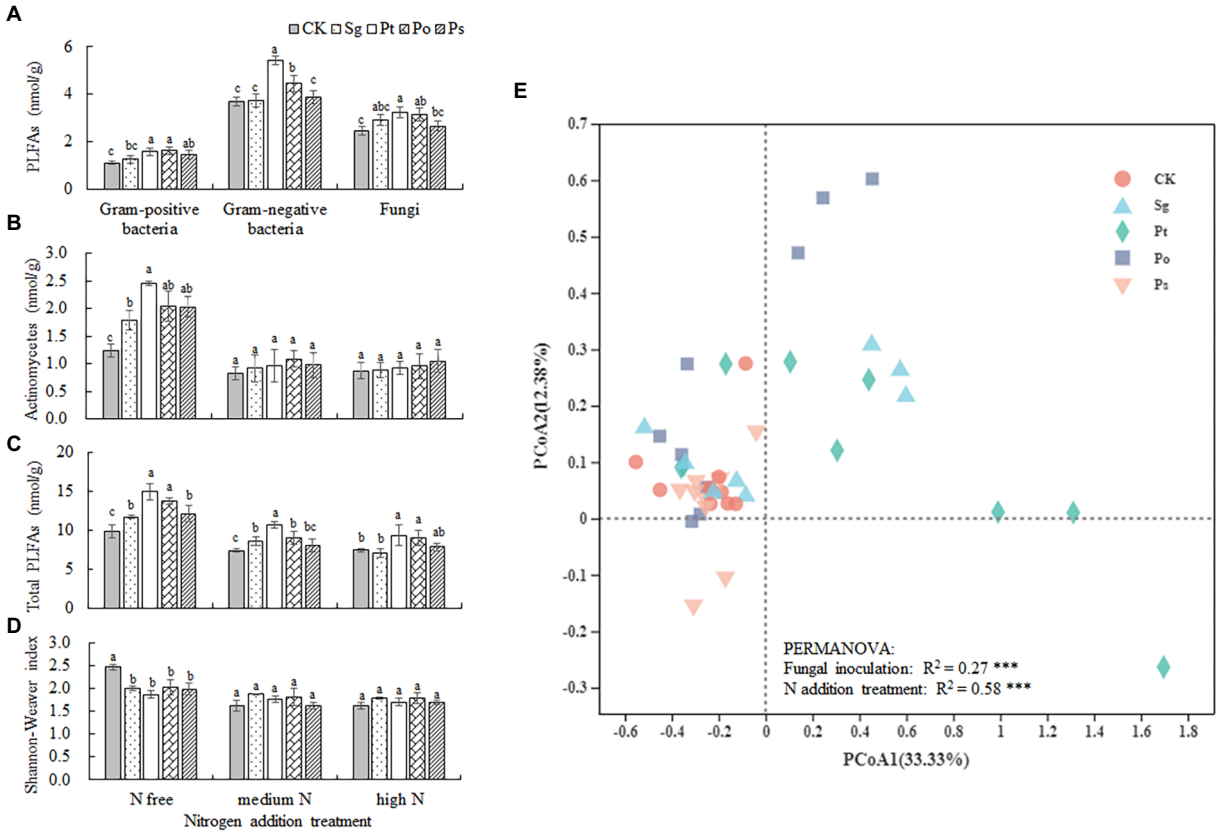

FIGURE 6
Soil microbial functional group abundance in the rhizosphere soil of inoculated *Pinus tabulaeformis* under the nitrogen addition treatments (N free, medium N, high N). Different letters above the error bars indicate a significant difference at $p<0.05$. **(A)**, PLFAs of gram-positive bacteria, gram-negative bacteria and fungi; **(B)**, PLFAs of actinomycetes; **(C)**, total PLFAs; and **(D)**, Shannon–Weaver index. **(E)**, Principal coordinate analysis (PCoA) of the soil microbial community. The data consisted of all of the PLFA markers. PERMANOVA statistics refer to significant effects of fungal inoculation and N addition treatment. Sg, *Suillus granulatus*; Pt, *Pisolithus tinctorius*; Po, *Pleotrichocladium opacum*; Ps, *Pseudopyrenochaeta* sp.; ***$p<0.001$.

2005; Högberg et al., 2010; Kjøller et al., 2012), while other studies have found that the mycorrhizal infection rate of plants remains unchanged or increases with increasing soil N availability (Wallenda and Kottke, 1998; Kou et al., 2015). Our results suggest that the response of host plants to fungal colonization under different N concentrations was related to the fungal species. The seedling colonization rates of Sg, Pt and Po increased with increasing N concentration, which was consistent with the results of in vitro culture, suggesting that high N availability may be beneficial to the growth and physiological metabolism of mycelia of these three fungi and thus promote their plant root colonization ability. The colonization rate of Ps under the high N treatment was significantly lower than that under the medium N treatment, which was in line with the cost–benefit theory based on reciprocal investments and biological markets (Corkidi et al., 2002; Smith and Read, 2008). With the increase in soil N availability, the dependence of the fungi on plant roots was reduced, and the host plants did not need to obtain more N from the mycorrhiza, resulting in a decrease in the fungal colonization rate.

In this study, inoculation with different fungi significantly promoted seedling height, ground diameter, root length and biomass under the N-free and medium N treatments compared with the CK treatment, while seedling growth indexes were reduced to varying degrees at high N levels compared with CK. The extramatrical mycelium of ectomycorrhizal fungi can increase the surface area for absorbing and could act as an extension of the root system, which is an efficient way to exploit larger volumes of soil beyond the root's N-depletion zone (Wu, 2011; Laliberté, 2017). Moreover, our results proved that dark septate endophytes can also increase nutritional availability for plants and thus resemble mycorrhizal symbiosis, enabling generally higher growth rates in plants. After plants are inoculated with exogenous fungi, inoculation treatment can help plants cope with the harm of N deficiency to a certain extent. In addition, the mycorrhizal growth response of all inoculation treatments was negative under the high N treatment, indicating that inoculation had an inhibitory effect on the seedling growth of *P. tabulaeformis*. Liao et al. (2010) conducted a nitrogen addition experiment on annual Chinese fir, and the results also showed that low nitrogen

promoted an increase in seedling biomass, while high nitrogen inhibited seedling growth. Under the condition of adequate soil N availability, the growth-promoting role of inoculated exogenous fungi on *P. tabulaeformis* seedlings can be fully played; however, excessive N addition weakens the ability of fungi to infect plant roots, thus affecting the growth of host plants (Wallenstein et al., 2006; Högberg et al., 2010). Therefore, the N input may change the symbiosis between fungi and host plants, as low N and normal N availability would strengthen the symbiosis between fungi and plants to improve the competitive ability of symbionts, while mycorrhizal benefits will be lowest when N, P or other belowground resources do not limit plant growth because plants will tend to reduce C allocation to roots and mycorrhizas in such an environment (Johnson et al., 2010).

The root system is the primary plant part that senses stress conditions, and roots can respond rapidly through changes in elongation (Li et al., 2019; Hou et al., 2020) and function (Shelden et al., 2016; Liese et al., 2018). Several plant growth-promoting microbes, including ectomycorrhizal fungi and dark septate endophytes, have also been shown to influence the root architecture of plants (López-Coria et al., 2016; González-Teuber et al., 2018; Liese et al., 2019; Hou et al., 2020). In this study, we found that the effects of fungal inoculation on the plant root system were dependent on soil N availability. The four fungi promoted the growth of the root system under low and normal N conditions, although the effects depended on the fungal species. Plants inoculated with Pt and Po exhibited a greater root length, and all of the fungi promoted a higher root volume than that of the control plants under the low N treatment. Significantly greater root length, surface area and volume were observed in the plants inoculated with these fungi under the medium N treatment when compared with the control plants, indicating positive effects on root growth. The development of a deep and extensive root system can regulate the absorption of water and nutrients in soil, which ultimately influences biomass production (Hund et al., 2009). This is one of the reasons why ectomycorrhizal fungal or dark septate endophytic inoculation of host plants enhanced the development of the root system under unstressed conditions (Domínguez-Núñez et al., 2006; Wu, 2011; Álvarez-Lafuente et al., 2018; Li et al., 2019; Xiong et al., 2021). In addition, ectomycorrhizal fungi and dark septate endophytes may alter auxin metabolism within the host root, which can regulate root development and change root architecture (Felten et al., 2009; Waqas et al., 2012; Vayssières et al., 2015; Splivallo et al., 2016; Priyadharsini and Muthukumar, 2017).

Nutrient uptake and plant growth are two parameters that are positively correlated. Most studies on ectomycorrhizal fungi-plant interactions revealed positive effects, and some ectomycorrhizal fungi can increase nutritional availability for plants, enabling generally higher growth rates in plants (Dynarski and Houlton, 2020). It has been suggested that dark septate endophytic inoculation also helped host plants absorb more P and N (Jumpponen et al., 1998), as dark septate endophytes can mineralize proteins and peptides in the soil, making N more available for uptake by plant roots (Upson et al., 2009; Vergara et al., 2017, 2018). Our results showed that the effects of fungal inoculation on the nutrient content of *P. tabulaeformis* seedlings were dependent on the fungal species and N availability. For all of the fungal inoculation treatments, the effect was almost always positive under the N-free and medium N treatments. A previous study using *P. tabulaeformis* found that seedlings inoculated with ectomycorrhizal fungi had a greater biomass and exhibited higher N, P and K contents than nonmycorrhizal seedlings (Lu et al., 2016); Pohjanen et al. (2014) also found that ectomycorrhizal fungi could increase nutrient uptake and growth of Scots pine (*Pinus sylvestris* L.) seedlings. Our study also provided direct evidence that dark septate endophytes may have a similar function to ectomycorrhizal fungi, forming a mutualistic symbiotic relationship with the host (Santos et al., 2021). A large number of extrinsic mycelia in rhizosphere soil can promote the transport, absorption and utilization of mineral elements such as N and P by plants. Dark septate endophytes can promote the growth and biomass accumulation of host plants by decomposing insoluble P and improving the utilization rate of N (Alberton et al., 2010; Vergara et al., 2018; Xu et al., 2020). Hence, the appropriate amount of N addition can increase the soil nutrient utilization of plants in forest ecosystems and reduce the limitation of N deficiency on plant growth.

The rhizosphere microbial community composition is reportedly dependent on the soil nutrient status (Leff et al., 2015; Haas et al., 2018; Chen et al., 2019) and the quantity and quality of root exudates (Marschner and Timonen, 2005; Xie et al., 2019). In this study, the soil microbial community composition could be significantly influenced by the interaction between fungal inoculation and nutrient inputs. The inoculation of the four fungi promoted the abundance of actinomycetes and total soil microorganisms under the N-free treatment, and Pt and Po significantly increased the abundance of soil fungi and G+ and G− bacteria regardless of N conditions. These changes could be related to the modification of growth and nutrient absorption of *P. tabulaeformis* after fungal inoculation, as some microbial groups are an important part of the rhizosphere microbial community that can promote plant growth and soil nutrient cycling (Artursson et al., 2006; Carrasco et al., 2010; Sreevidya et al., 2016; Hinojosa et al., 2019). Previous studies have shown that ectomycorrhizal fungi not only help the host plant to improve growth, nutrient conditions and stress tolerance (Smith and Read, 2008) but also recruit and enrich other microorganisms that are beneficial to themselves and/or plants (Cameron et al., 2013; Gupta and Aggarwal, 2018). Ectomycorrhizal fungi or dark septate endophytes may increase the relative abundances of beneficial rhizosphere fungi and bacteria, which are widely reported to promote plant growth through various mechanisms, including biological N fixation, mineral solubilization, iron chelation, and plant growth hormone secretion (He et al., 2019; Chu et al., 2021; Hou et al., 2021). In addition, our results showed that inoculation with exogenous fungi (ectomycorrhizal fungi or dark septate endophytes) reduced soil microbial species diversity under nutrient deficient conditions, which may be due to increased

competition between the original fungi and exogenous fungi (Chu et al., 2021).

In summary, our study suggests that the four fungi isolated from *P. tabulaeformis* showed good adaptability to different N levels *in vitro*, although the growth performance was dependent on the fungal species. Inoculation with the four fungi improved the growth, root development and nutrient absorption of host plants under the N-free and medium N treatments. However, a high N supply reduced the dependence of host plants on fungi and weakened the symbiotic relationship between fungi and plants. In addition, inoculation with ectomycorrhizal fungi and dark septate endophytes can alter the soil microbial community composition and increase the relative abundances of different microbial groups and total microbial biomass under N deficiency conditions, and these effects might contribute to the improved growth performance of *P. tabulaeformis* after fungal inoculation. Therefore, the rational application of N fertilizer and the inoculation of symbiotic fungi play an important role in improving the growth and afforestation of *P. tabulaeformis*. Future research needs to address the mechanisms behind the nutrient utilization capacity of root-associated fungi and their involvement in plant growth by a more effective way, such as isotopic leveling method.

Data availability statement

The original contributions presented in the study are included in the article/Supplementary material, further inquiries can be directed to the corresponding author.

Author contributions

YZ and XL conceived and designed the experiments and wrote the manuscript, LX, XN, and YYZ performed the research and analyzed the data. HF and QF revised the manuscript. All authors contributed to the article and approved the submitted version.

Funding

This work was supported by National Natural Science Foundation of China (32001112), Youth Natural Science Foundation of Hebei Province (C2020204169), and the starting Scientific Research Foundation for the introduced talents of Hebei Agricultural University (ZD201728).

Conflict of interest

The authors declare that the research was conducted in the absence of any commercial or financial relationships that could be construed as a potential conflict of interest.

Publisher's note

All claims expressed in this article are solely those of the authors and do not necessarily represent those of their affiliated organizations, or those of the publisher, the editors and the reviewers. Any product that may be evaluated in this article, or claim that may be made by its manufacturer, is not guaranteed or endorsed by the publisher.

Supplementary material

The Supplementary material for this article can be found online at: https://www.frontiersin.org/articles/10.3389/fmicb.2022.1013023/full#supplementary-material

References

Alberton, O., and Kuyper, T. W. (2009). Ectomycorrhizal fungi associated with *Pinus sylvestris* seedlings respond differently to increased carbon and nitrogen availability: implications for ecosystem responses to global change. *Glob. Chang. Biol.* 15, 166–175. doi: 10.1111/j.1365-2486.2008.01714.x

Alberton, O., Kuyper, T. W., and Summerbell, R. C. (2010). Dark septate root endophytic fungi increase growth of scots pine seedlings under elevated CO_2 through enhanced nitrogen use efficiency. *Plant Soil* 328, 459–470. doi: 10.1007/s11104-009-0125-8

Álvarez-Lafuente, A., Benito-Matías, L. F., Peñuelas-Rubira, J. L., and Suz, L. M. (2018). Multi-cropping edible truffles and sweet chestnuts: production of high-quality *Castanea sativa* seedlings inoculated with *tuber aestivum*, its ecotype *T. uncinatum*, *T. brumale*, and *T. macrosporum*. *Mycorrhiza* 28, 29–38. doi: 10.1007/s00572-017-0805-9

Andrade-Linares, D. R., Grosch, R., Restrepo, S., Krumbein, A., and Franken, P. (2011). Effects of dark septate endophytes on tomato plant performance. *Mycorrhiza* 21, 413–422. doi: 10.1007/s00572-010-0351-1

Artursson, V., Finlay, R. D., and Jansson, J. K. (2006). Interactions between arbuscular mycorrhizal fungi and bacteria and their potential for stimulating plant growth. *Environ. Microbiol.* 8, 1–10. doi: 10.1111/j.1462-2920.2005.00942.x

Ban, Y., Tang, M., Chen, H., Xu, Z., Zhang, H., and Yang, Y. (2012). The response of dark septate endophytes (DSE) to heavy metals in pure culture. *PLoS One* 7:e47968. doi: 10.1371/journal.pone.0047968

Ban, Y., Xu, Z. Y., Yang, Y., Zhang, H., Chen, H., and Tang, M. (2017). Effect of dark septate endophytic fungus *Gaeumannomyces cylindrosporus* on plant growth, photosynthesis and Pb tolerance of maize (*Zea mays* L.). *Pedosphere* 27, 283–292. doi: 10.1016/s1002-0160(17)60316-3

Bao, S. D. (2000). *Agrochemical Analysis of Soil (in Chinese)*. Beijing: Chinese Agricultural Press, 44–49.

Barrow, J. R. (2003). Atypical morphology of dark septate fungal root endophytes of Bouteloua in arid southwestern USA rangelands. *Mycorrhiza* 13, 239–247. doi: 10.1016/0014-5793(95)01196-L

Berthelot, C., Leyval, C., Chalot, M., and Blaudez, D. (2019). Interactions between dark septate endophytes, ectomycorrhizal fungi and root pathogens in vitro. *FEMS Microbiol. Lett.* 366:fnz158. doi: 10.1093/femsle/fnz158

Berthelot, C., Leyval, C., Foulon, J., Chalot, M., and Blaudez, D. (2016). Plant growth promotion, metabolite production and metal tolerance of dark septate endophytes isolated from metal-polluted poplar phytomanagement sites. *FEMS Microbiol. Ecol.* 92:fiw144. doi: 10.1093/femsec/fiw144

Blaško, R., Högberg, P., Bach, L. H., and Högberg, M. N. (2013). Relations among soil microbial community composition, nitrogen turnover, and tree growth in N-loaded and previously N-loaded boreal spruce forest. *For. Ecol. Manag.* 302, 319–328. doi: 10.1016/j.foreco.2013.02.035

Brundrett, M., Bougher, N., Dell, B., Grove, T., and Malajczuk, N. (1996). *Working With Mycorrhizas in Forestry and Agriculture*. Canberra: Australian Centre for International Agricultural Research.

Buyer, J. S., and Sasser, M. (2012). High throughput phospholipid fatty acid analysis of soils. *Appl. Soil Ecol.* 61, 127–130. doi: 10.1016/j.apsoil.2012.06.005

Cameron, D. D., Neal, A. L., van Wees, S. C., and Ton, J. (2013). Mycorrhiza induced resistance: more than the sum of its parts? *Trends Plant Sci.* 18, 539–545. doi: 10.1016/j.tplants.2013.06.004

Carrasco, L., Gattinger, A., Fliessbach, A., Roldan, A., Schloter, M., and Caravaca, F. (2010). Estimation by PLFA of microbial community structure associated with the rhizosphere of *Lygeum spartum* and *Piptatherum miliaceum* growing in semiarid mine tailings. *Microb. Ecol.* 60, 265–271. doi: 10.1007/s00248-009-9619-4

Chen, Y. L., Dunbabin, V. M., Diggle, A. J., Siddique, K. H. M., and Rengel, Z. (2012). Assessing variability in root traits of wild *Lupinus angustifolius* germplasm: basis for modelling root system structure. *Plant Soil* 354, 141–155. doi: 10.1007/s11104-011-1050-1

Chen, X., Hao, B., Jing, X., He, J., Ma, W., and Zhu, B. (2019). Minor responses of soil microbial biomass, community structure and enzyme activities to nitrogen and phosphorus addition in three grassland ecosystems. *Plant Soil* 444, 21–37. doi: 10.1007/s11104-019-04250-3

Chu, H., Tang, M., Wang, H., and Wang, C. (2018). Pinewood nematode infection alters root mycoflora of *Pinus tabulaeformis* Carr. *J. Appl. Microbiol.* 125, 554–563. doi: 10.1111/jam.13883

Chu, H., Wang, C., Wang, H., Chen, H., and Tang, M. (2016). Pine wilt disease alters soil properties and root-associated fungal communities in *Pinus tabulaeformis* forest. *Plant Soil* 404, 237–249. doi: 10.1007/s11104-016-2845-x

Chu, H. L., Wang, H. H., Zhang, Y. N., Li, Z. M., Wang, C. Y., Dai, D. Q., et al. (2021). Inoculation with ectomycorrhizal fungi and dark septate endophytes contributes to the resistance of *Pinus* spp. to pine wilt disease. *Front. Microbiol.* 12:687304. doi: 10.3389/FMICB.2021.687304

Compton, J. E., Watrud, L. S., Porteous, L. A., and Degrood, S. (2004). Response of soil microbial biomass and community composition to chronic nitrogen additions at Harvard forest. *For. Ecol. Manag.* 196, 143–158. doi: 10.1016/j.foreco.2004.03.017

Corkidi, L., Rowland, D. L., Johnson, N. C., and Allen, E. B. (2002). Nitrogen fertilization alters the functioning of arbuscular mycorrhizas at two semiarid grasslands. *Plant Soil* 240, 299–310. doi: 10.1023/A:1015792204633

Deng, X., Song, X., Halifu, S., Yu, W., and Song, R. (2020). Effects of dark septate endophytes strain A024 on damping-off biocontrol, plant growth and the rhizosphere soil environment of *Pinus sylvestris* var. *mongolica* annual seedlings. *Plants-Basel* 9:913. doi: 10.3390/plants9070913

Domínguez-Núñez, J. A., Serrano, J. S., Rodríguez Barreal, J. A., and Saiz de Omeñaca, J. A. (2006). The influence of mycorrhization with *tuber melanosporum* in the afforestation of a Mediterranean site with *Quercus ilex* and *Quercus faginea*. *For. Ecol. Manag.* 231, 226–233. doi: 10.1016/j.foreco.2006.05.052

Dynarski, K. A., and Houlton, B. Z. (2020). Isotopic constraints on plant nitrogen acquisition strategies during ecosystem retrogression. *Oecologia* 192, 603–614. doi: 10.1007/s00442-020-04606-y

Ekblad, A., Mikusinska, A., Ågren, G. I., Menichetti, L., Wallander, H., Vilgalys, R., et al. (2016). Production and turnover of ectomycorrhizal extramatrical mycelial biomass and necromass under elevated CO_2 and nitrogen fertilization. *New Phytol.* 211, 874–885. doi: 10.1111/nph.13961

Felten, J., Kohler, A., Morin, E., Bhalerao, R. P., Palme, K., Martin, F., et al. (2009). The ectomycorrhizal fungus *Laccaria bicolor* stimulates lateral root formation in poplar and Arabidopsis through auxin transport and signaling. *Plant Physiol.* 151, 1991–2005. doi: 10.1104/pp.109.147231

Frostegård, Å., Tunlid, A., and Bååth, E. (2010). Use and misuse of PLFA measurements in soils. *Soil Biol. Biochem.* 43, 1621–1625. doi: 10.1016/j.soilbio.2010.11.021

Gehring, C., Sevanto, S., Patterson, A., Ulrich, D. E. M., and Kuske, C. R. (2020). Ectomycorrhizal and dark septate fungal associations of pinyon pine are differentially affected by experimental drought and warming. *Front. Plant Sci.* 11:582574. doi: 10.3389/fpls.2020.582574

González-Teuber, M., Urzúa, A., Plaza, P., and Bascuñán-Godoy, L. (2018). Effects of root endophytic fungi on response of *Chenopodium quinoa* to drought stress. *Plant Ecol.* 219, 231–240. doi: 10.1007/s11258-017-0791-1

Gui, H., Hyde, K., Xu, J. C., and Mortimer, P. (2017). Arbuscular mycorrhiza enhance the rate of litter decomposition while inhibiting soil microbial community development. *Sci. Rep.* 7:42184. doi: 10.1038/srep42184

Gupta, M. M., and Aggarwal, A. (2018). "From mycorrhizosphere to rhizosphere microbiome: the paradigm shift" in *Root Biology*. eds. B. Giri, R. Parasad and A. Varma (Cham: Springer), 487–500.

Haas, J. C., Street, N. R., Sjödin, A., Lee, N. M., Högberg, M. N., Näsholm, T., et al. (2018). Microbial community response to growing season and plant nutrient optimisation in a boreal Norway spruce forest. *Soil Biol. Biochem.* 125, 197–209. doi: 10.1016/j.soilbio.2018.07.005

Hasselquist, N. J., and Högberg, P. (2014). Dosage and duration effects of nitrogen additions on ectomycorrhizal sporocarp production and functioning: an example from two N-limited boreal forests. *Ecol. Evol.* 4, 3015–3026. doi: 10.1002/ece3.1145

He, C., Liu, C., Liu, H. F., Wang, W. Q., Hou, J. L., and Li, X. N. (2022). Dual inoculation of dark septate endophytes and *Trichoderma viride* drives plant performance and rhizosphere microbiome adaptations of *Astragalus mongholicus* to drought. *Environ. Microbiol.* 24, 324–340. doi: 10.1111/1462-2920.15878

He, C., Wang, W. Q., and Hou, J. L. (2019). Plant growth and soil microbial impacts of enhancing licorice with inoculating dark septate endophytes under drought stress. *Front. Microbiol.* 10:2277. doi: 10.3389/fmicb.2019.02277

Hibbett, D. S., and Matheny, P. B. (2009). The relative ages of ectomycorrhizal mushrooms and their plant hosts estimated using Bayesian relaxed molecular clock analyses. *BMC Biol.* 7, 1–13. doi: 10.1186/1741-7007-7-13

Hinojosa, M. B., Laudicina, V. A., Parra, A., Albert-Belda, E., and Moreno, J. M. (2019). Drought and its legacy modulate the post-fire recovery of soil functionality and microbial community structure in a mediterranean shrubland. *Glob. Change Biol.* 25, 1409–1427. doi: 10.1111/gcb.14575

Högberg, M. N., Briones, M. J. I., Keel, S. G., Metcalfe, D. B., Campbell, C., Midwood, A. J., et al. (2010). Quantification of effects of season and nitrogen supply on tree below-ground carbon transfer to ectomycorrhizal fungi and other soil organisms in a boreal pine forest. *New Phytol.* 187, 485–493. doi: 10.1111/j.1469-8137.2010.03274.x

Hou, L., Li, X., He, X., Zuo, Y., and Zhao, L. (2021). Effect of dark septate endophytes on plant performance of *Artemisia ordosica* and associated soil microbial functional group abundance under salt stress. *Appl. Soil Ecol.* 165:103998. doi: 10.1016/J.APSOIL.2021.103998

Hou, L., Yu, J., Zhao, L. L., and He, X. L. (2020). Dark septate endophytes improve the growth and the tolerance of *Medicago sativa* and *Ammopiptanthus mongolicus* under cadmium stress. *Front. Microbiol.* 10:3061. doi: 10.3389/fmicb.2019.03061

Huang, Y., Li, T., Huang, Z. J., and Fei, Y. H. (2008). Ectomycorrhizal fungus-induced changes of cu and cd speciation in the rhizosphere of Chinese pine seedlings. *Pedosphere* 18, 758–765. doi: 10.1016/S1002-0160(08)60071-5

Hund, A., Ruta, N., and Liedgens, M. (2009). Rooting depth and water use efficiency of tropical maize inbred lines, differing in drought tolerance. *Plant Soil* 318, 311–325. doi: 10.1007/s11104-008-9843-6

Jin, X., Wang, Z., Wu, F., Li, X., and Zhou, X. (2022). Litter mixing alters microbial decomposer community to accelerate tomato root litter decomposition. *Microbiol. Spectr.* 10:e0018622. doi: 10.1128/spectrum.00186-22

Johnson, N. C., Wilson, G., Bowker, M. A., Wilson, J. A., and Miller, R. M. (2010). Resource limitation is a driver of local adaptation in mycorrhizal symbioses. *Proc. Natl. Acad. Sci. U. S. A.* 107, 2093–2098. doi: 10.1073/pnas.0906710107

Jumpponen, A. (2011). Dark septate endophytes—are they mycorrhizal? *Mycorrhiza* 11, 207–211. doi: 10.1007/s005720100112

Jumpponen, A., Mattson, K. G., and Trappe, J. M. (1998). Mycorrhizal functioning of *Phialocephala fortinii* with *Pinus contorta* on glacier forefront soil: interactions with soil nitrogen and organic matter. *Mycorrhiza* 7, 261–265. doi: 10.1007/s005720050190

Khastini, R. O., Ohta, H., and Narisawa, K. (2012). The role of a dark septate endophytic fungus, *Veronaeopsis simplex* Y34, in fusarium disease suppression in Chinese cabbage. *J. Microbiol.* 50, 618–624. doi: 10.1007/s12275-012-2105-6

Kjøller, R., Nilsson, L. O., Hansen, K., Schmidt, I. K., Vesterdal, L., and Gundersen, P. (2012). Dramatic changes in ectomycorrhizal community composition, root tip abundance and mycelial production along a stand-scale nitrogen deposition gradient. *New Phytol.* 194, 278–286. doi: 10.1111/j.1469-8137.2011.04041.x

Knapp, D. G., Pintye, A., and Kovacs, G. M. (2012). The dark side is not fastidious-dark septate endophytic fungi of native and invasive plants of semiarid sandy areas. *PLoS One* 7:8e32570. doi: 10.1371/journal.pone.0032570

Kou, L., Guo, D. L., Hao, Y., Gao, W. L., and Li, S. G. (2015). Growth, morphological traits and mycorrhizal colonization of fine roots respond differently to nitrogen addition in a slash pine plantation in subtropical China. *Plant Soil* 391, 207–218. doi: 10.1007/s11104-015-2420-x

Laliberté, E. (2017). Below-ground frontiers in trait-based plant ecology. *New Phytol.* 213, 1597–1603. doi: 10.1111/nph.14247

Landolt, M., Stroheker, S., Queloz, V., Gall, A., and Sieber, T. N. (2020). Does water availability influence the abundance of species of the *Phialocephala fortinii* s.l.–*Acephala applanata* complex (PAC) in roots of pubescent oak (*Quercus pubescens*) and scots pine (*Pinus sylvestris*)? *Fungal Ecol.* 44:100904. doi: 10.1016/j.funeco.2019.100904

Leff, J. W., Jones, S. E., Prober, S. M., Barberan, A., Borer, E. T., Firn, J. L., et al. (2015). Consistent responses of soil microbial communities to elevated nutrient inputs in grasslands across the globe. *Proc. Natl. Acad. Sci. U. S. A.* 112, 10967–10972. doi: 10.1073/pnas.1508382112

Li, X., He, C., He, X., Su, F., Hou, L., Ren, Y., et al. (2019). Dark septate endophytes improve the growth of host and non-host plants under drought stress through altered root development. *Plant Soil* 439, 259–272. doi: 10.1007/s11104-019-04057-2

Liao, Y. C., Fan, H. B., Li, Y. Y., Liu, W. F., and Yuan, Y. H. (2010). Effects of simulated nitrogen deposition on growth and photosynthesis of 1-year-old Chinese fir (*Cunninghamia lanceolata*) seedlings. *Acta Ecol. Sin.* 30, 150–154. doi: 10.1016/j.chnaes.2010.04.005

Liese, R., Leuschner, C., and Meier, I. C. (2019). The effect of drought and season on root life span in temperate arbuscular mycorrhizal and ectomycorrhizal tree species. *J. Ecol.* 107, 2226–2239. doi: 10.1111/1365-2745.13181

Liese, R., Lübbe, T., Albers, N. W., and Meier, I. C. (2018). The mycorrhizal type governs root exudation and nitrogen uptake of temperate tree species. *Tree Physiol.* 38, 83–95. doi: 10.1093/treephys/tpx131

Likar, M., and Regvar, M. (2013). Isolates of dark septate endophytes reduce metal uptake and improve physiology of *Salix caprea* L. *Plant Soil* 370, 593–604. doi: 10.1007/s11104-013-1656-6

Lilleskov, E. A., Fahey, T. J., Horton, T. R., and Lovett, G. M. (2002). Belowground ectomycorrhizal fungal community change over a nitrogen deposition gradient in Alaska. *Ecology* 83, 104–115. doi: 10.2307/2680124

Liu, N., Bao, G., and Bao, M. (2019). Response characteristics of Chinese pine (*Pinus tabulaeformis* Carr.) radial growth to climate and drought variability reconstruction in western Liaoning, Northeast China. *Forests* 10:752. doi: 10.3390/f10090752

Liu, X., Zhang, Y., Han, W., Tang, A., Shen, J., Cui, Z., et al. (2013). Enhanced nitrogen deposition over China. *Nature* 494, 459–462. doi: 10.1038/nature11917

López-Coria, M., Hernández-Mendoza, J. L., and Sánchez-Nieto, S. (2016). *Trichoderma asperellum* induces maize seedling growth by activating the plasma membrane H+-ATPase. *Mol. Plant-Microbe Interact.* 29, 797–806. doi: 10.1094/MPMI-07-16-0138-R

Lu, N., Yu, M., Cui, M., Luo, Z. J., Feng, Y., Cao, S., et al. (2016). Effects of different ectomycorrhizal fungal inoculates on the growth of *Pinus tabulaeformis* seedlings under greenhouse conditions. *Forests* 7:316. doi: 10.3390/f7120316

Maaroufi, N. I. (2019). Anthropogenic nitrogen enrichment enhances soil carbon accumulation by impacting saprotrophs rather than ectomycorrhizal fungal activity. *Glob. Change Biol.* 25, 2900–2914. doi: 10.1111/gcb.14722

Mandyam, K., and Jumpponen, A. (2005). Seeking the elusive function of the root-colonising dark septate endophytic fungi. *Stud. Mycol.* 53, 173–189. doi: 10.3114/sim.53.1.173

Mandyam, K., Loughin, T., and Jumpponen, A. (2010). Isolation and morphological and metabolic characterization of common endophytes in annually burned tallgrass prairie. *Mycologia* 102, 813–821. doi: 10.3852/09-212

Marschner, P., and Timonen, S. (2005). Interactions between plant species and mycorrhizal colonization on the bacterial community composition in the rhizosphere. *Appl. Soil Ecol.* 28, 23–36. doi: 10.1016/j.apsoil.2004.06.007

Mayerhofer, M. S., Kernaghan, G., and Harper, K. A. (2013). The effects of fungal root endophytes on plant growth: a meta-analysis. *Mycorrhiza* 23, 119–128. doi: 10.1007/s00572-012-0456-9

Mikusinska, A., Persson, T., Taylor, A. F., and Ekblad, A. (2013). Response of ectomycorrhizal extramatrical mycelium production and isotopic composition to in-growth bag size and soil fauna. *Soil Biol. Biochem.* 66, 154–162. doi: 10.1016/j.soilbio.2013.07.009

Nehls, U., and Plassard, C. (2018). Nitrogen and phosphate metabolism in ectomycorrhizas. *New Phytol.* 220, 1047–1058. doi: 10.1111/nph.15257

Newsham, K. K. (2011). A meta-analysis of plant responses to dark septate root endophytes. *New Phytol.* 190, 783–793. doi: 10.1111/j.1469-8137.2010.03611.x

Nilsson, L. O., Giesler, R., Baath, E., and Wallander, H. (2005). Growth and biomass of mycorrhizal mycelia in coniferous forests along short natural nutrient gradients. *New Phytol.* 165, 613–622. doi: 10.1111/j.1469-8137.2004.01223.x

Phillips, J. M., and Hayman, D. S. (1970). Improved procedures for clearing roots and staining parasitic and vesicular-arbuscular mycorrhizal fungi for rapid assessment of infection. *Trans. Br. Mycol. Soc.* 55, 158–IN18. doi: 10.1016/S0007-1536(70)80110-3

Phoenix, G. K., Emmett, B. A., Britton, A. J., Caporn, S. J. M., Dise, N. B., Helliwell, R., et al. (2012). Impacts of atmospheric nitrogen deposition: responses of multiple plant and soil parameters across contrasting ecosystems in long-term field experiments. *Glob. Change Biol.* 18, 1197–1215. doi: 10.1111/j.1365-2486.2011.02590.x

Pohjanen, J., Koskimaki, J. J., Sutela, S., Ardanov, P., Suorsa, M., Niemi, K., et al. (2014). Interaction with ectomycorrhizal fungi and endophytic Methylobacterium affects nutrient uptake and growth of pine seedlings in vitro. *Tree Physiol.* 34, 993–1005. doi: 10.1093/treephys/tpu062

Priyadharsini, P., and Muthukumar, T. (2017). The root endophytic fungus *Curvularia geniculata* from *Parthenium hysterophorus* roots improves plant growth through phosphate solubilization and phytohormone production. *Fungal Ecol.* 27, 69–77. doi: 10.1016/j.funeco.2017.02.007

Qiang, X. J., Ding, J. J., Lin, W., Li, Q. Z., Xu, C. Y., Zheng, Q., et al. (2019). Alleviation of the detrimental effect of water deficit on wheat (*Triticum aestivum* L.) growth by an indole acetic acid-producing endophytic fungus. *Plant Soil* 439, 373–391. doi: 10.1007/s11104-019-04028-7

Read, D. J., and Perez-Moreno, J. (2003). Mycorrhizas and nutrient cycling in ecosystems–a journey towards relevance? *New Phytol.* 157, 475–492. doi: 10.1046/j.1469-8137.2003.00704.x

Rodriguez, R. J., White, J. F. J., Arnold, A. E., and Redman, R. S. (2009). Fungal endophytes: diversity and functional roles. *New Phytol.* 182, 314–330. doi: 10.1111/j.1469-8137.2009.02773.x

Rojas, X., Guo, J. Q., Leff, J. W., McNear, J. D. H., Fierer, N., and McCulley, R. L. (2016). Infection with a shoot-specifc fungal endophyte (*Epichloë*) alters tall fescue soil microbial communities. *Microb. Ecol.* 72, 197–206. doi: 10.1007/s00248-016-0750-8

Ruotsalainen, A. L., Kauppinen, M., Wli, P. R., Saikkonen, K., Helander, M., and Tuomi, J. (2021). Dark septate endophytes: mutualism from by-products? *Trends Plant Sci.* 27, 247–254. doi: 10.1016/J.TPLANTS.2021.10.001

Santos, M., Cesanelli, I., Diánez, F., Sánchez-Montesinos, B., and Moreno-Gavíra, A. (2021). Advances in the role of dark septate endophytes in the plant resistance to abiotic and biotic stresses. *JoF.* 7:939. doi: 10.3390/JOF7110939

Santos, S. G. D., Silva, P. R. A. D., Garcia, A. C., Zilli, J., and Berbara, R. L. L. (2017). Dark septate endophyte decreases stress on rice plants. *Braz. J. Microbiol.* 48, 333–341. doi: 10.1016/j.bjm.2016.09.018

Schrijver, A. D., Frenne, P. D., Ampoorter, E., Nevel, L. V., Demey, A., Wuyts, K., et al. (2011). Cumulative nitrogen input drives species loss in terrestrial ecosystems. *Glob. Ecol. Biogeogr.* 20, 803–816. doi: 10.1111/j.1466-8238.2011.00652.x

Sebastiana, M., Duarte, B., Monteiro, F., Rui, M., and Matos, A. R. (2019). The leaf lipid composition of ectomycorrhizal oak plants shows a drought-tolerance signature. *Plant Physiol. Bioch.* 144, 157–165. doi: 10.1016/j.plaphy.2019.09.032

Shelden, M. C., Dias, D. A., Jayasinghe, N. S., Bacic, A., and Roessner, U. (2016). Root spatial metabolite profiling of two genotypes of barley (*Hordeum vulgare* L.) reveals differences in response to short-term salt stress. *J. Exp. Bot.* 67, 3731–3745. doi: 10.1093/jxb/erw059

Smith, S. E., and Read, D. (2008). *Mycorrhizal Symbiosis*. London: Academic Press.

Splivallo, R., Fischer, U., Göbel, C., Feussner, I., and Karlovsky, P. (2016). Truffles regulate plant root morphogenesis via the production of auxin and ethylene. *Plant Physiol.* 150, 2018–2029. doi: 10.1104/pp.109.141325

Sreevidya, M., Gopalakrishnan, S., Kudapa, H., and Varshney, R. H. (2016). Exploring plant growth-promotion actinomycetes from vermicompost and rhizosphere soil for yield enhancement in chickpea. *Braz. J. Microbiol.* 47, 85–95. doi: 10.1016/j.bjm.2015.11.030

Surono, S., and Narisawa, K. (2017). The dark septate endophytic fungus *Phialocephala fortinii* is a potential decomposer of soil organic compounds and a promoter of *Asparagus officinalis* growth. *Fungal Ecol.* 28, 1–10. doi: 10.1016/j.funeco.2017.04.001

Surono, S., and Narisawa, K. (2018). The inhibitory role of dark septate endophytic fungus *Phialocephala fortinii* against fusarium disease on the *Asparagus officinalis* growth in organic source conditions. *Biol. Control* 121, 159–167. doi: 10.1016/j.biocontrol.2018.02.017

Talbot, J. M., Allison, S. D., and Treseder, K. K. (2008). Decomposers in disguise: mycorrhizal fungi as regulators of soil C dynamics in ecosystems under global change. *Funct. Ecol.* 22, 955–963. doi: 10.1111/j.1365-2435.2008.01402.x

Terhonen, E., Sipari, N., and Asiegbu, F. O. (2016). Inhibition of phytopathogens by fungal root endophytes of Norway spruce. *Biol. Control* 99, 53–63. doi: 10.1016/j.biocontrol.2016.04.006

Upson, R., Read, D. J., and Newsham, K. K. (2009). Nitrogen form influences the response of *Deschampsia antarctica* to dark septate root endophytes. *Mycorrhiza* 20, 1–11. doi: 10.1007/s00572-009-0260-3

van der Heijden, M. G. A. (2002). "Arbuscular mycorrhizal fungi as a determinant of plant diversity: in search of underlying mechanisms and general principles" in *Mycorrhizal Ecology*. eds. M. G. A. Heijden and I. R. Sanders (New York, NY: Springer Berlin Heidelberg), 244–265.

van der Heijden, M. G. A., Martin, F. M., Selosse, M. A., and Sanders, I. R. (2015). Mycorrhizal ecology and evolution: the past, the present, and the future. *New Phytol.* 205, 1406–1423. doi: 10.1111/nph.13288

Vayssières, A., Pencík, A., Felten, J., Kohler, A., Ljung, K., Martin, F., et al. (2015). Development of the poplar-Laccaria bicolor ectomycorrhizal modifies root auxin metabolism, signaling, and response. *Plant Physiol.* 169, 890–902. doi: 10.1104/pp.114.255620

Vergara, C., Araujo, K. E. C., Alves, L. S., de Souza, S. R., Santos, L. A., Santa-Catarina, C., et al. (2018). Contribution of dark septate fungi to the nutrient uptake and growth of rice plants. *Braz. J. Microbiol.* 49, 67–78. doi: 10.1016/j.bjm.2017.04.010

Vergara, C., Araujo, K. E. C., Urquiaga, S., Schultz, N., Fdc, B., Ps, M., et al. (2017). Dark septate endophytic fungi help tomato to acquire nutrients from ground plant material. *Front. Microbiol.* 8:2437. doi: 10.3389/fmicb.2017.02437

Wallenda, T., and Kottke, I. (1998). Nitrogen deposition and ectomycorrhizas. *New Phytol.* 139, 169–187. doi: 10.1046/j.1469-8137.1998.00176.x

Wallenstein, M. D., Mcnulty, S., Fernandez, I. J., Boggs, J., and Schlesinger, W. H. (2006). Nitrogen fertilization decreases forest soil fungal and bacterial biomass in three long-term experiments. *For. Ecol. Manag.* 222, 459–468. doi: 10.1016/j.foreco.2005.11.002

Wang, Q., and Guo, L. D. (2010). Ectomycorrhizal community composition of *Pinus tabulaeformis* assessed by ITS-RFLP and ITS sequences. *Botany* 88, 590–595. doi: 10.1139/B10-023

Wang, Y., Zheng, J., Boyd, S. E., Xu, Z., and Zhou, Q. (2019). Effects of litter quality and quantity on chemical changes during eucalyptus litter decomposition in subtropical Australia. *Plant Soil* 442, 65–78. doi: 10.1007/s11104-019-04162-2

Waqas, M., Khan, A. L., Kamran, M., Hamayun, M., and Lee, I. J. (2012). Endophytic fungi produce gibberellins and indoleacetic acid and promotes host-plant growth during stress. *Molecules* 17, 10754–10773. doi: 10.3390/molecules170910754

Wen, Z., Shi, L., Tang, Y., Shen, Z., Xia, Y., and Chen, Y. (2017). Effects of *Pisolithus tinctorius* and *Cenococcum geophilum* inoculation on pine in copper-contaminated soil to enhance phytoremediation. *Int. J. Phytoremediation* 19, 387–394. doi: 10.1080/15226514.2016.1244155

Wu, T. H. (2011). Can ectomycorrhizal fungi circumvent the nitrogen mineralization for plant nutrition in temperate forest ecosystems? *Soil biol. Biochemist* 43, 1109–1117. doi: 10.1016/j.soilbio.2011.02.003

Xie, X. G., Zhang, F. M., Yang, T., Chen, Y., and Dai, C. C. (2019). Endophytic fungus drives nodulation and N_2 fixation attributable to specific root exudates. *MBio* 10, e728–e719. doi: 10.1128/mBio.00728-19

Xiong, H., Chen, P., Chen, W. Z., Yang, Y. H., Jin, Y. J., Tian, S. Y., et al. (2021). Effect of an ectomycorrhizal fungus on the growth of *Castanea henryi* seedlings and the *seasonal variation* of root tips' structure and physiology. *Forests* 12:1643. doi: 10.3390/f12121643

Xu, R., Li, T., Shen, M., Yang, Z. L., and Zhao, Z. W. (2020). Evidence for a dark septate endophyte (*Exophiala Pisciphila*, H93) enhancing phosphorus absorption by maize seedlings. *Plant Soil* 452, 249–266. doi: 10.1007/s11104-020-04538-9

Zeng, X., Wei, C., Liu, X., and Zhang, L. (2020). Qinghai spruce (*Picea crassifolia*) and Chinese pine (*Pinus tabuliformis*) show high vulnerability and similar resilience to early-growing-season drought in the Helan Mountains, China. *Ecol. Indic.* 110:105871. doi: 10.1016/j.ecolind.2019.105871

Zhang, Q., Gong, M., Yuan, J., Hou, Y., Zhang, H., Wang, Y., et al. (2017). Dark septate endophyte improves drought tolerance in sorghum. *Int. J. Agric. Biol.* 19, 53–60. doi: 10.17957/ijab/15.0241

Zhang, R., and Tang, M. (2012). Role of hydrogen peroxide and antioxidative enzymes in *Pinus tabulaeformis* seedlings inoculated with *amanita vaginata* and/or *Rhizoctonia solani*. *Eur. J. Plant Pathol.* 134, 381–389. doi: 10.1007/s10658-012-9996-2

Zhang, H., Yu, H., and Tang, M. (2017). Prior contact of *Pinus tabulaeformis* with ectomycorrhizal fungi increases plant growth and survival from damping-off. *New For.* 48, 855–866. doi: 10.1007/s11056-017-9601-9

Zhang, Z., Yuan, Y., Liu, Q., and Yin, H. (2019). Plant nitrogen acquisition from inorganic and organic sources via root and mycelia pathways in ectomycorrhizal alpine forests. *Soil Biol. Biochem.* 136:107517. doi: 10.1016/j.soilbio.2019.06.013

Zhou, Z., Wang, C., and Luo, Y. (2020). Meta-analysis of the impacts of global change factors on soil microbial diversity and functionality. *Nat. Commun.* 11:3072. doi: 10.1038/s41467-020-16881-7

frontiers | Frontiers in Microbiology

TYPE Original Research
PUBLISHED 15 November 2022
DOI 10.3389/fmicb.2022.1024128

OPEN ACCESS

EDITED BY
Punyasloke Bhadury,
Indian Institute of Science Education and Research Kolkata, India

REVIEWED BY
César Marín,
Santo Tomás University, Chile
Ashok Shukla,
Central Agroforestry Research Institute (CAFRI), India

*CORRESPONDENCE
Jiyu Jia
jiajiyu20110909@163.com
Heng Zhang,
471767070@qq.com

†These authors have contributed equally to this work

SPECIALTY SECTION
This article was submitted to Microbial Symbioses, a section of the journal Frontiers in Microbiology

RECEIVED 21 August 2022
ACCEPTED 24 October 2022
PUBLISHED 15 November 2022

CITATION
Qiao X, Sun T, Lei J, Xiao L, Xue L, Zhang H, Jia J and Bei S (2022) Arbuscular mycorrhizal fungi contribute to wheat yield in an agroforestry system with different tree ages.
Front. Microbiol. 13:1024128.
doi: 10.3389/fmicb.2022.1024128

Arbuscular mycorrhizal fungi contribute to wheat yield in an agroforestry system with different tree ages

Xu Qiao[1,2†], Tao Sun[2,3,4†], Junjie Lei[2], Li Xiao[2], Lihua Xue[2], Heng Zhang[2,3*], Jiyu Jia[1,5*] and Shuikuan Bei[1,5]

[1]Peking Union Medical College, Institute of Medicinal Plant Development, Chinese Academy of Medical Sciences, Beijing, China, [2]Key Laboratory of Desert-Oasis Crop Physiology, Ecology and Cultivation, MOARA/Institute of Grain Crops, Xinjiang Academy of Agricultural Sciences, Urumqi, China, [3]College of Water Conservancy and Civil Engineering, Xinjiang Agricultural University, Urumqi, China, [4]Institute of Agricultural Resources and Regional Planning, Chinese Academy of Agricultural Sciences, Beijing, China, [5]Key Laboratory of Plant-Soil Interactions, College of Resources and Environmental Sciences, Ministry of Education, National Academy of Agriculture Green Development, China Agricultural University, Beijing, China

Intercropping achieved through agroforestry is increasingly being recognized as a sustainable form of land use. In agroforestry, the roots of trees and crops are intermingled, and their interactions and the production of exudates alter the soil environment and soil microbial community. Although tree–crop interactions vary depending on the stand age of the trees, how stand age affects beneficial microorganisms, including arbuscular mycorrhizal fungi (AMF), and whether changes in soil microorganisms feed back on crop growth in agroforestry systems are unknown. We therefore conducted a long-term field study to compare changes in the soil microbial and AMF communities in a jujube/wheat agroforestry system containing trees of different stand ages: 3-year-old jujube, 8-year-old jujube, and 13-year-old jujube. Our results showed that by changing soil moisture and available phosphorus content, the stand age of the trees had a significant effect on the soil microbial and AMF communities. Soil moisture altered the composition of soil bacteria, in particular the proportions of Gram-positive and Gram-negative species, and available phosphorus had significant effects on the AMF community. A network analysis showed that older stands of trees reduced both AMF diversity and network complexity. An ordinary least squares regression analysis indicated that AMF diversity, network complexity, and stability contributed to wheat yield. Finally, structural equation modeling showed that changes in edaphic factors induced by tree age brought about significant variation in the soil microbial and AMF communities, in turn, affecting crop growth. Our study highlights the crucial roles of soil microorganisms, in particular AMF, in supporting plant growth in agroforestry systems as well as the need to consider stand age in the establishment of these systems.

KEYWORDS

agroforestry system, soil microbial community, arbuscular mycorrhizal fungi, stand age, yield

Introduction

Agroforestry, in which at least one woody perennial species is grown alongside a crop to increase crop diversity and productivity, is increasingly being recognized as a sustainable form of land use (Fentahun and Hager, 2010; Araujo et al., 2012). The ecological benefits of agroforestry include enhanced carbon sequestration (Baah-Acheamfour et al., 2014), improved soil quality (Dollinger and Jose, 2018), and increased microbial diversity (Bagyaraj et al., 2015; Duchene et al., 2017). Soil microbes regulate multiple ecosystem services, such as nutrient cycling (Rodrigues et al., 2013), organic matter decomposition (Kaiser et al., 2015), plant productivity (Tamburini et al., 2020), and plant disease control (Wei et al., 2019). Nevertheless, the impact of agroforestry on the structure of the soil microbial community is poorly understood, although information on the composition and diversity of microbial community and their determinants is critical to optimizing agroforestry systems (Liu et al., 2019).

The trees in an agroforestry system compete strongly with crops for soil nutrients, sunlight, moisture, and other available resources, which, in turn, could reduce both tree and crop production. The competition for resources increases with increasing tree growth because of the accompanying changes in spatiotemporal light patterns (Tscharntke et al., 2011; Liu et al., 2019). Therefore, in the establishment of an agroforestry system, the stand age of the trees must be taken into account (Peerawat et al., 2018). However, belowground competition would be more important than aboveground competition in many intercropping systems (Remison and Snaydon, 1980). In agroforestry, the roots of trees and crops are intermingled, and their interactions together with the production of exudates could alter both bulk soil and rhizosphere environments, such as the soil organic matter content and pH (Duchene et al., 2017), which would induce significant variation in the soil microbial community. In a study by Liu et al. (2019), bacterial communities in an agroforestry system exhibited obvious horizon-specific seasonal variation in response to spatial and temporal heterogeneity in edaphic factors. Conversely, microbial dynamics feeds back on plant fitness (Philippot et al., 2013; Hutchins et al., 2019). Yet the response of soil microbial communities to tree age, and which microbes in agroforestry systems play a crucial role in affecting plant growth are unknown.

Soil microorganisms, especially of beneficial microbes, modulate a number of processes in agroecosystems. For example, arbuscular mycorrhizal fungi (AMF), which act as key components of the soil microbial community, contribute to the development of healthy soils and agricultural sustainability (Jeffries et al., 2003; Guzman et al., 2021). AMF establishes associations with the majority of terrestrial plants, including most crops (Barrios, 2007; Turrini et al., 2018). In return for receiving carbon and energy from the host plant (Zhu and Miller, 2003; Bryla and Eissenstat, 2005), they provide plants with mineral nutrients (Wipf et al., 2019). Several studies have demonstrated that sustainable management practices, such as intercropping, positively influence the diversity and composition of AMF communities compared to conventional management (Meng et al., 2015). In agroforestry, the high plant diversity achieved with tree-based intercropping promotes the mycorrhizal network (Menezes et al., 2016; van Tuinen et al., 2020). However, little is known about the influence of tree-based intercropping systems on the diversity of AMF communities in tree and crop roots. The consensus is that native trees alter the soil dynamics of their rhizospheres and, in turn, influence the AMF community (Caravaca et al., 2020). And as tree grow, they further change the vegetation cover and the physicochemical attributes, such as soil moisture, available phosphorous, and available potassium, of the soil ecosystem in which mycorrhizas can be active (Sheng et al., 2017; Gao et al., 2019). This implies that the stand age of the trees indirectly shapes the composition of the AMF community and, by changing the properties of the soil, affects the successful establishment of AMF in the crops. In-depth knowledge of the roles of soil microbial and AMF communities in controlling plant productivity in agroforestry systems will help select a stand age that best contributes to the agroforestry system and that is able to maintain ecosystem stability.

Jujube agroforestry is extremely important in China. In the Xinjiang Uygur Autonomous Region (Northwest China), it covers >1.2 million hectares (Zhang et al., 2014). This area is characterized by with rich light and heat resources, large temperature difference between day and night, which is very suitable for fruit trees. With recent adjustments to planting systems in pursuit of high-yield and high-efficiency crops, jujube trees have been widely planted in farms within Xinjiang Province, China. These intercropping systems have considerable potential to provide food and nutritional security and to contribute to local economic development. However, as a consequence of tree aging, the change of planting structure will inevitably affect the cultivated soil quality and farmland ecological environment in this area, and will further affect the change of soil microbial community structure and function. Therefore, knowledge of the effects of tree age on soil microbial and AMF communities and of the role of these communities in promoting crop growth is critical to ensuring food security in the country. In this study, we conducted a field experiment designed to explore the soil microbial and AMF communities associated with jujube trees of different stand ages in an agroforestry system and resulting functional changes in crop growth. We hypothesized that (1) both the soil microbial community and the AMF community would be significantly affected by tree stand age because of the effects of tree age on soil properties, and (2) that variation in the composition and diversity of the soil microbial and AMF communities would predict changes in crop productivity.

Materials and methods

Study sites and sample collection

A field experiment was conducted in 2015 at the 4th Village of Zepu County with an altitude of about 1,300 m (38°05′N,

77°10′E), Kashi Prefecture, Xinjiang Uygur Autonomous Region, China. This area has a typical arid climate with an annual mean temperature of 11.6°C (1961–2008), an annual precipitation of 54.8 mm, and a potential evaporation of 2,079 mm. The mean frost-free period is 212 days.

The three planting patterns consisted of wheat intercropped with 3-year-old (IN3), 8-year-old (IN8), and 13-year-old (IN13) jujube trees (*Ziziphus jujuba Mill. Junzao*) were selected in 2015. Supplementary Figure S1A presents the growth stages of wheat and jujube trees. Jujube trees were planted in a North–South orientation. Basic information for the three jujube tree age groups is shown in Supplementary Table S1. Each intercropping plot included two rows (15 m length) of jujube trees and one wheat strip. There were three replicate plots per planting patterns. In all tree age plots, the row spacing was 500 cm, and there was 150 cm between within a row. The wheat strips in jujube intercropping systems were 3.3 m wide. Minimum distances between trees and wheat rows were 0.85 m for jujube, and intercropped wheat occupied 66% of the total area in the jujube-based system (Supplementary Figure S1B). Date trees are pruned from late February to mid-March in spring, keeping only the main branches and cutting off all the thinner branches. The pruned branches are carried out of the field. Each plot were each 0.4 ha in area and had a density of 425 wheat plants m^2. Row spacing for the intercropped wheat was 0.13 m.

Wheat (cv. Xindong 20) was sown on 3 October 2014, and harvested on 10 June 2015. The jujube trees with different tree ages were pruned annually. All fields were fertilized with urea, triple superphosphate, potassium sulfate, and farmyard manure (0.37% N, 0.41% P_2O_5, 0.46% K_2O) at concentrations of 15×10^3 kg ha^{-1} (farmyard manure), 275 kg ha^{-1} (N), 150 kg ha^{-1} (P_2O_5), and 275 kg ha^{-1} (K_2O). All farmyard manure, the P and K fertilizers, and 40% of the N fertilizer were applied evenly across the soil surface and then incorporated into the soil at a depth of 0–20 cm before the wheat was sown; the remaining 60% of the N fertilizer was spread when the wheat plants reached the stem elongation stage. The plots were irrigated three times across the whole growth period, with irrigation coinciding with the reviving, jointing, and filling stages of wheat growth. Each irrigation application included 90–100 mm (900–1,000 m^3 ha^{-1}).

The soils were sampled during the wheat filling stage, on May 20, 2015. After the removal of any crop residue, five soil cores were collected with an auger in each plot to a soil depth of 20 cm (5 cm diameter). Triplicate samples were collected. The sampling sites were 1.5 m away from the jujube trees. Immediately after their collection, the soil samples were transported on ice to the laboratory, where they were passed through a 2.0 mm mesh and divided into two subsamples. One subsample was stored at 4°C and later used to determine soil physicochemical properties, and the other subsample was stored at −20°C until it was used for DNA analysis. Ten wheat plants, five per transect (two transects in which jujube tree and wheat interact with each other), were excavated with a fork spade at each plot. The shoots were cut off at a height of ~ 5 cm, and all roots of a specific site were pooled in a plastic bag for subsequent processing. At the same time, 1-year-old young roots of jujube tree near the wheat plants were also cut off with a shovel and placed on ice in a cooler for transfer to the laboratory.

Soil parameter measurements

Soil parameters were measured according to standard methods as described in Page et al. (1982). Soil moisture (SM) was measured by drying fresh soil samples at 105°C to constant weight. Soil pH was measured in a soil:water (1:5) extract with a pH meter. Soil organic matter (SOM) and total nitrogen (TN) were measured using the Walkley–Black and Kjeldahl method. Soil total phosphorus (TP) was measured by colorimetric analysis after digestion with sulfuric acid and perchloric acid. Soil inorganic nitrogen was measured using a continuous flow analyzer (AutoAnalyzer-AA3, Seal Analytical, Norderstedt, Germany) after extraction with 2 mol L^{-1} KCl. Soil available phosphorous (AP) was determined by the Olsen method. Soil available potassium (AK) was extracted with neutral ammonium acetate and measured by atomic absorption spectrometry (ZL-5100, PerkinElmer, MA). Soil total potassium (TK) was measured by hydrofluoric acid digestion.

Phospholipid fatty acid

The total microbial biomass was the sum of all the biomarkers' values. The PLFAs i13:0, i14:0, a15:0, i15:0, i16:0, a17:0, i17:0, i18:0, i19:0, and a19:0 were used as the biomarkers for Gram-positive bacteria (G+), and 17:1 ω8c, 16:1 ω11c, 15:1 ω6c, 20:1 ω9c, 3OH 12:0, 2OH 14:0, i17:0 3OH, 2OH 16:0, i17:0 3OH, cy17:0, and cy19:0 ω8c were identified as the biomarker of Gram-negative bacteria (G-). Fungi were represented by 18:1 ω9c, 18:1 ω5c, 18:3 ω6c (6, 9, 12), 20:1 ω9c, and 16:1 ω5c. 10Me 17:0 and 10Me 18:0 were used to indicate Actinomycete (ACT)-derived fatty acids; 20:1 ω9c and 16:1 ω5c were indicative of Arbuscular mycorrhizal fungi (AMF); PLFA biomarker 20:4 ω6,9,12,15c was used to identify Protozoan-derived fatty acid. General bacteria were assessed by 12:0, 14:0, 15:0, 16:0, 17:0, i17:0 w5c, and 20:0 (Frostegård et al., 2011; Zhang et al., 2019a). The bacterial biomass of PLFA was the sum of the G+, G–, and General bacteria values. The ratio of different microbial PLFA values can represent the dynamic changes between microbial groups (Fanin et al., 2019). Saturated fatty acids included PLFAs12:0, 14:0, 15:0, 16:0, 17:0, and 20:0; PLFAs biomarkers i13:0, i14:0, i15:0, a15:0, i16:0, i17:0, a17:0, i18:0, i19:0, and a19:0 were included in Methyl-branched fatty acids. In this study, the ratios of fungi to bacteria (F/B), Gram-negative bacteria to Gram-positive bacteria (G−/G+), and Saturated fatty acids to monounsaturated fatty acids (S/M) were calculated to explain relative changes of microbial biomass and community to environmental change (Frostegård et al., 2011).

DNA extraction, PCR, and Illumina sequencing

The genomic DNA was extracted from 0.5 g of soil and 0.3 g wheat and jujube root using MoBio PowerSoil DNA Isolation Kit (MoBio Laboratories, Carlsbad, CA, United States). Genomic DNA was amplified using a nested polymerase chain reaction (PCR) procedure. The first amplification was performed in a final volume of 20 μl with 1.0 μl template DNA, 0.5 μl of each forward and reverse primer (16 pmol μl^{-1}), 10 μl of PCR SuperMix (TransGen Biotech Co., China), and 8.0 μl of sterile water with primer pair GeoA2-AML2 (White et al., 1990). Amplification procedure was conducted on a thermal cycler (Bio-Rad, United States) using the following conditions: 94°C for 3 min; 30 cycles of 94°C for 30 s; 40°C for 60 s; and 72°C for 1 min of extension, followed by 72°C for 10 min. Next, successful products of the first amplification were diluted at 1:100, and then was used as template in a second PCR with primer pair NS31 (Simon et al., 1992) and AMDGR (Sato et al., 2005). PCR reactions were performed under the same aforementioned conditions. Preparation of the amplicon libraries and pyrosequencing with Roche 454 GS-FLX technology were conducted at Personalbio in Shanghai, China.

The sequences were first filtered for quality and trimmed using mothur package to remove multiple identifiers and primers (version 1.31.2). And then, cleaned sequences (10,523 reads) were clustered into operational taxonomic units (OTUs) based on 97% similarity. Representative sequences from each OTU clade were blasted against the NCBI GenBank to obtain the most similar sequences from other studies. Finally, representative sequences for each OTU, blasted published sequences in the NCBI GenBank which were highly affiliated to each OTU, and representative sequences of major families of *Glomeromycotina* were used to construct a maximum likelihood tree.

Assessment of AMF root colonization

Mycorrhizal colonization of wheat roots and jujube root was determined by the quadrant intersection method (Giovannetti and Mosse, 1980).

Statistical analyses

All statistical analyses were performed in R 4.1.0 (R Core Team, 2020) unless otherwise noted. Indices of AMF diversity, including OTU richness, Chao1, and ACE, and of phylogenetic diversity were computed in the R package *vegan* (Oksanen et al., 2019). A principal coordinates analysis (PCoA) was performed to visualize the variation in the soil microbial and AMF communities across different tree stand ages, based on the Bray–Curtis dissimilarity. The relationships between the soil microbial and AMF communities and soil properties were determined in redundancy analyses (RDAs), also performed in the *vegan* package in R (Oksanen et al., 2019). Only environmental variables that correlated significantly ($p < 0.05$) with the RDA model were selected (calculated based on 999 permutations). Soil physicochemical parameters, AMF diversity, and the composition of the AMF community were analyzed in an ANOVA, and the least significant difference (LSD) was used to compare the means for each variable ($p < 0.05$). Co-occurrence networks of all OTUs of the AMF community were constructed based on Spearman rank correlations between OTUs to reveal significant positive correlations ($R > 0.3$ and $p < 0.05$). The results were visualized with Gephi (version 0.9.2; Li et al., 2015). A subgraph of each sample was obtained with the R package *igraph* (Csardi and Nepusz, 2006). This package was also used to calculate the topological network properties of each sample, including the total number of network nodes (representing OTUs), the total number of edges (connections between nodes representing significant positive correlations between OTUs), and the degree of co-occurrence (the number of direct correlations to a node). An ordinary least squares (OLS) linear regression model was used to test the relationship between topological network properties and wheat yield. The complex effects of abiotic and biotic factors on wheat yield were quantified by structural equation modeling (SEM) using AMOS 17.0 (SPSS, Chicago, IL, United States). Variables in the model included soil moisture, available phosphorus content, wheat yield, the proportion of Gram-positive (G+) to Gram-negative (G–) bacteria, and the degree of co-occurrence network (average degree). Maximum likelihood estimation was used to fit the covariance matrix to the model. The *a priori* theoretical model was adjusted according to the principle of the lowest chi-square, nonsignificant probability ($p > 0.05$), a high goodness-of-fit index (> 0.90), and root mean square error of approximation < 0.05 to ensure that the final model was adequately fitted (Grace and Keeley, 2006).

Results

Soil parameters, wheat yield, and aboveground biomass

Large differences were found in the physicochemical parameters of the soil across the three stands in the agroforestry system (Supplementary Table S2). Soil moisture, organic matter content, and available phosphorus content differed significantly with tree age and were highest in the soil of the IN3 treatment and lowest in the soil of the IN13 treatment. Total phosphorus and total potassium contents were highest in the IN3 treatment but did not differ significantly between the IN8 and IN13 treatments. Conversely, inorganic nitrogen content was highest in the IN13 treatment but did not differ significantly between the IN3 and IN8 treatments. There were no significant differences in soil pH, total nitrogen content, or available potassium content among the three treatments.

10.3389/fmicb.2022.1024128

Wheat yield and aboveground biomass differed significantly among treatments (Supplementary Table S3) and decreased significantly with increasing stand age. Consequently, wheat yield and aboveground biomass were highest in IN3 and lowest in IN13.

Soil microbial community

The Shannon diversity and Simpson diversity indices were significantly higher in IN8 and IN13 than in IN3 and were lowest in IN3 (Supplementary Table S4). The phospholipid fatty acid (PLFA) contents of the total and grouped soil microorganisms in the different treatments are shown in Table 1. PLFA diversity, which is used to characterize soil microbial communities, differed significantly among the three treatments. The total PLFA content was highest in IN8 and lowest in IN13. The trends in fungal biomass were similar to those of the total PLFA content, whereas AMF and protozoal biomass were lowest in IN13, and the differences between IN3 and IN8 were not significant. By contrast, the actinomycete content was lower in IN3 than in the other treatments. Bacteria accounted for a large proportion of the total PLFA content. The ratios of G+ to G– species and saturated to monounsaturated PLFA (S/M) showed a gradual upward trend from IN3 to IN13.

The PCoA provided further evidence that the soil microbial community was significantly distinct across the three stand ages (Figure 1). Three distinct clusters in the ordination graph were seen, with PCoA1 explaining 59.24% of the variance and PCoA2 explaining 27.23%. The PERMANOVA also showed significant effects of tree age and cropping system on soil microbial communities. A CCA was performed to determine the relationship between soil parameters and the microbial community. Soil moisture ($R^2 = 0.87$, $p < 0.01$), total phosphorus ($R^2 = 0.79$, $p = 0.01$), and available phosphorus ($R^2 = 0.66$, $p = 0.05$) had significant effects on the soil microbial community (Supplementary Figure S2A).

Composition of the AMF community

For the AMF, 68 OTUs representing seven genera were obtained. The two most abundant genera in soil and wheat root were *Funneliformis* (60.92 and 75.64%) and *Rhizophagus* (20.37 and 14.30%), whereas the most two abundant genera in jujube root were *Rhizophagus* (38.36%) and *Glomus* (32.35%; Figure 2A). In the soil AMF community, the relative abundances of *Diversispora*, *Funneliformis*, *Glomus*, and *Paraglomus* were significantly higher in IN3 than in IN8 or IN13, whereas the relative abundances of *Claroideoglomus* and *Rhizophagus* were much higher in IN13 than in IN3 or IN8 (Supplementary Figure S3). In the wheat root AMF community, the relative abundances of *Funneliformis* and *Rhizophagus* were much higher in IN8, and the abundances of *Diversispora* and *Claroideoglomus* were significantly higher in IN3 and IN13, respectively (Supplementary Figure S3). In jujube root, the

TABLE 1 Soil microorganism PLFA contents (nmol/g soil) across different tree ages. The same lowercase letters did not significantly differ among treatments at $P<0.05$ according to LSD test.

	Total PLFA	G+	G–	Bacterial	Fungi	Actinomycetes	AMF	Protozoan	G+/G–	F/B	S/M
IN3	32.37 ± 1.31b	6.77 ± 0.90a	4.96 ± 0.57a	23.02 ± 2.04a	3.90 ± 0.52ab	0.51 ± 0.06b	1.48 ± 0.08a	0.10 ± 0.00a	1.71 ± 0.09b	0.17 ± 0.01a	1.41 ± 0.09b
IN8	38.87 ± 1.21a	7.80 ± 0.28a	4.88 ± 0.26a	26.13 ± 0.91a	4.52 ± 0.24a	0.92 ± 0.10a	1.47 ± 0.07a	0.10 ± 0.00a	2.19 ± 0.06a	0.17 ± 0.01a	1.65 ± 0.07b
IN13	31.63 ± 1.83b	6.62 ± 0.53a	3.90 ± 0.38a	21.09 ± 2.46a	2.81 ± 0.34b	0.58 ± 0.05b	0.96 ± 0.06b	0.08 ± 0.01b	2.27 ± 0.06a	0.13 ± 0.00b	1.94 ± 0.05a

10.3389/fmicb.2022.1024128

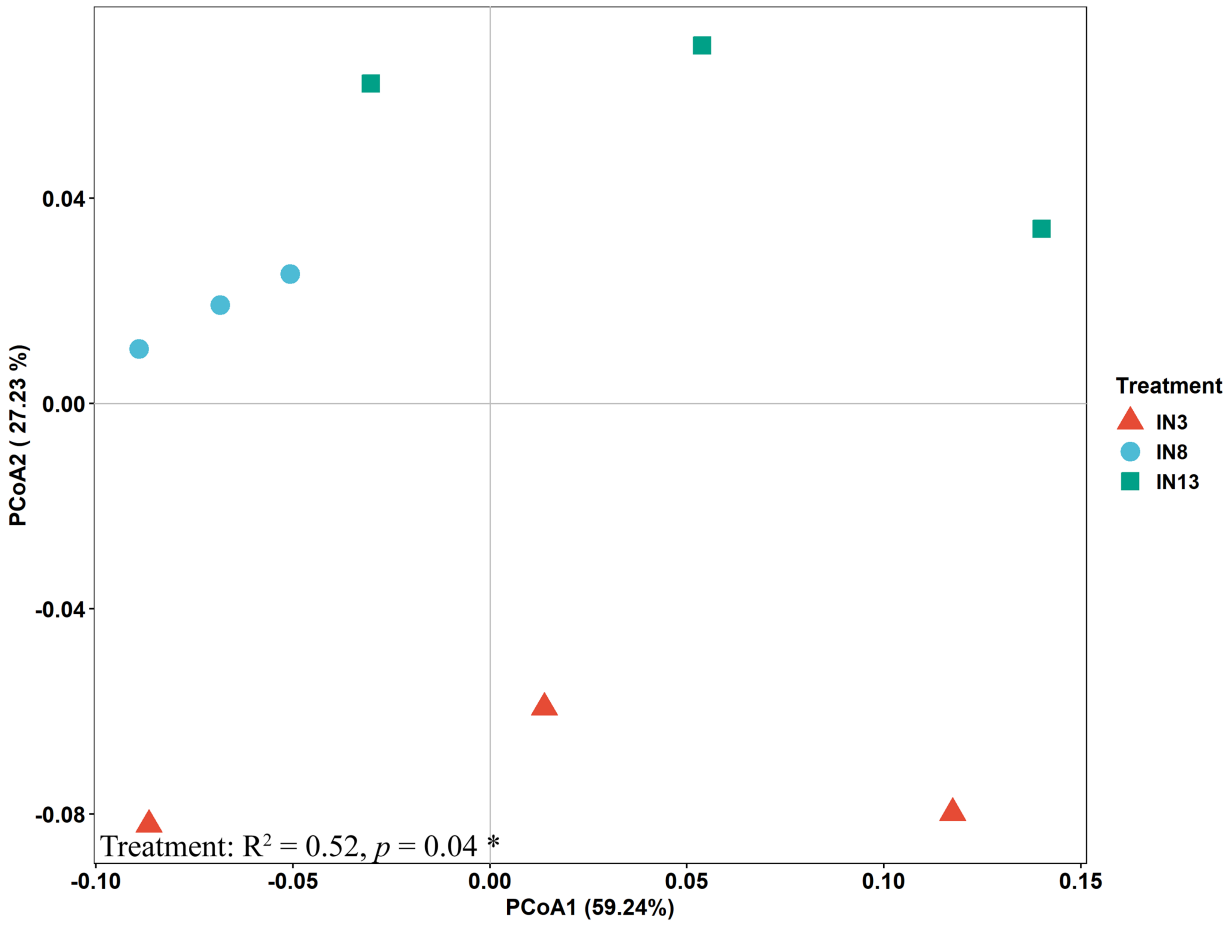

FIGURE 1
Principal coordinates analysis (PCoA) of soil microbial community based on the Bray–Curtis dissimilarities under different tree ages of intercropping systems.

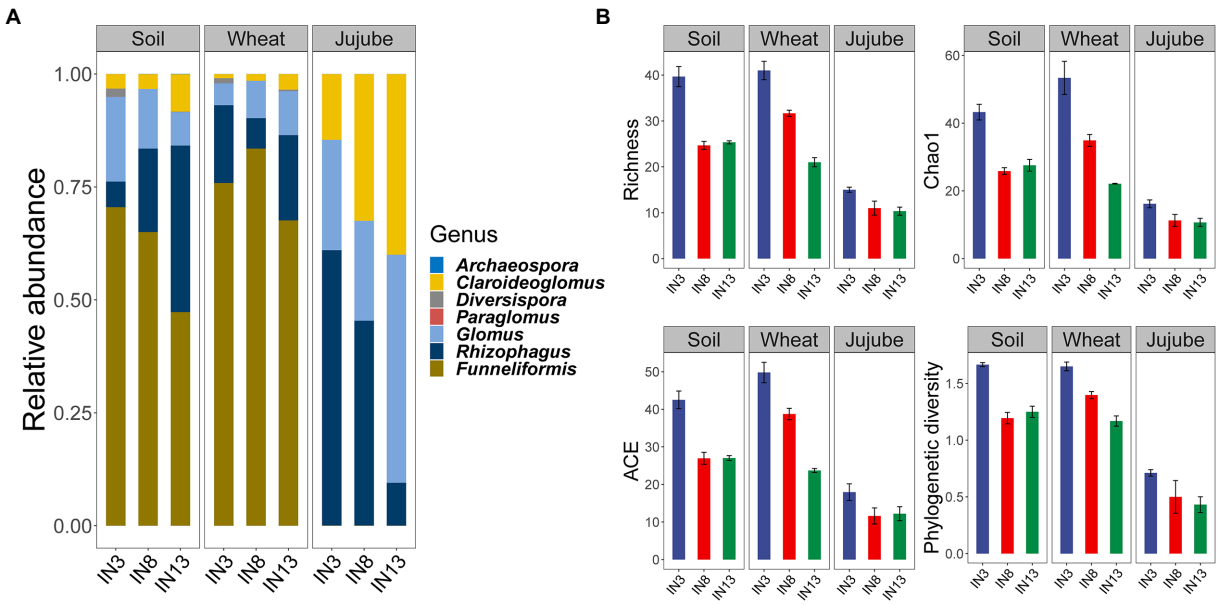

FIGURE 2
Relative abundance **(A)**, and α diversity **(B)**, of arbuscular mycorrhizal fungi in soil, wheat root and jujube root under different tree ages.

relative abundance of *Rhizophagus* was significantly higher in IN3, that of *Claroideoglomus* was significantly higher in IN8, and that of *Glomus* was significantly higher in IN13 (Supplementary Figure S3). The different treatments in the different niches also resulted in significantly distinct AMF diversity (Figure 2B). In soil and jujube root, richness, Chao1, ACE, and phylogenetic diversity were significantly higher in IN3 than in IN8 and IN13, although the differences between the latter two stands were not significant. However, all diversity indices showed a downward trend in jujube trees/wheat intercropping systems of increasing stand age (Figure 2B).

According to the PCoA, the AMF community did not differ significantly between soil and wheat root, whereas that in jujube root formed distinct clusters. PCoA1 and PCoA2 explained 65.89 and 21.14% of the variance, respectively (Figure 3A). The composition of the AMF communities in soil and wheat root varied significantly across the three stand ages, with PCoA1 explaining 75.82 and 67.64% of the variance and PCoA2 explaining 10.10 and 10.38%, respectively (Figures 3B, C). By contrast, the composition of the AMF community of jujube root did not differ significantly across the three stand ages (Figure 3D).

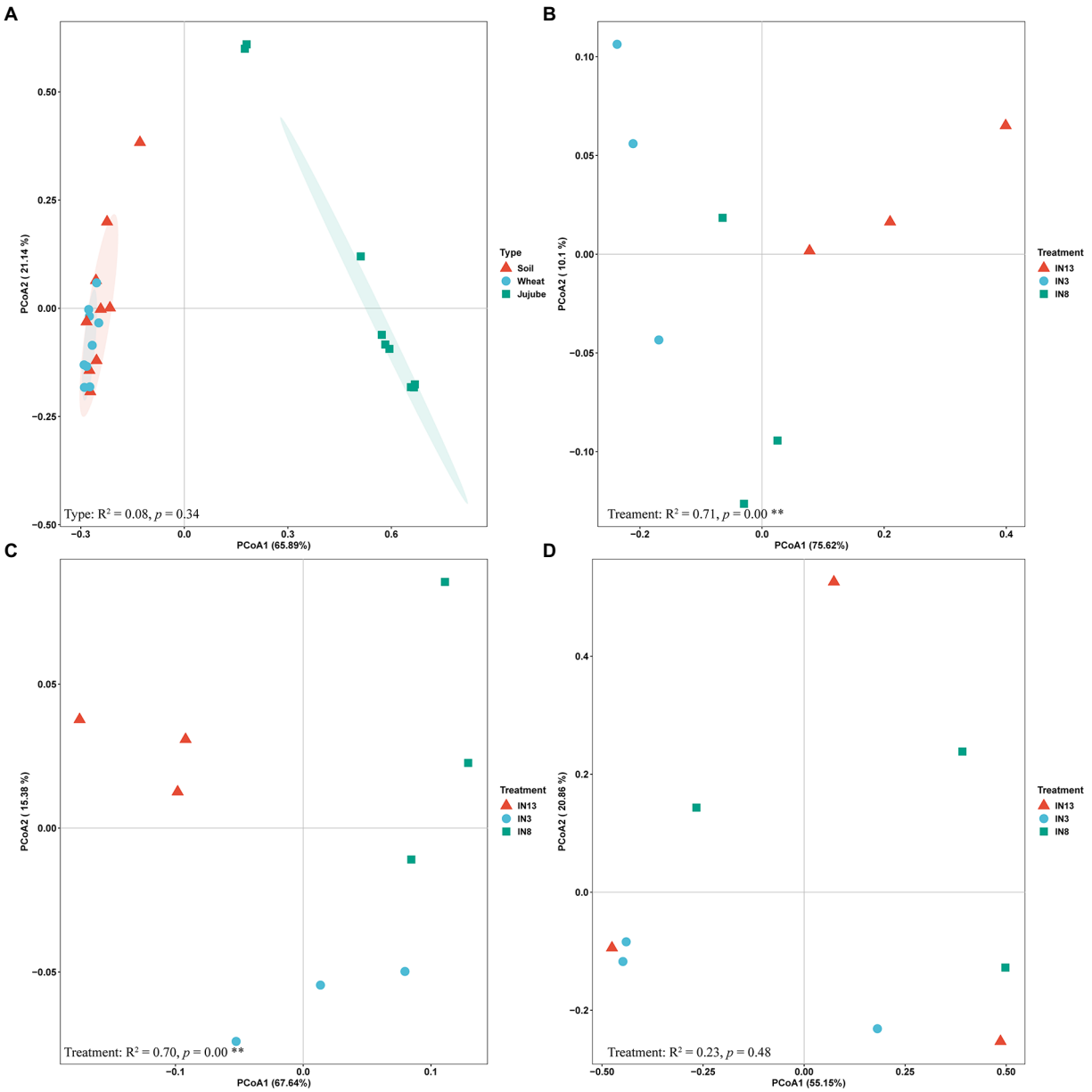

FIGURE 3
Principal coordinates analysis (PCoA) of arbuscular mycorrhizal fungi community based on the Bray–Curtis dissimilarities in different niches **(A)** and tree ages as well as cropping system of soil **(B)**, jujube **(C)** and wheat **(D)**.

The relationship between soil parameters and the AMF community was assessed in a CCA (Supplementary Figure S2). Significant effects on the AMF communities of soil and wheat root were found for total phosphorus ($R^2 = 0.77$, $p = 0.02$; $R^2 = 0.71$, $p = 0.03$), soil moisture ($R^2 = 0.74$, $p = 0.02$; $R^2 = 0.75$, $p = 0.02$), inorganic nitrogen ($R^2 = 0.71$, $p = 0.03$; $R^2 = 0.85$, $p = 0.01$), and available phosphorus ($R^2 = 0.67$, $p = 0.04$; $R^2 = 0.89$, $p < 0.01$; Supplementary Figures S2B,C). In addition, soil organic matter had a significant effect on the AMF community of wheat root, and available potassium and total potassium had a significant effect on the AMF community of jujube root (Supplementary Figure S2D).

Co-occurrence networks of AMF

Co-occurrence networks were constructed to investigate the effects of stand age on AMF interactions. A total of 68 nodes and 388 edges were detected (Figure 4). A subgraph of each sample was extracted, and the topological network parameters of node

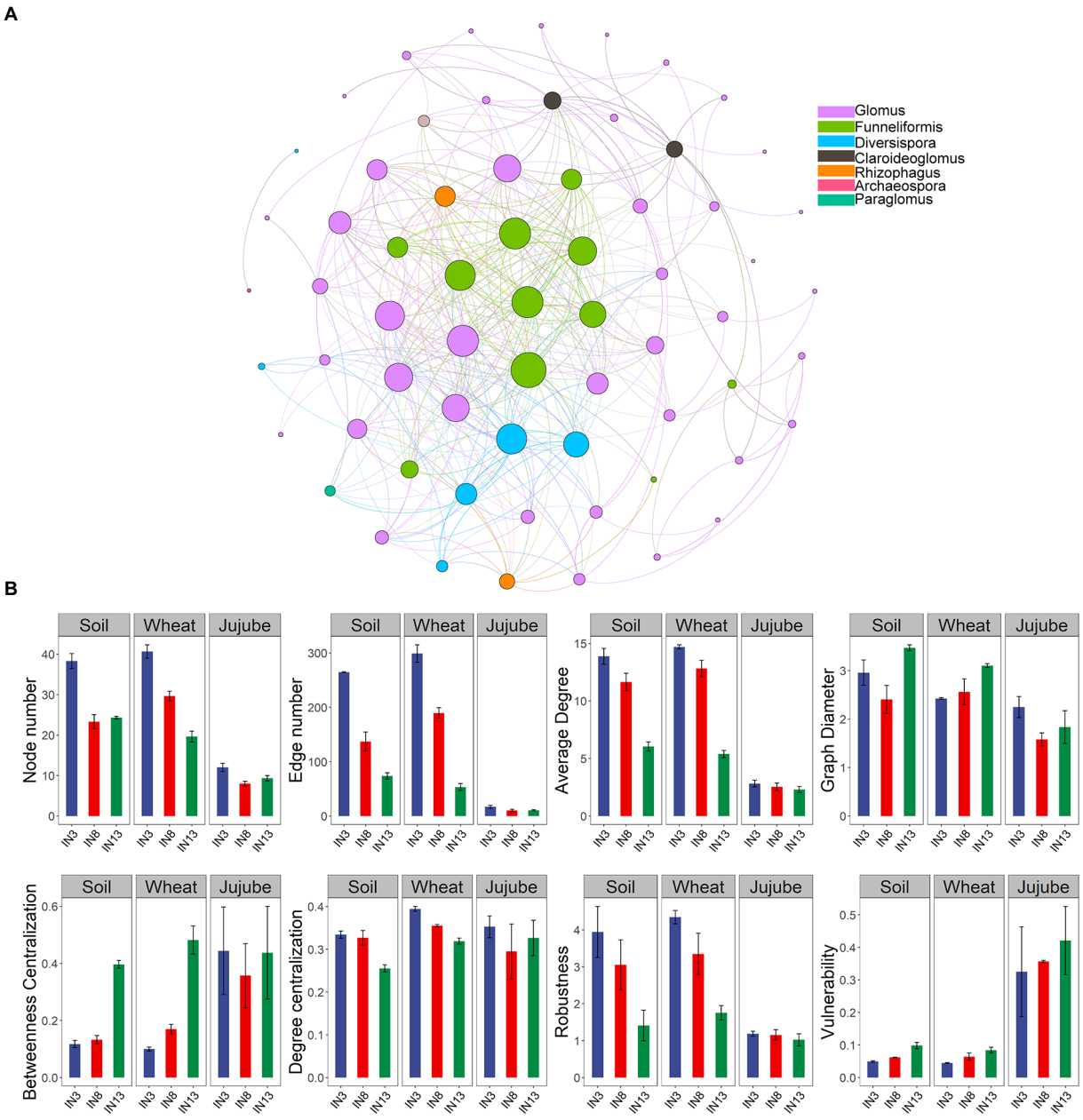

FIGURE 4
Co-occurrence network of arbuscular mycorrhizal fungi **(A)**. Topological parameters of arbuscular mycorrhizal fungal co-occurrence network in soil, wheat root and jujube root under different tree ages **(B)**.

and edge numbers, average degree, graph diameter, betweenness centralization, degree centralization, robustness, and vulnerability were calculated to assess the complexity and stability of the AMF network across the different treatments. Larger node and edge numbers, average degree, and degree centralization and smaller betweenness centralization represent greater network complexity. Higher robustness and lower vulnerability indicate greater network stability. For soil and wheat root, node and edge numbers, average degree, degree centralization, and robustness were highest in the IN3 treatment, which indicates its greater network complexity and stability (Figure 4B). Network complexity and stability showed a downward trend from IN3 to IN13 in wheat root (Figure 4B). These results strongly suggest that older stand age negatively affects AMF associations and reduces the complexity and stability of AMF community networks.

Relationship of soil microbial community, AMF diversity, and complexity and stability of co-occurrence networks to wheat yield and aboveground biomass

Positive and negative relationships were found between grouped PLFA contents, AMF diversity, network parameters, and both wheat yield and aboveground biomass. For example, the AMF content of the soil microbial community was positively related to wheat yield (Table 2), and both G+/G– and S/M were negatively related to wheat yield and aboveground biomass (Table 2). Wheat yield and aboveground biomass responded positively to the relative abundance of *Diversispora* and negatively to the relative abundance of *Rhizophagus* in the soil AMF community (Table 3). Positive responses of wheat yield and aboveground biomass to the relative abundances of *Funneliformis* and *Glomus*, respectively, were also found (Table 3). For the AMF community of wheat root, the relative abundance of *Rhizophagus* was related to wheat yield and aboveground biomass, whereas the relative abundance of *Claroideoglomus* responded negatively to wheat yield (Table 3). Significant positive relationships were found between soil AMF diversity (richness, Chao1, ACE, phylogenetic diversity) and wheat yield (Figure 5), and between soil AMF network complexity and stability and both wheat yield and aboveground biomass, which indicated that interactions between AMF communities promoted wheat growth (Figure 6).

TABLE 2 Pearson correlations between grouped PLFA contents and wheat yield as well as aboveground biomass.

PLFA contents	Yield		Aboveground biomass	
	R^2	p	R^2	p
Total PLFA	0.04	0.63	0.03	0.64
G+	0.07	0.48	0.07	0.49
G–	0.07	0.51	0.08	0.46
Bacterial	0.01	0.8	0.01	0.8
Fungi	0.04	0.59	0.03	0.69
Actinomycetes	0.09	0.43	0.22	0.21
AMF	**0.48**	**0.04***	0.4	0.06
Protozoan	0.36	0.08	0.31	0.12
G+/G–	**0.83**	**<0.01****	**0.9**	**<0.01****
F/B	0.28	0.14	0.19	0.23
S/M	**0.66**	**<0.01****	**0.59**	**0.02***

Value in bold indicates a significant difference. **indicates an extremely significant difference at $p < 0.01$, *indicates a significant difference at $p < 0.05$.

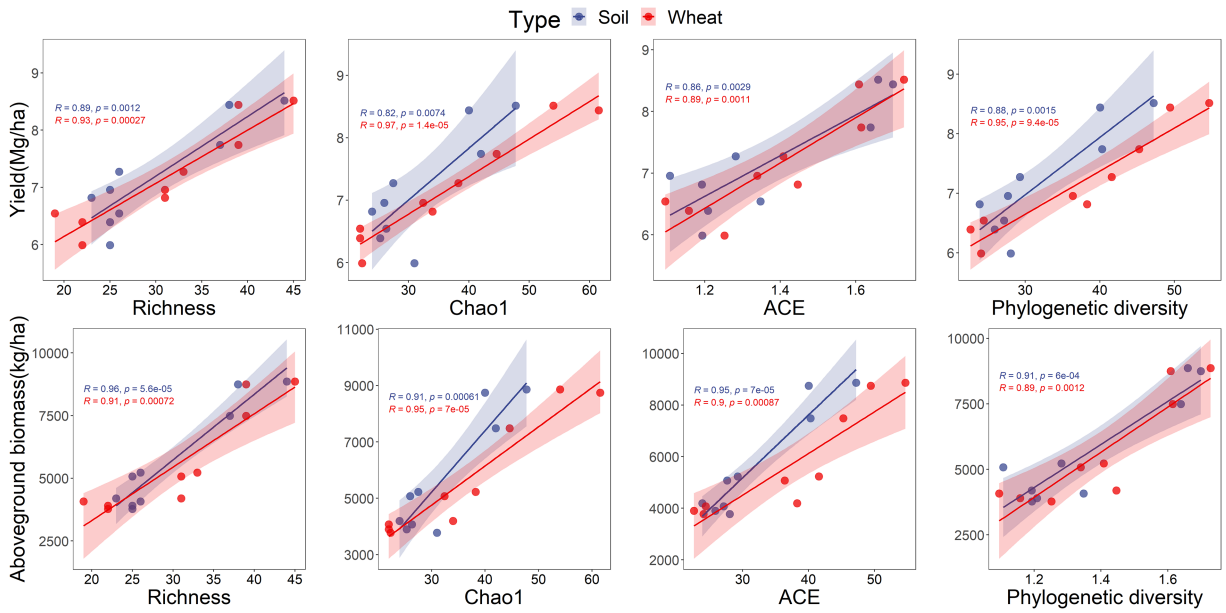

FIGURE 5
The relationships of wheat yield, aboveground biomass and α diversity of arbuscular mycorrhizal fungi.

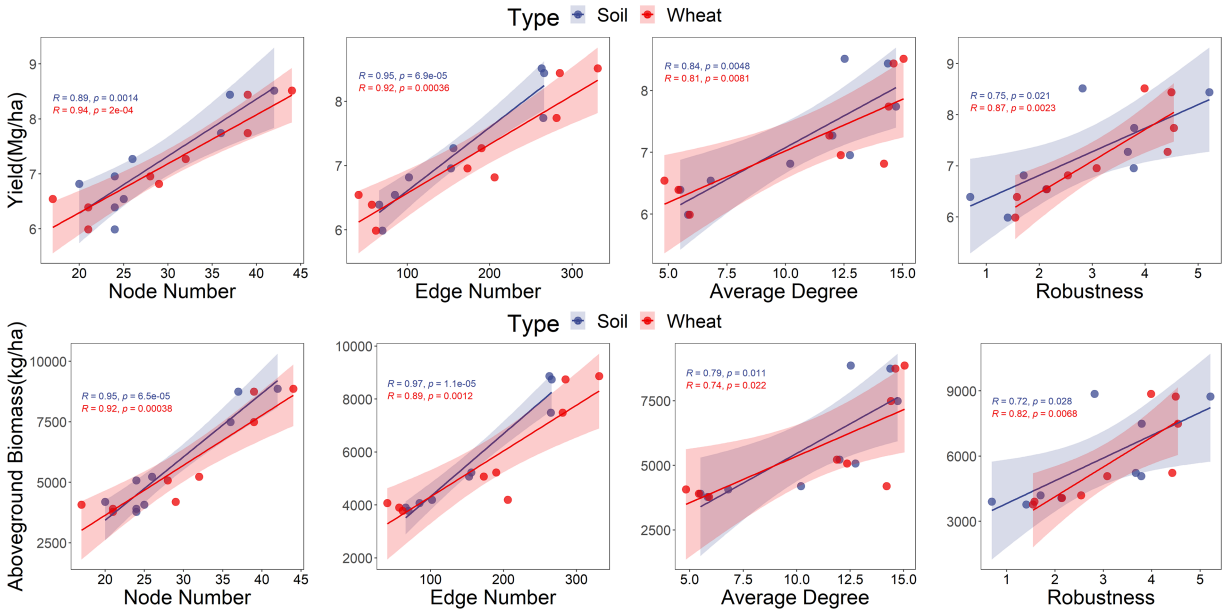

FIGURE 6
The relationships of wheat yield, aboveground biomass and topological parameters of arbuscular mycorrhizal fungi.

Structural equation modeling was performed to examine the hypothesized direct and indirect relationships between soil physicochemical parameters (soil moisture, available phosphorus), soil microbial community resistance (G+/G–), AMF network complexity (average degree), and wheat yield. The model explained 94.0% of the variance in wheat yield (Figure 7A). It also showed that stand age and G+/G– had negative indirect and direct effects, respectively, on wheat yield. Positive effects on wheat yield were found for soil moisture, available phosphorus content, and soil AMF network complexity (Figure 7B).

Discussion

The effects of stand age on the soil microbial community

Soil communities are extremely diverse (Robeson et al., 2011), as are their interactions with plants in supporting their growth (Compant et al., 2010; van Dam and Bouwmeester, 2016). In this study, the microbial communities of jujube stand of different ages in an agroforestry system were remarkably distinct (Figure 1), which supports our first hypothesis that soil microbial community could be affected by tree ages. Subsets of the microbial community can be defined based on specific microbial groups to identify variation in composition (Yao et al., 2016; Hugerth and Andersson, 2017). The total PLFA content, as well as the bacterial, G+, fungal, and actinomycete contents, was significantly higher in IN8 than in IN3 or IN13 (Table 1). Consistent with this result, the diversity of the soil microbial community was also highest in the IN8 treatment (Supplementary Table S4).

However, we also found that different groups of soil microorganisms responded differently to the increase in stand age. Thus, G+ was highest in IN8 and lowest in IN13, whereas G– showed a downward trend, differences that might have been due to different microbial life strategies and changes in soil parameters (Jing et al., 2019). Soil moisture is a major driver of the soil microbial community in agroforestry systems (Radhakrishnan and Varadharajan, 2016; Beule et al., 2020). The deeper soil water consumption by the roots of older trees significantly reduces water recharge to the soil and surface water, thus undermining the water supply available for crop growth (Ward et al., 2002). In addition, G+ communities are more resistant to drying/rewetting than G– communities due to their physiological characteristics such as the presence of a strong, thick, interlinked peptidoglycan cell wall (Schimel et al., 2007). Indeed, the G+/G– ratio has been recognized as a critical indicator to indicate resistance of microbial communities to perturbations (De Vries and Shade, 2013). A shift toward a greater presence of G+ (higher values of G+/G–) can be viewed as a mechanism allowing adaptation to a semi-arid climate as well as an indicator of a gradual change from copiotrophic to more oligotrophic conditions (Yao et al., 2006; Bastida et al., 2015). This may explain the upward trend in G+/G– with increasing stand age, and the significant negative relationship with soil moisture and soil phosphorus contents.

Significant variation in fungal biomass with tree growth was also found (Table 1). The contribution of fungi to the degradation of more recalcitrant material is larger than that of bacteria (Boer et al., 2005), such that the increase in fungal biomass in IN8 can be attributed to the competitive advantage to fungi conferred by the presence of stabilized substrates. The dramatic decline in

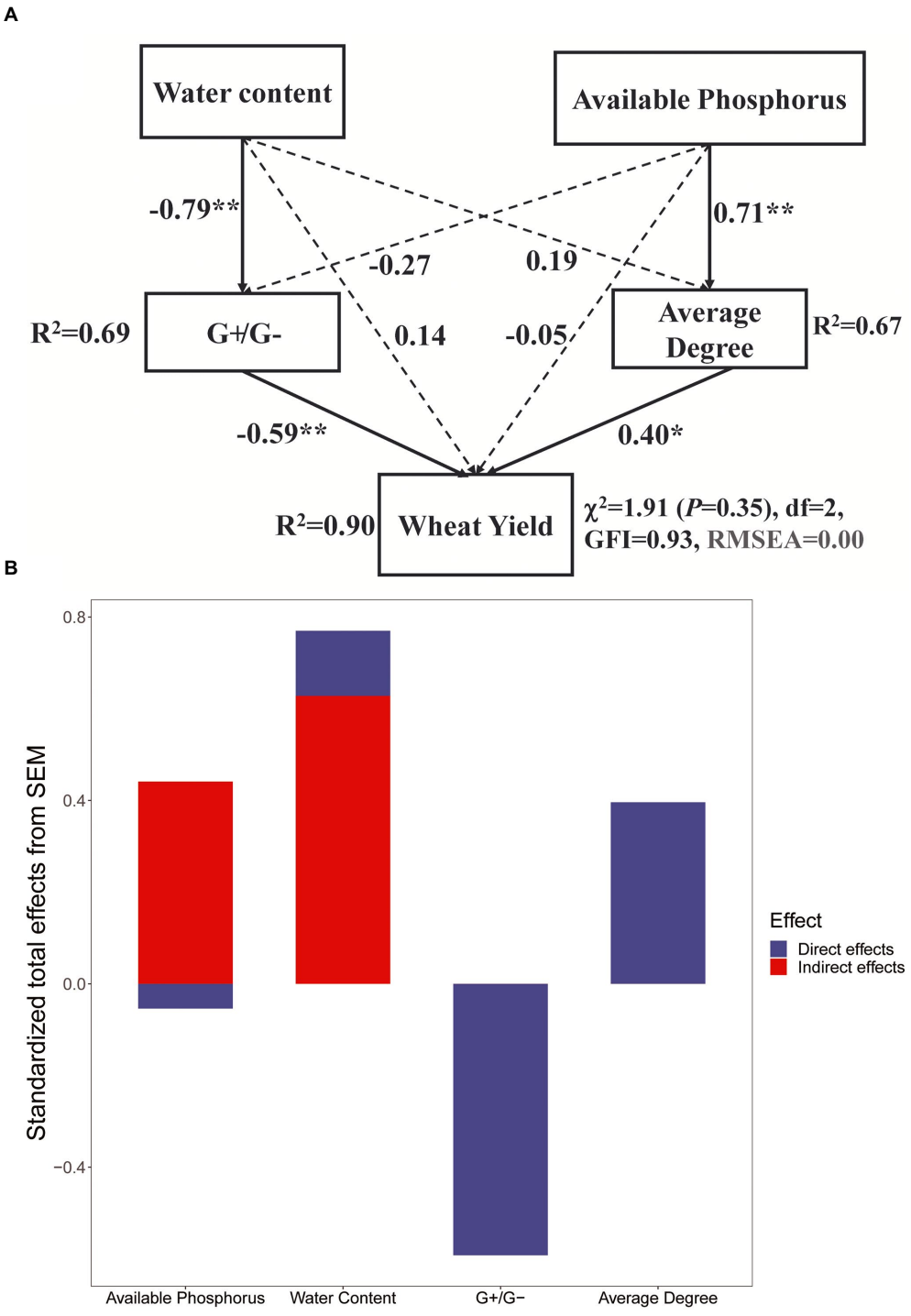

FIGURE 7
Effects of abiotic and biotic factors on wheat yield **(A)**. *indicates $p<0.05$; **indicates $p<0.01$. Continuous and dashed lines indicate significant and non-significant relationships, respectively. R^2 denotes the proportion of variance explained. **(B)** Standardized total effects (direct plus indirect effects) derived from the structural equation models depicted above.

fungal biomass in IN13 may have been due to adverse soil conditions, as a decline in soil moisture, soil nutrient, and organic matter adversely affect microbial growth (Bell et al., 2008; Köster et al., 2014). In fungi, the large amounts of energy needed to tolerate drought and low resource availability lead to a decline in fungal growth (Kempf and Bremer, 1998; Oren, 2008).

TABLE 3 Pearson correlations between relative abundance of AM fungi on genus level and wheat yield as well as aboveground biomass.

	Soil				Wheat root			
	Yield		Aboveground biomass		Yield		Aboveground biomass	
	R^2	p	R^2	p	R^2	p	R^2	p
Archaeospora	−0.39	0.3	−0.44	0.24	–	–	–	–
Claroideoglomus	−0.63	0.07	−0.6	0.09	**−0.66**	**0.05***	−0.64	0.07
Diversispora	**0.77**	**0.02***	**0.81**	**0.01***	–	–	–	–
Funneliformis	**0.74**	**0.02***	0.62	0.08	0.59	0.09	0.59	0.1
Glomus	0.64	0.06	**0.68**	**0.05***	−0.65	0.06	−0.53	0.14
Paraglomus	0.54	0.13	0.62	0.07	–	–	–	–
Rhizophagus	**−0.88**	**0.00****	**−0.8**	**0.01***	**−0.88**	**0.00****	**−0.8**	**0.01***

Value in bold indicates a significant difference. **indicates an extremely significant difference at $p < 0.01$, *indicates a significant difference at $p < 0.05$.

Variation in the AMF community across tree stands of different ages

The AMF community varied significantly among different niches (Figures 2, 3A). Although there is no host specificity between AM fungi and plants, different AM fungi have certain preferences for host plants (Campos et al., 2018). Plant species function as biotic filters, based on their preferences for specific AMF species (Kiers et al., 2011; Torrecillas et al., 2012). The AMF communities of soil and wheat were more similar than those of soil and jujube root (Figure 3). A possible explanation for this is that tillage before wheat planting destroyed jujube roots, and jujube, as a perennial plant, has slower root growth than wheat (Hailemariam et al., 2013). AMF obtain carbon from host plants and rely on plant photosynthetic capacity and the translocation of photosynthate to the root to meet their carbon needs (Shukla et al., 2009).

The significant changes in the community as a function of tree age further support our first hypothesis (Figures 2, 3). The downward trend in AMF diversity from IN3 to IN13 can be attributed to changes in the soil environment. In soil and in wheat root, community variation was induced by soil moisture as well as available phosphorus and inorganic nitrogen. Neither phosphorus nor nitrogen was lacking in the soil, which showed a negative relationship with AMF diversity, in contrast to soil moisture. Therefore, the absence of soil water would lead to the extinction of several species of AMF. Previous studies have shown that soil moisture acts as an abiotic filter that affects AMF community assembly by regulating AMF colonization and phylotype diversity (Deepika and Kothamasi, 2015). In jujube root, changes over time would include progressive lignification with increasing stand age, such that colonization by AMF would be increasingly challenging (Sheng et al., 2017), as evidenced by the observed changes in mycorrhizal colonization among the three jujube stands.

As the environment changed across the different treatments, so did the AMF communities colonizing the plant roots (Supplementary Figures S2, S3). AMF taxa can be classified according to their suitability to specific habitats, and their relative abundance in soil depends on the availability of suitable habitats and favorable host plants (Verbruggen et al., 2012). Different AMF taxa respond differently to variation in the abiotic environment (Sheng et al., 2017; Liu et al., 2019; Marro et al., 2022). For example, *Acaulosporaceae* and *Gigasporaceae* are more tolerant of acidic soil environments than most *Glomeraceae* (Veresoglou et al., 2013). However, some studies have shown that *Gigasporales* are sensitive to increased land-use intensity or disturbance, while *Glomerales* remain mostly unaffected under these conditions (Marro et al., 2022). Consistent with our results, Sheng et al. (2017) reported that a root-colonizing AMF community varied with stand age. In our study, we identified several significant relationships between soil parameters and the relative abundance of AMF at the genus level (Supplementary Figure S4). The relative abundance of *Glomus* was negatively related to soil moisture, whereas that of *Diversispora* was positively related to it in wheat root. These differences may have been due to the life strategies of different root-colonizing species of AMF (Sýkorová et al., 2007). *Glomus* species are often recognized as competitive root colonizers because they are able to colonize roots from spores (Herrmann et al., 2016), which could explain the increase in their relative abundance with increasing tree age. *Diversispora* prefer well-watered conditions (Cheng et al., 2021). *Rhizophagus*, a highly infective taxon and prolific producer of vesicles in roots, prefers roots (Souza, 2015; Knegt et al., 2016), which may explain its increased relative abundance in soil and wheat.

The contribution of AMF to wheat yield in agroforestry systems

Crop root systems have an inherent capability to adjust to complex soil environmental conditions (Malamy, 2005), including the secretion of a large array of primary or secondary plant metabolites into the soil to facilitate interactions with the biotic and abiotic environment (van Dam and Bouwmeester, 2016). In turn, host-specific changes in microbial composition

feedback on plant fitness (Bever, 2003). In this study, SEM suggested that the changes in soil parameters induced by tree age led to variation in the composition of soil microbial and AMF communities and therefore functional changes that ultimately affect crop growth (Figure 6). In our study, changes in soil moisture resulted in changes in the bacterial community, and available phosphorus had a positive effect on AMF network complexity. Changes in G+/G– and AMF network complexity had negative and positive effects, respectively, on wheat yield. The negative effects of bacteria on crop yield may reflect functional trade-offs between stress tolerance and the promotion of nutrient cycling. A previous study found an inverse relationship between the stability of the microbial community and the resistance of microbial biomass and activity (Piton et al., 2021). Therefore, a reorganization of the microbial community would promote ecosystem stability through functional compensation among species responding to environmental change (Allison and Martiny, 2008; Jurburg et al., 2017).

We also found that AMF content, diversity, and network complexity responded positively to wheat yield (Table 2), which supports our second hypothesis. AMF promote host plant growth by supplying nutrients, in particular N and P (Menezes et al., 2016; Guzman et al., 2021), and enhance the tolerance of plants to various stresses, such as drought and high temperature (Duc et al., 2018; Begum et al., 2019). The extracellular hyphae of AMF can facilitate the absorption and utilization of water by plants, which is important to preventing drought damage in plants (Bahadur et al., 2019). Other studies have found that drought resistance and the better performance of crops can be attributed to the accumulation of antioxidant enzymes (superoxide dismutase, peroxidase, and catalase) and soluble sugar produced by the AMF symbiosis (Zhang et al., 2019b). Besides, the lower colonization of AMF in older jujube root due to the lignification limited their diversity as well as the faster establishment of root colonization when switching from one crop to another (Mason and Wilson, 1994). Our results support the indispensable roles of soil microorganisms, in particular AMF, in promoting plant growth in agroforestry systems.

Conclusion

Soil microbial and AMF communities are significantly affected by the stand ages of trees in an agroforestry system. Soil moisture and the available phosphorus content related to tree age are the major drivers of these communities, which, in turn, affect crop growth. Our results also showed that AMF contribute to crop growth in agroforestry and are predictors of plant growth in agroforestry systems. However, according to a network analysis, AMF diversity and network complexity decrease with increasing stand age. Thus, stand age as well as the trade-offs among soil function, productivity, biodiversity, and economic benefits must be taken into account when establishing an agroforestry system.

Data availability statement

The data presented in the study are deposited in the NCBI repository, accession number PRJNA887214.

Author contributions

XQ, LHX, JL, LX, and HZ conducted the experiments. TS, JJ, and SB analyzed the data. XQ and HZ coordinated the long-term field experiments. XQ, TS, JJ, and SB wrote the manuscript. All authors contributed to the article and approved the submitted version.

Funding

This work was funded by the Key Cultivation Project of Scientific and Technological Innovation of Xinjiang Academy of Agricultural Sciences (xjkcpy-003), Key Research and Development Projects of Xinjiang (2021B02002), National Natural Science Foundation of China (Grant Nos. 31560587, 32160521, 32060433), The central government guides local funds for science and technology development (2060503), and the Modern Agricultural Industry Technology System (CARS-03-49).

Acknowledgments

We are grateful for the support from the Extension Centre of Agricultural Technology in Zepu County, Kashi Prefecture, Xinjiang. We also would like to thank the reviewers and the editors for their helpful comments.

Conflict of interest

The authors declare that the research was conducted in the absence of any commercial or financial relationships that could be construed as a potential conflict of interest.

Publisher's note

Supplementary material

The Supplementary material for this article can be found online at: https://www.frontiersin.org/articles/10.3389/fmicb.2022.1024128/full#supplementary-material

References

Allison, S. D., and Martiny, J. B. (2008). Resistance, resilience, and redundancy in microbial communities. *Proc. Natl. Acad. Sci. U. S.* 105, 11512–11519. doi: 10.1073/pnas.0801925105

Araujo, A. S. F., Leite, L. F. C., Iwata, B. F., Lira, M. A., Xavier, G. R., and Figueiredo, M. V. B. (2012). Microbiological process in agroforestry systems. A review. *Agron. Sustain. Dev.* 32, 215–226. doi: 10.1007/s13593-011-0026-0

Baah-Acheamfour, M., Carlyle, C. N., Bork, E. W., and Chang, S. X. (2014). Trees increase soil carbon and its stability in three agroforestry systems in Central Alberta, Canada. *Forest Ecol. Manag.* 328, 131–139. doi: 10.1016/j.foreco.2014.05.031

Bagyaraj, D. J., Thilagar, G., Ravisha, C., Kushalappa, C. G., Krishnamurthy, K. N., and Vaast, P. (2015). Below ground microbial diversity as influenced by coffee agroforestry systems in the Western Ghats, India. *Agric. Ecosyst. Environ.* 202, 198–202. doi: 10.1016/j.agee.2015.01.015

Bahadur, A., Batool, A., Nasir, F., Jiang, S., Mingsen, Q., Zhang, Q., et al. (2019). Mechanistic insights into arbuscular mycorrhizal fungi-mediated drought stress tolerance in plants. *Int. J. Mol. Sci.* 20:4199. doi: 10.3390/ijms20174199

Barrios, E. (2007). Soil biota, ecosystem services and land productivity. *Ecol. Econ.* 64, 269–285. doi: 10.1016/j.ecolecon.2007.03.004

Bastida, F., Selevsek, N., Torres, I. F., Hernández, T., and García, C. (2015). Soil restoration with organic amendments: linking cellular functionality and ecosystem processes. *Sci. Rep.* 5:15550. doi: 10.1038/srep15550

Begum, N., Qin, C., Ahanger, M. A., Raza, S., Khan, M. I., Ashraf, M., et al. (2019). Role of arbuscular mycorrhizal fungi in plant growth regulation: implications in abiotic stress tolerance. *Front. Plant Sci.* 10:1068. doi: 10.3389/fpls.2019.01068

Bell, C., McIntyre, N., Cox, S., Tissue, D., and Zak, J. (2008). Soil microbial responses to temporal variations of moisture and temperature in a Chihuahuan Desert grassland. *Microb. Ecol.* 56, 153–167. doi: 10.1007/s00248-007-9333-z

Beule, L., Lehtsaar, E., Corre, M. D., Schmidt, M., Veldkamp, E., and Karlovsky, P. (2020). Poplar rows in temperate agroforestry croplands promote bacteria, fungi, and denitrification genes in soils. *Front. Microbiol.* 10:3108. doi: 10.3389/fmicb.2019.03108

Bever, J. D. (2003). Soil community feedback and the coexistence of competitors: conceptual frameworks and empirical tests. *New Phytol.* 157, 465–473. doi: 10.1046/j.1469-8137.2003.00714.x

Boer, W., De Folman, L. B., Summerbell, R. C., and Boddy, L. (2005). Living in a fungal world: impact of fungi on soil bacterial niche development. *FEMS Microbiol. Rev.* 29, 795–811. doi: 10.1016/j.femsre.2004.11.005

Bryla, D. R., and Eissenstat, D. M. (2005). "Respiratory costs of mycorrhizal associations," in *Plant Respiration*. eds. H. Lambers and M. Ribas-Carbo (Dordrecht: Springer), 207–224.

Campos, C., Carvalho, M., Brígido, C., Goss, M. J., and Nobre, T. (2018). Symbiosis specificity of the preceding host plant can dominate but not obliterate the association between wheat and its arbuscular mycorrhizal fungal partners. *Front. Microbiol.* 9:2920. doi: 10.3389/fmicb.2018.02920

Caravaca, F., Rodriguez-Caballero, G., Campoy, M., Sanleandro, P. M., and Roldán, A. (2020). The invasion of semiarid Mediterranean sites by *Nicotiana glauca* mediates temporary changes in mycorrhizal associations and a permanent decrease in rhizosphere activity. *Plant Soil* 450, 217–229. doi: 10.1007/s11104-020-04497-1

Cheng, X. F., Wu, H. H., Zou, Y. N., Wu, Q. S., and Kuča, K. (2021). Mycorrhizal response strategies of trifoliate orange under well-watered, salt stress, and waterlogging stress by regulating leaf aquaporin expression. *Plant Physiol. Biochem.* 162, 27–35. doi: 10.1016/j.plaphy.2021.02.026

Compant, S., Clément, C., and Sessitsch, A. (2010). Plant growth-promoting bacteria in the rhizo- and endo-sphere of plants: their role, colonization, mechanisms involved and prospects for utilization. *Soil Biol. Biochem.* 42, 669–678. doi: 10.1016/j.soilbio.2009.11.024

Csardi, G., and Nepusz, T. (2006). The igraph software package for complex network research. *InterJ. Complex Syst.* 1695, 1–9. Available at: https://igraph.org

De Vries, F. T., and Shade, A. (2013). Control son soil microbial community stability under climate change. *Front. Microbiol.* 4, 1–16. doi: 10.3389/fmicb.2013.00265

Deepika, S., and Kothamasi, D. (2015). Soil moisture—a regulator of arbuscular mycorrhizal fungal community assembly and symbiotic phosphorus uptake. *Mycorrhiza* 25, 67–75. doi: 10.1007/s00572-014-0596-1

Dollinger, J., and Jose, S. (2018). Agroforestry for soil health. *Agrofor. Syst.* 92, 213–219. doi: 10.1007/s10457-018-0223-9

Duc, N. H., Csintalan, Z., and Posta, K. (2018). Arbuscular mycorrhizal fungi mitigate negative effects of combined drought and heat stress on tomato plants. *Plant Physiol. Biochem.* 132, 297–307. doi: 10.1016/j.plaphy.2018.09.011

Duchene, O., Vian, J. F., and Celette, F. (2017). Intercropping with legume for agroecological cropping systems: complementarity and facilitation processes and the importance of soil microorganisms. A review. *Agric. Ecosyst. Environ.* 240, 148–161. doi: 10.1016/j.agee.2017.02.019

Fanin, N., Kardol, P., Farrell, M., Nilsson, M. C., Gundale, M. J., and Wardle, D. A. (2019). The ratio of gram-positive to gram-negative bacterial PLFA markers as an indicator of carbon availability in organic soils. *Soil Biol. Biochem.* 128, 111–114. doi: 10.1016/j.soilbio.2018.10.010

Fentahun, M., and Hager, H. (2010). Integration of indigenous wild woody perennial edible fruit bearing species in the agricultural landscapes of Amhara region, Ethiopia. *Agrofor. Syst.* 78, 79–95. doi: 10.1007/s10457-009-9239-5

Frostegård, Å., Tunlid, A., and Bååth, E. (2011). Use and misuse of PLFA measurements in soils. *Soil Biol. Biochem.* 43, 1621–1625. doi: 10.1016/j.soilbio.2010.11.021

Gao, P., Zheng, X., Wang, L., Liu, B., and Zhang, S. (2019). Changes in the soil bacterial community in a chronosequence of temperate walnut-based intercropping systems. *Forests* 10:299. doi: 10.3390/f10040299

Giovannetti, M., and Mosse, B. (1980). An evaluation of techniques for measuring vesicular arbuscular mycorrhizal infection in roots. *New Phytol.* 84, 489–500. doi: 10.1111/j.1469-8137.1980.tb04556.x

Grace, J. B., and Keeley, J. E. (2006). A structural equation model analysis of postfire plant diversity in California shrublands. *Ecol. Appl.* 16, 503–514. doi: 10.1890/1051-0761(2006)016[0503:ASEMAO]2.0.CO;2

Guzman, A., Montes, M., Hutchins, L., DeLaCerda, G., Yang, P., Kakouridis, A., et al. (2021). Crop diversity enriches arbuscular mycorrhizal fungal communities in an intensive agricultural landscape. *New Phytol.* 231, 447–459. doi: 10.1111/nph.17306

Hailemariam, M., Birhane, E., Asfaw, Z., and Zewdie, S. (2013). Arbuscular mycorrhizal association of indigenous agroforestry tree species and their infective potential with maize in the rift valley, Ethiopia. *Agrofor. Syst.* 87, 1261–1272. doi: 10.1007/s10457-013-9634-9

Herrmann, L., Lesueur, D., Bräu, L., Davison, J., Jairus, T., Robain, H., et al. (2016). Diversity of root-associated arbuscular mycorrhizal fungal communities in a rubber tree plantation chronosequence in Northeast Thailand. *Mycorrhiza* 26, 863–877. doi: 10.1007/s00572-016-0720-5

Hugerth, L. W., and Andersson, A. F. (2017). Analysing microbial community composition through amplicon sequencing: from sampling to hypothesis testing. *Front. Microbiol.* 8:1561. doi: 10.3389/fmicb.2017.01561

Hutchins, D. A., Jansson, J. K., Remais, J. V., Rich, V. I., Singh, B. K., and Trivedi, P. (2019). Climate change microbiology—problems and perspectives. *Nat. Rev. Microbiol.* 17, 391–396. doi: 10.1038/s41579-019-0178-5

Jeffries, P., Gianinazzi, S., Perotto, S., Turnau, K., and Barea, J. M. (2003). The contribution of arbuscular mycorrhizal fungi in sustainable maintenance of plant health and soil fertility. *Biol. Fertil. Soils* 37, 1–16. doi: 10.1007/s00374-002-0546-5

Jing, Y., Wang, Y., Liu, S., Zhang, X., Wang, Q., Liu, K., et al. (2019). Interactive effects of soil warming, throughfall reduction, and root exclusion on soil microbial community and residues in warm-temperate oak forests. *Appl. Soil Ecol.* 142, 52–58. doi: 10.1016/j.apsoil.2019.05.020

Jurburg, S. D., Nunes, I., Stegen, J. C., Le Roux, X., Priemé, A., Sørensen, S. J., et al. (2017). Autogenic succession and deterministic recovery following disturbance in soil bacterial communities. *Sci. Rep.* 7, 1–11. doi: 10.1038/srep45691

Kaiser, M., Kleber, M., and Berhe, A. A. (2015). How air-drying and rewetting modify soil organic matter characteristics: an assessment to improve data interpretation and inference. *Soil Biol. Biochem.* 80, 324–340. doi: 10.1016/j.soilbio.2014.10.018

Kempf, B., and Bremer, E. (1998). Uptake and synthesis of compatible solutes as microbial stress responses to high-osmolality environments. *Arch. Microbiol.* 170, 319–330. doi: 10.1007/s002030050649

Kiers, E. T., Duhamel, M., Beesetty, Y., Mensah, J. A., Franken, O., Verbruggen, E., et al. (2011). Reciprocal rewards stabilize cooperation in the mycorrhizal symbiosis. *Science* 333, 880–882. doi: 10.1126/science.1208473

Knegt, B., Jansa, J., Franken, O., Engelmoer, D. J. P., Werner, G. D. A., Bücking, H., et al. (2016). Host plant quality mediates competition between arbuscular mycorrhizal fungi. *Fungal Ecol.* 20, 233–240. doi: 10.1016/j.funeco.2014.09.011

Köster, K., Berninger, F., Lindén, A., Köster, E., and Pumpanen, J. (2014). Recovery in fungal biomass is related to decrease in soil organic matter turnover time in a boreal fir chronosequence. *Geoderma* 235-236, 74–82. doi: 10.1016/j.geoderma.2014.07.001

Li, D., Liu, C. M., Luo, R., Sadakane, K., and Lam, T. W. (2015). MEGAHIT: an ultra-fast single-node solution for large and complex metagenomics assembly via succinct de Bruijn graph. *Bioinformatics* 31, 1674–1676. doi: 10.1093/bioinformatics/btv033

Liu, C., Jin, Y., Hu, Y., Tang, J., Xiong, Q., Xu, M., et al. (2019). Drivers of soil bacterial community structure and diversity in tropical agroforestry systems. *Agric. Ecosyst. Environ.* 278, 24–34. doi: 10.1016/j.agee.2019.03.015

Malamy, J. E. (2005). Intrinsic and environmental response pathways that regulate root system architecture. *Plant Cell Environ.* 28, 67–77. doi: 10.1111/j.1365-3040.2005.01306.x

Marro, N., Grilli, G., Soteras, F., Caccia, M., Longo, S., Cofré, N., et al. (2022). The effects of arbuscular mycorrhizal fungal species and taxonomic groups on stressed and unstressed plants: a global meta-analysis. *New Phytol.* 235, 320–332. doi: 10.1111/nph.18102

Mason, P. A., and Wilson, J. (1994). "Harnessing symbiotic associations: vesicular-arbuscular mycorrhizas," in *Tropical Trees: The Potential for Domestication and the Rebuilding of Forest Resources*. eds. R. R. B. Leakey and A. C. Newton (London: HMSO), 165–175.

Menezes, K. M., Silva, D. K., Queiroz, M. A., Félix, W. P., and Yano-Melo, A. M. (2016). Arbuscular mycorrhizal fungal communities in buffelgrass pasture under intercropping and shading systems in Brazilian semiarid conditions. *Agric. Ecosyst. Environ.* 230, 55–67. doi: 10.1016/j.agee.2016.05.024

Meng, L., Zhang, A., Wang, F., Han, X., Wang, D., and Li, S. (2015). Arbuscular mycorrhizal fungi and rhizobium facilitate nitrogen uptake and transfer in soybean/maize intercropping system. *Front. Plant Sci.* 6:339. doi: 10.3389/fpls.2015.00339

Oksanen, J., Blanchet, F. G., Friendly, M., Kindt, R., Legendre, P., McGlinn, D., et al. (2019). Vegan: Community ecology package, version 2.5–6.

Oren, A. (2008). Microbial life at high salt concentrations: phylogenetic and metabolic diversity. *Saline Syst.* 4, 2–13. doi: 10.1186/1746-1448-4-2

Page, A., Miller, R., and Keeney, D. (1982). *Methods of Soil Analysis, Part 2. Chemical and Microbiological Properties*. Madison, WI, American Society of Agronomy, Inc., Soil Science Society of America.

Peerawat, M., Blaud, A., Trap, J., Chevallier, T., Alonso, P., Gay, F., et al. (2018). Rubber plantation ageing controls soil biodiversity after land conversion from cassava. *Agric. Ecosyst. Environ.* 257, 92–102. doi: 10.1016/j.agee.2018.01.034

Philippot, L., Raaijmakers, J. M., Lemanceau, P., and van Der Putten, W. H. (2013). Going back to the roots: the microbial ecology of the rhizosphere. *Nat. Rev. Microbiol.* 11, 789–799. doi: 10.1038/nrmicro3109

Piton, G., Foulquier, A., Martinez-García, L. B., Legay, N., Arnoldi, C., Brussaard, L., et al. (2021). Resistance–recovery trade-off of soil microbial communities under altered rain regimes: an experimental test across European agroecosystems. *J. Appl. Ecol.* 58, 406–418. doi: 10.1111/1365-2664.13774

R Core Team (2020). R: a language and environment for statistical computing.

Radhakrishnan, S., and Varadharajan, M. (2016). Status of microbial diversity in agroforestry systems in Tamil Nadu, India. *J. Basic Microbiol.* 56, 662–669. doi: 10.1002/jobm.201500639

Remison, S. U., and Snaydon, R. W. (1980). A comparison of root competition and shoot competition between Dactylis glomerata and Holcus lanatus. *Grass Forage Sci.* 35, 183–187. doi: 10.1111/j.1365-2494.1980.tb01510.x

Robeson, M. S., King, A. J., Freeman, K. R., Birky, C. W., Martin, A. P., and Schmidt, S. K. (2011). Soil rotifer communities are extremely diverse globally but spatially autocorrelated locally. *Proc. Natl. Acad. Sci. U. S.* 108, 4406–4410. doi: 10.1073/pnas.1012678108

Rodrigues, J. L. M., Pellizari, V. H., Mueller, R., Baek, K., Da Jesus, E. C., Paula, F. S., et al. (2013). Conversion of the Amazon rainforest to agriculture results in biotic homogenization of soil bacterial communities. *Proc. Natl. Acad. Sci. U. S. A.* 110, 988–993. doi: 10.1073/pnas.1220608110

Sato, K., Suyama, Y., Saito, M., and Sugawara, K. (2005). A new primer for discrimination of arbuscular mycorrhizal fungi with polymerase chain reaction-denature gradient gel electrophoresis. *Grassl. Sci.* 51, 179–181. doi: 10.1111/j.1744-697X.2005.00023.x

Schimel, J., Balser, T. C., and Wallenstein, M. (2007). Microbial stress-response physiology and its implications for ecosystem function. *Ecology* 88, 1386–1394. doi: 10.1890/06-0219

Sheng, M., Chen, X., Zhang, X., Hamel, C., Cui, X., Chen, J., et al. (2017). Changes in arbuscular mycorrhizal fungal attributes along a chronosequence of black locust (*Robinia pseudoacacia*) plantations can be attributed to the plantation-induced variation in soil properties. *Sci. Total Environ.* 599-600, 273–283. doi: 10.1016/j.scitotenv.2017.04.199

Shukla, A., Kumar, A., Jha, A., Chaturvedi, O. P., Prasad, R., and Gupta, A. (2009). Effects of shade on arbuscular mycorrhizal colonization and growth of crops and tree seedlings in Central India. *Agrofor. Syst.* 76, 95–109. doi: 10.1007/s10457-008-9182-x

Simon, L., Lalonde, M., and Bruns, T. D. (1992). Specific amplification of 18S fungal ribosomal genes from vesicular arbuscular endomycorrhizal fungi colonizing roots. *Appl. Environ. Microbiol.* 58, 291–295. doi: 10.1128/aem.58.1.291-295.1992

Souza, T. (2015). "Glomeromycota classification," in *Handbook of Arbuscular Mycorrhizal Fungi* (Cham: Springer International Publishing), 87–128.

Sýkorová, Z., Ineichen, K., Wiemken, A., and Redecker, D. (2007). The cultivation bias: different communities of arbuscular mycorrhizal fungi detected in roots from the field, from bait plants transplanted to the field, and from a greenhouse trap experiment. *Mycorrhiza* 18, 1–14. doi: 10.1007/s00572-007-0147-0

Tamburini, G., Bommarco, R., Wanger, T. C., Kremen, C., van der Heijden, M. G., Liebman, M., et al. (2020). Agricultural diversification promotes multiple ecosystem services without compromising yield. *Sci. Adv.* 6:eaba1715. doi: 10.1126/sciadv.aba1715

Torrecillas, E., Alguacil, M. M., and Roldan, A. (2012). Host preferences of arbuscular mycorrhizal fungi colonizing annual herbaceous plant species in semiarid Mediterranean prairies. *Appl. Environ. Microbiol.* 78, 6180–6186. doi: 10.1128/AEM.01287-12

Tscharntke, T., Clough, Y., Bhagwat, S. A., Buchori, D., Faust, H., Hertel, D., et al. (2011). Multifunctional shade-tree management in tropical agroforestry landscapes–a review. *J. Appl. Ecol.* 48, 619–629. doi: 10.1111/j.1365-2664.2010.01939.x

Turrini, A., Avio, L., Giovannetti, M., and Agnolucci, M. (2018). Functional complementarity of arbuscular mycorrhizal fungi and associated microbiota: the challenge of translational research. *Front. Plant Sci.* 9:1407. doi: 10.3389/fpls.2018.01407

van Dam, N. M., and Bouwmeester, H. J. (2016). Metabolomics in the rhizosphere: tapping into belowground chemical communication. *Trends Plant Sci.* 21, 256–265. doi: 10.1016/j.tplants.2016.01.008

van Tuinen, D., Tranchand, E., Hirissou, F., Wipf, D., and Courty, P. E. (2020). Carbon partitioning in a walnut-maize agroforestry system through arbuscular mycorrhizal fungi. *Rhizosphere* 15:100230. doi: 10.1016/j.rhisph.2020.100230

Verbruggen, E., Van Der HEIJDEN, M. G., Weedon, J. T., Kowalchuk, G. A., and Röling, W. F. (2012). Community assembly, species richness and nestedness of arbuscular mycorrhizal fungi in agricultural soils. *Mol. Ecol.* 21, 2341–2353. doi: 10.1111/j.1365-294X.2012.05534.x

Veresoglou, S. D., Caruso, T., and Rillig, M. C. (2013). Modelling the environmental and soil factors that shape the niches of two common arbuscular mycorrhizal fungal families. *Plant Soil* 368, 507–518. doi: 10.1007/s11104-012-1531-x

Ward, P. R., Dunin, F. X., and Micin, S. F. (2002). Water use and root growth by annual and perennial pastures and subsequent crops in a phase rotation. *Agric. Water Manag.* 53, 83–97. doi: 10.1016/S0378-3774(01)00157-3

Wei, Z., Gu, Y., Friman, V. P., Kowalchuk, G. A., Xu, Y., Shen, Q., et al. (2019). Initial soil microbiome composition and functioning predetermine future plant health. *Sci. Adv.* 5:eaaw0759. doi: 10.1126/sciadv.aaw0759

White, T. J., Bruns, T., Lee, S. J. W. T., and Taylor, J. (1990). "Amplification and direct sequencing of fungal ribosomal RNA genes for phylogenetics," in *PCR Protocols: A Guide to Methods and Applications*. eds. M. A. Innis, D. H. Gelfand, J. J. Sninsky and T. J. White (San Diego, CA: Academic Press), 315e322.

Wipf, D., Krajinski, F., van Tuinen, D., Recorbet, G., and Courty, P. E. (2019). Trading on the arbuscular mycorrhiza market: from arbuscules to common mycorrhizal networks. *New Phytol.* 223, 1127–1142. doi: 10.1111/nph.15775

Yao, H., Jiao, X., and Wu, F. (2006). Effects of continuous cucumber cropping and alternative rotations under protected cultivation on soil microbial community diversity. *Plant Soil* 284, 195–203. doi: 10.1007/s11104-006-0023-2

Yao, Z., Xing, J., Gu, H., Wang, H., Wu, J., Xu, J., et al. (2016). Development of microbial community structure in vegetable-growing soils from open-field to plastic-greenhouse cultivation based on the PLFA analysis. *J. Soils Sediments* 16, 2041–2049. doi: 10.1007/s11368-016-1397-2

Zhang, D., Zhang, L., Liu, J., Han, S., Wang, Q., Evers, J., et al. (2014). Plant density affects light interception and yield in cotton grown as companion crop in young jujube plantations. *Field Crops Res.* 169, 132–139. doi: 10.1016/j.fcr.2014.09.001

Zhang, Z., Zhang, J., Xu, G., Zhou, L., and Li, Y. (2019b). b. Arbuscular mycorrhizal fungi improve the growth and drought tolerance of Zenia insignis seedlings under drought stress. *New For.* 50, 593–604. doi: 10.1007/s11056-018-9681-1

Zhang, Y., Zheng, N., Wang, J., Yao, H., Qiu, Q., and Chapman, S. J. (2019a). a. High turnover rate of free phospholipids in soil confirms the classic hypothesis of PLFA methodology. *Soil Biol. Biochem.* 135, 323–330. doi: 10.1016/j.soilbio.2019.05.023

Zhu, Y. G., and Miller, R. M. (2003). Carbon cycling by arbuscular mycorrhizal fungi in soil–plant systems. *Trends Plant Sci.* 8, 407–409. doi: 10.1016/S1360-1385(03)00184-5

frontiers | Frontiers in Microbiology

TYPE Original Research
PUBLISHED 22 December 2022
DOI 10.3389/fmicb.2022.1027428

OPEN ACCESS

EDITED BY
Yi Luo,
Nankai University,
China

REVIEWED BY
Sudhir K. Upadhyay,
Veer Bahadur Singh Purvanchal University,
India
Xinyu Wang,
Inner Mongolia University,
China
Shi Xin Jian,
Nankai University,
China

*CORRESPONDENCE
Hui Liu
✉ zhangxiushuang522@163.com

SPECIALTY SECTION
This article was submitted to Microbial Symbioses, a section of the journal Frontiers in Microbiology

RECEIVED 25 August 2022
ACCEPTED 01 December 2022
PUBLISHED 22 December 2022

CITATION
Liu H, Tang H, Ni X, Zhang J and Zhang X (2022) *Epichloë* endophyte interacts with saline-alkali stress to alter root phosphorus-solubilizing fungal and bacterial communities in tall fescue. *Front. Microbiol.* 13:1027428. doi: 10.3389/fmicb.2022.1027428

Epichloë endophyte interacts with saline-alkali stress to alter root phosphorus-solubilizing fungal and bacterial communities in tall fescue

Hui Liu*, Huimin Tang, Xiaozhen Ni, Jiazhen Zhang and Xi Zhang

College of Life Sciences, Dezhou University, Dezhou, China

Epichloë endophytes, present in aboveground tissues, modify belowground microbial community. This study was conducted to investigate endophyte (*Epichloë coenophialum*) associated with tall fescue (*Lolium arundinaceum*) interacted with an altered saline-alkali stress (0, 200 and 400mmol/l) to affect the belowground phosphorus solubilizing microorganisms including phosphorus solubilizing fungi (PSF) and bacteria (PSB). We found that a significant interaction between *E. coenophialum* and saline-alkali stress occurred in the diversity and composition of PSF in tall fescue roots. Under saline-alkali stress conditions (200 and 400mmol/l), *E. coenophialum* significantly increased the PSF diversity and altered its composition in the roots, decreasing the relative abundance of dominant *Cladosporium* and increasing the relative abundance of *Fusarium.* However, there was no significant interaction between *E. coenophialum* and saline-alkali stress on the PSB diversity in tall fescue roots. *E. coenophialum* significantly reduced the diversity of PSB in the roots, and *E. coenophialum* effects did not depend on the saline-alkali stress treatment. Structural equation modeling (SEM) showed that *E. coenophialum* presence increased soil available phosphorus concentration under saline-alkali stress primarily by affecting PSF diversity instead of the diversity and composition of PSB.

KEYWORDS

phosphorus solubilizing fungal (PSF) diversity, phosphorus solubilizing bacterial (PSB) diversity, soil available phosphorus, *Epichloë* endophyte, saline-alkali stress, tall fescue

1. Introduction

Plant tissues form a wide variety of symbiotic associations with above and belowground microorganisms, whose interactions range from parasitism to mutualism (Liu et al., 2021). An example of aboveground plant microorganisms that often occur worldwide between cool-season grasses such as perennial ryegrass and tall fescue are the fungal endophytes

(family Clavicipitaceae, genus *Epichloë*; Leuchtmann et al., 2014; Slaughter et al., 2018). In the grass-*Epichloë* endophytes symbiotic relationship, the grass provides the endophytes with nutrients and shelter, and in exchange, the endophytes promote grass growth and confer protection against abiotic such as drought and saline-alkali and biotic such as herbivores and foliar pathogens stressors (Chen et al., 2017; Liu et al., 2017, 2022a; Qin et al., 2019; Li et al., 2020; Yang et al., 2020). Although the consequences of *Epichloë* endophyte infection on the growth and resistance of host grasses have been well documented, to our knowledge, only a few papers have measured the impact of aboveground *Epichloë* endophytes on belowground components, especially on microorganisms (Arrieta et al., 2015; Vignale et al., 2016; Zhong et al., 2018; Liu et al., 2020, 2022b; Mahmud K. et al., 2021).

Roots are colonized, both internally and externally, by a wide range of root-associated microorganisms (Keim et al., 2014). Plant root secretes root exudates such as carbohydrates, proteins, secondary metabolites, etc. enhancing arbuscular mycorrhizal fungi (AMF) and plant growth-promoting rhizobacteria (PGPR) root colonization either directly or through regulating their gene expression (Singh P. et al., 2022; Upadhyay et al., 2022a). These root-associated microorganisms promote plant growth through root-hair proliferation, enhancing soil fertility; increase in nitrogen fixation ability; enhanced leaf surface area; improvement in vigor and biomass; increased indigenous plant hormones levels; and most importantly, by improving nutrient use efficiency (Fan et al., 2020; Mahmud A. A. et al., 2021; Singh R. K. et al., 2022). The most studied microorganisms that are affected by the *Epichloë* endophytes are AMF, and the results have shown that *Epichloë* endophytes can change the colonization, diversity and community of AMF (Vignale et al., 2016; Liu et al., 2020, 2022a,b; Terlizzi et al., 2022).

In addition to AMF, another important beneficial microbial group are phosphorus solubilizing microorganisms (PSMs) including phosphorus solubilizing fungi (PSF) and bacteria (PSB), and they may contribute to plant nutrition by increasing the pool of phosphorus (P) through the hydrolysis of organic P compounds and insoluble inorganic P sources, thereby making P available for plant assimilation (Arrieta et al., 2015; Kalayu, 2019; Yin et al., 2020). The mechanisms of organic and inorganic P solubilization made by PSMs involve synthesis of metabolites such as organic acids, chelation of cations, as well as synthesis of phosphatase enzymes that hydrolyse organic P forms to inorganic P (Rashid et al., 2004; Jarosch et al., 2019; Kalayu, 2019). Both PSF and PSB exhibit P solubilization (Bolo et al., 2021). The most powerful PSF include some species of the genera *Aspergillus* and *Penicillium* (Arrieta et al., 2015; Kalayu, 2019; Bolo et al., 2021). PSB in genera *Pseudomonas*, *Bacilli*, *Rhizobium* and *Agro-bacterium* also have P solubilizing abilities (Bolo et al., 2021).

To our knowledge, there are just a few studies that have evaluated the effects of *Epichloë* endophytes on PSMs. Arrieta et al. (2015) only focusing on PSF have demonstrated that *Epichloë* endophytes increase the diversity of PSF in rhizosphere soil of *Bromus auleticus*. In addition, many studies have emphasized that the key role of environmental context on the interaction of aboveground *Epichloë*-belowgroud microorganisms (Ding et al., 2021; Liu et al., 2022b). For example, Ding et al. (2021) in tall fescue found that *Epichloë* endophytes had a greater effect on rhizosphere general fungi under P limiting conditions. Liu et al. (2022b) showed that the effects of *Epichloë* endophytes on fungal and bacterial diversity occurred in 200 mmol/l saline-alkali stress but not in either non-saline-alkali or other saline-alkali stress conditions.

Soil salinization is a severe agronomical, ecological, and socioeco-nomic problem in most arid and semiarid regions worldwide (Munns and Tester, 2008; Estrada et al., 2013). Extensive fertilization, desertification processes, urbanization, uncon-trolled irrigation practices, etc. are the main factors triggering salinity (Abd-Alla et al., 2019; Upadhyay and Chauhan, 2022b). The salinization of the soil is increasing and more than 50% of the global arable land is predicted to be salinized by the year 2050 (Butcher et al., 2016). The belowground microbial communities were commonly influenced by saline-alkali conditions (Liu et al., 2021; Che et al., 2022). In this study, we focused on the effects of saline-alkali stress and *Epichloë* endophytes in the aboveground parts of tall fescue on belowground processes including PSF and PSB. Therefore, we hypothesize that (1) *Epichloë* endophyte will alter the belowground PSF and PSB diversity and community composition, and (2) that this effect will change with the level of saline-alkali stress.

2. Materials and methods

2.1. Plant material

The endophyte-infected (EI) and endophyte-free (EF) tall fescue seeds were provided by Professor Anzhi Ren at Nankai University. EI seeds were naturally infected with *Epichloë coenophialum* (Morganjones and Gams, 1982; Leuchtmann et al., 2014), and infection by *E. coenophialum* was verified by staining and microscopic analysis using aniline blue (Latch and Christensen, 1985) and by isolation of the fungus from plant leaf sheaths on potato dextrose agar (PDA) in Petri dishes. EF seeds were obtained by storing EI seeds at room temperature for 1 year to inactivate the endophyte.

2.2. Experimental design and harvest

Tall fescue plants were used in the experiments following a combined factorial design with two factors: (1) plants infected (EI) or not infected (EF) with the endophyte *E. coenophialum*, (2) plants grown under non-saline-alkali stress or saline-alkali stress conditions including two stress levels. Combinations of the two factors gave six different treatments (2 endophyte infection status × 3 saline-alkali stress levels) with a total of 30 pots (five replicates per treatment).

Seeds of tall fescue were sown at the soil surface at the rate of 20 seeds per pot in separate plastic pots (18 cm diameter × 16 cm height), each filled with 1.2 kg of normal soil. After germination (at 7 days), the plants were thinned to 12 uniform plants per pot. The growth conditions in the greenhouse at the College of Life Sciences, Dezhou University, China were as follows: 19–25°C, 40–50% relative humidity, and natural daylight.

After 6 weeks, seedlings were treated solution with or without saline-alkali (molar ratio of NaCl: Na_2SO_4: $NaHCO_3$: Na_2CO_3 = 9: 1: 1: 9, simulating mixed saline-alkali stress conditions according to the ion composition of saline-alkali soil in Northeast China). The EI and EF seedlings were subjected to the following saline-alkali stress: 200 and 400 mM. The saline-alkali levels determined in the experiment matched the range of natural environmental conditions without leading to extremely high mortality (Liu et al., 2022b). To avoid osmotic shock, 300 ml of each saline-alkali solution was gradually introduced by successively adding 100 ml every 2 days; an equal amount of distilled water was added to the control pots. The soil water content was controlled with a soil moisture probe (ECH_2O Check; Decagon Devices, Pullman, WA, United States) every day, and the lost water was supplemented with distilled water.

After 60 days exposure to saline-alkali stress, plant roots and rhizosphere soil samples were collected. The roots were carefully rinsed with distilled water and stored at −80°C before DNA extraction. The rhizosphere soil was collected by brushing the soil from the root surface with a sterilized soft-bristled paintbrush for available phosphorus determination.

2.3. Soil available phosphorus

The soil samples were air-dried and passed through a sieve (2 mm). The soil available phosphorus concentration was calculated by shaking the soil samples with $NaHCO_3$ solution (pH 8.5) and then colorimetrically analyzing the samples using the molybdenum blue method (Robertson et al., 1999).

2.4. DNA extraction, sequencing, and microbial community analysis

To analyze the composition of PSF and PSB communities in the root samples with different saline-alkali stress, microbial DNA from each sample was extracted by using the FastDNA® SPIN for soil kit (MP Biomedicals, Santa Ana, CA, United States). Extracted DNA was amplified using a ITS1F (5'-CTTGGTCATTTAGAGGAAGTAA-3′) and ITS2R (5'-GCTGCGTTCTTCATCGATGC-3′) universal primer set targeting the ITS1 region of the fungi as well as a 799F (5'-AACMGGATTAGATACCCKG-3′) and 1193R (5'-ACGTCATCCCCACCTTCC-3′) universal primer set targeting the V5–V7 region of the bacterial 16S rRNA. PCR products were purified and sequenced on an Illumina MiSeq platform (Illumina, San Diego, United States) by the standard protocols of Majorbio Bio-Pharm Technology Co. Ltd. (Shanghai, China).

The sequences among all reads were used to define operational taxonomic units (OTUs) using UPARSE (version 7.1[1]) with 97% sequence similarity. The sequences of all other samples were subsampled with the minimum number of reads to compare different samples at the same sequencing level (Fang et al., 2018). Final OTUs were taxonomically classified using the RDP Classifier algorithm[2] against the Unite7.2 ITS database and the Silva132 16S rRNA database at a confidence threshold of 70%.

2.5. Statistical analysis

The effects of the saline-alkali stress and *Epichloë* endophyte infection on the phosphorus solubilizing fungal (PSF) diversity, phosphorus solubilizing bacterial (PSB) diversity and soil available phosphorus (AP) concentration were analyzed using two-factor analysis of variance (ANOVA) with SPSS 20.0 (SPSS Inc., Chicago, IL, United States). When a significant effect was detected, the differences between the means of different treatments were determined using Duncan's multiple-range tests at $p = 0.05$. PSF and PSB diversity were estimated as the effective number of species using the exponential of Shannon diversity index. Variation in the PSF and PSB community composition was visualized using non-metric multidimensional scaling (NMDS) ordination, using the metaMDS function in the VEGAN package. Structural equation modeling (SEM) was fitted to our data using SPSS Amos 21.0 to identify potential causal relationships between explanatory variables (PSF and PSB diversity and community composition in roots) and soil AP concentration.

3. Results

3.1. Soil available phosphorus concentration

The soil available phosphorus (AP) concentration was significantly affected by saline-alkali stress ($F = 3.398$, $p = 0.050$) and *Epichloë* endophyte infection ($F = 11.645$, $p = 0.002$). The soil AP concentration was increased by *Epichloë* endophyte infection (16%, Figure 1A) but decreased by saline-alkali stress (11% on average, Figure 1B).

3.2. PSF and PSB diversity

The PSF diversity was significantly affected by saline-alkali stress, *Epichloë* endophyte infection and their interactions

1 http://drive5.com/uparse/

2 http://rdp.cme.msu.edu/

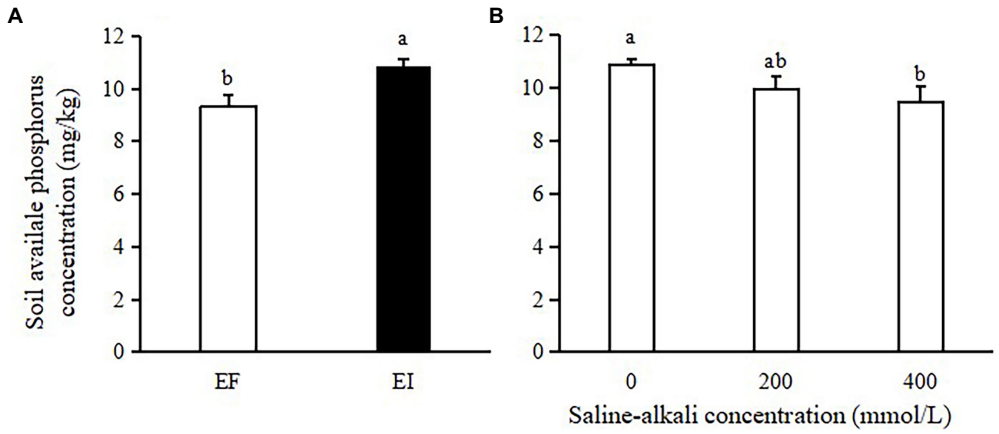

FIGURE 1
Effects of *Epichloë* endophyte **(A)** and saline-alkali stress **(B)** on soil available phosphorus concentration. Values are means±SE. Different letters denote means that are significantly different ($p<0.05$).

($F=12.272$, $p<0.001$). Under non-stress (0 mM) conditions, EI and EF tall fescue had similar PSF diversity. Saline-alkali stress significantly increased PSF diversity ($F=73.249$, $p<0.001$). *Epichloë* endophyte infection significantly increased the PSF diversity of tall fescue by 29 and 60% in the 200 and 400 mM saline-alkali stress conditions, respectively, (Figure 2A). The PSB diversity of tall fescue was significantly affected by the main effects of *Epichloë* endophyte ($F=22.380$, $p<0.001$), with *Epichloë* endophyte infection significantly decreasing the PSB diversity of tall fescue by 27% (Figure 2B). Saline-alkali stress also significantly decreased the PSB diversity (18% on average; $F=7.823$, $p=0.002$; Figure 2C).

3.3. PSF and PSB community composition

The 11 PSF genera covered by OTUs were *Acremonium*, *Aspergillus*, *Chaetomium*, *Cladosporium*, *Curvularia*, *Fusarium*, *Neocosmospora*, *Penicillium*, *Phoma*, *Talaromyces* and *Trichoderma*. *Cladosporium* was the dominant genus in all treatments, and its proportion ranged from 73.7 to 91.2%. *Epichloë* endophyte infection decreased the relative abundance of dominant *Cladosporium* and increased the relative abundance of *Fusarium* under saline-alkali stress conditions (Figure 3A). The PSB community comprised members of the genera *Arthrobacter*, *Bacillus*, *Flavobacterium*, *Pseudomonas* and *Streptomyces*. All treatments were dominated by the *Flavobacterium* (37.5% on average) and *Pseudomonas* (58.1% on average; Figure 3B).

NMDS based on the relative abundance of OTUs clustering by saline-alkali stress and *Epichloë* endophyte revealed that there was a significant effect of the interaction between saline-alkali stress and *Epichloë* endophyte on the community composition of PSF and PSB. Under non-stress (0 mM) conditions, there was not a significant difference either in PSF or PSB communities between EF and EI tall fescue. However, a clear separation in the PSF and PSB communities between EI and EF tall fescue was observed in 200 and 400 mM saline-alkali stress conditions (Figures 4A,B).

3.4. Relationship between PSF, PSB diversity, community composition and soil available phosphorus

We used SEM to assess the extent of direct and indirect effects of saline-alkali stress (S) and *Epichloë* endophyte infection (E) on the soil available phosphorus (AP) concentration of the tall fescue (Figures 5A,B). Saline-alkali stress and *Epichloë* endophyte infection had no direct effects on the soil AP concentration, but these two treatments increased the soil AP concentration by indirectly increasing the PSF diversity (PSFD; Figure 5A) but not by affecting PSB community diversity or composition (PSFC; Figure 5B).

4. Discussion

Soil salinization is detrimental to plant growth and yield in agroecosystems worldwide. One possible improvement strategy is to explore the potential of associated salt-tolerant microorganism to confer saline-alkali stress tolerance to plants (Moreira et al., 2020; Yang et al., 2020). The suitable root-associated microorganisms and components of root exudate interplay against stress (Singh P. et al., 2022; Upadhyay et al., 2022a). In our study, we found that the diversity of the PSF of saline-alkali stress conditions was higher than that in the non-saline-alkali stress conditions; however, the diversity of PSB showed the opposite direction, with higher diversity in non-saline-alkali stress than that in saline-alkali stress conditions. Therefore, compared with PSB, most PSF were saline-alkali tolerant. Among PSF, *Cladosporium* had the largest relative abundance and therefore an

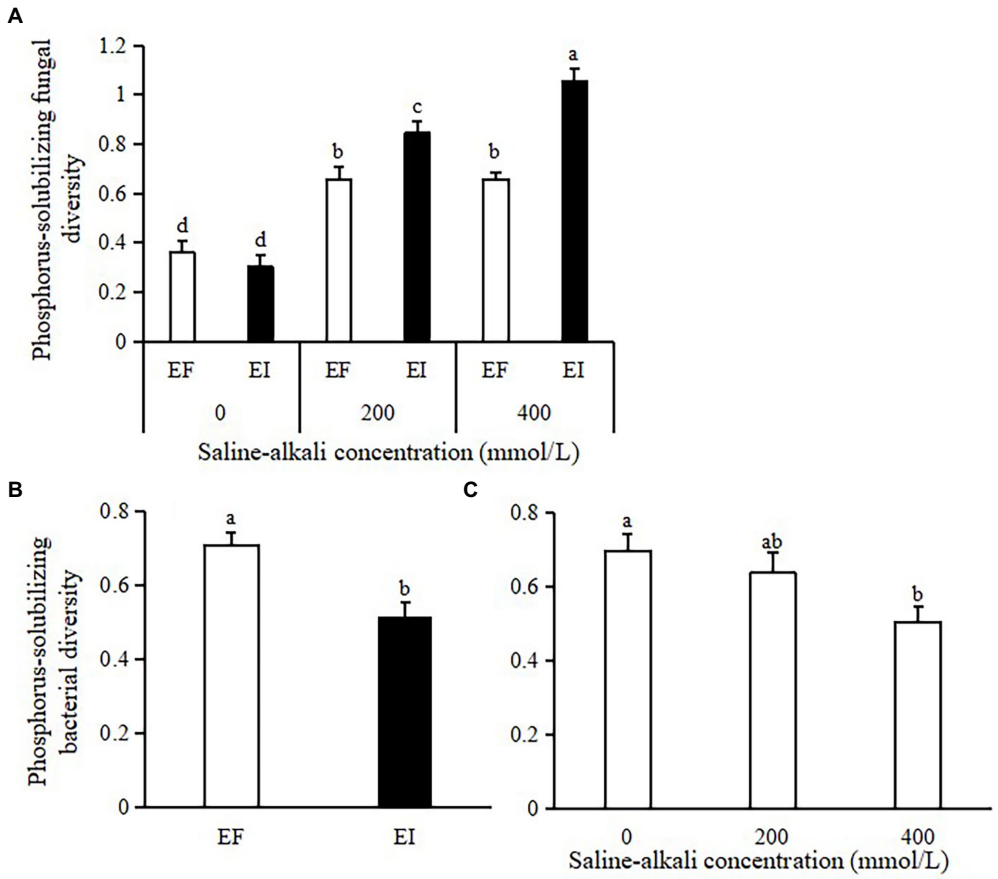

FIGURE 2
Effects of the interaction between *Epichloë* endophyte and saline-alkali stress on phosphorus solubilizing fungal (PSF) diversity in tall fescue roots **(A)**, and effects of *Epichloë* endophyte **(B)** and saline-alkali stress **(C)** on phosphorus solubilizing bacterial (PSB) diversity in tall fescue roots. Different letters denote means that are significantly different ($p<0.05$).

absolute advantage. The relative abundance of *Cladosporium* decreased with the increase of saline-alkali stress.

The *Epichloë* endophytes existing in the aboveground part of the host grass have been demonstrated that can produce effects on root microorganisms, and they can change the impact of environment condition on root microorganisms (Bell-Dereske et al., 2017; Slaughter et al., 2018; Zhong et al., 2021; Liu et al., 2022b). Bell-Dereske et al. (2017) in *Ammophila breviligulata* showed that with *Epichloë amarillans* infected, the diversity of root-associated bacteria declined with higher soil moisture, whereas in its absence, bacterial diversity increased with higher soil moisture. Slaughter et al. (2018) in tall fescue found that *E. coenophiala* significantly decreased the rate of AMF arbuscule formation in treatments without added precipitation, but had no significant effect in added precipitation treatments. Zhong et al. (2021) in *Achnatherum inebrians* showed that *Epichloë gansusensis* increased root-associated AMF diversity under drought conditions, while decreasing diversity under the water addition treatment. Liu et al. (2022b) demonstrated that the effects of *Epichloë* endophyte infection on AMF diversity shifted from neutral in non-saline-alkali stress to positive in 200 and 400 mmol/l saline-alkali stress. Little is known about the *Epichloë*-PSMs interaction and there is even less knowledge about the interaction *Epichloë*-PSMs-saline-alkali stress. Arrieta et al. (2015) in *B. auleticus* showed that *Epichloë pampeana* increased the diversity of PSF. In the present study, a synergistic effect occurred between *E. coenophiala* and saline-alkali stress on the diversity of PSF in tall fescue roots, and the PSF diversity of tall fescue roots infected with *E. coenophiala* under saline-alkali stress was significantly higher than that of tall fescue roots infected with *E. coenophiala* alone or treated with saline-alkali alone. In addition, *E. coenophiala* presence altered the relative abundance of several PSF groups, including decreasing the relative abundance of dominant *Cladosporium* and increasing the relative abundance of *Fusarium*. *Fusarium* has been previously recorded able to solubilize P. NMDS ordination revealed that a clear separation in the PSF communities between EI and EF plant roots was observed in 200 and 400 mmol/l saline-alkali stress conditions.

In contrast to PSF, there was no interaction between *E. coenophiala* and saline-alkali stress on the diversity of PSB in tall fescue roots. *E. coenophiala* decreased the diversity of

PSB in tall fescue roots regardless of saline-alkali stress level. However, a significant effect of the interaction between *E. coenophiala* and saline-alkali stress on the composition of PSB communities was observed. There was a clear separation between the PSB communities due to *E. coenophiala* presence that occurred both under 200 and 400 mmol/l saline-alkali stress conditions, whereas *E. coenophiala* presence had no obvious effect on the PSB community composition under non-stress conditions.

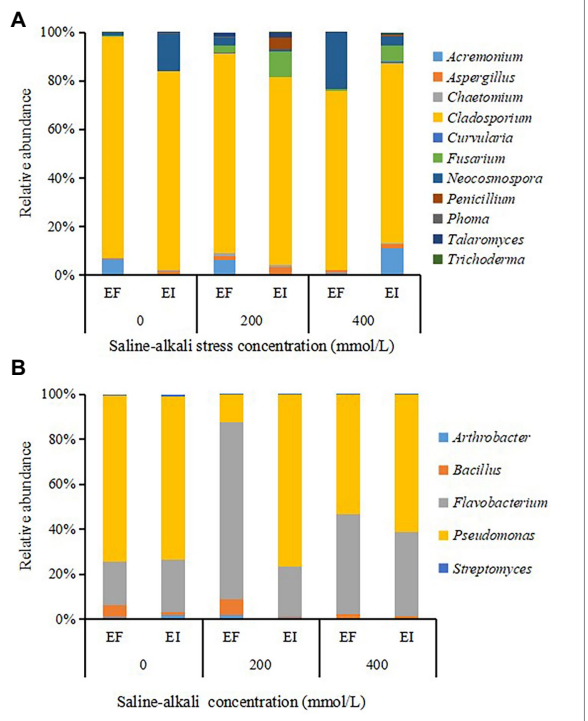

FIGURE 3
The composition of different genera of phosphorus solubilizing fungi (PSF) **(A)** and phosphorus solubilizing bacteria (PSB) **(B)** in roots of tall fescue with (EI) and without (EF) *Epichloë* endophyte under saline-alkali stress.

Phosphorus is an essential element for plant development and growth, making up about 0.2% of plant dry weight (Smith et al., 2011). Plants obtain phosphorus from soil solution in the form of phosphorus anion. However, phosphate anions react easily and are fixed by precipitation with cations such as Ca^{2+}, Mg^{2+}, Fe^{3+} and Al^{3+} under saline-alkali stress conditions due to high pH, becoming highly insoluble phosphate that is not available to plants (Machiavelli and Khurana, 2013; Singh P. et al., 2022; Upadhyay and Chauhan, 2022b). Rangseekaew et al. (2021) showed that rhizospheric bacteria promoted plants growth under NaCl stress resulted from the production of many plant-growth promoting attributes such as siderophore production, indole-3-acetic acid, and phosphate solubilization. In our study, saline-alkali stress and the presence of the *E. coenophiala* brought changes to the soil available phosphorus (AP), and a close association was also observed between the belowground phosphorus solubilizing microorganisms and soil AP. SEM results revealed that *E. coenophiala* presence had no direct effects on the soil AP, but increased the soil AP directly by increasing the diversity of PSF in tall fescue roots under saline-alkali stress conditions.

5. Conclusion

Our results demonstrated that *E. coenophiala* significantly increased the diversity of PSF and altered the community composition of PSF in tall fescue roots under saline-alkali stress conditions but did not affect those parameters mentioned above under non-stress conditions. By contrast, both *E. coenophiala* and saline-alkali stress significantly decreased the diversity of PSB in tall fescue roots. Furthermore, the positive effects of the

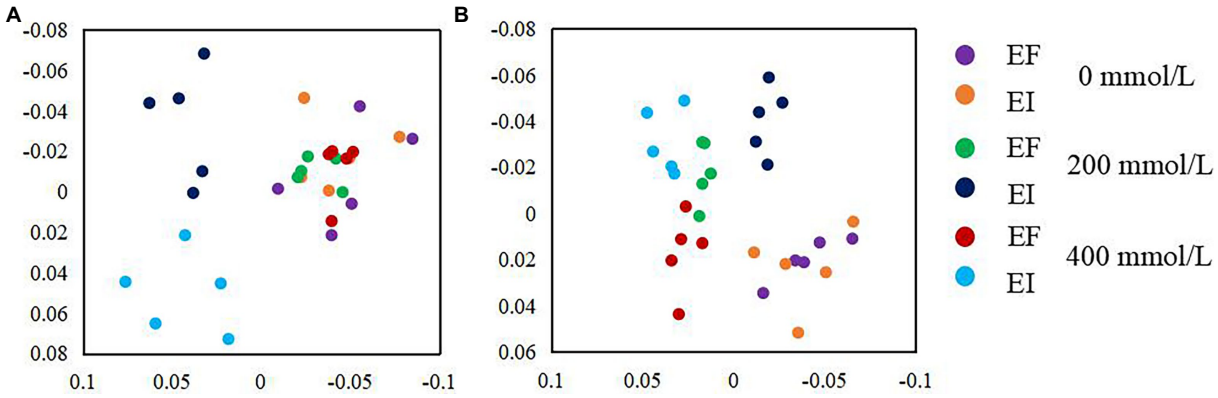

FIGURE 4
Non-metric multidimensional scaling (NMDS) ordination of PSF **(A)** and PSB **(B)** community composition in roots of tall fescue with (EI) and without (EF) *Epichloë* endophyte under saline-alkali stress.

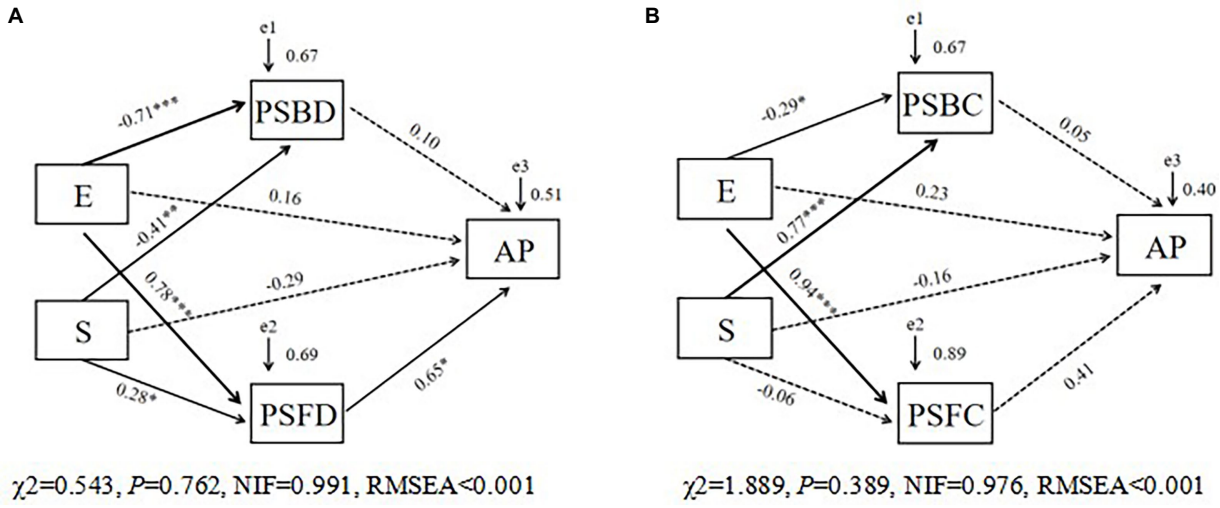

FIGURE 5
The structural equation model (SEM) showing the hypothesized causal relationships between explanatory factors [**(A)** PSF and PSB diversity; **(B)**, PSF and PSB community composition] and available phosphorus concentration in rhizosphere soil of tall fescue under saline-alkali stress. The width of arrows indicates the strength of the standardized path coefficient (***, $p<0.001$; **, $p<0.01$; *, $p<0.05$). The e-values represent residuals. E, endophyte infection status; S, saline-alkali stress; PSFD, phosphorus solubilizing fungal diversity; PSBD, phosphorus solubilizing bacterial diversity; PSFC, phosphorus solubilizing fungal community composition; PSBC, phosphorus solubilizing bacterial community composition.

E. coenophiala on PSF diversity, generate a significant increase in the phosphorus available to plants under saline-alkali stress conditions, making this a very interesting model to evaluate its impact on grasses of economic interest.

Data availability statement

The datasets presented in this study can be found in online repositories. The names of the repository/repositories and accession number(s) can be found below: NCBI - PRJNA883018.

Author contributions

HL designed the research. HT, XN, JZ, and XZ performed the experiments. HL and HT analyzed the data and wrote the manuscript. HL revised and polished the manuscript. All authors contributed to the article and approved the submitted version.

Funding

This work was supported by the National Natural Science Foundation of China (32001103) and Dezhou University Science Research Foundation (2019xjrc317).

Conflict of interest

The authors declare that the research was conducted in the absence of any commercial or financial relationships that could be construed as a potential conflict of interest.

Publisher's note

All claims expressed in this article are solely those of the authors and do not necessarily represent those of their affiliated organizations, or those of the publisher, the editors and the reviewers. Any product that may be evaluated in this article, or claim that may be made by its manufacturer, is not guaranteed or endorsed by the publisher.

References

Abd-Alla, M. H., Nafady, N. A., Bashandy, S. R., and Hassan, A. A. (2019). Mitigation of effect of salt stress on the nodulation, nitrogen fixation and growth of chickpea (*Cicer arietinum* L.) by triple microbial inoculation. *Rhizosphere* 10:100148. doi: 10.1016/j.rhisph.2019.100148

Arrieta, A. M., Iannone, L. J., Scervino, J. M., Vignale, M. V., and Novas, M. V. (2015). A foliar endophyte increases the diversity of phosphorus-solubilizing rhizospheric fungi and mycorrhizal colonization in the wild grass *Bromus auleticus*. *Fungal Ecol.* 17, 146–154. doi: 10.1016/j.funeco.2015.07.001

Bell-Dereske, L., Takacs-Vesbach, C., Kivlin, S. N., Emery, S. M., and Rudgers, J. A. (2017). Leaf endophytic fungus interacts with precipitation to alter belowground microbial communities in primary successional dunes. *FEMS Microbiol. Ecol.* 93, 1–16. doi: 10.1093/femsec/fix036

Bolo, P., Kihara, J., Mucheru-Muna, M., Njeru, E. M., Kinyua, M., and Sommer, R. (2021). Application of residue, inorganic fertilizer and lime affect phosphorus solubilizing microorganisms and microbial biomass under different tillage and cropping systems in a Ferralsol. *Geoderma* 390:114962. doi: 10.1016/j.geoderma.2021.114962

Butcher, K., Wick, A. F., De Sutter, T., Chatterjee, A., and Harmon, J. P. (2016). Soil salinity: a threat to global food securit. *Agron. J.* 108, 2189–2200. doi: 10.2134/agronj2016.06.0368

Che, J., Zhu, Y. L., Li, Y. H., Zhang, R., Ruan, Z. Y., and Zhang, W. (2022). Response of bacterial communities in saline-alkali soil to different pesticide stresses. *Environ. Sci. Pollut. R.* 29, 42709–42719. doi: 10.1007/s11356-021-16316-w

Chen, W., Liu, H., Wurihan Gao, Y. B., Card, S. D., and Ren, A. Z. (2017). The advantages of endophyte-infected over uninfected tall fescue in the growth and pathogen resistance are counteracted by elevated CO_2. *Sci. Rep.* 7:6952. doi: 10.1038/s41598-017-07183-y

Ding, N., Guo, H. C., Kupper, J. V., and McNear, D. H. Jr. (2021). Phosphorus source and *Epichloë coenophiala* strain interact over time to modify tall fescue rhizosphere microbial community structure and function. *Soil Biol. Biochem.* 154:108125. doi: 10.1016/j.soilbio.2020.108125

Estrada, B., Aroca, R., Maathuis, F. J. M., Barea, J. M., and Ruiz-Lozano, J. M. (2013). Arbuscular mycorrhizal fungi native from a Mediterranean saline area enhance maize tolerance to salinity through improved ion homeostasis. *Plant Cell Environ.* 36, 1771–1782. doi: 10.1111/pce.12082

Fan, D., Subramanian, S., and Smith, D. L. (2020). Plant endophytes promote growth and alleviate salt stress in *Arabidopsis thaliana*. *Sci. Rep.* 10:12740. doi: 10.1038/s41598-020-69713-5

Fang, D., Zhao, G., Xu, X., Zhang, Q., Shen, Q., Fang, Z., et al. (2018). Microbial community structures and functions of wastewater treatment systems in plateau and cold regions. *Bioresour. Technol.* 249, 684–693. doi: 10.1016/j.biortech.2017.10.063

Jarosch, K. A., Kandeler, E., Frossard, E., and Bünemann, E. K. (2019). Is the enzymatic hydrolysis of soil organic phosphorus compounds limited by enzyme or substrate availability? *Soil Biol. Biochem.* 139:107628. doi: 10.1016/j.soilbio.2019.107628

Kalayu, G. (2019). Phosphate solubilizing microorganisms: promising approach as biofertilizers. *Int. J. Agronomy* 2019, 1–7. doi: 10.1155/2019/4917256

Keim, J., Mishra, B., Sharma, R., Ploch, S., and Thines, M. (2014). Root-associated fungi of *Arabidopsis thaliana* and *Microthlaspi perfoliatum*. *Fungal Divers.* 66, 99–111. doi: 10.1007/s13225-014-0289-2

Latch, G. C. M., and Christensen, M. J. (1985). Artificial infection of grasses with endophytes. *Ann. Appl. Biol.* 107, 17–24. doi: 10.1111/j.1744-7348.1985.tb01543.x

Leuchtmann, A., Bacon, C. W., Schardl, C. L., White, J. F., and Tadych, M. (2014). Nomen-clatural realignment of *Neotyphodium* species with genus *Epichloë*. *Mycologia* 106, 202–215. doi: 10.3852/13-251

Li, F., Duan, T. Y., and Li, Y. Z. (2020). Effects of the fungal endophyte Epichloë festucae var. lolii on growth and physiological responses of perennial ryegrass cv. Fairway to combined drought and pathogen stresses. *Microorganisms* 8:1917. doi: 103390/microorganisms8121917

Liu, H., Chen, W., Wu, M., Wu, R. H., Zhou, Y., Gao, Y. B., et al. (2017). Arbuscular mycorrhizal fungus inoculation reduces the drought-resistance advantage of endophyte-infected versus endophyte-free *Leymus chinensis*. *Mycorrhiza* 27, 791–799. doi: 10.1007/s00572-017-0794-8

Liu, H. Q., Lu, X. B., Li, Z. H., Tian, C. Y., and Song, J. (2021). The role of root-associated microbes in growth stimulation of plants under saline conditions. *Land Degrad. Dev.* 32, 3471–3486. doi: 10.1002/ldr.3955

Liu, H., Tang, H. M., Ni, X. Z., Zhang, Y. J., and Wang, Y. C. (2022a). Interactive effects of *Epichloë* endophyte and arbuscular mycorrhizal fungi on saline-alkali stress tolerance in tall fescue. *Front. Microbiol.* 13:855890. doi: 10.3389/fmicb.2022.855890

Liu, H., Tang, H. M., Ni, X. Z., Zhang, Y. J., and Wang, Y. C. (2022b). Effects of the endophyte *Epichloë coenophiala* on the root microbial community and growth performance of tall fescue in different saline-alkali soils. *Fungal Ecol.* 57-58:101159. doi: 10.1016/j.funeco.2022.101159

Liu, H., Wu, M., Liu, J. M., Gao, Y. B., and Ren, A. Z. (2020). Endophyte infection influences arbuscular mycorrhizal fungi communities in rhizosphere soils of host as opposed to non-host grass. *Eur. J. Soil Sci.* 72, 995–1009. doi: 10.1111/ejss.12996

Machiavelli, S., and Khurana, S. M. P. (2013). An inoculating potential of phosphate-solubilising microbes as biofertilizers. *J. Biofertil. Biopestici.* 4:e100. doi: 10.4172/2155-6202.1000e110

Mahmud, K., Lee, K., Hill, N. S., Mergoum, A., and Missaoui, A. (2021). Influence of tall fescue *Epichloë* endophytes on rhizosphere soil microbiome. *Microorganisms* 9:1843. doi: 10.3390/microorganisms9091843

Mahmud, A. A., Upadhyay, S. K., Srivastava, A. K., and Bhojiya, A. A. (2021). Biofertilizers: a nexus between soil fertility and crop productivity under abiotic stress. *Curr. Res. Env. Sust.* 3:100063. doi: 10.1016/j.crsust.2021.100063

Moreira, H., Pereira, S. I. A., Vega, A., Castro, P. M. L., and Marques, A. P. G. C. (2020). Synergistic effects of arbuscular mycorrhizal fungi and plant growth-promoting bacteria benefit maize growth under increasing soil salinity. *J. Environ. Manag.* 257:109982. doi: 10.1016/j.jenvman.2019.109982

Morganjones, G., and Gams, W. (1982). Notes on Hyphomycetes. XLI. An endophyte of *Festuca arundinacea* and the anamorph of *Epichloë typhina*, new taxa in one of two new sections of Acremonium. *Mycotaxon* 50, 113–117.

Munns, R., and Tester, M. (2008). Mechanisms of salinity tolerance. *Annu. Rev. Plant Biol.* 59, 651–681. doi: 10.1146/annurev.arplant.59.032607.092911

Qin, J. H., Wu, M., Liu, H., Gao, Y. B., and Ren, A. Z. (2019). Endophyte infection and methyl jasmonate treatment increased the resistance of *Achnatherum sibiricum* to insect herbivores independently. *Toxins* 11, 7–19. doi: 10.3390/toxins11010007

Rangseekaew, P., Barros-Rodriguez, A., Pathom-aree, W., and Manzanera, M. (2021). Deep-Sea actinobacteria mitigate salinity stress in tomato seedlings and their biosafety testing. *Plan. Theory* 10:1687. doi: 10.3390/plants10081687

Rashid, M., Khalil, S., Ayub, N., Alam, S., and Latif, F. (2004). Organic acids production and phosphate solubilization by phosphate solubilizing microorganisms (PSM) under in vitro conditions. *Pak. J. Biol. Sci.* 7, 187–196. doi: 10.3923/pjbs.2004.187.196

Robertson, G., Coleman, D., Bledsoe, C., and Sollins, P. (1999). *Standard soil Methods for Long-Term Ecological Research*. Oxford University Press, New York.

Singh, P., Chauhan, P. K., Upadhyay, S. K., Singh, R. K., Dwivedi, P., Wang, J., et al. (2022). Mechanistic insights and potential use of siderophores producing microbes in rhizosphere for mitigation of stress in plants grown in degraded land. *Front. Microbiol.* 13:898979. doi: 10.3389/fmicb.2022.898979

Singh, R. K., Singh, P., Sharma, A., Guo, D. J., Upadhyay, S. K., Song, Q. Q., et al. (2022). Unraveling nitrogen fixing potential of endophytic Diazotrophs of different Saccharum species for sustainable sugarcane growth. *Int. J. Mol. Sci.* 23:6242. doi: 10.3390/ijms23116242

Slaughter, L. C., Nelson, J. A., Carlisle, E., Bourguignon, M., Dinkins, R. D., Phillips, T. D., et al. (2018). Climate change and *Epichloë coenophiala* association modify belowground fungal symbioses of tall fescue host. *Fungal Ecol.* 31, 37–46. doi: 10.1016/j.funeco.2017.10.002

Smith, S. E., Jakobsen, I., Gronlund, M., and Smith, F. A. (2011). Roles of arbuscular mycorrhizas in plant phosphorus nutrition: interactions between pathways of phosphorus uptake in arbuscular mycorrhizal roots have important implications for understanding and manipulating plant phosphorus acquisition. *Plant Physiol.* 156, 1050–1057. doi: 10.1104/pp.111.174581

Terlizzi, N. L., Rodríguez, M. A., Iannone, L. J., Lanari, E., and Novas, M. V. (2022). *Epichloë* endophyte affects the root colonization pattern of belowground symbionts in a wild grass. *Fungal Ecol.* 57-58:101143. doi: 10.1016/j.funeco.2022.101143

Upadhyay, S. K., and Chauhan, P. K. (2022b). Optimization of eco-friendly amendments as sustainable asset for salt-tolerant plant growth-promoting bacteria mediated maize (*Zea Mays* L.) plant growth, Na uptake reduction and saline soil restoration. *Environ. Res.* 211:113081. doi: 10.1016/j.envres.2022.113081

Upadhyay, S. K., Srivastava, A. K., Rajput, V. D., Chauhan, P. K., Bhojiya, A. A., Jain, D., et al. (2022a). Root exudates: mechanistic insight of plant growth promoting rhizobacteria for sustainable crop production. *Front. Microbiol.* 13:916488. doi: 10.3389/fmicb.2022.916488

Vignale, M. V., Iannone, L. J., Pinget, A. D., De Battista, J. P., and Novas, M. V. (2016). Effect of epichloid endophytes and soil fertilization on arbuscular mycorrhizal colonization of a wild grass. *Plant Soil* 405, 279–287. doi: 10.1007/s11104-015-2522-5

Yang, Y. R., Cao, Y. P., Li, Z. X., Zhukova, A., Yang, S. T., Wang, J. L., et al. (2020). Interactive effects of exogenous melatonin and *Rhizophagus intraradices* on saline-alkaline stress tolerance in *Leymus chinensis*. *Mycorrhiza* 30, 357–371. doi: 10.1007/s00572-020-00942-2

Yin, L. J., Liu, B., Wang, H. C., Zhang, Y., Wang, S., Jiang, F., et al. (2020). The rhizosphere microbiome of *Mikania micrantha* provides insight into adaptation and invasion. *Front. Microbiol.* 11:1462. doi: 10.3389/fmicb.2020.01462

Zhong, R., Xia, C., Ju, Y. W., Li, N. N., Zhang, X. X., Nan, Z. B., et al. (2018). Effects of *Epichloë gansuensis* on root-associated fungal communities of *Achnatherum inebrians* under different growth conditions. *Fungal Ecol.* 31, 29–36. doi: 10.1016/j.funeco.2017.10.005

Zhong, R., Xia, C., Ju, Y. W., Zhang, X. X., Duan, T. Y., Nan, Z. B., et al. (2021). A foliar *Epichloë* endophyte and soil moisture modified belowground arbuscular mycorrhizal fungal biodiversity associated with *Achnatherum inebrians*. *Plant Soil* 458, 105–122. doi: 10.1007/s11104-019-04365-7

frontiers | Frontiers in Microbiology

TYPE Original Research
PUBLISHED 16 February 2023
DOI 10.3389/fmicb.2023.1074468

OPEN ACCESS

EDITED BY
Juan Sun,
Qingdao Agricultural University,
China

REVIEWED BY
Mari Pent,
University of Tartu,
Estonia
Sudhir K. Upadhyay,
Veer Bahadur Singh Purvanchal University,
India

*CORRESPONDENCE
Yanfeng Han
✉ swallow1128@126.com

SPECIALTY SECTION
This article was submitted to Microbial Symbioses, a section of the journal Frontiers in Microbiology

RECEIVED 19 October 2022
ACCEPTED 30 January 2023
PUBLISHED 16 February 2023

CITATION
Ge W, Ren Y, Dong C, Shao Q, Bai Y, He Z, Yao T, Zhang Y, Zhu G, Deshmukh SK and Han Y (2023) New perspective: Symbiotic pattern and assembly mechanism of *Cantharellus cibarius*-associated bacteria. *Front. Microbiol.* 14:1074468. doi: 10.3389/fmicb.2023.1074468

New perspective: Symbiotic pattern and assembly mechanism of *Cantharellus cibarius*-associated bacteria

Wei Ge[1], Yulian Ren[1], Chunbo Dong[1], Qiuyu Shao[1], Yanmin Bai[1], Zhaoying He[1], Ting Yao[2], Yanwei Zhang[3], Guosheng Zhu[4], Sunil Kumar Deshmukh[5] and Yanfeng Han[1]*

[1]Institute of Fungus Resources, Department of Ecology/Key Laboratory of Plant Resource Conservation and Germplasm Innovation in Mountainous Region (Ministry of Education), College of Life Sciences/Institute of Agro-Bioengineering, Guizhou University, Guiyang, Guizhou, China, [2]Analysis and Test Center, Huangshan University, Huangshan, China, [3]School of Biological Sciences, Guizhou Education University, Guiyang, Guizhou, China, [4]Guizhou Key Laboratory of Edible Fungi Breeding, Institute of Crop Germplasm Resources, Guizhou Academy of Agricultural Sciences, Guiyang, Guizhou, China, [5]TERI-Deakin Nano Biotechnology Centre, The Energy and Resources Institute, New Delhi, India

Cantharellus cibarius, an ectomycorrhizal fungus belonging to the Basidiomycetes, has significant medicinal and edible value, economic importance, and ecological benefits. However, *C. cibarius* remains incapable of artificial cultivation, which is thought to be due to the presence of bacteria. Therefore, much research has focused on the relationship between *C. cibarius* and bacteria, but rare bacteria are frequently overlooked, and symbiotic pattern and assembly mechanism of the bacterial community associated with *C. cibarius* remain unknown. In this study, the assembly mechanism and driving factors of both abundant and rare bacterial communities of *C. cibarius* were revealed by the null model. The symbiotic pattern of the bacterial community was examined using a co-occurrence network. Metabolic functions and phenotypes of the abundant and rare bacteria were compared using METAGENassist2, and the impacts of abiotic variables on the diversity of abundant and rare bacteria were examined using partial least squares path modeling. In the fruiting body and mycosphere of *C. cibarius*, there was a higher proportion of specialist bacteria compared with generalist bacteria. Dispersal limitation dominated the assembly of abundant and rare bacterial communities in the fruiting body and mycosphere. However, pH, 1-octen-3-ol, and total phosphorus of the fruiting body were the main driving factors of bacterial community assembly in the fruiting body, while available nitrogen and total phosphorus of the soil affected the assembly process of the bacterial community in the mycosphere. Furthermore, bacterial co-occurrence patterns in the mycosphere may be more complex compared with those in the fruiting body. Unlike the specific potential functions of abundant bacteria, rare bacteria may provide supplementary or unique metabolic pathways (such as sulfite oxidizer and sulfur reducer) to enhance the ecological function of *C. cibarius*. Notably, while volatile organic compounds can reduce mycosphere bacterial diversity, they can increase fruiting body bacterial diversity. Findings from this study further, our understanding of *C. cibarius*-associated microbial ecology.

KEYWORDS

***Cantharellus cibarius*, mycosphere, diversity, community assembly, microbial interaction, volatile organic compounds**

1. Introduction

Mycorrhizal is one of the most common symbiotic forms in terrestrial ecosystems. More than 80% of plants in the world form mycorrhizal relationships by interacting with various types of fungi, such as ectomycorrhiza (Chauhan et al., 2022). The fungi that form ectomycorrhiza in symbiosis with plants are known as ectomycorrhizal fungi (EcMF) and include most Basidiomycota and Asomycota and some Zygomycota. These fungi predominantly associate with the roots of some plants in Pinaeceae, Cupressaceae, and Salicaceae to form EcMF with unique structures such as mantle, Harley reticulum, and extramatrical mycelia (Chot and Reddy, 2022). The development of the ecological niche of other soil microorganisms (such as bacteria) is thought to have been significantly influenced by the origin of coevolution between mycorrhizal fungi and land plants, leading to a number of antagonistic and reciprocal strategies (Boer et al., 2005). Mycorrhizal fungi have become a research hotspot in microbial ecology owing to the rapid development of various disciplines and microbial technologies, which have facilitated the gradual realization of the significance of fungus-related microbiota in fruiting body formation and development (Deveau et al., 2016; Pent et al., 2017). For instance, extensive research has been conducted on the microbiota of Ascomycetes (truffles) (Antony-Babu et al., 2014; Splivallo et al., 2015; Liu et al., 2021), while less is known about the microbiota of traditionally consumed Basidiomycetes. A group of EcMF known as *Cantharellus cibarius* is extensively distributed and has a delectable flavor and a high economic value. The presence of bacteria and other foreign microorganisms in the spores and tissues of the fruiting body, which complicates the intricate symbiotic relationship between the fruiting body and host tree, is thought to be the primary reason why artificial cultivation of *C. cibarius* is challenging (Kozarski et al., 2015). Consequently, rapidly developing high-throughput sequencing technologies have been employed to supplement the understanding of the microbial species associated with *C. cibarius* (Pent et al., 2017, 2020; Gohar et al., 2020; Ge et al., 2021). For instance, Gohar et al. (2020) found that the potential functional abundance of bacteria connected to *C. cibarius* varied with tissue and developmental phases. Ge et al. (2021) discovered differences in bacterial community composition and potential functional differentiation trends between fruiting bodies and rhizomorphs of *C. cibarius*. According to Pent et al. (2017, 2020), the main predominant factors influencing the bacterial diversity and community composition of *C. cibarius* were soil pH, host identity, and chemical composition of fruiting bodies. Saidi et al. (2016) isolated six strains of bacteria that could produce aroma from the fruiting body of *C. cibarius*, but it was unclear whether these bacteria were involved in the aroma synthesis of fungi. However, a similar situation has been demonstrated in Ascomycota such as truffles (Splivallo et al., 2015; Orban et al., 2023). Typically, the volatile organic compounds (VOCs) in the odor components of mushrooms are the primary factors affecting odor characteristics (Zhu et al., 2022). Such VOCs are low-molecular-weight substances (up to 500 Da) with high vapor pressure and a low boiling point. These properties are conducive to VOCs being volatilized and diffused in soil and air, even over long distances (Tyc et al., 2017; Orban et al., 2023). Consequently, VOCs are particularly suitable as signaling substances to assist mushrooms in being easily detected by animals or humans and completing their spore propagation strategy (Vahdatzadeh et al., 2019; Ge et al., 2021). VOCs also frequently mediate interactions between soil microorganisms, but there is limited information on whether VOCs also affect *C. cibarius*-associated microorganisms.

Many low-abundance taxa and a small number of dominating taxa make up soil microbial communities, according to an increasing number of studies (Zheng et al., 2021). Rare taxa frequently exhibit great diversity and functional redundancy as a member of the microbial "seed bank," and they play a significant ecological role in preserving species diversity and ecosystem function (Lynch and Neufeld, 2015; Jousset et al., 2017; Chen et al., 2020). They frequently exhibit considerable interactions with abundant taxa, forming an intricate ecological network (Jousset et al., 2017). Network analyses of symbiotic patterns provide new insights into such complex ecological networks, helping to reveal niche spaces or symbiotics shared by community members (Barberán et al., 2012; Faust and Raes, 2012). Therefore, exploring symbiotic patterns among microorganisms is beneficial to identify potential biological interactions, habitat affinity, or common physiology that can guide more targeted research or experimental settings (Barberán et al., 2012). Uncertainty about the interaction and symbiotic patterns of bacterial communities' results from the fact that many datasets of bacterial taxa related to *C. cibarius* do not directly show evidence for species interactions. Instead, they tend to focus on abundant taxa while ignore or delete rare taxa.

In recent years, researchers have found that microorganisms most likely participate in the whole process of EcMF from hyphal growth and ectomycorrhizal formation to fruiting body development (Antony-Babu et al., 2014; Li et al., 2018; Baragatti et al., 2019). For example, archaea, fungi, viruses, and protozoa can be symbiotic partners of mycorrhizal, hyphae, and fruiting bodies (Bomberg et al., 2003; Antony-Babu et al., 2014; Marupakula et al., 2017). The factors driving the assembly and symbiosis of these microorganisms may be caused by differences in host exudate composition or soil heterogeneity (host modification soil creation/soil intrinsic property); however, the factors that dominate the distribution and symbiotic patterns of microbial communities in the host and its unique habitat remain have yet to be elucidated (Ning et al., 2019; Jiao et al., 2020; Upadhyay et al., 2022). Soil contains rich and diverse bacterial communities, which provide a species pool for the microbiota of soil organisms (Antony-Babu et al., 2014; Deveau et al., 2016; Gohar et al., 2020). Thus, environmental forces that shape microbial community composition in the soil may indirectly contribute to the construction of microbial communities in fungal hyphae and fruiting bodies (Warmink et al., 2009; Antony-Babu et al., 2014). Studying the mechanisms underlying distribution patterns and species coexistence of microbial communities, however, remains a key issue in microbial ecology because the factors that lead to the formation of these microbial communities are poorly understood (Ning et al., 2019; Jiao and Lu, 2020; Dong et al., 2022). In recent years, there has been increasing use of community assembly to describe the distribution patterns of microbial communities, which are influenced by deterministic processes caused by microbial characteristics (e.g., phenotypic characteristics), interactions, and environmental conditions, and stochastic processes caused by microbial birth, death, colonization, extinction, and species formation (Chase and Myers, 2011; Chase, 2014; Zhou and Ning, 2017; Gao et al., 2020). However, the assembly process of unique bacterial communities in *C. cibarius* is still unknown.

This study used 12 fruiting bodies of *C. cibarius* and their corresponding mycosphere soil samples from three plots in Guiyang,

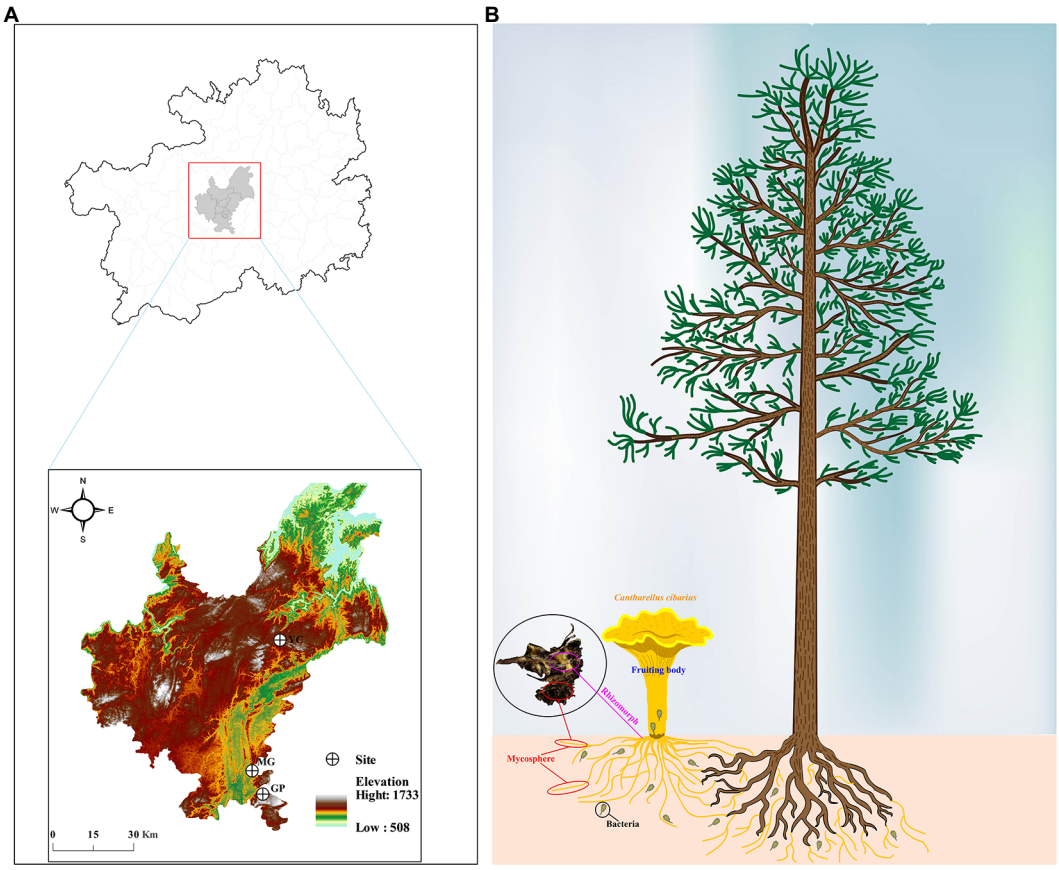

FIGURE 1
Information of the sampling site and part. **(A)** Geographic information of three sampling sites. **(B)** The habitat and sampling part of *Cantharellus cibarius*. GP, Gaopo Township; MG, Mengguan Township; YC, Yangchang Town.

Guizhou Province, China. The main objectives were (1) to explore the co-occurrence patterns and metabolic functions of abundant and rare bacteria in the fruiting bodies and mycosphere of *C. cibarius*; (2) to reveal the assembly mechanism of bacterial taxa in the fruiting body and mycosphere of *C. cibarius*; (3) to analyze the regulatory effects of various environmental factors on the diversity of abundant and rare bacteria in fruiting bodies and mycosphere. We hypothesized that: (1) the symbiotic pattern of the bacterial community in the mycosphere is more complex than the fruiting body, and the rare bacteria have some unique or complementary potential functions. (2) The assembly of abundant and rare bacterial communities in fruiting bodies and mycosphere was dominated by stochastic processes, but also influenced by different environmental factors. (3) The diversity of abundant and rare bacteria in fruiting bodies and mycosphere may be regulated differently by the same environmental factors.

2. Materials and methods

2.1. Sample collection and processing

The fruiting bodies and mycosphere samples were collected in August 2021 from the forest-soil region of three plots in Guiyang, Guizhou, China (see Figures 1A,B for detailed geographic information). Each fruiting body by using the measurement database[1] is evaluated in terms of its color and morphological characteristics (size, shape, and texture). Four fruiting body samples with the same developmental period (middle-aged) and their corresponding mycosphere soil (10 cm in diameter and 5 cm in depth) were collected from each plot. The spacing between samples was more than 50 m to ensure that samples came from different host plant roots. Samples were rapidly transported to the laboratory at 4°C for processing (Warmink and van Elsas, 2008; Oh et al., 2016). The fungal material was processed in the laboratory according to the methods of Ge et al. (2021). Briefly, the fruiting bodies were separated from the soil and the soil (~2 g) adhering to the rhizomorph (hyphae) was carefully removed. All samples were processed and placed in sterile centrifuge tubes for total DNA extraction. The remaining fruiting body tissue (cap and stipe) was dried in a freeze dryer and then ground to powder (<2 mm) for nutrient analysis and volatile composition determination (Kranabetter et al., 2019). The remaining portion of the mycosphere was air-dried and sieved on a 2-mm grid before being used for physicochemical analysis.

1 http://www.soortenbank.nl/

2.2. DNA extraction, PCR amplification, Illumina MiSeq sequencing, and processing of sequencing data

Total genomic DNA was extracted from fruiting bodies and mycosphere samples of *C. cibarius* using the E.Z.N.A. ® soil DNA Kit (Omega Bio-Tek, Norcross, GA, USA) according to the manufacturer's protocols. DNA concentration and purity were determined by NanoDrop 2000 UV-cis spectrophotometer (Thermo Scientific, Wilmington, USA). Variable V3-V4 regions of the 16S rRNA gene were amplified using the bacterial primers 338F (5′-ACTCCTACGGG AGGCAGCAG-3′) and 806R (5′-GGACTACHVGGGTWTCTAAT-3′) in the GeneAmp 9,700 PCR system (ABI, USA). The conditions and mixtures for PCR amplification were referenced in our previous method (Ge et al., 2021). Sequencing was performed on Illumina's Miseq PE300 platform (Shanghai Magi Biomedical Technology Co., LTD.).

Raw data files were quality-filtered by fastp[2] (Chen et al., 2018) and merged by FLASH[3] with the following criteria (Magoc and Salzberg, 2011): (1) reads were truncated at any site receiving an average quality score < 20 over a 50-bp sliding window; (2) according to the overlap relation between PE reads, pairs of reads were merged into a sequence with a minimum overlap length of 10 bp; (3) the maximum mismatch ratio allowed in the overlap region of the merged sequence was 0.2, and the non-conforming sequence was screened; (4) according to barcodes and primers at the beginning and end of the sequence, the samples were distinguished, and the sequence direction was adjusted. The allowable mismatch number of barcodes was 0, and the maximum primer mismatch number was 2. Sequences with ≥97% similarity were assigned to the same operational taxonomic units (OTUs), the chimeras were filtered by using UPARSE[4] (Stackebrandt and Goebel, 1994; Edgar, 2013) and the OTUs represented by less than two sequences were removed to avoid possible biases (Frøslev et al., 2017; Xiong et al., 2021). OTUs were classified and annotated by the RDP classifier (http://rdp.cme.msu.edu/version 2.2), then compared with the SILVA 16S rRNA database (v138), setting the comparison threshold at 70% (Wang et al., 2007). The raw data was uploaded to the NCBI database (BioProject ID: PRJNA871198; BioSample: SAMN30410437).

2.3. Analysis of climate, chemical composition of fruiting body, and soil physicochemical properties

Mean annual temperature (MAT), mean annual rainfall (MAR), relative humidity (RH), and sunshine duration (SD) in 2021 were obtained from meteorological data provided by the China Meteorological Data Service Center[5] and the mean values were calculated (Supplementary Table S1). According to the method of "Physical and Chemical Analysis of Soil Properties" (Ren et al., 2019), the soil physicochemical properties and the chemical composition of the fruiting body were determined. The total nitrogen in the soil (TN) and fruiting bodies (FTN) was measured with the semi-micro-Kelvin method (LY/T1228–1999). The total phosphorus in soil (TP) and fruiting bodies (FTP) was measured by the acid digestion Mo-Sb colorimetric method (LY/T1232-1999). The total potassium of soil (TK) and fruiting bodies (FTK) was measured by the base digestion-flame photometric method (LY/T1234-1999). Soil pH was measured with the potentiometric method (LY/T1239-1999). Soil organic matter (SOC) was measured with the potassium dichromate volumetric method (LY/T1237-1999). Soil available nitrogen (AN) was measured with the alkali N-proliferation (LY/T1229-1999). Soil available phosphorus (AP) was measured with the molybdenum-blue colorimetric method (GB12297-1990). Soil available potassium (AK) was measured by the flame photometric method (LY/T1236-1999). The data obtained for all indicators were shown in Supplementary Table S1.

2.4. Determination of volatile organic compounds in the fruiting bodies

According to Huang et al. (2018), there is a large amount of 1-octen-3-ol and unique β-ionone and dihydro-β-ionone in the VOCs of the fruiting body of *C. cibarius*. Therefore, these three VOCs were selected for analysis in this study. After the dried fruiting bodies were crushed, 0.5059 g was weighed into a 100-mL headspace injection bottle and 20 ml saturated sodium chloride solution was added. The extraction head was desorbed for 5 min (50/30 μm PDMS extraction head), inserted into the extraction bottle, and the headspace of 70°C water bath was extracted for 60 min at 1000 R/min speed. It was quickly inserted into the injection port of the gas chromatograph, desorbed at 250°C for 5 min, and simultaneously detected by gas chromatography–mass spectrometry (GC–MS). The chromatographic column was an Agilent HP-5MS elastic capillary column (30 m × 250 μm × 0.25 μm), and the column program was 40°C for 2 min; 5°C/min to 85°C for 2 min; 2°C/min to 110°C for 1 min; 3°C/min to 128°C for 1 min; 2°C/min to 145°C for 2 min; 5°C/min to 230°C for 8 min (total run time 69 min). The flow rate was 1.0 ml/min. The linear relationships were 0.1, 0.25, 0.5, 1.0, and 2.0 μl of standard solution, and with the injection volume as the abscissa (X) and the peak area (Y) as the ordinate, standard curves were generated and the contents of various VOCs were calculated, respectively. Data of all indexes are shown in Supplementary Table S1.

2.5. Habitat specialization

To help explain the pattern of beta diversity, we estimated Levins' niche breadth (B) index for the abundant and rare subcommunities (Levins, 1968):

$$B_j = \frac{1}{\Sigma_{i=1}^{N} P_{ij}^2}$$

where B_j represents the niche breadth of OUTj; N is the total number of communities; P_{ij} is the proportion of OTU j in the community i (Jiao et al., 2020). The B_j of the fruiting body and mycosphere samples were calculated, respectively, ($N = 12$ for both). The B index considered habitat utilization based on species abundance and evenness at the metacommunity scale. Higher B-values indicate a wider niche breadth for species existing in more habitats; lower B-values indicate a narrower niche breadth for species in fewer habitats. We calculated the average niche breadth index (B_m) for all taxa of a bacterial community to indicate

2 https://github.com/OpenGene/fastp, version 0.20.0
3 http://www.cbcb.umd.edu/software/flash, version 1.2.7
4 http://drive5.com/uparse/version7.1
5 http://data.cma.cn

the habitat utilization and divided each sub-community with an average B_m value based on 100 Bootstraps. According to the emergence of OTUs and using the permutation algorithms as implemented in EcolUtils (Salazar, 2015), OTUs were further classified as the generalist, specialist and neutral taxa (Zhang et al., 2018a).

2.6. Data analysis

To assess the role of abundant and rare bacteria in the fruiting body and mycosphere in community structure, the relative abundance of OTU ≥0.01% in samples was defined as abundant taxa (Dong et al., 2021), and the relative abundance of OTU <0.01% was defined as rare taxa (Jiao et al., 2017). The co-occurrence patterns of bacteria in the fruiting body and mycosphere were determined by network analysis. In order to increase statistical confidence, OTUs that were present in at least two-thirds (8 samples) of the samples were included in the network analysis, as stated by Du et al. (2020). In order to build the network, Spearman rank correlation coefficients between OTUs were determined using the "Hmisc" package (Harrell and Dupont, 2017). Only strongly correlated ($|r| > 0.8$) and statistically significant ($p < 0.01$) OTUs are present in the network (Hu et al., 2017; Du et al., 2020). The screened OTUs were visualized by Gephi (Version 0.9.2). The network topology parameters (including average clustering coefficient, average path distance, average degree, graph density, and modularity) are calculated in Gephi, version 0.9.2. In order to define the potential contribution of the deterministic and stochastic process to the assembly of microbial communities in the fruiting body and mycosphere, we used the null model in R (999 simulations) (Stegen et al., 2013) to calculate the β-nearest taxon index (|βNTI|), $|\beta NTI| \geq 2$ and $|\beta NTI| < 2$ represent the deterministic and stochastic process of the microbial community, respectively (Jiao et al., 2020). The relative influence of dispersal limitations was quantified as the fraction of pairwise comparisons with $|\beta NTI| < 2$ and $RC_{Bray} > 0.95$. The fraction of all pairwise comparisons with $|\beta NTI| < 2$ and $|RC_{Bray}| < 0.95$ was used to estimate the influence of the "undominant" (Zhou and Ning, 2017). To assess the major factors that affected the assembly processes for abundant and rare taxa, a Mantel test based on Spearman's correlation coefficients was conducted to compare the βNTI values with the Euclidean distance matrices for each of the variables (Vass et al., 2020; Zhao et al., 2022).

In order to compare the differences in the alpha diversity of the abundant and rare bacteria in the fruiting bodies and mycosphere, we calculated the alpha diversity indexes (Shannon, Richness) and Community Richness (ACE, Chao1) by Mothur software (Supplementary Table S2). ANOVA and T-test were used to analyze the differences in alpha diversity (Schloss et al., 2011). In Statistical Analysis of Metagenomic Profiles (STAMP), ANOVA was used to calculate the beta diversity of abundant and rare bacteria in fruiting bodies and mycosphere. It will be presented in the form of PCoA (Parks et al., 2014). The "Metacoder" function in the R package was used to generate a heat tree describing the taxon abundance of the top 50 abundant and rare bacterial operational taxonomic units (OTUs) in the fruiting body and mycosphere (Foster et al., 2017). To further understand the complex relationship between climate factors (RH, MAR, MAT, and SD), physicochemical properties (total nitrogen, total phosphorus, and total potassium) of the fruiting body, VOCs (1-octen-3-ol, dihydro-β-ionone, and β-ionone), and alpha diversity (Richness, Shannon, Pielou and Chao1 indexes) of abundant and rare bacteria in the fruiting body, a partial least squares model (PLS-PM) was constructed in SmartPLS3 (Ringle et al., 2015). Similarly, a PLS-PM was also used to further explain the influence process of climate factors, soil physicochemical properties (pH, organic matter, total nitrogen, available nitrogen, total phosphorus, available phosphorus, total potassium, available potassium) and VOCs on the alpha diversity of abundant and rare bacteria in the mycosphere (Richness, Shannon, Pielou and Chao1 indexes), respectively.

The metabolic functions, energy sources and biological relationships of abundant and rare bacteria in fruiting bodies and mycospheres soils were annotated based on METAGENassist2 (Arndt et al., 2012). The phenotype information of 11,000 organisms and the full sequences of about 1,800 organisms are collected in METAGENAssisted. In addition, phenotypic information contains approximately 20 categories for each microorganism, such as metabolism, habitat, energy, oxygen demand, and preferred temperature range (Dong et al., 2022).

3. Results

3.1. Analysis of community composition and diversity of abundant and rare bacteria in the fruiting body and mycosphere

After strict quality filtering, resulting sequences were gathered into OTUs with similarity ≥97%. In all, 3,456 OTUs and 2,165 OTUs were detected in the mycosphere and fruiting body, respectively. Although a large percentage of OTUs in fruiting bodies were recognized as rare taxa (average value =84.06%), they only made up 3.42% of the average relative abundance of each sample (Figure 2). In the mycosphere, a large percentage of OTUs were classified as rare taxa (average value =74.83%), however they only accounted for 6.81% of each sample's average relative abundance (Figure 2). The results showed that the abundant and rare

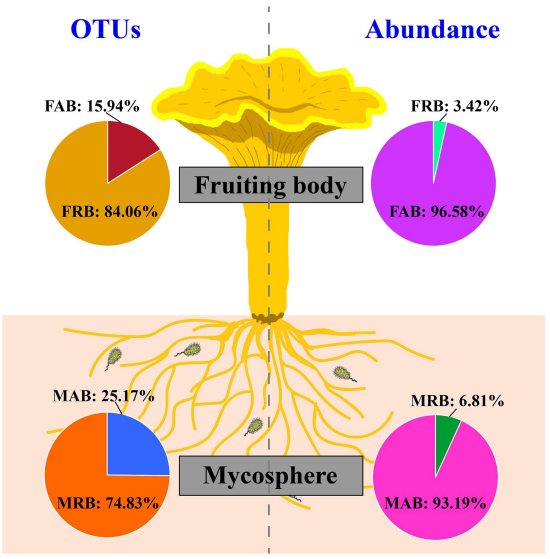

FIGURE 2
OTU and the relative abundance ratio of abundant and rare bacteria in the fruiting body and mycosphere. Abbreviation: FAB, abundant bacteria of the fruiting body; FRB, rare bacteria of the fruiting body; MAB, abundant bacteria of the mycosphere; MRB, rare bacteria of the mycosphere.

bacteria had obvious distribution patterns in both fruiting bodies and mycosphere.

To visualize the dominant taxa of abundant and rare bacteria in the fruiting body and mycosphere of *C. cibarius*, a heat tree was used to characterize the taxonomic information of the top 50 OTUs of abundant and rare bacteria in each sample. The abundant bacteria of the fruiting body (FAB) were mainly Proteobacteria, Acidobacteriota, and Patescibacteria at the phylum level, and *Allorhizobium-Neorhizobium-Pararhizobium-Rhizobium*, *Burkholderia-caballeronia-paraburkholderia*, *Serratia* and *Chitinophaga* were the dominant genera. The rare bacteria of the fruiting body (FRB) predominantly belonged to the phyla Planctomycetota, Firmicutes, and Actinobacteriota, and *Jatrophihabitans*, *Sphingomonas*, *Paenibacillus*, and *Reyranella* were the dominant genera (Figure 3A).

The abundant bacteria of the mycosphere (MAB)were mainly Proteobacteria, Actinobacteriota, and Acidobacteriota at the phylum level, and the dominant genera of abundant bacteria included *Acidipila*, *Bradyrhizobium*, *Devosia*, and *Crossiella*. In contrast, the rare bacteria of the mycosphere (MRB) predominantly belonged to the phyla Verrucomicrobiota, Myxococcota, Bacteroidota, and Chloroflexi, and the dominant genera of rare bacteria included *Chthoniobacter*, *Gemmatimonas*, *Cohnella*, and *Crossiella* (Figure 3B).

In addition, the diversity of abundant and rare taxa in different samples was analyzed. Alpha diversity index analysis showed that the diversity of MAB and MRB was significantly higher than that of fruiting bodies ($p < 0.05$) (Figures 4A–D). In both the fruiting body and mycosphere, the Shannon index of rare bacteria was substantially greater than that of abundant bacteria ($p < 0.05$) (Figure 4B). Additionally, the Pielou index of FRB was significantly higher than that of FAB ($p < 0.05$) (Figure 4C), and the Chao1 index of MRB was significantly higher than that of MAB ($p < 0.05$) (Figure 4D). Principal component analysis (PCoA) showed that abundant bacteria from different sites of the fruiting bodies and mycosphere clustered together, while rare bacteria also clustered together, and abundant and rare taxa were separated from each other (Figures 4E,F).

3.2. Analysis of community assembly, driving factors and niche breadth of the abundant and rare bacteria in the fruiting bodies and mycosphere

The null model shows the stochastic process for abundant and rare bacteria with a high relative contribution in the process of assembly (Figure 5A). For instance, in the stochastic process (dispersal limitation) of fruiting bodies, the relative contribution rate of the FAB (83.33%) was higher than that of the FRB (43.94%). In addition to being dominated by the dispersal limitation process, there were also some taxa in the "undominated" stochastic process in the fruiting bodies (Figure 5B). Similarly, the MAB and MRB were mainly restricted by the dispersal limitation of stochastic processes, but their proportion of deterministic processes (heterogeneous selection) was higher than that of the bacterial taxa in the fruiting bodies.

To explain the differences in the structure of abundant or rare bacterial communities in fruiting bodies and mycosphere of *C. cibarius*, the habitat specialization of the bacteria was examined. The niche breadth index of the OTU corresponding to the abundant and rare bacteria in the fruiting bodies and mycosphere, respectively, was estimated to further study the community structure. The niche breadth index of MAB was significantly higher than that of the FAB (Figure 5C). FAB (2.7 ± 0.084) had a significantly higher niche breadth index compared with that of the FRB (1.3801 ± 0.1527) ($p < 0.001$) (Figure 5C). MAB (5.19 ± 0.083) had a considerably larger niche breadth index compared with that that of MRB (2.54 ± 0.030) ($p < 0.001$) (Figure 5C).

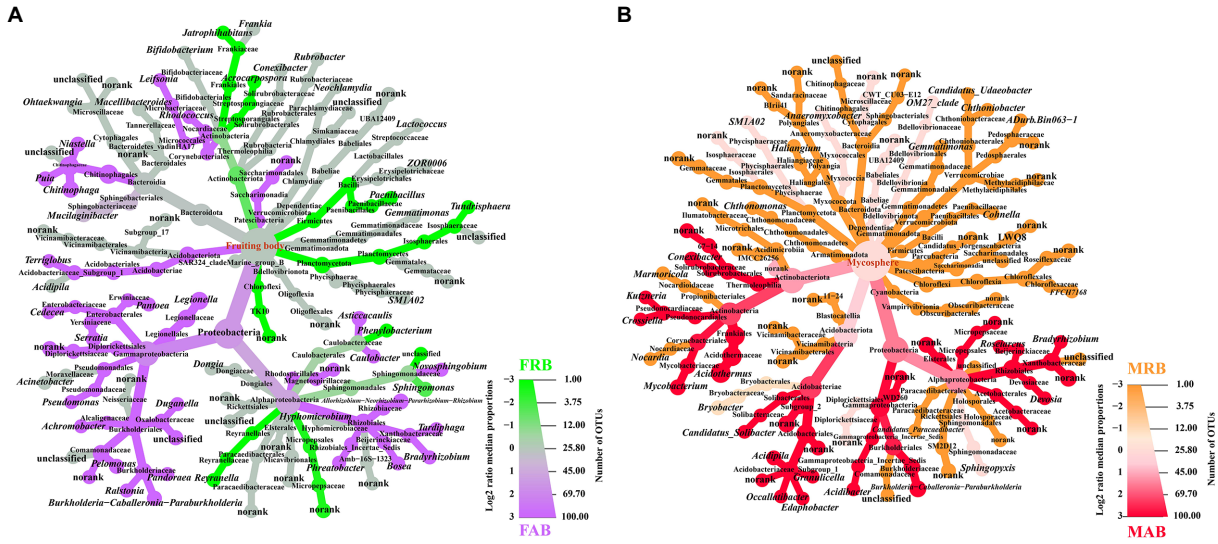

FIGURE 3
Heat tree of community classification and composition of the fruiting bodies and mycosphere. **(A)** Top 50 OTUs of abundant and rare bacteria of the fruiting body. **(B)** Top 50 OTUs of abundant and rare bacteria of the mycosphere. The size of the node is proportional to the number of OTUs within each taxon. Each figure shows the specific name of each classification level; the color scale and ruler on the right represent the log2 value of the median proportion and the number of OTUs, respectively; the colored picture shows the significantly different species compared between the two groups. Only the significantly different species will be colored, where purple represents the abundant bacteria of the fruiting body, green represents the rare bacteria of the fruiting body, red represents the abundant bacteria of the mycosphere, and orange represents the rare bacteria of the mycosphere. FAB, abundant bacteria of the fruiting body; FRB, rare bacteria of the fruiting body; MAB, abundant bacteria of the mycosphere; MRB, rare bacteria of the mycosphere.

10.3389/fmicb.2023.1074468

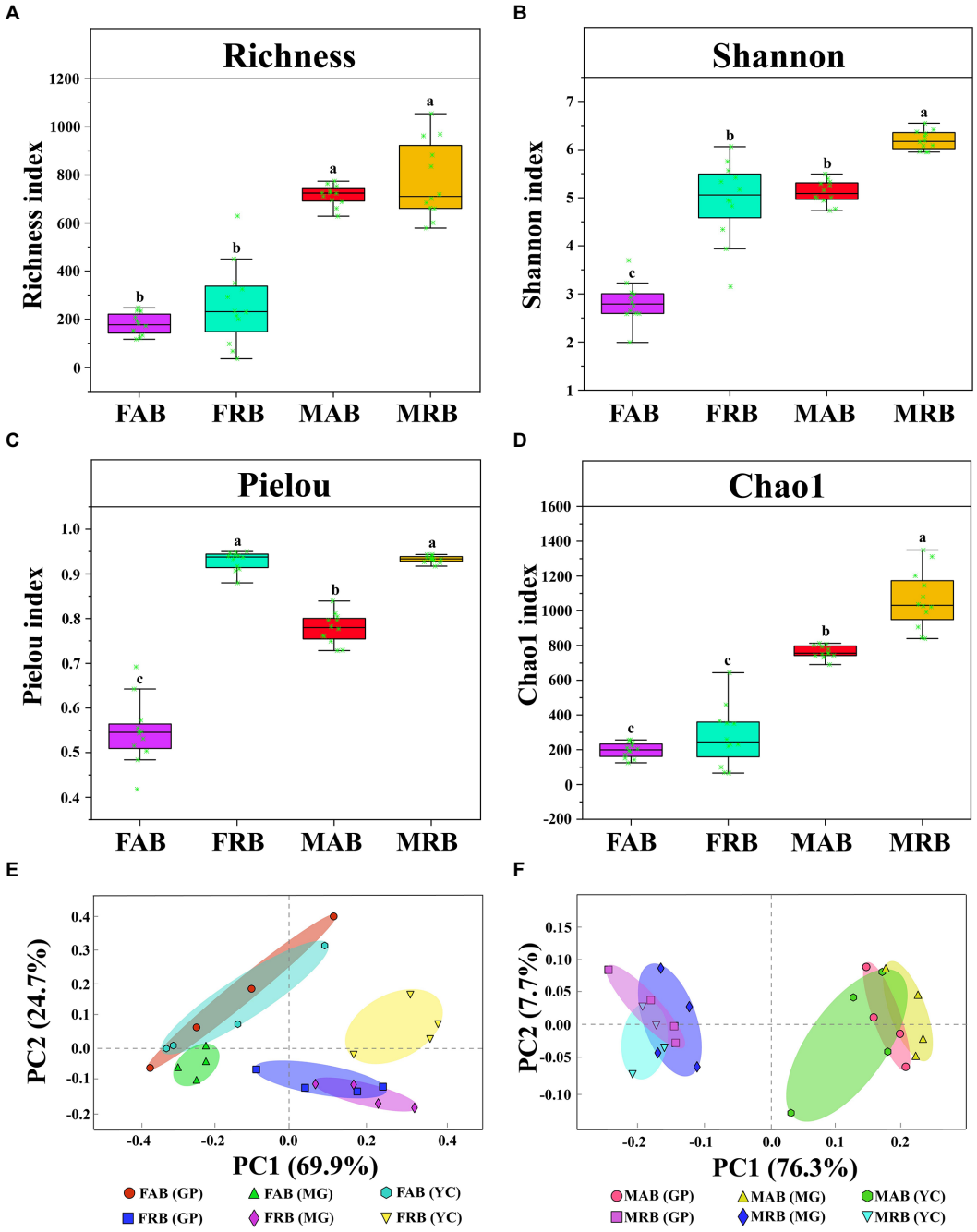

FIGURE 4
Alpha diversity and principal component analysis. **(A)** The Richness index of abundant and rare bacteria in the fruiting body and mycosphere. **(B)** The Shannon index of abundant and rare bacteria in the fruiting body and mycosphere. **(C)** The Pielou index of abundant and rare bacteria in the fruiting body and mycosphere. **(D)** The Chao1 index of abundant and rare bacteria in the fruiting body and mycosphere. **(E)** The principal component analysis of abundant and rare bacteria in the fruiting body. **(F)** The principal component analysis of abundant and rare bacteria in the mycosphere. Note: In Figures (A-D), there is no significant difference in Tukey's test for the same letter on the boxplot ($p>0.05$). Tukey's test showed significant differences in patterns with different letters ($p<0.05$). FAB, abundant bacteria of the fruiting body; FRB, rare bacteria of the fruiting body; MAB, abundant bacteria of the mycosphere; MRB, rare bacteria of the mycosphere; GP, Gaopo Township; MG, Mengguan Township; YC, Yangchang Town.

Furthermore, it is also important to distinguish between generalists and specialists to understand the assembly mechanisms of the microbial community. Therefore, we determined the generalist and specialist of abundant and rare bacteria in the two samples, respectively, depending on whether the niche breadth index was higher or lower than the simulated opportunity (Figure 5D). In the fruiting body and mycosphere, the proportion of specialists of abundant bacteria (FAB: 42.73%; MAB: 43.76%) was larger than that of rare bacteria (FRB: 0.05%; MRB: 13.23%), but the proportion of generalists of rare bacteria (FRB: 3.02%; MRB: 5.26%) was marginally higher than that of abundant bacteria (FAB: 0.29%; MAB: 0.52%) (Figure 5D).

To explore the major environmental factors that determined the assembly processes for abundant and rare taxa of the fruiting body and mycosphere, Mantel tests were conducted by comparing the βNTI values

10.3389/fmicb.2023.1074468

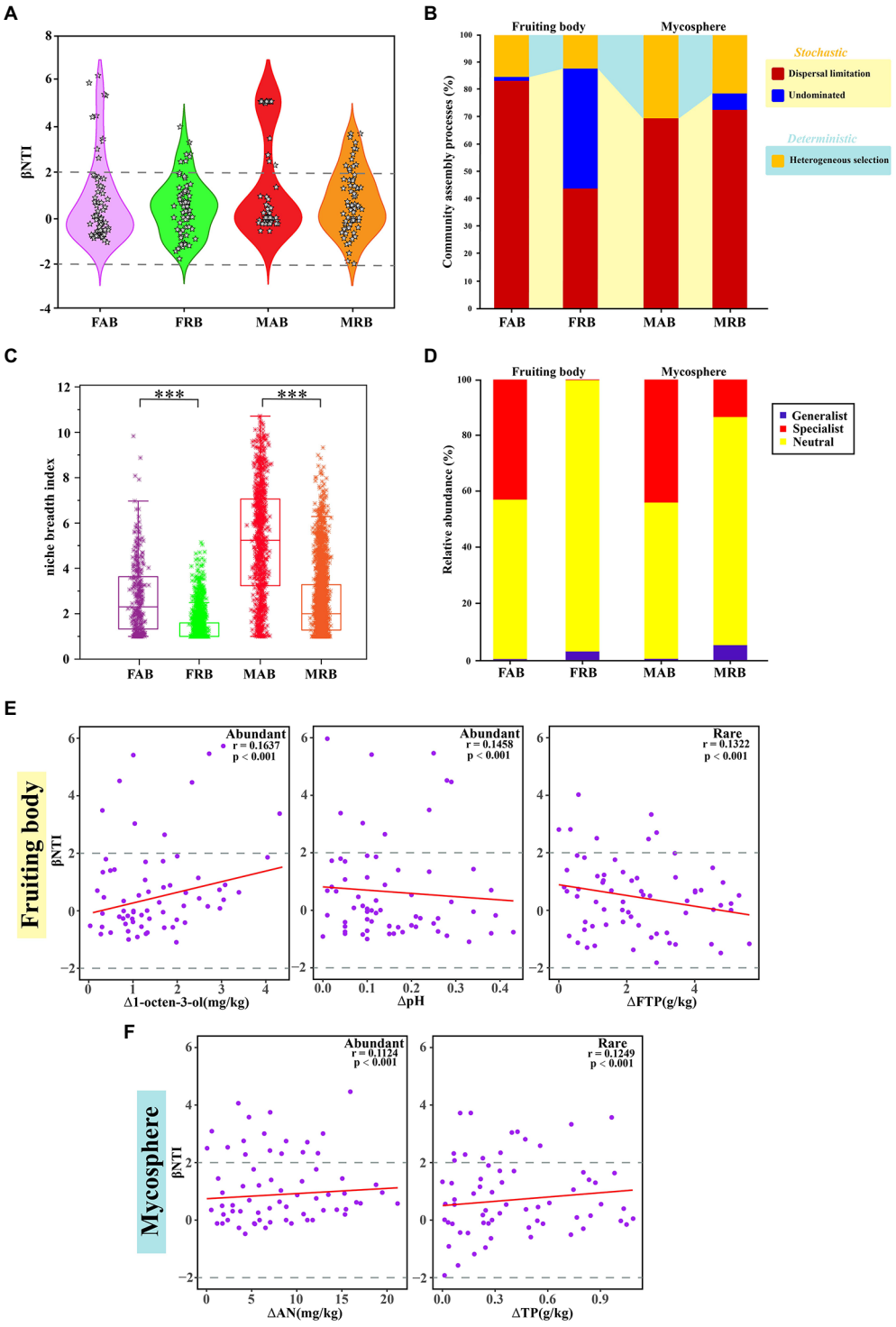

FIGURE 5
Null models and niche breadth index of the abundant and rare bacteria. **(A)** βNTI patterns of abundant and rare bacteria in the fruiting body and mycosphere. **(B)** The proportion of community assembly of the abundant and rare bacteria in the fruiting bodies and mycosphere is dominated by stochastic (dispersal limited and non-dominated) and partially deterministic (homogenous selection) processes. **(C)** Niche breadth of abundant and rare bacteria in fruitbody and mycosphere, these results were obtained based on the average of 100 bootstraps, and comparative analysis of abundant and rare bacteria within the sample was carried out using a *t*-test. * represent p <0.05, ** represent 0.001< p <0.01, *** represent p <0.001. **(D)** Relative abundance of the specialist, generalist, and neutral groups of abundant and rare bacteria in the fruiting bodies and mycosphere. **(E)** Spearman's correlations between β-nearest taxon index (βNTI) of communities in the fruiting body and changes in environmental variables. **(F)** Spearman's correlations between β-nearest taxon index (βNTI) of communities in the mycosphere soil and changes in environmental variables. FAB, abundant bacteria of the fruiting body; FRB, rare bacteria of the fruiting body; MAB, abundant bacteria of the mycosphere; MRB, rare bacteria of the mycosphere; FTP, total phosphorus of the fruiting body; AN, soil available nitrogen; TP, soil total phosphorus.

and each environmental variable (based on Euclidean distance matrices). The results suggested that many factors influenced the phylogenetic turnover of communities (Supplementary Table S3). The main explanatory variables were selected to determine the correlations between the assembly processes for different communities and environmental variables. The selected variables were 1-octen-3-ol and pH for FAB, FTP for FAB, AN for MAB, and TP for MRB (Supplementary Table S3). The significant positive correlation between 1-octen-3-ol and βNTI indicated that an increase in 1-octen-3-ol affected the assembly of the FAB (Figure 5E). However, the βNTI of FAB decreased with increasing pH (Figure 5E). Similar results were observed between βNTI and FTP in the FRB (Figure 5E). For the mycosphere, the βNTI of MAB decreased with the increase of AN, and the βNTI of MRB also showed a significant negative correlation with TP (Figure 5F).

3.3. Analysis of bacterial co-occurrence network between fruiting body and mycosphere

The co-occurrence networks of abundant and rare bacterial communities were further compared to assess their interactions. The results show that 107 nodes (OTUs) and 335 edges (correlations) were included in the samples of the fruiting body based on co-occurrence network analysis. Samples of the mycosphere contained 882 nodes and 7,825 edges. Other topological features were shown in Table 1. In the co-occurrence network, there were 318 edges and 104 nodes (97.2%) among the FAB, while the FRB had 3 nodes (2.8%) and 17 edges (Figure 6A). However, co-occurrence network of the MAB contained 7,443 edges and 685 nodes (77.34%). The overall number of MRB was 382 edges and 197 nodes (22.66%) (Figure 6E). Bacterial taxa in fruiting bodies and mycosphere are more likely to co-coexist (positive correlation, red line), rather than co-exclude (negative correlation, blue line). Negative correlations were 0 and 0.74% for the co-occurrence pattern of bacteria in the fruiting body and mycosphere, respectively, while positive correlations accounted for 100 and 99.26% in the co-occurrence network of the fruiting body and mycosphere (Figures 6A,E). Additionally, the predominant taxa in the fruiting body network were Proteobacteria (72.9%), Actinobacteriota (12.15%), and Bacteroidota (7.48%) (Figure 6B). Proteobacteria (28.20%), Actinobacteriota (17.12%), Acidobacteriota (12.10%), and Planctomycetota (8.05%) were the primary nodes in the network of the mycosphere (Figure 6F). The bacterial network in the fruiting body was clearly divided into six primary modules, according to the examination of network modularity data, and the proportion of OTUs in modules 1, 2, 3, and 4 was 18.69, 14.01, 13.08, and 12.15%, respectively (Figure 6C). However, the bacterial network in the mycosphere was divided into seven main modules, of which modules 1, 2, 3, and 4 accounted for 14.47, 11.34, 10.88, and 9.98% of the total OTUs, respectively (Figure 6G). Generalists, specialists, and neutral groups in the fruiting body and mycosphere were examined to assess the habitat specialization of the network. Most of the bacteria in both fruiting body and mycosphere samples belonged to neutral groups (F-neutral: 69.16%; M-neutral: 68.44%), and more specialists than generalists (F-generalist: 8.41%; M-generalist: 7.03%) were present (Figures 6D,H).

3.4. Correlation analysis of abundant and rare bacteria and environmental factors

Detailed exploration of the complex network of the relationship among climate, soil, VOCs, the chemical composition of the fruiting body, and the diversity of abundant and rare bacteria in the fruiting body and mycosphere was performed through PLS-PM of the fruiting body and mycosphere, respectively (Figure 7). The PLS-PM demonstrated a positive correlation between climate factors (MAT, MAR, SD, and RH) and the diversity of both FAB (0.934, $p < 0.05$) and FRB (0.567, $p < 0.05$) in the fruiting body. The diversity of both FAB (−0.983, $p < 0.05$) and FRB (−0.902, $p < 0.05$) was directly negatively impacted by the physicochemical properties of the fruiting bodies. However, the diversity of both FAB (0.033) and FRB (0.128) was positively impacted directly by VOCs (1-octen-3-ol, Dihydro-β-ionone, and β-ionone) (Figures 7A,B). Similarly, the climate factors were also positively correlated with the diversity of MAB (0.390, $p < 0.05$) and MRB (0.057, $p < 0.05$) in the mycosphere. The diversity of both MAB and MRB in the mycosphere was positively influenced by the soil physicochemical properties (pH, SOC, TN, TP, TK, AN, AP and AK) (0.280 and 0.245, respectively). However, VOCs exhibited adverse direct impacts on the diversity of MAB (−0.365, $p < 0.05$) and MAB (−0.452, $p < 0.05$) in the mycosphere (−0.365, $p < 0.05$; −0.452, $p < 0.05$) (Figures 7C,D).

3.5. Analysis of metabolic function, energy source, and symbiotic relationship of abundant and rare bacteria

From the analysis of potential biological relationships, most of the abundant and rare bacteria in the fruiting bodies and mycosphere were free-living, and the proportions of FAB (31.3%) and FRB (29.0%) in the fruiting bodies were higher than those in the mycosphere (MAB: 18.8%, MRB: 11.3%). In addition, the proportion of symbiosis in the MAB was relatively high (11.9%), which was higher than that in other taxa (Figure 8A). From the perspective of potential energy utilization, the FAB was heterotroph (17.8%), followed by diazotroph (3.3%) and autotroph (2.3%). The FRB was mainly heterotroph (5.9%) and autotroph (4.0%). However, the MAB was mainly photosynthetic (16.7%) and chemoorganotroph (5.2%). The MRB was mainly heterotroph (4.0%), and chemoorganotroph (1.8%) (Figure 8B). The results of potential metabolic functions showed that the FAB and FRB had similar functions, including ammonia oxidizer (FAB: 36.6%; FRB: 21.8%), nitrite reducer (FAB: 36.2%; FRB: 17.5%), sulfate reducer (FAB: 33.3%; FRB: 12.5%), dehalogenation (FAB: 27.3%; FRB: 20.1%) and chitin degradation (FAB:

TABLE 1 Topological features of bacterial co-occurrence network in the fruiting body and mycosphere.

Treatments	OTUs number	Node	Edge	Modularity	AD	ACC	APD	GD
Fruiting body	118	107	335	0.691 ± 0.03	5.678	0.678	2.911	0.049
Mycosphere	944	882	7,825	0.791 ± 0.02	17.724	0.539	4.865	0.02

AD, average degree; ACC, average clustering coefficient; APD, average path distance; GD, graph density.

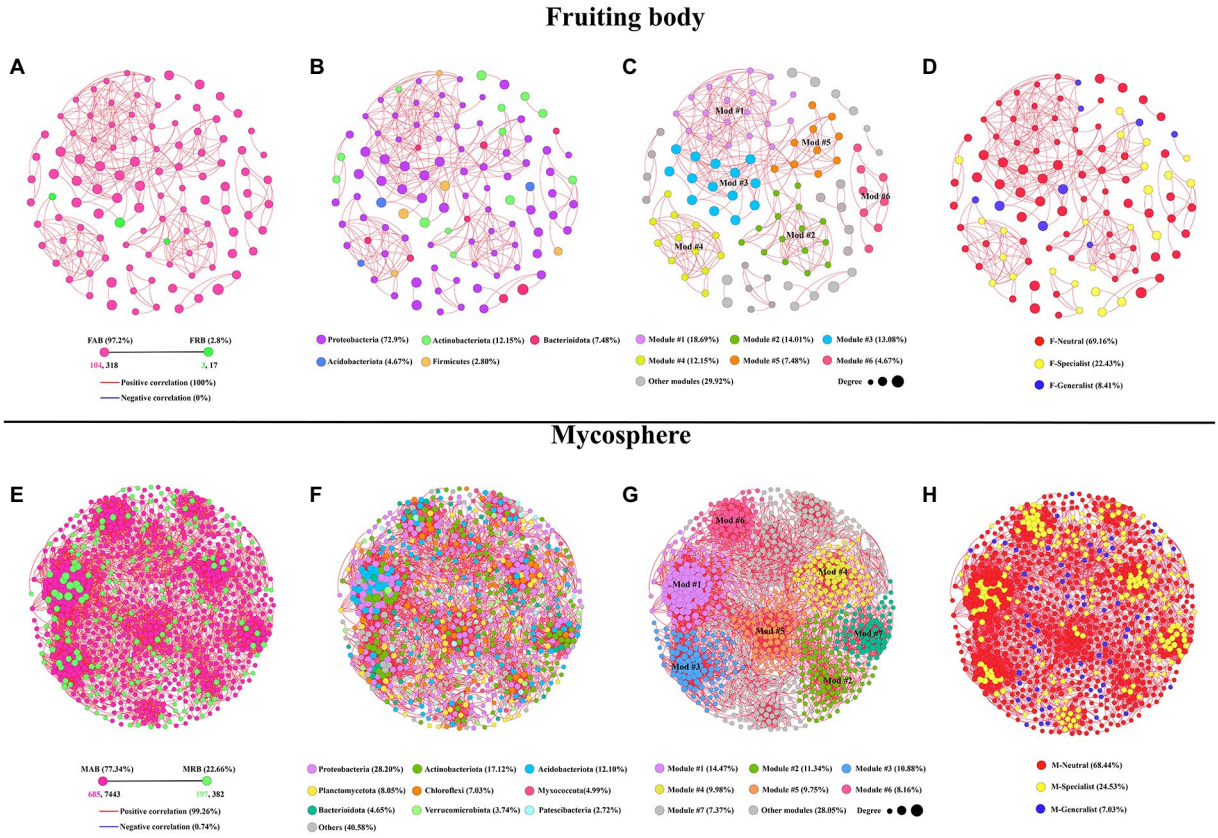

FIGURE 6
Analysis of the bacterial co-occurrence network between the fruiting body and mycosphere. **(A,E)** Depict the correlation co-occurrence network of abundant and rare bacteria in the fruiting body and mycosphere, respectively. **(B,F)** Depict the correlation co-occurrence network of bacterial taxonomic information in the fruiting body and mycosphere, respectively. **(C,G)** Depict the modularity of the bacterial correlation co-occurrence network of the fruiting body and microsphere, respectively. **(D,H)** Depict the type information of specialist, generalist, and neutral groups, respectively. Nodes of the network are colored according to abundant and rare bacteria information **(A,D)**, taxonomic information **(B,E)**, modularity **(C,F)**, and types of the generalist, specialist, and neutral group **(D,H)**. The size of the node depends on the degree of connectivity. Edge colors indicate positive (red) and negative (blue) correlations.

21.9%; FRB: 11.0%). The MAB in the mycosphere were mainly nitrogen fixation (16.6%), sulfate reducers (16.1%), chitin degradation (14.8%), nitrite reducers (13.7%), and stores polyhydroxybutyrate (9.7%). However, the MRB in the mycosphere were ammonia oxidizer (10.8%), dehalogenation (9.2%), and nitrite reducer (7.9%) (Figure 8C).

4. Discussion

Most studies on fruiting bodies and mycosphere at the moment concentrate on the dominant genera of abundant bacterial taxa (Pent et al., 2017, 2020; Ge et al., 2021). In this study, we also examined the community structure, assembly, and symbiotic patterns of abundant and rare bacteria in the fruiting body and mycosphere, and we offered fresh insights into how environmental factors affect bacterial diversity in the habitat of *C. cibarius*.

4.1. Rare bacteria are indispensable members of the unique habitat of *Cantharellus cibarius*

The abundant taxa have traditionally received the majority of attention in soil microbial studies since they are typically regarded as the most active and significant participants in the biogeochemical cycle (Cottrell and Kirchman, 2003). However, recent research has emphasized the significance of rare taxa as hidden regulators of microbiome function (Lynch and Neufeld, 2015). Therefore, the abundant bacteria in the fruiting body and mycosphere only accounted for a small portion of the microbial diversity, according to both the proportion of the abundant and rare bacteria in OTUs (Figure 2) and the comparison of their diversity (Figure 4), which was consistent with the results of Pedrós-Alió (2012). This highlights that rare bacteria are the dominant force in community composition and diversity supplementation.

In addition, since the community composition of rare bacteria was significantly different from that of abundant bacteria, it should not be ignored in the microbial community composition. Proteobacteria were the most significant dominant group among the FAB and MAB, and the increase in their richness may be related to the higher nutrient status of the fruiting bodies in comparison with the mycosphere (Torsvik and Øvreås, 2002). The fruiting body and mycosphere of *C. cibarius* frequently contain Acidobacteriota as dominant taxa (Pent et al., 2017; Ge et al., 2021). Burke et al. (2006) described Acidobacteriota as mycorrhizal helper bacteria, which are close to the Proteobacteria group physiologically and ecologically, and have similar ecological niches in the rhizosphere/mycosphere (Singh et al., 2007; Kielak et al., 2016). Its effect on the growth and development of *C. cibarius* could not

10.3389/fmicb.2023.1074468

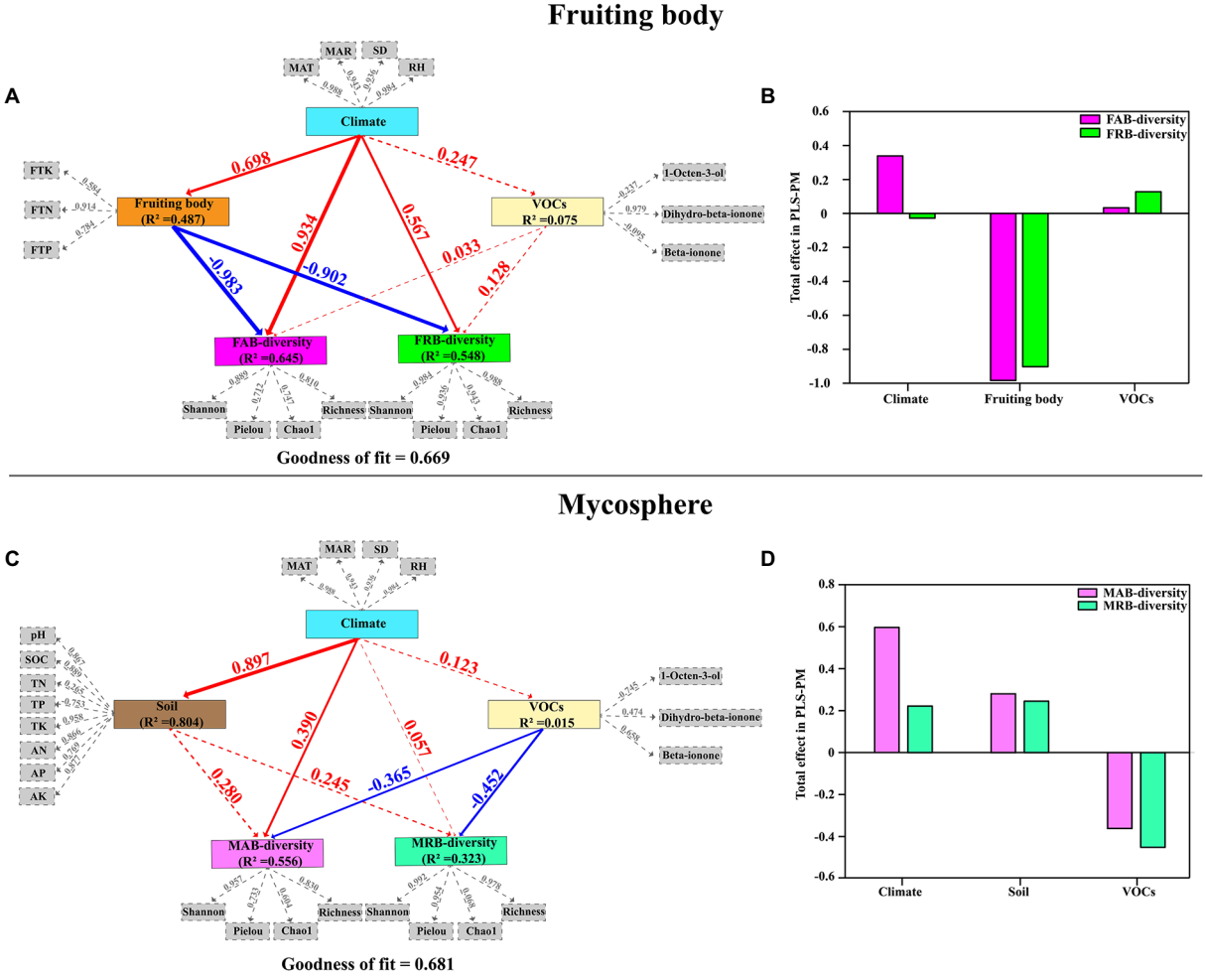

FIGURE 7
Partial least squares path modeling (PLS-PM) disentangling main pathways of climate, soil physicochemical properties, volatile organic compounds, and the chemical composition of the fruiting body on the diversity of abundant and rare bacteria in the fruiting body and mycosphere **(A,C)**; and the total effects of each variable on the diversity of abundant and rare bacteria in the fruiting body and mycosphere **(B,D)**. Each solid box represents a latent variable, and each gray dashed box represents an observed variable. The numbers on the arrow lines represent the normalized path coefficients, and the R^2 values represent the variance of the dependent variable explained by the internal model. The width of the arrow reflects the magnitude of the path coefficient. The blue and red arrows represent positive and negative impacts, respectively. Solid and dashed lines indicate a significant (p<0.05) and no significant (p>0.05) correlation, respectively. The goodness of fit (Gof) statistic was used to test the model, and the Gof values of the fruiting body and microsphere soil were 0.669 and 0.681, respectively. MAT, mean annual temperature; MAR, mean annual rainfall; RH, relative humidity; SD, sunshine duration; FTN, total nitrogen of the fruiting body; FTP, total phosphorus of the fruiting body; FTK, total potassium of the fruiting body; pH, soil pH; SOC, soil organic matter; TN, soil total nitrogen; TP, soil total phosphorus; TK, soil total potassium; AN, soil available nitrogen; AP, soil available phosphorus; AK, soil available potassium; FAB-diversity, alpha diversity index of abundant bacteria in fruiting body; FRB-diversity, alpha diversity index of rare bacteria in fruiting body; MAB-diversity, alpha diversity index of abundant bacteria in mycosphere; MRB-diversity, alpha diversity index of rare bacteria in mycosphere.

be ignored. In addition, Planctomycetota and Verrucomicrobiota which were two of the dominant phyla of rare bacteria in this study, are commonly found in the rhizosphere (Zul et al., 2007; da Rocha et al., 2009) and appear to have functionally strong rhizosphere capabilities, but their role in the growth and development of fruiting bodies remains to be demonstrated. Notably, Actinobacteriota and Firmicutes—two other dominant phyla of the rare bacteria in this study—were found to be associated with the production of VOCs in the study by Vahdatzadeh et al. (2015). Whether Actinobacteriota and Firmicutes are involved in the symbiosis of the unique aroma of *C. cibarius* deserves further study.

The dominant abundant bacteria of the fruiting bodies and mycosphere displays a trend toward functional type divergence (Ge et al., 2021). The findings of this study demonstrated that both abundant and rare bacteria had similar potential metabolic roles in the fruiting body and that the functional abundance of rare bacteria was not low. There is a difference in the functional distribution between the MAB and MRB in the mycosphere, which may be due to the diversity of rare bacteria increasing the functional redundancy of the mycosphere and providing complementary or unique metabolic pathways to support the function of the mycosphere ecosystem (Helliwell et al., 2013; Jousset et al., 2017). Potential energy utilization results revealed a high number of heterotrophs in both the FAB and FRB. This may be due to the exudates of the fruiting body and its underground hyphae (such as amino acids and trehalose), which serve as nutrient hotspots for numerous bacteria in soil and create diverse and unique ecological niches (Timonen et al., 1998; Rangel-Castro et al., 2002; Vellend, 2010). The abundant and rare bacteria in the fruiting body and mycosphere of *C. cibarius* were also discovered to be connected to the sulfur cycle in addition to the nitrogen cycle. This supports our first hypothesis and consistents with the findings of Liu et al. (2021) in the truffle, which

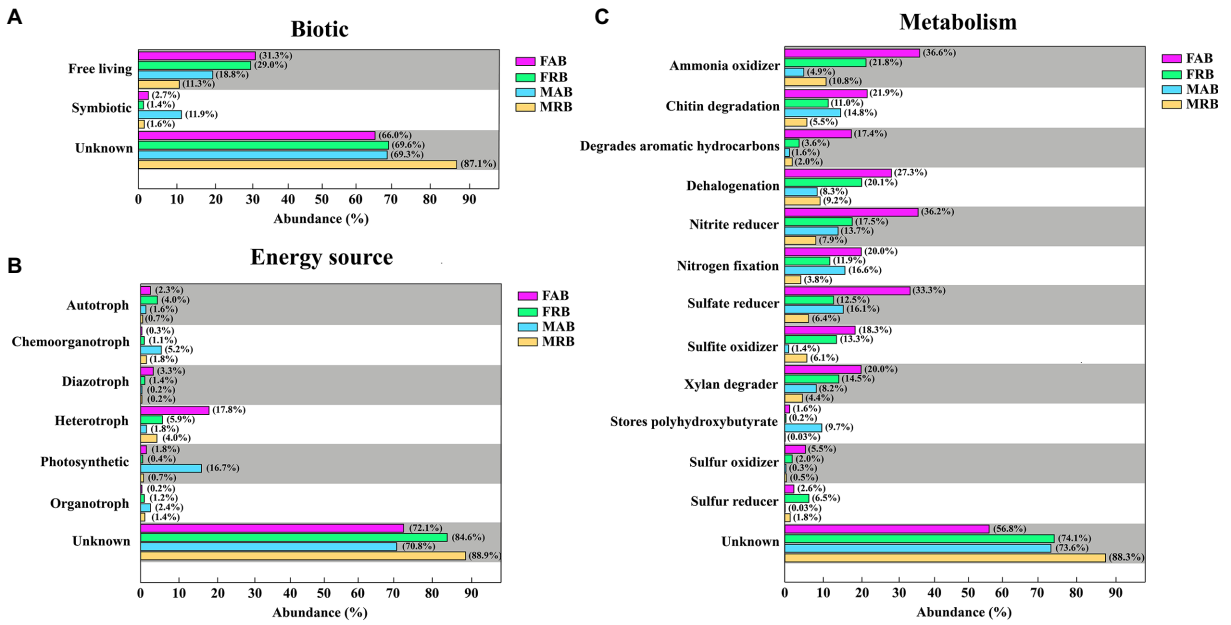

FIGURE 8
The potential phenotypic characteristics and metabolic functions of abundant and rare bacteria in the fruiting body and mycosphere. **(A)** Potential metabolism of abundant and rare bacteria in the fruiting bodies and mycosphere. **(B)** Energy sources of abundant and rare bacteria in the fruiting bodies and mycosphere. **(C)** Biological relationships between abundant and rare bacteria in the fruiting bodies and mycosphere. FAB, abundant bacteria of the fruiting bodies; FRB, rare bacteria of the fruiting bodies; MAB, abundant bacteria of the mycosphere; MRB, rare bacteria of the mycosphere.

suggest that bacteria of the fruiting bodies and mycosphere may have potential metabolic functions like sulfur cycling. Sulfur can be used by these bacteria as an energy source to support the development of fruiting bodies (Wang et al., 2019; Liu et al., 2021). From the analysis of potential biological relationships, most abundant and rare bacteria in the fruiting bodies and mycosphere of *C. cibarius* are free-living organisms, but there are some bacteria that are mainly in symbiotic, especially among the MAB in the mycosphere. The ability of fungal mycelia to actively migrate and grow in the soil may confer some specific resources that allow soil bacteria to respond positively to the growing mycosphere, select their preferred ecological niche, and form more symbiotic relationships (Noble et al., 2009; Warmink et al., 2009; Yun et al., 2013). Although fungal fruiting bodies and mycosphere structures may be transient (Haq et al., 2014), there is increasing evidence that bacteria play an important symbiotic function in specific fungal microflora (fruiting bodies and mycosphere) (Gohar et al., 2020; Yu et al., 2020; Ge et al., 2021). In summary, these findings reveal the importance of abundant and rare bacterial communities in the fruiting bodies and mycosphere of *C. cibarius*. In particular, the contributions of rare bacteria to community composition, diversity, and potential function cannot be ignored.

4.2. The assembly of abundant and rare bacterial communities in fruiting body and mycosphere is mainly a stochastic process but is also affected by different environmental factors

In this study, dispersal limitation was the main assembly process for the abundant and rare bacteria of the fruiting bodies and mycosphere of *C. cibarius*. Ma et al. (2017) and Xiao et al. (2018) also reported that soil bacteria were predominantly affected by dispersal limitation. Such stochastic processes allow species to coexist with overlapping niches and may regulate the diversity and ecosystem function of bacterial taxa in the fruiting body and mycosphere (Chase and Myers, 2011; Zhou and Ning, 2017). Additionally, some dormant bacteria can successfully serve as "seed banks" for bacterial sources when unfavorable circumstances restrict the growth of bacterial communities (Locey et al., 2020; Wisnoski et al., 2020). Thus, rare bacteria may contribute to the diversity of bacteria in the fruiting body and mycosphere of *C. cibarius*. However, compared with the mycosphere, the FAB and FRB in the fruiting body had a higher ratio of stochastic processes. This finding was consistent with a report by Chase (2014), which showed that the relative contribution of stochastic processes to the overall structure of soil microbial communities was increased over a small area. It is important to note that abundant bacteria were more affected by dispersal limitation in our current investigation compared with rare bacteria. This difference may be attributed to the different morphological characteristics of these bacterial taxa (an important integrated attribute of species related to their total abundance, growth rates, and range size) (Allen et al., 2006), and deterministic factors such as fruiting body habitat specificity (Hanson et al., 2012).

In the fruiting body and mycosphere samples, the proportion of specialists in the abundant bacteria was high (Figure 5D). This reflected that fruiting body and mycosphere habitat availability dominate specialists more than utilizing generalists with a wider range of habitat types, consistent with the findings of Munday et al. (1997) and Bean et al. (2002). It was recently reported that the symbiotic patterns of bacterial generalists differ in complexity and stability from those of specialists, which were more complex compared with those of generalists (Mo et al., 2020). In constast, we discovered that the proportion of generalists was higher in rare bacterial taxa, which were thought to have a wider niche breadth, stronger environmental tolerance, and more adaptable metabolic function (He Z. et al., 2022; He J. et al., 2022). These

results indicated that rare bacteria played an active role in maintaining the functional diversification and stability of the ecosystem of the fruiting body and its microbiota. Neutral groups were still the main groups in the abundant and rare bacteria of the fruiting bodies and mycosphere. This could be explained by the fact that the homogenous environment supplied by fruiting bodies and the mycosphere reduced species niche differentiation and increased the proportion of neutral species in community aggregation (Bar-Massada et al., 2014).

It is essential to reveal the factors that lead to the dominance of different microbial community assembly processes in community ecology (Tripathi et al., 2018; Vass et al., 2020). Previous studies have revealed that soil pH and nutrient concentrations are the major determinants of the microbiome structure and functions in fungal fruiting bodies (Pent et al., 2017, 2018, 2020). However, this study found that the βNTI of FAB was negatively correlated with soil pH, while the βNTI of FRB was positively correlated with FTP. These findings indicated that the assembly processes of the FAB and FRB may be regulated by different environmental factors. In addition to soil pH and FTP, 1-octen-3-ol may be involved in the community assembly of FAB; however, the mechanism underlying the promotion of the FAB requires further investigation to prove a direct link. There was also a high positive correlation between the βNTI of MAB and the AN, while the MRB was positively correlated with TP. The influence of soil physicochemical properties on the bacterial community structure has been well explained (Rousk et al., 2010; Bahram et al., 2018). However, in addition to theoretical correlation analysis, it is necessary to verify the actual impact of each indicator through rigorous scientific design. Nevertheless, these results are consistent with our second hypothesis that different environmental factors influence the assembly process of abundant and rare bacterial communities in fruiting bodies and mycosphere of *C. cibarius*. To summarize, the assembly of abundant and rare bacterial communities in the fruiting bodies and mycosphere of *C. cibarius* was affected by different environmental factors, although the dispersal limitation in stochastic processes is dominant.

4.3. The complex and diverse symbiotic patterns of the bacteria in the mycosphere support development and formation of the fruiting body

The distribution and ecological function of microbes were also impacted by microbe–microbe interactions (Barberán et al., 2012). Network analysis and topological characteristics in this study revealed that from the mycosphere to the fruiting body, the correlation, complexity, and modularity of microorganisms gradually decreased. The complexity of the truffle microbial community was found to steadily decline from the bulk soil to the soil–truffle interface, and then to the fruiting body, which is consistent with the results of Liu et al. (2021). The following aspects could explain this phenomenon similar to "ecological filtering": (1) the substrate released by fruiting bodies and their hyphae had an obvious influence on the resident bacteria, which was reflected in the marked difference of OTUs between fruiting bodies and the mycosphere; (2) the correlation was more significant in the mycosphere with higher microbial richness; (3) the bacterial community in the mycosphere had more functional modularity compared with that of the fruiting bodies, thus nutrient cycling and organic matter degradation were realized (Cong et al., 2015; Zhang et al., 2018b; Liu et al., 2021). This spatial heterogeneity may be crucial to understanding how different nutrient cycling processes at smaller spatial scales, including fruiting bodies and the mycosphere, are driven by more complex and diverse communities.

The bacterial co-occurrence network of the fruiting body and mycosphere of *C. cibarius* was consistently dominated by Proteobacteria and Actinobacteria, which may be more closely associated with metabolic processes such as nitrogen fixation and organic carbon consumption in the unique habitat of *C. cibarius* (Gohar et al., 2020; Ge et al., 2021). Additionally, the proportion of rare bacteria in the mycosphere was noticeably larger compared with that in the samples from fruiting bodies, which may be related to the intricacy of the mycosphere and the significance of rare bacteria in the global biogeochemical cycles (Hol et al., 2015; Jousset et al., 2017). In sum, the bacterial co-occurrence network of the mycosphere was more complex than that of the fruiting body, and this neework complexity may play an important role in the metabolism and nutrition needed for the growth and development of the fruiting body. In particular, the mechanism of the symbiosis of Proteobacteria still needs to be further evaluated.

4.4. The volatile organic compounds have different potential regulatory effects on bacterial diversity in the fruiting body and mycosphere

The diversity of abundant and rare bacteria in the fruiting body and mycosphere of *C. cibarius* in response to environmental conditions and host features were systematically evaluated by using PLS-PM. For both FAB and FRB in the fruiting bodies, their diversity was positively regulated by climate factors. Previous studies have shown that appropriate temperature, humidity, rainfall, and sunshine duration can increase soil microbial diversity and are also important conditions for the normal growth of soil fungal fruiting bodies (Xia et al., 2016; Wang et al., 2017; Sun et al., 2018; Yuichi, 2018). However, this study found that these appropriate climate factors also increase bacterial diversity in the fruiting body. This promoting effect may be a direct effect of climate factors, or it may be that climate factors stimulate *C. cibarius* to increase the production of soluble carbohydrates, thereby affecting the bacterial taxa depending on these compounds (Rangel-Castro et al., 2002). In contrast, the diversity of abundant and rare bacterial taxa was negatively regulated by the chemical composition of fruiting bodies. Previous studies have shown that the chemical composition of fungal fruiting bodies has a stronger influence on the diversity and community structure of specific bacteria in the fruiting bodies compared with the soil physicochemical properties (Pent et al., 2020). The ratios of N%, P%, C%, and C: N in fruiting bodies exhibit different degrees of influence on bacterial diversity (Pent et al., 2020). However, in this study, TN, TP, and TK of the fruiting body negatively regulated the diversity of both abundant and rare bacterial taxa. This may be because *C. cibarius* affect the composition and diversity of the microbial community near their fruiting bodies by changing soil conditions, thus forming small-scale and nutrient-rich hot spots (Pent et al., 2020). This would attract bacterial taxa with specific symbiotic functions to colonize the fruiting bodies and exclude other irrelevant bacteria, so as to effectively control the bacterial diversity. VOCs have a beneficial effect on the bacterial diversity of fruiting bodies. Relevant reports stated that the aromas of 1-octen-3-ol, dihydro-β-ionone, and β-ionone all had the potential to be attractive, having advantageous effects on luring animals and insects, and recruiting specific bacteria to colonize fruiting bodies (Thakeow et al., 2008; Sharma et al., 2012; Vahdatzadeh et al., 2015; Splivallo et al., 2019; Xu et al., 2019).

Similar to EcMF, further research has been conducted on the interactions between VOCs and the microorganisms that are found in truffles, such as *Tuber melanosporium* and *Thelephora* (Antony-Babu et al., 2014; Vahdatzadeh et al., 2015; Benucci and Bonito, 2016; Splivallo et al., 2019). By generating VOCs, *Lyphyllum* attracted the colonization of *Burkholderia terrae* BS001(Haq et al., 2014). Thus, the fruiting body site of *C. cibarius* may be a significant aromatic dense niche that attracts particular bacteria. This is supported by bacteria with potential aromatic compound metabolic functions (Splivallo et al., 2015; Vahdatzadeh et al., 2015; Ge et al., 2021) and the PLS-PM results of this study (Figure 8), which show a close relationship between VOCs and diversity of the fruiting body and mycosphere. However, not all VOCs are synthesized by mycorrhizal fungi themselves, and endofungal bacteria in their fruiting bodies may also be involved in aroma formation (Splivallo and Ebeler, 2015; Saidi et al., 2016). In this process, bacteria can produce a variety of VOCs, and some VOCs have strong antibacterial activity (Ghasemi et al., 2021; Orban et al., 2023), which may have an opposite role on bacterial diversity of the fruiting body. For instance, Ghasemi et al. (2021) discovered that the VOCs produced by endofungal bacteria *Pseudomonas* sp. Bi1, *Bacillus* sp. De3, *Pantoea* sp. Ma3 and *Pseudomonas* sp. De1 isolated from wild growing mushrooms inhibited the activity of *Pseudomonas tolaasii* Pt18, the causal agent of mushroom brown blotch disease. Interestingly, the unique bacterial taxa in the fruiting body of *C. cibarius* can co-exist in the fruiting body of *C. cibarius* with many bacteria that produce antimicrobial metabolites such as antibiotics and VOCs. Further studies should be performed to determine whether it carries resistance genes or other symbiotic mechanisms.

The diversity of abundant and rare bacteria in the mycosphere of *C. cibarius* was also positively regulated by climate factors and soil physicochemical properties but had a significant negative correlation with VOCs ($p < 0.05$). This is consistent with our third hypothesis. Climate factors such as temperature, humidity, rainfall, and sunshine duration were reported as important factors affecting soil microbial diversity (Xia et al., 2016; Wang et al., 2017; Sun et al., 2018). Similarly, the positive regulation of soil physicochemical properties on bacteria in mycosphere has been documented in previous studies (Pent et al., 2017; Yu et al., 2020). However, it is more noteworthy that VOCs negatively regulate the diversity of abundant and rare bacteria in the mycosphere. Such results are similar to the recent hot phenomenon of "allelopathic inhibition." Allelopathic inhibition, put simply, generally implies that the host species (plants, fungus, or microbes) will exhibit a variety of interaction processes and control species diversity when an organism introduces damaging macromolecules (allelopathic chemicals) into the environment (Rice, 1984). In relation to this, the compounds in this study—1-octen-3-ol and β-ionone—have been shown to exhibit antibacterial and antiviral properties (Beltran-Garcia et al., 1997; Zhu et al., 2010; Sharma et al., 2012; Kertesz and Thai, 2018). *Volvariella volvacea* was found to have the important fragrance component dihydro-ionone (Xu et al., 2019). Data from Vahdatzadeh et al. (2019) have further shown that there is a significant relationship between specific microbial classes and VOCs. Therefore, *C. cibarius* may release some VOCs to regulate the categories and diversity of bacteria in the mycosphere, so as to ensure the normal growth, development, and health of the fruiting body. Furthermore, it is claimed that *C. cibarius* have evolved a successful environmental strategy for acquiring and controlling the space they require to survive and reproduce (Warmink et al., 2009; Pent et al., 2017; Gohar et al., 2020; Pent et al., 2020; Ge et al., 2021). In this space, unique bacterial communities were assembled according to host identity, host chemical composition, physicochemical properties of the mycosphere, function guild, or other nutritional effects (Warmink et al., 2009; Pent et al., 2017; Gohar et al., 2020; Pent et al., 2020; Ge et al., 2021). Therefore, we speculated that VOCs of *C. cibarius* may provide another novel explanation for the competitiveness of *C. cibarius* and the formation of unique bacterial communities in the fruiting body and mycosphere, which will be further verified in the future studies. In summary, bacterial diversity in the fruiting bodies and mycosphere of *C. cibarius* is regulated by different environmental factors. Although VOCs are correlated with bacterial diversity in different ways, correlation does not always imply causation, and more data are needed to verify the specific interaction mechanism(s).

Data availability statement

The datasets presented in this study can be found in online repositories. The names of the repository/repositories and accession number(s) can be found in the article/Supplementary material.

Author contributions

YH, YZ, and GZ: conceptualization and funding acquisition. WG, YR, and CD: data acquisition. QS, YB, ZH, and TY: formal analysis. WG: writing the first draft. YH and SD: writing, review, and editing the manuscript. All authors have read and agreed to the published version of the manuscript.

Funding

This work was financially supported by "Hundred" Talent Projects of Guizhou Province (Qian Ke He [2020] 6005), the Project of Guizhou Province Science and Technology (Qiankehe Platform for talents [2019] 5105), the Natural Science Foundation of China (Nos. 32160007, 32060011, 32260003), and Construction Program of Biology First-class Discipline in Guizhou (GNYL [2017] 009).

Conflict of interest

The authors declare that the research was conducted in the absence of any commercial or financial relationships that could be construed as a potential conflict of interest.

Publisher's note

Supplementary material

The Supplementary material for this article can be found online at: https://www.frontiersin.org/articles/10.3389/fmicb.2023.1074468/full#supplementary-material

References

Allen, C. R., Garmestani, A. S., Havlicek, T. D., Marquet, P. A., Peterson, G. D., Restrepo, C., et al. (2006). Patterns in body mass distributions: sifting among alternative hypotheses. *Ecol. Lett.* 9, 630–643. doi: 10.1111/j.1461-0248.2006.00902.x

Antony-Babu, S., Deveau, A., van Nostrand, J. D., Zhou, J., le Tacon, F., Robin, C., et al. (2014). Black truffle-associated bacterial communities during the development and maturation of *Tuber melanosporum* ascocarps and putative functional roles. *Environ. Microbiol.* 16, 2831–2847. doi: 10.1111/1462-2920.12294

Arndt, D., Xia, J., Liu, Y., Zhou, Y., Guo, A. C., Cruz, J. A., et al. (2012). METAGENassist: a comprehensive web server for comparative metagenomics. *Nucleic Acids Res.* 40, W88–W95. doi: 10.1093/nar/gks497

Bahram, M., Hildebrand, F., Forslund, S. K., Anderson, J. L., Soudzilovskaia, N. A., Bodegom, P. M., et al. (2018). Structure and function of the global topsoil microbiome. *Nature* 560, 233–237. doi: 10.1038/s41586-018-0386-6

Baragatti, M., Grollemund, P. M., Montpied, P., Dupouey, J. L., Gravier, J., Murat, C., et al. (2019). Influence of annual climatic variations, climate changes, and sociological factors on the production of the Périgord black truffle (*Tuber melanosporum* Vittad.) from 1903-1904 to 1988-1989 in the Vaucluse (France). *Mycorrhiza* 29, 113–125. doi: 10.1007/s00572-018-0877-1

Barberán, A., Bates, S. T., Casamayor, E. O., and Fierer, N. (2012). Using network analysis to explore co-occurrence patterns in soil microbial communities. *ISME J.* 6, 343–351. doi: 10.1038/ismej.2011.119

Bar-Massada, A., Kent, R., and Carmel, Y. (2014). Environmental heterogeneity affects the location of modelled communities along the niche-neutrality continuum. *Proc. Biol. Sci.* 281:20133249. doi: 10.1098/rspb.2013.3249

Bean, K., Jones, G. P., and Caley, M. J. (2002). Relationships among distribution, abundance and microhabitat specialization in a guild of coral reef triggerfish (family Balistidae). *Mar. Ecol. Prog. Ser.* 233, 263–272. doi: 10.3354/meps233263

Beltran-Garcia, M. J., Estarron-Espinosa, M., and Ogura, T. (1997). Volatile compounds secreted by the oyster mushroom (*Pleurotus ostreatus*) and their antibacterial activities. *J. Agric. Food Chem.* 45, 4049–4052. doi: 10.1021/JF960876I

Benucci, G., and Bonito, G. M. (2016). The truffle microbiome: species and geography effects on bacteria associated with fruiting bodies of *Hypogeous Pezizales*. *Microb. Ecol.* 72, 4–8. doi: 10.1007/s00248-016-0755-3

Boer, W., Folman, L. B., Summerbell, R. C., and Boddy, L. (2005). Living in a fungal world: impact of fungi on soil bacterial niche development. *FEMS Microbiol. Rev.* 29, 795–811. doi: 10.1016/j.femsre.2004.11.005

Bomberg, M., Jurgens, G., Saano, A., Sen, R., and Timonen, S. (2003). Nested PCR detection of archaea in defined compartments of pine mycorrhizospheres developed in boreal forest humus microcosms. *FEMS Microbiol. Ecol.* 43, 163–171. doi: 10.1111/j.1574-6941.2003.tb01055.x

Burke, D. J., Kretzer, A. M., Rygiewicz, P. T., and Topa, M. A. (2006). Soil bacterial diversity in a loblolly pine plantation: influence of ectomycorrhizas and fertilization. *FEMS Microbiol. Ecol.* 57, 409–419. doi: 10.1111/j.1574-6941.2006.00125.x

Chase, J. M. (2014). Spatial scale resolves the niche versus neutral theory debate. *J. Veg. Sci.* 25, 319–322. doi: 10.1111/jvs.12159

Chase, J. M., and Myers, J. A. (2011). Disentangling the importance of ecological niches from stochastic processes across scales. *Philos. Trans. R. Soc. Lond. Ser. B Biol. Sci.* 366, 2351–2363. doi: 10.1098/rstb.2011.0063

Chauhan, S., Mahawar, S., Jain, D., Udpadhay, S. K., Mohanty, S. R., Singh, A., et al. (2022). Boosting sustainable agriculture by arbuscular mycorrhiza under stress condition: mechanism and future prospective. *Biomed. Res. Int.* 2022:5275449. doi: 10.1155/2022/5275449

Chen, Q. L., Ding, J., Zhu, D., Hu, H. W., Delgado-Baquerizo, M., Ma, Y. B., et al. (2020). Rare microbial taxa as the major drivers of ecosystem multifunctionality in long-term fertilized soils. *Soil Biol. Biochem.* 141:107686. doi: 10.1016/j.soilbio.2019.107686

Chen, S., Zhou, Y., Chen, Y., and Gu, J. (2018). Fastp: an ultra-fast all-in-one FASTQ preprocessor. *Bioinformatics* 34, i884–i890. doi: 10.1093/bioinformatics/bty560

Chot, E., and Reddy, M. S. (2022). Role of ectomycorrhizal symbiosis behind the host plants ameliorated tolerance against heavy metal stress. *Front. Microbiol.* 13:855473. doi: 10.3389/fmicb.2022.855473

Cong, J., Yang, Y., Liu, X., Lu, H., Liu, X., Zhou, J., et al. (2015). Analyses of soil microbial community compositions and functional genes reveal potential consequences of natural forest succession. *Sci. Rep.* 5:10007. doi: 10.1038/srep10007

Cottrell, M. T., and Kirchman, D. L. (2003). Contribution of major bacterial groups to bacterial biomass production (thymidine and leucine incorporation) in the Delaware estuary. *Limnol. Oceanogr.* 48, 168–178. doi: 10.4319/lo.2003.48.1.0168

da Rocha, U. N., van Overbeek, L., and van Elsas, J. D. (2009). Exploration of hitherto-uncultured bacteria from the rhizosphere. *FEMS Microbiol. Ecol.* 69, 313–328. doi: 10.1111/j.1574-6941.2009.00702.x

Deveau, A., Antony-Babu, S., Le Tacon, F., Robin, C., Frey-Klett, P., and Uroz, S. (2016). Temporal changes of bacterial communities in the *Tuber melanosporum* ectomycorrhizosphere during ascocarp development. *Mycorrhiza* 26, 389–399. doi: 10.1007/s00572-015-0679-7

Dong, C. B., Shao, Q. Y., Ren, Y. L., Ge, W., Yao, T., Hu, H. Y., et al. (2022). Assembly, core microbiota, and function of the rhizosphere soil and bark microbiota in *Eucommia ulmoides*. *Front. Microbiol.* 13:855317. doi: 10.3389/fmicb.2022.855317

Dong, C. B., Zhang, Z. Y., Shao, Q. Y., Yao, T., Liang, Z. Q., and Han, Y. F. (2021). Mycobiota of *Eucommia ulmoides* bark: diversity, rare biosphere and core taxa. *Fungal Ecol.* 53:101090. doi: 10.1016/j.funeco.2021.101090

Du, S., Dini-Andreote, F., Zhang, N., Liang, C., Yao, Z., Zhang, H., et al. (2020). Divergent co-occurrence patterns and assembly processes structure the abundant and rare bacterial communities in a salt marsh ecosystem. *Appl. Environ. Microbiol.* 86, e00322–e00320. doi: 10.1128/AEM.00322-20

Edgar, R. C. (2013). UPARSE: highly accurate OTU sequences from microbial amplicon reads. *Nat. Methods* 10, 996–998. doi: 10.1038/nmeth.2604

Faust, K., and Raes, J. (2012). Microbial interactions: from networks to models. *Nat. Rev. Microbiol.* 10, 538–550. doi: 10.1038/nrmicro2832

Foster, Z. S., Sharpton, T. J., and Grünwald, N. J. (2017). Metacoder: an R package for visualization and manipulation of community taxonomic diversity data. *PLoS Comput. Biol.* 13:e1005404. doi: 10.1371/journal.pcbi.1005404

Frøslev, T. G., Kjøller, R., Bruun, H. H., Ejrnæs, R., Brunbjerg, A. K., Pietroni, C., et al. (2017). Algorithm for post-clustering curation of DNA amplicon data yields reliable biodiversity estimates. *Nat. Commun.* 8, 1188–1111. doi: 10.1038/s41467-017-01312-x

Gao, C., Montoya, L., Xu, L., Madera, M., Hollingsworth, J., Purdom, E., et al. (2020). Fungal community assembly in drought-stressed sorghum shows stochasticity, selection, and universal ecological dynamics. *Nat. Commun.* 11:34. doi: 10.1038/s41467-019-13913-9

Ge, W., Zhang, Z. Y., Dong, C. B., Han, Y. F., Deshmukh, S. K., and Liang, Z. Q. (2021). Bacterial community analysis and potential functions of core taxa in different parts of the fungus *Cantharellus cibarius*. *Pol. J. Microbiol.* 70, 373–385. doi: 10.33073/pjm-2021-035

Ghasemi, S., Harighi, B., Mojarrab, M., and Azizi, A. (2021). Response of *Pseudomonas tolaasii*, the causal agent of mushroom brown blotch disease to the volatile compounds produced by endofungal bacteria. *BioControl* 66, 421–432. doi: 10.1007/s10526-020-10071-6

Gohar, D., Pent, M., Põldmaa, K., and Bahram, M. (2020). Bacterial community dynamics across developmental stages of fungal fruiting bodies. *FEMS Microbiol. Ecol.* 96:fiaa175. doi: 10.1093/femsec/fiaa175

Hanson, C. A., Fuhrman, J. A., Horner-Devine, M. C., and Martiny, J. B. (2012). Beyond biogeographic patterns: processes shaping the microbial landscape. *Nat. Rev. Microbiol.* 10, 497–506. doi: 10.1038/nrmicro2795

Haq, I. U., Zhang, M., Yang, P., and van Elsas, J. D. (2014). The interactions of bacteria with fungi in soil: emerging concepts. *Adv. Appl. Microbiol.* 89, 185–215. doi: 10.1016/B978-0-12-800259-9.00005-6

Harrell, F.E. Jr.and Dupont, C. (2017). Hmisc: Harrell Miscellaneous. R Package Version 4.0-3 Online Publication. Available at: https://rdocumentation.org/packages/Hmisc/versions/4.0-3

He, Z., Liu, D., Shi, Y., Wu, X., Dai, Y., Shang, Y., et al. (2022). Broader environmental adaptation of rare rather than abundant bacteria in reforestation succession soil. *Sci. Total Environ.* 828:154364. doi: 10.1016/j.scitotenv.2022.154364

He, J., Zhang, N., Muhammad, A., Shen, X., Sun, C., Li, Q., et al. (2022). From surviving to thriving, the assembly processes of microbial communities in stone biodeterioration: a case study of the West Lake UNESCO World Heritage area in China. *Sci. Total Environ.* 805:150395. doi: 10.1016/j.scitotenv.2021.150395

Helliwell, K. E., Wheeler, G. L., and Smith, A. G. (2013). Widespread decay of vitamin-related pathways: coincidence or consequence? *Trends Genet.* 29, 469–478. doi: 10.1016/j.tig.2013.03.003

Hol, W. H., Garbeva, P., Hordijk, C., Hundscheid, P. J., Gunnewiek, P. J., Van Agtmaal, M., et al. (2015). Non-random species loss in bacterial communities reduces antifungal volatile production. *Ecology* 96, 2042–2048. doi: 10.1890/14-2359.1

Hu, A., Ju, F., Hou, L., Li, J., Yang, X., Wang, H., et al. (2017). Strong impact of anthropogenic contamination on the co-occurrence patterns of a riverine microbial community. *Environ. Microbiol.* 19, 4993–5009. doi: 10.1111/1462-2920.13942

Huang, L. L., Chen, G., and Yu, F. Q. (2018). Analysis on volatile components from five edible wild mushrooms. *Edible Fungi* 40, 80–84.

Jiao, S., and Lu, Y. (2020). Abundant fungi adapt to broader environmental gradients than rare fungi in agricultural fields. *Glob. Chang. Biol.* 26, 4506–4520. doi: 10.1111/gcb.15130

Jiao, S., Luo, Y., Lu, M., Xiao, X., Lin, Y., Chen, W., et al. (2017). Distinct succession patterns of abundant and rare bacteria in temporal microcosms with pollutants. *Environ. Pollut.* 225, 497–505. doi: 10.1016/j.envpol.2017.03.015497e505

Jiao, S., Yang, Y., Xu, Y., Zhang, J., and Lu, Y. (2020). Balance between community assembly processes mediates species coexistence in agricultural soil microbiomes across eastern China. *ISME J.* 14, 202–216. doi: 10.1038/s41396-019-0522-9

Jousset, A., Bienhold, C., Chatzinotas, A., Gallien, L., Gobet, A., Kurm, V., et al. (2017). Where less may be more: how the rare biosphere pulls ecosystems strings. *ISME J.* 11, 853–862. doi: 10.1038/ismej.2016.174

Kertesz, M. A., and Thai, M. (2018). Compost bacteria and fungi that influence growth and development of *Agaricus bisporus* and other commercial mushrooms. *Appl. Microbiol. Biotechnol.* 102, 1639–1650. doi: 10.1007/s00253-018-8777-z

Kielak, A. M., Barreto, C. C., Kowalchuk, G. A., van Veen, J. A., and Kuramae, E. E. (2016). The ecology of Acidobacteria: moving beyond genes and genomes. *Front. Microbiol.* 7:744. doi: 10.3389/fmicb.2016.00744

Kozarski, M., Klaus, A., Vunduk, J., Zizak, Z., Niksic, M., Jakovljevic, D., et al. (2015). Nutraceutical properties of the methanolic extract of edible mushroom *Cantharellus cibarius* (Fries): primary mechanisms. *Food Funct.* 6, 1875–1886. doi: 10.1039/c5fo00312a

Kranabetter, J. M., Harman-Denhoed, R., and Hawkins, B. J. (2019). Saprotrophic and ectomycorrhizal fungal sporocarp stoichiometry (C: N: P) across temperate rainforests as evidence of shared nutrient constraints among symbionts. *New Phytol.* 221, 482–492. doi: 10.1111/nph.15380

Levins, R. (1968). *Evolution in Changing Environments: Some Theoretical Explorations*. New Jersey *Princeton University Press*

Li, Q., Yan, L., Ye, L., Zhou, J., Zhang, B., Peng, W., et al. (2018). Chinese black truffle (*Tuber indicum*) alters the ectomycorrhizosphere and endoectomycosphere microbiome and metabolic profiles of the host tree *Quercus aliena*. *Front. Microbiol.* 9:2202. doi: 10.3389/fmicb.2018.02202

Liu, D., Pérez-Moreno, J., He, X., Garibay-Orijel, R., and Yu, F. (2021). Truffle microbiome is driven by fruit body compartmentalization rather than soils conditioned by different host trees. *mSphere* 6:e0003921. doi: 10.1128/mSphere.00039-21

Locey, K. J., Muscarella, M. E., Larsen, M. L., Bray, S. R., Jones, S. E., and Lennon, J. T. (2020). Dormancy dampens the microbial distance-decay relationship. *Philos. Trans. R. Soc. Lond. Ser. B Biol. Sci.* 375:20190243. doi: 10.1098/rstb.2019.0243

Lynch, M. D., and Neufeld, J. D. (2015). Ecology and exploration of the rare biosphere. *Nat. Rev. Microbiol.* 13, 217–229. doi: 10.1038/nrmicro3400

Ma, B., Dai, Z., Wang, H., Dsouza, M., Liu, X., He, Y., et al. (2017). Distinct biogeographic patterns for archaea, bacteria, and fungi along the vegetation gradient at the continental scale in eastern China. *mSystems* 2:e00174-16. doi: 10.1128/mSystems.00174-16

Magoc, T., and Salzberg, S. L. (2011). FLASH: fast length adjustment of short reads to improve genome assemblies. *Bioinformatics* 27, 2957–2963. doi: 10.1093/bioinformatics/btr507

Marupakula, S., Mahmood, S., Jernberg, J., Nallanchakravarthula, S., Fahad, Z. A., and Finlay, R. D. (2017). Bacterial microbiomes of individual ectomycorrhizal *Pinus sylvestris* roots are shaped by soil horizon and differentially sensitive to nitrogen addition. *Environ. Microbiol.* 19, 4736–4753. doi: 10.1111/1462-2920.13939

Mo, Y., Zhang, W., Wilkinson, D. M., Yu, Z., Xiao, P., and Yang, J. (2020). Biogeography and co-occurrence patterns of bacterial generalists and specialists in three subtropical marine bays. *Limnol. Oceanogr.* 66, 793–806. doi: 10.1002/lno.11643

Munday, P. L., Jones, G. P., and Caley, M. J. (1997). Habitat specialisation and the distribution and abundance of coral-dwelling gobies. *Mar. Ecol. Prog. Ser.* 152, 227–239. doi: 10.3354/meps152227

Ning, D., Deng, Y., Tiedje, J. M., and Zhou, J. (2019). A general framework for quantitatively assessing ecological stochasticity. *Proc. Natl. Acad. Sci. U. S. A.* 116, 16892–16898. doi: 10.1073/pnas.1904623116

Noble, R., Dobrovin-Pennington, A., Hobbs, P. J., Pederby, J., and Rodger, A. (2009). Volatile C8 compounds and pseudomonads influence primordium formation of *Agaricus bisporus*. *Mycologia* 101, 583–591. doi: 10.3852/07-194

Oh, S. Y., Fong, J. J., Park, M. S., and Lim, Y. W. (2016). Distinctive feature of microbial communities and bacterial functional profiles in *Tricholoma matsutake* dominant soil. *PLoS One* 11:e0168573. doi: 10.1371/journal.pone.0168573

Orban, A., Jerschow, J. J., Birk, F., Suarez, C., Schnell, S., and Rühl, M. (2023). Effect of bacterial volatiles on the mycelial growth of mushrooms. *Microbiol. Res.* 266:127250. doi: 10.1016/j.micres.2022.127250

Parks, D. H., Tyson, G. W., Hugenholtz, P., and Beiko, R. G. (2014). STAMP: statistical analysis of taxonomic and functional profiles. *Bioinformatics* 30, 3123–3124. doi: 10.1093/bioinformatics/btu494

Pedrós-Alió, C. (2012). The rare bacterial biosphere. *Annu. Rev. Mar. Sci.* 4, 449–466. doi: 10.1146/annurev-marine-120710-100948

Pent, M., Bahram, M., and Põldmaa, K. (2020). Fruitbody chemistry underlies the structure of endofungal bacterial communities across fungal guilds and phylogenetic groups. *ISME J.* 14, 2131–2141. doi: 10.1038/s41396-020-0674-7

Pent, M., Hiltunen, M., Põldmaa, K., Furneaux, B., Hildebrand, F., Johannesson, H., et al. (2018). Host genetic variation strongly influences the microbiome structure and function in fungal fruiting bodies. *Environ. Microbiol.* 20, 1641–1650. doi: 10.1111/1462-2920.14069

Pent, M., Põldmaa, K., and Bahram, M. (2017). Bacterial communities in boreal forest mushrooms are shaped both by soil parameters and host identity. *Front. Microbiol.* 8:836. doi: 10.3389/fmicb.2017.00836

Rangel-Castro, J. I., Danell, E., and Pfeffer, P. E. (2002). A 13C-NMR study of exudation and storage of carbohydrates and amino acids in the ectomycorrhizal edible mushroom *Cantharellus cibarius*. *Mycologia* 94, 190–199. doi: 10.2307/3761795

Ren, Y. L., Lu, M., Fan, F. X., and Peng, S. X. (2019). The relationship between soil fungi and physicochemical properties in swamp meadow of plateau wetlands. *Ecolog. Sci.* 39, 42–49. doi: 10.14108/j.cnki.1008-8873.2019.01.006

Rice, E. L. (1984). *Allelopathy*, *2nd* Academic Press, New York.

Ringle, C.M., Wende, S., and Becker, J.M. (2015). SmartPLS 3. SmartPLS GmbH, Boenningstedt. Available at: http://www.smartpls.com

Rousk, J., Bååth, E., Brookes, P. C., Lauber, C. L., Lozupone, C., Caporaso, J. G., et al. (2010). Soil bacterial and fungal communities across a pH gradient in an arable soil. *ISME J.* 4, 1340–1351. doi: 10.1038/ismej.2010.58

Saidi, N., Deshaware, S., Romdhane, I. B., Nadim, M., Laaribi, M., Ltifi, A., et al. (2016). Endogenous starter bacteria associated to chanterelle mycelia enhance aroma, color and growth of mycelia. *Int. J. Eng. Appl. Sci.* 3, 58–65.

Salazar, G. (2015). EcolUtils: utilities for community ecology analysis. R package version 0.1. Available at: https://github.com/GuillemSalazar/EcolUtils

Schloss, P. D., Gevers, D., and Westcott, S. L. (2011). Reducing the effects of PCR amplification and sequencing artifacts on 16S rRNA-based studies. *PLoS One* 6:e27310. doi: 10.1371/journal.pone.0027310

Sharma, V., Singh, G., Kaur, H., Saxena, A. K., and Ishar, M. P. (2012). Synthesis of β-ionone derived chalcones as potent antimicrobial agents. *Bioorg. Med. Chem. Lett.* 22, 6343–6346. doi: 10.1016/j.bmcl.2012.08.084

Singh, B. K., Munro, S., Potts, J. M., and Millard, P. (2007). Influence of grass species and soil type on rhizosphere microbial community structure in grassland soils. *Appl. Soil Ecol.* 36, 147–155. doi: 10.1016/j.apsoil.2007.01.004

Splivallo, R., Deveau, A., Valdez, N., Kirchhoff, N., Frey-Klett, P., and Karlovsky, P. (2015). Bacteria associated with truffle-fruiting bodies contribute to truffle aroma. *Environ. Microbiol.* 17, 2647–2660. doi: 10.1111/1462-2920.12521

Splivallo, R., and Ebeler, S. E. (2015). Sulfur volatiles of microbial origin are key contributors to human-sensed truffle aroma. *Appl. Microbiol. Biotechnol.* 99, 2583–2592. doi: 10.1007/s00253-014-6360-9

Splivallo, R., Vahdatzadeh, M., Maciá-Vicente, J. G., Molinier, V., Peter, M., Egli, S., et al. (2019). Orchard conditions and fruiting body characteristics drive the microbiome of the black truffle *Tuber aestivum*. *Front. Microbiol.* 10:1437. doi: 10.3389/fmicb.2019.01437

Stackebrandt, E., and Goebel, B. M. (1994). Taxonomic note: a place for DNA-DNA reassociation and 16s rRNA sequence analysis in the present species definition in bacteriology. *Int. J. Syst. Evol. Microbiol.* 44, 846–849. doi: 10.1099/00207713-44-4-846

Stegen, J. C., Lin, X., Fredrickson, J. K., Chen, X., Kennedy, D. W., Murray, C. J., et al. (2013). Quantifying community assembly processes and identifying features that impose them. *ISME J.* 7, 2069–2079. doi: 10.1038/ismej.2013.93

Sun, D., Bi, Q., Li, K., Dai, P., Yu, Y., Zhou, W., et al. (2018). Significance of temperature and water availability for soil phosphorus transformation and microbial community composition as affected by fertilizer sources. *Biol. Fertil. Soils* 54, 229–241. doi: 10.1007/s00374-017-1252-7

Thakeow, P., Angeli, S., Weissbecker, B., and Schütz, S. (2008). Antennal and behavioral responses of cis boleti to fungal odor of *Trametes gibbosa*. *Chem. Senses* 33, 379–387. doi: 10.1093/chemse/bjn005

Timonen, S., Jrgensen, K. S., Haahtela, K., and Sen, R. (1998). Bacterial community structure at defined locations of Pinus sylvestris-Suillus bovinus and Pinus sylvestris-Paxillus involutus mycorrhizospheres in dry pine forest humus and nursery peat. *Can. J. Microbiol.* 44, 499–513. doi: 10.1139/w98-035

Torsvik, V., and Øvreås, L. (2002). Microbial diversity and function in soil: from genes to ecosystems. *Curr. Opin. Microbiol.* 5, 240–245. doi: 10.1016/s1369-5274(02)00324-7

Tripathi, B. M., Stegen, J. C., Kim, M., Dong, K., Adams, J. M., and Lee, Y. K. (2018). Soil pH mediates the balance between stochastic and deterministic assembly of bacteria. *ISME J.* 12, 1072–1083. doi: 10.1038/s41396-018-0082-4

Tyc, O., Song, C., Dickschat, J. S., Vos, M., and Garbeva, P. (2017). The ecological role of volatile and soluble secondary metabolites produced by soil bacteria. *Trends Microbiol.* 25, 280–292. doi: 10.1016/j.tim.2016.12.002

Upadhyay, S. K., Srivastava, A. K., Rajput, V. D., Chauhan, P. K., Bhojiya, A. A., Jain, D., et al. (2022). Root exudates: mechanistic insight of plant growth promoting rhizobacteria for sustainable crop production. *Front. Microbiol.* 13:916488. doi: 10.3389/fmicb.2022.916488

Vahdatzadeh, M., Deveau, A., and Splivallo, R. (2015). The role of the microbiome of truffles in aroma formation: a meta-analysis approach. *Appl. Environ. Microbiol.* 81, 6946–6952. doi: 10.1128/AEM.01098-15

Vahdatzadeh, M., Deveau, A., and Splivallo, R. (2019). Are bacteria responsible for aroma deterioration upon storage of the black truffle *Tuber aestivum*: a microbiome and volatilome study. *Food Microbiol.* 84:103251. doi: 10.1016/j.fm.2019.103251

Vass, M., Székely, A. J., Lindström, E. S., and Langenheder, S. (2020). Using null models to compare bacterial and microeukaryotic metacommunity assembly under shifting environmental conditions. *Sci. Rep.* 10:2455. doi: 10.1038/s41598-020-59182-1

Vellend, M. (2010). Conceptual synthesis in community ecology. *Q. Rev. Biol.* 85, 183–206. doi: 10.1086/652373

Wang, Q., Garrity, G. M., Tiedje, J. M., and Cole, J. R. (2007). Naive Bayesian classifier for rapid assignment of rRNA sequences into the new bacterial taxonomy. *Appl. Environ. Microbiol.* 73, 5261–5267. doi: 10.1128/AEM.00062-07

Wang, R., Lin, J. Q., Liu, X. M., Pang, X., Zhang, C. J., Yang, C. L., et al. (2019). Sulfur oxidation in the acidophilic autotrophic *Acidithiobacillus* spp. *Front. Microbiol.* 9:3290. doi: 10.3389/fmicb.2018.03290

Wang, X. B., Lü, X. T., Yao, J., Wang, Z. W., Deng, Y., Cheng, W. X., et al. (2017). Habitat-specific patterns and drivers of bacterial beta-diversity in China's drylands. *ISME J.* 11, 1345–1358. doi: 10.1038/ismej.2017.11

Warmink, J. A., Nazir, R., and van Elsas, J. D. (2009). Universal and species-specific bacterial 'fungiphiles' in the mycospheres of different basidiomycetous fungi. *Environ. Microbiol.* 11, 300–312. doi: 10.1111/j.1462-2920.2008.01767.x

Warmink, J. A., and van Elsas, J. D. (2008). Selection of bacterial populations in the mycosphere of *Laccaria proxima*: is type III secretion involved? *ISME J.* 2, 887–900. doi: 10.1038/ismej.2008.41

Wisnoski, N. I., Muscarella, M. E., Larsen, M. L., Peralta, A. L., and Lennon, J. T. (2020). Metabolic insight into bacterial community assembly across ecosystem boundaries. *Ecology* 101:e02968. doi: 10.1002/ecy.2968

Xia, Z., Bai, E., Wang, Q., Gao, D., Zhou, J., Jiang, P., et al. (2016). Biogeographic distribution patterns of bacteria in typical Chinese forest soils. *Front. Microbiol.* 7:1106. doi: 10.3389/fmicb.2016.01106

Xiao, X., Liang, Y., Zhou, S., Zhuang, S., and Sun, B. (2018). Fungal community reveals less dispersal limitation and potentially more connected network than that of bacteria in bamboo forest soils. *Mol. Ecol.* 27, 550–563. doi: 10.1111/mec.14428

Xiong, C., He, J. Z., Singh, B. K., Zhu, Y. G., Wang, J. T., Li, P. P., et al. (2021). Rare taxa maintain the stability of crop mycobiomes and ecosystem functions. *Environ. Microbiol.* 23, 1907–1924. doi: 10.1111/1462-2920.15262

Xu, X., Xu, R., Jia, Q., Feng, T., Huang, Q., Ho, C. T., et al. (2019). Identification of dihydro-β-ionone as a key aroma compound in addition to C8 ketones and alcohols in *Volvariella volvacea* mushroom. *Food Chem.* 293, 333–339. doi: 10.1016/j.foodchem.2019.05.004

Yu, F., Liang, J. F., Song, J., Wang, S. K., and Lu, J. K. (2020). Bacterial community selection of *Russula griseocarnosa* mycosphere soil. *Front. Microbiol.* 11:347. doi: 10.3389/fmicb.2020.00347

Yuichi, S. (2018). Influences of environmental factors on fruiting body induction, development and maturation in mushroom-forming fungi. *Fungal Biol. Rev.* 32, 236–248. doi: 10.1016/j.fbr.2018.02.003

Yun, Y. B., Park, S. W., Cha, J. S., and Kim, Y. K. (2013). Biological characterization of various strains of *Pseudomonas tolaasii* that causes brown blotch disease. *Appl. Biol. Chem.* 56, 41–45. doi: 10.1007/s13765-012-2242-y

Zhang, J., Jiao, S., and Lu, Y. (2018a). Biogeographic distribution of bacterial, archaeal and methanogenic communities and their associations with methanogenic capacity in Chinese wetlands. *Sci. Total Environ.* 622-623, 664–675. doi: 10.1016/j.scitotenv.2017.11.279

Zhang, J., Zhang, B., Liu, Y., Guo, Y., Shi, P., and Wei, G. (2018b). Distinct large-scale biogeographic patterns of fungal communities in bulk soil and soybean rhizosphere in China. *Sci. Total Environ.* 644, 791–800. doi: 10.1016/j.scitotenv.2018.07.016

Zhao, Z. Y., Ma, Y. T., Feng, T. Y., Kong, X., Wang, Z. H., Zheng, W., et al. (2022). Assembly processes of abundant and rare microbial communities in orchard soil under a cover crop at different periods. *Geoderma* 406:115543. doi: 10.1016/j.geoderma.2021.115543

Zheng, W., Zhao, Z., Lv, F., Wang, R., Wang, Z., Zhao, Z., et al. (2021). Assembly of abundant and rare bacterial and fungal sub-communities in different soil aggregate sizes in an apple orchard treated with cover crop and fertilizer. *Soil Biol. Biochem.* 156:108222. doi: 10.1016/j.soilbio.2021.108222

Zhou, J., and Ning, D. (2017). Stochastic community assembly: does it matter in microbial ecology? *Microbiol. Mol. Biol. Rev.* 81, e00002–e00017. doi: 10.1128/MMBR.00002-17

Zhu, R., Wen, Y., Wu, W., Zhang, L., Salman Farid, M., Shan, S., et al. (2022). The flavors of edible mushrooms: a comprehensive review of volatile organic compounds and their analytical methods. *Crit. Rev. Food Sci. Nutr.*, 1–15. doi: 10.1080/10408398.2022.2155798

Zhu, J., Zhang, L., Jin, X., Han, X., Sun, C., and Yan, J. (2010). Beta-ionone-induced apoptosis in human osteosarcoma (U2os) cells occurs via a p53-dependent signaling pathway. *Mol. Biol. Rep.* 37, 2653–2663. doi: 10.1007/s11033-009-9793-y

Zul, D., Denzel, S., Kotz, A., and Overmann, J. (2007). Effects of plant biomass, plant diversity, and water content on bacterial communities in soil lysimeters: implications for the determinants of bacterial diversity. *Appl. Environ. Microbiol.* 73, 6916–6929. doi: 10.1128/AEM.01533-07

frontiers | Frontiers in Microbiology

TYPE Original Research
PUBLISHED 22 February 2023
DOI 10.3389/fmicb.2023.979835

OPEN ACCESS

EDITED BY
Juan Sun,
Qingdao Agricultural University,
China

REVIEWED BY
Sudhir K. Upadhyay,
Veer Bahadur Singh Purvanchal University,
India
Samantha Chandranath Karunarathna,
Qujing Normal University,
China

*CORRESPONDENCE
Wen Wang
✉ wenwang@nwpu.edu.cn

†These authors share first authorship

SPECIALTY SECTION
This article was submitted to
Microbial Symbioses,
a section of the journal
Frontiers in Microbiology

RECEIVED 28 June 2022
ACCEPTED 02 February 2023
PUBLISHED 22 February 2023

CITATION
Zhang C, Shi X, Zhang J, Zhang Y and
Wang W (2023) Dynamics of soil microbiome
throughout the cultivation life cycle of morel
(*Morchella sextelata*).
Front. Microbiol. 14:979835.
doi: 10.3389/fmicb.2023.979835

Dynamics of soil microbiome throughout the cultivation life cycle of morel (*Morchella sextelata*)

Chen Zhang[1†], Xiaofei Shi[2†], Jiexiong Zhang[1], Yesheng Zhang[3] and Wen Wang[1*]

[1]School of Ecology and Environment, Northwestern Polytechnical University, Xi'an, China, [2]The Germplasm Bank of Wild Species, Yunnan Key Laboratory for Fungal Diversity and Green Development, Kunming Institute of Botany, Chinese Academy of Sciences, Kunming, China, [3]Shandong Junsheng Biotechnologies Co., Ltd., Liaocheng, China

Although *Morchella sextelata* (morel) is a well-known, edible, and medicinal fungus widely cultivated in China, the dynamics and roles of its soil microbiome during cultivation are unclear. Using rhizosphere soil samples collected throughout the *M. sextelata* cultivation life cycle, we conducted a high-throughput metagenomic sequencing analysis, with an emphasis on variations in soil microbial composition, characteristic biomarkers, and ecological functions. We found that microbial relative abundance, alpha diversity, and structure varied significantly among fungal growth stages. A total of 47 stage-associated biomarkers were identified through a linear discriminant analysis of effect size. In addition, horizontal comparison of soil microbiomes exhibiting successful and failed primordium formation further confirmed primordium-associated microbes with possible key roles in primordium formation. A microbial function analysis revealed that nutrient metabolism-related pathways were enriched during mycelium and fruiting body stages, whereas the signal transduction pathway was enriched during the primordium stage. This result indicates that diverse microbes are required at different growth stages of *M. sextelata*. Our research has revealed the dynamic scenario of the soil microbiome throughout the cultivation life cycle of *M. sextelata*. The high-resolution microbial profiles uncovered in the present study provide novel insights that should contribute to the improvement of morel cultivation using microbial inoculants.

KEYWORDS

metagenomics, microbial community, morel (*Morchella sextelata*), primordium formation, fruiting body maturation

1. Introduction

Morels (*Morchella* spp.) are well-known, edible, and medicinal fungi with unique, honeycomb-like fertile tissues (Pilz et al., 2007) and an abundance of amino acids, polysaccharides, and trace elements (Tietel and Masaphy, 2018). According to various studies, morels are beneficial to human health, with significant tumor-inhibitory, immune-enhancing, and antioxidant and antibacterial properties (Heleno et al., 2013; Wu et al., 2020; Sunil and Xu, 2022).

Morel cultivation has been a research focus worldwide, with an early indoor cultivation of *M. rufobrunnea* in the 1980s in the United States (Ower, 1982). In recent decades, the cultivation area of several black morels (*M. sextelata, M. importuna,* and *M. exima*) in China has rapidly expanded to 10,000 ha, with an average yield more than 3,000 kg/ha (Tang et al., 2021; Zhao et al., 2021). The cultivation process includes sowing of cultured spawn in soil, coverage with exogenous nutrients for approximately 10–15 days (until the soil surface is covered with mycelia), and management of fruiting bodies under appropriate growth conditions (Li et al., 2016). In a recent study of *M. importuna*, the carbon used to support fruiting body growth was initially transferred from exogenous nutrient bags to the soil, whereas required nitrogen seemed to originate directly from soil (Tan et al., 2019). Although large-scale cultivation of morels has been achieved in China, several major obstacles still exist, including yield instability (Du and Yang, 2021), susceptibility to pathogen infection (Guo et al., 2016; He et al., 2017, 2018), and environmental fluctuations. To address these challenges and improve commercial morel cultivation in the field, an understanding of the soil microbiome during the cultivation life cycle of morels would be useful.

Soil microbiome structure and function affect plant development (Edwards et al., 2015; Chen et al., 2019; Xiong et al., 2021). Numerous studies have clarified mechanisms of plant growth-promoting rhizobacteria (Nerva et al., 2022; Singh R. K. et al., 2022; Upadhyay et al., 2022) and highlighted the great potential of microbial inoculants (Deng et al., 2022; Singh P. et al., 2022; Upadhyay and Chauhan, 2022). Soil microbes also have important functions in the growth of mushrooms, such as *Agaricus bisporus* (Wang et al., 2016), *Ganoderma lucidum* (Zhang et al., 2018), *Phlebopus portentosus* (Yang et al., 2019), and *Stropharia rugosoannulata* (Gong et al., 2018). Possible key functions of the soil microbiome during mushroom growth are the following: (i) conversion of lignocellulosic feedstock into a selective, nutrient-rich fertilizer for mushroom growth; (ii) interaction with the mushroom itself during mycelial elongation and proliferation stages; and (iii) induction of primordium and ascocarp formation during cultivation (Kertesz and Thai, 2018). In contrast, some bacterial and fungal taxa in soil substrates can act as pathogens of cultivated mushrooms, leading to reduced yield and severe quality loss.

The nutritional types of *Morchella* vary from soil-saprophytic to symbiotic (Larson et al., 2016; Longley et al., 2019). The three main cultivated species (*M. sextelata*, *M. importuna,* and *M. exima*) are soil-saprophytic, which must be covered with soil during cultivation while the mycelium acquires nutrients from soil and surrounding substrate. Longley et al. (2019) analyzed the composition of soil bacteria and fungi associated with *M. rufobrunnea* at primordium and fruiting body stages by 16S rRNA and ITS amplicon sequencing and found that *Gilmaniella* and *Bacillus* were predominant in substrates. In addition, Benucci et al. (2019) examined the microbial community composition of *M. sextelata* ascocarps and soils beneath the ascocarps by 16S rRNA and ITS amplicon sequencing, and Orlofsky et al. (2021) studied the composition and function of the soil microbiome beneath young and mature fruiting bodies of *M. rufobrunnea* in the field. Furthermore, Tan et al. (2021) comparatively analyzed soil microbial composition, nutrient transformation, and key enzyme activities after inoculation of *M. importuna* into semi-synthetic substrates and proposed a conceptual illustration of the ecophysiological factors influencing morel fructification. Despite these advances in elucidating the effect of the soil microbiome, a comprehensive understanding of soil microbiome dynamics from seeding to harvesting, i.e., during mycelium elongation, primordium formation, and ascocarp maturation, is lacking, as current 16S rRNA and ITS amplicon sequencing methods cannot easily identify functional genes of the soil microbiome in detail. A life cycle investigation of the soil microbiome across all morel growth stages is crucial to: (1) determine how the soil microbiome dynamically varies with growth stages during morel cultivation, (2) identify key biomarkers associated with variations shaping the soil microbiome, (3) understand the ecological functions of these soil microbes, and (4) reveal how these microbes affect morel growth and development.

In this study, we hypothesized that the soil microbiome changes significantly along with morel growth, especially the primordium and fruiting body stages. We also hypothesized that microbiota drive changes in soil ecological functions associated with morel growth and development. To test these hypotheses, we analyzed the dynamic succession of the soil microbiome and identified stage-associated characteristic biomarkers from sowing to harvesting in *M. sextelata* during mycelium (days 1, 10, and 23), primordium (day 40), and fruiting body (days 55, 65, and 90) stages. We also compared functional pathways of the soil microbiome at different growth stages to understand the ecological functions and potential mechanisms of microbes promoting morel growth and development.

2. Materials and methods

2.1. Morel cultivation and soil sampling

Morels (*M. sextelata*) were cultivated in a plastic greenhouse in Jinji, Longyang County (25.16° N, 99.24° E; 1,600 m above sea level), Yunnan, China, in the Winter of 2020. The cultivation procedure followed a standard technical protocol (Liu et al., 2017). During the key growth stages of *M. sextelata*, representative rhizosphere soil samples were collected around *M. sextelata* mycelium (days 01, 10, and 23), primordium (day 40), and fruiting body (days 55, 65, and 90; Figure 1; Supplementary Table S1). After removal of the top 2 cm of soil, rhizosphere soil at a depth of 2–8 cm was collected with a 10-cm soil auger from three sites located 2–3 m apart on a ridge, with the three samples then thoroughly mixed as one composite sample. At each sampling period, we collected three composite samples as replicates from three different ridges. A total of 21 composite samples were collected at seven time points. We also collected five composite soil samples between days 55 and 65 with failed primordium formation from a nearby, separate greenhouse (distance < 500 m) in which morels were sown at approximately the same time (Supplementary Table S1) and cultivated similarly (Liu et al., 2017). All samples were rapidly frozen with liquid nitrogen and stored at −80°C for subsequent DNA extraction.

2.2. DNA extraction and shotgun metagenomic sequencing

DNA extraction and shotgun metagenomic sequencing were performed by Novogene (Beijing, China). Total DNA was extracted from samples using a PowerSoil DNA extraction kit (MO BIO, Carlsbad, CA, United States) and then qualified and quantified by

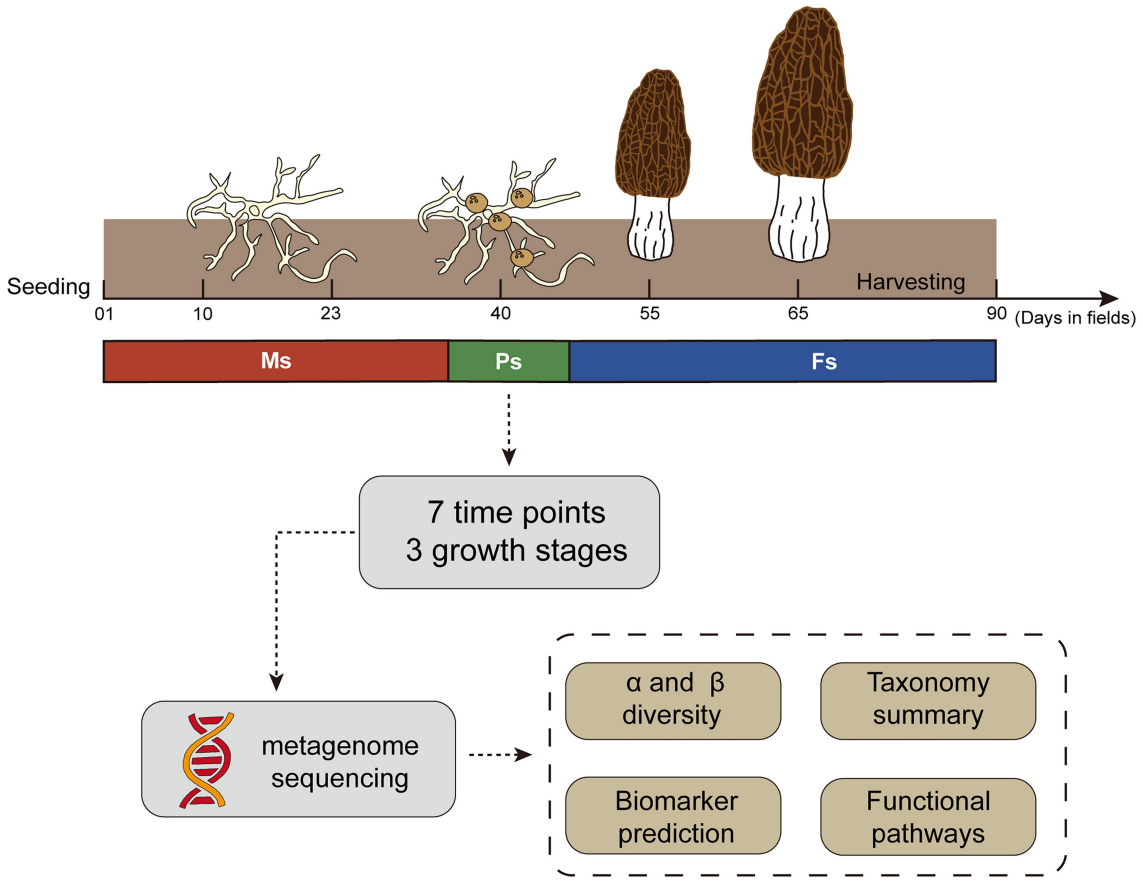

FIGURE 1
Outline of the study design and sampling strategy used throughout the *Morchella sextelata* cultivation life cycle. Ms, mycelium stage; Ps, primordium stage; Fs, fruiting body stage.

agarose gel electrophoresis and nano-spectrophotometry. Qualified DNA was used for construction of a metagenomic sequencing library, which was analyzed on the Illumina NovaSeq 6000 platform (Illumina, San Diego, CA, United States) with a sequencing read length of 150 bp and an insert fragment size of 350 bp. All sequence data were deposited at NCBI under BioProject accession number PRJNA841746.

2.3. Bioinformatic analyses

After removal of adapter sequences and trimming of low-quality sequences based on a 5-bp sliding window (quality < 20, read accuracy < 99%), sequences longer than 50 bp were retained for further analysis (Bolger et al., 2014). The sequencing data were aligned to the reference genome of *M. sextelata* using the Kneaddata v0.7.4 pipeline with Bowtie2 (Langmead and Salzberg, 2012), and the sequences from *M. sextelata* genome were then removed. The processed data were assembled with Megahit v1.2.9 using the deBruijn graph method (Li et al., 2015). The metagenome assembly results were evaluated in Quast v5.0.2 (Gurevich et al., 2013). Coding sequences were predicted with Prodigal v2.6.3 and further clustered using CD-HIT v4.8.1, with 95% amino acid identity used as a criterion, to obtain a non-redundant gene catalog (Hyatt et al., 2010; Fu et al., 2012). Gene abundance was calculated in Salmon v1.4.0 based on coverage of metagenomic gene regions (Patro et al., 2017). Accurate *k-mer* matching against the NCBI-NT database was performed with Kraken2 v2.1.1, and annotated microbial taxonomic profiles were generated by the lowest common ancestor method (Wood et al., 2019). Non-redundant gene sequences were compared against the eggNOG v5.0 database using Diamond v0.9.36 for annotation of microbial functional profiles (Buchfink et al., 2015; Huerta-Cepas et al., 2019). Finally, soil microbiome taxonomic and functional composition tables were obtained for further statistical analyses and visualization.

2.4. Statistical analyses and visualization

Prior to analysis, data were quality filtered to remove microbial taxa with a relative abundance < 0.01%. Rarefaction curves were used to assess data richness from the results of sampling. The top 10 phyla at different time points were visualized using the histogram function in the R package ggplot2 (Ginestet, 2011). Alpha diversity based on Shannon's and Simpson's indexes was evaluated using the R package vegan (Dixon, 2003). Microbiome structure (beta diversity) was calculated based on Bray–Curtis distances (Ricotta and Podani, 2017) and visualized by principal coordinate analysis (PCoA) and non-metric multidimensional scaling (NMDS). A linear discriminant analysis of effect size (LEFSe) with p-value < 0.05 and LDA score > 2

thresholds was conducted to identify characteristic biomarkers at different *M. sextelata* growth stages (Segata et al., 2011). Biomarkers were sorted by LDA score from largest to smallest, and the R package pheatmap was used to display the average relative abundance of biomarkers at each growth stage. STAMP v2.1.3 was used to examine the abundance of functional pathways between different growth stages (Parks et al., 2014), and significant differences among samples were assessed with a *t*-test. The QIIME2 v2021.11.0 pipeline and R v4.1.1 were used throughout the study for data processing, analysis, and visualization (Bolyen et al., 2019).

3. Results

3.1. Soil microbiome composition during *Morchella sextelata* cultivation

A total of 306.59 GB of clean sequence data (11.17–21.32 GB per sample) were obtained from 21 samples (Supplementary Table S2), from which 21 phyla, 56 classes, 129 orders, 263 families, 717 genera, and 2,307 species were identified (Supplementary Table S3). Rarefaction analysis indicated that the sequencing depth was sufficient to cover most microbial taxa (Supplementary Figure S1). The most dominant phyla were *Proteobacteria* and *Actinobacteria*, with a total abundance of 83.30%–95.09%. The abundances of other phyla were as follows: *Bacteroidetes* (0.61%–9.08%), *Planctomycetes* (0.83%–3.39%), *Firmicutes* (0.71%–1.99%), and *Acidobacteria* (0.50%–1.56%). As shown in Figure 2A, where the top 10 phyla with the highest relative abundances are displayed as a stacked bar plot, the relative abundance of different soil microbes fluctuated over time at different growth stages of *M. sextelata*; this was especially true at the primordium stage (day 40), an obvious turning point.

Phyla with a relative abundance > 1% but significantly differing over time are shown in Figure 2. The relative abundance of *Proteobacteria* continuously increased from mycelium (days 01, 10, and 23) to primordium (day 40) stages and decreased during the fruiting body stage (days 55, 65, and 90; $p = 2.81 \times 10^{-9}$, Figure 2B). The fluctuation in abundance of *Proteobacteria* mainly took place in the families *Burkholderiaceae*, *Comamonadaceae*, *Pseudomonadaceae*, *Sphingomonadaceae,* and *Xanthomonadaceae*. The abundance of *Actinobacteria* (*Nocardioidaceae*, *Pseudonocardiaceae,* and *Streptomycetaceae*) continuously decreased from mycelium (days 01, 10, and 23) to primordium (day 40) stages and increased during the fruiting body stage (days 55, 65, and 90; $p = 2.47 \times 10^{-7}$, Figure 2C). The relative abundance of *Bacteroidetes* was similar to *Proteobacteria* ($p = 0.094$, Figure 2D). *Planctomycetes* ($p = 5.86 \times 10^{-3}$, Figure 2E), *Firmicutes* ($p = 2.39 \times 10^{-4}$, Figure 2F), and *Acidobacteria* ($p = 6.63 \times 10^{-5}$, Figure 2G) had higher abundances during the fruiting body stage (days 55, 65, and 90) than at the other two stages.

3.2. Community diversity of the soil microbiome across the three growth stages of *Morchella sextelata*

Soil microbial alpha diversity was significantly different among different growth stages ($p < 0.01$; Figures 3A,B). Shannon's and Simpson's index values were lowest at the primordium stage and highest at the fruiting body stage (Figures 3A,B). PCoA based on Bray–Curtis distances uncovered significant shifts in microbial community composition between stages (Figure 3C). In particular, soil microbial community compositions clustered into three groups closely correlated with mycelium, primordium, and fruiting body stages, which were separated along the main coordinate axis. Similar patterns were also observed in the NMDS analysis (Figure 3D). These results indicate that soil microbial community composition and structure varied during the different *M. sextelata* growth stages.

3.3. Key microbial biomarkers associated with *Morchella sextelata* growth stages

The LEFSe analysis was conducted to identify characteristic biomarkers associated with *M. sextelata* growth stages. Because the soil microbiome immediately after sowing mostly reflected the original status of the soil (before mycelial growth) and thus could have biased the stage-associated results, samples from day 01 were not included in the analysis. A total of 47 microbial biomarkers (LDA > 3), mainly from *Actinobacteria*, *Bacteroidetes,* and *Proteobacteria* were identified (Figure 4A). Two of 17 characteristic microbial taxa associated with the mycelium stage, namely *Sphingomonas* and *Bradyrhizobium*, had LDA values >4. We identified 16 microbial biomarkers associated with the primordium stage; among them, *Pseudomonas* and *Massilia* had the highest LDA values (>4). Finally, 14 microbial biomarkers were associated with the fruiting body stage, including *Hydrogenophaga* and *Burkholderia* with LDA values > 3. Each characteristic biomarker had its highest abundance at a specific *M. sextelata* growth stage (Figure 4B). As representative microbes of different stages, these biomarkers may extensively interact and play important roles in mycelium elongation, primordium formation, and fruiting body maturation to promote *M. sextelata* growth and development.

3.4. Validation of primordium-associated microbial biomarkers through comparison of soil samples with and without primordium formation

For use as controls, we collected five soil samples from a nearby greenhouse (distance < 500 m) in which *M. sextelata* had been sown at approximately the same time but with no primordium formation taking place (Supplementary Table S1). These soil samples had been managed and collected in the same way as the other samples in this study. To verify the characteristic biomarkers associated with the primordium stage, we horizontally compared the rhizosphere soil microbiome of the five control samples with that of samples with primordium formation.

Alpha diversity was significantly different between the two sample groups (Shannon's index, $p = 0.0044$; Simpson's index, $p = 0.024$; Supplementary Figure S2). Microbial community structure differed significantly as well (Figure 5A). NMDS separated the samples into two independent groups, i.e., with and without primordium formation (Figure 5A). In addition, we predicted 16 primordium-associated biomarkers by LEFSe (Figure 4A) and further visualized their relative abundances with a heatmap (Figure 5B). Compared with their

10.3389/fmicb.2023.979835

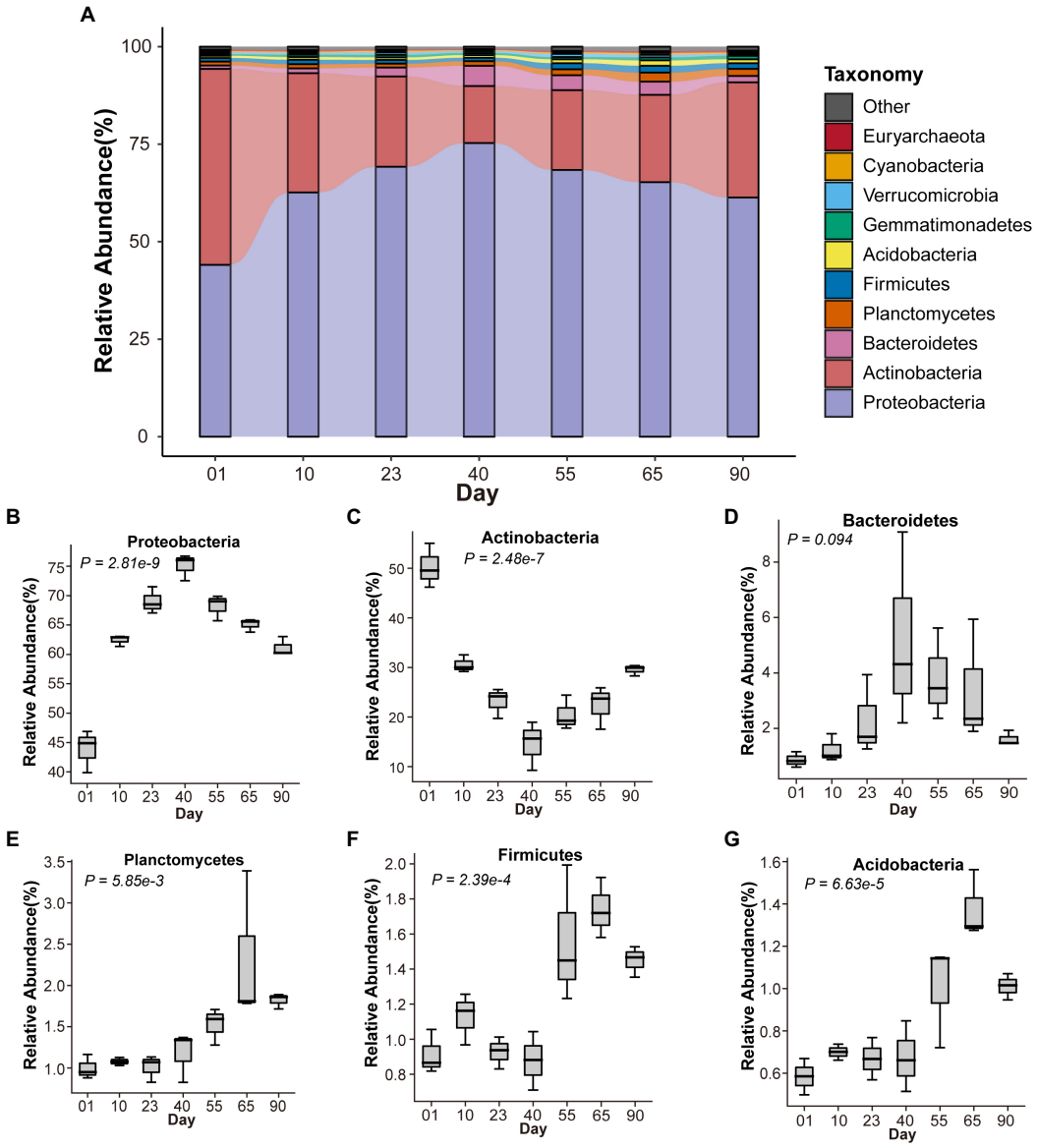

FIGURE 2
Composition of the soil microbiome at different growth stages of *Morchella sextelata*. **(A)** Relative abundances of the top 10 most abundant phyla at different time points. **(B–G)** Variation in microbial phyla during *M. sextelata* cultivation.

abundances in soil without primordium formation, all 16 biomarkers were significantly more abundant in soil with primordium formation. The absence of synergy among these microbes might be correlated with the failure of primordia to form.

3.5. Functional analysis of the soil microbiome across the three growth stages of *Morchella sextelata*

To explore biological functions of the soil microbiome during the life cycle of cultivated *M. sextelata*, we performed a functional annotation analysis at different *M. sextelata* growth stages based on the KEGG orthology database. The majority of enriched KEGG pathways were related to metabolism (55.47%), followed by environmental information processing (8.27%), genetic information processing (7.69%), human diseases (7.58%), cellular processes (7.20%), organismal systems (3.30%), and those not included in KEGG pathway or BRITE databases (10.49%; Supplementary Figure S3). Soil microbiome functional pathways are listed in Supplemental Table S4. Alpha diversity based on Shannon's and Simpson's indexes was significantly higher at the primordium stage than at mycelium and fruiting body stages (Supplementary Figure S4), thus indicating that the soil microbial community was functionally more diverse at the primordium stage. Principal component analysis (PCA) revealed that ecological functions of the soil microbiome varied among *M. sextelata* growth stages, with samples from the primordium stage found to be strikingly different from those of mycelium and fruiting body stages (Supplementary Figure S4).

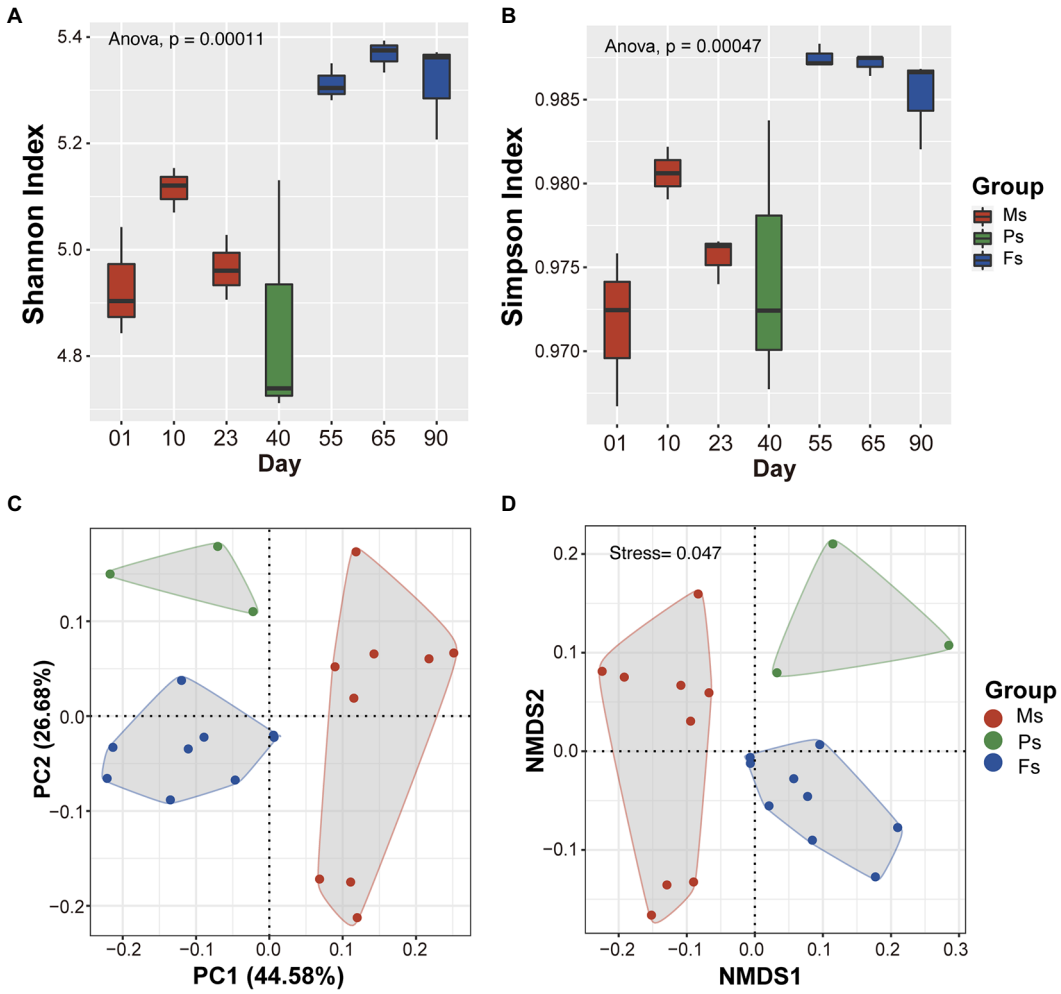

FIGURE 3
Variation in soil microbial diversity among *Morchella sextelata* growth stages. **(A,B)** Changes in microbial community alpha diversity based on Shannon's and Simpson's indexes. **(C,D)** PCoA and NMDS plots of microbial community diversity based on Bray–Curtis distances. Mycelium, primordium, and fruiting body stages are depicted in red, green, and blue, respectively. Ms, mycelium stage; Ps, primordium stage; Fs, fruiting body stage.

Pairwise comparative analysis of level-2 KEGG pathways was used to characterize the functional pathways differing among the three *M. sextelata* growth stages (Figure 6). Pathways related to carbohydrate, amino acid, and energy metabolism were enriched at the mycelium stage (Figures 6A,B), an observation supporting the idea that the soil microbiome helps *M. sextelata* mycelium absorb and transform large-scale nutrients from surrounding substrate. At the primordium stage, the soil microbiome was enriched in signal transduction-related pathways (Figures 6A,C), including those associated with the mitogen-activated protein kinase signaling pathway and the bacterial two-component regulatory system. This result suggests that soil microbes can transmit information through signal transduction molecules to transform rhizosphere microbes during primordium formation, a critical step in morel cultivation. At the fruiting body stage, ascocarp development and maturity were accompanied by a significant increase in enriched pathways related to carbohydrate, amino acid, and energy metabolism, thus reflecting potential nutrient demand during morel fruiting.

4. Discussion

4.1. Microbial community dynamics across three *Morchella sextelata* growth stages

The main components of the soil microbiome during the three growth stages of *M. sextelata* were *Proteobacteria* and *Actinobacteria*, followed by *Bacteroidetes*, *Planctomycetes*, *Firmicutes*, and *Acidobacteria* (Figure 2A). These phyla are also the major constituents of the soil microbial community in the natural habitat of *M. rufobrunnea* (Orlofsky et al., 2021) and in semi-synthetic substrates of *M. importuna* (Tan et al., 2021), which indicates that these microbes are indispensable during the morel life cycle. Nevertheless, the composition of the soil microbiome was marked by significant differences among mycelium, primordium, and fruiting body stages (Figures 3C,D). In particular, the relative abundances of *Proteobacteria* and *Bacteroidetes* increased until the primordium stage and then decreased, whereas the opposite was true of *Actinobacteria* (Figures 2B,C). Similar patterns have been observed in studies of

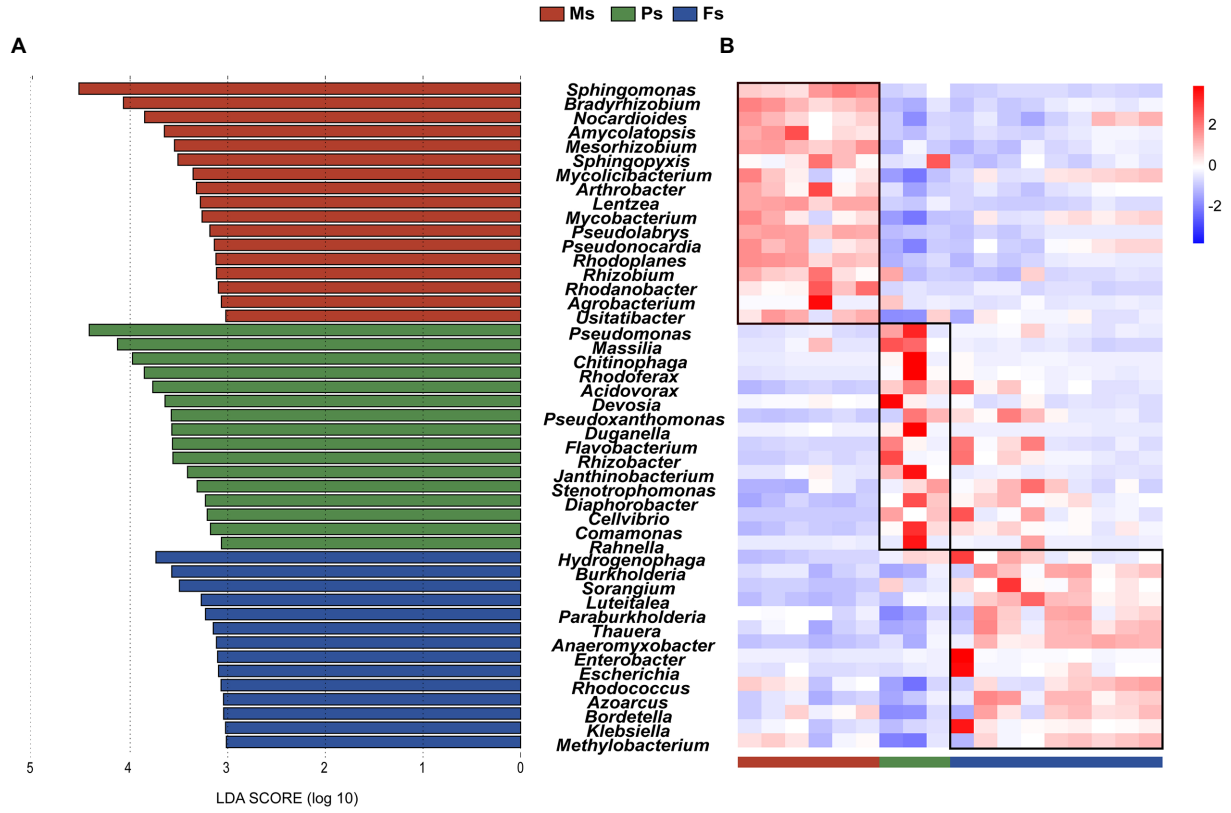

FIGURE 4
Identification of key microbial biomarkers associated with *Morchella sextelata* growth stages. **(A)** LEfSe to identify characteristic biomarkers between different stages. Only microbial taxa with a LDA score > 3 are shown. **(B)** Heatmap showing the relative abundances (*Z*-scores) of 47 stage-associated biomarkers identified by LEfSe. Ms, mycelium stage; Ps, primordium stage; Fs, fruiting body stage.

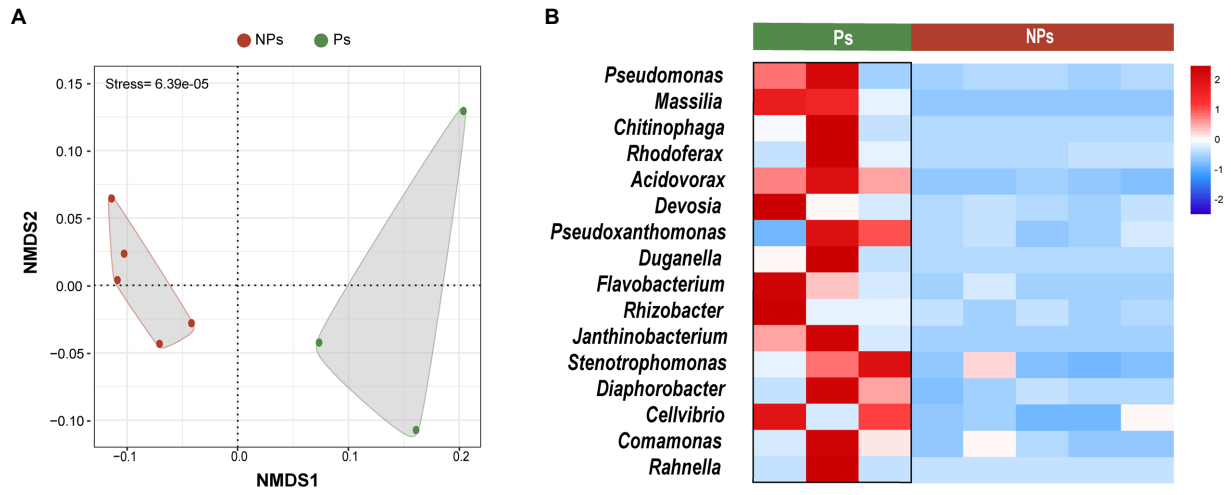

FIGURE 5
Comparative analysis of the soil microbiome with and without primordium formation. **(A)** NMDS plots of microbial community diversity based on Bray–Curtis distances. **(B)** Heatmap showing the relative abundances (*Z*-scores) of 16 primordium-associated biomarkers. Ps, samples with primordium formation (sampling at day 40). NPs, samples without primordium formation (sampling between days 55 and 65).

rhizosphere microbiomes of *A. bisporus* (Kertesz and Thai, 2018), *G. lucidum* (Zhang et al., 2018), and *P. portentosus* (Yang et al., 2019), with *Proteobacteria* more abundant at the primordium stage than at other growth stages. The fact that microbiome structure varied significantly among growth stages strongly suggests that morels can shape the soil microbiome and that normal morel growth requires specific microbes. These findings may be useful for the future improvement of morel cultivation through microbial inoculants.

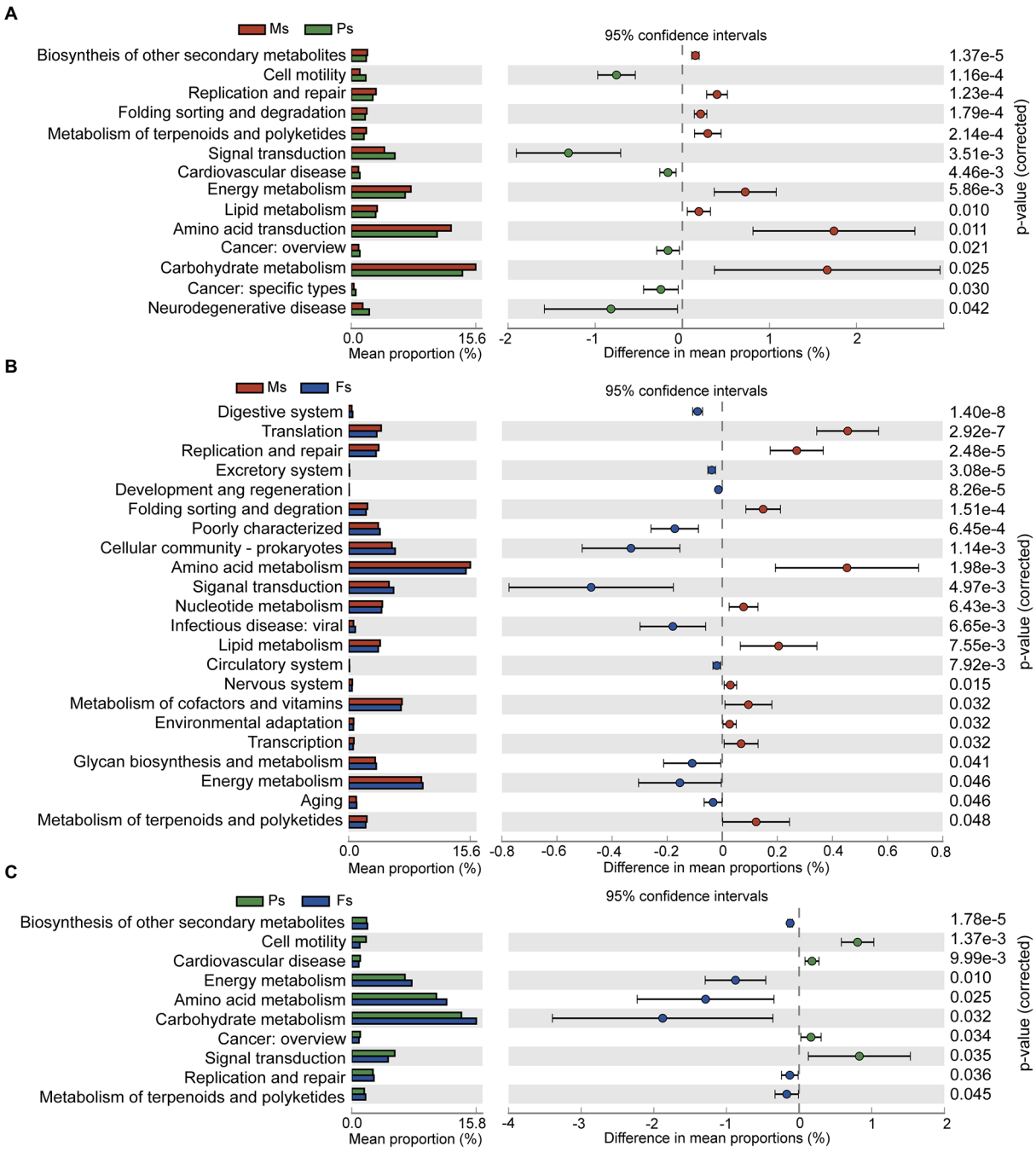

FIGURE 6
Variations in KEGG functions of the soil microbiome during mycelium, primordium, and fruiting body stages of *Morchella sextelata*. **(A–C)** Comparisons of mycelium and primordium stages **(A)**, mycelium and fruiting body stages **(B)**, and primordium and fruiting body stages **(C)**. Ms, mycelium stage; Ps, primordium stage; Fs, fruiting body stage.

4.2. Keystone microbes and their functions during *Morchella sextelata* growth

To further explore microbiota having critical effects on the growth of *M. sextelata*, we identified 47 characteristic biomarkers associated with specific growth stages (Figure 4A). Among them, *Sphingomonas* and *Bradyrhizobium* were significantly abundant at the mycelium stage and thus might contribute to the mycelium elongation and nutrient metabolism of morels. Interestingly, *Sphingomonas* and *Bradyrhizobium* are considered to be beneficial to the growth of mushrooms, which can multiply during composting and have strong lignocellulose degradation ability (Vajna et al., 2012; Zhang et al., 2014; Gohar et al., 2022). In this way, the surrounding substrate can be degraded to release more nutrients for mushroom growth.

At the primordium stage, *Pseudomonas* was the main biomarker (Figure 4A). *Pseudomonas* promotes mycelium growth, primordium formation, and high yield in *A. bisporus*

(Noble et al., 2009; Zarenejad et al., 2012; Chen et al., 2013), *Pleurotus eryngii* (Kim et al., 2008), and *Pleurotus ostreatus* (Cho et al., 2003), which suggests that *Pseudomonas* can also interact directly with morels to induce primordium formation. This hypothesis is supported by the fact that *Pseudomonas* was significantly more abundant in our study in soil with primordium formation than in soil with failed primordium formation (Figures 5A,B). *Burkholderiaceae* (*Hydrogenophaga* and *Burkholderia*) was present in higher abundance in the fruiting body stage (Figure 4A). Members of *Burkholderiaceae* have been associated with the formation of *P. portentosus* (Yang et al., 2019) and *Tricholoma matsutake* (Kataoka et al., 2012; Li et al., 2016), which suggests that this phylum promotes the growth of morel ascocarps. Given the important functions of these keystone microbes in morel growth and development, the use of inoculants containing such microbes may be a practical way to promote mycelium elongation, primordium formation, and ascocarp maturation in morels.

4.3. Potential pathogenic microbes during *Morchella sextelata* cultivation

Soil-borne pathogenic fungi and bacteria have been reported in morel cultivation (Guo et al., 2016; He et al., 2017, 2018). We thus note that some members of *Pseudomonas*, aside from their benefits, have ecologically harmful effects and can cause mushroom diseases. For example, mushroom brown spot disease due to *Pseudomonas tolaasii* has caused yield losses in *A. bisporus* (Largeteau and Savoie, 2010), *Pleurotus ostreatus* (Lo Cantore and Iacobellis, 2014), and *Flammulina velutipes* (Han et al., 2012). In our study, *Pseudomonas* was significantly enriched at the primordium stage (Figure 4B) and was more abundant in soil with primordium formation (Figure 5B). This result suggests that this genus plays an important role in promoting primordium formation. The application of growth-promoting bacteria as microbial inoculants is a promising method (Nerva et al., 2022; Upadhyay et al., 2022; Upadhyay and Chauhan, 2022). Consequently, the addition of specific beneficial microbial taxa to promote growth and enhance the resistance of *M. sextelata* is worthy of further investigation.

In conclusion, our study has revealed the dynamics of the soil microbiome throughout the *M. sextelata* cultivation life cycle. We uncovered significant changes in the microbial community during *M. sextelata* growth and identified stage-associated biomarkers. Our functional analysis of the soil microbiome revealed that diverse functional strategies are required for different growth stages of *M. sextelata*. The presented data provide novel insights for future application of microbial inoculants and soil improvement for stable morel cultivation.

Data availability statement

The data presented in the study are deposited in the NCBI repository (https://www.ncbi.nlm.nih.gov/), accession number PRJNA841746.

Author contributions

CZ, XS, and WW conceived and designed the research. CZ, JZ, and YZ coordinated the sampling. CZ and XS processed, analyzed, and interpreted the data and wrote the original draft. All authors contributed to the article and approved the submitted version.

Funding

This work was supported by the National Key Research and Development Program of China (2021YFD1600404) and the Postdoctoral Directional Training Foundation of Yunnan Province.

Acknowledgments

We acknowledge the technical assistance of Zhongkai Wang in the laboratory. We are deeply grateful to Fuqiang Yu and Xinhua He for their improvements to the manuscript.

Conflict of interest

YZ was employed by the company Shandong Junsheng Biotechnologies Co., Ltd.

The remaining authors declare that the research was conducted in the absence of any commercial or financial relationships that could be construed as a potential conflict of interest.

Publisher's note

Supplementary material

The Supplementary material for this article can be found online at: https://www.frontiersin.org/articles/10.3389/fmicb.2023.979835/full#supplementary-material

References

Benucci, G. M. N., Longley, R., Zhang, P., Zhao, Q., Bonito, G., and Yu, F. Q. (2019). Microbial communities associated with the black morel *Morchella sextelata* cultivated in greenhouses. *PeerJ* 7:e7744. doi: 10.7717/peerj.7744

Bolger, A. M., Lohse, M., and Usadel, B. (2014). Trimmomatic: a flexible trimmer for Illumina sequence data. *Bioinformatics* 30, 2114–2120. doi: 10.1093/bioinformatics/btu170

Bolyen, E., Rideout, J. R., Dillon, M. R., Bokulich, N., Abnet, C. C., Al-Ghalith, G. A., et al. (2019). Reproducible, interactive, scalable and extensible microbiome data science using QIIME 2. *Nat. Biotechnol.* 37, 852–857. doi: 10.1038/s41587-019-0209-9

Buchfink, B., Xie, C., and Huson, D. H. (2015). Fast and sensitive protein alignment using DIAMOND. *Nat. Methods* 12, 59–60. doi: 10.1038/nmeth.3176

Chen, S. C., Qiu, C. W., Huang, T., Zhou, W. W., Qi, Y. C., Gao, Y. Q., et al. (2013). Effect of 1-aminocyclopropane-1-carboxylic acid deaminase producing bacteria on the hyphal growth and primordium initiation of *Agaricus bisporus*. *Fungal Ecol.* 6, 110–118. doi: 10.1016/j.funeco.2012.08.003

Chen, S. M., Waghmode, T. R., Sun, R. B., Kuramae, E. E., Hu, C. S., and Liu, B. B. (2019). Root-associated microbiomes of wheat under the combined effect of plant development and nitrogen fertilization. *Microbiome* 7:136. doi: 10.1186/s40168-019-0750-2

Cho, Y. S., Kim, J. S., Crowley, D. E., and Cho, B. G. (2003). Growth promotion of the edible fungus *Pleurotus ostreatus* by fluorescent pseudomonads. *FEMS Microbiol. Lett.* 218, 271–276. doi: 10.1016/S0378-1097(02)01144-8

Deng, X. H., Zhang, N., Li, Y. C., Zhu, C. Z., Qu, B. Y., Liu, H. J., et al. (2022). Bio-organic soil amendment promotes the suppression of *Ralstonia solanacearum* by inducing changes in the functionality and composition of rhizosphere bacterial communities. *New Phytol.* 235, 1558–1574. doi: 10.1111/nph.18221

Dixon, P. (2003). VEGAN, a package of R functions for community ecology. *J. Veg. Sci.* 14, 927–930. doi: 10.1111/j.1654-1103.2003.tb02228.x

Du, X. H., and Yang, Z. L. (2021). Mating systems in true morels (*Morchella*). *Microbiol. Mol. Biol. R.* 85, e0022020–e0000220. doi: 10.1128/MMBR.00220-20

Edwards, J., Johnson, C., Santos-Medellin, C., Lurie, E., Podishetty, N. K., Bhatnagar, S., et al. (2015). Structure, variation, and assembly of the root-associated microbiomes of rice. *Proc. Natl. Acad. Sci. U. S. A.* 112, E911–E920. doi: 10.1073/pnas.1414592112

Fu, L. M., Niu, B. F., Zhu, Z. W., Wu, S. T., and Li, W. Z. (2012). CD-HIT: accelerated for clustering the next-generation sequencing data. *Bioinformatics* 28, 3150–3152. doi: 10.1093/bioinformatics/bts565

Ginestet, C. (2011). ggplot2: elegant graphics for data analysis. *J. R. Stat. Soc.* 174, 245–246. doi: 10.1111/j.1467-985X.2010.00676_9.x

Gohar, D., Poldmaa, K., Tedersoo, L., Aslani, F., Furneaux, B., Henkel, T. W., et al. (2022). Global diversity and distribution of mushroom-inhabiting bacteria. *Environ. Microbiol. Rep.* 14, 254–264. doi: 10.1111/1758-2229.13045

Gong, S., Chen, C., Zhu, J. X., Qi, G. Y., and Jiang, S. X. (2018). Effects of wine-cap *Stropharia* cultivation on soil nutrients and bacterial communities in forestlands of northern China. *PeerJ* 6:e5741. doi: 10.7717/peerj.5741

Guo, M. P., Chen, K., Wang, G. Z., and Bian, Y. B. (2016). First report of stipe rot disease on *Morchella importuna* caused by *fusarium incarnatum*—F. equiseti species complex in China. *Plant Dis.* 100:2530. doi: 10.1094/Pdis-05-16-0633-Pdn

Gurevich, A., Saveliev, V., Vyahhi, N., and Tesler, G. (2013). QUAST: quality assessment tool for genome assemblies. *Bioinformatics* 29, 1072–1075. doi: 10.1093/bioinformatics/btt086

Han, H. S., Jhune, C. S., Cheong, J. C., Oh, J. A., Kong, W. S., Cha, J. S., et al. (2012). Occurrence of black rot of cultivated mushrooms (*Flammulina velutipes*) caused by pseudomonas tolaasii in Korea. *Eur. J. Plant Pathol.* 133, 527–535. doi: 10.1007/s10658-012-9941-4

He, P. X., Li, C. C., Cai, Y. L., Zhang, Y., Bian, Y. B., and Liu, W. (2018). First report of pileus rot disease on cultivated *Morchella importuna* caused by *Diploospora longispora* in China. *J. Gen. Plant Pathol.* 84, 65–69. doi: 10.1007/s10327-017-0754-3

He, X. L., Peng, W. H., Miao, R. Y., Tang, J., Chen, Y., Liu, L. X., et al. (2017). White mold on cultivated morels caused by *Paecilomyces penicillatus*. *FEMS Microbiol. Lett.* 364:fnx037. doi: 10.1093/femsle/fnx037

Heleno, S. A., Stojkovic, D., Barros, L., Glamoclija, J., Sokovic, M., Martins, A., et al. (2013). A comparative study of chemical composition, antioxidant and antimicrobial properties of *Morchella esculenta* (L.) Pers. from Portugal and Serbia. *Food Res. Int.* 51, 236–243. doi: 10.1016/j.foodres.2012.12.020

Huerta-Cepas, J., Szklarczyk, D., Heller, D., Hernandez-Plaza, A., Forslund, S. K., Cook, H., et al. (2019). eggNOG 5.0: a hierarchical, functionally and phylogenetically annotated orthology resource based on 5090 organisms and 2502 viruses. *Nucleic Acids Res.* 47, D309–D314. doi: 10.1093/nar/gky1085

Hyatt, D., Chen, G. L., LoCascio, P. F., Land, M. L., Larimer, F. W., and Hauser, L. J. (2010). Prodigal: prokaryotic gene recognition and translation initiation site identification. *BMC Bioinformatics* 11:119. doi: 10.1186/1471-2105-11-119

Kataoka, R., Siddiqui, Z. A., Kikuchi, J., Ando, M., Sriwati, R., Nozaki, A., et al. (2012). Detecting nonculturable bacteria in the active mycorrhizal zone of the pine mushroom *Tricholoma matsutake*. *J. Microbiol.* 50, 199–206. doi: 10.1007/s12275-012-1371-7

Kertesz, M. A., and Thai, M. (2018). Compost bacteria and fungi that influence growth and development of *Agaricus bisporus* and other commercial mushrooms. *Appl. Microbiol. Biotechnol.* 102, 1639–1650. doi: 10.1007/s00253-018-8777-z

Kim, M. K., Math, R. K., Cho, K. M., Shin, K. J., Kim, J. O., Ryu, J. S., et al. (2008). Effect of *pseudomonas* sp P7014 on the growth of edible mushroom *Pleurotus eryngii* in bottle culture for commercial production. *Bioresour. Technol.* 99, 3306–3308. doi: 10.1016/j.biortech.2007.06.039

Langmead, B., and Salzberg, S. L. (2012). Fast gapped-read alignment with bowtie 2. *Nat. Methods* 9, 357–359. doi: 10.1038/Nmeth.1923

Largeteau, M. L., and Savoie, J. M. (2010). Microbially induced diseases of *Agaricus bisporus*: biochemical mechanisms and impact on commercial mushroom production. *Appl. Microbiol. Biotechnol.* 86, 63–73. doi: 10.1007/s00253-010-2445-2

Larson, A. J., Cansler, C. A., Cowdery, S. G., Hiebert, S., Furniss, T. J., Swanson, M. E., et al. (2016). Post-fire morel (*Morchella*) mushroom abundance, spatial structure, and harvest sustainability. *Forest Ecol. Manag.* 377, 16–25. doi: 10.1016/j.foreco.2016.06.038

Li, Q., Li, X. L., Chen, C., Li, S. H., Huang, W. L., Xiong, C., et al. (2016). Analysis of bacterial diversity and communities associated with *Tricholoma matsutake* fruiting bodies by barcoded pyrosequencing in Sichuan Province, Southwest China. *J. Microbiol. Biotechnol.* 26, 89–98. doi: 10.4014/jmb.1505.05008

Li, D. H., Liu, C. M., Luo, R. B., Sadakane, K., and Lam, T. W. (2015). MEGAHIT: an ultra-fast single-node solution for large and complex metagenomics assembly via succinct de Bruijn graph. *Bioinformatics* 31, 1674–1676. doi: 10.1093/bioinformatics/btv033

Liu, W., Zhang, Y., and He, P. X. (2017). *Morel biology and cultivation*. Changchun: Jilin science and Technology Press.

Lo Cantore, P., and Iacobellis, N. S. (2014). Characterization of fluorescent pseudomonads responsible for the yellowing of oyster mushroom (*Pleurotus ostreatus*). *Phytopathol. Mediterr.* 53, 54–65. doi: 10.14601/Phytopathol_Mediterr-12292

Longley, R., Benucci, G. M. N., Mills, G., and Bonito, G. (2019). Fungal and bacterial community dynamics in substrates during the cultivation of morels (*Morchella rufobrunnea*) indoors. *FEMS Microbiol. Lett.* 366:fnz215. doi: 10.1093/femsle/fnz215

Nerva, L., Sandrini, M., Moffa, L., Velasco, R., Balestrini, R., and Chitarra, W. (2022). Breeding toward improved ecological plant-microbiome interactions. *Trends Plant Sci.* 27, 1134–1143. doi: 10.1016/j.tplants.2022.06.004

Noble, R., Dobrovin-Pennington, A., Hobbs, P. J., Pederby, J., and Rodger, A. (2009). Volatile C8 compounds and pseudomonads influence primordium formation of Agaricus bisporus. *Mycologia* 101, 583–591. doi: 10.3852/07-194

Orlofsky, E., Zabari, L., Bonito, G., and Masaphy, S. (2021). Changes in soil bacteria functional ecology associated with *Morchella rufobrunnea* fruiting in a natural habitat. *Environ. Microbiol.* 23, 6651–6662. doi: 10.1111/1462-2920.15692

Ower, R. (1982). Notes on the development of the morel ascocarp: *Morchella esculenta*. *Mycologia* 74, 142–144. doi: 10.1080/00275514.1982.12021480

Parks, D. H., Tyson, G. W., Hugenholtz, P., and Beiko, R. G. (2014). STAMP: statistical analysis of taxonomic and functional profiles. *Bioinformatics* 30, 3123–3124. doi: 10.1093/bioinformatics/btu494

Patro, R., Duggal, G., Love, M. I., Irizarry, R. A., and Kingsford, C. (2017). Salmon provides fast and bias-aware quantification of transcript expression. *Nat. Methods* 14, 417–419. doi: 10.1038/nmeth.4197

Pilz, D., Mclain, R., Villarreal-Ruiz, L., Berch, S., Wurtz, T. L., Parks, C. G., et al. (2007). *Ecology and management of morels harvested from the forests of Western North America*. Portland: United States Department of Agriculture.

Ricotta, C., and Podani, J. (2017). On some properties of the bray-Curtis dissimilarity and their ecological meaning. *Ecol. Complex.* 31, 201–205. doi: 10.1016/j.ecocom.2017.07.003

Segata, N., Izard, J., Waldron, L., Gevers, D., Miropolsky, L., Garrett, W. S., et al. (2011). Metagenomic biomarker discovery and explanation. *Genome Biol.* 12:R60. doi: 10.1186/gb-2011-12-6-r60

Singh, P., Chauhan, P. K., Upadhyay, S. K., Singh, R. K., Dwivedi, P., Wang, J., et al. (2022). Mechanistic insights and potential use of siderophores producing microbes in rhizosphere for mitigation of stress in plants grown in degraded land. *Front. Microbiol.* 13:898979. doi: 10.3389/fmicb.2022.898979

Singh, R. K., Singh, P., Sharma, A., Guo, D. J., Upadhyay, S. K., Song, Q. Q., et al. (2022). Unraveling nitrogen fixing potential of endophytic diazotrophs of different saccharum species for sustainable sugarcane growth. *Int. J. Mol. Sci.* 23:6242. doi: 10.3390/ijms23116242

Sunil, C., and Xu, B. J. (2022). Mycochemical profile and health-promoting effects of morel mushroom *Morchella esculenta* (L.)—a review. *Food Res. Int.* 159:111571. doi: 10.1016/j.foodres.2022.111571

Tan, H., Kohler, A., Miao, R. Y., Liu, T. H., Zhang, Q., Zhang, B., et al. (2019). Multi-omic analyses of exogenous nutrient bag decomposition by the black morel *Morchella importuna* reveal sustained carbon acquisition and transferring. *Environ. Microbiol.* 21, 3909–3926. doi: 10.1111/1462-2920.14741

Tan, H., Yu, Y., Tang, J., Liu, T., Miao, R., Huang, Z., et al. (2021). Build your own mushroom soil: microbiota succession and nutritional accumulation in semi-synthetic substratum drive the fructification of a soil-saprotrophic morel. *Front. Microbiol.* 12:656656. doi: 10.3389/fmicb.2021.656656

Tang, J., Wang, Y., Xu, Y. Y., Tan, H., He, X. L., Yu, Y., et al. (2021). Research progress on key issues of morel industry development. *J. Fungal Res.* 19, 217–231. doi: 10.13341/j.jfr.2021.1466. (in Chinese)

Tietel, Z., and Masaphy, S. (2018). True morels (*Morchella*) nutritional and phytochemical composition, health benefits and flavor: a review. *Crit. Rev. Food Sci.* 58, 1888–1901. doi: 10.1080/10408398.2017.1285269

Upadhyay, S. K., and Chauhan, P. K. (2022). Optimization of eco-friendly amendments as sustainable asset for salt-tolerant plant growth-promoting bacteria mediated maize (*Zea Mays L.*) plant growth, Na uptake reduction and saline soil restoration. *Environ. Res.* 211:113081. doi: 10.1016/j.envres.2022.113081

Upadhyay, S. K., Srivastava, A. K., Rajput, V. D., Chauhan, P. K., Bhojiya, A. A., Jain, D., et al. (2022). Root exudates: mechanistic insight of plant growth promoting rhizobacteria for sustainable crop production. *Front. Microbiol.* 13:916488. doi: 10.3389/fmicb.2022.916488

Vajna, B., Szili, D., Nagy, A., and Marialigeti, K. (2012). An improved sequence-aided T-RFLP analysis of bacterial succession during oyster mushroom substrate preparation. *Microb. Ecol.* 64, 702–713. doi: 10.1007/s00248-012-0063-5

Wang, L., Mao, J. G., Zhao, H. J., Li, M., Wei, Q. S., Zhou, Y., et al. (2016). Comparison of characterization and microbial communities in rice straw- and wheat straw-based compost for *Agaricus bisporus* production. *J. Ind. Microbiol. Biotechnol.* 43, 1249–1260. doi: 10.1007/s10295-016-1799-6

Wood, D. E., Lu, J., and Langmead, B. (2019). Improved metagenomic analysis with kraken 2. *Genome Biol.* 20:257. doi: 10.1186/s13059-019-1891-0

Wu, G. G., Sun, Y., Deng, T. S., Song, L. L., Li, P., Zeng, H. J., et al. (2020). Identification and functional characterization of a novel immunomodulatory protein from *Morchella conica* SH. *Front. Immunol.* 11:559770. doi: 10.3389/fimmu.2020.559770

Xiong, C., Singh, B. K., He, J. Z., Han, Y. L., Li, P. P., Wan, L. H., et al. (2021). Plant developmental stage drives the differentiation in ecological role of the maize microbiome. *Microbiome* 9:171. doi: 10.1186/s40168-021-01118-6

Yang, R. H., Bao, D. P., Guo, T., Li, Y., Ji, G. Y., Ji, K. P., et al. (2019). Bacterial profiling and dynamic succession analysis of *Phlebopus portentosus* casing soil using MiSeq sequencing. *Front. Microbiol.* 10:1927. doi: 10.3389/fmicb.2019.01927

Zarenejad, F., Yakhchali, B., and Rasooli, I. (2012). Evaluation of indigenous potent mushroom growth promoting bacteria (MGPB) on *Agaricus bisporus* production. *World J. Microbiol. Biotechnol.* 28, 99–104. doi: 10.1007/s11274-011-0796-1

Zhang, B., Yan, L. J., Li, Q., Zou, J., Tan, H., Tan, W., et al. (2018). Dynamic succession of substrate-associated bacterial composition and function during *Ganoderma lucidum* growth. *PeerJ* 6:e4975. doi: 10.7717/peerj.4975

Zhang, X., Zhong, Y. H., Yang, S. D., Zhang, W. X., Xu, M. Q., Ma, A. Z., et al. (2014). Diversity and dynamics of the microbial community on decomposing wheat straw during mushroom compost production. *Bioresour. Technol.* 170, 183–195. doi: 10.1016/j.biortech.2014.07.093

Zhao, Q., Lv, M. L., Li, L., Huang, W., Zhang, Y. F., and Hao, Z. (2021). Temptation and trap of morel industry in China. *J. Fungal Res.* 19, 232–237. doi: 10.13341/j.jfr.2021.1447. (in Chinese)

Frontiers in Microbiology

Explores the habitable world and the potential of microbial life

The largest and most cited microbiology journal which advances our understanding of the role microbes play in addressing global challenges such as healthcare, food security, and climate change.

Discover the latest Research Topics

See more →

Frontiers

Avenue du Tribunal-Fédéral 34
1005 Lausanne, Switzerland
frontiersin.org

Contact us

+41 (0)21 510 17 00
frontiersin.org/about/contact